

# **Design, Synthesis and Evaluation of a Shape-Diverse Fragment Library**

**Rong Zhang**

Submitted in accordance with the requirements for  
the degree of Doctor of Philosophy

The University of Leeds

School of Chemistry

March 2017



The candidate confirms that the work submitted is her own and that appropriate credit has been given where reference has been made to the work of others.

This copy has been supplied on the understanding that it is copyright material and that no quotation from the thesis may be published without proper acknowledgement.

**© 2017 The University of Leeds and Rong Zhang**

The right of Rong Zhang to be identified as Author of this work has been asserted by her in accordance with the Copyright, Designs and Patents Act 1988.

## Acknowledgements

I would like to thank my supervisor Professor Adam Nelson for his support and teachings throughout my time at the University of Leeds. I have thoroughly enjoyed undertaking my PhD project and feel proud of my achievements, and this would not have been possible without Adam's encouragement and constant guidance.

I would also like to thank my co-supervisor Dr. Stuart Warriner for his invaluable help and notable ideas throughout my project, as I never imagined I would be able to employ the depth of computational chemistry as I have done within my PhD, and the worthwhile knowledge which I can now take forwards.

None of the biological aspect of my PhD would have been possible without the work conducted by Dr. Daniel Foley, and Patrick McIntyre in the X-ray crystallographic screen of my fragment library. I would also like to thank Dr. Patrick Collins and Diamond Light source for their facilities and collaboration on my project.

I want to thank my friends and colleagues within the Nelson group, not only those who are still here now, but also those who have come and gone in these three and a half years, including the MChem, MSc and summer students whom have made my time here so memorable.

One of the key reasons for which I chose to complete a PhD was due to inspiration from my father, who is also an organic chemist. I'd like to thank my parents for both their loving support and helping me make the right decisions in life.

Lastly, I would like to thank the EPSRC for providing funding for my project.

## **Abstract**

This thesis describes the development of a fragment library in order to identify the value of shape-diverse molecules in their ability to target novel areas of shape-space.

Chapter 1 introduces known approaches to ligand discovery as well as the concept of chemical space and molecular shape diversity. Chapter 2 describes the computational tools and protocols used to identify fragments of interest from both commercial and Leeds libraries, that fulfil the criteria of maximum coverage of reference shapes as well as high shape-diversity. The synthesis of fragments based on Leeds chemistry is described in Chapter 3, focusing on four key chemistries established within the Nelson group, as well as the reselection of molecules to overcome synthetic challenges. Chapter 4 describes the screen of the library of fragments using high-throughput X-ray crystallography, as well as the development of a novel fragment hit against Aurora A kinase. Overall my fragment library was successful in its ability to investigate unexplored shape-space and presented valuable hits against a useful target.

# Contents

Abbreviations .....	1
1. Introduction.....	3
1.1    Approaches to Ligand Discovery .....	5
1.2    Biophysical Methods for Fragment Screening .....	10
1.3    Chemical Space.....	12
1.4    Scaffold Diversity.....	18
1.5    Shape Diversity .....	19
1.6    Project Aims.....	24
2. Design of a Shape-Diverse Fragment Library.....	26
2.1    Use of the Terms “Building block,” “Scaffold,” and “Fragment” .....	26
2.2    Enumeration of the Compounds .....	27
2.3    Identification of a Suitable Heavy Atom Filter .....	34
2.4    Principal Moment of Inertia (PMI) Analysis.....	39
2.5    Identification of Reference Shapes for the Library and Generation of Shape Fingerprints.....	39
2.6    Identification of a Library of Synthetic Targets .....	42
2.7    Analysis of the Chosen Library .....	54
2.8    Purchase of Commercial Fragments.....	63
3. Synthesis of a Shape-Diverse Fragment Library .....	71
3.1    Shape-Similar Alternative Fragments.....	74
3.2    Alternative Fragment Libraries .....	75
3.3    Synthesis of Fragments Using the Ugi Reaction as a Key Step.....	79
3.4    Synthesis of Fragments Using Amino Acid Chemistry .....	95

3.5	Synthesis of Fragments Using the Mitsunobu Reaction as a Key Step.....	102
3.6	Synthesis of Fragments Using Iridium Chemistry.....	107
4.	Evaluation of a Shape-Diverse Fragment Library .....	111
4.1	Screening of Fragment Library using X-ray Crystallography.....	111
4.2	Aurora A Kinase as a Protein Target.....	112
4.3	Fragment Hits against Aurora A Kinase .....	115
4.4	Design of a Library of Analogues of a Hit Compound .....	120
4.5	Synthesis of a Library of Analogues of a Hit Compound.....	122
4.6	Screening of Library of Analogues against Aurora A Kinase .....	132
4.7	Project Summary.....	135
5.	Experimental .....	136
5.1	General Experimental .....	136
5.2	General Procedures.....	138
5.3	High-Throughput Protein Crystallography.....	145
5.4	Synthesis of Building Blocks .....	146
5.5	Connection of Building Blocks.....	163
5.6	Synthesis of Scaffolds.....	182
5.7	Synthesis of Fragments .....	201
	Appendix.....	248
	References.....	297



## Abbreviations

$\delta$	chemical shift
ATR	attenuated total reflectance
Boc	<i>tert</i> -butyl oxy carbonyl
Bu	butyl
CAN	ceric ammonium nitrate
CDI	carbonyldiimidazole
conc.	concentrated
COSY	correlation spectroscopy
DCE	dichloroethane
DCM	dichloromethane
DDQ	2,3-dichloro-5,6-dicyano-1,4-benzoquinone
DEAD	diethyl azodicarboxylate
DEPT	distortionless enhancement by polarisation transfer
DIAD	diisopropyl azodicarboxylate
DIBAL-H	diisobutylaluminium hydride
DIPEA	<i>N,N</i> -diisopropylethylamine
DMAP	4-dimethylaminopyridine
DMF	<i>N,N</i> -dimethylformamide
DMS	dimethyl sulfide
DMSO	dimethyl sulfoxide
ES	electrospray
Et	ethyl
ether	diethyl ether
HMBC	heteronuclear multiple bond correlation
HMQC	heteronuclear multiple quantum coherence
HRMS	high resolution mass spectroscopy
FT-IR	fourier transform infra-red
<i>J</i>	coupling constant
LCMS	liquid chromatography mass spectroscopy
<i>m/z</i>	mass to charge ratio
Me	methyl
m.p	melting point

NMR	nuclear magnetic resonance
NOE	nuclear Overhauser effect
petrol	petroleum spirit (b.p. 40-60 °C)
PMB	<i>para</i> -methoxybenzyl
RCM	ring-closing metathesis
sat.	saturated
TBDPS	<i>tert</i> -butyldiphenylsilyl
TFA	trifluoroacetic acid
THF	tetrahydrofuran
THP	tetrahydropyran

# 1 Introduction

Our ability to address the issues which determine drug success or failure is reliant on possessing synthetic chemistry methodology to make the right molecules quickly and predictably. A chemical lead is a molecule with good potency in biological assays, and reflects the targeted mechanism. The absorption, distribution and metabolism profile (ADME) of a chemical lead could be determined; a drug must achieve high and sustained plasma concentrations after oral dosing to exert the desired effect.<sup>1</sup>

Initial starting points (*i.e.* “hits” or “leads”) are often found by screening of compounds from chemical libraries which are usually reliant on robust chemical methodology for their production. Such methodology includes reductive aminations, acylations, Pd-mediated cross-couplings and  $S_NAr$  reactions.<sup>2</sup> Once initial hits have been identified, the lead optimisation process aims to improve their drug-like profile and activity through the synthesis of many designed analogues. Once a single clinical candidate molecule has been identified, scale-up and process chemistry then devises cost-effective and efficient syntheses to deliver the final compound on multi-kilogram scales.<sup>3</sup> The drug discovery process is summarised in Figure 1.

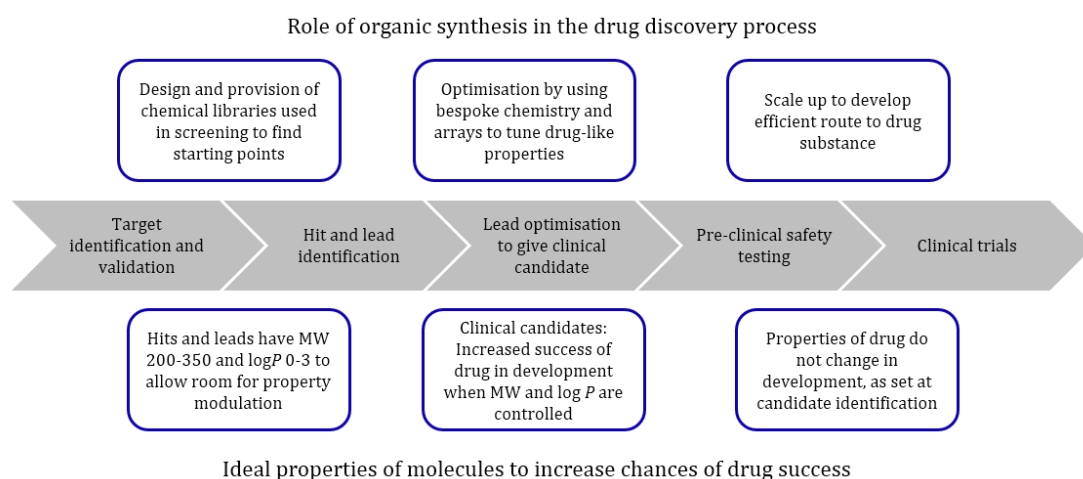


**Figure 1** An overview of the drug discovery process highlighting the role of organic synthesis and the ideal properties of molecules at each stage. MW = molecular weight in Da,  $\log P$  =  $\log$ (partition coefficient in *n*-octanol/water). Adapted from <sup>3</sup>

Oral drugs usually obey the Lipinski rule of five<sup>i</sup> (MW <500 Da,  $\log P$  <5, no. of hydrogen bond donors  $\leq 5$ ) in order to be easily absorbed.<sup>4</sup> More recent studies have shown however, that compounds close to the limits defined by Lipinski actually have a

<sup>i</sup> Lipinski states that it is possible to fail one of the guidelines and still produce a successful drug.

lower probability of success in development, with significantly lower MW and  $\log P$  values favoured in successful medicines. These observations have led to several revised guidelines suggesting, for example, that molecules with  $\log P < 3$  and polar surface area  $> 75$  will show greater safety in pre-clinical studies or that molecules with MW  $< 400$  and  $\log P < 4$  appear to be more successful in a range of assays of drug-like character.<sup>3</sup> The drug optimization process is illustrated in Figure 2.

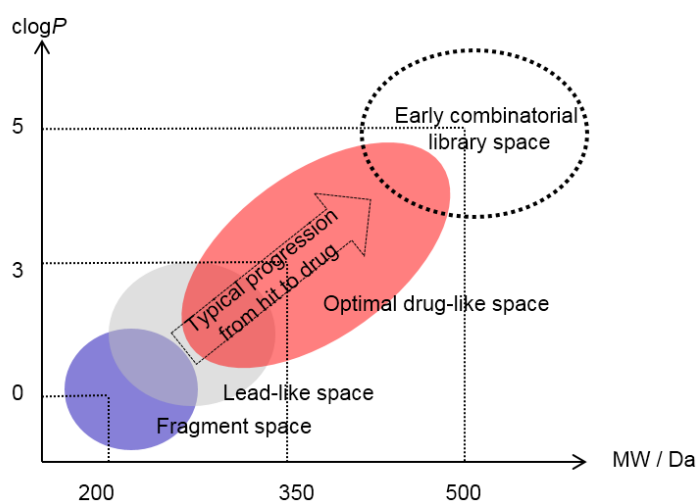


**Figure 2** Optimal oral drug-like space can be defined by the central red oval. As optimization tends to progress by addition of complexity and lipophilicity (arrow), starting points should be in lead-like (or fragment-like) areas of property space for the progression to end in drug-like space. Adapted from <sup>3</sup>

The strategy of increasing lipophilicity to gain better binding to a drug target is often used to increase apparent drug potency but can also result in a greater probability of binding to other, undesired, drug targets.<sup>3</sup> Controlling the lipophilicity of drug substances is thus pivotal to the drug discovery process and  $\log P$  values in the range 1 to 3 are now thought to give the best balance of properties for most oral drugs. Other factors to take into consideration include the number of aromatic rings and the fraction of  $sp^3$ -hybridised carbons.<sup>5,6</sup>

Though the degree of aromaticity may also be related to the  $\log P$  of molecules, excessive levels of aromaticity are usually associated with undesirable outcomes. This leads to suggestions that aromatic rings on lead-like molecules should be limited to a maximum of three, and a lower proportion of  $sp^2$ -hybridised carbon atoms should be incorporated than typical historically. Many functional groups are undesirable due to chemical stability issues (*e.g.* acid chlorides, many Michael acceptors, most organometallics), as well as the potential for toxicity, unwanted interactions with biological systems or general instability.<sup>3</sup>

## 1.1 Approaches to Ligand Discovery

Chemical technologies that have impacted drug discovery in previous decades include computational methods such as quantitative structure-activity relationships and combinatorial chemistry.<sup>1</sup> Different approaches that are currently used to obtain chemical leads include from an existing lead or drug, from a natural product, and high throughput screening (HTS, described in Figure 3). The preclinical drug-discovery cascade, starting from HTS and moving into the launched drug phase requires the screening of the order of one million compounds to find a suitable lead for one ultimately successful outcome.<sup>7</sup> Fragment-based drug discovery (FBDD) is a new approach, increasingly used in the pharmaceutical industry, for reducing attrition and providing leads for challenging biological targets.<sup>8</sup>

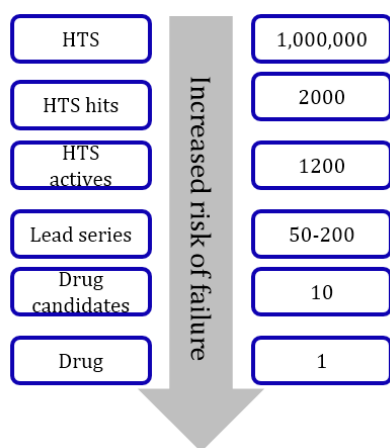


**Figure 3** A typical drug discovery cascade using HTS, showing the number of compounds assessed at each stage (for illustrative purposes only). A 40% false positive rate is assumed in evaluating HTS hits, and one in two to five leads are assumed to progress from lead identification to drug candidate. The risk of failure increases as a molecule becomes a drug candidate because of high costs in clinical trials. Adapted from <sup>7</sup>

### 1.1.1 Traditional Approaches

There are several traditional approaches to the discovery of drug molecules. The most widespread traditional methods include the use of combinatorial libraries and HTS. The combinatorial chemistry approach is pursued in the hope to gain quick access to novel pharmaceuticals, through the rapid generation and screening of vast collections of molecules.<sup>9</sup> A wide variety of high-speed and parallel synthetic techniques are applied such as solid-phase synthesis, and separation techniques in order to effect an easy purification of intermediates and final products.<sup>10</sup> Combinatorial libraries consist of static populations of discrete molecules, derived from a set of units connected in various sequences by the repetitive application of specific chemical reactions, with the aim of producing as high a structural diversity as possible.<sup>11</sup> The rapid increase in the availability of compound libraries drove the development of methods for faster and more efficient screening of lead molecules. HTS is based on robotic handling of small amounts

of materials, and equivalent advances in the detection of relevant signals and interpretation of the data.<sup>12</sup>

The reality of drug-receptor interactions, at the molecular level, is too complex to provide a fail-safe *in silico* technology for drug discovery. Beyond ligand-receptor interactions, there is the complexity of multiple binding modes, accessible conformational states (whether static or dynamic) for both ligand and receptor, affinity vs. selectivity, plasma protein binding, metabolic stability, ADME, as well as *in vivo* vs. *in vitro* properties of model compounds.

In the combinatorial chemistry field, differences in the reactivity of similar, yet diverse reagents, often leads to impurity, or failure to synthesise the compounds at all. In combination with inadequate or missing synthetic blocks, this has resulted in moderately successful lead-finding combinatorial libraries focused more on forming carbon-heteroatom bonds and less on forming carbon-carbon bonds.<sup>13</sup> In comparison, mixtures of compounds per well in HTS do not generally yield reliable results compared to one compound per well, and screening potentially reactive species is often a cause of false hits.<sup>14</sup> Furthermore, single dose/single test procedures require repeat experiments in order to eliminate the false positives and to confirm the structure and biological activity of the HTS hits. The stability of the compounds in solid form, or in solution, coupled with the compounds' availability for future HTS, add further challenges.

Permeability and solubility are properties increasingly being screened for with computational and experimental methods, prior to choosing candidate leads for further optimisation. Virtual screening has emerged as an adaptive response to HTS, as Lipinski's rule<sup>4</sup> implemented early on in drug discovery could potentially increase the chance of success in drug discovery projects. Compound filtering according to Lipinski rule of five can save time in the process of synthesis planning, and opens up the possibility of exploring large numbers of reagents - since post-enumeration property estimation is usually much more time-consuming.

Filtering also avoids large numbers of reactive halogens in the products, the presence of highly flexible unsubstituted, unbranched alkyl chains, the formation of compounds that exceed the maximum accepted number of rings, or ionisable groups, in the product library. More importantly, molecules that are reactive toward protein targets can also be removed, such as Michael acceptors, ketones and aldehydes. Such compounds would not yield leads or hits, but would likely turn out to be false HTS positives.<sup>13</sup> Finally, if changes that influence binding affinity and ADME properties were simultaneously monitored, there would be much more reduced chance of prediction errors and the approach is likely to converge on interesting compounds more rapidly.<sup>15</sup> This could be a

less resource-demanding strategy and is especially useful in the absence of experimental hits from already existing drugs.

It is notable that most drugs found in compiled databases were classically discovered and developed using biological assays, selective cytotoxicity assays and animal models of disease, not using biochemical (*e.g.* HTS) assays. Today, there is a risk that high-throughput experiments reduce the opportunity for innovative and iterative thinking, as millions of molecules are screened simultaneously without the possibility of interpretation and analysis between the traditional rounds of experiments for this number of data points.<sup>7</sup>

### **1.1.2 Fragment-Based Drug Discovery**

Fragment-based drug discovery identifies low MW ligands (typically 150-300 Da) that bind to biologically important macromolecules.<sup>1</sup> A recent analysis<sup>16</sup> suggests that projects involving fragment screening generate smaller, less lipophilic hits and leads than those identified through the use of other hit discovery techniques, such as HTS. Compared with HTS, the fragment approach requires fewer compounds to be screened due to better coverage of chemical space, *i.e.* the space spanned by all possible chemical compounds in all possible topology isomers.<sup>17</sup> As a result, fragment screening offers more efficient and successful optimization campaigns, despite the lower initial potency of the screening hits.<sup>1</sup> Furthermore, reducing the numbers of molecules screened in the individual steps is desirable for academic groups or start-up companies that do not have the same screening capacities as large pharmaceutical companies.<sup>8</sup>

The first and second fragment-based drugs, Zelboraf and Venclexta can be seen in Figure 4. Zelboraf<sup>18</sup> functions as a B-Raf enzyme inhibitor and is used to treat metastatic melanoma. Zelboraf was discovered at Plexxikon and developed in partnership with Roche; the drug was approved in August 2011 and reached market in just six years. Venclexta<sup>19</sup> functions as a Bcl-2 PPI inhibitor and is used to treat chronic lymphocytic leukaemia; the drug was co-developed by AbbVie and Genentech and approved in April 2016.

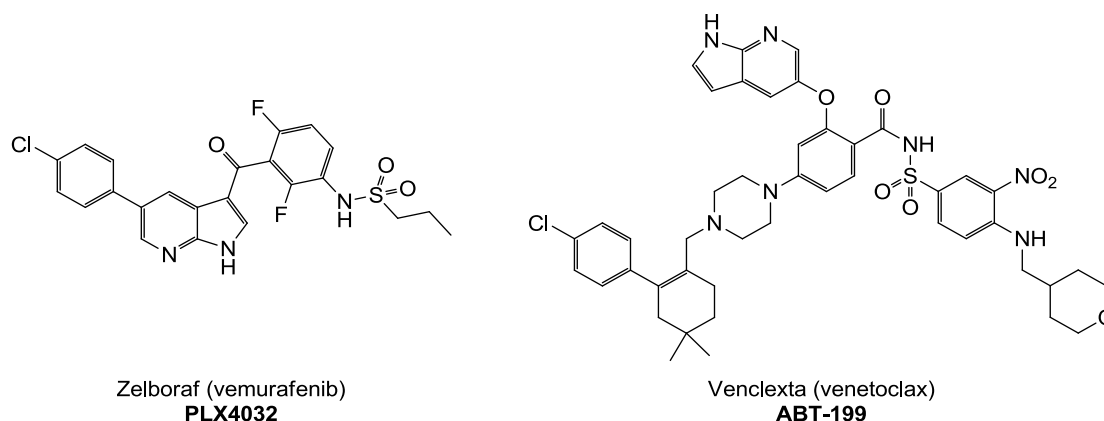
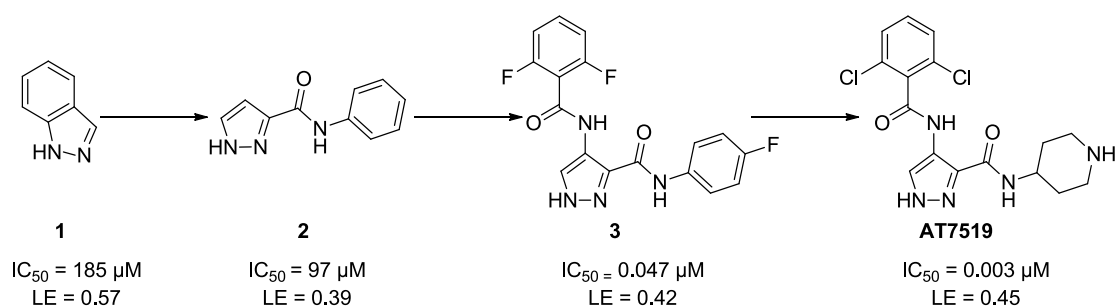


**Figure 4** The first and second drugs discovered using FBDD, Zelboraf and Venclexta.

In FBDD, the optimization process starts from a small and efficiently binding fragment in which each atom in the molecule is involved in the desired binding interactions. Thus, the size, complexity and physical properties of the molecule can be more easily controlled than when starting from a higher-affinity HTS hit that contains groups not essential to the desired binding. If the “weak” fragment forms part of a potent drug, and still forms the same interactions with the protein, then the fragment in fact contributes over half<sup>1</sup> the favourable binding energy despite being tens of thousands of times weaker in affinity.

Ligand efficiency ( $LE = \Delta G^\circ \div N$ , the binding energy per heavy atom of a ligand to its binding partner) of a fragment can be maintained during a fragment-to-lead chemistry campaign, provided structural information about binding interactions is available.<sup>20</sup> This can be achieved by growing the fragment synthetically to a proximal binding site, or by linking two fragments together. An example of a fragment to drug campaign can be described in the discovery of **AT7519**, an inhibitor of cyclin-dependent kinases (CDK)<sup>21</sup> (Scheme 1). The  $\log P$  (calculated  $\log P$ ) changes of the compound at each different stage of development is shown (Figure 5). Binding energy is proportional to  $\log(IC_{50})$ , thus it can be shown that as binding energy of the compound increased (became more negative), LE against CDK was maintained, represented by the exponential relationship between  $IC_{50}$  and number of heavy atoms (Figure 6). This is generally the case for high LE fragments.<sup>1</sup>



**Scheme 1** The discovery of **AT7519**. Fragment **1** was identified from an X-ray screen as binding to the hinge region of the kinase, and this interaction was consolidated with the amide in **2**. Growing into a proximal binding pocket and using di-*ortho* substitution to induce a twist in the second phenyl ring led to structure **3**, the lead molecule. To improve cell-based activity and *in vivo* efficacy, a piperidine solubilizing group was incorporated into the final candidate structure, **AT7519**.<sup>21</sup>

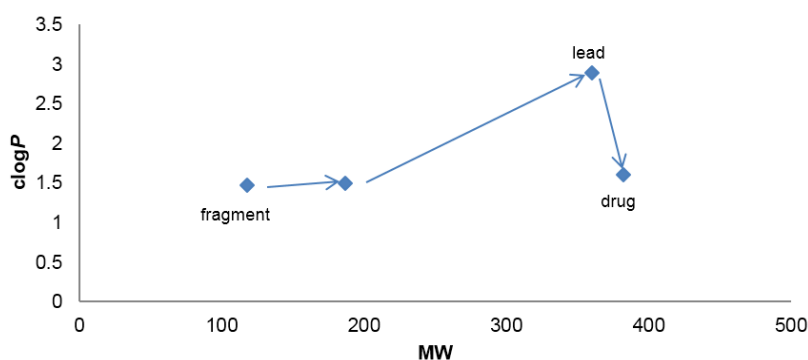


**Figure 5** Relationship between  $clogP$  and MW as the fragment is developed into a higher MW lead compound, before polar groups are incorporated into the final drug in order to optimise ADME (Scheme 1).

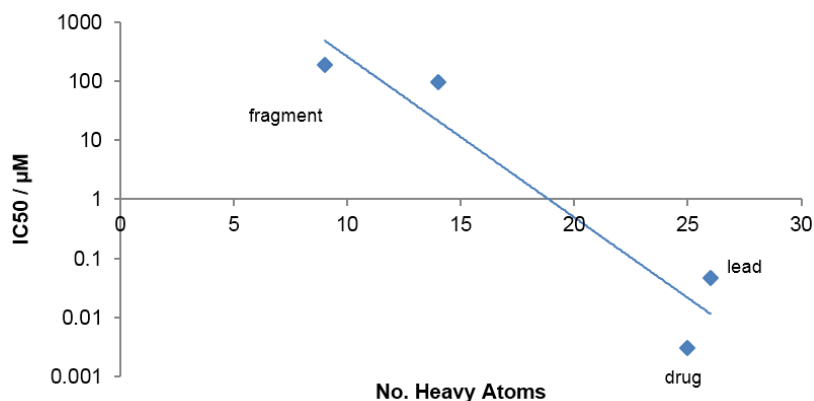


**Figure 6** Relationship between  $IC_{50}$  and number of heavy atoms as the fragment is developed into a higher MW lead and drug compound (Scheme 1). Since  $\log(IC_{50})$  is proportional to the binding energy of the ligand to its binding partner, the logarithmic trend observed between  $IC_{50}$  and number of heavy atoms indicates unchanged LE throughout this process *i.e.* the gradient is constant.

In most cases, a co-crystal structure is necessary in order to fix the binding mode of the fragment before growing it. This often reduces fragment screens to targets that have a soakable crystallography system established. Unfortunately, the fragment or

analogues of the fragment may not be amenable to synthesis. There is frequently a need for chemical synthesis to access a compound with potency similar to a compound that might be identified through other means such as HTS. Secondly, it is hard to imagine certain types of chemotypes ever being obtained through FBDD, for example, a complex natural product with a few fused rings or a macrocyclic compound.<sup>8</sup>

Due to their weaker affinity, specialized techniques are required to screen for fragments. Biophysical methods such as X-ray diffraction, NMR spectroscopy, surface plasmon resonance (SPR), isothermal calorimetry and mass spectrometry have been exploited.<sup>22</sup> There also continues to be a key role for more traditional biochemical screening formats such as fluorescence anisotropy or time-resolved fluorescence energy transfer, though the preferred configuration of such assays for fragment screening may need to be different from the format used in, for example, HTS.<sup>23</sup>

These techniques usually require specialized equipment, personnel with specific expertise, supporting informatics infrastructure, and access to large amounts of purified protein (>10 mg). The fragments also need to be soluble at the high concentrations used for screening, and this may be an advantage in the subsequent lead optimization stage.<sup>1</sup> Thus, in fragment screening, tolerance to large amounts of organic material is often necessary whereas in HTS the emphasis is on miniaturisation and cost reduction.<sup>23</sup> Previous difficult experiences in optimizing  $\mu\text{M}$  HTS hits created the assumption that it would be harder to start from a lower potency. In practice, the high LE and the high quality interactions of fragments to the target protein make them much more optimisable.<sup>1</sup>

## 1.2 Biophysical Methods for Fragment Screening

Key structural methods such as X-ray crystallography or NMR spectroscopy can be used to rationalise fragment binding and direct synthetic modifications to the chemical scaffolds, allowing a rapid increase in affinity towards the target. This also enables other properties, such as selectivity, to be explored at an early stage.<sup>24</sup> Surface plasmon resonance (SPR) is another primary biophysical method for the screening of low molecular weight fragment libraries. SPR biosensor technology is used to identify the binding of compounds to protein targets, as well as provide accurate information on the affinity and kinetics of molecular interactions.<sup>25</sup> Other fragment screening methods include techniques such as isothermal titration calorimetry<sup>26</sup> and mass spectrometry.<sup>22</sup>

### **1.2.1 Fragment Screening by Surface Plasmon Resonance**

SPR is a label-free technology used to monitor biomolecular interactions.<sup>27</sup> This technique is highly sensitive and capable of detecting fragments with molecular weights as low as 100 Da bound to biomolecular targets.<sup>28</sup> SPR is very attractive due to its low protein consumption,<sup>29</sup> rapid assay development and kinetic and thermodynamic validation of hits.<sup>28</sup> The protein is first immobilized onto a chip surface, which enables as many as thousands of molecules to be sequentially screened using the same surface before the protein needs to be renewed.<sup>29</sup> In an SPR experiment, the change in the surface plasmon resonance angle upon interaction of the fragment with the immobilized protein creates the detected response. The response in SPR is proportional to the fraction of bound protein.<sup>30</sup>

It is important to note that protein-fragment interactions can be only be detected when working at fragment concentrations comparable to the dissociation rate constant of the fragment. This is crucial when screening targets for which the fragments do not have a large binding efficiency index, such as some inhibitors of protein-protein interactions.<sup>29</sup> Nevertheless, SPR allows the analysis of binding kinetics, thus providing the association and dissociation rate constant of the interactions.<sup>31</sup> In addition, SPR-based fragment screening has potential to eliminate all nonspecific binders, and another advantage is the availability of multiple biosensor channels, meaning multiple proteins can be screened in parallel.<sup>28</sup>

### **1.2.2 Fragment Screening by NMR**

NMR-based fragment screening offers a large dynamic range and is capable of capturing very weak interactions.<sup>29</sup> Detection of binding by NMR may be achieved using techniques such as chemical shift perturbation, differential line broadening, transfer NOE, and diffusion-based methods. These methods can be distinguished by those that monitor NMR signals from the protein, and those that monitor signals from the ligands.<sup>32</sup> The relatively low sensitivity of NMR detection can be partially offset by the high compound concentrations used when studying weak protein-fragment interactions,<sup>33</sup> and this is the case even when the compounds are used at concentrations orders of magnitude lower than their dissociation binding constants. Screening by NMR offers the benefit of identification of hits that are insoluble at the concentrations required for detection by other biophysical techniques.<sup>29</sup> In addition, the ability for NMR to detect changes in the concentrations and aggregation states of the fragments significantly reduces the number of false positives compared to biochemical assays.<sup>33</sup> Nevertheless, it is ideal for

complementary screening techniques to be applied for supporting evidence.<sup>29</sup>

### 1.2.3 Fragment Screening by X-Ray Crystallography

In order to use X-ray crystallography as a method for fragment screening, it is necessary to prepare and analyse large numbers of crystalline complexes.<sup>33</sup> This is done by exposing the protein to the fragments, and solving the crystal structures of the resulting complexes. One technique involves growing crystals of the target protein and then soaking them in solutions of the fragments; a soakable system is thus essential. This could be done either for single compounds or as cocktails of compounds.<sup>34</sup> Screening by X-ray crystallography requires the production of diffraction quality crystals, which need to be generated reproducibly and to a similar size and quality on a large scale. Thus, optimisation of the processes from protein production to crystallisation is necessary.

Systems for efficient collection of X-ray diffraction data is key for rapid progression in the screening process. A principal step in solving structures of protein–ligand complexes is the placement of the ligand into the experimentally observed electron density,<sup>33</sup> and final binding evidence is provided by the X-ray structure of the fragment bound to the receptor. In addition, this delivers the relevant structural information toward any fragment optimization in a medicinal chemistry campaign. However, it can be difficult to observe electron density of fragment hits bound to their receptor due to various experimental causes.<sup>29</sup>

## 1.3 Chemical Space

Compared with higher MW molecules used in methods such as HTS or lead-oriented synthesis, the fragment approach requires fewer compounds to be screened. This is because smaller, less complex molecules sample chemical space more efficiently and have a greater chance of fitting a given drug binding site. It has been estimated<sup>35</sup> that for every extra heavy atom added to an organic molecule, the number of potential structures increase by around a factor of 10 *i.e.* there are approximately  $10^7$  more molecules with MW 400 relative to those with MW 300. Thus, by screening sets of lower MW compounds, a relatively greater proportion of accessible chemical space can be sampled thereby increasing the chance of finding hit molecules. By analogy to the Lipinski Rule of five,<sup>4</sup> fragments are often described using a modified Rule of three (MW <300 Da,  $\log P < 3$ , no. of hydrogen bonds  $\leq 3$ ).<sup>3,36</sup>

Knowledge of active fragments can be used in data-mining analyses of the output from an HTS screen, and the ready availability of significant numbers of analogues in an HTS screening collection can provide rapid structure-activity relationships around

fragment hits.<sup>23</sup> Molecular complexity is discussed in detail in this section, and its relevance to fragment screening. Examples of library synthesis methods which allow the optimal coverage of chemical space include combinatorial variation of scaffolds used in lead and diversity-oriented synthesis, and chemistry and biology-based expansion in fragment screening.

### 1.3.1 Molecular Complexity

The molecular complexity model is based around the theory that a ligand binds to a receptor if there is an exact match between all of their interaction features (Figure 7). It was found that the probability of binding decreases rapidly as the complexity of the ligand increases, since there are many fewer ways of obtaining a match than a mismatch. In addition, the probability of finding a unique binding event, *i.e.* where the ligand matches the receptor in one way only, passes through a maximum, as very simple ligands can find multiple binding modes (Figure 8).<sup>23</sup>

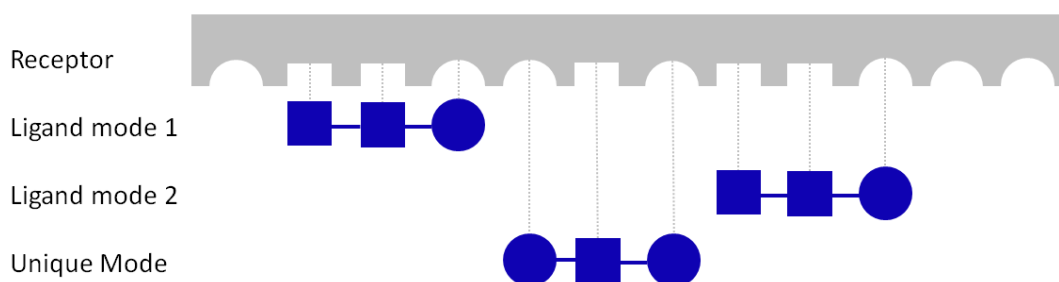


**Figure 7** The complexity model where ligands are represented as linear strings of circles and squares and their receptor is represented as a combination of circular and square clefts. A match corresponds to exactly complementing features of ligand and receptor. Some ligands can match more than one way (modes 1, 2), and other ligands only show a unique mode.

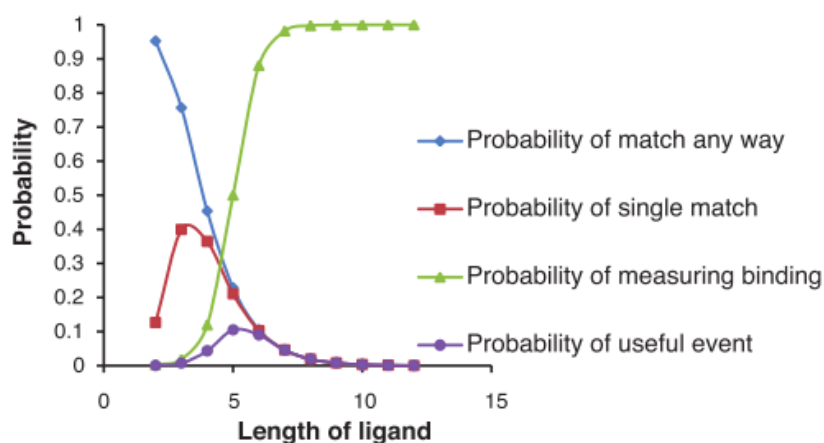


**Figure 8** Data for random receptors of length 12. This model shows that the probability of a ligand binding to a receptor in at least one mode decreases rapidly with ligand length (blue). The probability of matching in one way only goes

through a maximum (red, at ligand length 3). Combined with the probability of physically detecting a binding event (green, the longer the ligand the more easily it is detected), gives the overall probability of a “useful event” (purple, where the ligand binds in a single binding mode and can be detected). Reproduced from <sup>23</sup>

Moreover, the physicochemical properties of larger, more complex molecules mean they are not compatible with good medicinal chemistry starting points due to the tendency for these properties to increase further during lead optimisation. Key limitations to the model include the restriction to a binary interaction type (charge, shape, desolvation, polarisation, *etc.*), the one-dimensional nature of the representation and the requirement for all features to match.

Ligand promiscuity can be calculated by determining the number of targets to which a given ligand binds. Compounds with higher MW exhibit on average higher promiscuity, alongside increased lipophilicity. A way of incorporating promiscuity into the model is to require only a threshold number of matches between ligand and receptor, ignoring any additional mismatches. Under this approach it is found that the probability of a ligand interacting with a receptor increases with the size of the ligand, because there is a higher likelihood of finding suitable matching substrings in a longer ligand, although with lower potency (using the number of matches as a surrogate for potency). In drug discovery the emphasis is on optimising the activity of a lead series against the primary target of interest whilst minimising activity at other targets; and since such compounds will tend to concentrate in lipid bilayers which are home to many key signalling systems, the likelihood of off-target interactions and ultimately toxicities will also be increased.<sup>23</sup>

### 1.3.2 Lead-Oriented Synthesis

In general, lead-like molecules have  $\log P$  values in the range  $-1$  to  $3$  and MW in the ideal range  $200$  to  $350 \text{ g mol}^{-1}$  (approximately  $14$  to  $26$  non-hydrogen atoms).<sup>3</sup> Lead-oriented synthesis must be able to deliver molecules with specific molecular properties, while also maintaining the synthetic efficiency to allow their cost-effective utilization. It does this by focusing on the physicochemical and functional group properties of the target molecules.<sup>3</sup> The concept and methods related to lead-likeness are very intuitive and fit with the current experience of what typically happens in lead optimization.<sup>7</sup>

Unprotected polar functionality is often poorly compatible with many reagents due to high reactivity, insolubility in non-polar solvents, or coordination to a catalyst.<sup>37</sup> The pharmaceutical industry seeks to identify molecules able to efficiently interact with biological systems, frequently through polar or hydrogen bonding interactions; unfortunately, these polar interactions rely on functional groups such as weakly acidic OH and NH bonds or Lewis base/hydrogen bond acceptors. Lead-oriented syntheses should ideally be able to mediate novel transformations in the presence of such biologically relevant functional groups. But whilst these reactive groups can introduce further functionality or diversification, they also leave undesired structural features. Similarly,

protecting groups often remain in reaction products requiring extra chemical steps for their removal which may severely limit the practical application in arrays. Lead-oriented syntheses which do not leave residual undesired reactive centres or protecting groups are therefore of particular value.<sup>3</sup>

In contrast, diversity-oriented synthesis targets scaffold diversity mainly in drug-like space, by using cascades which produce large numbers of molecular scaffolds using a small set of transformations.<sup>3,38,39</sup> Unlike lead-oriented synthesis, diversity-oriented synthesis shows little consideration towards molecular properties. Other methods include target-oriented synthesis, which targets just one compound, and combinatorial chemistry, which targets large numbers of compounds. Early combinatorial synthesis libraries relied on diverse capping groups for their overall diversity, but the addition of multiple points of diversity in order to build a large library often meant the molecules lie outside of lead-like space on grounds of size and lipophilicity.<sup>3</sup> Examples of generic structures considered for a reduced complexity screening set is shown in Figure 9.

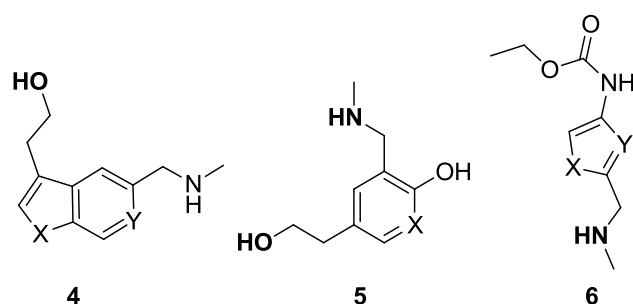
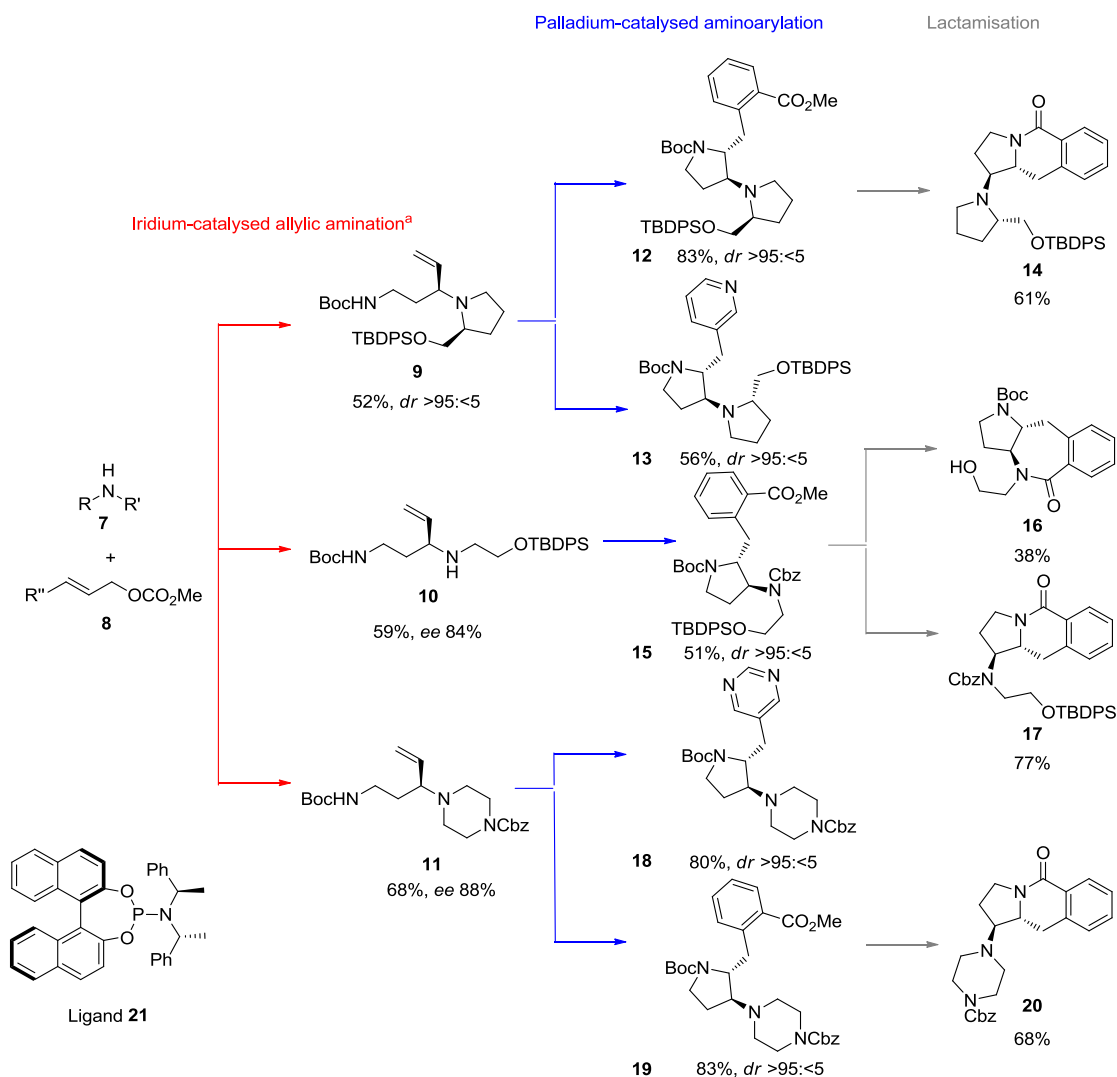


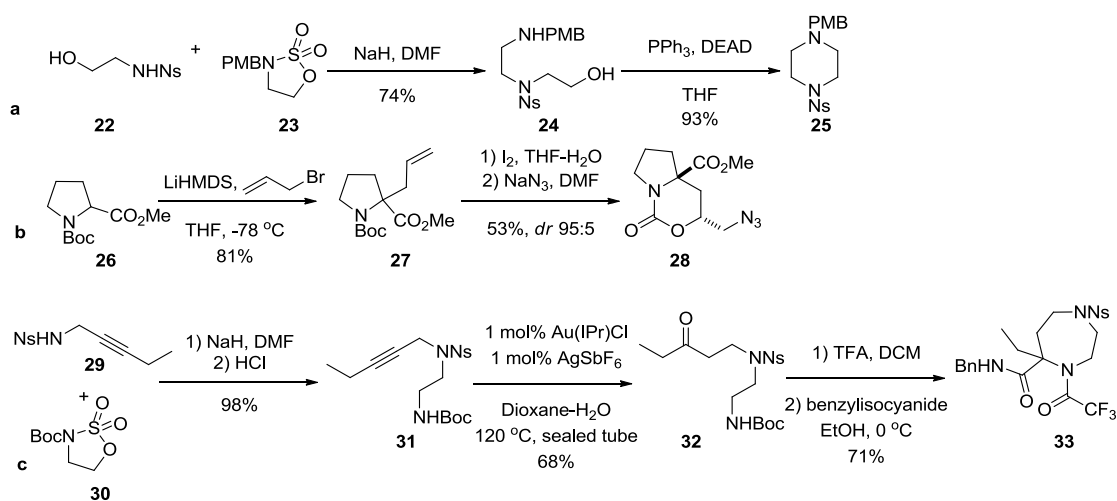
**Figure 9** Examples of generic structures considered for a reduced complexity screening set. X and Y indicate possible heteroatoms. Synthetic handles are shown in bold.<sup>7</sup>

### 1.3.2.1 Examples of Lead-Oriented Synthesis

Methodology that allows the connectivity of building blocks to be varied whilst maintaining a common approach are particularly valuable *e.g.* an Iridium catalysed allylic amination reaction (Scheme 2). Synthetic approaches to diverse lead-like molecular scaffolds are more powerful if more bonds are formed to individual building blocks, or if more building blocks are used.<sup>40</sup> It should also be possible to vary all of the building blocks independently. Finally, the value of specific synthetic approaches depends on the accessibility of the starting materials, the increased molecular complexity of the product scaffolds, the structural diversity of the product scaffolds, and the molecular properties of the derivatives.<sup>5</sup> Further examples of advantageous synthetic approaches include scaffolds formed using Mitsunobu reactions, amino acid chemistry, and Ugi reactions (Scheme 3).



**Scheme 2** Synthesis of example lead molecules using iridium-catalysed allylic amination reactions. a) 2 mol% [Ir(dbcot)Cl]<sub>2</sub>, 4 mol% ligand **21**, 4 mol% <sup>n</sup>BuNH<sub>2</sub>, DMSO, 55 °C. dbcot = dibenzo[*a,e*]cyclooctatetraene.<sup>41</sup>

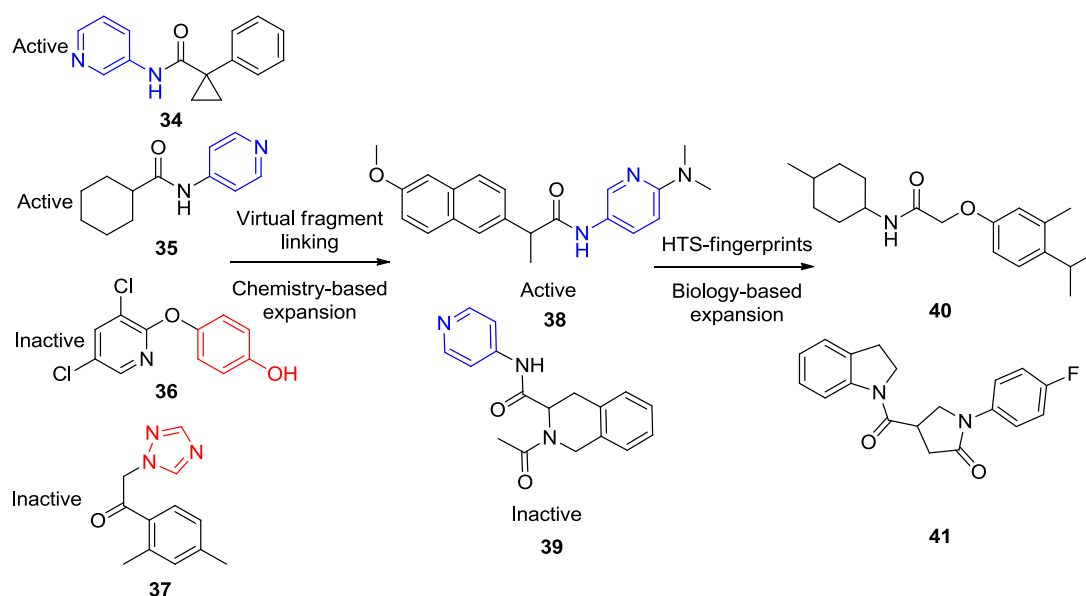


**Scheme 3** Synthesis of example lead molecules using key reactions including a) Mitsunobu chemistry<sup>42</sup>, b) amino acid chemistry<sup>43</sup> and c) Ugi chemistry<sup>44</sup>.

### 1.3.3 Fragment Development

Evaluation of several fragment libraries shows that they are predominantly populated with (hetero)aromatic-derived chemotypes, which might bias their success for certain targets.<sup>16</sup> By combining fragment-based screening with virtual fragment linking and HTS fingerprints, another effective strategy has been developed not only to expand from low-affinity hits to potent compounds but also to hop in chemical space to substantially novel chemotypes.

One approach<sup>8</sup> (Scheme 4) involved information about desirable substructures being firstly extracted from a fragment screen, and this information is used to select larger compounds containing these substructures (chemistry-based expansion). In the next step, the larger compounds are tested for activity, and information regarding the biological and biochemical activity enriched in the active compounds is used to select a subsequent set of small molecules for evaluation (biology-based expansion). It was found that in the chemistry-based expansion the desirable linking of the fragment substructures is revealed. Furthermore, in the second step, the biological fingerprints of the active hits were able to be uncovered, and by expanding on the basis of these fingerprints, active compounds were identified that contain chemotypes not covered by the original fragment library.



**Scheme 4** Fragment-hit expansion strategies, virtual fragment linking and HTS fingerprinting, use a combination of chemistry and biology-based expansion to select small molecules for testing. In the first step, chemical features (highlighted in red and in blue) are extracted from the active and inactive fragment pool and used to generate conditions applied to the screening collection. The top-ranked molecules are screened and then divided into an active and inactive sets to build a second classifier according to bioactivity profiles. Adapted from <sup>8</sup>

Compounds that are identified from biological expansion often contain substructures that had been enriched in fragment hits in the hot-spot region, while exploring other parts of the binding pocket with substructures that fragment-based screening identified as unfavourable for the hotspot. Although it might be by chance that these unfavourable substructures are present in the biological expansion hits, it is notable because the presence of the unfavourable substructures would preclude them from being identified earlier during the chemical expansion.

Chemistry-based expansion of fragment hits was able to identify only active compounds concentrated in a very narrow area of chemical space. However, as non-structural descriptors, HTS-fingerprinting in biology-based expansion was able to reach out to active compounds further away in chemical space. These observations show that it is the combination of orthogonal views on molecular similarity (chemical and biological) in the two hit-expansion steps that is crucial for a successful follow-up on fragment hits. Since random compound selection in the first step led to the identification of rather structurally diverse active molecules, the subsequent chemistry-based expansion was not biased toward a particular region but was able to retrieve active molecules scattered over large parts of chemical space.<sup>8</sup>

## 1.4 Scaffold Diversity

Assessing chemical diversity requires each structure to be characterized by one or more descriptors. These can be molecular descriptors such as physicochemical properties or topological indexes. Larger substructures such as ring systems can also be used; an advantage of using large features like rings is that structures having such features in common often belong to the same chemical family. The framework is obtained by removing all side-chain atoms, *i.e.* non-ring atoms not on a direct path between two ring systems. As a result, the framework of a structure is described by all of the ring systems and all the linkers. Typically, the framework describes only molecular topology, *i.e.* contains no three-dimensional (3D) or stereochemical information. Part of the reason this concept is useful in medicinal chemistry is that it describes the arrangement of rings in a structure, and rings are key building blocks in the design of drugs.<sup>45</sup>

In order to identify the framework of each structure in a compound set, an iterative algorithm proceeds by flagging all terminal atoms, then every atom adjacent to a flagged atom unless it is adjacent to more than one unflagged atom; the process is repeated until no more atoms can be flagged. When finished, the unflagged atoms and the bonds between them constitute the framework. The graph level has connectivity information but ignores element and bond types, the graph/node level has connectivity

and element information but ignores bond types, and finally, the graph/node/bond level has connectivity, element, and bond type information (Figure 10). Next, a procedure looks for a match between each new framework and all previously found frameworks; this procedure builds a portfolio of frameworks each of which is assigned a unique identifier. Acyclic substances are ignored here because the framework definition is not applicable to these compounds.

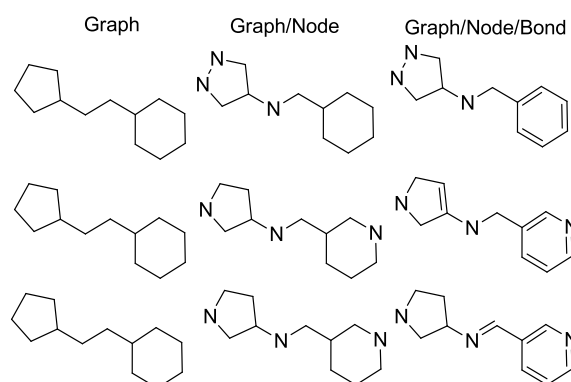


**Figure 10** The frameworks shown for three different compounds at the graph level, the graph/node level, and the graph/node/bond level. All three compounds are identical at the graph level and two of the three compounds are identical at the graph/node level. Adapted from <sup>46</sup>

If many compounds derived from a framework have already been synthesised, these derivatives can serve as potential starting materials for further syntheses. This suggests there is considerable overlap between the most common shapes of drugs and organic compounds in general, and contributing factors include chemical stability and synthetic accessibility.<sup>46</sup> A method to assess the diversity of a screening collection uses the NC50C descriptor, which has been derived from a plot describing the density (percentage of classified compounds) of each class or framework, which was then transformed into a cumulative plot allowing interpolation of the percentage of frameworks required to describe 50% of classified compounds, or PC50C. Since this metric is independent of the size of a library, it can be used to compare collections of different sizes.<sup>47</sup>

The use of frameworks as the basis for diversity analysis has certain limitations in that it excludes acyclic compounds and the part of the structural diversity associated with acyclic side chains attached to the framework. Nevertheless, this is a conceptually simple way to assess diversity for a large structure database. A lack of structural diversity among test compounds is a potential drawback in the drug discovery process.<sup>48</sup>

## 1.5 Shape Diversity

Molecular 3D shape can be defined using their lowest-energy 3D conformer, which can then be used to calculate the proportion of “rod-like”, “disc-like” and “sphere-like” characteristics belonging to the molecule, otherwise known as their principal

moment of inertia (PMI). Some believe<sup>49</sup> that these shape characteristics of a molecule together with its size constitutes the first, most basic level in a hierarchy of molecular descriptors. On top of that, an abundance of secondary descriptors are necessary to refine the information with a more spatial view to the potential for interactions, such as polar surface area, hydrogen-bonding surface potential, surface charge distribution, or presence and location of specific pharmacophoric elements.

The shape space coverage has been found to originate mainly from the nature and the 3D geometry (but not the size) of the central scaffold, while the number and nature of the peripheral substituents and conformational aspects were shown to be of minor importance. It could also be argued that molecular shape is related to the scaffold only in the limit that the scaffold is large with respect to the entire molecule, meaning that the influence of the scaffold on the overall shape will disappear with decreasing size. Surprisingly, results indicate that even very small scaffolds exert a highly distinctive effect on the molecular shape distribution of the respective libraries.<sup>50</sup> On the other hand, shape complementarity is necessary, but alone not sufficient for a compound to productively interact with a target, suggesting that molecules with similar shapes will not necessarily produce similar biological activities. A second layer of complexity is added by the fact that many biological targets contain several different sites prone to interaction with small molecules.

Another way of analysing chemical shape is based on comparing molecular shapes with a set of reference shapes.<sup>51</sup> This relationship can be captured in the form of a binary string, or a fingerprint.<sup>ii</sup> If there is similarity between the molecule and the reference shape above a predefined threshold, then the corresponding bit is switched on in the binary string. The generated fingerprints can be used to identify similarities between two compounds by extracting common bits within their fingerprint. Essentially, it is the number of reference shapes used which determines the number of bits set in a fingerprint.<sup>52</sup>

### 1.5.1 Principal Moment of Inertia (PMI)

Chemists often reason that compounds with greater 3D characteristics will be more complex as a result of higher numbers of sp<sup>3</sup> centres, stereochemical relations *etc.*, and will have lower hit rates in fragment screens.<sup>16</sup> However, a recent analysis<sup>53</sup> showed that addition of a methyl group can produce significant improvements in potency (and

---

<sup>ii</sup> This is different to biological fingerprints (Section 1.3.3).

ligand efficiency), primarily through conformational changes, generating more shape analogues.

In order to calculate the proportion of “rod-like”, “disc-like” and “sphere-like” characteristics, normalized ratios of PMI<sup>50</sup> are plotted into two-dimensional triangular graphs, where the vertices (1,1), (0.5, 0.5), (0,1) correspond to the “envelope” shapes of spheres, disks, and rods, respectively (Figure 11). The plot is then used to compare the shape space covered by different compound sets, such as combinatorial libraries of varying size and composition.

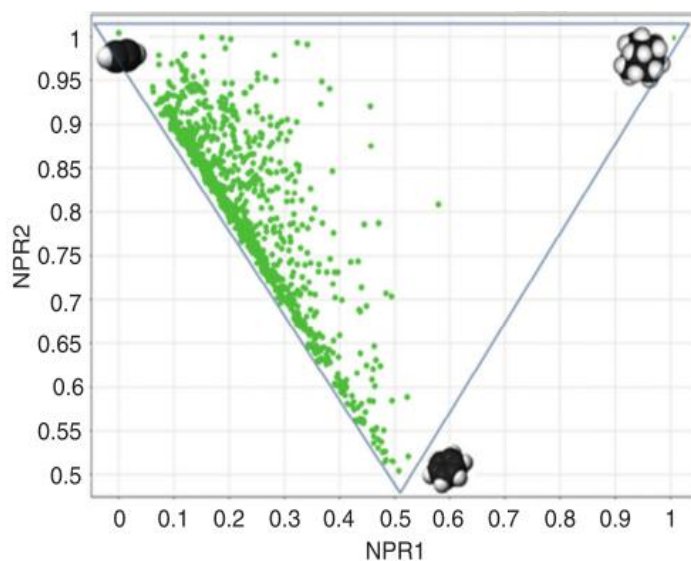


**Figure 11** PMI of a 3D fragment consortium members' library (approximately 1000 fragments), which is representative of commercial fragment space. Reproduced from <sup>16</sup>

Molecular descriptors or properties need to be correlated with, and predictive for, biological activity, (back-)translatable into chemical structure terms, and fast to calculate. 3D molecular shape intuitively meets the above criterion. This is simply because a compound will only modulate the activity of a biological target, if its 3D shape can match the appropriate cavities, clefts, or bulges presented by the biological counterpart. 3D shapes are generated based on standard bond lengths, bond angles, and ring conformations, taking into account atom type, hybridization state, and bond order.<sup>50</sup> PMIs on their own derived either computationally or experimentally from IR or microwave spectra, have previously been used to assess molecular properties such as shape, geometry, and conformational parameters.<sup>54</sup>

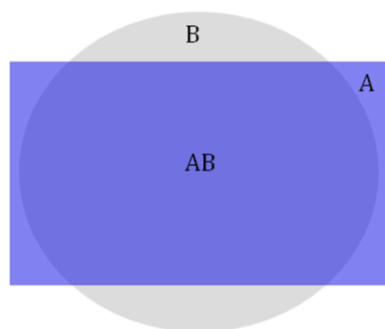
It can be seen from Figure 11 that some areas of the triangle remain entirely unpopulated, such as the region around the right-hand corner, indicating the absence of fragments with 3D shapes. However, the pharmaceutical track record of discoid molecules is undisputed, as evaluation of several fragment libraries show that they are predominantly populated with (hetero)aromatic-derived chemotypes.<sup>16</sup> Results may have been distorted by restricting the shape analysis to only one conformation per

compound, considering that the 3D structure determined from crystals of the small-molecule alone is not necessarily congruent with that adopted in a complex with the biological target.<sup>50</sup> Nevertheless, molecular flexibility can be fairly represented when a large library has been used.

Fundamentally, it is beneficial for primary screening collections to strive for maximum shape diversity, because it is highly desirable to identify several distinct chemical series active on a given target, to predict potential downstream issues often encountered with one chemical family, such as toxicity or poor pharmacokinetics. The envelope shape analysis offers a rapid way to assess and compare compound collections for their biological diversity, despite limitations such as the fact that it appears to disregard any information related to the situation on the inside of the molecular envelope. However, further studies<sup>50</sup> have since shown that such “degenerate” situations are extremely rare and restricted only to highly symmetrical, unsubstituted molecules.

### 1.5.2 Comparison of Shape Similarity

3D similarity methods use geometric constraints and are valued for their ability to find compounds belonging to diverse chemical families.<sup>55</sup> ROCS performs rapid overlays of 3D chemical structures using atom-centered Gaussians to compute geometric overlap.<sup>56</sup> Shape similarity can be determined by similarity scores calculated using the Tanimoto equation.



$$\text{Tanimoto} = \frac{O_{AB}}{O_A + O_B - O_{AB}}$$

**Figure 12** The rectangle and oval shapes represent two different shaped molecules A and B respectively, placed in positions of maximum overlap.  $O_{AB}$  is the volume overlap between conformer A and conformer B,  $O_A$  is conformer A volume, and  $O_B$  is conformer B volume. A Tanimoto score of 1 indicates complete overlap.<sup>57</sup>

Figure 12 shows a rectangle and oval which represent two different shaped molecules A and B, placed in positions of maximum overlap. Here,  $O_{AB}$  is the volume overlap between conformer A and conformer B,  $O_A$  is conformer A volume, and  $O_B$  is conformer B volume. A Tanimoto score of 1 indicates complete overlap. These shapes can then be used to identify a small set of diverse reference shapes representative of the entire library, and a binary fingerprint can be generated for each molecule in the library

in the form of bit strings. Within every bit string, each bit corresponds to a computed similarity above a predefined threshold between the fragment and the reference shape.<sup>58</sup> Table 1 shows molecular fingerprints for two hypothetical molecules A and B, generated using ten reference shapes (1-10). The ten reference shapes give rise to the 10 bits shown, where 1 indicates a correlation between the molecule and the reference shape, and 0 indicates a lack of correlation. This process is described in detail in Section 2.5.

<b>Reference Shape</b>	<b>1</b>	<b>2</b>	<b>3</b>	<b>4</b>	<b>5</b>	<b>6</b>	<b>7</b>	<b>8</b>	<b>9</b>	<b>10</b>
<b>Molecule A</b>	1	0	0	1	0	0	0	1	0	0
<b>Molecule B</b>	1	0	1	0	0	0	0	0	0	0

**Table 1** Molecular fingerprints for two hypothetical molecules A and B, generated using ten reference shapes (1-10). The ten reference shapes give rise to the 10 bits shown, with each bit corresponding to a computed similarity between the molecule and the reference shape. Here, 1 indicates a correlation between the molecule and the reference shape, and 0 indicates a lack of correlation.

## 1.6 Project Aims

My project aims to use novel methodology to design a fragment library in which the molecules will not only have distinct shapes, they will also be highly three-dimensional. Synthesis of the fragments will be completed and screened using biophysical methods in combination with a representative library of commercial fragments. By covering under-explored areas of chemical space, I hope to identify high-quality novel hits towards biologically relevant targets without the need to synthesise a large number of molecules, where the high shape-diversity of the library is key in order to reduce attrition rates in drug discovery.

### 1.6.1 To design a virtual fragment library (Chapter 2)

A range of scaffolds synthesised using chemistry validated in Leeds will be identified; based on these scaffolds, a virtual library of novel structures will be enumerated using established chemical routes. A heavy atom range will be selected which allows the most diverse range of fragments to be included. The library will next be combined with 100,000 randomly selected commercial molecules from the ZINC library<sup>59</sup> (which will also be filtered for the same heavy atom range) and a set of reference shapes will be identified by ROCS to represent the library. These reference shapes will then be filtered for fragment-like properties using  $\text{clog}P$  values of  $-1$  to  $3$ .

A simulated annealing protocol will be used to perform set comparison, allowing the most effective selection of 80 shape-diverse fragments based on different weightings of composition of virtual compounds, coverage of reference shapes, and diversity of fragments. It will be decided here what proportion of the compounds would be virtual and what proportion of the compounds would be bought commercially. Three-dimensionality of the final library will be investigated using a PMI plot, an example of which can be seen in Figure 13 (following page). It is hoped that the virtual compounds will exhibit higher 3D characteristics compared to commercial compounds.

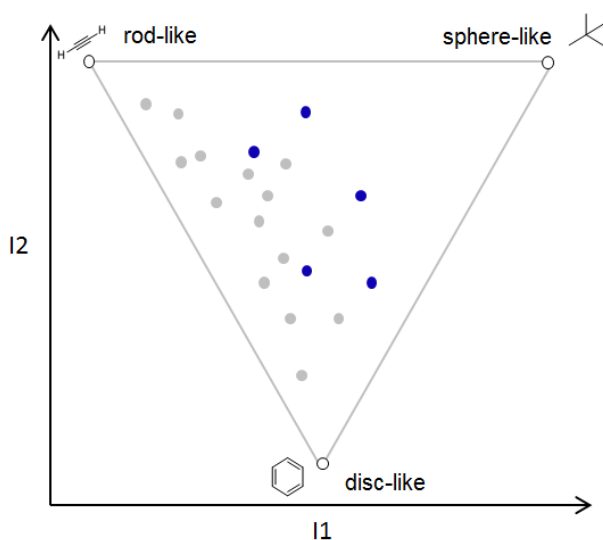


**Figure 13** Example PMI plot where blue represents virtual compounds and grey represents commercial compounds.

### 1.6.2 To synthesise a set of shape-diverse fragments (Chapter 3)

A retrosynthetic analysis of different virtual sets will allow selection of a set of molecules with the most established chemistry for synthesis; the key chemistries which will be investigated include iridium-catalysed allylic amination, amino acid chemistry, Mitsunobu chemistry and Ugi chemistry. Synthetic challenges will be overcome by generating alternative libraries of 80 compounds without compromising on the coverage of reference shapes, and diversity of fragments

### 1.6.3 To assess the biological properties of the library of fragments (Chapter 4)

All 80 molecules will be screened against a number of established targets in a biophysical evaluation of their viability as fragments. High-throughput X-ray crystallography will be used to observe binding interactions and indicate whether more 3D Leeds fragments exhibit better binding compared to flatter commercial molecules. The project is summarised in Figure 14.

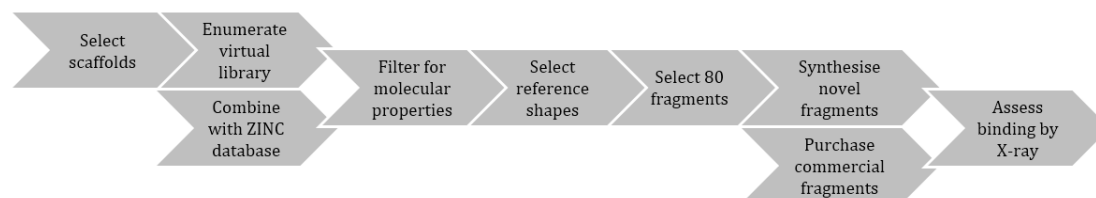


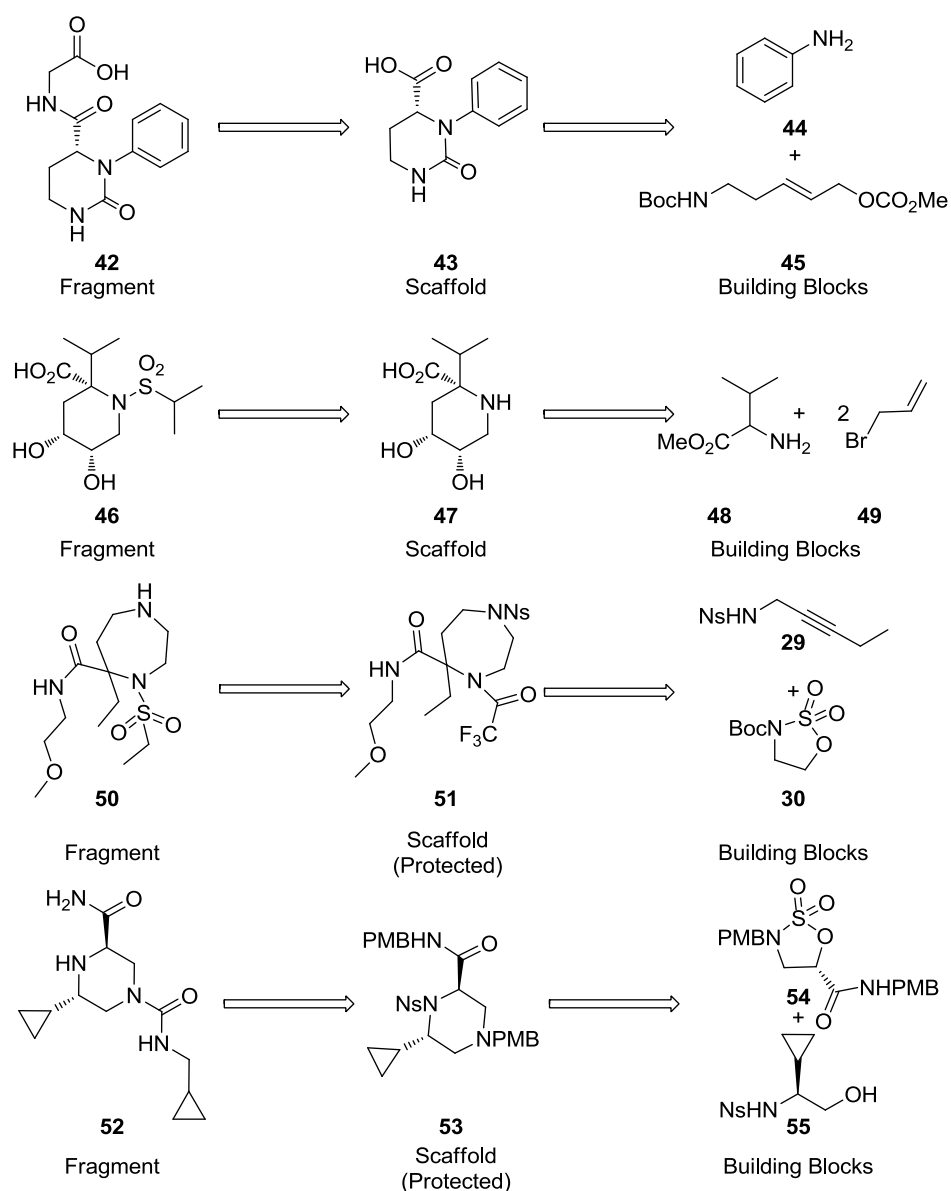
**Figure 14** Summary of each step of the project.

## 2 Design of a Shape-Diverse Fragment Library

This Chapter discusses the enumeration of a virtual library using scaffolds closely related to those previously synthesised by the group. By varying the building blocks, virtual scaffolds could be identified, as well as undergo derivatisation to maximise their shape diversity. Next, taking fragment-like properties into consideration, a heavy atom filter was selected. ROCS was used to identify a range of reference shape molecules for the combined libraries of ZINC (commercial, 100,000 selected at random) and compounds based on Leeds chemistry. Next, a selection protocol allowed a library of 80 compounds to be identified, of which 20 were virtual; the properties which were considered in the selection process included composition of virtual compounds, coverage of reference shapes, and diversity of fragments. Finally, retrosynthetic analysis of fragments allowed the selection of the 20 compounds with the best-established chemistry for synthesis.

### 2.1 Use of the Terms “Building block,” “Scaffold,” and “Fragment”

Below are examples of the chemistries which will be discussed, shown via the retrosynthesis of target fragments which may later play a role in drug discovery. First, the scaffold from which fragments are derivatised can be seen, followed by the building blocks of the reaction. The underpinning chemistries which have been selected include iridium-catalysed allylic amination<sup>41</sup>, amino acid chemistry<sup>43</sup>, the Ugi reaction<sup>44</sup> and the Mitsunobu reaction<sup>42</sup> (Scheme 5).



**Scheme 5** Retrosynthesis of exemplified fragments.

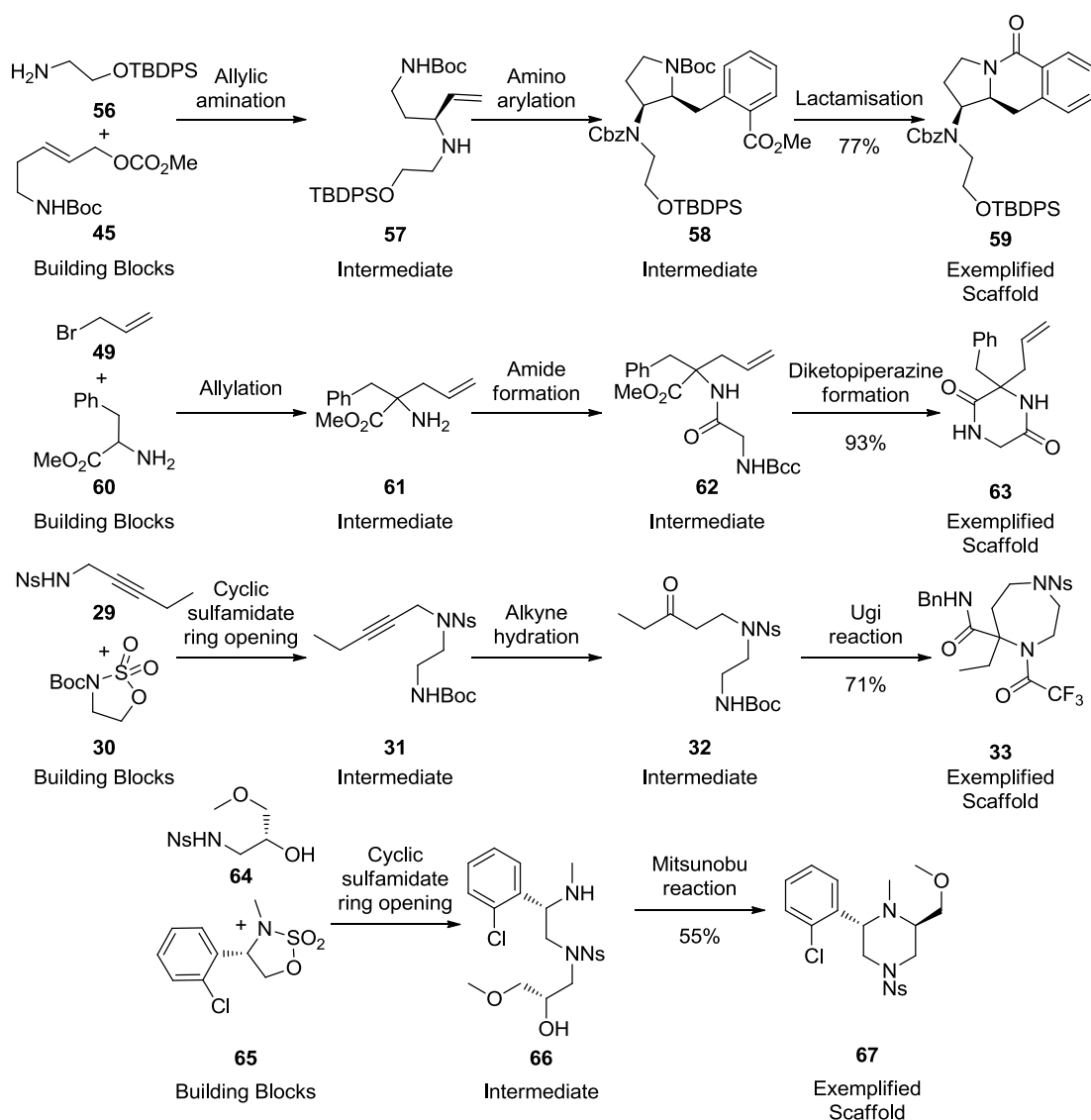
## 2.2 Enumeration of the Compounds

This section discusses the generation of virtual scaffolds using previously prepared scaffolds by the Nelson group, by changing building blocks as well as converting less desirable functional groups into those which are more versatile. Derivatising the virtual scaffolds resulted in a virtual fragment library with high shape diversity.

### 2.2.1 Identification of Scaffolds Previously Prepared

Successful reactions previously completed by members of the Nelson group were summarised in order to gather a selection of reliable methodologies. These involved cyclisation reactions such as aminoarylation, ring-closing metathesis, gold-mediated

hydroamination and the Heck, Ugi and Mitsunobu reactions. Connective reactions preceding cyclisation involved transformations such as *N*-allylation, allylic and reductive amination, using building blocks such as allylic carbonates, amino acids and cyclic sulfamidates. Scaffolds synthesised from each different starting material were grouped and tabulated for ease of reference. These scaffolds were formed in reasonable yields with a well-adapted selection of methodologies; some examples can be seen in Scheme 6, and a full range can be found in the Appendix (Table 31).

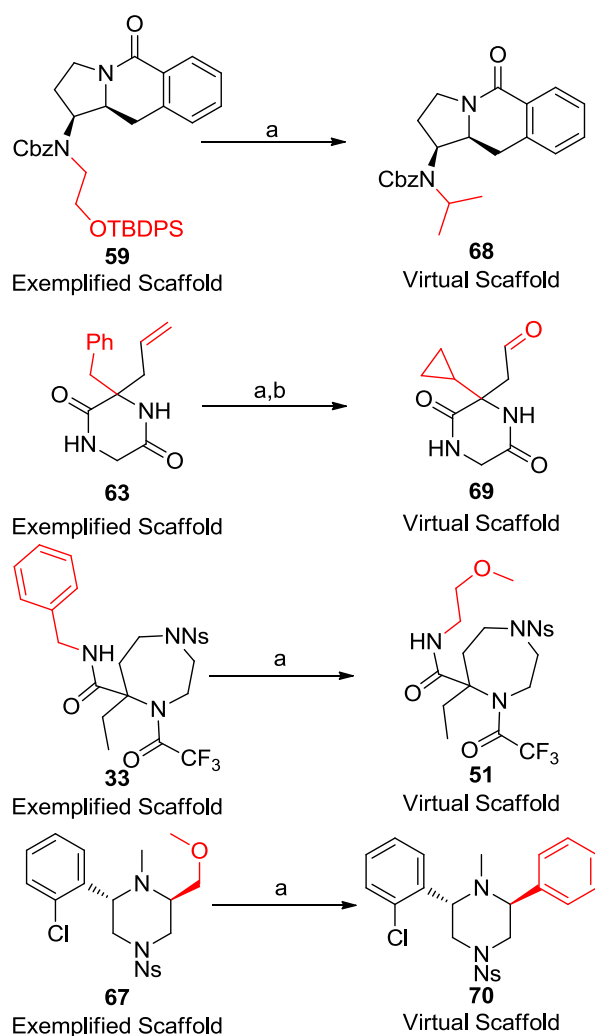


**Scheme 6** Methodologies for formation, and yields of exemplified scaffolds.

## 2.2.2 Identification of Virtual Scaffolds Potentially Synthesisable Using Previously Established Methods

A range of small groups was chosen to replace interchangeable aryl and alkyl groups within the scaffolds with the intention of reducing the number of rotatable bonds.

This could be accomplished for example by using an alternative electron-deficient aryl bromide for the aminoarylation reaction or by changing the substituent on an amino acid building block. By making only small alterations to the building blocks, it is presumed that the virtual scaffolds would largely remain synthetically accessible based on the precedent provided by the exemplified scaffolds. Furthermore, less versatile groups such as alkenes were converted into more useful functionalities such as aldehydes and carboxylic acids - which practically would require a simple one step conversion. Working retrosynthetically, it was important to ensure that the new desired building blocks were commercially available for synthetic practicality. Some example conversions can be seen in Scheme 7 and a full range of building blocks and functional group interconversions can be found in the Appendix (Table 32).



**Scheme 7** Examples of exemplified and virtual scaffolds generated by a) changing substituents on building blocks and b) converting undesirable functional groups into more useful ones for derivatisation. The original and changed substitutions are shown in red.

Each virtual scaffold was enumerated using Pipeline Pilot (PLP); Figure 15 shows an example protocol used to enumerate a range of virtual scaffolds based on amino acid chemistry. Setting the reactant property allowed the enumerated compounds to be labelled according to the numeric identifier for each exemplified scaffold, and thus it was

possible to see which exemplified scaffold gave the largest number of virtual scaffolds. These transformations involved changing alkene functionalities into more useful ketone, diol, aldehyde, acid or alcohol groups, whilst various substituents were diversified according to changes in the building block *i.e.* changing the nucleophile, isocyanate and initial amino acid. By placing the components one after the other, it ensured that more than one enumeration could be done in parallel, generating a diverse range of compounds.

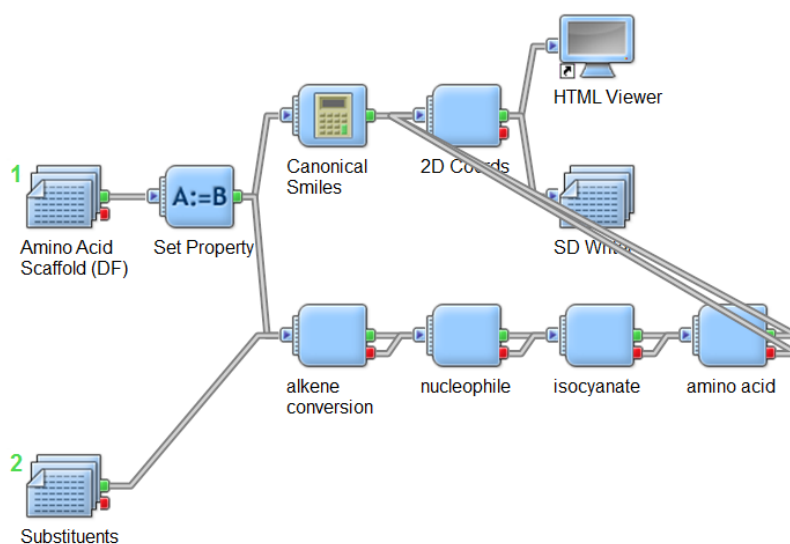


**Figure 15** Example Pipeline Pilot (PLP) protocol used to enumerate exemplified scaffolds to give virtual scaffolds, by using alternative starting materials (nucleophiles, isocyanates and amino acids) as well as converting undesirable functional groups (alkenes) into those which provide a better synthetic handle for novel derivatisation.

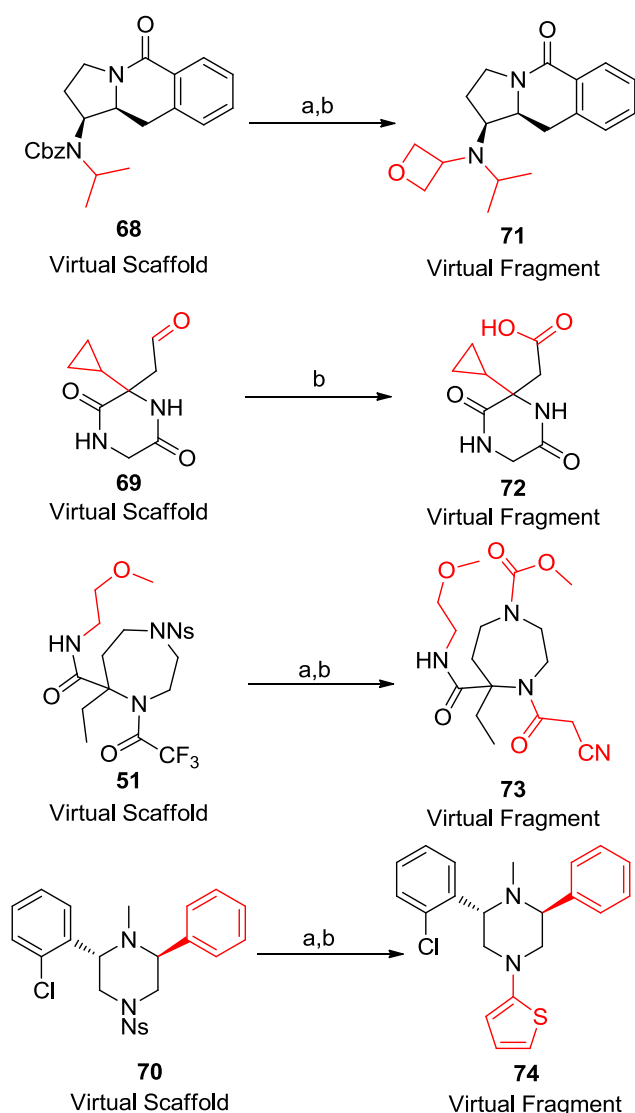
The 2D co-ordinates component allowed the compounds to be easily visualised on an HTML viewer and the SD (structure-data) writer allowed the compounds to be stored as an SD file and later combined with other scaffolds. Connecting the unchanged scaffolds directly to the SD writer meant that the exemplified scaffolds were not lost in the final list of compounds, whilst the canonical smiles component allowed the originator compound to be traced and appear as a 2D reference structure. In addition, slight modifications were made to the exemplified scaffolds in order to prevent undesirable functional groups being fed into the resulting compounds. Modifications included hydrolysis of unstable ester groups, removal of the trifluoroacetamide capping groups used in Mitsunobu chemistry as well as removal of reactive azide and iodide functional groups.

### 2.2.3 Derivatisation of Virtual Scaffolds

The SD files for all virtual scaffolds were next fed into a new protocol via the SD reader, which allowed derivatisation to occur using a range of small capping groups.

These decoration reactions included amide formation, reductive amination, sulfonamide formation, as well as *N*- and *O*-alkylation/arylation. As seen in the protocol in Section 2.3, Figure 17, the first-row component simply deprotected the scaffolds allowing the undecorated compounds to be captured in the library. The second-row derivatisation component allowed *O*-alkylation to occur as well as decorations involving a primary amine as the capping group *i.e.* amide coupling to a carboxylic acid functionality in the scaffold, and reductive amination of an aldehyde or ketone functionality in the scaffold.

In contrast, the third-row derivatisation component allowed decoration of secondary amine functionalities already present within the scaffold, *i.e.* amide coupling to a small acid chloride, reductive amination using a small ketone/aldehyde, sulfonamide formation and finally, *N*-alkylation. The complete range of virtual derivatisations can be found in the Appendix (Table 33), selected at random from the eMolecules online database using the lowest heavy atom filter available that still generated a reasonable number of capping molecules. Some example fragments can be seen in Scheme 8.



**Scheme 8** Examples of virtual fragments generated by a) deprotecting and b) derivatising scaffolds. The parts of the virtual scaffold shown in red highlight substituents which have been changed from the exemplified scaffold, and the parts of the virtual fragment shown in red highlight substituents which have been changed from the exemplified scaffold as well as the virtual scaffold.

The deprotection steps are split between *N*- and *O*-deprotection in the third row of the PLP protocol due to the special case of some nitrogens in the scaffold requiring deprotection to undergo decoration. In addition, unlike individual diversification components for different sets of chemistries *e.g.* amino acid chemistry, derivatisation for the entire virtual scaffold library can be combined into a single component, since only one decoration is allowed per compound. This allowed shape diversity to be added whilst minimising extra molecular weight. The stereoisomers component enumerated all possible stereoisomers for those which are undefined - this is especially common within the amino acid building blocks, where the products are racemic. Finally, undesired functionalities such as any untransformed alkenes and unreacted aldehydes were removed as well as any duplicate molecules, thus forming the final library of 66,814 compounds. Plots showing lipophilicity vs. number of heavy atoms of the final virtual library as well as 100,000 randomly selected ZINC compounds show that virtual compounds tend to be less lipophilic (Figure 16). The mean value for  $AlogP^{iii}$  (the generated value for lipophilicity offered by PLP) of commercial compounds lies at 2.9446 whereas the mean  $AlogP$  of virtual compounds lies at 0.91321.

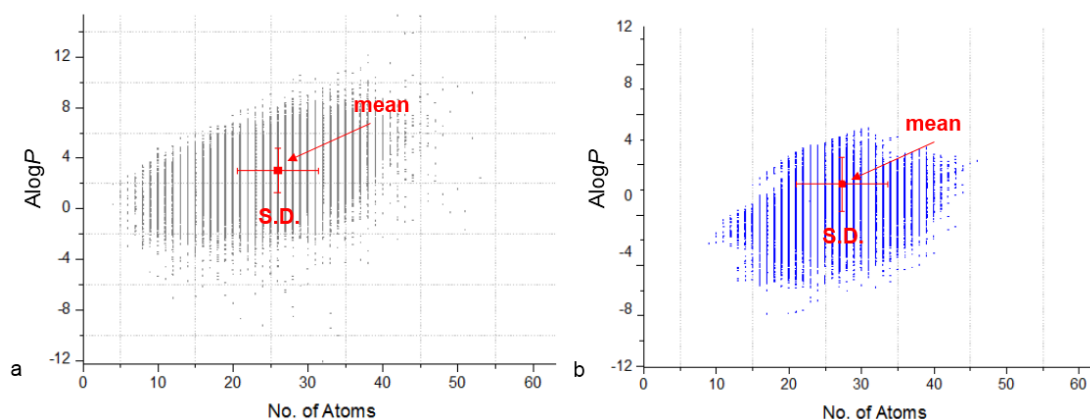


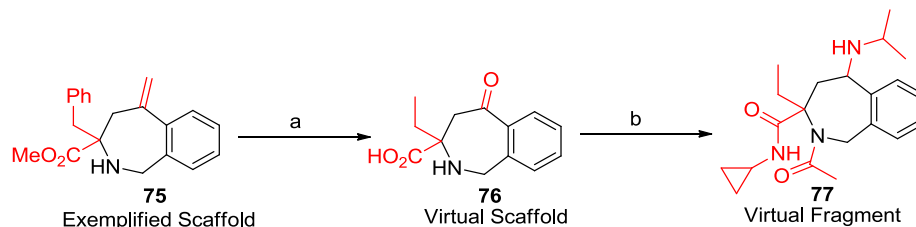
**Figure 16** Lipophilicity vs. number of heavy atoms of a) 100,000 ZINC compounds (grey) and b) the final virtual library (blue). It can be seen from the mean and standard deviation of the libraries here that virtual compounds tend to be less lipophilic.

#### 2.2.4 Summary of Route for Fragment Design

Seen in Scheme 9 is a summary of conversion from the exemplified scaffold to a virtual fragment. The benzyl group in the exemplified scaffold is interchangeable by changing the amino acid building block substituent to an ethyl group. The undesirable alkene functionality is oxidised to a ketone and the undesirable ester functionality is

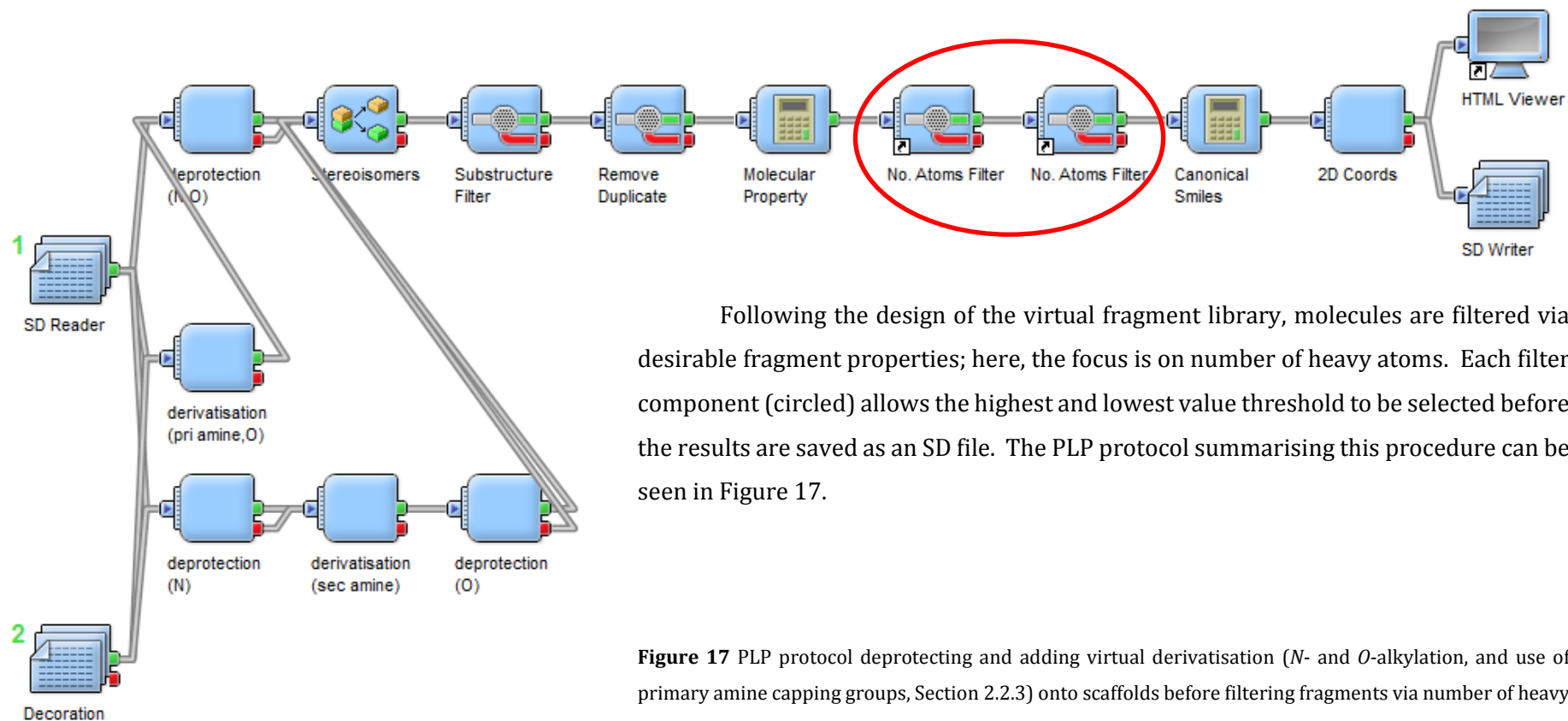
<sup>iii</sup>  $AlogP$  is similar to  $clogP$  but atomic-based as opposed to fragment-based.

hydrolysed to give the virtual scaffold. Next, the still reactive secondary amine functional group is capped by acetyl chloride, while the carboxylic acid group is capped by cyclopropylamine and the ketone group is subjected to reductive amination with isopropylamine to give the virtual fragment.



**Scheme 9** Summary of route used to form a virtual fragment from an exemplified scaffold. Here, the novel substituents and functionalities are highlighted in red in the virtual scaffold, as well as their predecessor, in the exemplified scaffold; a) The benzyl group in the exemplified scaffold **75** is interchangeable by changing the amino acid building block. The undesirable alkene functionality is oxidised to a ketone and the undesirable ester functionality is hydrolysed to give the virtual scaffold **76**; b) The still reactive secondary amine group is capped by a range of acid chlorides, and the carboxylic acid and ketone groups can react with a range of primary amine capping groups to undergo both amide formation and reductive amination to give virtual fragment **77** (final derivatisations are also shown in red).

## 2.3 Identification of a Suitable Heavy Atom Filter

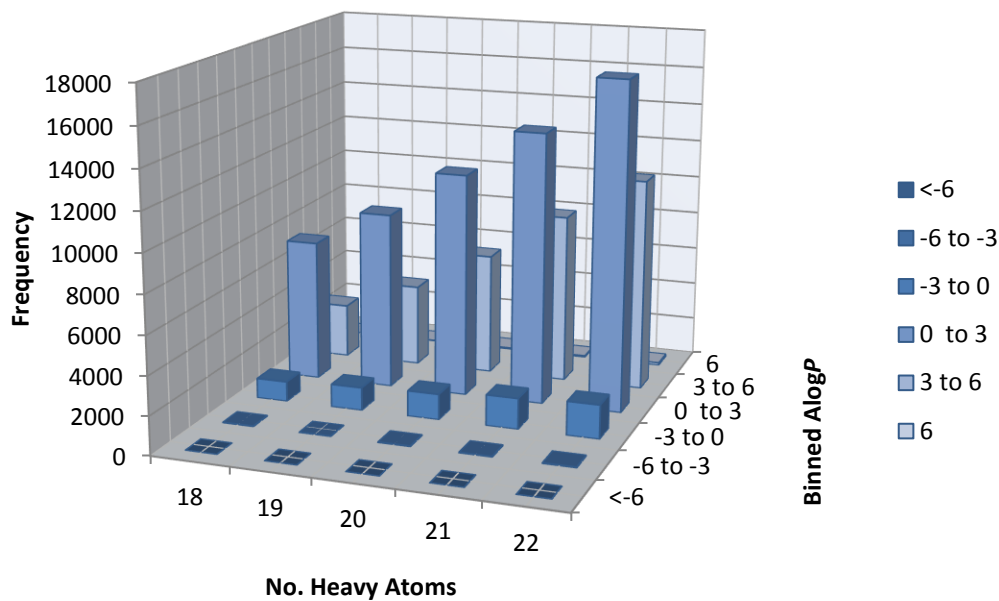


Following the design of the virtual fragment library, molecules are filtered via desirable fragment properties; here, the focus is on number of heavy atoms. Each filter component (circled) allows the highest and lowest value threshold to be selected before the results are saved as an SD file. The PLP protocol summarising this procedure can be seen in Figure 17.

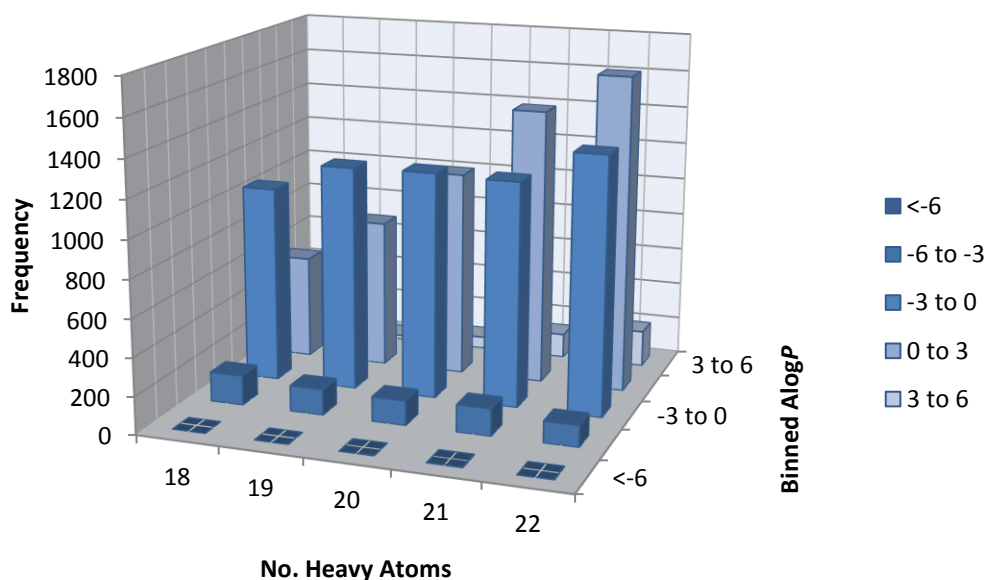
**Figure 17** PLP protocol deprotecting and adding virtual derivatisation (*N*- and *O*-alkylation, and use of primary amine capping groups, Section 2.2.3) onto scaffolds before filtering fragments via number of heavy atoms (components circled).

Fragment-like molecules usually lie within the region of 16-24 heavy atoms, leaving a total of 22,975 molecules in the virtual library which fit within the criteria. It was important to select a more restricted heavy atom range, *i.e.* 16-20, 18-22 or 20-24 to allow shape diversity analysis. In order to identify which range covered the greatest number of scaffolds and thus maximised scaffold diversity, the following analysis was carried out evaluating the number of scaffolds available with heavy atom counts in the ranges 16-20, 18-22 and 20-24 heavy atoms. In order to do this, the scaffolds which were not covered at all (shown as 0% of fragments covered per scaffold) have been highlighted in the Appendix for each heavy atom range (Table 34, along with the complete range of scaffolds).

It is clear that although not the most prolific, the most shape-diverse set of fragments (containing the highest number of scaffolds) appear under the heavy atom range 18-22, with 12,715 molecules, some examples of which can be seen in Table 2. It is key to note here that for individual scaffolds, the percentage total of generated fragments covered by each heavy atom range is not important as long as it is more than 0%. Only one scaffold has not been covered by the heavy atom range 18-22, with three scaffolds excluded by the heavy atom range 16-20, and seven scaffolds excluded by the heavy atom range 20-24. Comparing frequency plots of lipophilicity vs. number of heavy atoms of the ZINC commercial library against the virtual library, both of which contain only compounds with 18-22 heavy atoms, it could be observed that again, virtual compounds tend to be less lipophilic (Figure 18). This is because the majority of virtual compounds reside in the  $AlogP$  ranges of -3 to 0 and 0 to 3 whereas in the case of the ZINC commercial library the majority of compounds tend to reside in the  $AlogP$  ranges of 0 to 3 and 3 to 6.

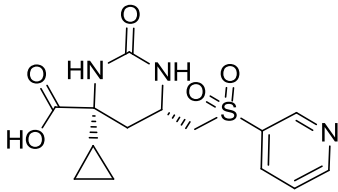
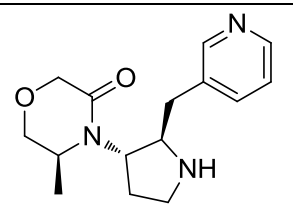
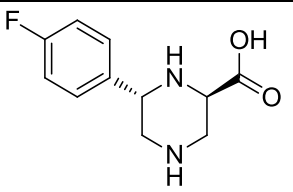


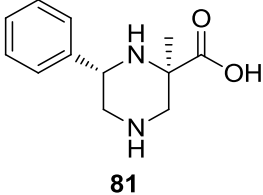
a



b

**Figure 18** Lipophilicity vs. number of heavy atoms of a) the ZINC commercial library and b) the virtual library, after both have been filtered for compounds with 18-22 heavy atoms. The compounds have been binned into five AlogP ranges with frequency plotted against each. It can be seen here that the majority of virtual compounds reside in the AlogP ranges of -3 to 0 and 0 to 3 whereas the majority of commercial compounds tend to reside in the AlogP ranges of 0 to 3 and 3 to 6.

Key chemistry for formation	Example scaffold	No. fragments based on scaffold	16-20 HA	Percentage of total fragments	18-22 HA	Percentage of total fragments	20-24 HA	Percentage of total fragments
Amino acid chemistry	 <p><b>78</b></p>	128	6	4.7%	50	39.1%	122	95.3%
Iridium-catalysed allylic amination reaction	 <p><b>79</b></p>	106	4	3.8%	22	20.8%	105	99.1%
Mitsunobu reaction	 <p><b>80</b></p>	1315	783	59.5%	751	57.1%	660	50.2%

Ugi reaction	 <b>81</b>	334	13	3.9%	71	21.3%	329	98.5%
--------------	--	-----	----	------	----	-------	-----	-------

**Table 2** Percentage of molecules belonging to each HA (heavy atom) range, of the total number of fragments derivatised from example scaffolds. It was on this basis that the heavy atom range 18-22 was chosen in order to incorporate the most diverse range of fragments.

## 2.4 Principal Moment of Inertia (PMI) Analysis

Principal moment of inertia is directional, and its values in the x, y, and z directions can be determined for the lowest energy 3D conformer of each molecule. The smallest and second smallest of these three values are normalised, where  $\frac{\text{smallest PMI}}{\text{biggest PMI}} = I_1$  and  $\frac{\text{second smallest PMI}}{\text{biggest PMI}} = I_2$ . This eliminates the dependence of the representation of the library on the size of the molecules in question, which eases the need for decorrelation procedures when used in combination with other descriptors such as molecular weight, volume, or surface area.<sup>50</sup>  $I_2$  can then be plotted against  $I_1$  generating a 2D scatter chart (Figure 19), where corners of the triangular distribution contain the reference shapes rod (0, 1), disc (0.5, 0.5) and sphere (1, 1). It could be seen from the mean values of the libraries that the majority of molecules lie towards rod/disc-like shape space, and that in comparison to commercial compounds (grey), virtual compounds (blue) are moving away from rod/disc-like shape space and stretching towards more 3D shape space.

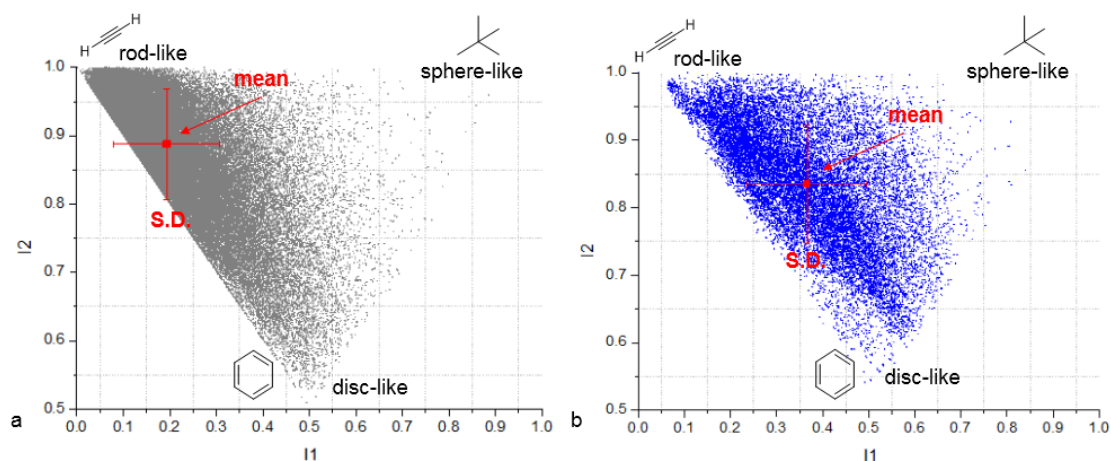


**Figure 19** PMI plots showing the distribution of a) commercial and b) virtual compounds in shape space, where  $\frac{\text{smallest PMI}}{\text{biggest PMI}} = I_1$  and  $\frac{\text{second smallest PMI}}{\text{biggest PMI}} = I_2$ . Commercial compounds are shown in grey and virtual compounds are shown in blue, with mean values and standard deviations of the libraries clearly indicated. It can be seen here that virtual compounds are moving away from the rod/disc edge, where most commercial compounds reside, and into more 3D shape space.

## 2.5 Identification of Reference Shapes for the Library and Generation of Shape Fingerprints

In order to identify which fragment shapes are novel and suitable to target, reference shapes were generated from a combined library including virtual fragments and commercial fragments from the ZINC library. ZINC fragments were filtered for 18-22 heavy atoms, with duplicate molecules as well as salts being removed; around 100,000 of

these molecules were then randomly selected. The 3D shapes of the combined library were generated using the CORINA 3D structure generator<sup>60</sup> and the reference shapes were generated by ROCS.

The process of reference shape selection is illustrated in Figure 20, where the axes are arbitrary molecular shape descriptors and the library of molecules (black dots) fills the entire graph. In order to generate reference shapes, one fragment (1) is selected at random, with fragments which map within 0.8 Tanimoto similarity of itself removed (area shaded grey and black dots hollowed out). Here, Tanimoto is a measure of shape overlap and a score of 0-1 is calculated, where a score of 0 indicated no shape match and a score of 1 indicates exact shape match (Section 1.5.2). The value 0.8 Tanimoto was chosen as an arbitrary indication of similarity which allowed a reasonable number of reference shapes to be generated as a result. Next, a second fragment (2) is selected which is least similar in shape to fragment 1, and fragments which map within 0.8 Tanimoto of (2) are again removed. This action is repeated until all available shape space has been covered - by a total of 2477 reference shapes (only eight shown here, 1-8, highlighted as blue circles).

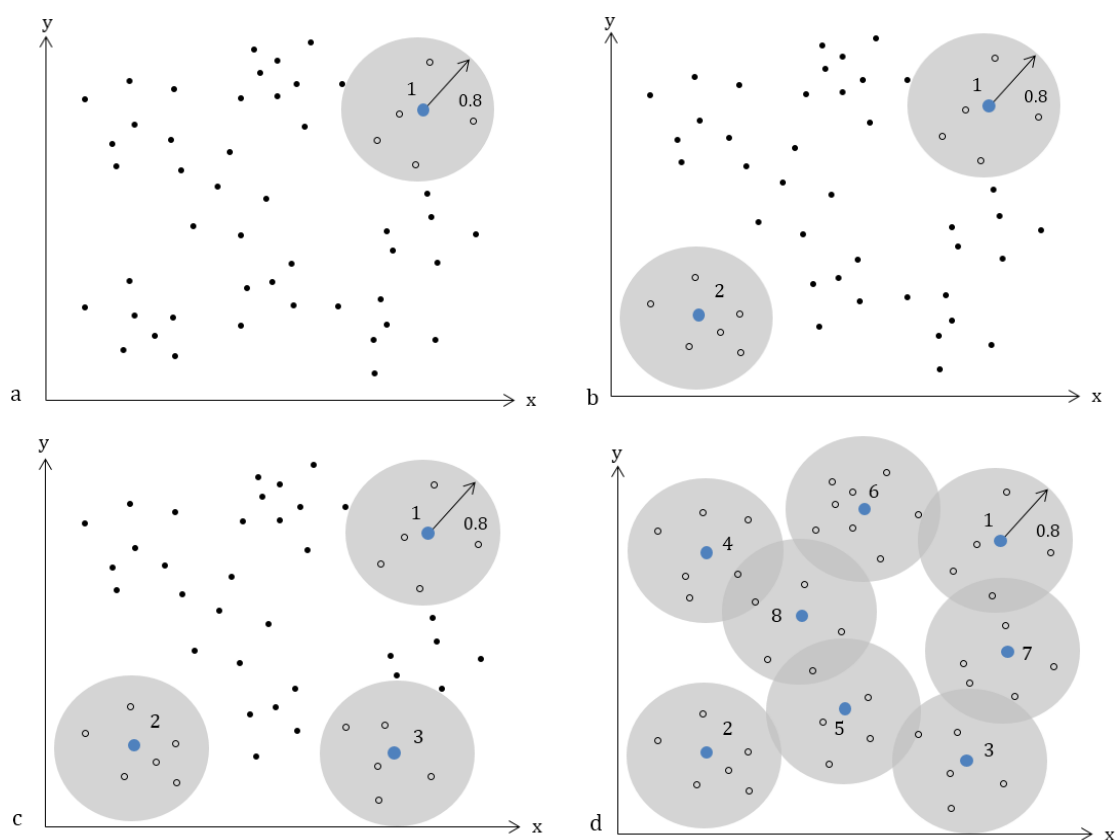


**Figure 20** Tanimoto plots to show how reference shapes are generated. The axes are arbitrary molecular shape descriptors, black dots are fragments, blue circles are reference shapes (1-8) and grey circles cover fragments within 0.8 Tanimoto of the reference shape. a) One fragment (1) is selected at random, with

fragments which map within 0.8 Tanimoto similarity of itself removed (area shaded grey and black dots hollowed out). b) A second fragment (2) is selected which is least similar in shape to fragment 1, with fragments which map within 0.8 Tanimoto of itself removed. c) A third fragment (3) is selected which is least similar in shape to fragment 2, with fragments which map within 0.8 Tanimoto of itself removed. d) This action is repeated until all available shape space has been covered (reference shape fragments 1-8). It can be seen here that although reference shapes are far apart from one another, some fragments map onto several reference shapes, making them less shape-diverse than those which map onto a singular reference shape (Section 2.6.1).

The aim of the project is to synthesise a small and manageable library of molecules, which, in combination with those available commercially, are able to cover the vast majority of shape space. It is possible to select this smaller library by using ROCS to perform full shape comparison of molecules from the rest of the combined library; however, this is computationally demanding and instead, ROCS is used to generate a fingerprint for each molecule as an alternative representation. Fingerprint scoring is then performed by PLP to compare the rest of the combined library against one another and this can be done much more rapidly than full shape comparison (see simulated annealing in Section 2.6.1). Generation of fingerprints by mapping molecules in the combined library onto reference shapes is shown using Tanimoto plots in Figure 21. Here, the axes are arbitrary molecular shape descriptors, dark blue circles are reference shapes (1-8) and pale blue circles cover fragments within 0.7 Tanimoto of the reference shape. The value 0.7 Tanimoto was chosen since it was smaller than but close to the 0.8 Tanimoto used to generate reference shapes. One fragment (A) is selected at random, with reference shapes which map within 0.7 Tanimoto similarity of itself identified (area shaded pale blue and blue dots hollowed out). A different fragment (B) is selected at random, with reference shapes which map within 0.7 Tanimoto similarity of itself identified (area shaded pale blue and blue dots hollowed out).

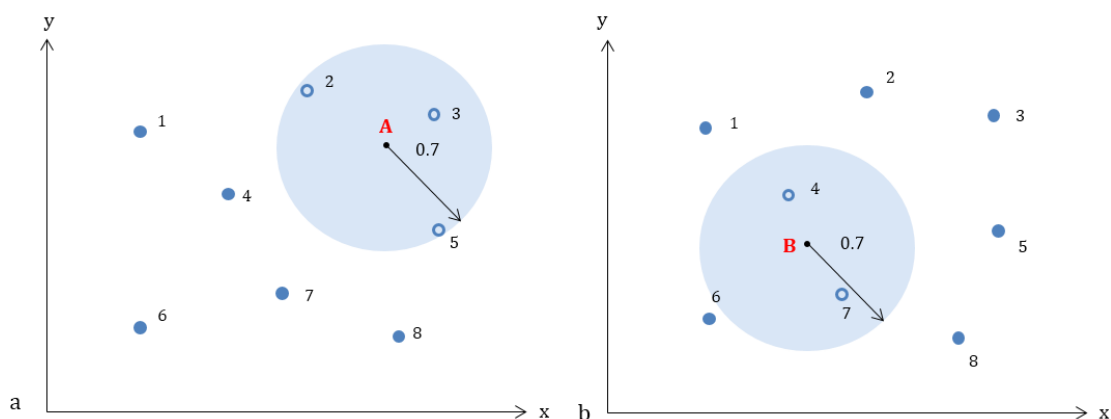


**Figure 21** Tanimoto plots to show how fingerprints are generated using reference shapes. The axes are arbitrary molecular shape descriptors; dark blue circles are reference shapes (1-8) and pale blue circles cover

fragments within 0.7 Tanimoto of the reference shape. a) One fragment (A) is selected at random, with reference shapes which map within 0.7 Tanimoto similarity of itself identified (area shaded pale blue and blue dots hollowed out). b) A different fragment (B) is selected at random, with reference shapes which map within 0.7 Tanimoto similarity of itself identified (area shaded pale blue and blue dots hollowed out).

The fingerprint generation for fragments A and B (Figure 21) can be seen in Table 3, with each set bit in the bit string corresponding to 0.7 Tanimoto similarity or higher between the fragment and the reference shape.<sup>58</sup> Here, fragment A covers reference shapes 2, 3, and 5, and fragment B covers reference shapes 4 and 7. “1” as part of the bit string indicates the fragment’s correlation with the specific reference shape and “0” indicates a lack of correlation. It is clear that even when only eight reference shapes are used, two fragments still give rise to very different fingerprints.

Reference Shape	1	2	3	4	5	6	7	8
Fragment A	0	1	1	0	1	0	0	0
Fragment B	0	0	0	1	0	0	1	0

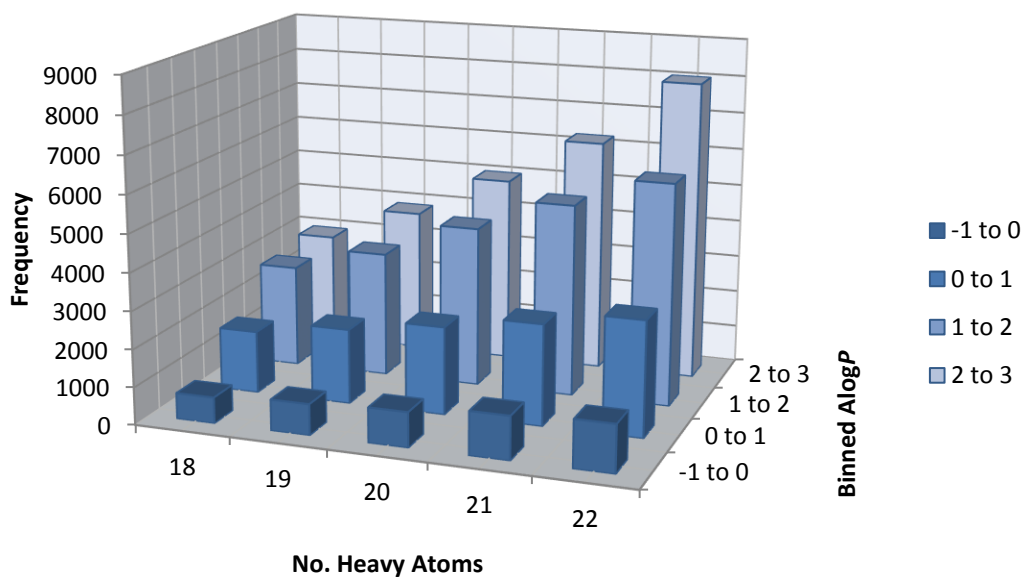
**Table 3** Fingerprint generation of fragments A and B (Figure 21), with each set bit corresponding to 0.7 Tanimoto similarity or higher between the fragment and the reference shape (8 reference shapes, *i.e.* 8 bits). Here, fragment A covers reference shapes 2, 3, and 5, and fragment B covers reference shapes 4 and 7. “1” as part of the bit string indicates the fragment’s correlation with the specific reference shape and “0” indicates a lack of correlation.

## 2.6 Identification of a Library of Synthetic Targets

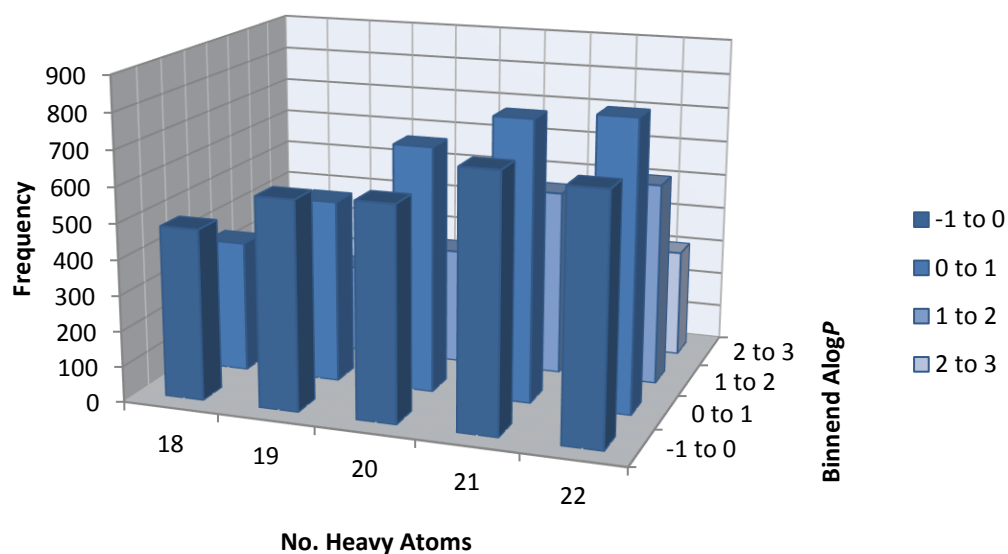
A target number of 80 compounds was decided upon for my fragment library, which will ideally represent all the shape space covered by the 2477 reference shapes, as well as being highly diverse. Within these compounds, there will be a fraction of which will be based on chemistry validated in Leeds, and the rest will be commercially available. In order to ensure the most appropriate and unbiased selection of compounds, a simulated annealing protocol, which effectively compares sets of compounds against one another, was applied using PLP.

Before identifying the best conditions for selection, the library of molecules was filtered by *AlogP*, using the fragment-like range of -1 to 3, giving 73,031 molecules for the input file. Plots of lipophilicity vs. number of heavy atoms of the ZINC commercial library as well as the virtual library, each containing only compounds with 18 to 22 heavy atoms and *AlogP* -1 to 3 have been produced, to show frequency of fragments in each category (Figure 22). This indicated that overall the libraries skew towards containing more heavy

atoms. In addition, virtual compounds are less lipophilic as the majority reside in the  $AlogP$  of 0 to 1 category whereas the majority of commercial compounds reside in the  $AlogP$  of 2 to 3 category.



a



b

**Figure 22** Lipophilicity vs. number of heavy atoms of a) the ZINC commercial library and b) the virtual library after filtering for compounds with heavy atoms 18-22 and  $AlogP$  -1-3. The compounds have been binned into four  $AlogP$  ranges and in addition, plotted against frequency. It can be seen here that the majority of virtual compounds reside in the  $AlogP$  range of 0 to 1 whereas the majority of commercial compounds reside in the  $AlogP$  range of 2 to 3. In the case of both libraries, fragments skew towards containing a higher number of heavy atoms.

### 2.6.1 Optimising Conditions for Compound Selection

In order to identify the best conditions for the protocol to be run, trial runs were completed for different weightings of composition, coverage and diversity. The scores of each trial run were then compared. The optimal conditions (ideal weightings of composition, coverage and diversity) were then applied to the 73,031 filtered molecules (represented as bit strings for rapid computational analysis) in order to source the ideal library of 80 compounds. Here, composition score is an indication of whether the ideal percentage of virtual compounds have been matched, coverage score indicates the fraction of reference shapes hit by the chosen set (where the more shapes hit the better), and diversity score indicates the shape diversity of the set *i.e.* it would be better to hit more reference shapes with the same number of fragments.

In practical terms, composition score is calculated as the magnitude deviation of the set from the ideal percentage of virtual compounds hence a value of 0 indicates that the target value is matched. Coverage score is calculated as 1 minus the fraction of bits which are switched on in the whole set hence a value of 0.1 implies 90% of the bits are covered by the set, *i.e.* the set contains molecules which would match with 90% of the reference set. The diversity score is the average overlap of fingerprints considering all pairwise combinations within the set, normalised to the size of the set, whereby lower values equal less overlap.

The final score is a result of a coefficient multiplied by a score for composition, coverage and diversity, where the lower the score in each section the better the result. The coefficients weight each part of the score in the final score. Each run is optimised using a maximum of 5000 iterations with a cooling rate of 0.98, where 20 attempts are taken per temperature. Cooling rate defines the speed of convergence of the process to minimum scores, where the higher the number the slower the cooling. 20 attempts will be taken per temperature in order to find a better set (with lower scores) before cooling is applied. Here, temperature determines the percentage of compounds altered from the previous set when a new set of compounds is selected, and as it cools, that percentage decreases. The initial temperature is set to alter a maximum of 30% of compounds in the initial set, and approaches 0 as the run converges to the optimum set.

The process of set comparison begins with a comparison of the final score for two initial sets of compounds, sets 1 and 2. The lower score is desirable so if the score of set 2 is lower than set 1, set 2 becomes the new chosen set. If, however, this is not the case, the probability of set 2 becoming the new chosen set is determined by the switch probability.

$$\text{Switch Probability} = e^{\frac{-1 \times (\text{set 2} - \text{set 1})}{\text{temperature}}}$$

Once switch probability is calculated, it is then compared to a generated random number between 0 and 1. If the switch probability is higher than the random number, set 2 becomes the new chosen set. Switch probability is calculated based on pseudo thermodynamics, where the smaller the difference between sets 1 and 2, and the higher the temperature, the more likely that set 2, despite having a higher score, will become the new chosen set. The reason this protocol is in place is in order to avoid a local minimum early in the run, which would prevent a better set with a lower score to be identified. This is illustrated later in Figure 24.

The simulated annealing scoring process uses fingerprint comparison, which is much less computationally demanding than 3D shape matching using ROCS. For illustration purposes, this can be explained using Tanimoto graphs (Figure 23). Here, the axes are arbitrary molecular shape descriptors and the library of molecules (black dots) including the generated reference shapes (blue dots, 1-8) fill the entire graph. Four fragments are selected at random (A-D), with reference shapes which map within 0.7 Tanimoto similarity of each identified (area shaded pale blue and blue dots hollowed out). In plot a, only seven out of the eight reference shapes have been covered (reference shape 6 has been left out), therefore the generated fragments exhibit low coverage. In plot b, all eight reference shapes have been covered by the new set of fragments A, C, D, E, but reference shapes 2, 4 and 5 have been covered by more than one fragment. Therefore, the generated fragments exhibit maximum coverage but low diversity. In plot c, all eight reference shapes have been covered by the new set of fragments D, F, G, H, and each reference shape is only covered by one fragment. Therefore, the generated fragments in plot c exhibit maximum coverage and high diversity, making it the most desirable set of four compounds.

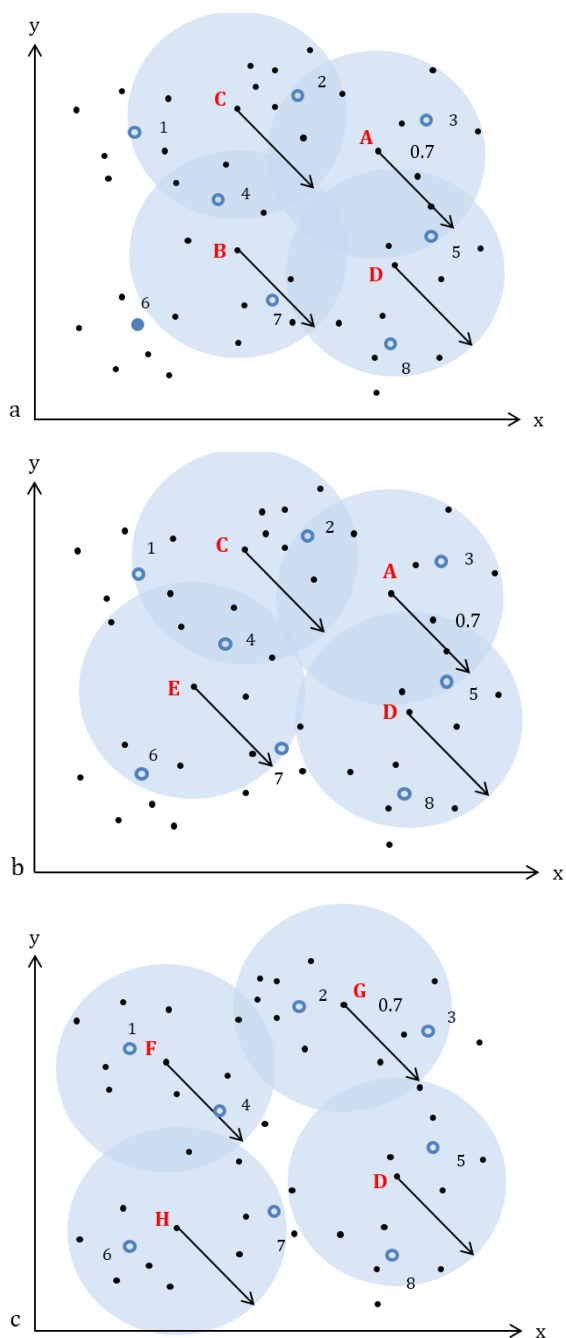


**Figure 23** Tanimoto plots showing how the library of 80 fragments are selected (example shows library of four only). The axes are arbitrary molecular shape descriptors, black dots are fragments, dark blue circles are reference shapes (1-8) and pale blue circles cover fragments within 0.7 Tanimoto of the reference shape. a) Four fragments (A-D) are selected at random, with reference shapes which map within 0.7 Tanimoto similarity of each identified (area shaded pale blue and blue dots hollowed out). Only seven out of eight reference shapes have been covered (reference shape 6 left out); the generated fragments exhibit low coverage. b) All eight reference shapes have been covered by the new set of fragments A, C, D, E, but reference shapes 2, 4 and 5 have been covered by more than one fragment. The generated fragments exhibit maximum coverage but low diversity. c) All eight reference shapes have been covered by the new set of fragments D, F, G, H, and each reference shape is only covered by one fragment. The generated fragments exhibit maximum coverage and high diversity.

The chosen fragments from the libraries shown in Figure 23, plot a-c (libraries 1-3, respectively) is next converted into fingerprints in Table 4, with each set bit corresponding to a similarity of 0.7 Tanimoto or higher between the fragment and the reference shape. Here, 1 indicates the fragment's correlation with the specific reference shape and 0 indicates a lack of correlation. The coverage of each reference shape is then summarised for the library by indicating if they hit at least one fragment (where 1 indicates yes and 0 indicates no).

<b>Library 1 (Figure 23, plot a)</b>								
<b>Reference Shape</b>	<b>1</b>	<b>2</b>	<b>3</b>	<b>4</b>	<b>5</b>	<b>6</b>	<b>7</b>	<b>8</b>
<b>Fragment A</b>	0	1	1	0	1	0	0	0
<b>Fragment B</b>	0	0	0	1	0	0	1	0
<b>Fragment C</b>	1	1	0	1	0	0	0	0
<b>Fragment D</b>	0	0	0	0	1	0	0	1
<b>Hits <math>\geq 1</math> fragment</b>	1	1	1	1	1	0	1	1
<b>Library 2 (Figure 23, plot b)</b>								
<b>Fragment A</b>	0	1	1	0	1	0	0	0
<b>Fragment C</b>	1	1	0	1	0	0	0	0
<b>Fragment D</b>	0	0	0	0	1	0	0	1
<b>Fragment E</b>	0	0	0	1	0	1	1	0
<b>Hits <math>\geq 1</math> fragment</b>	1	1	1	1	1	1	1	1
<b>Library 3 (Figure 23, plot c)</b>								
<b>Fragment D</b>	0	0	0	0	1	0	0	1
<b>Fragment F</b>	1	0	0	1	0	0	0	0
<b>Fragment G</b>	0	1	1	0	0	0	0	0
<b>Fragment H</b>	0	0	0	0	0	1	1	0
<b>Hits <math>\geq 1</math> fragment</b>	1	1	1	1	1	1	1	1

**Table 4** Fingerprint analysis of libraries shown in Figure 23, plot a-c (libraries 1-3, respectively), with each set bit corresponding to a similarity of 0.7 Tanimoto or higher between the fragment and the reference shape (there are 8 reference shapes, *i.e.* 8 bits). Here, 1 indicates the fragment's correlation with the specific reference shape and 0 indicates a lack of correlation. The coverage of each reference shape is then summarised for the library by indicating if they hit at least one fragment (where 1 indicates yes and 0 indicates no).

The number of reference shapes that are hit by at least 1 fragment ( $\geq 1$  Hit) is then totalled and used in calculations for reference shape coverage (Table 6). The composition score is 0 for all three libraries as the target value of 4 fragments per library was matched. The coverage score can be calculated; where coverage is " $\geq 1$  Hit" as a fraction of the total number of reference shapes (8 in this example). The coverage scores of 0 calculated for libraries 2 and 3 indicate the maximum coverage of reference shapes by the library.

$$\text{Coverage Score} = 1 - \text{Coverage}$$

Diversity score is calculated based on the number of reference shapes that hit 2 fragments (A&B) as a fraction of the number of reference shapes that hit at least 1 fragment (A|B), and this is calculated for each pair of fragments individually and then summed. These pairwise interactions can be illustrated by the overlap matrix showing  $\frac{A\&B}{A|B}$  for fragments A-D in library 1 (Table 5), where  $\sum(\frac{A\&B}{A|B})$  refers to the sum of the values above the matrix diagonal (diagonal showing each fragment overlapping with itself to give 1 Tanimoto) and these values are also mirrored underneath the diagonal. The matrix sum as a fraction of the number of entries (excluding the entries in the diagonal) gives rise to the diversity score (below and Table 6). The score of 0 calculated for library 3 indicates maximum diversity, with library 2 the second most diverse. Thus, library 3 is the most ideal out of the three.

Fragment	A	B	C	D
A	1	0	$\frac{1}{5}$	$\frac{1}{4}$
B	0	1	$\frac{1}{4}$	0
C	$\frac{1}{5}$	$\frac{1}{4}$	1	0
D	$\frac{1}{4}$	0	0	1

$$\text{Diversity Score} = \frac{\sum(\frac{A\&B}{A|B}) \times 2}{\text{Total} \times (\text{Total} - 1)}$$

**Table 5**  $\frac{A\&B}{A|B}$  values showing pairwise relationships for fragments A-D in library 1, where A&B is the number of reference shapes that hit 2 fragments and A|B is the number of reference shapes that hit at least 1 fragment.

Library	≥1 Hit	Coverage	$\sum(\frac{A\&B}{A B})$	Coverage Score	Diversity Score
1	7	$\frac{7}{8}$	$\frac{7}{10}$	0.125	0.117
2	8	1	$\frac{13}{20}$	0	0.108
3	8	1	0	0	0

**Table 6** The number of reference shapes that are hit by at least 1 fragment (≥1 Hit) are totalled for libraries 1-3 and used to calculate the coverage score of the libraries using  $\text{Coverage Score} = 1 - \text{Coverage}$ . Here, coverage is “≥1 Hit” as a fraction of the total number of reference shapes (8 in this example). The scores of 0 calculated for libraries 2 and 3 indicate the maximum coverage of reference shapes by the library.  $\sum(\frac{A\&B}{A|B})$  values showing pairwise relationships are also calculated for fragments in libraries 1-3, and used to calculate the diversity score of the libraries using  $\text{Diversity Score} = \frac{\sum(\frac{A\&B}{A|B}) \times 2}{\text{Total} \times (\text{Total} - 1)}$ . Here, A&B is the number of

reference shapes that hit 2 fragments, and  $A|B$  is the number of reference shapes that hit at least 1 fragment.  $\sum \binom{A \& B}{A|B}$  Refers to the sum of the values above the diagonal of the matrix shown in Table 5 and total is the number of fragments. The score of 0 calculated for library 3 indicates maximum diversity, with library 2 the second most diverse. Thus, library 3 is the most ideal out of the three.

Seven sets of conditions were attempted for different weightings of composition, coverage and diversity, and calculation of library scores were averaged over 10 trial runs for each set of conditions (Table 7). Initially, the composition target was set to 25% virtual molecules, or 20 molecules out of the library of 80 fragments. The scores given are the lowest scores out of the 5000 iterations, where average defines the average number of fragment hits per reference shape, with a lower average suggesting the fragment shapes are more unusual. Lower standard deviation indicates higher consistency for the number of fragment hits per reference shape, and fewer zero hits mean that a greater number of reference shapes are hit by the selected fragments, or a greater fraction of shape space is covered.

Highlighted in Table 7 are the lowest values per score column, where composition score = 0 means the target number of compounds in the chosen set has been matched, coverage score = 0 means the molecules in the chosen set hit 100% of those in the reference set, and diversity score = 0 means no overlap and maximum shape diversity. It could be seen that although the weighting for composition : coverage : diversity = 1 : 10 : 100 gave the same number of lowest values as composition : coverage : diversity = 1 : 100 : 10, the former has a substantially higher number of reference shapes not hit by a fragment (higher zero hits) as well as deviates from the target number of virtual molecules (composition score doesn't equal zero) - both factors which play an important role in the library. As a result, the latter weighting was carried forward in order to find the ideal number of virtual target molecules (Table 8). Again, these values were averaged over 10 trial runs for each set of conditions.

Composition Weighting	Composition Score	Coverage Weighting	Coverage Score	Diversity Weighting	Diversity Score	Average	Standard Deviation	Zero Hits
10	0	10	0.0082	10	0.052	7.3	3.5	21.0
1	0.015	10	0.0120	100	0.041	5.9	2.8	35.9
1	0	100	0.0049	10	0.060	8.2	4.0	12.2
10	0	1	0.0150	100	0.044	6.3	3.1	42.4
100	0	1	0.0140	10	0.049	6.8	3.3	39.6
10	0	100	0.0065	1	0.063	8.3	4.1	16.1
100	0	10	0.0068	1	0.064	8.5	4.2	16.9

**Table 7** A comparisons of library scores achieved for differing weightings of composition, coverage and diversity, along with the average number of fragment hits per reference shape, standard deviation of fragment hits per reference shape and number of reference shapes which were not hit by fragments (zero hits). For a detailed explanation of these terms, refer to the opening of Section 2.6.1. Highlighted in the table are the lowest values per score column, and it was on this basis that the weighting composition : coverage : diversity = 1 : 100 : 10 was carried forward.

<b>% Virtual Compounds</b>	<b>Composition Score</b>	<b>Coverage Score</b>	<b>Diversity Score</b>	<b>Normalised Total</b>	<b>Average</b>	<b>Standard Deviation</b>	<b>Zero Hits</b>
0	0.070	0.0048	0.0597	0.0103	8.12	4.04	11.8
10	0	0.0053	0.0602	0.0102	8.12	3.98	13.1
25	0	0.0049	0.0603	0.0099	8.19	4.01	12.2
50	0.016	0.0054	0.0657	0.0110	8.62	4.51	13.4
<b>Production run using 25%</b>	0	0.0035	0.0488	0.0076	6.97	3.28	8.8

**Table 8** A comparison of composition, coverage and diversity scores achieved for differing percentages of virtual compounds in the library, along with the total scores normalised to be independent of the weighting for each, average number of fragment hits per reference shape, standard deviation of fragment hits per reference shape and number of reference shapes which were not hit by a fragment (zero hits). For a detailed explanation of these terms, refer to the opening of Section 2.6.1. Highlighted in the table are the lowest values per score column, and it was on this basis that 25% composition of virtual molecules was chosen for the production run, along with an increased number of iterations (10,000) and a slower cooling rate (0.99).

Here, by focusing on only runs which gave a composition score of 0, the highlighted lowest values in runs consisting of 10 and 25% virtual molecules show an equal number of lowest scores. Taking into consideration that 20 is a suitable number of compounds for synthesis, 25% was selected as the composition target. Next, ten production runs were executed with the final set of conditions *i.e.* composition : coverage : diversity = 1 : 100 : 10, with a target of 25% virtual compounds. An increased number of iterations (10,000) and a slower cooling rate (0.99, see Section 2.6.1) was used and the convergence value was also decreased to accommodate these changes in conditions, lowering the scores further.

The graphs for one of the runs (Figure 24) illustrate the normalised combined score against number of iterations, and the frequency of hits per reference shape (with each reference shape represented as a bit string). As predicted, smooth convergence can be observed in the run with some random jumps in score towards the beginning (plot a), which is desirable in order to prevent a premature local minimum, and an even spread of frequency of hits can also be seen (plot b).

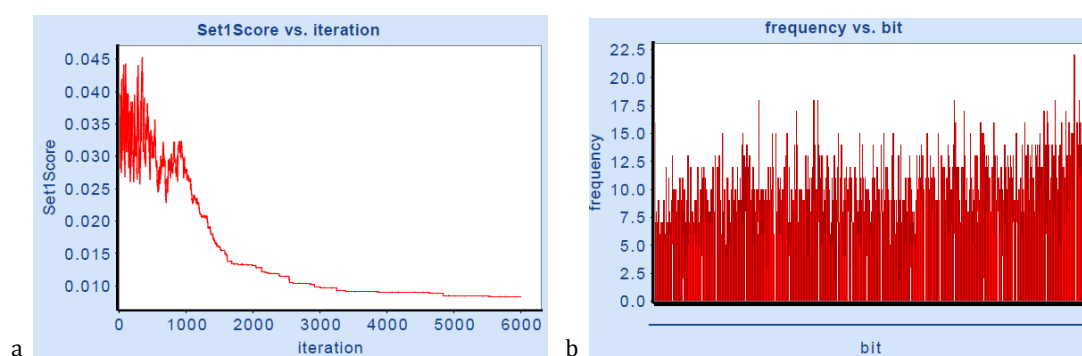
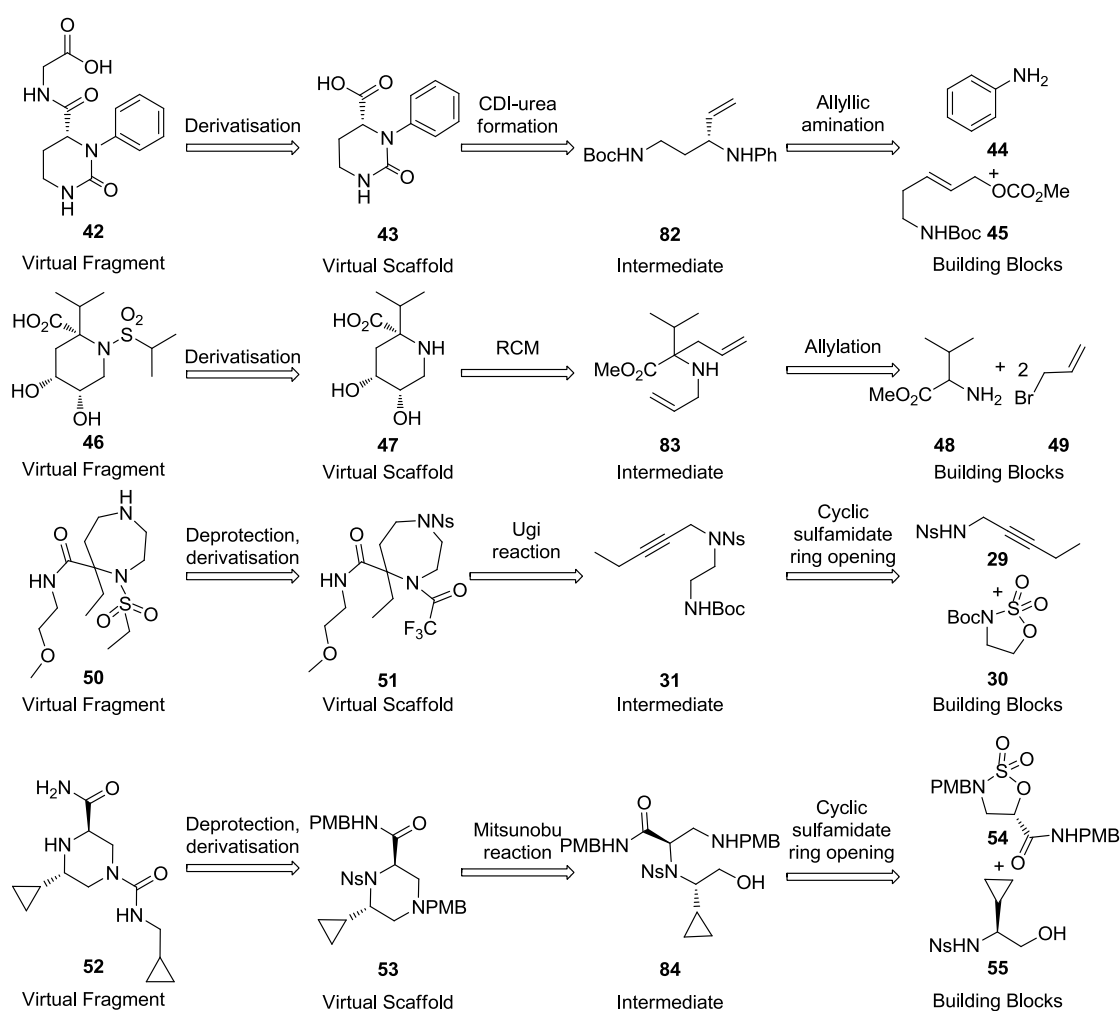


**Figure 24** a) Initial jumps in the score of a chosen set followed by smooth convergence. b) A consistent frequency of hits per reference shape indicates an even coverage of reference shapes.

Most libraries were discarded at this point due to stereochemistry of compounds that would be difficult to control, as a result of new stereocentres generated via a virtual derivatisation step. This was the case with unsymmetrical ketone capping groups used in the final reductive amination step for many of the Ugi scaffolds. In retrospect, if unsymmetrical ketones had been omitted from the enumeration, the final library would offer a more synthetically accessible selection of molecules. Nevertheless, libraries from two runs were carried forward for the next stage of analysis.

## 2.6.2 Retrosynthetic Analysis of Fragments of Interest

Retrosynthetic analysis of molecules from two compound libraries of interest (Section 2.6.1) were undertaken, with building blocks, key intermediates and reactions completed identified for each virtual molecule. This is in order to evaluate the commercial availability of necessary reagents as well as the viability of the chemistry involved. Shown in Scheme 10 are example compounds from one library (run 1); for the complete retrosynthetic analysis of compounds from the two libraries, refer to the Appendix (Table 35). Molecules produced by run 1 were taken forward for synthesis due to their chemistry being more developed than those produced by run 2. A PMI and properties plot of the chosen library (Figure 25) indicates that Leeds fragments (blue) exhibit a higher 3D character than commercial fragments (grey), and slightly lower *AlogP*.



**Scheme 10** Detailed retrosynthetic analysis of example fragments.

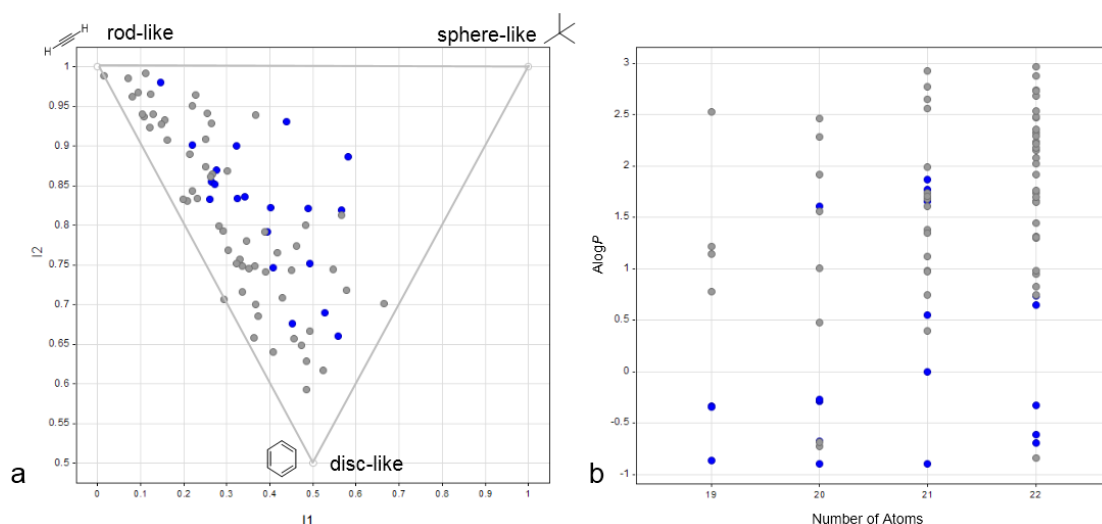


**Figure 25** a) PMI plot of the chosen library of 80 fragments. It can be seen here that Leeds fragments (blue) exhibit a higher 3D character than commercial fragments (grey). b) Lipophilicity vs. number of heavy atoms of the chosen library of 80 fragments. It can be seen here that the Leeds fragments (blue) are slightly lower in  $AlogP$  than commercial fragments (grey).

## 2.7 Analysis of the Chosen Library

In order to further verify the shape diversity of the chosen set of compounds, two new PLP protocols were devised in order to compare the chosen set against randomly selected sets of compounds. The first protocol focuses on the Tanimoto score of the library calculated using fingerprint comparison, where a lower score indicates higher shape diversity. The second method analyses the number of frameworks present in the library, as well as the number of compounds per framework. Here, framework is used as a unique identifier (refer to Section 1.4) for shape analysis. Finally, the value added by the virtual fragments to the combined library of both virtual and ZINC fragments is investigated.

### 2.7.1 Shape Diversity Analysis

The shape diversity of the chosen set of compounds can be verified by calculating a shape similarity score for the library, where a lower score indicates lower similarity, or higher shape diversity. All 80 compounds were scored against one another using shape fingerprint comparison. Tanimoto similarity scores ( $\frac{A \& B}{A | B}$ , where  $A \& B$  is the number of bits switched on in both fragments and  $A | B$  is the number of bits switched on in at least 1 fragment, Section 2.6.1) were calculated where compound 1 was scored against compounds 1 to 80, and then compound 2 was scored against compounds 1 to 80 until this was completed for all 80 compounds.

The scores were then totalled for each compound, and where shape match is identical for compound 1 against itself, and compound 2 against itself *etc.*, the score value of 1 per compound, or 80 per library, was removed from this total. Next, the average score per compound was calculated as a determinant of the shape diversity of the set, where the lower score would mean higher shape diversity (less overlap). The resulting score for the chosen library was calculated to be 3.5936. The same process was applied to ten libraries of 80 random compounds, which gave an average of 8.6842 per library, with a standard deviation of 0.4733. This is significantly more than two standard deviations higher than that of the target 80 compounds; therefore, it is true to say that the objective of identifying a shape-diverse set of 80 fragments has been reached.

### 2.7.2 Framework Analysis

Another way in which diversity can be evaluated is by identifying the different frameworks present in the library and the frequency of compounds containing each framework. A new PLP protocol was therefore devised and applied to the combined library of 73,031 compounds as well as the chosen library of 80 compounds. The framework type used to score, or categorize the libraries was “graph” only, which considers the connectivity of the molecule (Section 1.4). The frameworks were ordered in decreasing frequency of compounds that contained each one, and those frequencies were then normalised in order to make them independent of the library size (Table 9). The same was done for a random library of 80 compounds (Appendix, Table 36) in order to compare the relationship between frequency of frameworks in the combined library to both the chosen and random library of 80.

**Table 9** For each framework type in the chosen library of 80 fragments, the frequency of compounds containing the framework has been summarised, as well as the corresponding frequency of compounds containing the same framework in the combined library. The frameworks were ordered in decreasing frequency of compounds present in the chosen library of 80, and those frequencies were then normalised in order to make them independent of the library size. (Seen on the following page)

Framework (Smiles)	Frequency in Chosen Library of 80	Normalised Frequency	Frequency in Combined Library of 73,031	Normalised Frequency
C1CCCC1	13	0.1625	6714	0.0919
C1CCC(CC1)C2CCCC2	4	0.0500	2331	0.0319
C1CCC(CC1)C2CCCC2	3	0.0375	2490	0.0341
C(C1CCCC1)C2CCCC2	3	0.0375	2209	0.0302
C(CCC1CCCC1)CCC2CCCC2	3	0.0375	1589	0.0218
C(CC1CCCC1)C2CCCC2	2	0.0250	3156	0.0432
C(C1CCCC1)C2CCCC2	2	0.0250	178	0.0024
C(CC1CCCC1)C2CC2	2	0.0250	426	0.0058
C1CCCC1	2	0.0250	846	0.0116
C(CC1CCCC1)C2CCCC2	2	0.0250	112	0.0015
C(CCC1CCCC1)CC2CCCC2	2	0.0250	2299	0.0315
C(CC1CCCC1C2CCCC2)C3CCCC3	1	0.0125	31	0.0004
C1CCC(CC1)C2CCCC(C2)C3CCCC3	1	0.0125	90	0.0012
C(CC1CCCC1)CC2CCCC2	1	0.0125	400	0.0055
C(C1CCCC1)C2CCC(CC3CCCC3)C2	1	0.0125	48	0.0007
C(CC1CCCC1)CC2CCC(C2)C3CCCC3	1	0.0125	83	0.0011
C(C1CCCC1)C2CCC3CCCC3C2	1	0.0125	219	0.0030
C(CCC1CCCC1)CCC2CCC(C2)C3CCCC3	1	0.0125	13	0.0002
C(CC1CCCC1)C(CCC2CCCC2)C3CCCC3	1	0.0125	3	0
C(CC1CCCC1)CC2CCC(CC3CCCC3)CC2	1	0.0125	19	0.0003
C(CCCC1CCCC1)CCC2CCCC2	1	0.0125	749	0.0103
C(CC1CCC2CCCC2C1)C3CCCC3	1	0.0125	328	0.0045
C(CC1CCCC1)CC2CCC(CC3CCCC3)C2	1	0.0125	15	0.0002
C(CC(CC1CCCC1)C2CC2)CC3CCCC3	1	0.0125	8	0.0001
C(C1CCCC1)C2CCC(CC3CCCC3)CC2	1	0.0125	49	0.0007

C(CCCC1CC2CCCC2C1)CCC3CCCC3	1	0.0125	3	0
C(CC1CCCC1)CC2CCCC2	1	0.0125	2809	0.0385
C(CC1CCC2CCCC2C1)C3CCCC3	1	0.0125	370	0.0051
C(C1CCCC1)C2CCCC2CC3CCCC3	1	0.0125	27	0.0004
C(CC1CCCC1CCC2CCCC2)C3CCCC3	1	0.0125	2	0
C(CC1CCCCC1)C2CC2	1	0.0125	79	0.0011
C(C1CC1)C2CCCC2	1	0.0125	206	0.0028
C(CC1CCCC1)CC2CCCC2	1	0.0125	100	0.0014
C(CC1CCCC1)CC2CCCC(CC3CC3)C2	1	0.0125	8	0.0001
C(CC1CCCC1)CC2CCCC(C2)C3CCCC3	1	0.0125	9	0.0001
C1CCC(CC1)C2CCCC(C2)C3CCCC3	1	0.0125	16	0.0002
C(CC1CC1)CC2CCCC(C2)C3CC3	1	0.0125	2	0
C(CC1CC1)CC2CCCC2CCC3CC3	1	0.0125	5	0.0001
C(C1CCCC1)C2CCCC(C2)C3CC3	1	0.0125	14	0.0002
C1CCCCC1	1	0.0125	328	0.0045
C(C1CCCC1)C2CCCC(C2)C3CCCC3	1	0.0125	62	0.0008
C(CCC1CCCC1)CCC2CCCC2	1	0.0125	1205	0.0165
C(CCC1CCCC1)CC2CCCC2	1	0.0125	2402	0.0329
C(C1CCCC1)C2CCCC2	1	0.0125	2498	0.0342
Linear	1	0.0125	187	0.0026
C(CCCCC1CCCC1)CCCC2CCCC2	1	0.0125	9	0.0001
C(CC1CCCC1)C2CCCC2	1	0.0125	271	0.0037
C1CC2CCCC2C1	1	0.0125	68	0.0009
C1CCC2CCCC2C1	1	0.0125	1639	0.0224
C(CC1CCCC1)CC2CC3CCCC3C2	1	0.0125	31	0.0004
C1CCCCC2(CCCCC1)CCCC2	1	0.0125	2	0
C(CCC1CCCC1)CCC2CCCC2	1	0.0125	305	0.0042
C(CCCC1CCCC1)CCCC2CCCC2	1	0.0125	150	0.0021

Plots to show the relationship between normalised frequencies of each framework present in a) the combined library and the chosen library of 80 and b) the combined library and a random library of 80 (Figure 26). It is clear that a closer relationship can be observed in plot b than in plot a, suggesting that the chosen library is more framework-diverse, whereas the random library has been selected simply based on the how frequently a framework appears in the combined library.

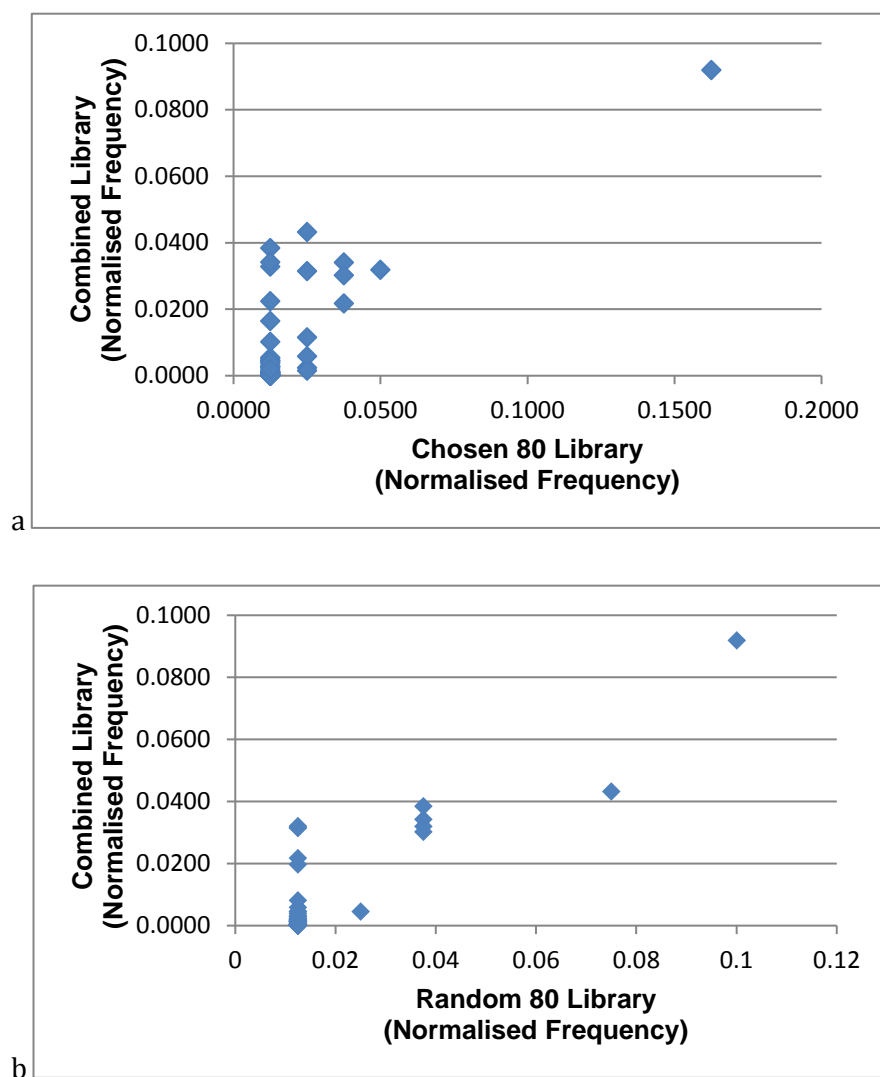


**Figure 26** Plots to show the relationship between normalised frequencies of each framework in a) the combined library and the chosen library of 80 and b) the combined library and a random library of 80. A closer relationship can be observed in plot b than in plot a, suggesting that the chosen library is more framework-diverse; whereas the random library has been selected simply based on the how frequently a framework appears in the combined library.

PC50C is a value which indicates the fraction of frameworks required to cover half of the total library of compounds, and can be an indicator of framework diversity, where the higher PC50C indicates a more framework-diverse library.<sup>47</sup> Since the chosen library

of 80 contains a total of 53 frameworks, and 13 frameworks are required to cover 40 of the compounds (calculated using the cumulative total of compounds starting from the most frequently occurring framework, in decreasing order), its PC50C is calculated to be  $13 \div 53 = 0.245$ . The same was done to ten randomly selected libraries of 80 molecules, seen in Table 10 and displayed graphically in Figure 27, which gave an average PC50C of 0.254 and a standard deviation of 0.0319.

Random Library	No. Frameworks	No. Frameworks Covering 50% Compounds	PC50C
1	53	14	0.264
2	48	11	0.229
3	59	19	0.322
4	52	13	0.250
5	50	11	0.220
6	53	13	0.245
7	51	11	0.216
8	56	16	0.286
9	53	13	0.245
10	50	13	0.260
<b>Average</b>	52.5	13.4	0.254

**Table 10** The total number of frameworks as well as the number of frameworks needed to cover 50% of compounds in each library was identified for ten random libraries of 80 molecules, and their PC50C values were calculated using  $\frac{\text{No. Frameworks Covering 50\% Compounds}}{\text{Total No. Frameworks}}$ . The data gave an average PC50C of 0.254 for the ten random libraries and a standard deviation of 0.0319.

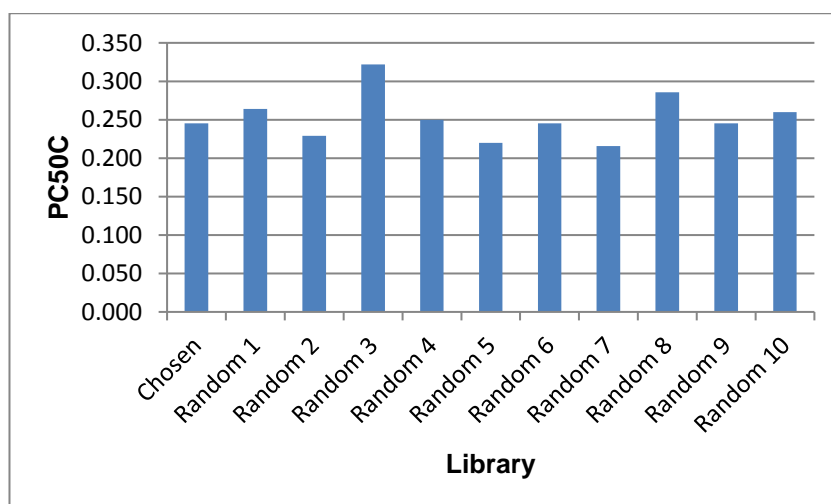


**Figure 27**  
A comparison of PC50C of the chosen library with the 10 randomly selected libraries of 80 molecules (Table 10).

The PC50C values for the chosen library of 80 differs from the mean PC50C of the random libraries by much less than two standard deviations, showing no significant difference between the framework diversity of the libraries (Figure 27). Although it might have been expected that the chosen library would have a higher PC50C due to its high

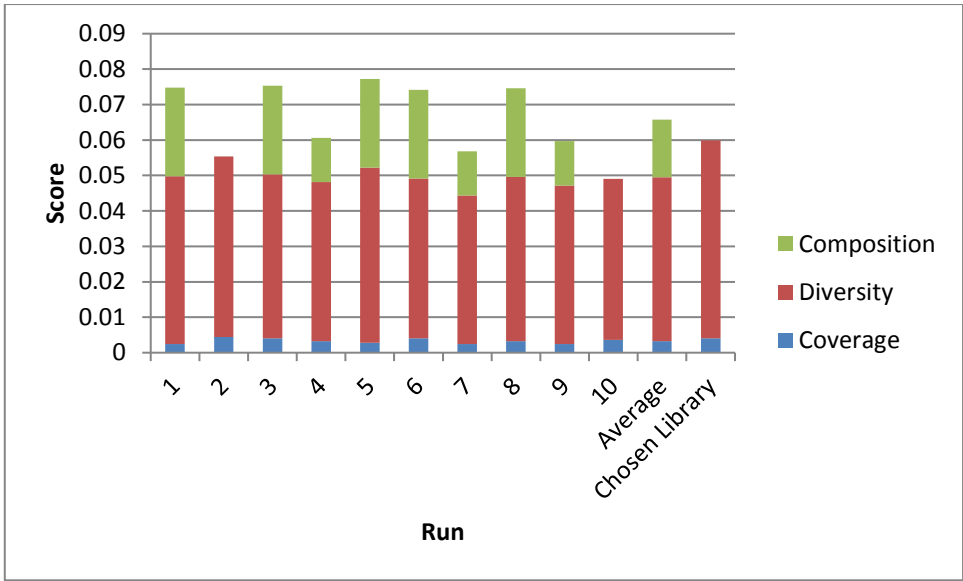
shape diversity, the similar values could be explained by that frameworks are not necessarily indicative of shape.

### **2.7.3 Comparison of Virtual Compounds to Commercial Compounds**

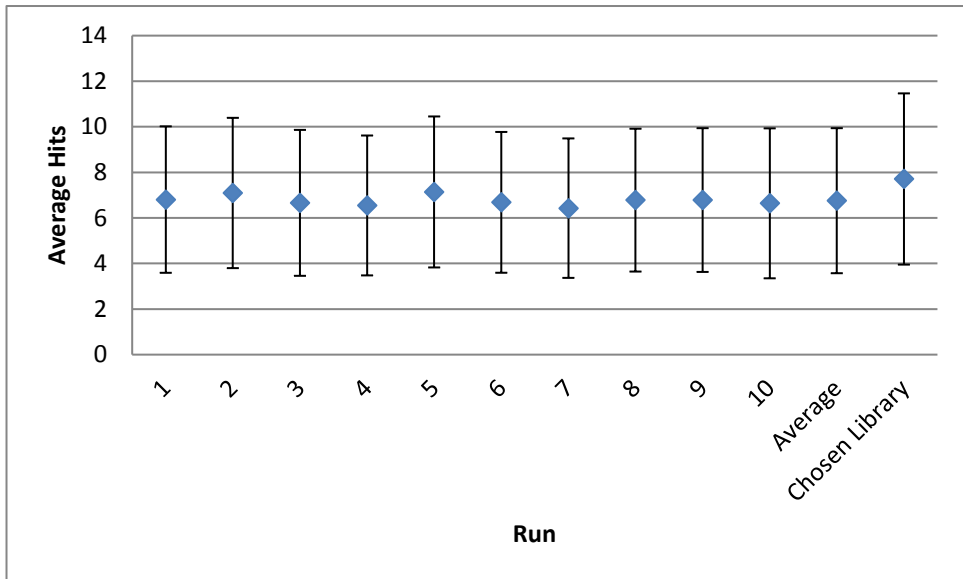
In order to investigate the value added by the 20 virtual fragments to the 80-compound library of both virtual and ZINC fragments, the score of the chosen library was compared to the score of a library of fragments selected when only commercial ZINC molecules are available. This was done by generation of ten libraries of 80 fragments from the ZINC library using the same conditions for compound selection as that used for the chosen set. It was observed that on average the ZINC set were unable to achieve a composition score of 0 (Table 11), a fundamental property of the chosen library (highlighted). This indicates that under the same selection conditions, it is not possible to select 80 fragments from the ZINC library whilst achieving maximum reference shape coverage and maximum shape diversity (Section 2.6.1), thus proving the value of virtual fragments in the library. A graphical display of Table 11 is seen in Figure 28.

<b>Run</b>	<b>Composition Score</b>	<b>Coverage Score</b>	<b>Diversity Score</b>	<b>Average Hits</b>	<b>Standard Deviation</b>	<b>Zero Hits</b>
<b>1</b>	0.025	0.0024223	0.047319	6.8050	3.2142	6
<b>2</b>	0	0.0044409	0.050952	7.0949	3.2977	11
<b>3</b>	0.025	0.0040371	0.046308	6.6605	3.2023	10
<b>4</b>	0.0125	0.0032297	0.044882	6.5470	3.0699	8
<b>5</b>	0.025	0.002826	0.049372	7.1397	3.313	7
<b>6</b>	0.025	0.0040371	0.045083	6.6831	3.0893	10
<b>7</b>	0.0125	0.0024223	0.041917	6.4287	3.0603	6
<b>8</b>	0.025	0.0032297	0.046375	6.7804	3.1342	8
<b>9</b>	0.0125	0.0024223	0.044761	6.7840	3.1547	6
<b>10</b>	0	0.0036334	0.045401	6.6399	3.2907	9
<b>Average</b>	0.01625	0.0032701	0.046237	6.7563	3.1826	8.1
<b>Chosen Library</b>	0	0.0040371	0.055811	7.7085	3.7569	10

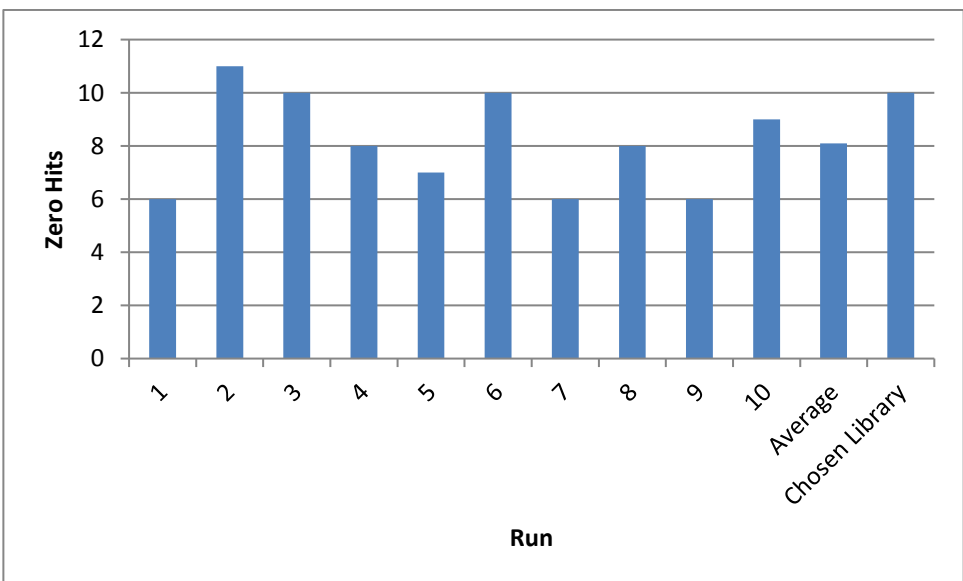
**Table 11** Scores for ten libraries selected using only commercial fragments from ZINC. Displayed scores include composition, coverage and diversity, along with average number of fragment hits per reference shape, standard deviation of fragment hits per reference shape and number of references shapes which were not hit by a fragment (zero hits); this is shown graphically in Figure 27. For a detailed explanation of these terms, refer to the opening of Section 2.6.1. The average score has been calculated, indicating that a composition score of 0 is unable to be achieved (highlighted), unlike within the chosen library.



a



b



c

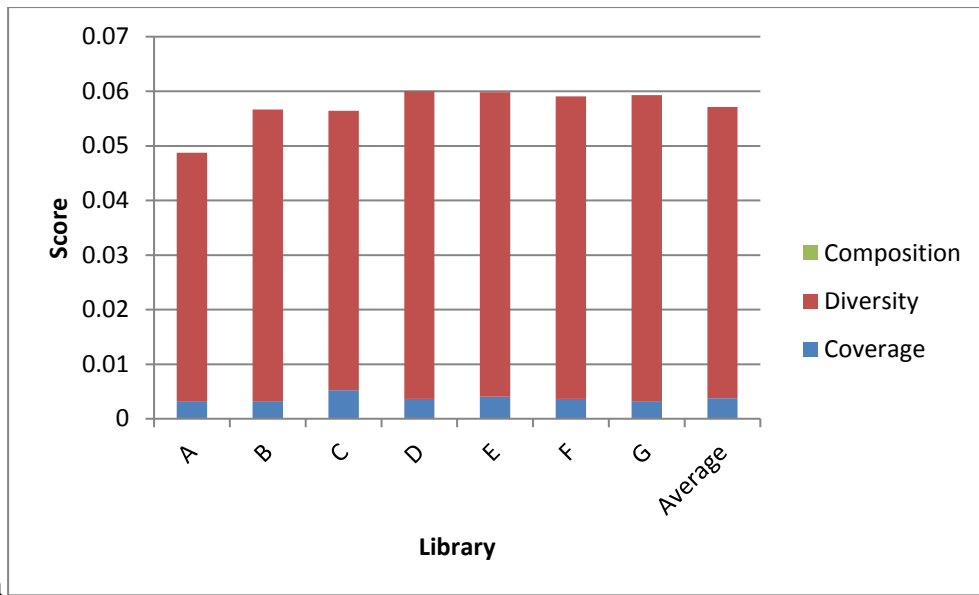
**Figure 28** Graphical representation of properties of ten libraries selected using only commercial fragments from ZINC, seen in Table 11. These include a) composition, coverage and diversity scores; b) average number of fragment hits per reference shape with standard deviations shown as error bars and c) number of references shapes which were not hit by a fragment (zero hits). For a detailed explanation of these terms, refer to the opening of Section 2.6.1. The average values have been calculated for each property and have been included in all three plots as well as the same properties for the chosen library. This clearly indicates that a composition score of 0 is unable to be achieved using only commercial fragments from ZINC, unlike within the chosen library.

## 2.8 Purchase of Commercial Fragments

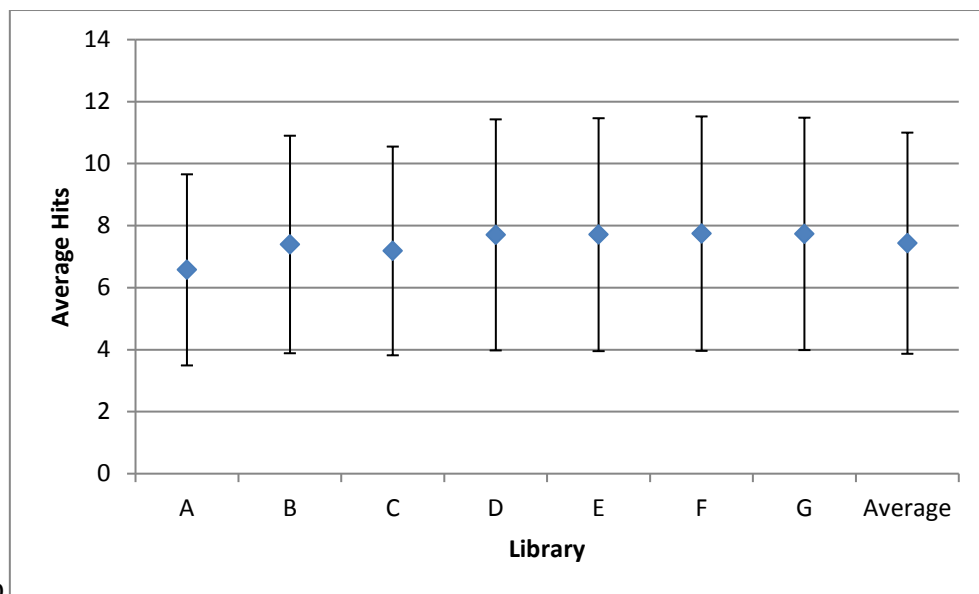
With the 20 fragments synthesised using Leeds chemistry completed, an attempt to source the remaining 60 commercial fragments revealed challenges due to high cost or lack of availability. As a result, commercial fragments were reselected for the final library to overcome these issues, and this was done a total of three times (libraries E-G). During each reselection of commercial molecules, ten alternative libraries were generated with the fragments already in hand remaining unaltered. The library with the lowest composition, coverage and diversity score (Section 2.6.1) was selected until all compounds were successfully sourced. The similar scores of the library of 80 compounds in each round of reselection (Section 3.2 describes how libraries A-D are directed at reselection of fragments synthesised using Leeds chemistry; here libraries E-G are described for reselection of commercial fragments) indicate that the shape-diversity of the final library has not been compromised from the initial target fragments (Table 12). This is denoted by the fact that all scores for libraries A-G contain values within two standard deviations of the average library score. A graphical display of Table 12 can be seen in Figure 29.

<b>Library</b>	<b>Composition Score</b>	<b>Coverage Score</b>	<b>Diversity Score</b>	<b>Average Hits</b>	<b>Standard Deviation</b>	<b>Zero Hits</b>
<b>A</b>	0	0.0032297	0.045488	6.5733	3.0824	8
<b>B</b>	0	0.0032297	0.053412	7.3924	3.5084	8
<b>C</b>	0	0.0052483	0.051173	7.1841	3.3662	13
<b>D</b>	0	0.0036334	0.056421	7.7017	3.7268	9
<b>E</b>	0	0.0040371	0.055811	7.7085	3.7569	10
<b>F</b>	0	0.0036334	0.055451	7.7416	3.7811	9
<b>G</b>	0	0.0032297	0.056052	7.7344	3.7480	8
<b>Average</b>	0	0.0037488	0.053401	7.4337	3.5671	9.3
<b>Standard Deviation</b>	0	0.0006726	0.003659	0.4030	0.2446	1.7

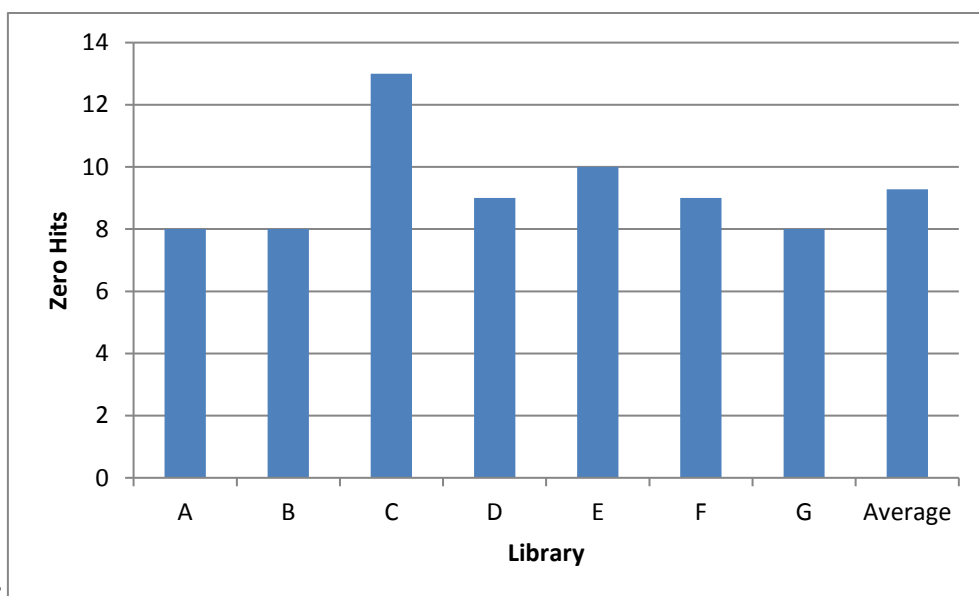
**Table 12** A comparison of scores for the initial library (Library A), each regenerated library (Libraries B-F) and the final library (Library G). Displayed scores include composition, coverage and diversity, along with the average number of fragment hits per reference shape, standard deviation of fragment hits per reference shape and number of reference shapes not hit by a fragment (zero hits); this is shown graphically in Figure 28. For a detailed explanation of these terms, refer to the opening of Section 2.6.1. The column averages and standard deviations of each property have also been calculated.



a



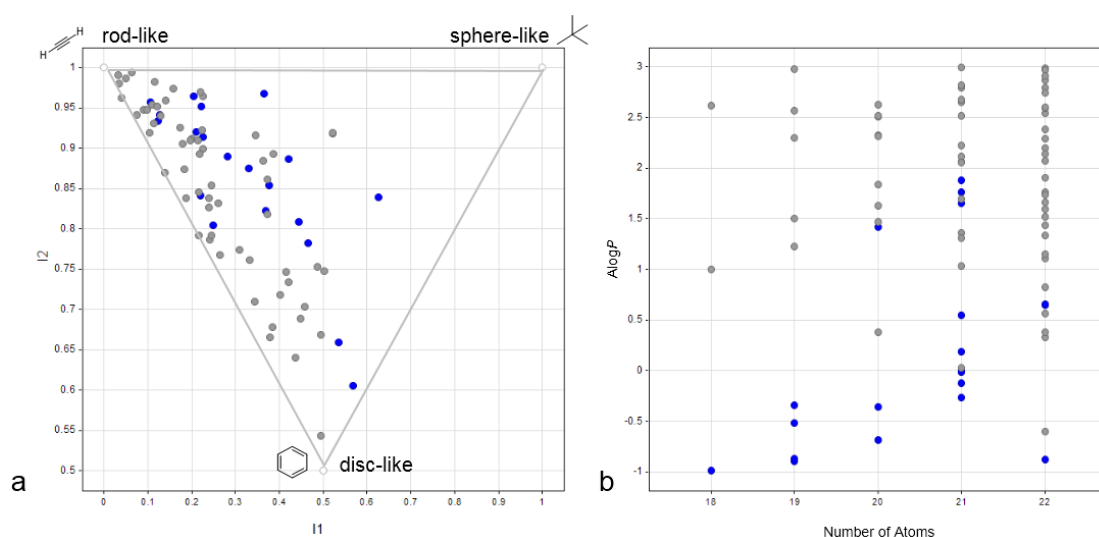
b



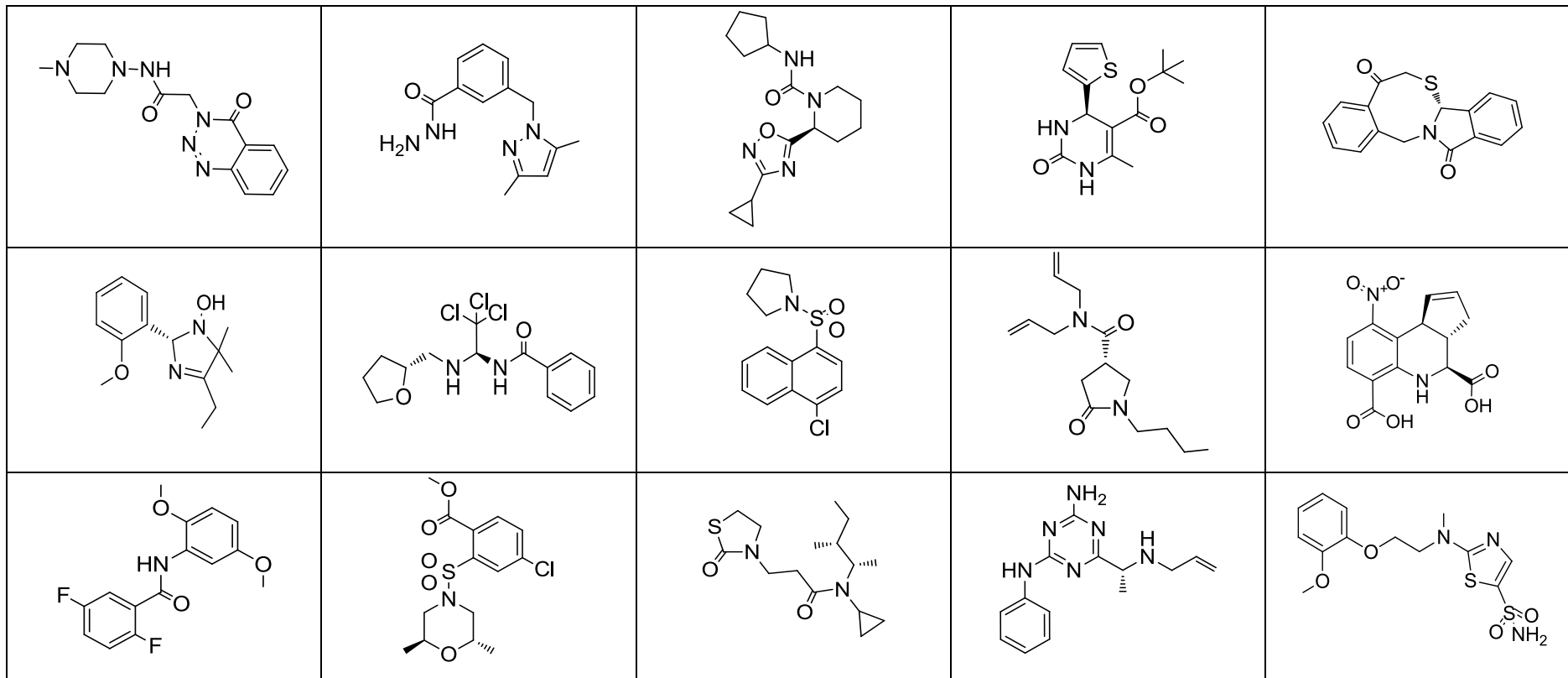
c

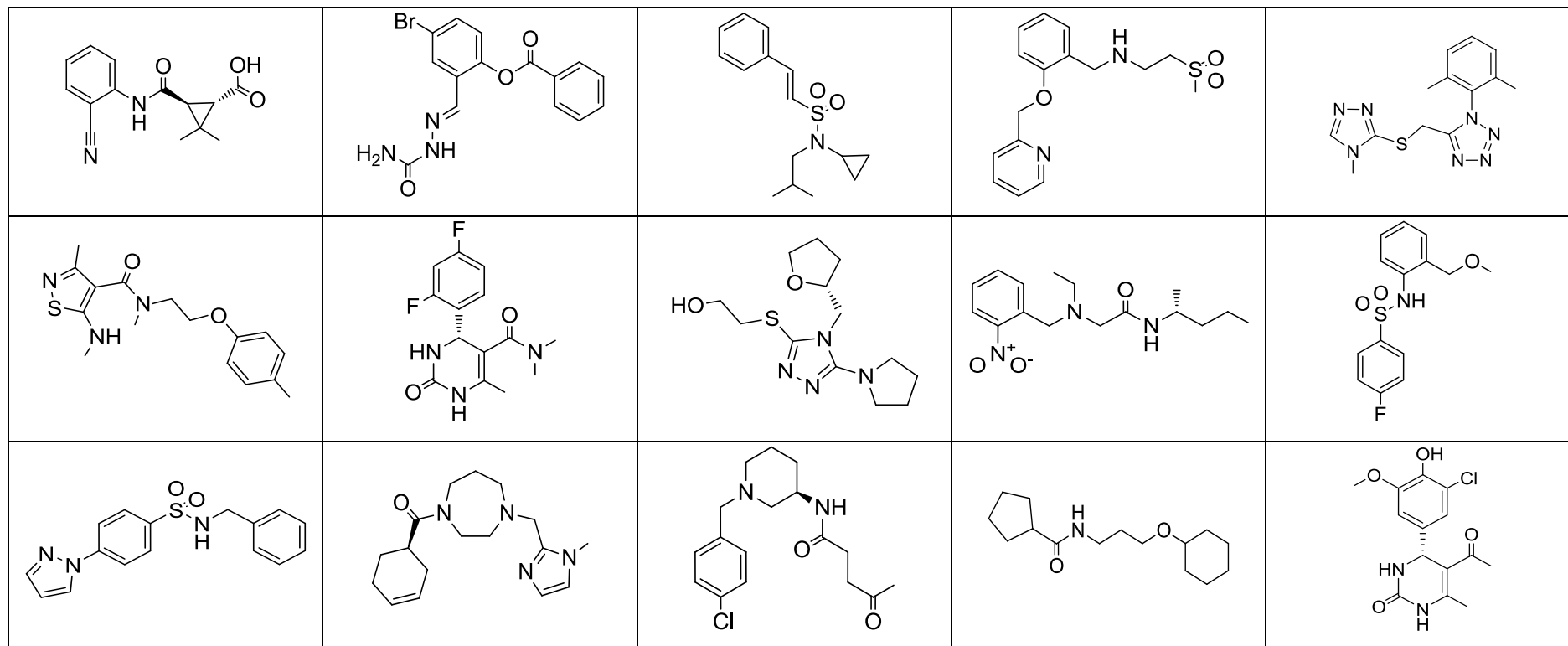
**Figure 29** Graphical representation of properties of the initial chosen library (Library A), each regenerated library (Libraries B-F) and the final library (Library G), seen in Table 12. These include a) composition, coverage and diversity scores; b) average number of fragment hits per reference shape with standard deviations shown as error bars and c) number of reference shapes not hit by a fragment (zero hits). For a detailed explanation of these terms, refer to the opening of Section 2.6.1. The average values have been calculated for each property and have been included in all three plots, indicating that properties of each library are comparable.

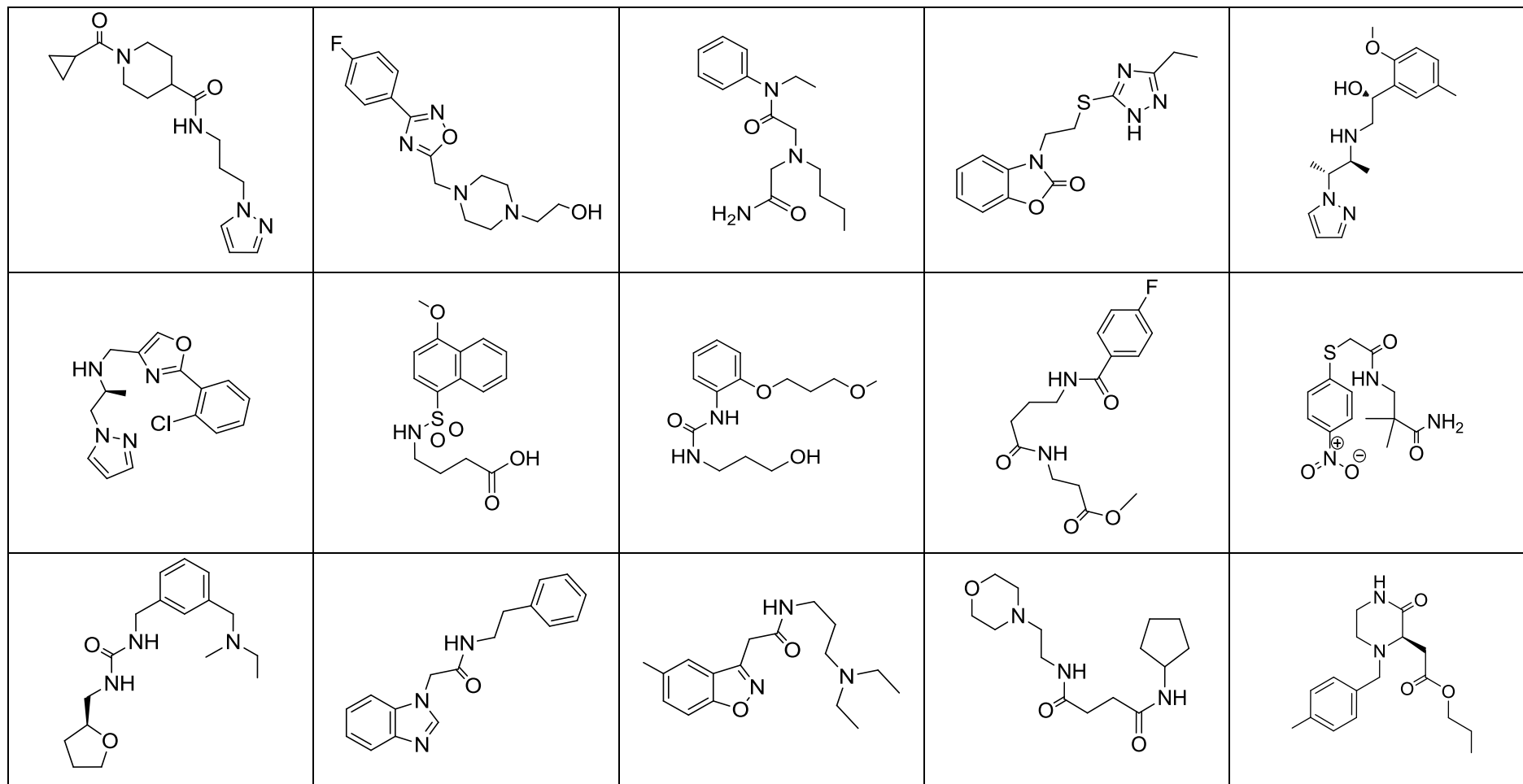
A PMI and properties plot of the final library, or Library G (Figure 30) indicates that Leeds fragments (blue) exhibit a higher 3D character than commercial fragments (grey), and slightly lower  $AlogP$ . The structures for all 60 commercially purchased fragments can be seen in Table 13.



**Figure 30** a) PMI plot of Library G, the final library of 80 fragments. It can be seen here that Leeds fragments (blue) exhibit a higher 3D character than commercial fragments (grey). b) Lipophilicity vs. number of heavy atoms of Library G. It can be seen here that the Leeds fragments (blue) are slightly lower in  $AlogP$  than commercial fragments (grey).



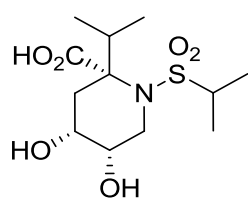
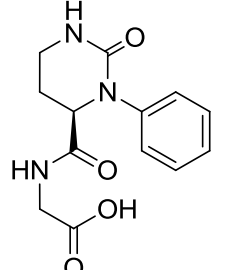
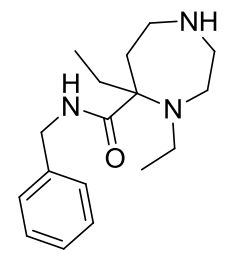
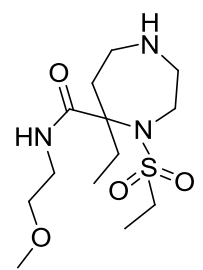
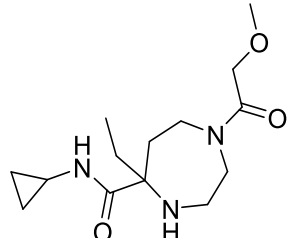
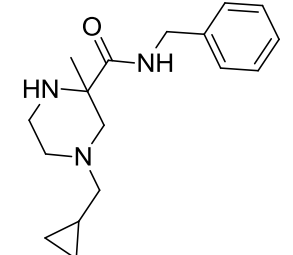
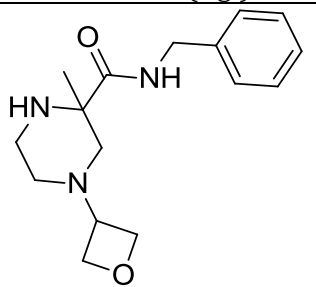
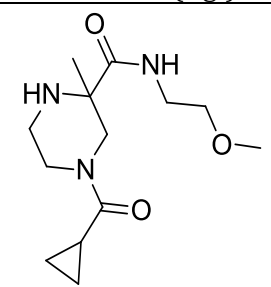
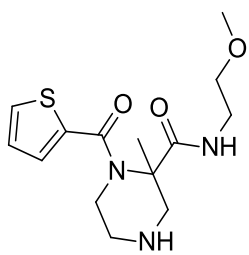
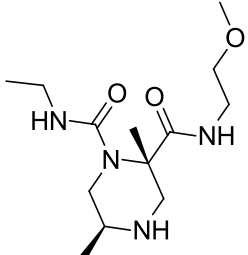






### **3 Synthesis of a Shape-Diverse Fragment Library**

This Chapter focuses on the work I have completed on the 20 synthetic compounds (Table 14) within my shape-diverse library of 80. The Chapter has been divided into four sections focusing on the key chemistries for fragment formation. Section 3.3 describes fragments synthesised using Ugi chemistry, Section 3.4 describes fragments synthesised using amino acid chemistry, Section 3.5 describes fragments synthesised using Mitsunobu chemistry, and finally Section 3.6 describes fragments synthesised using iridium chemistry, in a key step for formation. Each section is divided into sub-sections for the synthesis of building blocks, the key reaction connecting those building blocks together, the formation of scaffolds, and finally deprotection and decoration of the scaffolds in order to form the desired fragments.

scaffold 1 (Amino acid)	scaffold 2 (Iridium)	scaffold 3 (Ugi)	scaffold 4 (Ugi)	scaffold 5 (Ugi)
				
scaffold 6 (Ugi)	scaffold 6 (Ugi)	scaffold 7 (Ugi)	scaffold 7 (Ugi)	scaffold 8 (Ugi)
				

scaffold 9 (Ugi)	scaffold 10 (Ugi)	scaffold 11 (Ugi)	scaffold 11 (Ugi)	scaffold 12 (Ugi)
scaffold 13 (Ugi)	scaffold 14 (Mitsunobu)	scaffold 15 (Mitsunobu)	scaffold 16 (Mitsunobu)	scaffold 17 (Mitsunobu)

**Table 14** The original library of 20 fragments selected for synthesis using chemistry developed at Leeds. Each fragment has been labelled with the scaffold from which they originate as well as the chemistry used for their key stage for formation.

### 3.1 Shape-Similar Alternative Fragments

During encounters with fragments whose synthetic routes were exhausted and unsuccessful, an attempt was made to identify a shape-similar fragment. Using PLP, shape-similar fragments to **50** (Section 3.3.4.1.2) was identified by calculating the Tanimoto score between the bit string of the target fragment's fingerprint and that of the rest of the fragments in the Leeds library. Tanimoto scores lie in the region of 0-1, where a score of 1 equates to an identical fragment in terms of shape and 0 equates to a complete lack of shape similarity. The calculation is shown below (analogous to that used in Section 2.7.1), where each bit indicates a match with a specific reference shape. Here, "number of [and] bits" refers to the number of reference shapes covered by both the target fragment and the suggested alternative fragment, and "number of [or] bits" refers to the number of reference shapes covered by either the target fragment or the suggested alternative fragment.

$$\text{Tanimoto score} = \frac{\text{number of [and] bits}}{\text{number of [or] bits}}$$

The three highest similarity fragments could be identified by allowing the protocol to only select molecules which matched the target fragment with Tanimoto scores of >0.5 (Figure 31). Unfortunately, two of these fragments **85** and **86** require decorations with an unreactive alkyl sulfonyl chloride capping group, similar to **50**. The synthesis of the third fragment **87** involves a reductive amination reaction that would likely result in a mixture of two diastereomers which would be challenging to separate. By using the same protocol to trial locating shape-similar alternative fragments for other compounds from the library, it was suggested that the target molecule **50** resided in an especially unpopulated area of shape space. As a result, a new simulated annealing protocol was applied which selects a new library of 20 fragments with high coverage of reference shapes and diversity; this protocol would allow completed compounds to be included without relying on specific compounds similar in shape to problematic fragments such as **50**.

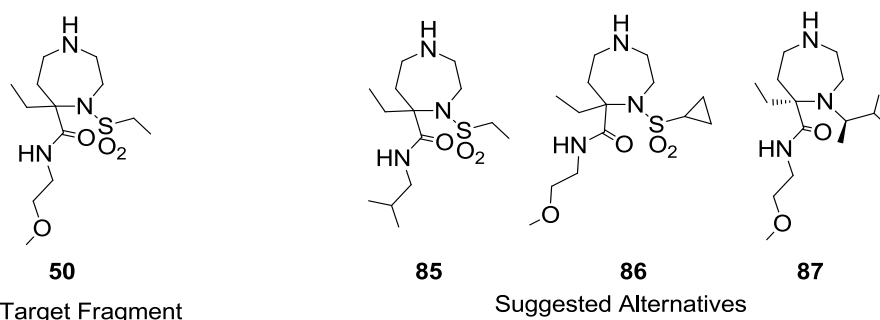


**Figure 31** The target fragment **50** for which a replacement is required and the proposed alternatives **85-87** by PLP.

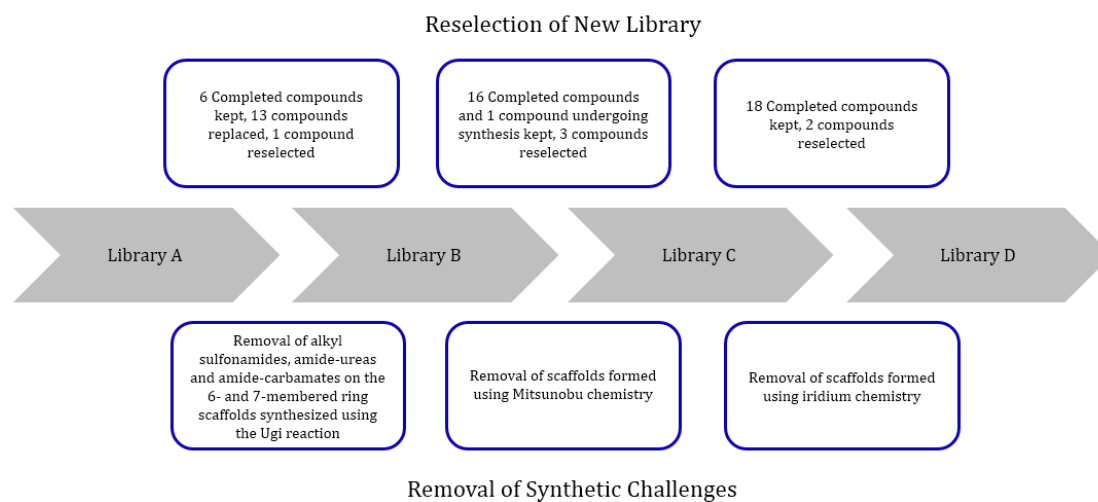
### 3.2 Alternative Fragment Libraries

An improved method to using a PLP protocol to locate shape-similar fragments was to generate a new simulated annealing protocol. This was able to produce an alternative library of 20 fragments (Library B) to the original (Library A) selected from the Leeds virtual fragment library, with optimum coverage of reference shapes and diversity. Alternative libraries were generated three times in total (libraries B-D), each time allowing completed compounds to be included whilst implementing new filters. Library B allowed removal of alkyl sulfonamides on the 6-membered and 7-membered ring scaffolds synthesised using the Ugi reaction, on the most hindered nitrogen within the ring (to avoid synthetically unfeasible fragments such as **50**, Section 3.3.4.1.2). On these same nitrogens, amide-ureas and amide-carbamates were also removed (to avoid synthetically unfeasible fragments leading to side-products such as **159**, Section 3.3.4.3.2). Ten virtual fragment libraries were generated using the new filters where Library B was selected based on low reagent cost and ease of synthesis, as well as familiarity of the chemistry.

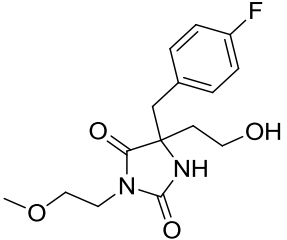
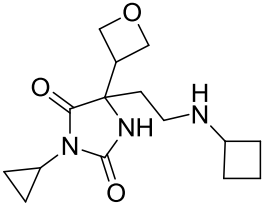
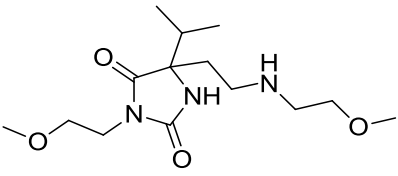
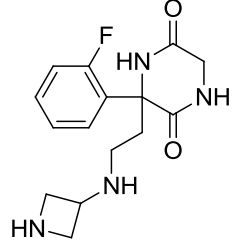
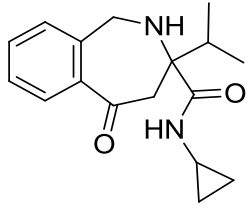
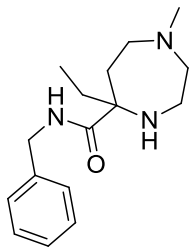
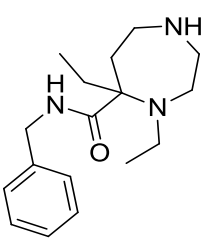
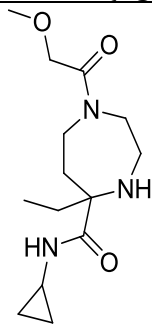
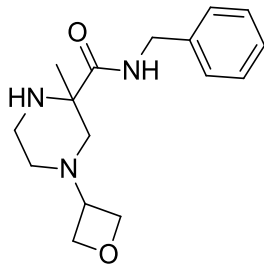
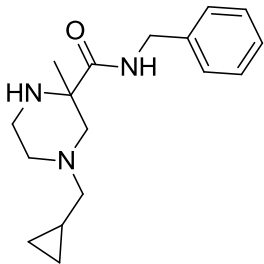
Based on Library B, new challenges were identified and the same replacement process was implemented. Library C was selected after exclusion of scaffolds formed using Mitsunobu cyclisation chemistry. This was due to the unsuccessful connection of building blocks (Section 3.5.2), epimerisation of stereocentres as well as unsuccessful deprotection reactions (Section 3.5.4). Library C was selected from a set of 10 new libraries generated by PLP.

Based on Library C, new challenges were identified during formation of intermediates using the iridium-catalysed allylic amination reaction, and the same replacement process was implemented. It was observed on one occasion that the iridium-catalysed reaction was unable to selectively promote formation of the desired alkene (Section 3.6.2), and unfortunately the following aminoarylation reactions were also

unsuccessful. Library D was selected after exclusion of scaffolds formed using iridium chemistry in a key step (Table 15). A summary of the library reselection process is shown in Figure 32 and libraries A-D can be seen in the Appendix (Table 37). The synthesis of fragments as a result of the original as well as regenerated libraries has been discussed throughout.



**Figure 32** Summary of the library reselection process from Library A to Library D, including number of compounds kept and replaced in each round of selection as well as the synthetic challenges which were removed. Library D was ultimately prepared.

scaffold 1 (Amino acid)	scaffold 2 (Amino acid)	scaffold 3 (Amino acid)	scaffold 4 (Amino acid)	scaffold 5 (Amino acid)
				
scaffold 6 (Ugi)*	scaffold 6 (Ugi)	scaffold 7 (Ugi)*	scaffold 8 (Ugi)*	scaffold 8 (Ugi)*
				

scaffold 8 (Ugi)	scaffold 9 (Ugi)*	scaffold 9 (Ugi)*	scaffold 10 (Ugi)	scaffold 11 (Ugi)
scaffold 12 (Ugi)	scaffold 12 (Ugi)	scaffold 13 (Ugi)	scaffold 13 (Ugi)*	scaffold 14 (Ugi)

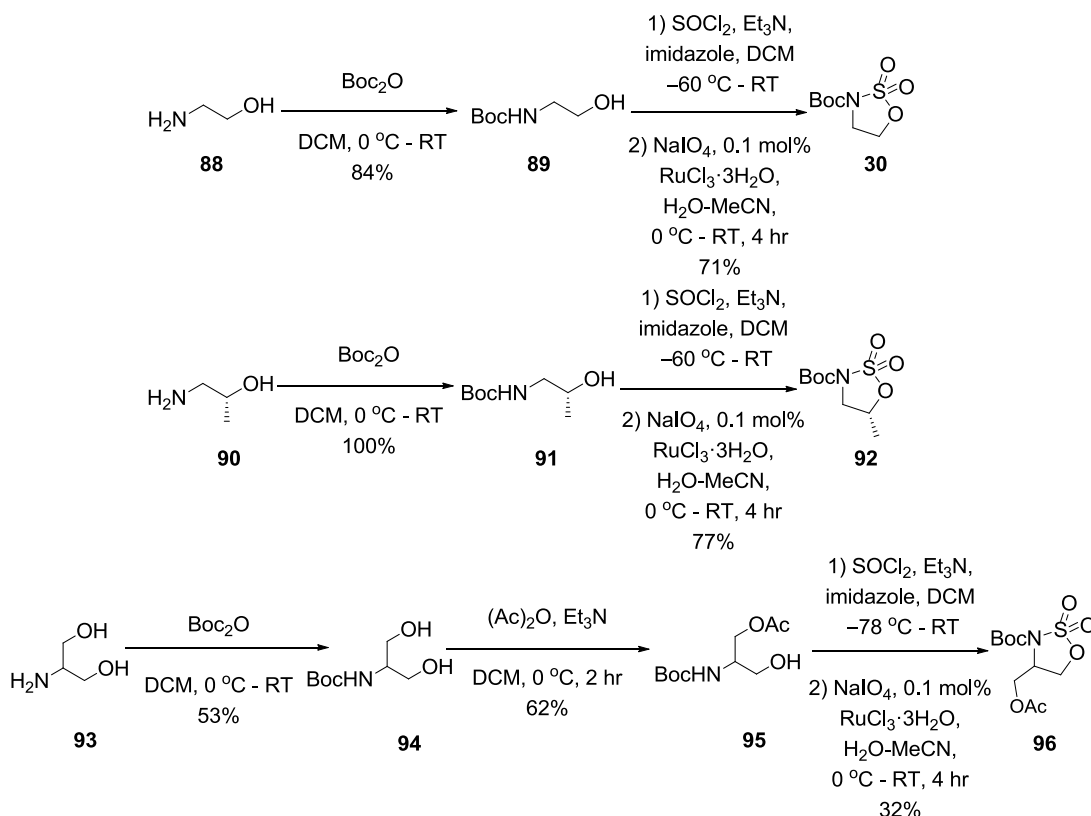
**Table 15** Library D, the final library of 20 fragments selected from the Leeds virtual fragment library. Each fragment has been labelled with the scaffold from which they originate as well as the chemistry used for their key stage for formation. \*Fragments that have remained from the original library.

### 3.3 Synthesis of Fragments Using the Ugi Reaction as a Key Step

#### 3.3.1 Synthesis of Building Blocks

##### 3.3.1.1 Cyclic sulfamidates

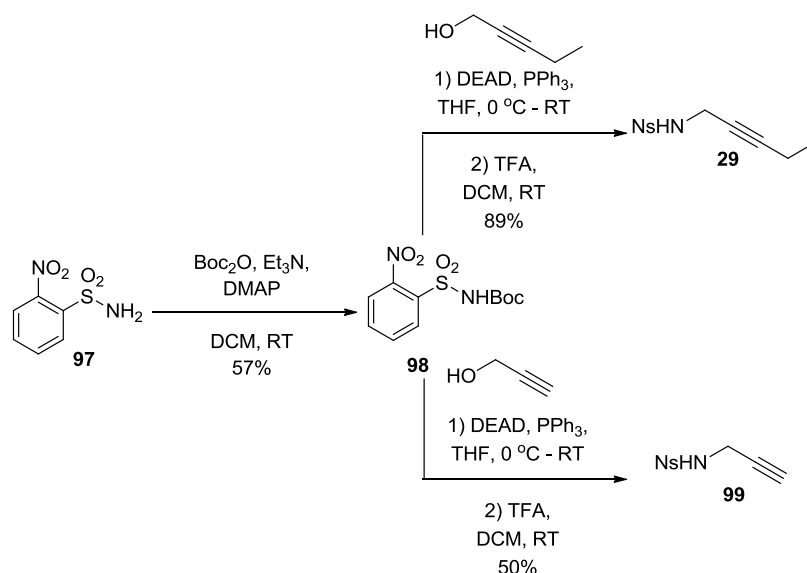
The formation of the cyclic sulfamidates **30**, **92** and **96** (Scheme 11) began with Boc-protection<sup>61</sup> of the corresponding commercially available amines followed by reaction with thionyl chloride, giving the cyclic sulfamidite. A ruthenium-catalysed oxidation using sodium periodate yielded the cyclic sulfamidates on 10 g scales.<sup>62,63</sup> The sulfamidate ring formation reaction was repeated on Boc-ethanolamine using 2.2 equivalents of NaIO<sub>4</sub> instead of 1.1 equivalents, where it was discovered that the oxidation step completed in just 4 hours whereas it is normally left to react overnight. The yield improved from 23% to 71% and the crude material was pure enough to carry through to the next step after aqueous workup. The formation of the cyclic sulfamidate **96** proceeded via an acetylated<sup>64</sup> intermediate **95**. A mixture of mono-acylated intermediate and di-acylated side product was recovered in this step.



**Scheme 11** Synthesis of cyclic sulfamidates.

### 3.3.1.2 Alkynyl sulfonamides

Boc-protection of 2-nitrobenzenesulfonamide and a DEAD-promoted Mitsunobu reaction<sup>iv</sup> with corresponding alkynyl alcohols was followed by Boc-deprotection to yield sulfonamides **29** and **99** on 25 g scales (Scheme 12). Purification of the propargyl sulfonamide **99** was difficult due to large amounts of triphenylphosphine oxide being present; the majority of which was removed by filtration prior to flash chromatography.



**Scheme 12** Synthesis of alkynyl sulfonamides.

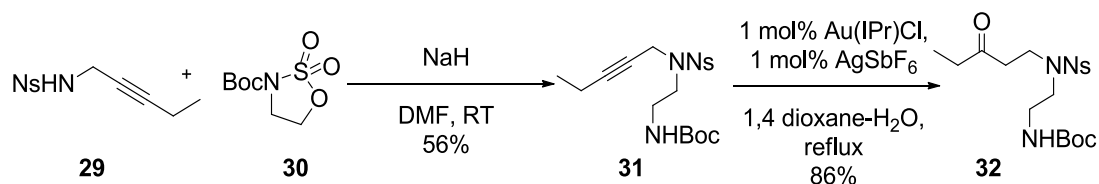
### 3.3.2 Connection of Building Blocks

Cyclic sulfamidate ring opening of **30** with pentynyl sulfonamide **29** under basic conditions gave the sulfonamide **31**. Gold-mediated alkyne hydration<sup>65-68</sup> of sulfonamide **31**, performed over 3 hr in a sealed tube at  $120\text{ }^\circ\text{C}$ , gave the ketone **32** regioselectively.<sup>44,69-71</sup> Larger scale alkyne hydration (1 g scale) proved difficult to drive to completion due to the small size of reaction tubes available. One solution was to complete the reaction at reflux, using a longer reaction time (overnight) to compensate for the lower reaction temperature ( $100\text{ }^\circ\text{C}$ ). This proved possible and the reaction was completed on a 6 g scale, where yield of the ketone **32** also improved from 56% to 86% (Scheme 13).

The cyclic sulfamidate ring opening reaction was repeated using a range of other sulfamidates and sulfonamides, followed by gold-mediated hydroamination<sup>72-76</sup> to give the desired tetrahydropyrazine. Sulfonamide **100** was produced on a 4 g scale, followed by cyclisation to produce **101** (Table 16, Entry 1). The methyl-substituted sulfonamide **102** was produced as a presumed single enantiomer, with inversion of configuration at

<sup>iv</sup> DIAD was initially used in place of DEAD however this caused issues in purification.

the stereogenic centre. The sulfonamide **102** then reacted in a gold-mediated hydroamination reaction to give the tetrahydropyrazine **103** on a 2 g scale (Table 16, Entry 2). The same ring opening reaction using an acetate-substituted cyclic sulfamidate produced sulfonamide **104**, which upon hydroamination yielded the tetrahydropyrazine **105** on a 2 g scale (Table 16, Entry 3).



**Scheme 13** Synthesis of ketone **32**.

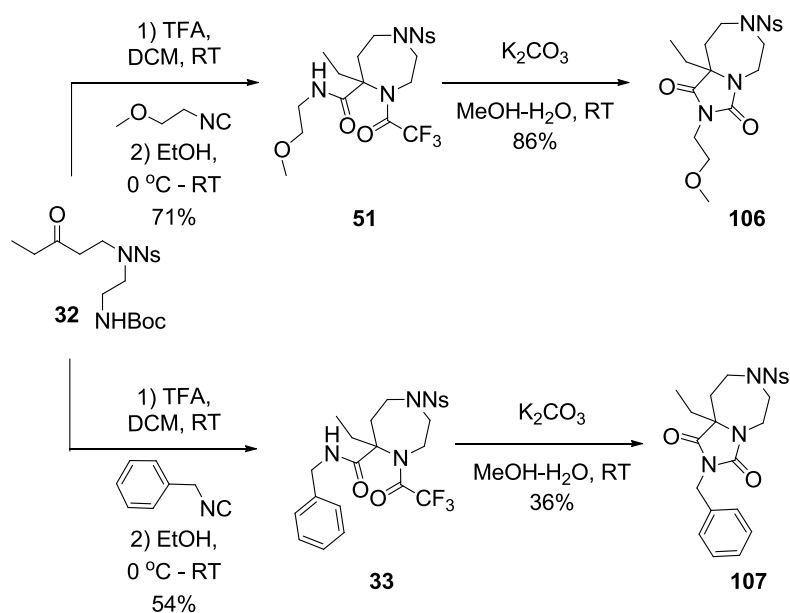
Entry	Sulfonamide	Cyclic Sulfamidate	Product <sup>a</sup>	Yield / %	Product <sup>b</sup>	Yield / %
1				61		62
2				49		95
3				58		73

**Table 16** Yields of products from the cyclic sulfamidate ring opening reaction and the following gold-mediated hydroamination reaction; a) Conditions: NaH, DMF, RT; b) Conditions: 5 mol% Au(PPh<sub>3</sub>)Cl, 5 mol% AgSbF<sub>6</sub>, 1,4-dioxane, 100 °C.

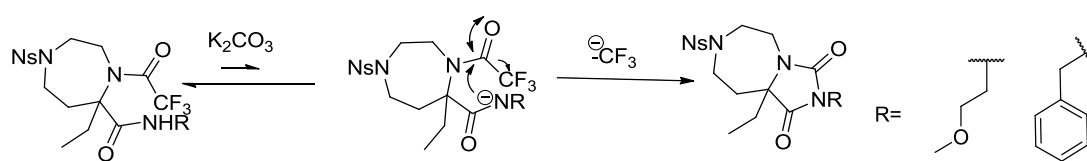
### 3.3.3 Synthesis of Scaffolds

The two novel scaffolds **51** and **33** were generated using the Ugi reaction from the ketone **32** and two different isocyanides, proceeding via an iminium intermediate. Scaffold **51** was formed on a 600 mg scale and scaffold **33** was formed on a 1 g scale (Scheme 14). Attempts were made to remove the trifluoroacetamide group via base

hydrolysis, using NaOH as well as K<sub>2</sub>CO<sub>3</sub> in H<sub>2</sub>O–MeOH (30:70). Fluorine NMR showed disappearance of fluorine atoms, and a slight shift in proton NMR could be observed. However, it was not possible to assign one additional peak in the carbon NMR at 156 ppm, and a mass peak of 26 greater than the product mass. This was the case for both intermediates. Upon further investigation it was identified that the reaction formed hydantoin **106** and **107** via an addition-elimination mechanism from the nucleophilic amide nitrogen, with the <sup>-</sup>CF<sub>3</sub> anion as the leaving group. This structure was confirmed by both HRMS and carbon NMR. The proposed mechanism for the formation of the hydantoin structure<sup>77</sup> can be seen in Scheme 15.



**Scheme 14** Synthesis of hydantoin **106** and **107**.



**Scheme 15** Mechanism for the formation of the hydantoin structure.

The structures of the hydantoin **106** and **107** were assigned on the basis of their IR and HMBC spectra. The characteristic amide C=O peaks for hydantoin structures<sup>78</sup> around 1780 cm<sup>-1</sup> and 1720 cm<sup>-1</sup> were present in both IR spectra and the structure was also verified by HMBC, where correlations were seen between the carbonyl carbon previously belonging to the trifluoroacetamide group, and nearby protons (Figure 33).

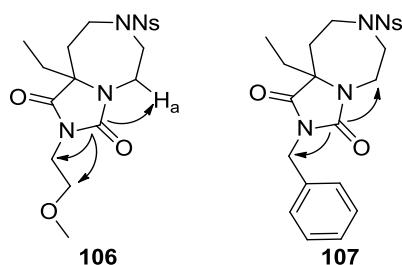
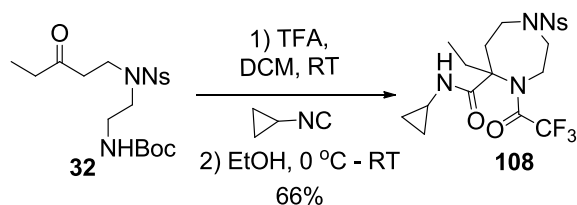


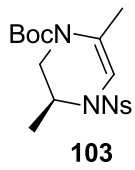
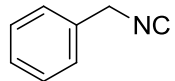
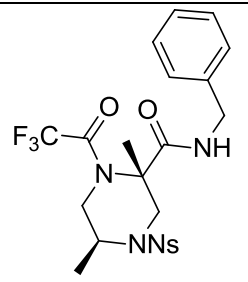
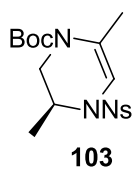
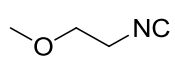
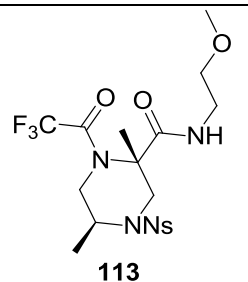
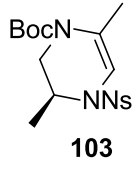
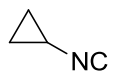
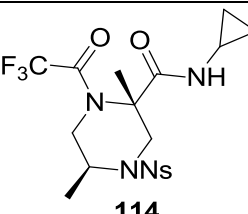
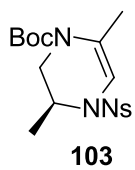
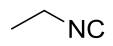
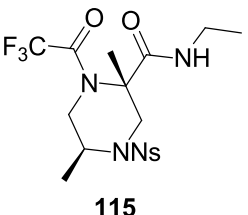
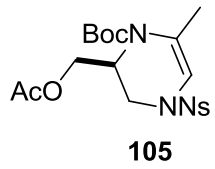
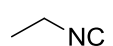
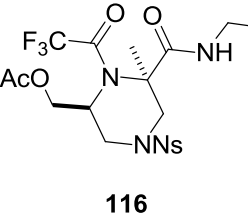
**Figure 33** HMBC correlations shown via arrows between the carbonyl carbon previously belonging to the trifluoroacetamide group, and nearby protons in hydantoin **106** and **107**.

Novel scaffold **108** synthesised using the Ugi reaction has been formed on a 1 g scale from ketone **32** (Scheme 16). The 6-membered ring hydroamination product **101** was also used in three Ugi reactions to give scaffold **109** (Table 17, Entry 1) on a 500 mg scale, and **110** (Table 17, Entry 2) and **111** (Table 17, Entry 3) on 1 g scales.



**Scheme 16** Synthesis of scaffold **108**.

Entry	Tetrahydropyrazine	Isocyanide	Product <sup>a</sup>	Yield / %
1	 <b>101</b>		 <b>109</b>	60
2	 <b>101</b>		 <b>110</b>	11
3	 <b>101</b>		 <b>111</b>	69

4	 <b>103</b>		 <b>112</b>	77
5	 <b>103</b>		 <b>113</b>	81
6	 <b>103</b>		 <b>114</b>	49
7	 <b>103</b>		 <b>115</b>	71
8	 <b>105</b>		 <b>116</b>	49

**Table 17** Yields of products from the Ugi reaction; a) Conditions: 1) TFA, DCM, RT, 2) isocyanide, EtOH, 0 °C - RT.

The piperazines **112-115** (Table 17, Entry 4-7) were synthesised diastereoselectively from tetrahydropyrazine **103** using three different isocyanides, on 200 mg - 1.5 g scales.<sup>79</sup> The tetrahydropyrazine **105** was treated with 18 equivalents of TFA- three times the amount of previous reactions to effect iminium formation- before undergoing the Ugi reaction with ethyl isocyanide to yield piperazine **116** on a 1 g scale (Table 17, Entry 8). In the case of the piperazine **116**, the relative configuration was determined by NOESY analysis (Figure 34); where an NOE was observed between the

methyl protons and the proton in the 6-membered ring attached to the same carbon as the methyl acetate substituent, they are indicated to be on the same face of the ring.

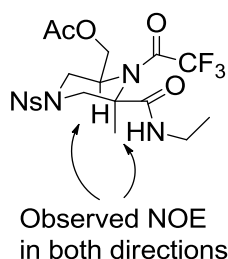


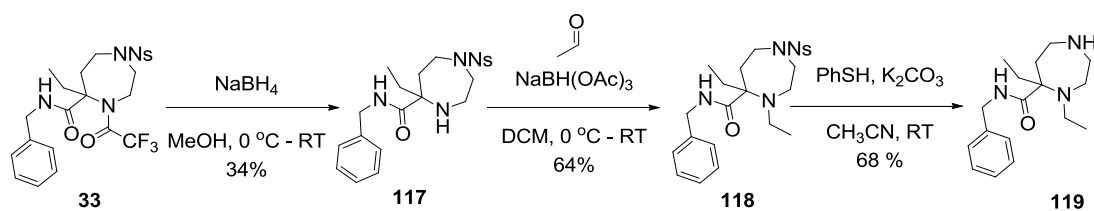
**Figure 34** Determination of configuration of scaffold **116**.

### 3.3.4 Synthesis of Fragments

#### 3.3.4.1 7-Membered ring fragments

##### 3.3.4.1.1 Benzylamide-substituted 7-membered rings

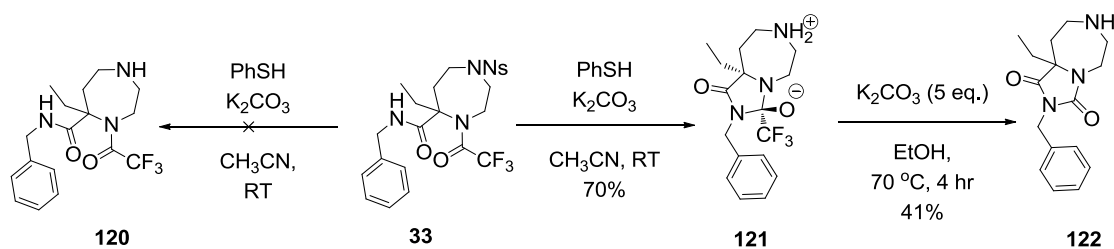
One method to prevent the formation of hydantoins **106** and **107** (Section 3.3.3) would be to change the trifluoroacetyl protecting group in scaffolds **51** and **33**. However, this is difficult to achieve due to the nature of the Ugi reaction. Instead, completing the reaction under reductive conditions using  $\text{NaBH}_4$  proved successful in the removal of the trifluoroacetamide group.<sup>80,81</sup> The deprotected diazepane **117** was next decorated on the secondary amine by reductive amination<sup>82</sup> using acetaldehyde to give the alkylated product **118** on a 300 mg scale. The alkylated intermediate **118** was deprotected to remove the sulfonyl group,<sup>83</sup> producing fragment **119** on a 1 g scale (Scheme 17).



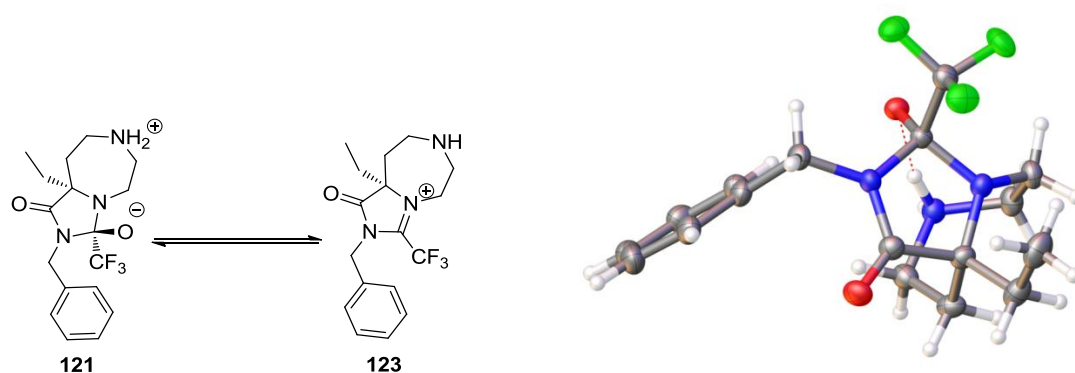
**Scheme 17** Synthesis of fragment **117**.

Sulfonyl deprotection on scaffold **33** was completed to produce a negligible amount of the desired intermediate **120** as well as a major side-product with a mass of  $[\text{M}-18]^+$ . X-ray crystallography enabled determination of the structure of the side-product as cyclic zwitterion **121**, which under conditions on the LCMS gave rise to the charged iminium species **123**, accounting for the  $[\text{M}-18]^+$  peak observed (Scheme 19). The formation of zwitterion **121** is promoted by the presence of a hydrogen bond between the oxy and ammonium ions stabilising the structure (Figure 35). **121** was subjected to

excess base which gave the expected hydantoin **122** (Scheme 18), suggesting it is an intermediate in the hydantoin formation reaction.<sup>84</sup>



**Scheme 18** Synthesis of hydantoin **122** via zwitterion **121** using sulfonyl deprotection conditions.

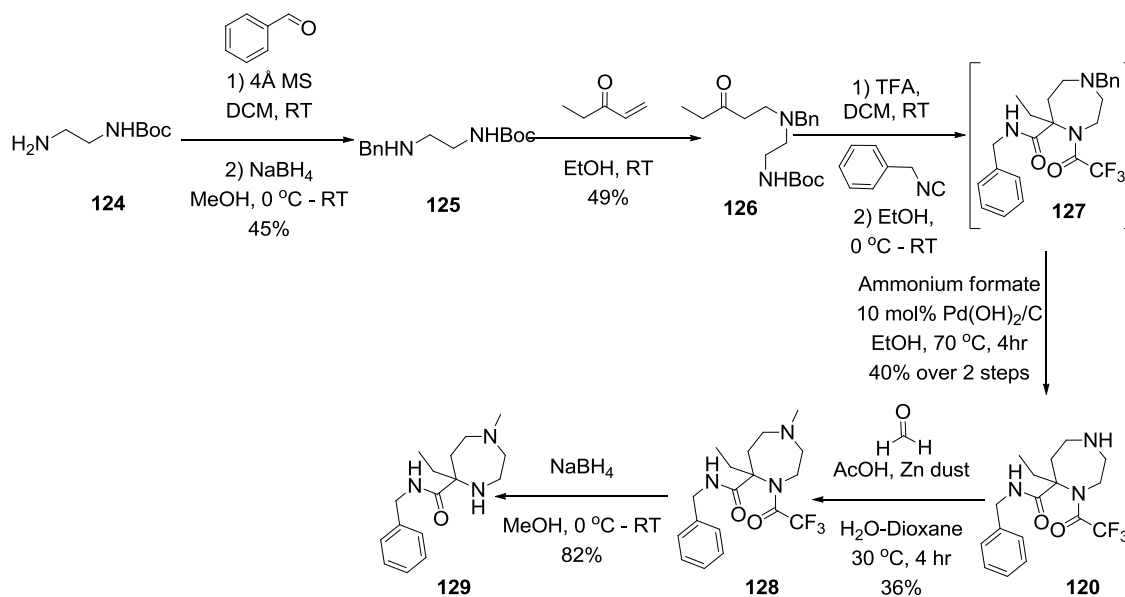


**Scheme 19** Formation of the  $[M-18]^+$  mass ion **123** from zwitterion **121**.

**Figure 35** X-ray crystal structure of zwitterion **121**.

An alternative route was used to remake scaffold **33** using a benzyl protecting group in place of the sulfonyl group. This route began with reductive amination of Boc-ethylene diamine in the presence of benzaldehyde, followed by reaction with ethyl vinyl ketone to produce ketone **126** which reacted in an Ugi cyclisation to produce scaffold **127** in three steps. Scaffold **127** was used as crude in a transfer hydrogenation reaction to give the de-benzylated intermediate **120** on a 500 mg scale. The following methylation of **120** using MeI regenerated the starting material.<sup>v</sup> The alternative reductive amination however was successful, giving fragment **129** on a 50 mg scale after the final trifluoroacetyl reduction (Scheme 20).

<sup>v</sup> Methylation of Boc-ethylene diamine using MeI was attempted to produce a building block where the methyl substituent can be used as a protecting group as well as being present in the final fragment. Unfortunately, the majority product isolated was dimethylated Boc-ethylene diamine. Methylation was reattempted using formaldehyde under reductive conditions in order to prevent dimethylation but this was unsuccessful.

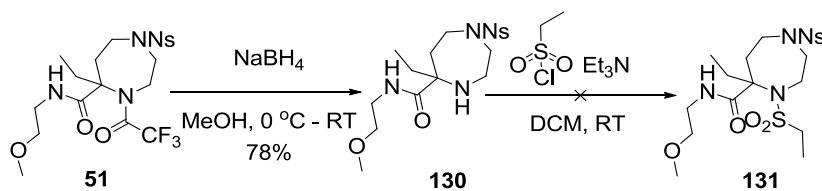


**Scheme 20** Synthesis of fragment **129**.

### 3.3.4.1.2 2-Methoxyethylamide-substituted 7-membered rings

The trifluoroacetyl group on scaffold **51** was removed by reduction to give the intermediate **130** on a 500 mg scale, which next required decoration. The conditions in Table 18 were attempted for the formation of the sulfonlated<sup>85</sup> diazepane **131** shown in Scheme 21. Sulfonation of intermediate **130** at the secondary amine under basic conditions either reproduced the starting material or caused decomposition of the reagents. The reaction was attempted with bases DIPEA and Et<sub>3</sub>N, at room temperature and at reflux in reaction solvents DCM, MeCN and DMF. A catalytic amount of DMAP was added in order to activate the sulfonyl chloride and the reaction was also attempted using benzylsulfonyl chloride in place of ethylsulfonyl chloride. This was in order to test the reaction viability, as aromatic sulfonyl chlorides are known to have higher reactivity than its alkyl counterparts. After heating at reflux overnight, the product peak could be observed, but decomposition occurred when the temperature was increased to 120 °C.

As a result, the sulfonation was repeated with 8 equivalents of ethylsulfonyl chloride at a lower temperature of 100 °C over two days in order to promote the reaction, using DIPEA as the reaction solvent, before later being heated in a microwave at 100 °C for 30 mins and later at 110 °C for 1 hr. In summary, a small amount of product could be detected when using benzylsulfonyl chloride in the reaction, but no product nor identifiable by-product could be detected when the reaction was attempted using ethylsulfonyl chloride. As a result, this reaction has been abandoned for an alternative fragment which was identified using a new PLP protocol (discussed in Section 3.1).



**Scheme 21** The attempted synthesis of intermediate **131**.<sup>86</sup>

Entry	Sulfonyl chloride (eq.)	Base (eq.)	Catalyst	Solvent	Temperature / °C	Time
1	Ethyl (1.5)	Et <sub>3</sub> N (2)		DCM	25	overnight
2	Ethyl (1.5)	DIPEA (2)		DCM	25	overnight
3	Ethyl (3)	DIPEA (4)		DCM	40 (reflux)	overnight
4	Ethyl (1.5)	DIPEA (2)	DMAP	MeCN	80 (reflux)	overnight
5	Benzyl (1.5)	DIPEA (2)	DMAP	MeCN	80 (reflux)	overnight
6	Benzyl (1.5)	DIPEA (2)	DMAP	DMF	120	overnight
7	Ethyl (8)	DIPEA (10)	DMAP		100	2 days
8	Ethyl (8)	DIPEA (10)	DMAP		100 (μW)	30 mins
9	Ethyl (8)	DIPEA (10)	DMAP		110 (μW)	1 hr

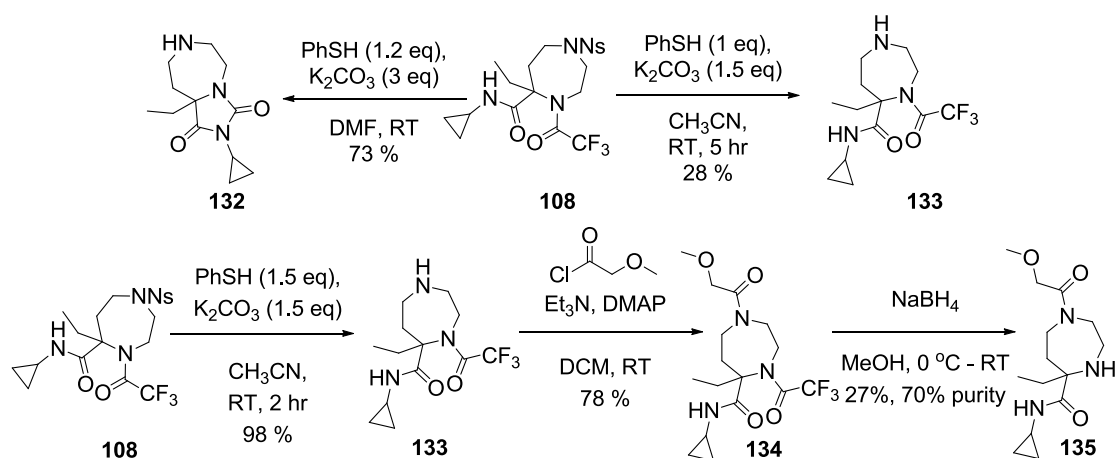
**Table 18** Conditions attempted for the synthesis of intermediate **131**.

### 3.3.4.1.3 Cyclopropylamide-substituted 7-membered rings

Whilst attempting to remove the sulfonyl group on scaffold **108**, it was found that the product was water soluble; therefore, changing the solvent from DMF to MeCN allowed ease of solvent removal due to the much lower boiling point of MeCN, without compromising on solvent polarity. An unwanted hydantoin formed as the major product in the presence of base; in order to overcome this, the amount of base was reduced, and also added only after the addition of PhSH, allowing the -SPh anion to act as a buffer in the reaction solution. Reagent amounts were changed from 1.2 equivalents of PhSH with 3 equivalents of K<sub>2</sub>CO<sub>3</sub> to 1 equivalent of PhSH with 1.5 equivalents of K<sub>2</sub>CO<sub>3</sub>. The reaction was carefully monitored and stopped after 5 hours with no formation of hydantoin observed, although the unwanted cyclic zwitterion, analogous to **121** (Section 3.3.4.1.1) was present. The reaction is found to complete faster (2 hr instead of 5 hr) by increasing PhSH from 1 equivalent to 1.5 equivalents and the yield improved drastically (by 70%) by changing the purification method from flash chromatography to basic SCX.

The following acylation<sup>87</sup> of **133** using methoxyacetyl chloride yielded intermediate **134** which was reduced to give the crude fragment **135** on a 2 g scale (Scheme 22). Unfortunately, attempted purification of **135** using basic SCX cartridge,

flash chromatography as well as preparative HPLC failed to produce the pure compound, which decomposed under high temperature NMR. Nevertheless, it is possible to use fragment **135** in a biological screen at its known purity of 70%.



**Scheme 22** Synthesis of fragment **135**.

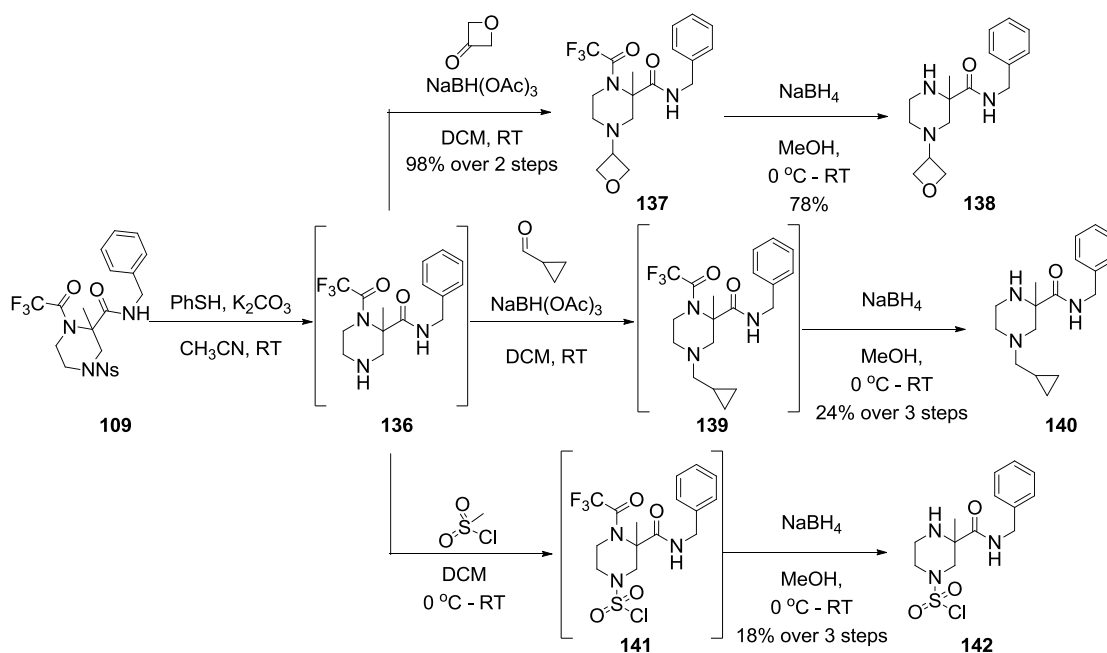
### 3.3.4.2 6-Membered ring fragments

#### 3.3.4.2.1 Benzylamide-substituted 6-membered rings

The sulfonyl deprotection product of scaffold **109** was difficult to purify using basic SCX, flash chromatography or preparative HPLC due to the desired product **136** decomposing into the undesired zwitterion, analogous to **121** (Section 3.3.4.1.1). Intermediate **136** was therefore used as crude in an alkylation reaction with 2-bromooxetane in order to form the desired product **137**.<sup>vi</sup> The alkylation of intermediate **136** was completed using oxetan-3-one, under reductive amination conditions, and the following trifluoroacetyl deprotection worked in good yield, giving **138** on a 500 mg scale (Scheme 23).

The same piperazine **136** was used as crude for the reductive amination reaction using cyclopropyl carboxaldehyde to give **139**, but a mixture of two inseparable products with the same mass was formed. As a result, **139** was used as crude for the final reduction step to produce fragment **140** on a 50 mg scale for which purification was completed by preparative HPLC. **136** was also used as crude in a sulfonylation reaction which was unable to reach completion due to lack of base used as a preventative measure to avoid hydantoin formation. Intermediate **141** was then used as crude and reduced to remove the trifluoroacetyl protecting group to yield **142** successfully on a 1.5 g scale (Scheme 23).

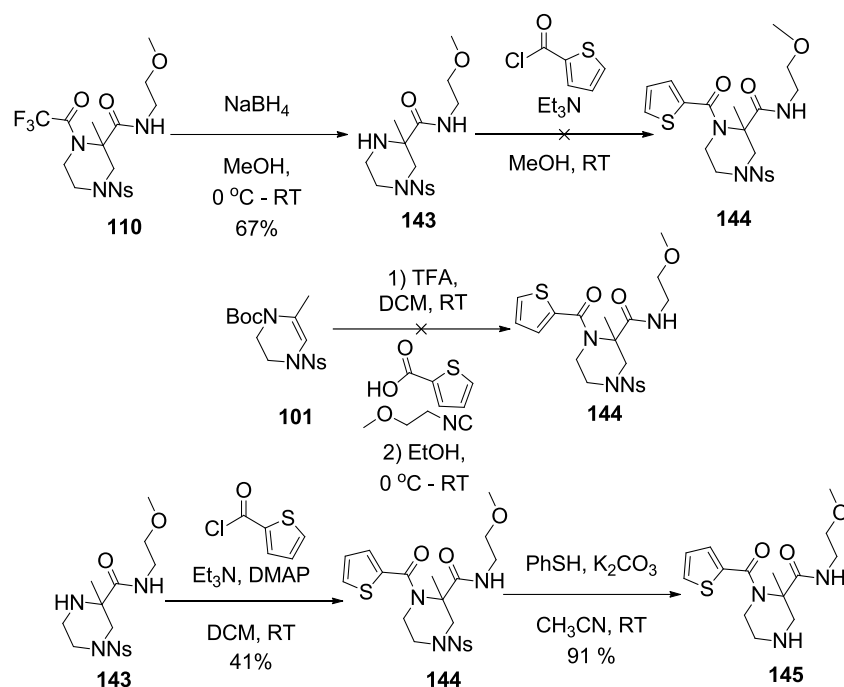
<sup>vi</sup> The reaction carried out with 1.5 eq. Cs<sub>2</sub>CO<sub>3</sub> whilst heating at 60 °C in DMF resulted in formation of the hydantoin. Additionally, no reaction occurred when this method was attempted without base, and by heating in ether at reflux.



**Scheme 23** Synthesis of fragments **138**, **140** and **142**.

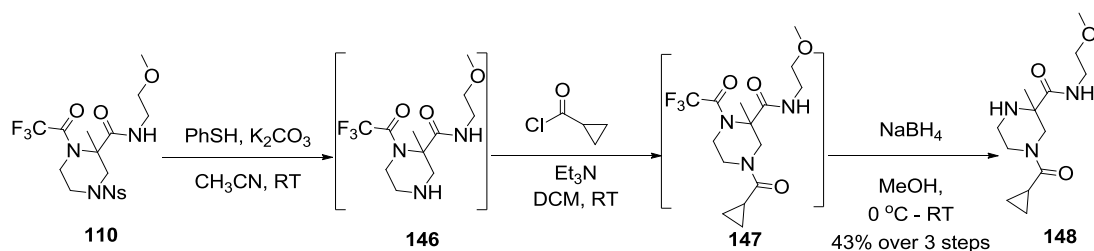
### 3.3.4.2.2 2-Methoxyethylamide-substituted 6-membered rings

Scaffold **110** was reduced to remove its trifluoroacetamide protecting group giving intermediate **143** on an 80 mg scale. The following acylation product was unable to be isolated by flash chromatography or preparative HPLC. An alternative synthesis was attempted in which 2-thiophene carboxylic acid was added in excess (2 eq.) to tetrahydropyrazine **101** in the Ugi reaction after formation of the imine intermediate. Unfortunately, the majority product formed was the original scaffold **110**. The sulfonylation was repeated using 2-thiophenecarbonyl chloride as before but changing the solvent from MeOH to DCM with a catalytic amount of DMAP. The reaction was successful and intermediate **144** was formed in good yield, before undergoing sulfonyl deprotection to produce the final fragment **145** (Scheme 24).



**Scheme 24** Synthesis of fragment **145**.

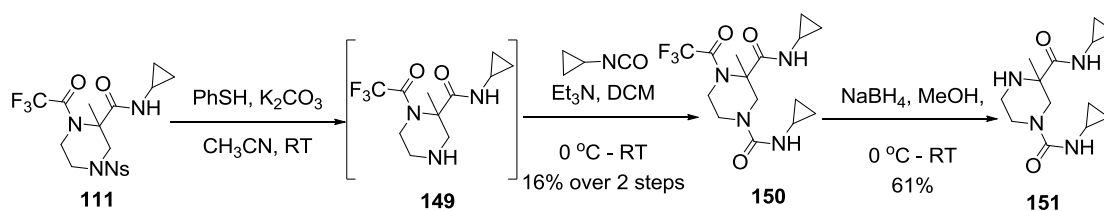
The sulfonyl deprotection product of scaffold **110** proved difficult to purify by basic SCX, flash chromatography or preparative HPLC. Intermediate **146** was used as crude for the following acylation reaction using cyclopropyl carbonyl chloride, and **147** was purified by preparative HPLC. Any rotameric forms which may have been present decomposed when subjected to high temperature NMR thus **147** was used as crude successfully for the final reduction to produce fragment **148** (Scheme 25).



**Scheme 25** Synthesis of fragment **148**.

### 3.3.4.2.3 Cyclopropylamide-substituted 6-membered rings

The sulfonyl deprotection product of scaffold **111** was used as crude in a urea formation reaction with cyclopropyl isocyanate<sup>88</sup> to produce intermediate **150**. The final reduction to remove the trifluoroacetyl protecting group was completed to yield **151** on a 300 mg scale (Scheme 26).

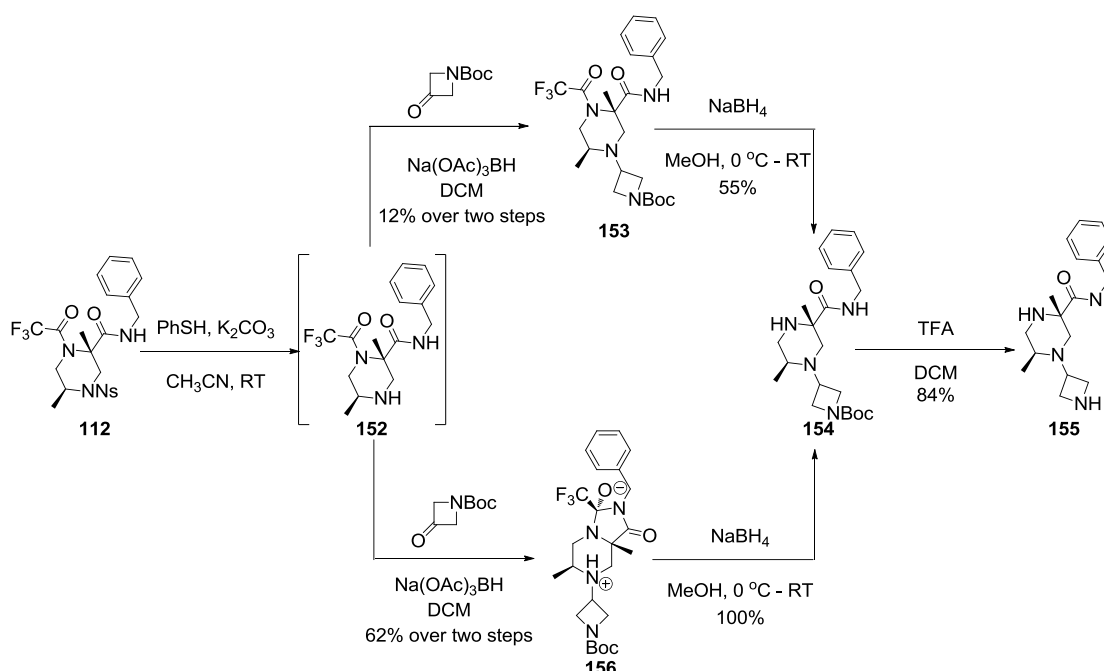


**Scheme 26** Synthesis of fragment **151**.

### 3.3.4.3 Enantiomerically-enriched fragments

#### 3.3.4.3.1 Benzylamide-substituted 6-membered rings

Sulfonyl deprotection of the dimethyl-substituted piperazine scaffold **112** on a 1 g scale produced a mixture of the trifluoroacetamide as well as the cyclised zwitterion. The two products were able to be separated after the following reductive amination reaction with Boc-azetidinone to give **153** and the cyclised zwitterion **156**. Interestingly, both **153** and **156** formed the same desired product after reduction of the trifluoroacetyl protecting group. A final Boc-deprotection of intermediate **154** produced the desired fragment **155** (Scheme 27).

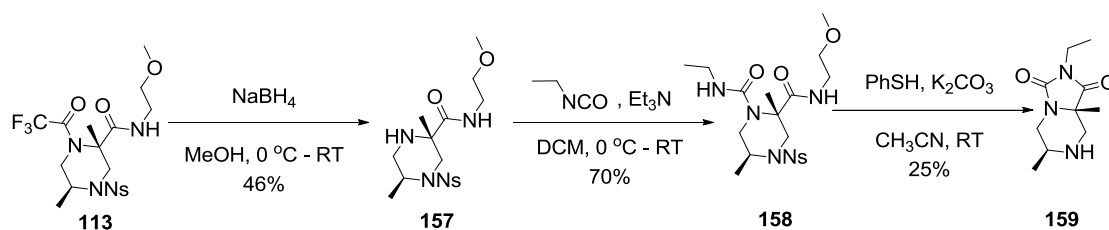


**Scheme 27** Synthesis of fragment **155**.

#### 3.3.4.3.2 2-Methoxyethylamide-substituted 6-membered rings

Reduction was completed on scaffold **113** in order to remove the trifluoroacetyl protecting group and the following urea formation was successful, producing **158** on a 300 mg scale. However, although the final sulfonyl deprotection showed the product formation, **158** was unstable to cyclisation and only the undesired hydantoin **159** could

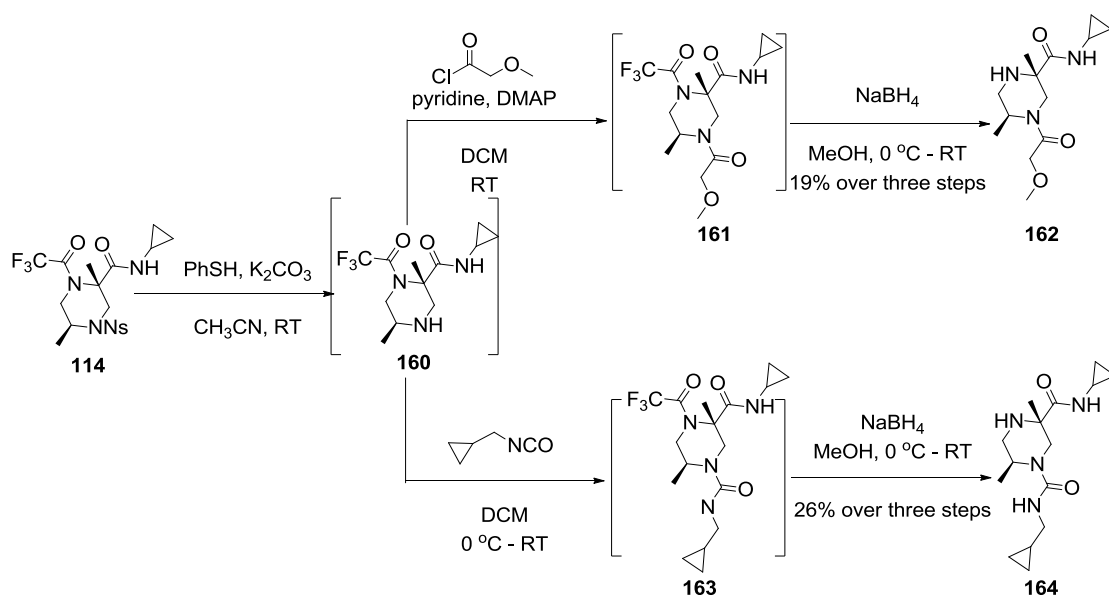
be isolated (Scheme 28). Since the direct cyclisation with amides has been preceded for isocyanates, this compound was abandoned for an alternative in the newly generated library (discussed in Section 3.2).



**Scheme 28** Synthesis of hydantoin **159**.

### 3.3.4.3.3 Cyclopropylamide-substituted 6-membered rings

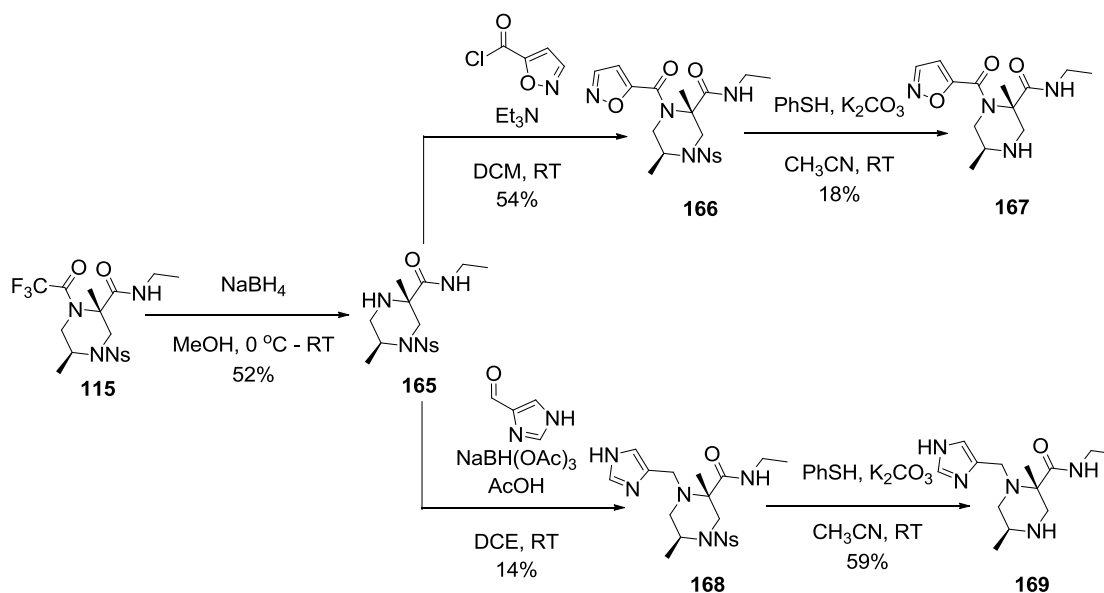
Sulfonyl deprotection was performed on the dimethyl-substituted piperazine scaffold **114** on an 800 mg scale and the following decorated intermediates were used as crude for the final reduction reactions to produce fragments **162** and **164** (Scheme 29).



**Scheme 29** Synthesis of fragments **162** and **164**.

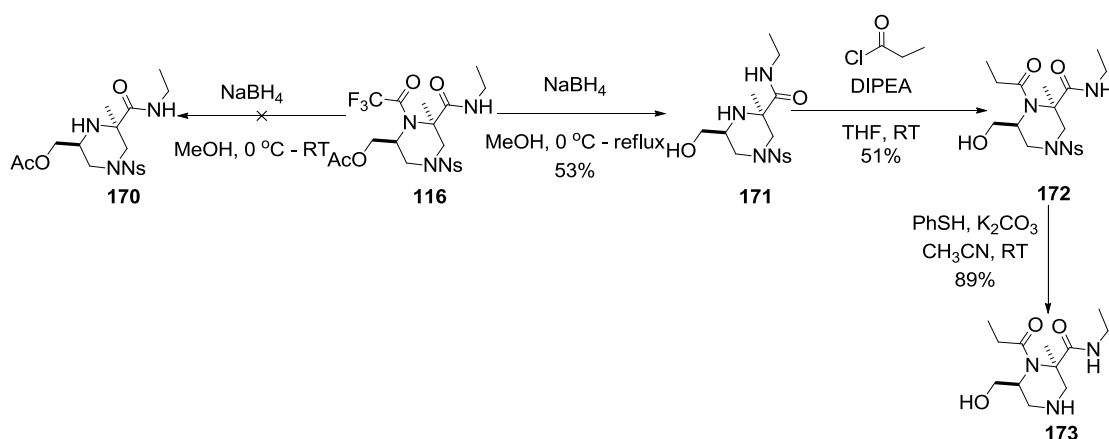
### 3.3.4.3.4 Ethylamide-substituted 6-membered rings

Reduction was completed on scaffold **115** in order to remove the trifluoroacetyl protecting group, and the following acylation with isoxazole-5-carbonyl chloride was successful to produce intermediate **166**. The final sulfonyl deprotection step yielded fragment **167** on a 200 mg scale. Intermediate **165** was also reacted with 4-imidazolecarboxaldehyde in order to produce **168**, which gave fragment **169** on a 100 mg scale upon deprotection (Scheme 30).



**Scheme 30** Synthesis of fragments **167** and **169**.

Unfortunately, the trifluoroacetyl group on scaffold **116** could not be removed by reaction with a large excess of  $\text{NaBH}_4$  at room temperature, possibly due to the hindered nature of the nitrogen centre. Thus, this reaction was heated to reflux overnight in MeOH where the acetate group was observed to undergo reduction followed by removal of the trifluoroacetyl group to produce **171**. This reduces the number of deprotection steps to the final fragment with no selectivity issues in the following acylation using propionyl chloride, as no increase in shift of the alkyl protons neighbouring the hydroxyl group was observed upon acylation. The final sulfonyl deprotection yielded fragment **173** on a 300 mg scale (Scheme 31).



**Scheme 31** Synthesis of fragment **173**.

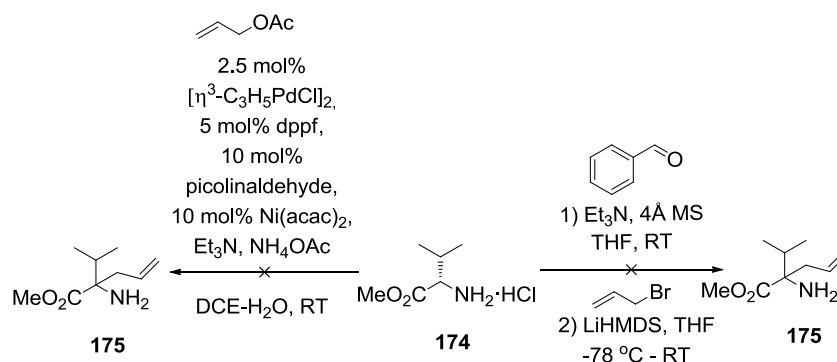
## 3.4 Synthesis of Fragments Using Amino Acid Chemistry

### 3.4.1 Synthesis of Building Blocks

#### 3.4.1.1 Identification of a suitable method

Formation of the amino ester **175** was attempted using a palladium- and nickel-catalysed allylation of valine methyl ester hydrochloride in the presence of allyl acetate.<sup>89</sup> The desired product was isolated as crude; however, attempted purification by basic SCX cartridge caused the product to decompose. The reaction was repeated in the hope of using the material as crude but unfortunately product formation was inconsistent. The procedure was attempted once more using anhydrous DCE for the formation of the palladium complex and each reagent was added in quick succession; however, no material was isolatable.

The synthesis of amino ester **175** was re-attempted using an alternative route, which began with imine formation before LiHMDS was used to deprotonate the acidic  $\alpha$ -proton. The anion intermediate was quenched with allyl bromide and finally the imine functionality was hydrolysed using a citric acid work-up. However, it appeared that any product which may have formed was unstable and only a small amount of non-allylated imine intermediate could be isolated. The reaction was repeated with 3 equivalents of LiHMDS instead of 1.5 but again minimal product formation was observed (Scheme 32).

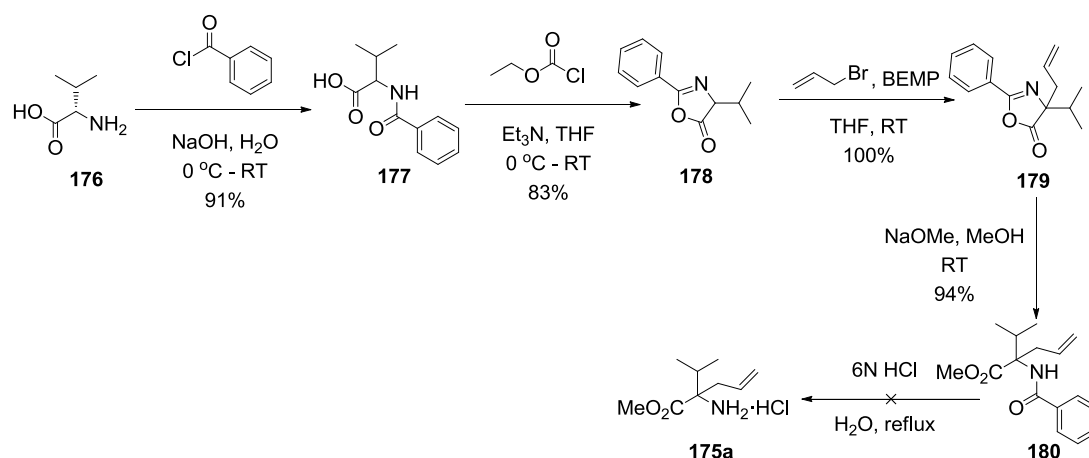


**Scheme 32** Attempted synthesis of amino ester **175**.

The synthesis of amino ester **175** was next attempted via formation of the azalactone intermediate **178**.<sup>90</sup> This route began with benzoyl protection of valine followed by cyclisation in the presence of ethyl chloroformate to produce azalactone **178**. Allylation to produce intermediate **179** proceeded with ease in the presence of BEMP<sup>vii</sup> due to the increased reactivity of the  $\alpha$ -carbon, before the azalactone ring is opened to

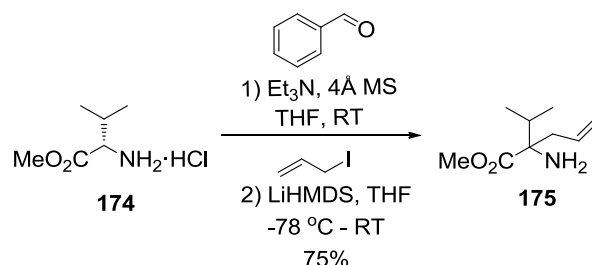
<sup>vii</sup> BEMP is the abbreviated name for the phosphazene base 2-*tert*-butylimino-2-diethylamino-1,3-dimethyl-perhydro-1,3,2-diazaphosphorine.

give the allylated amino ester **180** formed on a 5 g scale. Unfortunately, reflux in HCl over two days in an attempt to remove the benzoyl protecting group yielded an undesired benzoyl derivative as well as a side product with loss of the methoxy group (Scheme 33).



**Scheme 33** Attempted synthesis of amino ester **175a**.

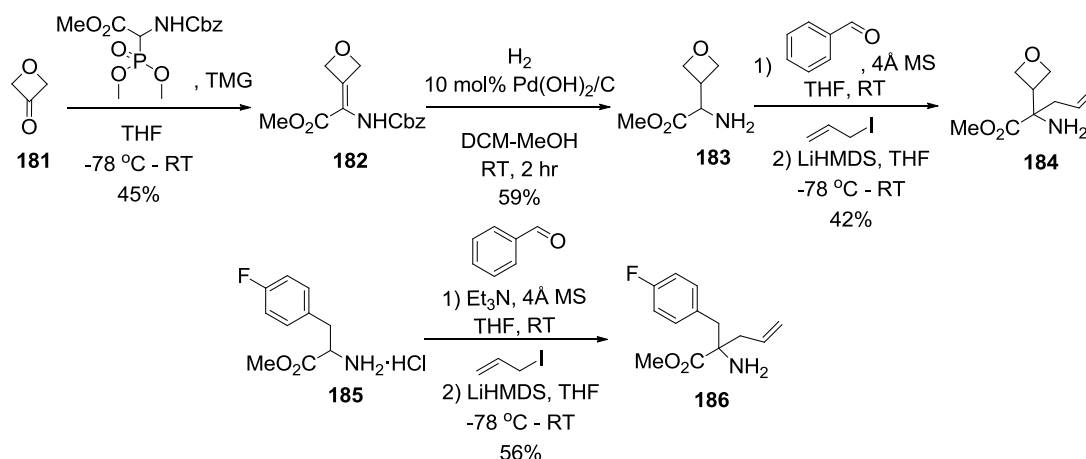
The formation of building block **175** via an imine intermediate was re-attempted using allyl iodide instead of allyl bromide in order to explore electrophiles with increased reactivity. The desired amino ester **175** was isolated successfully on a 500 mg scale, which was used directly after aqueous workup (Scheme 34).



**Scheme 34** Synthesis of amino ester **175**.

### 3.4.1.2 Alkylation of amino esters

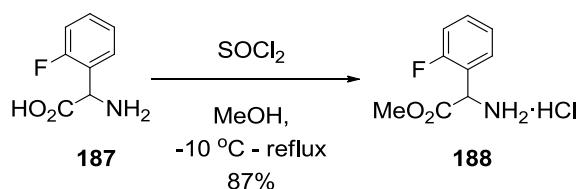
Alkylation of amino esters **183** and **185** gave **184** and **186** on 2 g and 500 mg scales respectively (Scheme 35). The formation of amino ester **183** began with commercially available 3-oxetanone, which reacted with *Z*-phosphonoglycine trimethyl ester to yield an alkenic intermediate **182**. **182** produced the desired amino ester **183** upon hydrogenation of the alkene functionality and removal of the Cbz protecting group.<sup>91</sup>



**Scheme 35** Synthesis of amino esters.

### 3.4.1.3 Amino ester formation

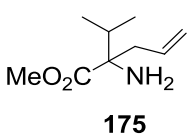
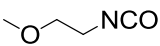
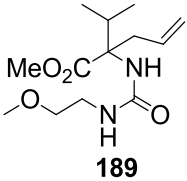
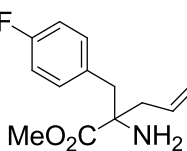
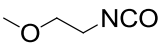
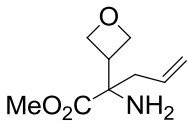
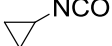
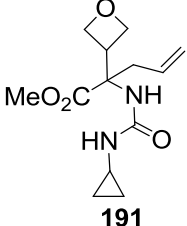
Methylation of amino acid **187** produced methyl ester **188** on a 1 g scale (Scheme 36).<sup>92</sup>



**Scheme 36** Synthesis of amino ester **188**.

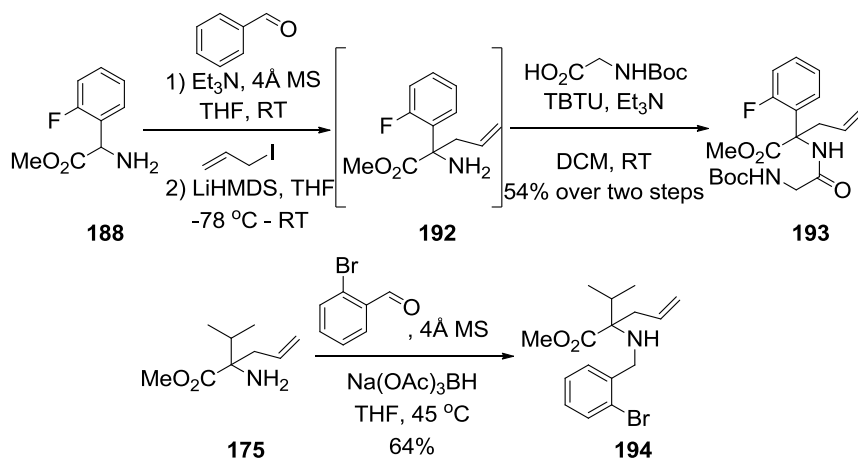
### 3.4.2 Connection of Building Blocks

Ureas<sup>93</sup> were synthesised via the reaction of a range of amino esters and isocyanates in the presence of base. The ureas **189** and **190** were synthesised by reaction with methoxyethyl isocyanate (Table 19, Entries 1 and 2, respectively) and urea **191** was synthesised by reaction with cyclopropyl isocyanate (Table 19, Entry 3).

Entry	Amino Ester	Isocyanate	Product <sup>a</sup>	Yield / %
1	 <b>175</b>		 <b>189</b>	58
2	 <b>186</b>		 <b>190</b>	52
3	 <b>184</b>		 <b>191</b>	40

**Table 19** Yields of products from the urea formation reaction; a) Conditions: Et<sub>3</sub>N, DCM, 0°C - RT.

Allylation of amino ester **188** produced intermediate **192** which was used as crude in the formation of amide **193** via a TBTU- catalysed coupling reaction<sup>94,95</sup> on a 500 mg scale. Reductive amination of amino ester **175** with 2-bromobenzaldehyde produced the desired intermediate **194** on a 1 g scale (Scheme 37).



**Scheme 37** Synthesis of intermediates **193** and **194**.

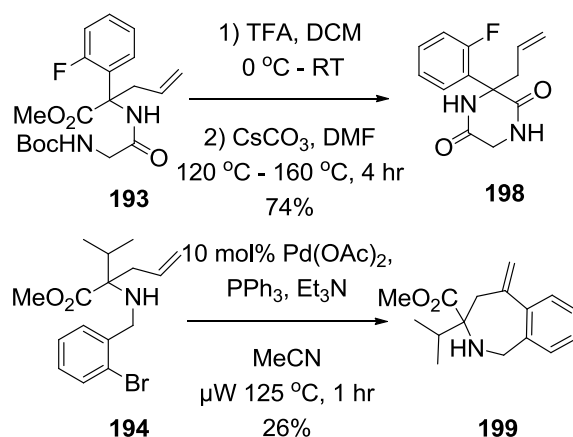
### 3.4.3 Synthesis of Scaffolds

Hydantoins **195-197** (Table 20, Entry 1-3) were synthesised from the intramolecular cyclisation of ureas in the presence of base.

Entry	Urea	Product <sup>a</sup>	Yield / %
1	 <b>189</b>	 <b>195</b>	67
2	 <b>190</b>	 <b>196</b>	80
3	 <b>191</b>	 <b>197</b>	92

**Table 20** Yields of products from the hydantoin formation reaction; a) Conditions: NaO<sup>t</sup>Bu, toluene, 100 °C.

Boc-deprotection<sup>96</sup> of **193** revealed a free amine which was able to undergo intramolecular base-mediated cyclisation with the ester functionality present, producing diketopiperazine scaffold **198** on a 500 mg scale. An intramolecular Heck reaction<sup>97</sup> of alkene **194** under microwave conditions produced benzazepine scaffold **199** in moderate yield, on a 1 g scale (Scheme 38).

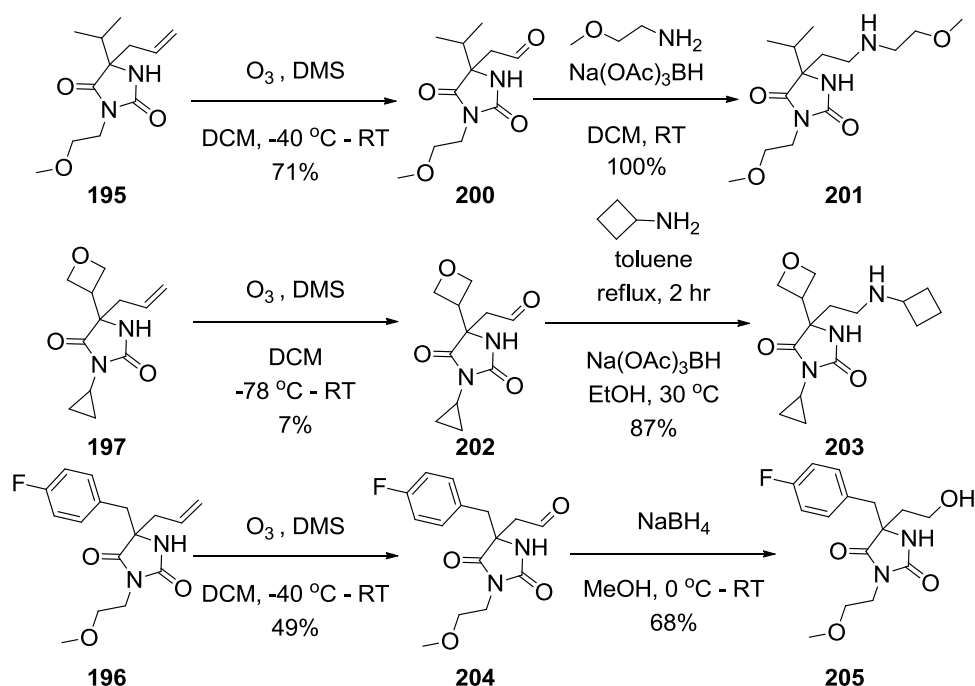


**Scheme 38** Synthesis of scaffolds **198** and **199**.

### 3.4.4 Synthesis of Fragments

#### 3.4.4.1 Hydantoin

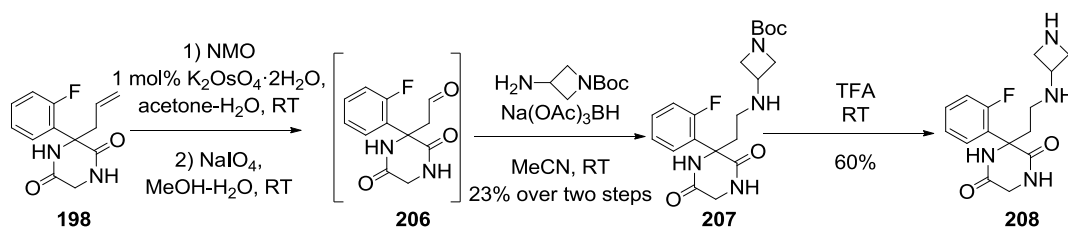
The synthesis of fragments **201** and **203** proceeded via the ozonolysis<sup>98</sup> of scaffolds **195** and **197** to produce corresponding aldehydes, which later reacted in reductive aminations with alternate amines to produce fragments **201** and **203**, on 50 mg scales. The ozonolysis of scaffold **196** followed by reduction of the aldehyde intermediate produced fragment **205** on a 50 mg scale (Scheme 39).



**Scheme 39** Synthesis of hydantoin fragments.

#### 3.4.4.2 Diketopiperazine

The alkene **198** was subjected to ozonolysis on a 100 mg scale; however the starting material was regenerated. Alternatively, dihydroxylation followed by oxidative cleavage<sup>99</sup> of **198** was difficult to monitor and the next reductive amination step with 1-Boc-3-(amino)azetidines was carried out on the crude intermediate to give **207**. The final Boc-deprotection reached completion when TFA was used as the reaction solvent to produce fragment **208** (Scheme 40).



Scheme 40 Synthesis of fragment **208**.

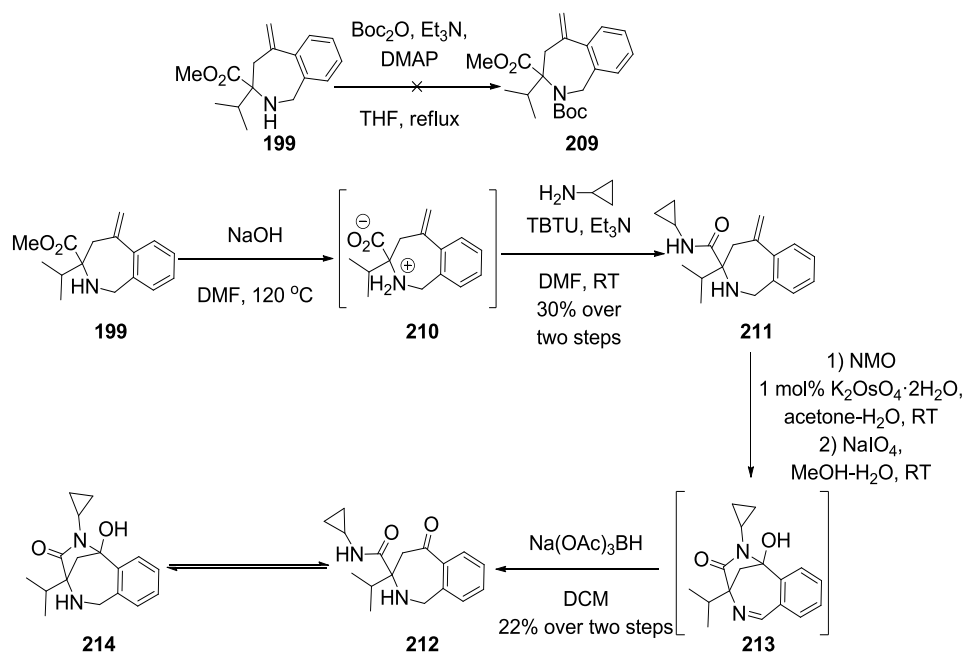
#### 3.4.4.3 Tetrahydrobenzazepine

Boc-protection was attempted on the tetrahydrobenzazepine scaffold **199** in order to produce an acid chloride intermediate for amide formation. Unfortunately, no reaction was observed when using a stoichiometric amount of DMAP alongside Et<sub>3</sub>N, and by heating the solution at reflux in THF. Scaffold **199** was next hydrolysed on a 100 mg scale in order to attempt a classical amide coupling route where it was found that heating the reaction was necessary due to the hindered nature of the ester. Only a small amount of acid **210** formed after heating the reaction mixture at reflux in MeOH; however, heating the reaction mixture at 120 °C in DMF resulted in reaction completion.

Removal of excess NaOH was difficult due to the zwitterionic nature of **210** and it was therefore carried forward to the next reaction. The following amide coupling reaction was completed using a large excess of cyclopropylamine and by adding TBTU last to the reaction mixture in order to prevent polymerisation. Purification using basic SCX was unsuccessful but the amide **211** was able to be isolated using aqueous workup followed by flash chromatography. The final oxidation step to produce ketone **212** was attempted using ozonolysis on a 30 mg scale, unfortunately no significant product formation was observed along with a mixture of side-products.

An osmium-mediated dihydroxylation and oxidative cleavage was attempted on alkene **211**. The mass of the dihydroxylated intermediate was observed, however the major isolated product after oxidative cleavage appeared to be the non-preventable over-oxidised imine product **213** containing a cyclised hemiaminal. Imine **213** was later reduced in the hope that the product conformation would be preferential for the ketone

**212** over the hemiaminal **214**, but unfortunately a mixture of the two could still be observed despite disappearance of the double bond (Scheme 41).



**Scheme 41** Synthesis of fragment **212**.

## 3.5 Synthesis of Fragments Using the Mitsunobu Reaction as a Key Step

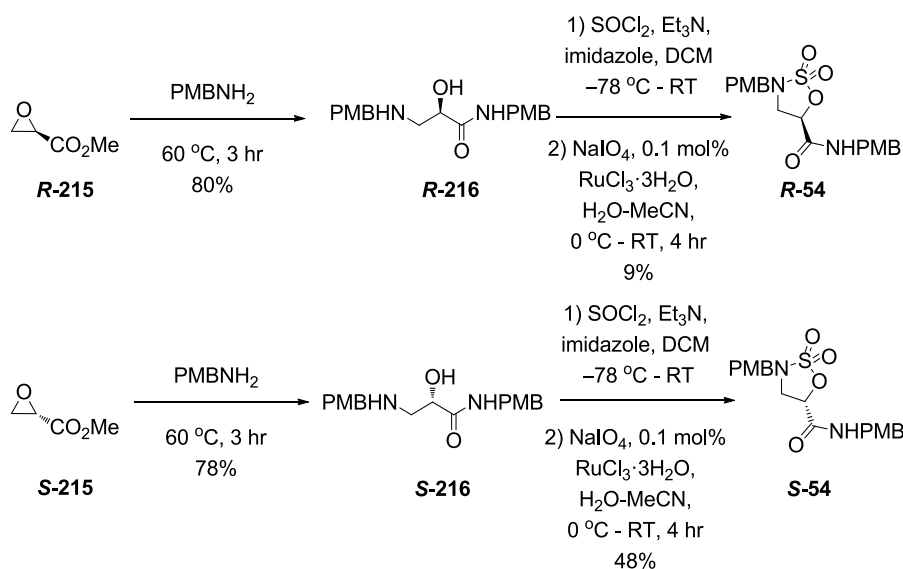
### 3.5.1 Synthesis of Building Blocks

#### 3.5.1.1 Cyclic Sulfamidates

Formation of cyclic sulfamidates **R-54** and **S-54** began with ring opening of corresponding epoxides<sup>100</sup> followed by cyclic sulfamidate ring formation to give the desired products on 5 g scales. The cyclic sulfamidate ring formation from amide **R-216** proceeded via a sulfamidite intermediate; it was noted that although the intermediate formed fully, the following oxidation step was low-yielding, possibly due to the PMB protecting group being susceptible to undesired oxidation. No oxidation was observed after 6 hours and starting material **R-216** was regained overnight along with a mixture of side-products. The oxidation step to form sulfamidate **R-54** was repeated by reducing the amount of  $\text{NaIO}_4$  used from 2 equivalents to 1 in order to prevent over-oxidation. The reaction reached completion after three days with no improvement in yield.

During the formation of cyclic sulfamidate **S-54**, oxidation of the sulfamidite intermediate produced a mixture of side-products after 4 hours with consumption of starting material **S-216**. The synthesis was reattempted using new  $\text{NaIO}_4$  as well as ruthenium catalyst and yield improved from 8 to 19%. It was found that when remaking

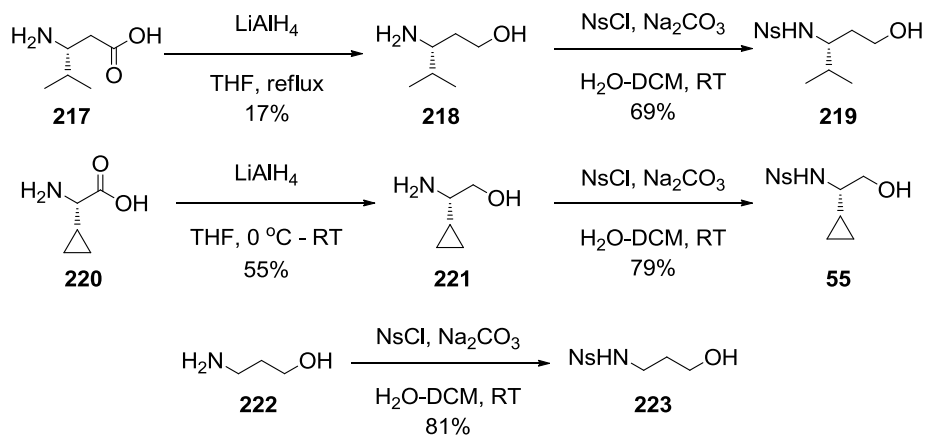
the cyclic sulfamidate building block, using 4 equivalents of periodate instead of 2 in fact consumed the starting material in just three hours with only the desired product formed and none of the over-oxidised side-product. This led to the conclusion that the cyclic sulfamidate must be the kinetic product whilst the over-oxidised side-product is thermodynamically favourable. Pleasingly, the yield of **S-54** more than doubled to 48% (Scheme 42).



**Scheme 42** Synthesis of cyclic sulfamidates.

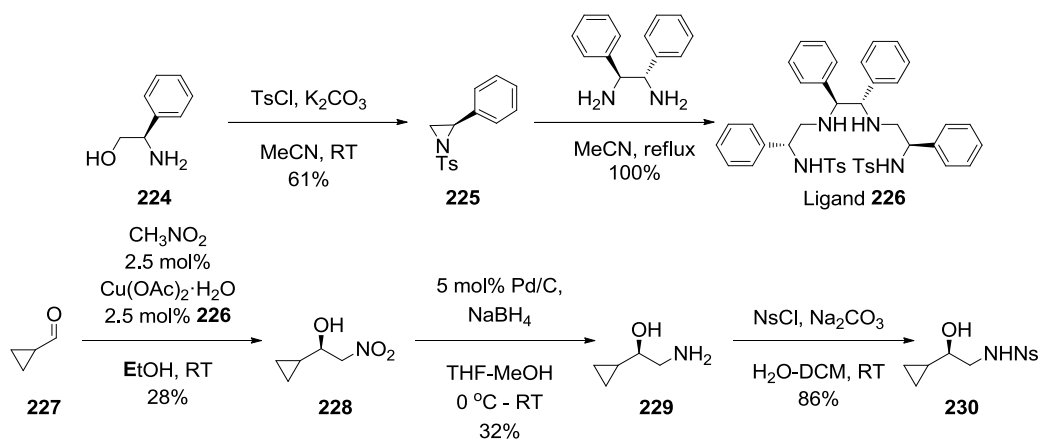
### 3.5.1.2 Amino alcohols

The enantiomerically-enriched amino alcohols **218** and **221** were synthesised by reduction of their acid precursors **217** and **220** in the presence of  $\text{LiAlH}_4$ ,<sup>101,102</sup> and later sulfonyl protection yielded amino alcohols **219** and **55** on 3 g and 500 mg scales, respectively. The commercially available 3-amino-1-propanol was also protected to yield amino alcohol **223** on a 500 mg scale (Scheme 43).



**Scheme 43** Synthesis of amino alcohols.

Amino alcohol **229** was synthesised via a nitro intermediate, with the aid of the chiral ligand **226**. Protection of (*R*)-2-phenylglycinol followed by opening of the aziridine ring with diphenylethylenediamine produced ligand **226** on a 1 g scale. **226** was used to aid a copper-catalysed reaction of cyclopropyl carboxaldehyde with nitromethane to yield nitro intermediate **228**. Reduction of **228** produced the desired amine **229** which was later protected to yield building block **230** on a 1 g scale (Scheme 44).

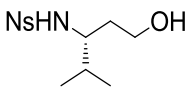
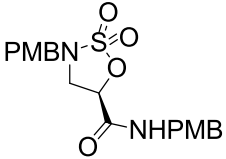
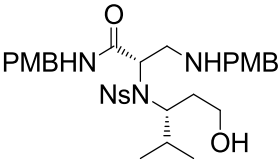
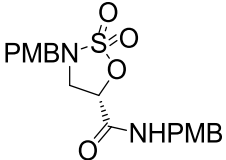
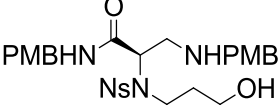
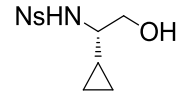
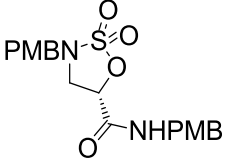
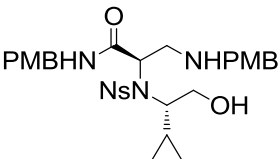
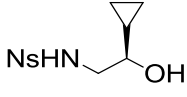
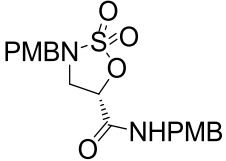
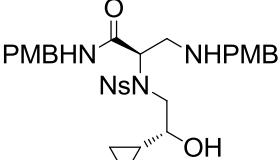


**Scheme 44** Synthesis of amino alcohol **230**.

### 3.5.2 Connection of Building Blocks

The cyclic sulfamidate ring opening reaction between **R-54** and amino alcohol **219** did not proceed at room temperature. The reaction was heated to 70 °C overnight; the limiting reagent sulfamidate **R-54** was consumed but only sulfonamide starting material **219** could be isolated (Table 21, Entry 1). It is likely that the reaction is challenging due to steric hindrance from the substituted carbon of attack on cyclic sulfamidate **R-54**, as well as the bulky  $\alpha$ -substituent of amino alcohol **219**.<sup>42</sup> This theory was validated by the ring opening reaction between sulfamidate **S-54** and unsubstituted amino alcohol **223**, which proceeded in reasonable yield (Table 21, Entry 2).

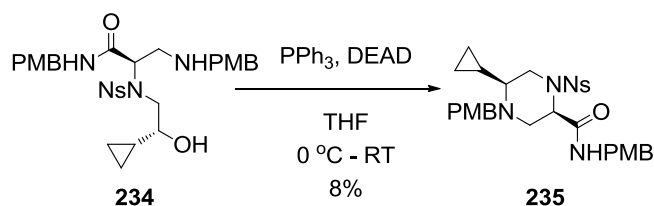
It was hoped that the reduced steric bulk from the cyclopropyl ring in amino alcohol **55** compared to the isopropyl group in **219** would result in a successful ring opening with **S-54**; however, the product was unable to be isolated cleanly (Table 21, Entry 3). The  $\beta$ -substituted amino alcohol **230** used in a sulfamidate ring opening reaction with **S-54** on a 300 mg scale gave a mixture of diastereoisomers due to possible epimerisation under the reaction conditions. These diastereoisomers were able to be separated (25% and 19% yield respectively) with the major product being carried forward (Table 21, Entry 4).

Entry	Nucleophile	Electrophile	Desired Product	Conditions	Outcome
1	 <b>219</b>	 <b>R-54</b>	 <b>231</b>	NaH, DMF, 70 °C	Sulfonamide starting material isolated
2	 <b>223</b>	 <b>S-54</b>	 <b>232</b>	NaH, DMF, 70 °C	32 % product isolated
3	 <b>55</b>	 <b>S-54</b>	 <b>233</b>	NaH, DMF, 70 °C	Mixture formed
4	 <b>230</b>	 <b>S-54</b>	 <b>234</b>	NaH, DMF, RT	25% product isolated

**Table 21** Conditions attempted for the cyclic sulfamidate ring opening reaction.

### 3.5.3 Synthesis of Scaffolds

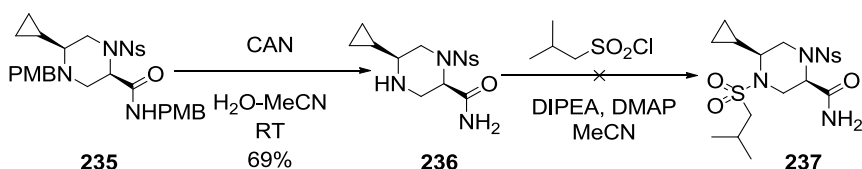
Intermediate **234** was used in a Mitsunobu cyclisation<sup>103,104</sup> reaction on a 200 mg scale to produce a mixture of diastereoisomers.<sup>105,106</sup> This was possibly due to epimerisation of the chiral centre alpha to the carbonyl group, under reaction conditions. The two diastereoisomers were separated by preparative HPLC and NOESY was used to confirm the stereochemistry of the major product as the desired scaffold **235** (Scheme 45). Unfortunately, purification by preparative HPLC meant the product yield was significantly reduced.



Scheme 45 Synthesis of scaffold **235**.

### 3.5.4 Synthesis of Fragments

CAN was used to deprotect the PMB group<sup>107</sup> of scaffold **235** on a 10 mg scale and it was observed on LCMS that each PMB group was removed in turn and the reaction only completed after a total of 8 equivalents of CAN was used; the product **236** was isolated using preparative HPLC. CAN deprotection was repeated on the piperazine scaffold, where the Mitsunobu product **235** was carried forward as a mixture of diastereoisomers in order to avoid loss of material using preparative HPLC. A white solid by-product was removed by filtration and the filtrate was purified by flash chromatography. The isolated deprotected piperazine **236** was used as crude for the following sulfonylation step, which did not yield any isolatable products (Scheme 46).



Scheme 46 Attempted synthesis of intermediate **237**.

Transfer hydrogenation<sup>108</sup> in an attempt to remove the PMB groups from scaffold **235** resulted in an unsurprising reduction of the nitrophenyl group to aniline, as well as removal of only one PMB group, presumably on the amine (Table 22, Entry 1). Both reflux in TFA (Table 22, Entry 2) and DDQ oxidation<sup>109</sup> (Table 22, Entry 3) showed starting

material remaining as well as the formation of an unknown side product. In addition, the DDQ oxidation reaction also showed removal of only one PMB group, after reflux overnight. It was decided at this stage that synthesis of fragments using Mitsunobu cyclisation chemistry would be abandoned and alternatives would be generated (discussed in Section 3.2).

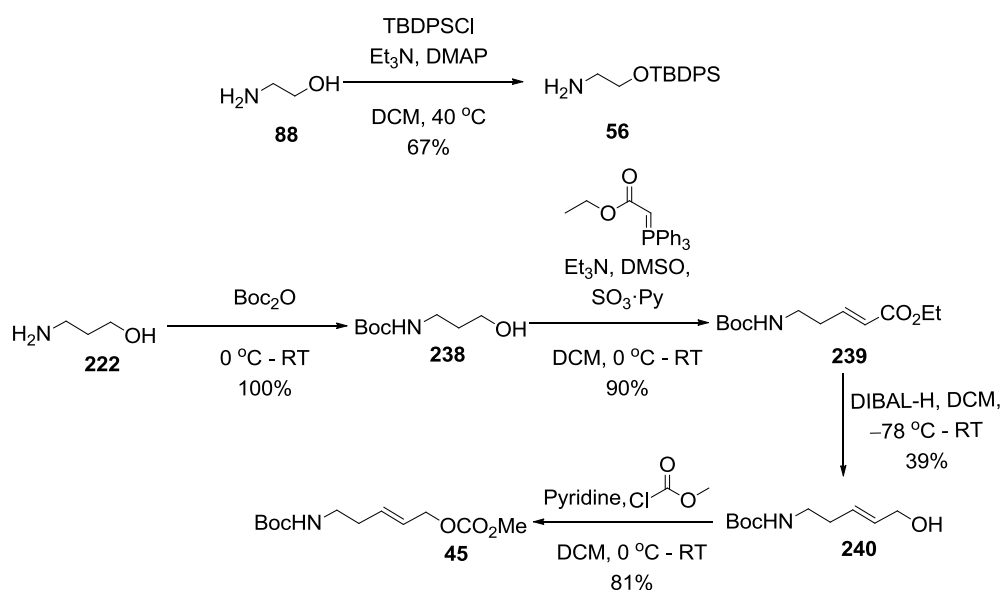
Entry	Conditions	Outcome
1	Ammonium formate, 5 mol% Pd(OH) <sub>2</sub> /C, EtOH, 70 °C	Reduction of nitro group
2	TFA, DCM, reflux	Unknown product formed
3	DDQ, H <sub>2</sub> O-DCM, 0 °C - 45 °C	Removal of one PMB group

**Table 22** Range of conditions attempted for PMB deprotection.

### 3.6 Synthesis of Fragments Using Iridium Chemistry

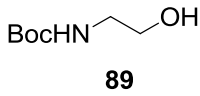
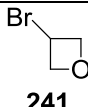
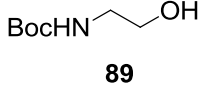
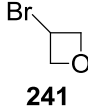
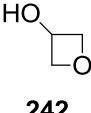
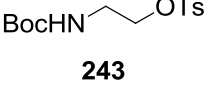
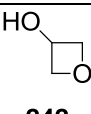
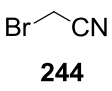
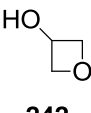
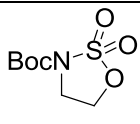
#### 3.6.1 Synthesis of Building Blocks

The silyl-protected<sup>110</sup> alcohol **56** was produced on a 10 g scale. Boc-protection of 3-amino-propanol was followed by a one-pot Parikh Doering oxidation<sup>111</sup> to give the aldehyde *in situ*, before being quenched by carbethoxymethylene triphenyl phosphorane in a Wittig reaction to give the  $\alpha,\beta$ -unsaturated ester **239**. The ester **239** was reduced<sup>110</sup> and later took part in an addition-elimination reaction with methyl chloroformate to give the allylic carbonate **45** on a 10 g scale (Scheme 47).

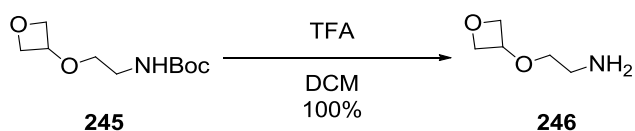


**Scheme 47** Synthesis of amino alcohol **56** and allylic carbonate **45**.

A range of conditions were attempted in order to synthesise an alternative building block to **56**; this would result in the desired fragment formed using fewer steps as the amino alcohol building block **246** is pre-decorated with the desired oxetane substituent. Unfortunately, heating of the amino alcohol **89** (synthesis discussed in Section 3.3.1.1) overnight with bromooxetane resulted in loss of the Boc group only (Table 23, Entry 1). The same reaction under phase transfer conditions at a lower temperature reproduced the starting material (Table 23, Entry 2). A substitution reaction combining nucleophile 3-oxetanol with tosyl-protected amine **243** was equally unsuccessful (Table 23, Entry 3). An attempt to form the acetonitrile derivative by reacting 3-oxetanol with bromoacetonitrile which could later be reduced to give the desired amine **246** gave a mixture of starting materials (Table 23, Entry 4). Pleasingly, synthesis via a cyclic sulfamidate ring opening reaction with sulfamidate **30** (synthesis discussed in Section 3.3.1.1) and 3-oxetanol was successful, producing **245** in reasonable yield (Table 23, Entry 5). Boc-deprotection yielded the desired amine **246** on a 2 g scale (Scheme 48).

Entry	Nucleophile	Electrophile	Conditions	Outcome
1	 <b>89</b>	 <b>241</b>	Cs <sub>2</sub> CO <sub>3</sub> , DMF, 60 °C	Loss of Boc group
2	 <b>89</b>	 <b>241</b>	Bu <sub>4</sub> NOH, H <sub>2</sub> O-MeCN, 40 °C	Amino alcohol recovered
3	 <b>242</b>	 <b>243</b>	Cs <sub>2</sub> CO <sub>3</sub> , DMF, 50- 100 °C	Mixture formed
4	 <b>242</b>	 <b>244</b>	K <sub>2</sub> CO <sub>3</sub> , acetone, 60 °C, 4 hr	Starting materials recovered
5	 <b>242</b>	 <b>30</b>	NaH, DMF, RT	41% yield

**Table 23** Range of conditions attempted for the synthesis of amine **245**.

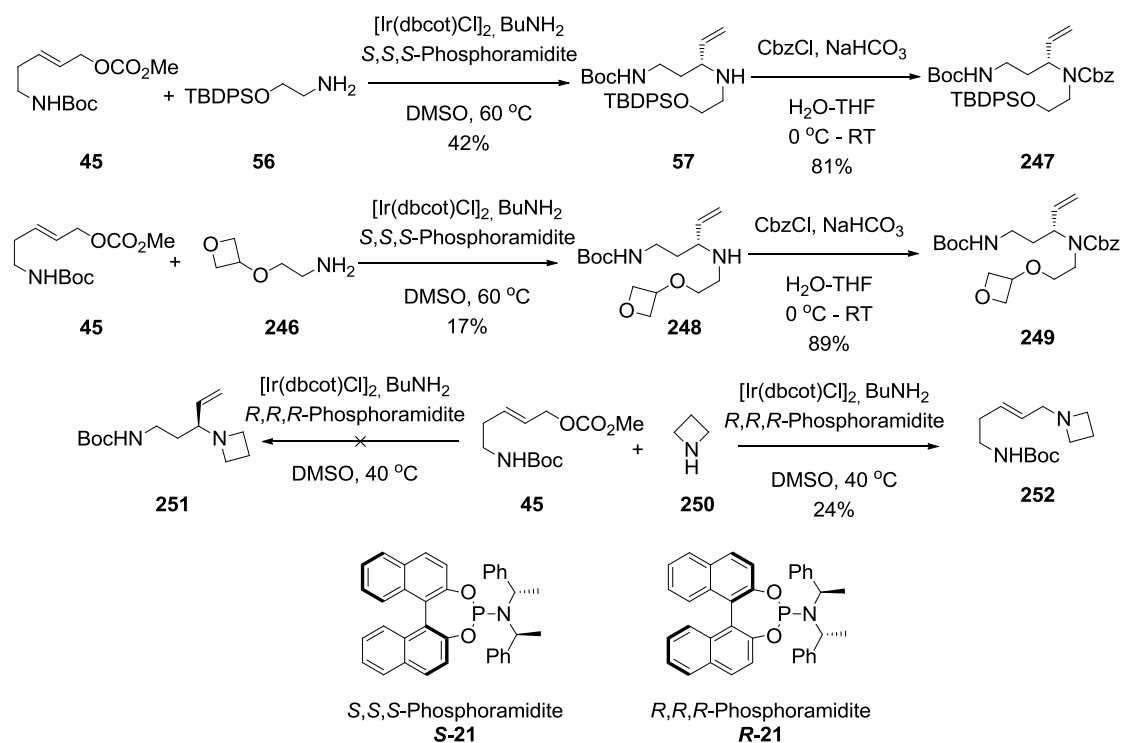


**Scheme 48** Synthesis of amine **246**.

### 3.6.2 Connection of Building Blocks

An iridium-catalysed allylic amination reaction between allylic carbonate **45** and amine **56** produced the alkene **57** enantioselectively on a 1 g scale. Cbz-protection<sup>112</sup> of alkene **57** on a 500 mg scale gave intermediate **247** as a mixture of rotamers. The same allylic amination reaction using the alkylated amino alcohol **246** was unable to react to completion, producing alkene **248** in 17% yield on a 500 mg scale; this was later Cbz-protected to produce **249**.

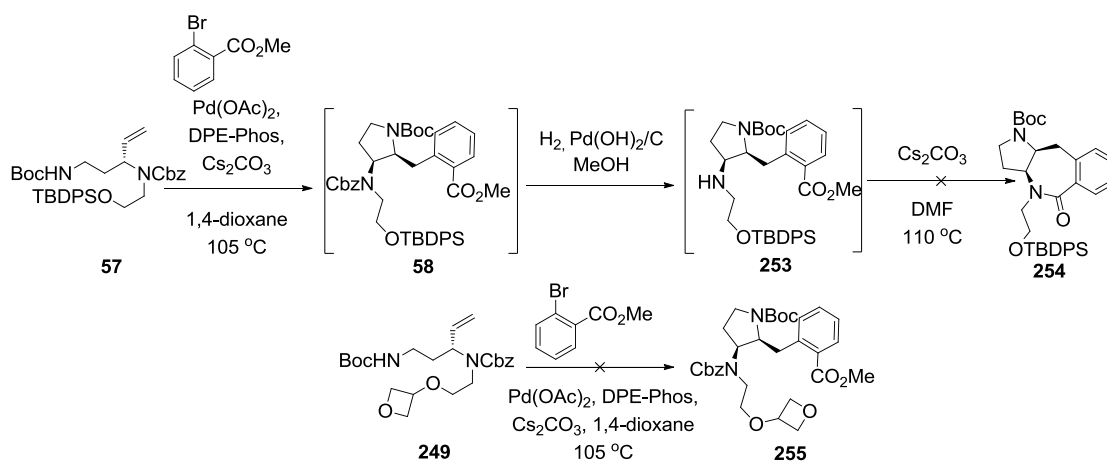
The allylic amination reaction using allylic carbonate **45** and azetidine was conducted at 40 °C instead of the 60 °C used in previous reactions. The reduced temperature was implemented as well as a large excess of amine in order to prevent loss by evaporation of the volatile azetidine. It was found in this instance that the undesired internal alkene was the only isolatable product as a result of an alternate mechanistic pathway (Scheme 49). Thus, a replacement for the fragment based on intermediate **251** was necessary (this procedure is discussed in Section 3.2).



**Scheme 49** Synthesis of alkenes.

### 3.6.3 Synthesis of Scaffolds

Intermediate **57** was used in an aminoarylation reaction with 2-bromobenzoate, producing intermediate **58** as a mixture which was used as crude for the following hydrogenation step, where two major products were isolated. The first isolated compound corresponded to the protonated mass of the product (617) and the second corresponded to an unknown compound of two mass units greater (619). The free amine **253** was used as crude in a base-mediated intramolecular cyclisation reaction where an unknown side-product was isolated that did not contain either the Boc or TBDPS group. An alternative route would be to avoid use of the silyl protecting group and begin synthesis with the oxetane decoration pre-installed on the oxygen, such as in alkene **249**. Unfortunately, an unknown mixture was isolated from the aminoarylation reaction (Scheme 50). It was decided at this stage that synthesis of fragments using iridium-catalysed allylic aminations would be abandoned and alternatives would be generated (discussed in Section 3.2).



**Scheme 50** Attempted synthesis of intermediates **254** and **255**.

## 4 Evaluation of a Shape-Diverse Fragment Library

### 4.1 Screening of Fragment Library using X-ray Crystallography

X-ray crystallography is an ideal screening technique because it reveals the experimental binding mode of weakly binding compounds, offering a useful starting point for fragment optimisation. Biochemical and other biophysical techniques are also widely used but disadvantages include reduced sensitivity, high rates of false positives and screening concentrations are limited to the low micromolar range.<sup>113</sup> In addition, hits generated using other biophysical techniques might yield compounds with physical properties that are less likely to give rise to X-ray hits. An example of this would be where lower solubility fragments can be screened using ligand-detected NMR, this could yield hits which are more lipophilic than X-ray hits.<sup>114</sup>

Although X-ray crystallography is ideal for detecting weakly binding fragments, it is a technique which has previously been time-consuming and low-throughput. However, in recent years the efficiency of X-ray crystallography has increased greatly due to the introduction of robotics, improved algorithms and detectors, and technical advances at synchrotron facilities. For example, at beamline I04-1 at Diamond Light Source (Harwell, UK), recent developments around soaking, harvesting and data analysis can allow the screening of a 1000-compound fragment library to be completed within a week. More importantly, this enables the possibility of screening by soaking single compounds per crystal, rather than cocktails, allowing screening concentrations of >100 mM to be possible.<sup>113</sup> Structure-based ligand design can then be used to improve the potency of fragment hits through iterative cycles of design, synthesis and screening.<sup>114</sup>

The fragment screen used for my library was completed at Diamond Light Source by Dr. Daniel Foley (University of Leeds) and Patrick McIntyre (University of Leicester), with the assistance of Dr. Patrick Collins (Diamond Light Source) using high-throughput X-ray crystallography. Protein crystals were firstly soaked with individual fragments, before being picked and later analysed using automated X-ray diffraction. Fragment hits were confirmed through detection of additional electron density. This process has been summarised in Figure 36 and has been described in more detail in Section 4.2.1.<sup>115</sup>

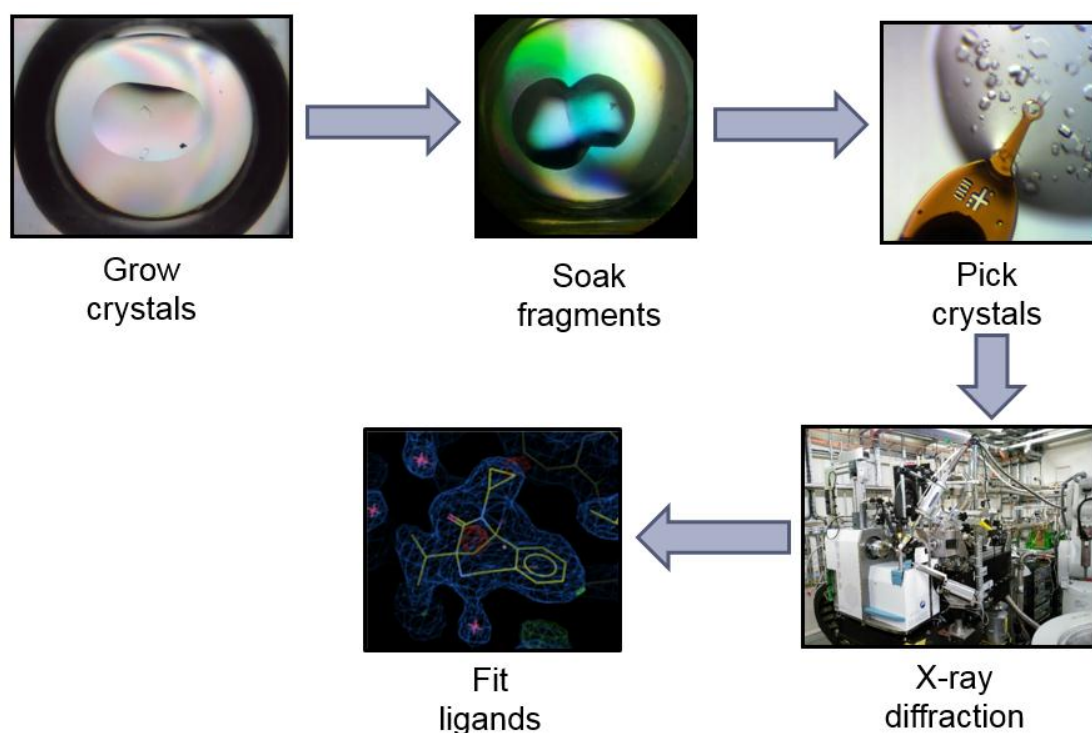


**Figure 36** The screening process at Diamond Light Source, where protein crystals were grown, soaked in solutions of individual fragments before being picked and analysed using X-ray diffraction. Bound fragments were further investigated using electron density mapping. The screening process was conducted by Dr. Daniel Foley (University of Leeds) and Patrick McIntyre (University of Leicester), with the assistance of Dr. Patrick Collins (Diamond Light Source).<sup>115</sup>

## 4.2 Aurora A Kinase as a Protein Target

During the process of mitosis, errors in chromosome segregation can lead to change in the number of chromosomes, a distinct property of human tumour cells.<sup>116</sup> Cyclin-dependent kinases (CDKs) are renowned regulators of cell-cycle progression. In addition to the CDKs, a number of other protein kinases also act as mitotic regulators, functioning either directly or in cooperation with CDKs.<sup>117</sup> One example of a group of these is the Aurora kinase family, which has recently emerged as key mitotic regulators required for genome stability.

Aurora A is a serine/ threonine kinase overexpressed in a wide range of different human tumours, indicating its essential role in tumour formation or progression, making Aurora A a useful therapeutic target. The Aurora kinases have been conserved throughout eukaryotic evolution and members of this family have been studied at length in various model organisms. The first discovery of Aurora A arose due to its overexpression in primary breast and colon tumour samples.<sup>116</sup>

Molecules that target the active site of Aurora A often mimic the planar adenine base of ATP;<sup>114</sup> previously reported inhibitors from fragment screens include ZM447439,

Hesperadin and VX-680.<sup>116</sup> The binding pose of ATP within the hinge region of the protein can be seen in Figure 37.<sup>118</sup> Within the active site, oxygen atoms in the ATP phosphate backbone are able to form hydrogen bonds (H-bonds) with adjacent polar atoms in residues K162, K143, D274 and N261.

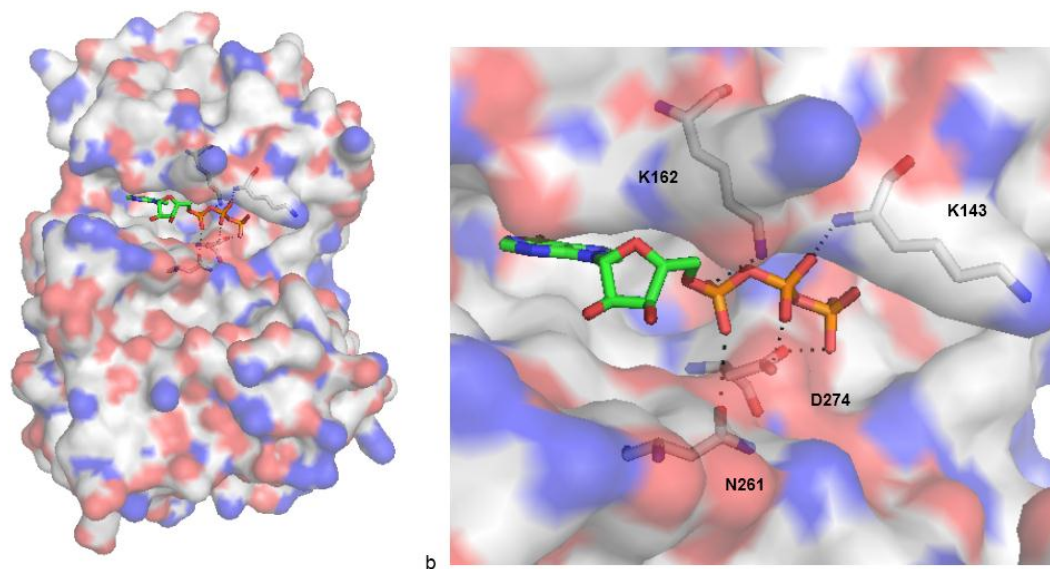


**Figure 37** a) The binding pose of ATP (green) within the hinge region of the protein. b) Within the active site, oxygen atoms in the ATP phosphate backbone are able to form H-bonds with adjacent polar atoms in residues K162, K143, D274 and N261, shown as black dotted lines. Adapted from <sup>118</sup>

The kinase activity of Aurora A is also regulated by the binding of a protein called TPX2. AurkinA was recently published as a novel chemical inhibitor of the Aurora A-TPX2 interaction.<sup>118</sup> AurkinA has been observed crystallographically to bind to a hydrophobic 'Y'-shaped pocket in the protein that normally accommodates a conserved YSY motif from TPX2, blocking the Aurora A-TPX2 interaction as a result (Figure 38).

Further analysis suggests that AurkinA is able to form hydrophobic interactions between its quinoline and phenyl substituents and the hydrophobic base of the 'Y' pocket created by residues L178, V182, V206 and L208. In addition, an ionic interaction is present between the carboxylic acid of AurkinA and the basic side chain of residue K166. More importantly, the binding of AurkinA to the 'Y' pocket has been reported to induce structural changes in Aurora A that inhibit catalytic activity *in vitro* and in cells, without affecting the binding of ATP to the active site, demonstrating a mechanism of allosteric inhibition.<sup>118</sup>

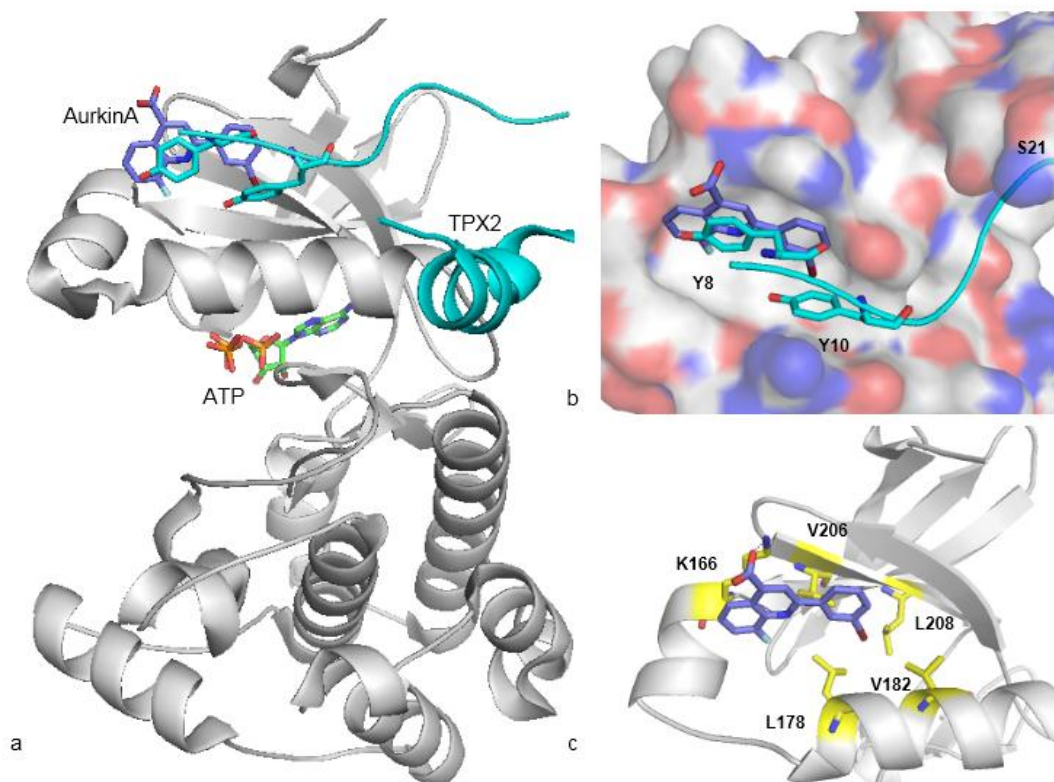


**Figure 38** a) Crystal structure of Aurora A liganded with ATP (green) and AurkinA (purple), overlaid with TPX2 (blue). AurkinA is bound to the ‘Y’ pocket of Aurora A, which sits above the ATP site. b) Detailed structure of AurkinA and TPX2 binding in the ‘Y’ pocket, a binding site of the YSY motif of TPX2. c) Interaction of AurkinA with different residues within the ‘Y’ pocket, where hydrophobic interactions can be seen between its quinoline and phenyl substituents and the hydrophobic base of the cavity created by residues L178, V182, V206 and L208. An ionic interaction is also present between the carboxylic acid of AurkinA and the basic side chain of residue K166 (shown using a black dotted line). Adapted from <sup>118</sup>

#### 4.2.1 Screening of Fragment Library against Aurora A Kinase

All 20 Leeds fragments synthesised by myself (which will be referred to as “Leeds fragments” from hereon in) were screened at Diamond Light Source along with 60 commercially purchased molecules against protein target Aurora A Kinase, using high-throughput X-ray crystallography. The screening team consisted of Dr. Daniel Foley (University of Leeds), Patrick McIntyre (University of Leicester) and Dr. Patrick Collins (Diamond Light Source). Protein crystals were firstly soaked with individual fragments; Aurora A was used at 450  $\mu$ M concentration in combination with 5mM ADP, Leeds and commercial fragments were soaked at 200 mM and 80 mM respectively. The presence of ATP bound to the Aurora A active site increases the likelihood of fragment binding in alternative binding pockets.

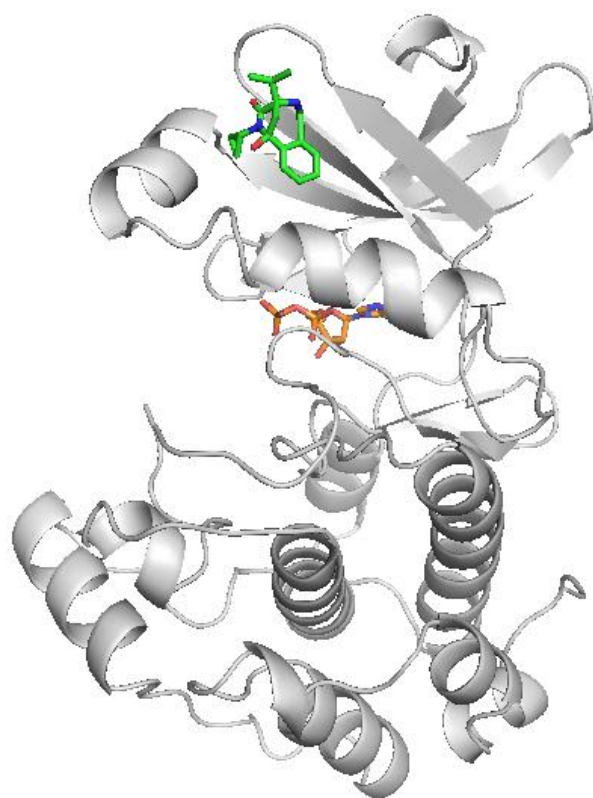
Crystals were then picked before being analysed using automated X-ray diffraction. Diffraction data were collected on beamline I04-1 at the Diamond Light Source and processed using XChem Explorer and PanDDA (Pan-Dataset Density

Analysis).<sup>115</sup> Fragment hits were confirmed through detection of additional electron density; polar and hydrophobic interactions with the protein were also identified using PyMOL.

### 4.3 Fragment Hits against Aurora A Kinase

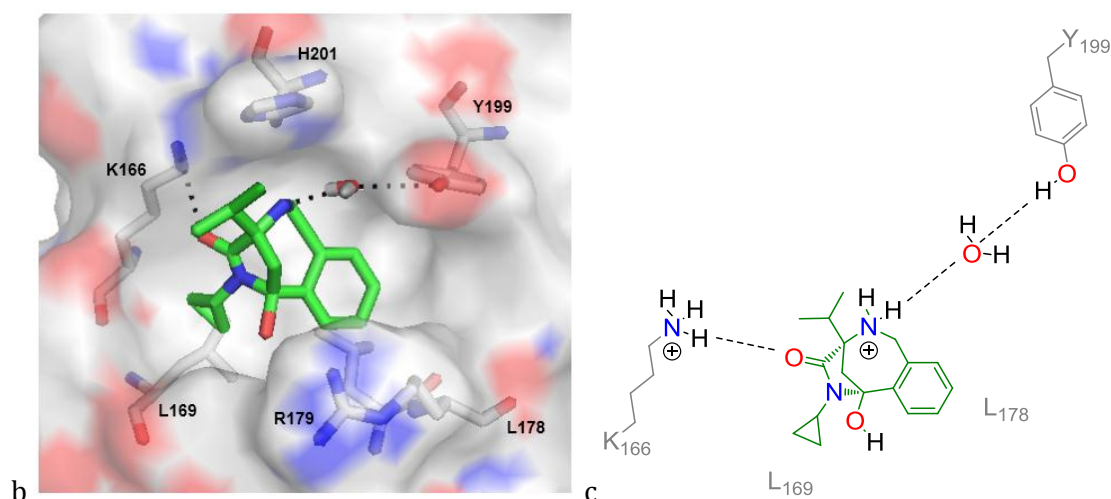
#### 4.3.1 Hit from Leeds Library against Aurora A Kinase

**214** was identified as a key novel hit against Aurora A Kinase, revealed to target the same site as that targeted by AurkinA, offering new opportunities for allosteric modulation of the enzyme. The X-ray crystal structure of Aurora A with the ligand and ATP bound, as well as the detailed binding pose of **214** within the allosteric pocket can be seen in Figure 39. Within the binding cavity, hydrophobic interactions were observed between the cyclopropyl and phenyl substituents of **214**, and protein residues L169 and L178, respectively. In addition, hydrogen bonding interactions can be identified between the amide CO of the fragment to residue K166, and the amine NH to Y199; here, the latter interaction is mediated by a water molecule. More importantly, the H-bond between K166 and the amide CO in **214** mirrors that of the ionic interaction between the same residue and the carboxylic acid of Aurkin A. The phenyl rings in both small molecules also exhibit hydrophobic interactions with L178 in Aurora A.



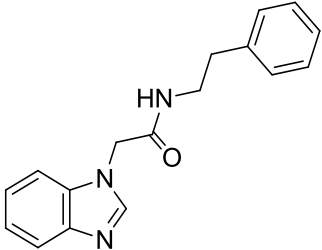
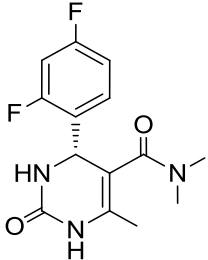
a

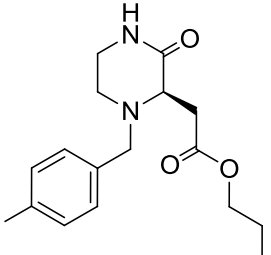
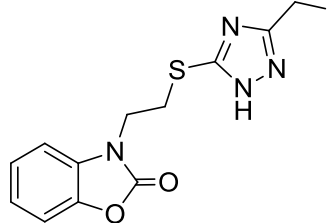
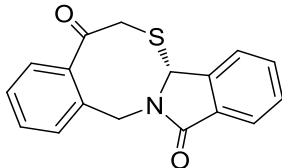
**Figure 39** a) The X-ray crystal structure of Aurora A with the bound hit compound **214** (green) and ATP (orange). b) The detailed X-ray crystal structure of the allosteric binding pocket of Aurora A in which the hit molecule **214** is bound. c) A schematic illustration of interactions of **214** with nearby amino acid residues, where hydrophobic interactions have been observed between the cyclopropyl and phenyl substituents to L169 and L178, respectively, and hydrogen bonding interactions ( $\leq 3.5$  Å) have been observed between the amide CO of **214** to residue K166, and the amine NH of **214** to Y99 via a bridging water molecule.



### 4.3.2 Hits from ZINC Commercial Library against Aurora A Kinase

Nine fragments were found to target Aurora A from the library of 60 commercial fragments, where the fragment hits are bound to the protein with varying occupancy levels. Table 24 summarises five hits which provided clear crystal densities, along with an evaluation of their binding modes. The remaining fragment hits can be found in Table 38 of the Appendix along with an observation of their respective electron densities. Three of the five fragments shown in Table 24 were found to target the 'Y' pocket as **214** did (site 1); fragment **259** was observed to target a second site (site 2) on the same face of the protein. Site 3 is another pocket situated on the opposite face of Aurora A, targeted by **260**. Figure 40 shows a comparison of sites 1-3, using exemplar fragments to demonstrate binding. The binding modes of all five fragments can be seen in detail in Figure 41.

Compound	Site of Target	Binding Mode
 <p><b>256</b></p>	1	<p>A H-bond is observed between the amide CO and R179. <math>\pi</math>-Stacking interactions are observed between the benzimidazole ring and Y199 and finally, hydrophobic interactions are observed between the phenyl ring and L178.</p>
 <p><b>257</b></p>	1	<p>Hydrophobic interactions are observed between the difluorophenyl ring and L178.</p>

 <p style="text-align: center;"><b>258</b></p>	1	<p>A H-bond is observed between the lactam CO and Y199. Hydrophobic interactions are also observed between the propyl side chain and L178, as well as between the tolyl ring and L169.</p>
 <p style="text-align: center;"><b>259</b></p>	2	<p>The benzene ring is observed to participate in a <math>\pi</math>-stacking interaction with F157 as well as an edge to face interaction with Y197.</p>
 <p style="text-align: center;"><b>260</b></p>	3	<p>Hydrophobic interactions are observed between the benzene ring and P138, as well as between the isoindolinone functionality and F165.</p>

**Table 24** Five hits from the library of 60 commercial fragments which showed clear electron densities, along with an evaluation of their binding modes.

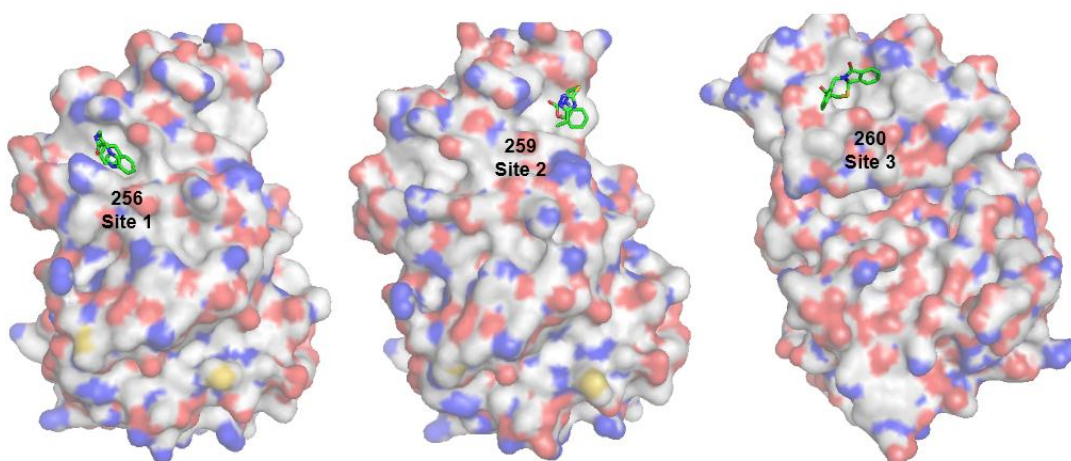


**Figure 40** The three different pockets in Aurora A targeted by commercial fragments (green), shown using example hit molecules. Here, site 1 is the 'Y' pocket also targeted by **214**, shown using **256**, site 2 is situated on the same face as site 1, occupied by **259** and site 3 is situated on the opposite face of the protein, occupied by **260**.

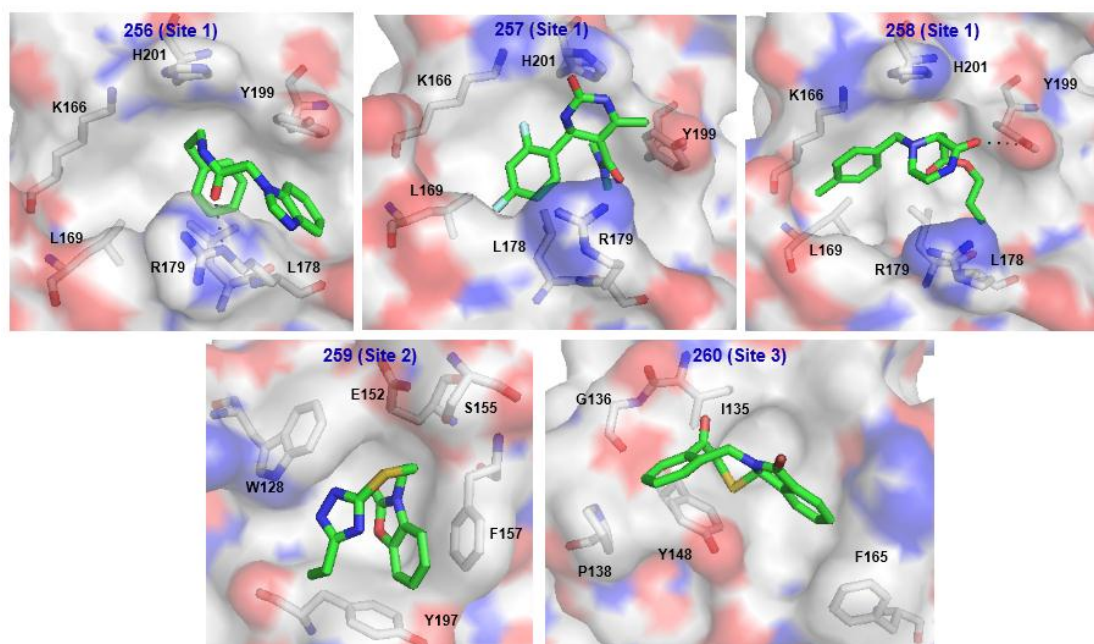


**Figure 41** Binding modes of five hits (green) from the library of 60 commercial fragments which showed clear electron densities, targeting sites 1-3 within Aurora A. The interactions of the fragments are described in detail in Table 24 and hydrogen bonds are shown using black dotted lines.

Affinity measurements are challenging on small fragments due to their weak binding, as these are only starting points to a potent lead compound. In the case of compounds from the ZINC commercial library, it could be argued that the better resolved a ligand's density, the tighter it is bound to the protein; however, other factors are involved which influence the final electron density of the observed crystal structures. Nevertheless, it is clear to say that the 'Y' pocket, or site 1, remains a popular allosteric

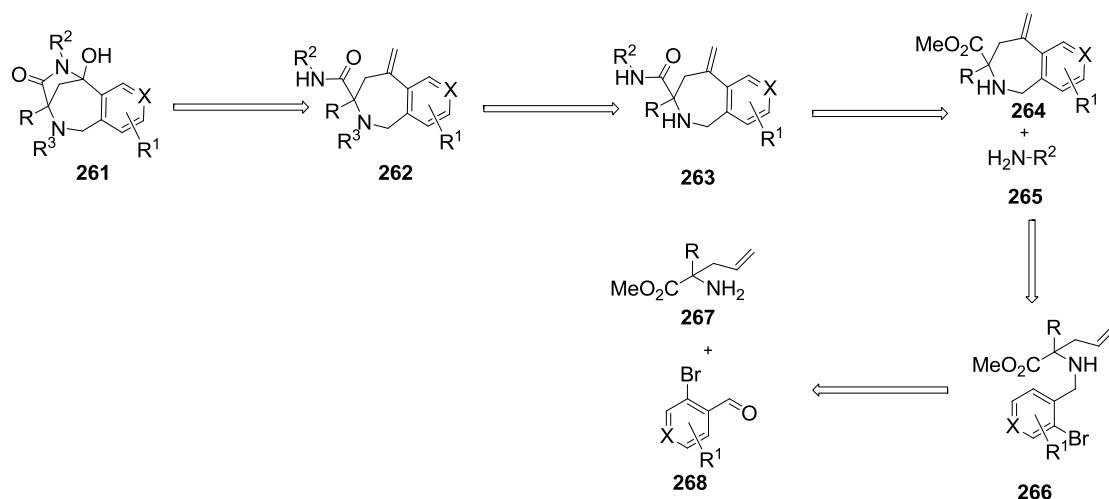
target site, with sites 2 and 3 being identified as a novel binding pockets. Subsequent follow up by biophysical measurement of the affinity of the fragments for the protein would allow definitive prioritisation of hits for elaboration.

#### 4.4 Design of a Library of Analogues of a Hit Compound

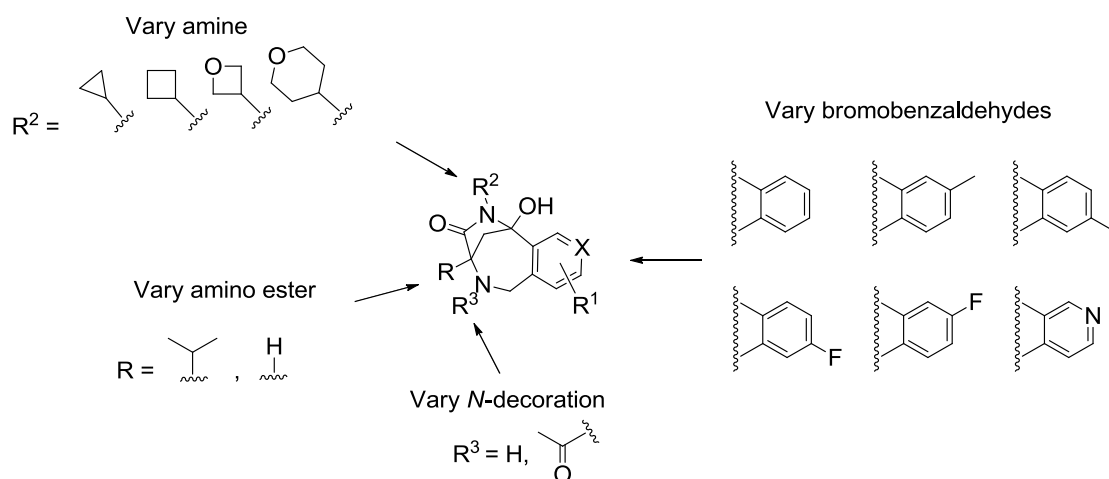
The electron density of **214** in the region of the binding pocket was well-defined and allowed scope for fragment growth. Potential analogues of **214** were identified to allow optimisation of compound affinity to the allosteric cavity by exploiting structure activity relationships. The retrosynthetic analysis of **214** can be seen in Scheme 51, where possible variation for substituents has been labelled as 'R,' and 'X' has been used in place of possible heteroatoms. A range of commercially available, and functionality-compatible bromoaldehydes were identified to install a single substituent on the aryl ring of **214**, and a range of cyclic amines was identified in the hope of exploring the space around its amide functionality. Allylated glycine methyl ester was also used as a building block to explore compounds with reduced steric hindrance as well as to allow possible further decoration on the secondary amine functionality. Furthermore, this would be able to confirm whether the presence of the isopropyl substituent on this series of compounds is important for the activity of the fragment.

Modifications on **214** are summarised in Scheme 52, where different cyclic amide substituents ( $R^2$ ) can be used to explore the visible space around L169 in the 'Y' pocket. The isopropyl group (R) could also be substituted by hydrogen, which would allow further decoration on the adjacent secondary amine ( $R^3$ ) to explore the pocket in a new direction.  $R^1$  substitutions point downwards in the binding pocket towards L178 which could be explored with small groups on the arene. In addition, by installing a nitrogen heteroatom on position X, it is possible to explore interactions with the adjacent Y199 in the binding pocket. The proposed analogues can be seen in Scheme 53, all of which are synthesisable using commercially available reagents and based on established chemistry.

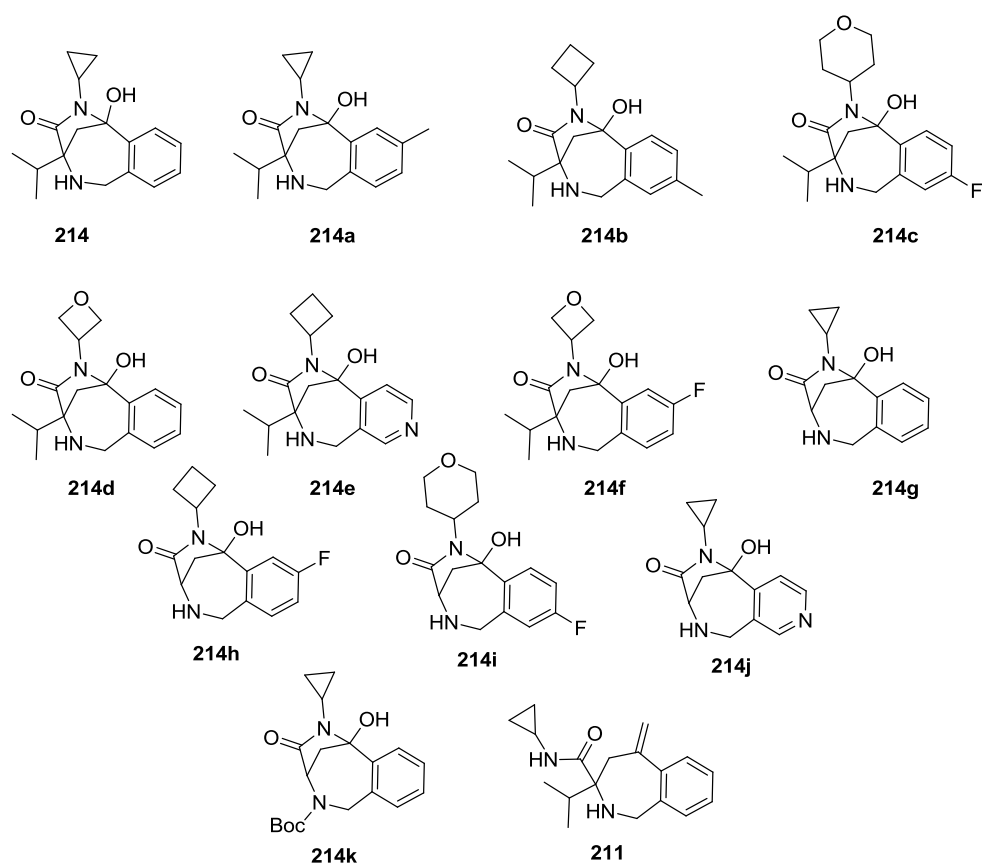
The original hit **214** was remade and screened alongside intermediates **211** and **214k**. The alkene intermediate **211** allowed the uncyclised amide precursor of **214** to be investigated, highlighting possible value of the cyclised hemiaminal motif within the final fragment. Here, not only is **214k** a precursor to analogue **214g**, the Boc protecting group fulfils the role of an acyl decoration on the secondary amine. Finally, the compounds shown in Scheme 53 were all screened as racemates.



**Scheme 51** Retrosynthetic analysis of **214**, where functionalities available for variation have been labelled using R groups, and X represents the presence of a possible heteroatom.



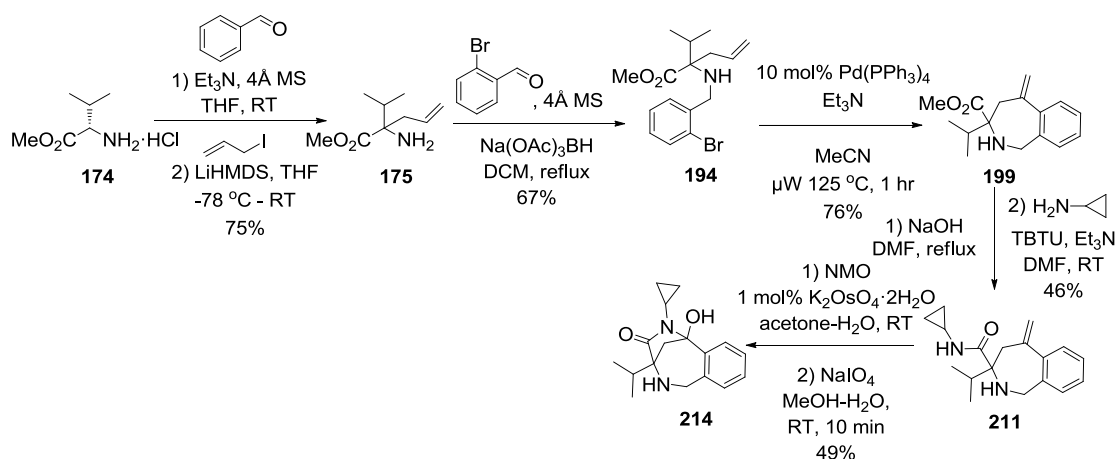
**Scheme 52** Modifications on **214** in different positions in order to produce a library of analogues. These include varying the amino ester, bromobenzaldehyde and amine building blocks, as well as using different decorations on the secondary amine functionality.



**Scheme 53** Proposed analogues of **214** to be synthesised.

#### 4.5 Synthesis of a Library of Analogues of a Hit Compound

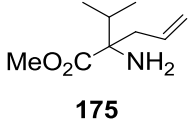
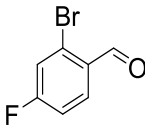
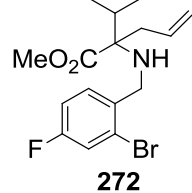
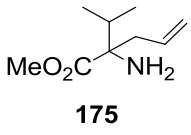
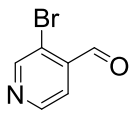
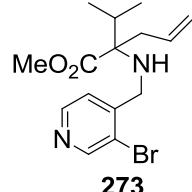
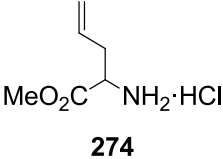
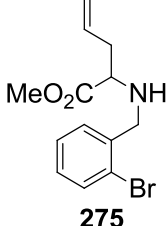
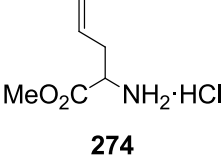
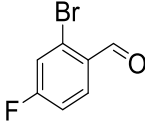
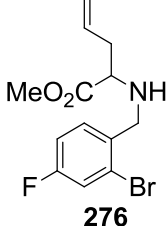
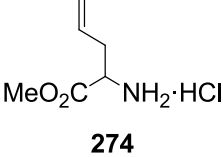
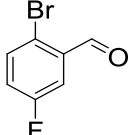
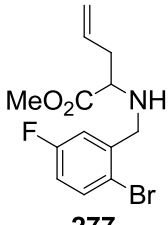
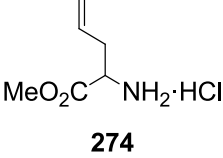
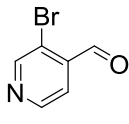
The synthetic sequence for reproduction of the original hit compound **214** can be seen in Scheme 54. A slight improvement in yield was observed when changing reductive amination conditions from heating at 45 °C in THF to heating at reflux in DCM. The yield for the Heck reaction improved from 26% to 76% by changing the catalyst and ligand from 10 mol% Pd(OAc)<sub>2</sub> with PPh<sub>3</sub> to 10 mol% Pd(PPh<sub>3</sub>)<sub>4</sub>. Next, completing the hydrolysis of **199** at reflux in DMF instead of at 120 °C ensured the reaction consistently reached completion overnight resulting in an improved yield. Finally, the oxidative cleavage step following dihydroxylation of **211** was monitored carefully and it was found that after 10 minutes, virtually no over-oxidation to the imine occurred and thus the yield increased from 22% over two steps (which included an additional imine reduction, see Section 3.4.4.3) to 49%, where the major product observed was the cyclised hemiaminal. The synthetic route shown in Scheme 54 was completed on a 700 mg scale.



**Scheme 54** Resynthesis of fragment **214**.

Reductive amination was completed on both substituted (Table 19, Entry 1 to 5) and unsubstituted amino esters (Table 19, Entry 6 to 9), using a range of bromoaldehydes. The procedure was performed in the presence of  $\text{Na}(\text{OAc})_3\text{BH}$  and 4Å MS (20% w/w), using DCM as the reaction solvent and by heating the mixture at reflux overnight. In the case of entries 6 to 9, **274** also required the addition of 1 equiv.  $\text{Et}_3\text{N}$  due to the presence of the hydrochloride salt. The secondary amine products were isolated in good yields.

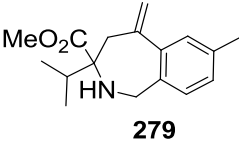
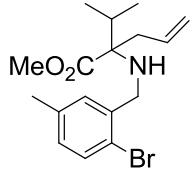
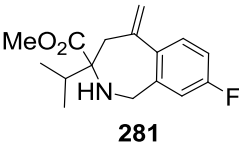
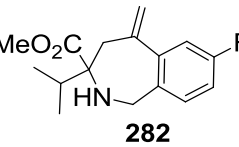
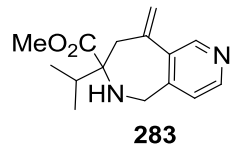
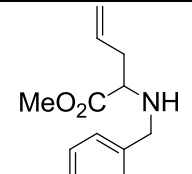
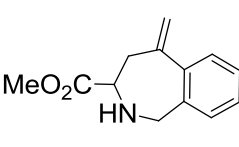
Entry	Amino Ester	Bromoaldehyde	Product <sup>a</sup>	Yield / %
1				66
2				80
3				64

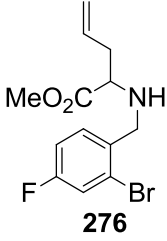
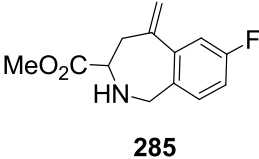
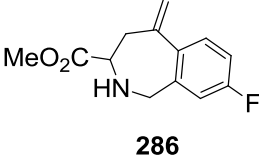
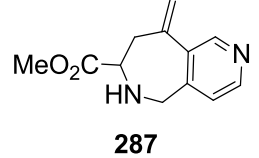
4	 <b>175</b>		 <b>272</b>	65
5	 <b>175</b>		 <b>273</b>	57
6	 <b>274</b>		 <b>275</b>	40 <sup>b</sup>
7	 <b>274</b>		 <b>276</b>	46 <sup>b</sup>
8	 <b>274</b>		 <b>277</b>	50 <sup>b</sup>
9	 <b>274</b>		 <b>278</b>	54 <sup>b</sup>

**Table 25** Yields of products from the reductive amination reaction; a) Conditions: 4Å MS, Na(OAc)<sub>3</sub>BH, DCM, reflux; b) Additional 1 equiv. Et<sub>3</sub>N used.

Benzazepines and pyridoazepines were synthesised using Heck cyclisation reactions of both substituted (Table 26, Entry 1 to 5) and unsubstituted secondary amines (Table 26, Entry 6 to 9). The catalyst used for the Heck reaction was Pd(PPh<sub>3</sub>)<sub>4</sub> (10 mol%)

in the presence of Et<sub>3</sub>N. MeCN was used as the reaction solvent and the cyclisation completed after 1 hr, by heating at 125 °C under microwave conditions. Excellent yields were achieved for the isopropyl substituted amines, with good yields achieved for the unsubstituted secondary amines.

Entry	Secondary Amine	Product <sup>a</sup>	Yield / %
1	 <p><b>269</b></p>	 <p><b>279</b></p>	81
2	 <p><b>270</b></p>	 <p><b>280</b></p>	88
3	 <p><b>271</b></p>	 <p><b>281</b></p>	91
4	 <p><b>272</b></p>	 <p><b>282</b></p>	92
5	 <p><b>273</b></p>	 <p><b>283</b></p>	91
6	 <p><b>275</b></p>	 <p><b>284</b></p>	57

7	 <p style="text-align: center;"><b>276</b></p>	 <p style="text-align: center;"><b>285</b></p>	52
8	 <p style="text-align: center;"><b>277</b></p>	 <p style="text-align: center;"><b>286</b></p>	84
9	 <p style="text-align: center;"><b>278</b></p>	 <p style="text-align: center;"><b>287</b></p>	81

**Table 26** Yields of products from the Heck cyclisation reaction; a) Conditions: 10 mol% Pd(PPh<sub>3</sub>)<sub>4</sub>, Et<sub>3</sub>N, MeCN,  $\mu$ W, 125 °C, 1 hr.

Amide coupling was completed on both substituted (Table 27, Entry 1 to 4) and unsubstituted benzazepines (Table 27, Entry 5 to 7), using a range of commercially available amines. The first part of the procedure involved ester hydrolysis in the presence of NaOH, performed at reflux in DMF. The harsh conditions used proved reliable, and necessary in the presence of the hindered centre adjacent to the ester functionality, for benzazepines in entries 1 to 4. The second part of the one-pot procedure involved amide coupling in the presence of the desired amine, which was used in large excess, and using Et<sub>3</sub>N as base. The procedure concluded with addition of the coupling agent TBTU, in order to avoid polymerisation of the starting material. The reaction completed at RT overnight producing the desired amides in reasonable yields, except for **290** which was isolated in particularly high yield.

The amide coupling of pyridoazepines **283** and **287** were unsuccessful due to the instability of the pyridine functionality during hydrolysis conducted at high temperatures. In addition, amide coupling between benzazepine **199** and 4-aminoxetane was also unsuccessful. Due to time restraint, analogues **214d**, **214e** and **214j** (see Section 4.4, Scheme 53) were abandoned.

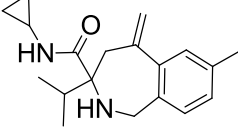
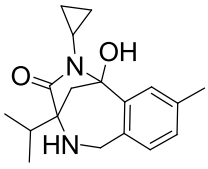
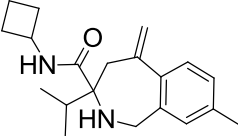
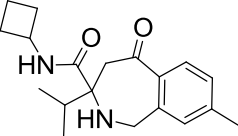
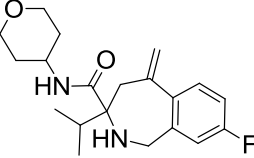
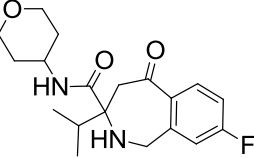
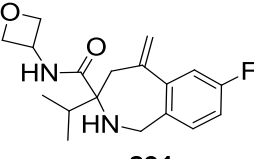
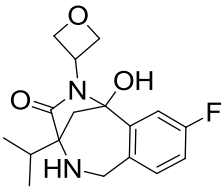
Entry	Benzazepine	Amine	Product <sup>a</sup>	Yield / %
1	 <b>279</b>		 <b>288</b>	20
2	 <b>280</b>		 <b>289</b>	38
3	 <b>281</b>		 <b>290</b>	72
4	 <b>282</b>		 <b>291</b>	37
5	 <b>284</b>		 <b>292</b>	39
6	 <b>285</b>		 <b>293</b>	<i>b</i>
7	 <b>286</b>		 <b>294</b>	18

**Table 27** Yields of products from the amide coupling reaction; a) Conditions: 1) NaOH, DMF, reflux; 2) amine, Et<sub>3</sub>N, TBTU, DMF, RT; b) The crude reaction mixture was used without purification (See Table 29, Entry 2).

Dihydroxylation followed by oxidative cleavage was completed on a range of substituted benzazepines (Table 28), with synthesis of fragment **214f** requiring an additional imine reduction step as over-oxidation seemed to occur simultaneously to

ketone formation (see Section 3.4.4.3). Conditions for dihydroxylation involved use of oxidising agent  $K_2OsO_4 \cdot 2H_2O$  (1mol%) in the presence of NMO. The reaction was performed in an acetone- $H_2O$  solvent mixture and completed at RT overnight.

The second part of the one-pot procedure involved oxidative cleavage of the diol product using 4 equiv.  $NaIO_4$  in a MeOH- $H_2O$  solvent mixture. The reaction completed in 10 min at room temperature and great care was taken to stop the reaction immediately after completion. The desired fragments in entries 1 to 3 were isolated in good yields. In the case of the benzazepine **291**, over-oxidation to the imine side-product was observed within the same period and an extra reduction step was required to provide the final desired fragment in reasonable yield.

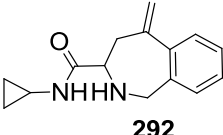
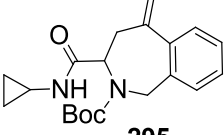
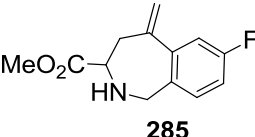
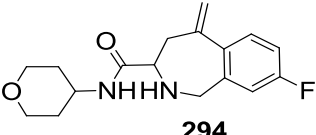
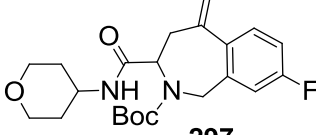
Entry	Benzazepine	Product <sup>a</sup>	Yield / %
1	 <b>288</b>	 <b>214a</b>	36
2	 <b>289</b>	 <b>214ba</b>	66
3	 <b>290</b>	 <b>214ca</b>	83
4	 <b>291</b>	 <b>214f</b>	16% over two steps <sup>b</sup>

**Table 28** Yields of products from the dihydroxylation and oxidative cleavage reactions; a) Conditions: 1) NMO, 1 mol%  $K_2OsO_4 \cdot 2H_2O$ , acetone- $H_2O$ , RT; 2)  $NaIO_4$ , MeOH- $H_2O$ , RT, 10 min; b) Extra reduction step required due to over-oxidation to the imine side-product, conditions: 3)  $Na(OAc)_3BH$ , DCM, RT.

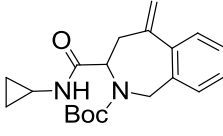
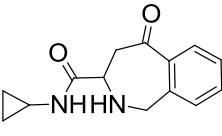
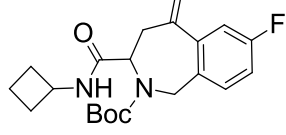
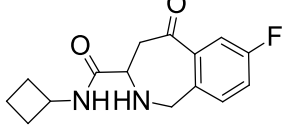
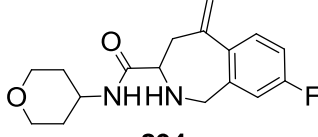
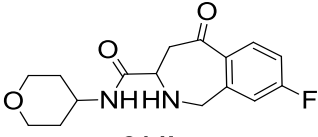
The same osmium-mediated dihydroxylation reaction was unsuccessful for the unsubstituted benzazepine **292**, thus ozonolysis was attempted in order to convert the terminal alkene to a ketone. Unfortunately, no identifiable product was observed.

Ozonolysis was then reattempted on Boc-amine **295** after protection of benzazepine **292** on a 100 mg scale, with half of intermediate **214ka** (see Scheme 56) being submitted for X-ray screening in order to identify any value to substitution on the secondary amine functionality.

Boc-protection was later performed on a range of unsubstituted benzazepines (Table 29), followed by ozonolysis and finally deprotection (Table 30). Boc-protection was completed in good yields in the presence of Boc<sub>2</sub>O, using DCM as reaction solvent with the mixture left at RT overnight. Next, ozonolysis was completed at -78 °C-RT, using DCM as the reaction solvent and DMS as the reducing agent. The final Boc-deprotection was performed *in situ*, using TFA as the reaction solvent to yield the final desired fragments in good to excellent yields.

Entry	Benzazepine	Product <sup>a</sup>	Yield / %
1	 <b>292</b>	 <b>295</b>	70
2	 <b>285</b>	 <b>296</b>	31% over two steps <sup>b</sup>
3	 <b>294</b>	 <b>297</b>	<i>c</i>

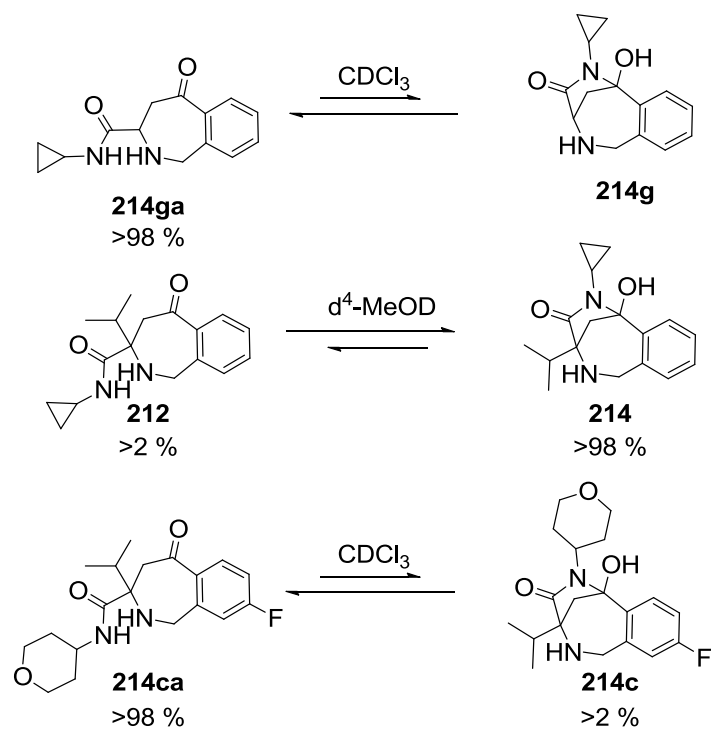
**Table 29** Yields of products from Boc-protection reactions; a) Conditions: Boc<sub>2</sub>O, DCM, RT; b) See Table 27, Entry 6; c) The crude reaction mixture was used without purification (See Table 30, Entry 3).

Entry	Boc-amine	Product <sup>a</sup>	Yield / %
1	 <b>295</b>	 <b>214ga</b>	41
2	 <b>296</b>	 <b>214ha</b>	100
3	 <b>294</b>	 <b>214ia</b>	100% over two steps <sup>b</sup>

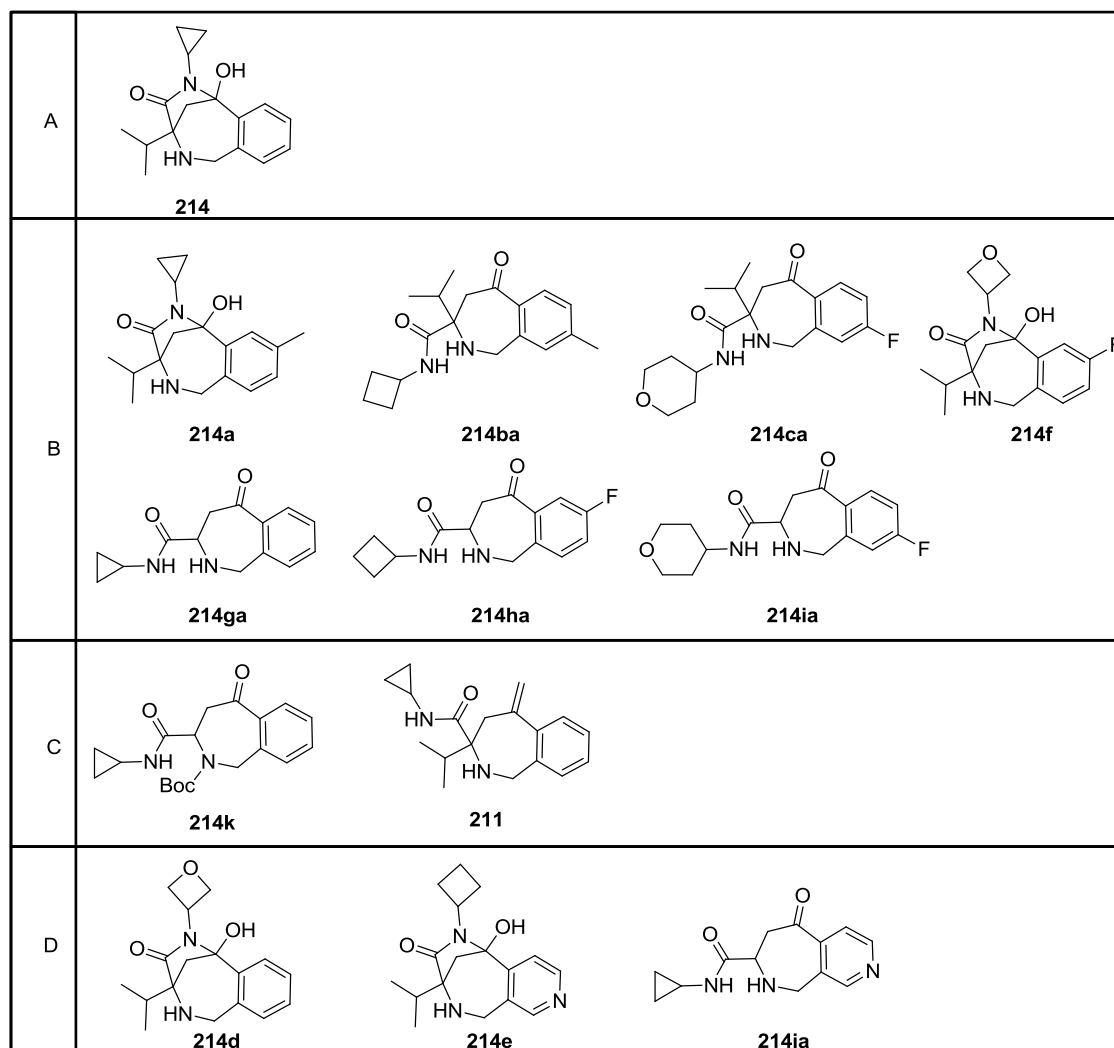
**Table 30** Yields of products from ozonolysis and Boc-deprotection reactions; a) Conditions: 1) O<sub>3</sub>, DMS, DCM, -78 °C-RT, 2) TFA, RT; b) See Table 29, Entry 3.

One notable observation was that in the case of fragments without an isopropyl substituent adjacent to the amide, the product favoured the open chain ketone form rather than the closed chain hemiaminal form. This could be attributed to the Thorpe-Ingold effect where the increasing number of substituents favours cyclisation to form the hemiaminal structure. However, the open chain ketone form was favoured in the case where a larger substituent than the cyclopropyl group on the amide was present, such as in fragment **214ca**, which contains a tetrahydropyran ring. This is a possible result of steric clash between the large rings on the amide and the OH of the hemiaminal.

The effects on the equilibrium between the open and closed chain forms of comparable fragments could also be due to solvent effects, where CDCl<sub>3</sub> appears to favour formation of the cyclic hemiaminal and presence of MeOD appears to favour formation of the open chain amide, shown in Scheme 55. A summary of the final submitted analogues, intermediates as well as the original hit can be seen in Scheme 56, shown as their major cyclised/uncyclised forms. Fragments which were not synthesised have also been highlighted.



**Scheme 55** Equilibrium observed between the open and close chain forms of fragments **214g**, **214** and **214c**. Here, the presence of the isopropyl substituent in **214** promotes formation of the cyclised hemiaminal. However, increased steric bulk such as from the tetrahydropyran substituent in **214ca** means that the open chain amide form is favoured. The solvents in which the structural NMR data was obtained have been indicated, as this could also affect the position of equilibrium.



**Scheme 56** Analogues of **214** shown as their major cyclised/uncyclised forms; A: Original hit molecule, B: successfully synthesised analogues, C: successfully synthesised intermediates, D: Fragments which were not prepared.

#### 4.6 Screening of Library of Analogues against Aurora A Kinase

After conducting an X-ray screen of completed fragment analogues in Scheme 56, five molecules from the library were found to also target the 'Y' pocket of Aurora A. Three of these hits showed clear electron densities and the remaining hits can be found in Table 38 of the Appendix along with their observed electron densities. One of the three binders is the resynthesized hit molecule **214**, whose binding mode was replicated, another is the alkene precursor to **214**, **211**, and the final hit is a new analogue, **214b**. Within fragments **211** and **214b**, the cyclic amide substituents and benzene rings belonging to both compounds exhibit hydrophobic interactions towards L169 and L178, respectively. In addition, a H-bond is observed between the amide CO of **214b** and K166. These binding

interactions can be seen crystallographically in Figure 42, as well as their overlaid structures with **214**.

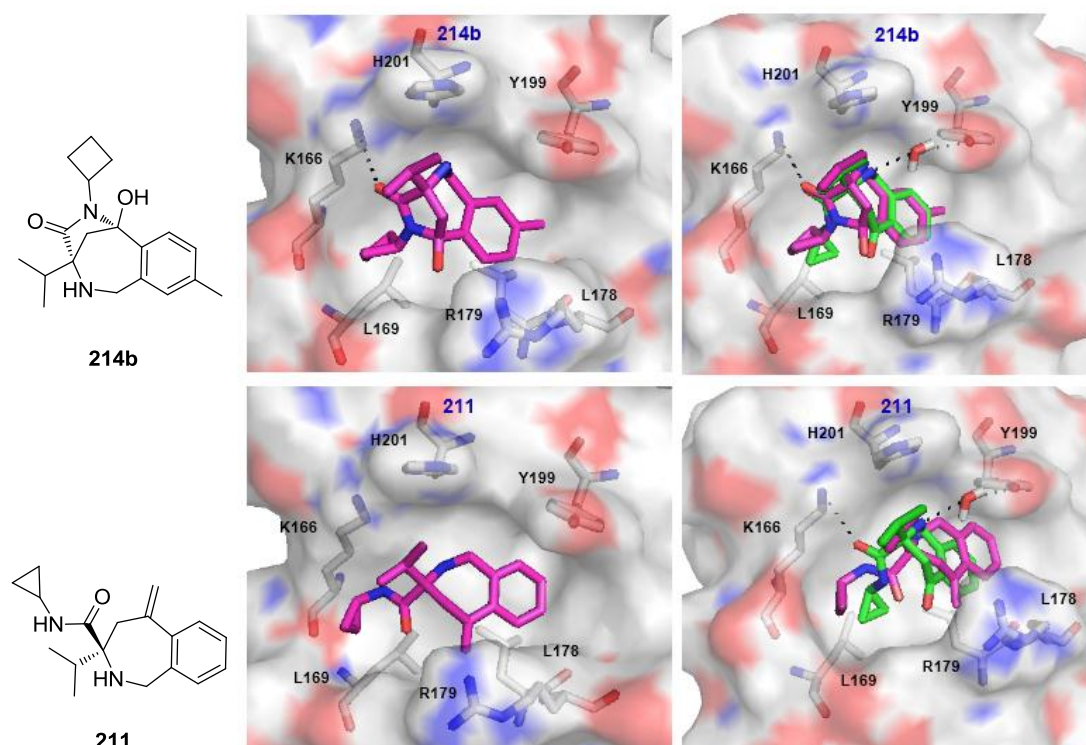


**Figure 42** The interactions of **214b** and **211** (pink) within the Aurora A ‘Y’ binding pocket as well as the overlaid hits with **214** (green). H-bonds formed between polar atoms of the fragment and nearby protein residues are marked using black dotted lines.

Through initial evaluation of crystal density of the hits shown in Figure 42, **214b** appears to be the most promising fragment within those screened against the Aurora A ‘Y’ pocket, producing electron density with clarity comparable to that of the initial hit molecule **214**. Although **214b** was isolated as the uncyclised ketone in its major form (see Section 4.5, Scheme 56), X-ray crystallography proves the active compound is in fact the hemiaminal structure.

The superior crystal structure of **214b** within the library of analogues is unsurprising since both **214b** and **214** contain the cyclic hemiaminal motif. Secondly, the binding poses of the two fragments overlap almost exactly, with the extra methyl substituent on the benzene ring of **214b** reinforcing hydrophobic interactions with L178. In addition, the larger cyclobutyl substituent on the amide of **214b** in place of the cyclopropyl group on **214** can further explore hydrophobic interactions with L169. Unsurprisingly, **211** produced weaker electron density than **214b**, and little overlap exists between its binding pose and that of **214**. This is due to the contrasting open chain

amide motif of **211** as well as the lack of polar atom in the alkenic position, resulting in reduced potential polar interactions.

#### 4.6.1 Future Hit Development

It would be worthwhile to further develop **214b** into a potent lead compound, and one way to do this might be to explore larger substituents on the benzene ring to optimise hydrophobic interactions with L178 in the Aurora A 'Y' pocket. Overlaying the binding modes of commercial fragment **256** with **214b** (Figure 43, a) shows an almost exact overlap between the benzene rings of the two fragments. The conserved position of the benzene groups in the binding cavity is due to hydrophobic interactions with protein residue L178 as well as the H-bond observed between R179 and the amide CO of **256**.

The addition of a small methyl substituent when developing **214** to **214b** simply grows the fragment in one plane. However, the use of larger substitutions on the benzene ring would be ideal in order to explore potential  $\pi$ -stacking interactions, exhibited between the benzimidazole ring of **256** and Y199. The position of the benzimidazole ring is also attributed to the amide CO of **256** interacting with R179, a useful motif to consider. It is clear in this case that the three-dimensional character of the molecule offers useful vectors along which to explore, and one of these might be functionalisation of the secondary amine, although challenges such as steric hindrance of the nitrogen centre must be considered. Another viable position for fragment growth could be on the bridging CH<sub>2</sub> of the 7-membered ring. Possible positions for further functionalisation of **214b** has been highlighted in yellow (Figure 43, b).

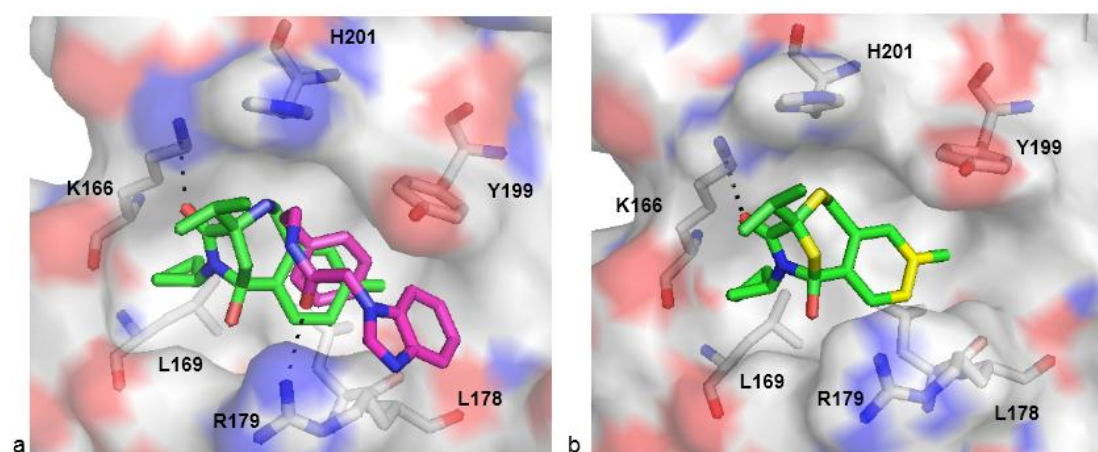


**Figure 43** a) The overlaid structures of commercial fragment **256** (pink) with analogue **214b** (green), where H-bonds are shown using black dotted lines. b) Analogue **214b** with key positions for further fragment growth highlighted in yellow. These include using larger substituents on the benzene ring, as well as substitutions on the amine NH and fragment growth via the bridging CH<sub>2</sub> of the 7-membered ring.

## 4.7 Project Summary

Within this project, a set of 80 shape-diverse fragments was selected, 20 of which were synthesised using two key Leeds chemistry methodologies and 60 of which were purchased commercially. These 80 molecules were successfully screened against the kinase target Aurora A using high-throughput X-ray crystallography. A total of ten hits was identified, nine of which belonged to the ZINC commercial library and one of which was from the Leeds library. The 'Y' binding site in Aurora A is of interest due to its known role in allosteric modulation of the protein target; **214** was found to target this key site along with five molecules from the ZINC commercial library. Four other fragments from the ZINC commercial library was found to target two other novel binding sites within Aurora A.

The hit compound **214** from the Leeds library was further developed through investigation of the 'Y' binding site for potential structure activity relationships. A library of ten molecules was synthesized and screened as a result- seven of which were analogues to **214**, two of which were intermediates to final fragments and one of which was the repeated synthesis of **214**. Five hits were identified from the X-ray screen of these ten molecules, in which the initial hit **214** was reconfirmed along with the alkene intermediate **211** and three analogue molecules. Evaluation of crystal densities of these binders allowed an initial hierarchy of fragment hits to be proposed, where analogue **214b** appears to bind comparably to **214**, allowing new opportunities for hit elaboration along useful vectors.

### 4.7.1 Wider Outlook

Based on the array of hits provided by the X-ray fragment screen it could be concluded that the library of 80 molecules was successful in its ability to investigate unexplored shape-space and present valuable hits against a worthwhile target. However, since a higher hit rate was produced by the commercial library, it could be argued that the increased 3-dimensionality of the Leeds library has yet to prove its value. Nevertheless, 80 is a small number for a screening collection compared to that generally used in industry and it is only possible to confirm this observation when a much larger fragment collection is used. In addition, it is necessary to branch out onto screening a wider range of targets in order to determine whether the fragments synthesised by myself add value to commercial fragments.

## 5 Experimental

### 5.1 General Experimental

All non-aqueous reactions were performed under an atmosphere of nitrogen. Solvents were removed *in vacuo* using a Büchi rotary evaporator and a Vacuubrand PC2001 Vario diaphragm pump. THF, DCM, MeOH, EtOH, toluene and MeCN were dried and purified by means of a Pure Solv MD solvent purification system (Innovative Technology Inc.). Anhydrous DMF, DMSO and 1,4-dioxane was obtained in Oxford sure/seal™ bottles from Sigma-Aldrich and all other solvents used were of chromatography or analytical grade. Quantities of solvents and wash solutions were calculated with respect to the limiting reagent. Commercially available starting materials were obtained from Acros Organics, Alfa Aesar, Fisher Scientific, Fluka, Fluorochem, Lancaster, Maybridge or Sigma-Aldrich. Several isocyanides and isocyanates were obtained from Insight Biotechnology and the majority of screening compounds were sourced from Enamine.

Ozonolysis was carried out using a LAB2B laboratory ozone generator (0.4-0.6 psi). Thin layer chromatography was carried out on aluminium backed silica (Merck silica gel 60 F254) plates supplied by Merck and visualisation of the plates was achieved using an ultraviolet lamp ( $\lambda_{\text{max}} = 254 \text{ nm}$ ), and  $\text{KMnO}_4$ . Flash chromatography was carried out using silica gel 60 (35-70  $\mu\text{m}$  particles). Infrared spectra were recorded on a Bruker Alpha-P ATR FT-IR spectrometer. Optical rotation measurements were carried out at the sodium D-line (589 nm) on an Optical Activity AA-1000 polarimeter instrument. Melting points were determined on a Reichert hot stage microscope and are uncorrected.

Proton, carbon and fluorine NMR data were collected on an Advance 500, Bruker DPX500, DPX400 and DPX300 spectrometer. All shifts were recorded against an internal standard of tetramethylsilane.  $\text{CDCl}_3$ , MeOD and  $\text{DMSO-d}_6$  used for NMR experiments were obtained from Sigma-Aldrich. Splitting patterns in this report have been recorded in an abbreviated manner; s (singlet), d (doublet), t (triplet), q (quartet), quint (quintet), hept (heptet) and m (multiplet). NMR data was recorded in the following format; ppm (number of protons, splitting pattern, coupling constant (Hz), proton ID). Signal assignments were made with the aid of DEPT 135, COSY, HMQC, HMBC and NOESY, and signals of substituents were assigned using the compound IUPAC name. Where the compound exists as a mixture of two different forms, numbering of substituents were completed via their major form.

Low resolution mass spectra data were recorded on an Agilent 1200 series LC system comprising a Bruker HCT Ultra ion trap mass spectrometer, a high vacuum degasser, a binary pump, a high performance autosampler, an autosampler thermostat, a thermostated column compartment and a diode array detector. The system used two 121 solvent systems; MeCN-H<sub>2</sub>O + 0.1% formic acid with a Phenomenex Luna C18 50 × 2 mm 5 micron column or MeCN-H<sub>2</sub>O with a Phenomenex Luna C18 50 × 2 mm 5 micron column. High resolution mass spectrometry, using electrospray ionisation, was recorded on a Bruker Maxis Impact.

## 5.2 General Procedures

### A. 2-Nitrobenzenesulfonyl protection

2-Nitrobenzenesulfonyl chloride (1.0 eq.) was added to a solution of the amino alcohol (1.05 eq.) and Na<sub>2</sub>CO<sub>3</sub> (1.05 eq.) in 1:1 H<sub>2</sub>O–DCM (0.8 M solution with respect to the limiting reagent). The resulting mixture was stirred at room temperature overnight before being acidified to pH<2 and extracted with DCM (3 × *ca.* 10 mL/mmol). The combined organic phases were washed with brine (*ca.* 10 mL/mmol), dried (MgSO<sub>4</sub>) and concentrated *in vacuo* to yield the crude product.

### B. Boc-protection

Boc<sub>2</sub>O (1.0 eq.) was slowly added to a solution of the amine (1.0 eq.) in DCM (0.3 M solution with respect to the limiting reagent) at 0 °C and the resulting solution was warmed to room temperature and stirred overnight. The residue was diluted with sat. K<sub>2</sub>CO<sub>3</sub> (0.3 M solution with respect to the limiting reagent) and stirred for 2 hr to remove excess Boc<sub>2</sub>O, before being diluted with water. The aqueous layer was extracted with DCM (3 × *ca.* 10 mL/mmol) and the combined organic phases were washed with sat. K<sub>2</sub>CO<sub>3</sub> (*ca.* 10 mL/mmol), water (*ca.* 10 mL/mmol), brine (*ca.* 10 mL/mmol), dried (MgSO<sub>4</sub>), and concentrated *in vacuo* to yield the crude product.

### C. Epoxide ring-opening

A solution of 4-methoxybenzylamine (4.0 eq.) and the epoxide (1.0 eq.) was stirred at 60 °C for 3 hr. The reaction mixture was diluted with 1:1 MeOH–DCM (*ca.* 10 mL/mmol), filtered and the solid collected to yield the crude product.

### D. Cyclic sulfamidate ring formation

The protected amine (1.0 eq.) in DCM (0.8 M solution with respect to the limiting reagent) was added slowly to a stirred solution of SOCl<sub>2</sub> (1.1 eq.), Et<sub>3</sub>N (2.2 eq.) and imidazole (4.0 eq.) in DCM (0.2 M solution with respect to the limiting reagent), at –60 °C. The reaction mixture was stirred at –60 °C for 3 hr then at room temperature overnight, before being quenched with water. The aqueous phase was extracted with DCM (3 × *ca.* 10 mL/mmol) and the combined organic phases were washed with brine (*ca.* 10 mL/mmol), dried (MgSO<sub>4</sub>), and concentrated *in vacuo* to give the crude cyclic sulfamidite. The residue was dissolved in MeCN (0.3 M solution with respect to the

limiting reagent) and cooled to 0 °C before NaIO<sub>4</sub> (2.0 eq.), RuCl<sub>3</sub>·3H<sub>2</sub>O (0.1 mol%) and water (0.3 M solution with respect to the limiting reagent) were added sequentially and the resulting mixture stirred for 4 hr. The reaction mixture was diluted with water (*ca.* 10 mL/mmol) and the aqueous phase was extracted with Et<sub>2</sub>O (3 × *ca.* 10 mL/mmol). The combined organic phases were washed with brine (*ca.* 10 mL/mmol), dried (MgSO<sub>4</sub>), and concentrated *in vacuo* to yield the crude product.

#### E. Alkynyl sulfonamide formation

DEAD (1.3 eq.) was added to a solution of the alcohol (1.0 eq.), sulfonamide (1.1 eq.) and PPh<sub>3</sub> (1.3 eq.) in THF (0.1 M solution with respect to the limiting reagent) at 0 °C. The resulting solution was warmed to room temperature and stirred overnight, before being concentrated *in vacuo* to give a residue which was purified by flash chromatography (SiO<sub>2</sub>, 25:25:50 Petrol–Et<sub>2</sub>O–CHCl<sub>3</sub>). TFA (10 eq.) was added to a solution of the intermediate sulfonamide in DCM (0.1 M solution with respect to the limiting reagent) at room temperature and stirred overnight. The reaction mixture was quenched by addition of sat. K<sub>2</sub>CO<sub>3</sub> to pH>11 and the organic layer was extracted with DCM (3 × *ca.* 10 mL/mmol). The combined organic phases were washed with brine (*ca.* 10 mL/mmol), dried (MgSO<sub>4</sub>), and concentrated *in vacuo* to yield the crude product.

#### F. Cyclic sulfamidate ring opening

NaH (60% in oil, 1.1 eq.) was added to a solution of the sulfonamide (1.1 eq.) in DMF (0.2 M solution with respect to the limiting reagent) and stirred for 10 min. The cyclic sulfamidate (1.0 eq.) was added and the resulting solution was stirred at room temperature overnight. The reaction mixture was cooled to 0 °C, acidified with aq. HCl (5 M, 6 eq.), stirred for 1 hr and basified to pH>12 with sat. K<sub>2</sub>CO<sub>3</sub>. The aqueous layer was extracted with EtOAc (3 × *ca.* 10 mL/mmol), the combined organic phases were washed with brine (*ca.* 10 mL/mmol), dried (MgSO<sub>4</sub>) and concentrated *in vacuo* to give the crude product.

#### G. Gold-mediated alkyne hydration

Au(IPr)Cl (1 mol%), AgSbF<sub>6</sub> (1 mol%) and the sulfonamide (1.0 eq.) were combined in 1,4-dioxane (0.5 M solution with respect to the limiting reagent). Water (0.8 M solution with respect to the limiting reagent) was added, and the resulting solution was stirred at 100 °C overnight. The reaction mixture was cooled to room temperature and concentrated *in vacuo* to yield the crude product.

#### H. Gold-mediated hydroamination

Au(PPh<sub>3</sub>)Cl (5 mol%), AgSbF<sub>6</sub> (5 mol%) and the sulfonamide (1.0 eq.) were combined in 1,4-dioxane (0.2 M solution with respect to the limiting reagent) and stirred at 100 °C overnight. The reaction mixture was cooled to room temperature and concentrated *in vacuo* to give the crude product.

#### I. Allylic amination

<sup>n</sup>BuNH<sub>2</sub> (4 mol%) was added to a solution of [Ir(dbcot)Cl]<sub>2</sub> (2 mol%) and phosphoramidite (4 mol%) in DMSO (1.0 M solution with respect to the limiting reagent). The mixture was stirred and heated to 60 °C for 30 min. A solution of the allylic carbonate (1.0 eq.) and the amine (1.3 eq.) in DMSO (2.0 M solution with respect to the limiting reagent) was added and the resulting reaction mixture was stirred at 60 °C overnight, before being purified by basic SCX cartridge to give the crude product.

#### J. Cbz-protection

CbzCl (1.05 eq.) was added dropwise to a suspension of the amine (1.0 eq.) and NaHCO<sub>3</sub> (2.0 eq.) in 1:1 THF–H<sub>2</sub>O (0.15 M solution with respect to the limiting reagent) at 0 °C and the resulting solution was warmed to room temperature and stirred overnight. The reaction mixture was acidified with HCl (1M) to pH<2 and extracted with EtOAc (3 × *ca.* 10 mL/mmol). The combined organic phases were washed with brine (*ca.* 10 mL/mmol), dried (MgSO<sub>4</sub>) and concentrated *in vacuo* to give the crude product.

#### K. Ugi reaction

TFA (6.0 eq.) was added to a solution of the substrate (1.0 eq.) in DCM (0.1 M solution with respect to the limiting reagent) at room temperature, and stirred overnight. The crude reaction mixture was concentrated *in vacuo* to give an intermediate TFA salt. The isocyanide (2.0 eq.) was added to a solution of the salt in EtOH (0.05 M solution with respect to the limiting reagent) at 0 °C and stirred at room temperature overnight. The reaction mixture was concentrated *in vacuo* to give the crude product.

#### L. Trifluoroacetamide reduction

NaBH<sub>4</sub> (7.0 eq.) was added to a solution of the protected diazepane (1.0 eq.) in MeOH (0.1 M solution with respect to the limiting reagent) at 0 °C. The reaction mixture was stirred at room temperature overnight before the solvent was removed *in vacuo* and the residue was treated with water (*ca.* 10 mL/mmol). The aqueous layer was extracted

with EtOAc ( $3 \times ca. 10 \text{ mL/mmol}$ ) and the combined organic phases were dried ( $\text{MgSO}_4$ ) and concentrated *in vacuo*.

#### M. Reductive amination

The aldehyde (4.0 eq. if commercial, 1.0 eq. if novel) and  $\text{NaBH}(\text{OAc})_3$  (6.0 eq.) was added to a solution of the amine (1.0 eq. if novel, 4.0 eq. if commercial) in DCM (0.1 M solution with respect to the limiting reagent), and the reaction was stirred at room temperature overnight. Water (*ca.* 10 mL/mmol) was added and the aqueous layer was extracted with DCM ( $3 \times ca. 10 \text{ mL/mmol}$ ). The combined organic phases were washed with brine (*ca.* 10 mL/mmol), dried ( $\text{MgSO}_4$ ) and concentrated *in vacuo*.

#### N. Reductive amination (II)

The aldehyde (2.0 eq.) was added to a mixture of the amino ester (1.0 eq.) in DCM (0.1 M solution with respect to the limiting reagent) in the presence of 4 Å mol. sieves (0.2 w/w).  $\text{NaBH}(\text{OAc})_3$  (6.0 eq.) was added and the mixture stirred at reflux overnight. Water (*ca.* 10 mL/mmol) was added and the aqueous layer was extracted with DCM ( $3 \times ca. 10 \text{ mL/mmol}$ ). The combined organic layers were washed with water (*ca.* 10 mL/mmol), dried ( $\text{MgSO}_4$ ) and concentrated *in vacuo*.

#### O. 2-Nitrobenzenesulfonyl deprotection

$\text{K}_2\text{CO}_3$  (1.5 eq.) was added to a stirred solution of the protected diazepane (1.0 eq.) and PhSH (1.5 eq.) in MeCN (0.1 M solution with respect to the limiting reagent), and the mixture was stirred at room temperature until completion was observed by TLC. Excess  $\text{K}_2\text{CO}_3$  was removed by filtration and the reaction mixture was concentrated *in vacuo* to yield the crude product.

#### P. Amino ester allylation

Benzaldehyde (1.0 eq.) was added to a suspension of the methyl ester hydrochloride (1.0 eq.),  $\text{Et}_3\text{N}$  (1.0 eq.) and 4 Å mol. sieves (0.2 w/w) in THF (0.2 M solution with respect to the limiting reagent). The reaction mixture was stirred overnight before being filtered and concentrated *in vacuo*. The residue was dissolved in THF (0.2 M solution with respect to the limiting reagent) and LiHMDS (1 M in THF, 3.0 eq.) was added dropwise at  $-78^\circ\text{C}$ . The reaction mixture was stirred for 15 min then allyl iodide (1.5 eq.) was added dropwise. The reaction mixture was stirred at  $-78^\circ\text{C}$  for 1 hr and at room temperature overnight. Citric acid (30 wt% in water, 0.2 M solution with respect to the

limiting reagent) was added and the reaction was stirred for 1 hr before being partitioned with Et<sub>2</sub>O (3 × *ca.* 10 mL/mmol). The aqueous layer was neutralised with NaHCO<sub>3(s)</sub> and extracted with DCM (3 × *ca.* 10 mL/mmol). The combined organic layers were dried (MgSO<sub>4</sub>) and concentrated *in vacuo* to give the crude product.

#### Q. Urea formation

Et<sub>3</sub>N (2 eq.) and the isocyanate (1.5 eq.) were added to a solution of the amine (1.0 eq.) in DCM (0.1 M solution with respect to the limiting reagent) at 0 °C. The reaction mixture was stirred for 1 hr at 0 °C and then at room temperature overnight. The reaction mixture was diluted with water (*ca.* 10 mL/mmol) and the aqueous layer was extracted with DCM (3 × *ca.* 10 mL/mmol). The combined organic layers were washed with water (*ca.* 10 mL/mmol), brine (*ca.* 10 mL/mmol), dried (MgSO<sub>4</sub>) and concentrated *in vacuo* to give the crude product.

#### R. Hydantoin formation

NaO<sup>t</sup>Bu (1.0 eq.) was added to a solution of the urea (1.0 eq.) in toluene (0.1 M solution with respect to the limiting reagent) and the reaction mixture was stirred at 100 °C for 8 hr, before being concentrated *in vacuo* to give the crude product.

#### S. Heck reaction

Et<sub>3</sub>N (2.5 eq.) was added to a stirred solution of the amino ester (1.0 eq.) and Pd(PPh<sub>3</sub>)<sub>4</sub> (10 mol%) in MeCN (0.1 M solution with respect to the limiting reagent). The reaction mixture was heated at 125 °C under μW for 1 hr before being concentrated *in vacuo*.

#### T. Acylation

Et<sub>3</sub>N (2.0 eq.) was added to a solution of the amine (1.0 eq.) and the acid chloride (2.0 eq.) in DCM (0.4 M solution with respect to the limiting reagent) at 0 °C. DMAP (1 mol%) was added and the reaction was stirred at room temperature overnight. The solvent was removed *in vacuo* to give the crude product.

#### U. Ozonolysis

The alkene (1.0 eq.) was dissolved in DCM (0.1 M solution with respect to the limiting reagent) and O<sub>3</sub> was bubbled through the solution at -78 °C until saturation was indicated by the appearance of a blue solution, and then stirred for a further 10 min. The

solution was purged with O<sub>2</sub> until it turned colourless, before DMS (1.1 eq.) was added and the reaction mixture stirred overnight. Water (*ca.* 10 mL/mmol) was added and the aqueous layer was extracted with DCM (3 × *ca.* 10 mL/mmol), the combined organic layers were dried (MgSO<sub>4</sub>) and concentrated *in vacuo* to give the crude product.

#### V. Amide coupling

The amino ester (1.0 eq.) was dissolved in DMF (0.1 M solution with respect to the limiting reagent) and NaOH (6.0 eq.) was added. The reaction mixture was stirred at reflux overnight before being cooled to room temperature. Et<sub>3</sub>N (3.0 eq.) and the amine (10 eq.) was added to the solution, before TBTU (1.5 eq.) was then added and the reaction mixture stirred overnight. Water (*ca.* 10 mL/mmol) and EtOAc (*ca.* 10 mL/mmol) were added and the aqueous layer was extracted with EtOAc (3 × *ca.* 10 mL/mmol). The combined organic layers were washed with water (3 × *ca.* 10 mL/mmol), brine (3 × *ca.* 10 mL/mmol), dried (MgSO<sub>4</sub>) and concentrated *in vacuo*.

#### W. Osmium-mediated dihydroxylation and oxidative cleavage

Potassium osmate dihydrate (1 mol%) was added to a solution of the alkene (1.0 eq.) and NMO (1.3 eq.) in a mixture of acetone (0.7 M solution with respect to the limiting reagent) and water (6 M solution with respect to the limiting reagent), and the mixture was stirred overnight at room temperature. Sodium hydrosulfite (*ca.* 100 mg/mmol) was added and the mixture stirred for 30 min before being filtered through Celite. The filtrate was concentrated *in vacuo* and dissolved in a mixture of MeOH (0.5 M solution with respect to the limiting reagent) and water (5 M solution with respect to the limiting reagent). NaIO<sub>4</sub> (1.5 eq.) was added and the reaction mixture stirred overnight, before being concentrated *in vacuo* to yield the crude product.

#### X. Osmium-mediated dihydroxylation and oxidative cleavage (II)

Potassium osmate dihydrate (1 mol%) was added to a solution of the alkene (1.0 eq.) and NMO (1.3 eq.) in a mixture of acetone (0.7 M solution with respect to the limiting reagent) and water (6 M solution with respect to the limiting reagent), and the mixture was stirred overnight at room temperature. Sodium hydrosulfite (*ca.* 100 mg/mmol) was added and the mixture stirred for 30 min before being filtered through Celite. The filtrate was concentrated *in vacuo* and dissolved in a mixture of MeOH (0.5 M solution with respect to the limiting reagent) and water (5 M solution with respect to the limiting reagent). NaIO<sub>4</sub> (4.0 eq.) was added and the reaction mixture stirred for

ten minutes before water (*ca.* 10 mL/mmol) and EtOAc (*ca.* 10 mL/mmol) were added. The aqueous layer was extracted with EtOAc (3 × *ca.* 10 mL/mmol) and the combined organic layers were washed with water (*ca.* 10 mL/mmol), brine (*ca.* 10 mL/mmol), dried (MgSO<sub>4</sub>) and concentrated *in vacuo*.

#### Y. Boc-deprotection

The protected amine (1 eq.) was dissolved in TFA (0.1 M solution with respect to the limiting reagent) and stirred at room temperature overnight. The reaction mixture was concentrated *in vacuo* and purified by basic SCX cartridge.

### 5.3 High-Throughput Protein Crystallography

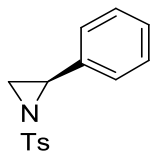
High-throughput protein crystallography was completed at Diamond Light Source (Harwell, UK) by Dr. Daniel Foley (University of Leeds) and Patrick McIntyre (University of Leicester), with the assistance of Dr. Patrick Collins (Diamond Light Source).

Protein crystals were soaked with individual fragments; Aurora A was used at 450  $\mu$ M concentration in combination with 5mM ADP. The protein buffer used was 20 mM tris at pH 7.0, 200 mM NaCl, 5 mM MgCl<sub>2</sub> and 10% glycerol. The protein solution was mixed in a 1:1 ratio with the crystallisation buffer which contained 100 mM tris at pH 8.5, 500 mM NaCl, 200 mM MgCl<sub>2</sub> and 32.5% PEG 3350. The stock concentration of the commercial fragments was 200 mM, soaked at a final concentration of 80 mM, and the stock concentration of the Leeds fragments was 500 mM, soaked at a final concentration of 200 mM. Both sets of compounds contained 40% deuterated DMSO.

200 nL droplets were used for diffraction and image resolution was 2.2 Å on average. X-ray diffraction data were collected on beamline I04-1 at the Diamond Light Source and processed using XChem Explorer and PanDDA (Pan-Dataset Density Analysis).<sup>115</sup> Where racemates were screened, both enantiomers were fitted to the electron density in the PanDDA event maps using COOT (Crystallographic Object-Oriented Toolkit),<sup>119</sup> then the enantiomer with the best fit was chosen.

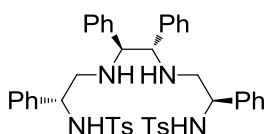
## 5.4 Synthesis of Building Blocks

### (2R)-1-(4-Methylbenzenesulfonyl)-2-phenylaziridine, **225**



Tosyl chloride (3.06 g, 16.0 mmol) was added slowly to a solution of (*R*)-2-phenylglycinol (1.00 g, 7.29 mmol) and  $K_2CO_3$  (4.03 g, 29.2 mmol) in MeCN (70 mL, 0.1 M) and stirred at room temperature overnight. Toluene (35 mL) was added and any solid was removed by filtration. The filtrate was concentrated *in vacuo* to give a crude residue which was purified by flash chromatography ( $SiO_2$ , 60:40 Petrol–EtOAc) to yield the aziridine<sup>120</sup> **225** (1.21 g, 61%) as a white solid,  $R_f = 0.53$  (40:60 Petrol–EtOAc);  $\delta_H$  (500 MHz,  $CDCl_3$ ) 7.64 (2H, d,  $J$  8.3, tolyl 2-H and tolyl 6-H), 7.25–7.22 (3H, m, phenyl 3-H, phenyl 4-H and phenyl 5-H), 7.20 (2H, d,  $J$  8.3, tolyl 3-H and tolyl 5-H), 7.12 (2H, dd,  $J$  6.3 and 3.2, phenyl 2-H and phenyl 6-H), 5.50 (1H, d,  $J$  6.7, 3- $H_a$ ), 4.44 (1H, dd,  $J$  11.4 and 6.7, 3- $H_b$ ), 3.79–3.76 (1H, m, 2-H) and 2.40 (3H, s, methyl);  $\delta_C$  (126 MHz,  $CDCl_3$ ) 143.4 (tolyl C-1), 137.9–137.6 (1H, m, 2-H) and 2.40 (3H, s, methyl);  $\delta_C$  (126 MHz,  $CDCl_3$ ) 143.4 (tolyl C-1), 137.6 (tolyl C-4), 137.1 (phenyl C-1), 129.5 (phenyl C-3 and phenyl C-5), 128.6 (phenyl C-2 and phenyl C-6), 128.0 (phenyl C-4), 127.2 (tolyl C-2 and tolyl C-6), 126.9 (tolyl C-3 and tolyl C-5), 66.3 (C-2), 59.5 (C-3) and 21.5 (methyl).

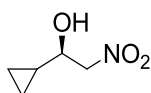
### 4-Methyl-*N*-[(1*R*)-2-[(1*S*, 2*S*)-2-[(2*R*)-2-(4-methylbenzenesulfonamido)-2-phenylethyl] amino]-1,2-diphenylethyl] amino]-1-phenylethyl] benzene-1-sulfonamido, **226**



(1*S*, 2*S*)-1,2-diphenylethane-1,2-diamine (471 mg, 2.22 mmol) was added to the aziridine **225** (1.21 g, 4.43 mmol) in MeCN (50 mL, ~0.1 M) and stirred at reflux overnight. The solvent was removed *in vacuo* to give the tetramine<sup>121</sup> **226** (1.68 g, 100%) as a bright yellow solid which was used without purification,  $R_f = 0.72$  (80:20 Petrol–EtOAc);  $\delta_H$  (500 MHz,  $CDCl_3$ ) 7.63 (4H, d,  $J$  8.2, tolyl 2- $H_2$  and tolyl 6- $H_2$ ), 7.33–7.25 (10H, m, ethylphenyl 2- $H_2$ , ethylphenyl 3- $H_2$ , ethylphenyl 5- $H_2$ , ethyldiphenyl 3- $H_2$  and ethyldiphenyl 5- $H_2$ ), 7.25–7.21 (6H, m, ethylphenyl 6- $H_2$ , ethyldiphenyl 2- $H_2$  and ethyldiphenyl 6- $H_2$ ), 7.19 (4H, d,  $J$  8.2, tolyl 3- $H_2$  and tolyl 5- $H_2$ ), 7.15–7.09 (4H, m, ethylphenyl 4- $H_2$  and ethyldiphenyl 4- $H_2$ ),

4.48-4.39 (2H, m, phenylethyl 1-H<sub>2</sub>), 4.12 (2H, s, diphenylethyl 1-H<sub>2</sub>), 3.79-3.70 (4H, m, phenylethyl 2-H<sub>4</sub>) and 2.40 (6H, s, methyl), analysis given to one of the two identical halves of the molecule;  $\delta_{\text{C}}$  (126 MHz, CDCl<sub>3</sub>) 143.3 (tolyl C-1), 143.0 (ethylphenyl C-1), 137.7 (ethyldiphenyl C-1), 137.2 (tolyl C-4), 129.5 (tolyl C-2 and tolyl C-6), 128.6 (ethylphenyl C-3 and ethylphenyl C-5), 128.3 (ethyldiphenyl C-3 and ethyldiphenyl C-5), 127.9 (ethylphenyl C-4), 127.2 (ethylphenyl C-2 and ethylphenyl C-6), 127.2 (ethyldiphenyl C-4), 126.9 (ethyldiphenyl C-2 and ethyldiphenyl C-6), 126.9 (tolyl C-3 and tolyl C-5), 66.1 (phenylethyl C-2), 61.8 (diphenylethyl C-1), 59.6 (phenylethyl C-1) and 21.5 (methyl), analysis given to one of the two identical halves of the molecule.

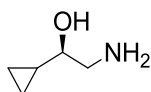
### (1R)-1-Cyclopropyl-2-nitroethan-1-ol, **228**



The ligand **226** (330 mg, 2.5 mol%) and Cu(OAc)<sub>2</sub>·H<sub>2</sub>O (86.8 mg, 2.5 mol%) were suspended in EtOH (30 mL, ~0.5 M) and stirred at room temperature for 30 min. Cyclopropyl carboxaldehyde (1.29 mL, 17.2 mmol), then nitromethane (9.32 mL, 172 mmol) were added and stirred overnight. The reaction mixture was concentrated *in vacuo* and purified by flash chromatography (SiO<sub>2</sub>, 60:40 Petrol-EtOAc) to yield the *nitroalcohol* **228** (670 mg, 30%) as a colourless oil,  $R_{\text{f}} = 0.55$  (60:40 Petrol-EtOAc);  $\nu_{\text{max}}/\text{cm}^{-1}$  (ATR) 3397 (br), 3010, 1247, 1378, 1079, 1051 and 1024;  $[\alpha]_{\text{D}}^{24} -0.19$  ( $c = 1.90$ , CHCl<sub>3</sub>);  $\delta_{\text{H}}$  (500 MHz, CDCl<sub>3</sub>) 4.58-4.48 (2H, m, 2-H<sub>2</sub>), 3.65 (1H, td,  $J$  8.2 and 4.1, 1-H), 2.96 (1H, br s, OH), 1.00-0.87 (1H, m, cyclopropyl 1-H), 0.66-0.56 (2H, m, cyclopropyl 2-H<sub>2</sub>), 0.48-0.43 (1H, m, cyclopropyl 3-H<sub>a</sub>) and 0.36-0.30 (1H, m, cyclopropyl 3-H<sub>b</sub>);  $\delta_{\text{C}}$  (126 MHz, CDCl<sub>3</sub>) 80.4 (C-2), 73.0 (C-1), 14.3 (cyclopropyl C-1), 3.1 (cyclopropyl C-2) and 2.2 (cyclopropyl C-3); HRMS found  $[2\text{M}]^{\text{H}^+}$ , 263.1544. C<sub>5</sub>H<sub>9</sub>NO<sub>3</sub> requires  $[2\text{M}]^{\text{H}}$ , 263.1242.

*ee.* not determined in this case; an example *ee.* can be seen in literature<sup>122</sup>.

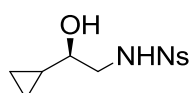
### (1R)-2-Amino-1-cyclopropylethan-1-ol, **229**



NaBH<sub>4</sub> (1.03 g, 27.2 mmol) was added to a suspension of nitroalcohol **228** (890 mg, 6.79 mmol) and Pd/C (361 mg, 5 mol%) in 1:1 MeOH-THF (70 mL, 0.1 M) at 0 °C. The reaction mixture was stirred at 0 °C for 2 hr and then at room temperature overnight, before being filtered through Celite and washed with MeOH. The filtrate was concentrated *in vacuo* and the residue was purified by flash chromatography (SiO<sub>2</sub>, 20:80

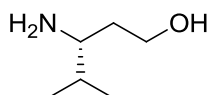
sat.  $\text{NH}_3$  in MeOH-DCM) to yield the *amino alcohol* **229** (450 mg, 66%) as a colourless oil,  $R_f = 0.63$  (30:70 sat.  $\text{NH}_3$  in MeOH-DCM);  $[\alpha]_D^{24} -0.87$  ( $c = 0.51$ ,  $\text{CHCl}_3$ );  $\nu_{\text{max}}/\text{cm}^{-1}$  (ATR) 3348 (br), 2954, 1643, 1393, 1274, 1121 and 1017;  $\delta_{\text{H}}$  (500 MHz,  $\text{CDCl}_3$ ) 2.74 (1H, d,  $J$  11.1, 2- $\text{H}_a$ ), 2.64 (1H, td,  $J$  8.2 and 3.3, 1-H), 2.51 (1H, dd,  $J$  11.1 and 8.2, 2- $\text{H}_b$ ), 1.84 (3H, br s,  $\text{NH}_2$  and OH), 0.74-0.56 (1H, m, cyclopropyl 1-H), 0.36-0.23 (2H, m, cyclopropyl 2- $\text{H}_2$ ), 0.13 (1H, ddd,  $J$  8.9, 6.6 and 4.0, cyclopropyl 3- $\text{H}_a$ ) and 0.00 (1H, dt,  $J$  8.9 and 4.7, cyclopropyl 3- $\text{H}_b$ );  $\delta_{\text{C}}$  (126 MHz,  $\text{CDCl}_3$ ) 76.7 (C-1), 47.3 (C-2), 15.0 (cyclopropyl C-1), 2.4 (cyclopropyl C-2) and 1.8 (cyclopropyl C-3).

### (2R)-2-Cyclopropyl-2-hydroxy-5-(4-nitrophenyl)ethane-1-sulfonamido, **230**



By general procedure A, amino alcohol **229** (160 mg, 1.58 mmol) gave the protected *amino alcohol* **230** (370 mg, 86%) as a yellow oil which was used without further purification,  $R_f = 0.54$  (30:70 Petrol-EtOAc);  $\nu_{\text{max}}/\text{cm}^{-1}$  (ATR) 3527 (br), 3342 (br), 2883, 1537, 1360, 1337 and 1163;  $[\alpha]_D^{25} 0.11$  ( $c = 0.53$ ,  $\text{CHCl}_3$ );  $\delta_{\text{H}}$  (500 MHz,  $\text{CDCl}_3$ ) 8.19-8.15 (1H, m, nitrophenyl 3-H), 7.93-7.87 (1H, m, nitrophenyl 6-H), 7.81-7.74 (2H, m, nitrophenyl 4-H and nitrophenyl 5-H), 5.82 (1H, t,  $J$  4.3, NH), 3.39 (1H, ddd,  $J$  12.6, 7.5 and 4.3, 1- $\text{H}_a$ ), 3.16 (1H, ddd,  $J$  12.6, 7.5 and 4.3, 1- $\text{H}_b$ ), 3.06 (1H, td,  $J$  7.5 and 3.3, 2-H), 1.89 (1H, br s, OH), 0.99-0.84 (1H, m, cyclopropyl 1-H), 0.60-0.51 (2H, m, cyclopropyl 2- $\text{H}_2$ ), 0.37-0.32 (1H, m, cyclopropyl 3- $\text{H}_a$ ) and 0.29-0.25 (1H, m, cyclopropyl 3- $\text{H}_b$ );  $\delta_{\text{C}}$  (126 MHz,  $\text{CDCl}_3$ ) 148.1 (nitrophenyl C-2), 133.64 (nitrophenyl C-1), 133.58 (nitrophenyl C-5), 132.7 (nitrophenyl C-4), 131.1 (nitrophenyl C-6), 125.4 (nitrophenyl C-3), 75.0 (C-2), 48.9 (C-1), 15.1 (cyclopropyl C-1), 2.7 (cyclopropyl C-2) and 2.3 (cyclopropyl C-3); HRMS found  $\text{MH}^+$ , 287.0693.  $\text{C}_{11}\text{H}_{14}\text{N}_2\text{O}_5\text{S}$  requires  $\text{MH}$ , 287.0701.

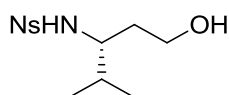
### (3R)-3-Amino-4-methylpentan-1-ol, **218**



Homovaline (2.50 g, 19.1 mmol) in THF (50 mL, ~0.4 M) was added dropwise to  $\text{LiAlH}_4$  (7.20 g, 191 mmol) in THF (150 mL, ~0.1 M) at 0 °C. The reaction mixture was warmed to reflux and heated at reflux overnight before being cooled to 0 °C. The reaction mixture was quenched with water (8 mL), followed by 4 M NaOH (8 mL), then water (24 mL), and stirred for 30 min. The mixture was filtered and the filtrate concentrated *in vacuo* to give a residue which was purified by flash chromatography ( $\text{SiO}_2$ , 15:85 sat.  $\text{NH}_3$

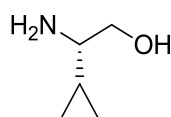
in MeOH–DCM) to yield the amino alcohol<sup>123</sup> **218** (370 mg, 17%) as a colourless amorphous solid,  $R_f = 0.42$  (20:80 sat.  $\text{NH}_3$  in MeOH–DCM);  $\delta_{\text{H}}$  (500 MHz,  $\text{CDCl}_3$ ) 3.81–3.68 (2H, m, 1- $\text{H}_2$ ), 2.77 (3H, br s,  $\text{NH}_2$ , OH), 2.63 (1H, ddd,  $J$  10.5, 5.0 and 2.7, 3-H), 1.59–1.48 (2H, m, 2- $\text{H}_2$ ), 1.47–1.36 (1H, m, 4-H), 0.84 (3H, d,  $J$  6.7, 5- $\text{H}_3$ ) and 0.81 (3H, d,  $J$  6.7, methyl);  $\delta_{\text{C}}$  (126 MHz,  $\text{CDCl}_3$ ) 62.6 (C-1), 57.8 (C-3), 35.1 (C-4), 34.6 (C-2), 18.6 (C-5) and 17.2 (methyl);  $m/z$  (ES) 118.2 (80%,  $\text{MH}^+$ ) and 217.3 (100%).

### (3R)-1-Hydroxy-4-methyl-5-(2-nitrophenyl)pentane-3-sulfonamido, **219**



By general procedure A, amino alcohol **218** (370 mg, 3.16 mmol) gave the protected *amino alcohol* **219** (660 mg, 69%) as a colourless solid which was used without further purification, m.p. 110–112 °C;  $R_f = 0.38$  (40:60 Petrol–EtOAc);  $\nu_{\text{max}}$ /  $\text{cm}^{-1}$  (ATR) 3339 (br), 2962, 2877, 1539, 1362, 1164 and 600;  $[\alpha]_{\text{D}}^{28}$  152 ( $c = 0.23$ ,  $\text{CHCl}_3$ );  $\delta_{\text{H}}$  (500 MHz,  $\text{CDCl}_3$ ) 8.20–8.12 (1H, m, nitrophenyl 3-H), 7.93–7.86 (1H, m, nitrophenyl 6-H), 7.81–7.68 (2H, m, nitrophenyl 4-H and nitrophenyl 5-H), 5.36 (1H, d,  $J$  9.0, NH), 3.93–3.78 (1H, m, 3-H), 3.77–3.67 (1H, m, 1- $\text{H}_a$ ), 3.64–3.51 (1H, m, 1- $\text{H}_b$ ), 2.18 (1H, t,  $J$  6.0, OH), 1.85–1.77 (1H, m, 2- $\text{H}_a$ ), 1.77–1.70 (1H, m, 2- $\text{H}_b$ ), 1.60–1.49 (1H, m, 4-H), 0.85 (3H, d,  $J$  6.9, 5- $\text{H}_3$ ) and 0.77 (3H, d,  $J$  6.8, methyl);  $\delta_{\text{C}}$  (126 MHz,  $\text{CDCl}_3$ ) 147.9 (nitrophenyl C-2), 135.4 (nitrophenyl C-1), 133.2 (nitrophenyl C-5), 132.7 (nitrophenyl C-4), 130.3 (nitrophenyl C-6), 125.2 (nitrophenyl C-3), 58.8 (C-1), 57.6 (C-3), 35.1 (C-2), 32.3 (C-4), 18.7 (C-5) and 17.8 (methyl); HRMS found  $\text{MH}^+$ , 303.1020.  $\text{C}_{12}\text{H}_{18}\text{N}_2\text{O}_5\text{S}$  requires  $\text{MH}$ , 303.1014.

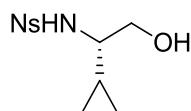
### (S)-2-Amino-2-cyclopropylethanol, **221**



L-Cyclopropylglycine (0.380 mL, 4.30 mmol) was dissolved in THF (5 mL, 1 M) and cooled to 0 °C.  $\text{LiAlH}_4$  (8.69 mL, 1 M in THF) was added dropwise and the reaction mixture warmed to room temperature and stirred at room temperature overnight. Water (5 mL) was added to quench the reaction mixture along with Celite (1 g), before any solid was removed by filtration through a pad of Celite. The filtrate was concentrated *in vacuo* to yield the amino alcohol<sup>124</sup> **221** (242 mg, 55%) as a yellow oil which was used without further purification,  $\nu_{\text{max}}$ /  $\text{cm}^{-1}$  (ATR) 3349 (br), 3280, 3002, 2862, 1584, 1372, 1049 and 1017;  $\delta_{\text{H}}$  (300 MHz,  $\text{CDCl}_3$ ) 3.69 (1H, dd,  $J$  10.6 and 3.9, 1- $\text{H}_a$ ), 3.44 (1H, dd,  $J$  10.6 and 7.8, 1- $\text{H}_b$ ), 2.10 (1H, ddd,  $J$  8.8, 7.8 and 3.9, 2-H), 1.99 (3H, br s,  $\text{NH}_2$ , OH), 0.82–0.65 (1H, m,

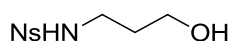
cyclopropyl 1-H), 0.54-0.43 (2H, m, cyclopropyl 2-H<sub>2</sub>) and 0.25-0.13 (2H, m, cyclopropyl 3-H<sub>2</sub>);  $\delta_c$  (126 MHz, CDCl<sub>3</sub>) 66.8 (C-1), 57.9 (C-2), 15.2 (cyclopropyl C-1), 2.5 (cyclopropyl C-2) and 2.2 (cyclopropyl C-3); HRMS found MH<sup>+</sup>, 102.0909. C<sub>5</sub>H<sub>11</sub>NO requires *MH*, 102.0919.

### (1S)-1-Cyclopropyl-2-hydroxy-S-(2-nitrophenyl)ethane-1-sulfonamido, 55



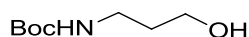
By general procedure A, amino alcohol **221** (242 mg, 2.39 mmol) gave the protected *amino alcohol* **55** (513 mg, 79%) as a brown oil which was used without further purification,  $R_f = 0.38$  (40:60 Petrol–EtOAc);  $\nu_{\max}/\text{cm}^{-1}$  (ATR) 3345 (br), 3008, 2883, 1539, 1361, 1164 and 589;  $[\alpha]_D^{28}$  68 ( $c = 0.097$ , CHCl<sub>3</sub>);  $\delta_H$  (500 MHz, CDCl<sub>3</sub>) 8.21-8.15 (1H, m, nitrophenyl 3-H), 7.95-7.91 (1H, m, nitrophenyl 6-H), 7.82-7.75 (2H, m, nitrophenyl 4-H and nitrophenyl 5-H), 5.79 (1H, d,  $J$  6.8, NH), 3.79 (1H, dd,  $J$  11.3 and 3.8, 2-H<sub>a</sub>), 3.72 (1H, dd,  $J$  11.3 and 5.5, 2-H<sub>b</sub>), 2.82-2.72 (1H, m, 1-H), 2.04 (1H, br s, OH), 1.05-0.92 (1H, m, cyclopropyl 1-H), 0.63-0.51 (1H, m, cyclopropyl 2-H<sub>a</sub>), 0.44-0.33 (1H, m, cyclopropyl 2-H<sub>b</sub>), 0.27 (1H, td,  $J$  10.1 and 5.0, cyclopropyl 3-H<sub>a</sub>) and 0.00 (1H, td,  $J$  10.2 and 5.0, cyclopropyl 3-H<sub>b</sub>);  $\delta_c$  (126 MHz, CDCl<sub>3</sub>) 148.0 (nitrophenyl C-2), 135.1 (nitrophenyl C-1), 133.3 (nitrophenyl C-5), 132.6 (nitrophenyl C-4), 130.8 (nitrophenyl C-6), 125.3 (nitrophenyl C-3), 65.3 (C-2), 61.8 (C-1), 13.2 (cyclopropyl C-1), 3.52 (cyclopropyl C-2) and 3.48 (cyclopropyl C-3); HRMS found MH<sup>+</sup>, 287.0695. C<sub>11</sub>H<sub>14</sub>N<sub>2</sub>O<sub>5</sub>S requires *MH*, 287.0701.

### 3-Hydroxy-S-(2-nitrophenyl)propane-1-sulfonamido, 223



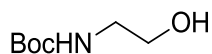
By general procedure A, 3-amino-1-propanol (0.510 mL, 6.66 mmol) gave the protected *amino alcohol* **223** (1.34 g, 81%) as a colourless oil which was used without further purification,  $R_f = 0.24$  (40:60 Petrol–EtOAc);  $\nu_{\max}/\text{cm}^{-1}$  (ATR) 3329 (br), 2946, 2884, 1537, 1334, 1161 and 588;  $\delta_H$  (500 MHz, CDCl<sub>3</sub>) 8.07-7.99 (1H, m, nitrophenyl 3-H), 7.78-7.72 (1H, m, nitrophenyl 6-H), 7.68-7.59 (2H, m, nitrophenyl 4-H and nitrophenyl 5-H), 5.74 (1H, t,  $J$  5.4, NH), 3.66 (2H, t,  $J$  5.4, 1-H<sub>2</sub>), 3.15 (2H, q,  $J$  6.1, 3-H<sub>2</sub>) and 1.73-1.61 (2H, m, 2-H<sub>2</sub>);  $\delta_c$  (126 MHz, CDCl<sub>3</sub>) 148.2 (nitrophenyl C-2), 133.9 (nitrophenyl C-1), 133.4 (nitrophenyl C-5), 132.6 (nitrophenyl C-4), 131.0 (nitrophenyl C-6), 125.2 (nitrophenyl C-3), 60.3 (C-1), 41.4 (C-3) and 31.8 (C-2); HRMS found MH<sup>+</sup>, 261.0560. C<sub>9</sub>H<sub>12</sub>N<sub>2</sub>O<sub>5</sub>S requires *MH*, 261.0545.

### ***tert*-Butyl(3-hydroxypropyl)carbamate, 238**



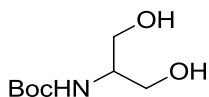
By general procedure B, 3-amino-propanol (10.0 g, 133 mmol) gave the protected amino alcohol<sup>125</sup> **238** (23.3 g, 100%) as a colourless oil which was used without further purification,  $R_f = 0.31$  (30:70 Petrol–EtOAc);  $\nu_{\max}/\text{cm}^{-1}$  (ATR) 3354 (br), 2937, 1691, 1531 and 1173;  $\delta_{\text{H}}$  (500 MHz,  $\text{CDCl}_3$ ) 4.98 (1H, s, NH), 3.61 (2H, q,  $J$  5.9, 3- $\text{H}_2$ ), 3.37 (1H, t,  $J$  5.9, OH), 3.23 (2H, q,  $J$  5.9, 1- $\text{H}_2$ ), 1.63 (2H, quint,  $J$  5.9, 2- $\text{H}_2$ ) and 1.40 (9H, s, Boc);  $\delta_{\text{C}}$  (126 MHz,  $\text{CDCl}_3$ ) 157.2 (CO), 79.6 (Boc), 59.4 (C-3), 37.1 (C-1), 32.9 (C-2) and 28.5 (Boc);  $m/z$  (ES) 198.1 (100%,  $\text{MNa}^+$ ).

### ***tert*-Butyl *N*-(2-hydroxyethyl)carbamate, 89**



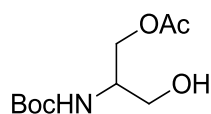
By general procedure B, ethanolamine (9.88 mL, 164 mmol) gave the protected amino alcohol<sup>125</sup> **89** (25.1 g, 95%) as a yellow oil which was used without further purification,  $R_f = 0.30$  (50:50 Petrol–EtOAc);  $\nu_{\max}/\text{cm}^{-1}$  (ATR) 3336, 2977, 1685, 1514, 1167 and 1066;  $\delta_{\text{H}}$  (500 MHz,  $\text{CDCl}_3$ ) 5.08 (1H, br s, NH), 3.70 (2H, q,  $J$  4.9, 2- $\text{H}_2$ ), 3.29 (2H, q,  $J$  4.9, 1- $\text{H}_2$ ), 2.87 (1H, br s, OH) and 1.46 (9H, s, Boc);  $\delta_{\text{C}}$  (126 MHz,  $\text{CDCl}_3$ ) 146.9 (CO), 85.3 (Boc), 62.7 (C-2), 43.3 (C-1) and 28.5 (Boc);  $m/z$  (ES) 184.0 (100%,  $\text{MNa}^+$ ).

### ***tert*-Butyl(1,3-dihydroxypropan-2-yl)carbamate, 94**



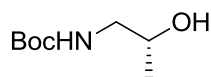
By general procedure B, serinol (10.0 g, 110 mmol) gave a crude residue which was purified by flash chromatography ( $\text{SiO}_2$ , 10:90 MeOH–DCM) to yield Boc-serinol<sup>44</sup> **94** (11.1 g, 53%) as a colourless amorphous solid,  $R_f = 0.35$  (100% EtOAc);  $\delta_{\text{H}}$  (500 MHz,  $\text{CDCl}_3$ ) 5.35 (1H, d,  $J$  7.6, 2-H), 3.87-3.79 (2H, m, 1- $\text{H}_2$ ), 3.79-3.72 (2H, m, 3- $\text{H}_2$ ), 3.69 (1H, br s, NH), 3.26 (2H, br s, OH) and 1.47 (9H, s, Boc);  $\delta_{\text{C}}$  (126 MHz,  $\text{CDCl}_3$ ) 156.4 (CO), 80.0 (Boc), 63.4 (C-1 and C-3), 53.1 (C-2) and 28.4 (Boc);  $m/z$  (ES) 214.0 (100%,  $\text{MNa}^+$ ).

## 2-[[*tert*-Butoxy]carbonyl]amino}-3-hydroxypropyl acetate, **95**



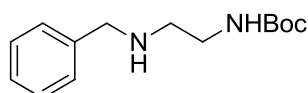
Acetic anhydride (6.58 mL, 69.7 mmol) was added dropwise to a solution of the carbamate (11.1 g, 57.9 mmol) and Et<sub>3</sub>N (16.1 mL, 116 mmol) in DCM (550 mL, 0.1 M) at 0 °C and the resulting solution was stirred at 0 °C for 2 hr. The reaction mixture was warmed to room temperature, quenched by addition of aq. HCl (1 M) to pH<2 and extracted with DCM (3 × 300 mL). The combined organic phases were washed with brine (300 mL), dried (MgSO<sub>4</sub>) and concentrated *in vacuo*. The residue was purified by flash chromatography (SiO<sub>2</sub>, 60:40 Petrol–EtOAc) to yield the acetylated amino alcohol<sup>44</sup> **95** (8.36 g, 62%) as a colourless oil, *R*<sub>f</sub> = 0.57 (30:70 Petrol–EtOAc); δ<sub>H</sub> (500 MHz, CDCl<sub>3</sub>) 5.04-5.05 (1H, m, 2-H), 4.21 (2H, d, *J* 5.6, 1-H<sub>2</sub>), 3.90 (1H, br s, NH), 3.72-3.66 (1H, m, 3-H<sub>a</sub>), 3.66-3.60 (1H, m, 3-H<sub>b</sub>), 2.81 (1H, br s, OH), 2.10 (3H, s, methyl) and 1.46 (9H, s, Boc); δ<sub>C</sub> (126 MHz, CDCl<sub>3</sub>) 171.4 (acetyl CO), 155.8 (Boc CO), 79.9 (Boc), 63.1 (C-1), 61.9 (C-3), 51.1 (C-2), 28.3 (Boc) and 20.8 (methyl); *m/z* (ES) 256.0 (100%, MNa<sup>+</sup>).

## (*R*)-1-*N*[(1,1-dimethylethoxy)carbonyl]amino-2-propanol, **91**



By general procedure B, (*R*)-(-)-1-amino-2-propanol (10.4 mL, 133 mmol) gave the protected *amino alcohol* **91** (23.3 g, 100%) as a yellow oil, which was used without further purification, *R*<sub>f</sub> = 0.52 (30:70 Petrol–EtOAc); ν<sub>max</sub>/ cm<sup>-1</sup> (ATR) 3343 (br), 2976, 1684, 1520, 1366, 1249 and 1168; [α]<sub>D</sub><sup>27</sup> -11 (c = 1.1, MeOH); δ<sub>H</sub> (500 MHz, CDCl<sub>3</sub>) 5.12 (1H, br s, NH), 3.99-3.79 (1H, m, 1-H<sub>a</sub>), 3.41-3.17 (1H, m, 1-H<sub>b</sub>), 3.12-2.86 (2H, m, 2-H and OH), 1.45 (9H, s, Boc) and 1.17 (3H, d, *J* 6.3, 3-H<sub>3</sub>); δ<sub>C</sub> (126 MHz, CDCl<sub>3</sub>) 156.8 (CO), 79.5 (Boc), 67.5 (C-2), 48.0 (C-1), 28.4 (Boc) and 20.6 (C-3); HRMS found MNa<sup>+</sup>, 198.1102. C<sub>8</sub>H<sub>17</sub>NO<sub>3</sub> requires *MNa*, 198.1106.

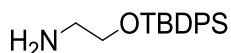
## *N*α-Benzyl-*N*ω-*tert*-butoxycarbonyl ethylene diamine, **125**



Benzaldehyde (3.49 mL, 34.3 mmol) was added dropwise to a stirred suspension of *N*-Boc-ethylenediamine (4.94 mL, 31.2 mmol) and 4 Å mol. sieves (5 g) in DCM (50 mL, 0.7 M) at room temperature and stirred overnight. The reaction mixture was filtered and

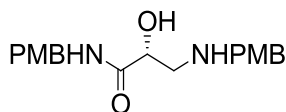
washed with DCM (50 mL), before being concentrated *in vacuo*. The residue was dissolved in MeOH (50 mL, 0.7 M) and cooled to 0 °C. NaBH<sub>4</sub> (2.36 g, 62.4 mmol) was added portion-wise over 10 min and the resulting solution was warmed to room temperature and stirred for 2 hr before being concentrated *in vacuo*. The residue was diluted with water (50 mL) and aq. HCl (1 M) was added to acidify the solution. EtOAc (50 mL) was added and the aqueous layer extracted with EtOAc (2 × 50 mL) to remove organic impurities before being basified with aq. NaOH (2 M) and extracted with DCM (3 × 50 mL). The combined organic layers were dried (MgSO<sub>4</sub>) and concentrated *in vacuo* to yield the diamine<sup>126</sup> **125** (3.54 g, 45%) as a colourless amorphous solid which was used without further purification, *R*<sub>f</sub> = 0.09 (30:70 Petrol–EtOAc); δ<sub>H</sub> (500 MHz, CDCl<sub>3</sub>) 7.46-7.40 (2H, m, benzyl 3-H and benzyl 5-H), 7.40-7.35 (2H, m, benzyl 2-H and benzyl 6-H), 7.34-7.30 (1H, m, benzyl 4-H), 5.48 (2H, br s, NH), 3.92 (2H, s, benzylic-H<sub>2</sub>), 3.35 (2H, dd, *J* 12.5 and 6.5, 2-H<sub>2</sub>), 2.88 (2H, app t, *J* 5.3, 1-H<sub>2</sub>) and 1.45 (9H, s, Boc); δ<sub>C</sub> (126 MHz, CDCl<sub>3</sub>) 156.2 (CO), 135.9 (benzyl C-1), 129.0 (benzyl C-3 and benzyl C-5), 128.8 (benzyl C-2 and benzyl C-6), 128.1 (benzyl C-4), 79.5 (Boc), 52.6 (C-2), 48.0 (benzylic-C), 39.0 (C-1) and 28.4 (Boc); *m/z* (ES) 195.0 (100%) and 251.0 (36%, MH<sup>+</sup>).

#### (2-Aminoethoxy)(*tert*-butyl)diphenylsilane, **56**



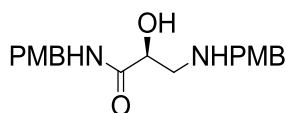
Et<sub>3</sub>N (12.6 mL, 90.0 mmol), DMAP (5.00 g, 41.0 mmol) and TBDPSCl (23.4 mL, 90.0 mmol) were added to a solution of ethanolamine (4.94 mL, 81.9 mmol) in DCM (150 mL, 0.5 M). The reaction mixture was stirred at 40 °C overnight before being quenched with water (500 mL). The organic phase was separated and washed with water (3 × 500 mL) and brine (500 mL), before being dried (MgSO<sub>4</sub>) and concentrated *in vacuo*. The residue was purified by flash chromatography (SiO<sub>2</sub>, 5:95 MeOH–DCM) to yield the protected alcohol<sup>127</sup> **56** (16.3 g, 67%) as a yellow oil, *R*<sub>f</sub> = 0.27 (10:90 MeOH–DCM); δ<sub>H</sub> (500 MHz, CDCl<sub>3</sub>) 7.75-7.70 (4H, m, phenyl 3-H and phenyl 5-H), 7.50-7.39 (6H, m, phenyl 2-H, phenyl 4-H and phenyl 6-H), 3.72 (2H, t, *J* 5.3, 1-H<sub>2</sub>), 2.85 (2H, t, *J* 5.3, 2-H<sub>2</sub>), 1.49 (2H, s, NH<sub>2</sub>) and 1.11 (9H, s, <sup>t</sup>Bu); δ<sub>C</sub> (126 MHz, CDCl<sub>3</sub>) 135.6 (phenyl C-3 and phenyl C-5), 133.7 (phenyl C-1), 129.69 (phenyl C-4), 127.72 (phenyl C-2 and phenyl C-6), 66.2 (C-1), 44.3 (C-2), 26.9 (<sup>t</sup>Bu) and 19.3 (Si-C).

**(2R)-2-Hydroxy-N-[(4-methoxyphenyl)methyl]-3-[[4-methoxyphenyl)methyl]amino} propanamide, R-216**



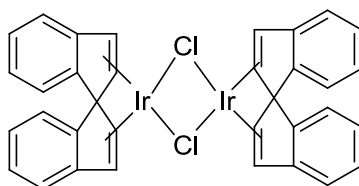
By general procedure C, methyl (2R)-glycidate (5.00 g, 49.0 mmol) gave the amide<sup>100</sup> **R-216** (13.5 g, 80%) as a colourless amorphous solid which was used without further purification,  $R_f = 0.68$  (5:95 MeOH-DCM);  $\delta_H$  (500 MHz,  $CDCl_3$ ) 7.53 (1H, s, NH), 7.22 (2H, d,  $J$  8.5, 1-PMB 2-H and 3-PMB 2-H), 7.16 (2H, d,  $J$  8.5, 1-PMB 6-H and 3-PMB 6-H), 6.91-6.84 (4H, m, 1-PMB 3-H, 1-PMB 5-H, 3-PMB 3-H and 3-PMB 5-H), 4.41 (2H, d,  $J$  5.8, amide benzylic- $H_2$ ), 4.06 (1H, t,  $J$  6.0, 2-H), 3.83 (1H, s, OH), 3.83 (6H, s, 1-PMB methyl and 3-PMB methyl), 3.76-3.68 (2H, m, amine benzylic- $H_2$ ) and 3.06 (1H, dd,  $J$  12.3 and 6.0, 3- $H_a$ ), 2.99 (1H, dd,  $J$  12.3 and 6.0, 3- $H_b$ );  $\delta_C$  (126 MHz,  $CDCl_3$ ) 172.8 (C-1), 159.2 (1-PMB C-4), 159.1 (3-PMB C-4), 131.6 (1-PMB C-1), 130.3 (3-PMB C-1), 129.2 (1-PMB C-2 and 3-PMB C-2), 129.0 (1-PMB C-6 and 3-PMB C-6), 114.2 (1-PMB C-3 and 3-PMB C-3), 114.1 (1-PMB C-5 and 3-PMB C-5), 69.2 (C-2), 55.3 (1-PMB methyl), 55.3 (3-PMB methyl), 52.9 (amide benzylic C-2), 51.2 (amine benzylic C-2) and 42.7 (C-3);  $m/z$  (ES) 345.4 (100%,  $MH^+$ ).

**(2S)-2-Hydroxy-N-[(4-methoxyphenyl)methyl]-3-[[4-methoxyphenyl)methyl]amino} propanamide, S-216**



By general procedure C, methyl (2S)-glycidate (5.00 g, 49.0 mmol) gave the amide<sup>100</sup> **S-216** (13.1 g, 78%) as a colourless amorphous solid which was used without further purification; analytical data as **R-216**.

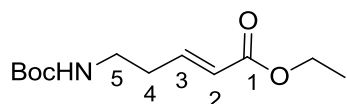
**Chloro(dibenzo[a,e]cyclooctatetraene)iridium(I)dimer, 298**



An oven-dried flask under  $N_2$  was charged with  $[Ir(COD)Cl]_2$  (510 mg, 0.760 mmol) and DCM (10 mL,  $\sim 0.1$  M) was added. A solution of dbcot (303 mg, 1.48 mmol) in DCM (10 mL,  $\sim 0.1$  M) was added dropwise over 30 min. The reaction mixture was stirred for

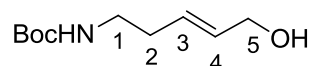
45 min before being cooled to 0 °C, filtered and washed with cyclohexane, before being dried *in vacuo* to yield the iridium dimer<sup>41</sup> **298** (162 mg, 25%) as a bright yellow solid,  $\delta_{\text{H}}$  (500 MHz,  $\text{C}_6\text{D}_6$ ) 6.57 (8H, dd,  $J$  5.4 and 3.3, dbcot 1,4, 7 and 10- $\text{H}_8$ ), 6.38 (8H, dd,  $J$  5.4 and 3.3, dbcot 2, 3, 8 and 9- $\text{H}_8$ ) and 5.12 (8H, s, dbcot 5, 6, 11 and 12- $\text{H}_8$ ).

**(E)-Ethyl 5-((tert-butoxycarbonyl)amino)pent-2-enoate, 239**



DMSO (98.0 mL, 1.38 mmol),  $\text{Et}_3\text{N}$  (105 mL, 752 mmol) and  $\text{SO}_3\cdot\text{Py}$  complex (59.9 g, 376 mmol) were added to a 0 °C solution of the alcohol **238** (22.0 g, 125 mmol) in DCM (250 mL,  $\sim 0.5$  M). The reaction mixture was warmed to room temperature and stirred for 1 hr before carbethoxymethylene triphenyl phosphorane (87.4 g, 251 mmol) was added at 0 °C. The reaction mixture was warmed to room temperature and stirred overnight, where it changed from yellow to red. Water was added (100 mL) and the pH of the reaction mixture adjusted to  $\sim 3$  using conc. HCl before the layers were separated and the aqueous phase was extracted with DCM ( $3 \times 100$  mL). The combined organic phases were washed with aq. HCl (1 M, 100 mL), sat.  $\text{NaHCO}_3$  (100 mL), brine (100 mL), dried ( $\text{MgSO}_4$ ) and concentrated *in vacuo* to give a red oil which was purified by flash chromatography ( $\text{SiO}_2$ , 80:20 Petrol–EtOAc) to yield the  $\alpha$ ,  $\beta$ -unsaturated ester<sup>128</sup> **239** (27.6 g, 90%) as a pale yellow oil,  $R_f = 0.68$  (60:40 Petrol–EtOAc);  $\nu_{\text{max}}/\text{cm}^{-1}$  (ATR) 3373, 2979, 1719, 1655, 1523 and 1174;  $\delta_{\text{H}}$  (500 MHz,  $\text{CDCl}_3$ ) 6.87 (1H, dt,  $J$  15.7 and 6.4, 3-H), 5.86 (1H, d,  $J$  15.7, 2-H), 4.63 (1H, s, NH), 4.17 (2H, q,  $J$  7.1, ethyl 1- $\text{H}_2$ ), 3.25 (2H, q,  $J$  6.4, 5- $\text{H}_2$ ), 2.38 (2H, q,  $J$  6.4, 4- $\text{H}_2$ ), 1.42 (9H, s, Boc) and 1.27 (3H, t,  $J$  7.1, ethyl 2- $\text{H}_3$ );  $\delta_{\text{C}}$  (126 MHz,  $\text{CDCl}_3$ ) 166.4 (Boc CO), 155.9 (C-1), 145.5 (C-3), 123.5 (C-2), 79.6 (Boc), 60.5 (ethyl C-1), 39.2 (C-5), 32.9 (C-4), 28.5 (Boc) and 14.4 (ethyl C-2);  $m/z$  (ES) 266.1 (100%,  $\text{MNA}^+$ ).

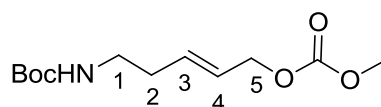
**(E)-tert-Butyl(5-hydroxypent-3-en-1-yl)carbamate, 240**



DIBAL-H (340 mL, 1 M in hexane) was added via cannula to a solution of the  $\alpha$ ,  $\beta$ -unsaturated ester **239** (27.6 g, 113 mmol) in DCM (250 mL,  $\sim 0.5$  M), at  $-78$  °C over 30 min. The resulting mixture was stirred at  $-78$  °C for 1 hr and warmed to room temperature and stirred for 3 hr. The reaction mixture was quenched with sat.  $\text{NH}_4\text{Cl}$  (300 mL) at  $-78$  °C over 30 min, and warmed to room temperature and stirred overnight. The resulting salts were filtered through a pad of Celite and the aqueous layer was extracted with DCM

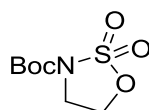
(3 × 300 mL). The combined organic phases were washed with sat. NH<sub>4</sub>Cl (300 mL), brine (300 mL), dried (MgSO<sub>4</sub>), and concentrated *in vacuo* to yield the allylic alcohol<sup>129</sup> **240** (8.94 g, 39%) as a yellow oil, which was used without further purification, *R*<sub>f</sub> = 0.26 (60:40 Petrol–EtOAc);  $\nu_{\max}/\text{cm}^{-1}$  (ATR) 3346, 2977, 2931, 1691, 1528 and 1172;  $\delta_{\text{H}}$  (500 MHz, CDCl<sub>3</sub>) 5.70 (1H, dt, *J* 15.6 and 4.9, 4-H<sub>2</sub>), 5.63 (1H, dt, *J* 15.6 and 6.5, 3-H<sub>2</sub>), 4.62 (1H, s, NH), 4.09 (2H, t, *J* 4.9, 5-H<sub>2</sub>), 3.17 (2H, q, *J* 6.5, 1-H<sub>2</sub>), 2.23 (2H, q, *J* 6.5, 2-H<sub>2</sub>), 1.83 (1H, s, OH) and 1.44 (9H, s, Boc);  $\delta_{\text{C}}$  (126 MHz, CDCl<sub>3</sub>) 156.0 (Boc CO), 131.6 (C-4), 129.0 (C-3), 79.2 (Boc), 63.3 (C-5), 39.9 (C-1), 32.8 (C-2) and 28.4 (Boc); *m/z* (ES) 425.3 (100%, 2MNa<sup>+</sup>).

### (*E*)-tert-Butyl(5-((methoxycarbonyl)oxy)pent-3-en-1-yl)carbamate, **45**



Methyl chloroformate (3.78 mL, 48.9 mmol) was added to a 0 °C solution of the allylic alcohol **240** (8.94 g, 44.4 mmol) and pyridine (3.96 mL, 48.9 mmol) in DCM (100 mL, ~0.5 M). The resulting mixture was stirred for 1 hr at 0 °C, before being warmed to room temperature and stirred overnight. Pyridine (3.59 mL, 44.4 mmol) and methyl chloroformate (1.72 mL, 22.2 mmol) was added at 0 °C and stirred for 1 hr at room temperature. Sat. NH<sub>4</sub>Cl (50 mL) was added and the aqueous phase was extracted with DCM (3 × 50 mL), the combined organic phases were washed with water (50 mL), brine (50 mL), dried (MgSO<sub>4</sub>), and concentrated *in vacuo* to give a residue which was purified by flash chromatography (SiO<sub>2</sub>, 70:30 Petrol–EtOAc) to yield the allylic carbonate<sup>130</sup> **45** (9.31 g, 81%) as a colourless oil, *R*<sub>f</sub> = 0.64 (50:50 Petrol–EtOAc);  $\nu_{\max}/\text{cm}^{-1}$  (ATR) 3383, 2977, 1749, 1713, 1520 and 1270;  $\delta_{\text{H}}$  (500 MHz, CDCl<sub>3</sub>) 5.74 (1H, dt, *J* 15.6 and 6.6, 4-H<sub>2</sub>), 5.68–5.59 (1H, m, 3-H<sub>2</sub>), 4.56 (2H, d, *J* 6.6, 5-H<sub>2</sub>), 3.76 (3H, s, methyl), 3.17 (2H, q, *J* 6.4, 1-H<sub>2</sub>), 2.23 (2H, q, *J* 6.4, 2-H<sub>2</sub>) and 1.41 (9H, s, Boc);  $\delta_{\text{C}}$  (126 MHz, CDCl<sub>3</sub>) 156.0 (Boc CO), 155.7 (Carbonate CO), 133.4 (C-4), 125.9 (C-3), 79.3 (Boc), 68.3 (C-5), 54.8 (methyl), 39.7 (C-1), 32.9 (C-2) and 28.5 (Boc); *m/z* (ES) 282.2 (100%, MNa<sup>+</sup>).

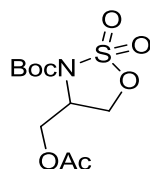
### tert-Butyl 2,2-dioxo-1,2,3-oxathiazolidine-3-carboxylate, **30**



By general procedure D, the protected amino alcohol **89** (5.84 g, 36.2 mmol) gave the cyclic sulfamidate<sup>44</sup> **30** (5.74 g, 71%) as a colourless solid, which was used without

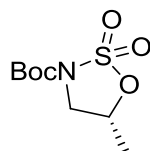
further purification,  $R_f = 0.54$  (50:50 Petrol–EtOAc);  $\nu_{\max}/\text{cm}^{-1}$  (ATR) 2985, 1713, 1351, 1332, 1152 and 806;  $\delta_{\text{H}}$  (500 MHz,  $\text{CDCl}_3$ ) 4.61 (2H, t,  $J$  6.4, 5- $\text{H}_2$ ), 4.04 (2H, t,  $J$  6.4, 4- $\text{CH}_2$ ) and 1.56 (9H, s, Boc);  $\delta_{\text{C}}$  (126 MHz,  $\text{CDCl}_3$ ) 148.7 (CO), 85.6 (Boc), 65.5 (C-5), 45.3 (C-4) and 27.9 (Boc);  $m/z$  (ES) 469.5 (100%,  $2\text{MNa}^+$ ).

***tert*-Butyl-4-[(acetyloxy)methyl]-2,2-dioxo-1,2λ,3-oxathiazolidine-3-carboxylate, **96****



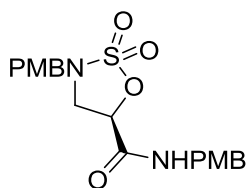
By general procedure F, the protected amino alcohol **95** (8.36 g, 35.8 mmol) gave the cyclic sulfamidate<sup>44</sup> **96** (3.38 g, 32%) as a colourless amorphous solid, which was used without further purification,  $R_f = 0.19$  (30:70 Petrol–EtOAc);  $\delta_{\text{H}}$  (500 MHz,  $\text{CDCl}_3$ ) 4.70 (1H, dd,  $J$  9.7 and 6.4, 4-methyl- $\text{H}_a$ ), 4.59–4.52 (2H, m, 4-methyl- $\text{H}_b$  and 4-H), 4.47 (1H, dd,  $J$  11.5 and 6.1, 5- $\text{H}_a$ ), 4.33 (1H, dd,  $J$  11.5 and 3.7, 5- $\text{H}_b$ ), 2.14 (3H, s, acetyl) and 1.59 (9H, s, Boc);  $\delta_{\text{C}}$  (126 MHz,  $\text{CDCl}_3$ ) 170.5 (acetyl CO), 148.3 (Boc CO), 86.1 (Boc), 67.6 (4-methyl), 61.5 (C-5), 55.5 (C-4), 27.9 (Boc) and 20.6 (acetyl);  $m/z$  (ES) 261.9 (100%,  $\text{MH}^+$ ).

**(*R*)-5-Methyl-2,2-dioxo[1,2,3]oxathiazolidine-3-carboxylic acid *tert*-butyl ester, **92****



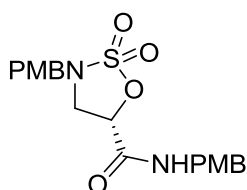
By general procedure F, the protected amino alcohol **91** (23.3 g, 133 mmol) gave the *cyclic sulfamidate* **92** (24.4 g, 77%) as an orange amorphous solid, which was used without further purification,  $R_f = 0.56$  (100% DCM);  $\nu_{\max}/\text{cm}^{-1}$  (ATR) 2983, 1716, 1366, 1329, 1194, 1144 and 825;  $[\alpha]_{\text{D}}^{27} -17$  ( $c = 0.28$ , MeOH);  $\delta_{\text{H}}$  (500 MHz,  $\text{CDCl}_3$ ) 4.83–4.64 (1H, m, 5-H), 3.86 (1H, dd,  $J$  10.0 and 5.6, 4- $\text{H}_a$ ), 3.43 (1H, app t,  $J$  10.0, 4- $\text{H}_b$ ), 1.36 (3H, d,  $J$  6.2, methyl) and 1.33 (9H, s, Boc);  $\delta_{\text{C}}$  (126 MHz,  $\text{CDCl}_3$ ) 148.7 (CO), 85.4 (Boc), 76.2 (C-5), 51.7 (C-4), 27.9 (Boc) and 18.1 (methyl); HRMS found  $\text{MNa}^+$ , 260.0563.  $\text{C}_8\text{H}_{15}\text{NO}_5\text{S}$  requires  $\text{MNa}$ , 260.0569.

**(5R)-N,3-bis[(4-methoxyphenyl)methyl]-2,2-dioxo-1,2λ<sup>6</sup>,3-oxathiazolidine-5-carboxamide, R-54**



By general procedure D, the protected amino alcohol **R-216** (7.16 g, 20.7 mmol) gave a crude residue which was purified by flash chromatography (SiO<sub>2</sub>, 60:40 Petrol-EtOAc) to yield the cyclic sulfamidate<sup>42</sup> **R-54** (720 mg, 9%) as a colourless amorphous solid, *R<sub>f</sub>* = 0.76 (30:70 Petrol-EtOAc); δ<sub>H</sub> (500 MHz, CDCl<sub>3</sub>) 7.24 (4H, d, *J* 8.3, 1-PMB 2-H, 1-PMB 6-H, 3-PMB 2-H and 3-PMB 6-H), 6.91 (4H, d, *J* 8.3, 1-PMB 3-H, 1-PMB 5-H, 3-PMB 3-H and 3-PMB 5-H), 6.80 (1H, br s, NH), 4.95 (1H, dd, *J* 7.6 and 5.3, 5-H), 4.50-4.40 (2H, m, amide benzylic-H<sub>2</sub>), 4.18 (2H, s, sulfamidate benzylic-H<sub>2</sub>), 3.85 (3H, s, 1-PMB methyl), 3.84 (3H, s, 3-PMB methyl), 3.72 (1H, dd, *J* 10.6 and 7.6, 4-H<sub>a</sub>) and 3.59 (1H, dd, *J* 10.6 and 5.3, 4-H<sub>b</sub>); δ<sub>C</sub> (126 MHz, CDCl<sub>3</sub>) 166.4 (CO), 160.1 (1-PMB C-4), 159.5 (3-PMB C-4), 130.1 (1-PMB C-2 and 3-PMB C-2), 129.1 (1-PMB C-1), 129.0 (1-PMB C-6 and 3-PMB C-6), 125.5 (3-PMB C-1), 114.5 (1-PMB C-3 and 3-PMB C-3), 114.4 (1-PMB C-5 and 3-PMB C-5), 75.5 (C-5), 55.3 (1-PMB methyl and 3-PMB methyl), 51.4 (amide benzylic-C), 49.8 (sulfamidate benzylic-C) and 43.0 (C-4); *m/z* (ES) 428.9 (100%, MNa<sup>+</sup>).

**(5S)-N,3-bis[(4-methoxyphenyl)methyl]-2,2-dioxo-1,2λ<sup>6</sup>,3-oxathiazolidine-5-carboxamide, S-54**



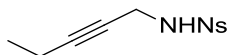
By general procedure D (with an additional 2 eq. of NaIO<sub>4</sub> to promote formation of the kinetic product), the protected amino alcohol **S-216** (2.08 g, 6.04 mmol) gave a crude residue which was purified by flash chromatography (SiO<sub>2</sub>, 50:50 Petrol-EtOAc) to yield the cyclic sulfamidate<sup>42</sup> **S-54** (1.18 g, 48%) as a colourless amorphous solid; data as **R-54**.

***tert*-Butyl-*N*-[(2-nitrophenyl)sulfonyl]carbamate, **98****



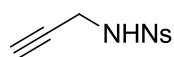
DMAP (450 mg, 0.370 mmol) was added to a stirred suspension of 2-nitrobenzenesulfonamide (25.0 g, 124 mmol), Boc<sub>2</sub>O (27.0 g, 124 mmol) and Et<sub>3</sub>N (25.9 mL, 186 mmol) in DCM (125 mL, ~1 M), and the resulting solution was stirred at room temperature overnight. The reaction mixture was quenched with aq. HCl (2 M) until pH <2 and extracted with DCM (6 × 50 mL). The combined organic phases were washed with water (50 mL), brine (50 mL), dried (MgSO<sub>4</sub>) and concentrated *in vacuo* to yield the protected sulfonamide<sup>44</sup> **98** (27.1 g, 73%) as a pale brown solid which was used without further purification, *R*<sub>f</sub> = 0.75 (50:50 Petrol-EtOAc); *v*<sub>max</sub>/ cm<sup>-1</sup> (ATR) 3256, 2983, 1747, 1721, 1544, 1361 and 1149; *δ*<sub>H</sub> (500 MHz, CDCl<sub>3</sub>) 8.38-8.32 (1H, m, 3-H), 7.89-7.85 (1H, m, 6-H), 7.83-7.76 (2H, m, 4-H and 5-H), 7.58 (1H, s, NH) and 1.43 (9H, s, Boc); *δ*<sub>C</sub> (126 MHz, CDCl<sub>3</sub>) 148.6 (C-2), 134.7 (C-5), 133.3 (C-4), 132.5 (C-6), 132.0 (C-1), 125.1 (C-3), 84.8 (Boc) and 27.9 (Boc), Boc CO not observed; *m/z* (ES) 301.0 (100%, [M-H]<sup>-</sup>).

**2-Nitro-*N*-(pent-2-yn-1-yl)benzene-1-sulfonamide, **29****



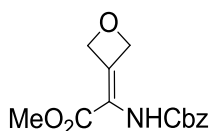
By general procedure E, 2-pentyn-1-ol (3.61 mL, 39.0 mmol), and sulfonamide **98** (13.0 g, 42.9 mmol) gave a crude product which was recrystallized from Petrol to yield the pentynyl sulfonamide<sup>44</sup> **29** (9.30 g, 89%) as a yellow solid, *R*<sub>f</sub> = 0.74 (50:50 Petrol-EtOAc); *v*<sub>max</sub>/ cm<sup>-1</sup> (ATR) 3336, 3098, 2978, 1537, 1343 and 1165; *δ*<sub>H</sub> (500 MHz, CDCl<sub>3</sub>) 8.23-8.17 (1H, m, 3-H), 7.95-7.88 (1H, m, 6-H), 7.79-7.72 (2H, m, 4-H and 5-H), 5.60 (1H, t, *J* 6.2, NH), 3.97 (2H, dt, *J* 6.2 and 2.2, pentynyl 1-H<sub>2</sub>), 1.83 (2H, qt, *J* 7.5 and 2.2, pentynyl 4-H<sub>2</sub>) and 0.82 (3H, t, *J* 7.5, pentynyl 5-H<sub>3</sub>); *δ*<sub>C</sub> (126 MHz, CDCl<sub>3</sub>) 148.1 (C-2), 134.5 (C-1), 133.7 (C-5), 132.9 (C-4), 131.8 (C-6), 125.5 (C-3), 87.4 (pentynyl C-2), 73.1 (pentynyl C-3), 34.1 (pentynyl C-1), 13.5 (pentynyl C-4) and 12.1 (pentynyl C-5); *m/z* (ES) 423.5 (100%) and 291.1 (67%, MNa<sup>+</sup>).

## 2-Nitro-*N*-(prop-2-yn-1-yl)benzene-1-sulfonamide, **99**



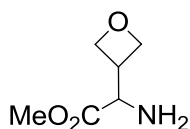
By general procedure E, propargyl alcohol (1.78 mL, 30.6 mmol) and sulfonamide **98** (10.2 g, 33.6 mmol) gave a crude product which was recrystallized from 50:50 Petrol-CHCl<sub>3</sub> to give the propargyl sulfonamide<sup>44</sup> **99** (5.85 g, 80%) as a colourless solid,  $R_f = 0.55$  (50:50 Petrol-EtOAc);  $\nu_{\max}/\text{cm}^{-1}$  (ATR) 3294, 3094, 1536, 1415, 1368, 1332, 1162, 1072 and 605;  $\delta_{\text{H}}$  (500 MHz, CDCl<sub>3</sub>) 8.29-8.15 (1H, m, nitrophenyl 3-H), 8.01-7.88 (1H, m, nitrophenyl 6-H), 7.82-7.76 (2H, m, nitrophenyl 4-H and nitrophenyl 5-H), 5.73 (1H, t,  $J$  5.5, NH), 4.05 (2H, dd,  $J$  5.5 and 2.5, 1-H<sub>2</sub>) and 2.00 (1H, t,  $J$  2.5, 3-H);  $\delta_{\text{C}}$  (126 MHz, CDCl<sub>3</sub>) 148.0 (nitrophenyl C-1), 134.0 (nitrophenyl C-2), 133.8 (nitrophenyl C-5), 132.9 (nitrophenyl C-4), 131.6 (nitrophenyl C-6), 125.5 (nitrophenyl C-3), 77.4 (C-3), 73.3 (C-2) and 33.4 (C-1);  $m/z$  (ES) 263.0 (100%, MNa<sup>+</sup>).

## *N*-Benzyloxycarbonyl- $\alpha$ - $\beta$ -didehydro-(3-oxetanyl)-glycine, methyl ester, **182**



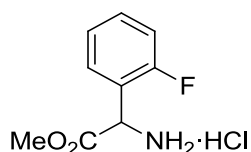
1,1,3,3-Tetramethylguanidine (1.80 mL, 14.4 mmol) was added to a solution of *N*-benzyloxycarbonyl-(phosphonoglycine)-trimethyl ester (5.00 g, 15.1 mmol) in THF (30 mL, ~0.5 M) at -78 °C, and stirred at -78 °C for 1 hr. 3-Oxetanone (0.920 mL, 14.4 mmol) was added and the reaction mixture was stirred at room temperature overnight, before being diluted with EtOAc (50 mL), filtered and washed. The combined organic phases were washed with 1% citric acid (3 × 50 mL), brine (50 mL), dried (MgSO<sub>4</sub>) and concentrated *in vacuo*. The residue was purified by flash chromatography (SiO<sub>2</sub>, 30:70 Petrol-EtOAc) to give the alkene<sup>91</sup> **182** (1.80 g, 45%) as a colourless amorphous solid,  $R_f = 0.67$  (30:70 Petrol-EtOAc);  $\delta_{\text{H}}$  (500 MHz, CDCl<sub>3</sub>) 7.46-7.34 (5H, m, benzyl-H), 6.79 (1H, s, NH), 5.48 (2H, s, benzylic-H<sub>2</sub>), 5.46-5.41 (2H, m, oxetanyl 2-H<sub>a</sub> and oxetanyl 4-H<sub>a</sub>), 5.14 (2H, app s, oxetanyl 2-H<sub>b</sub> and oxetanyl 4-H<sub>b</sub>) and 3.83 (3H, s, methyl);  $\delta_{\text{C}}$  (126 MHz, CDCl<sub>3</sub>) 197.9 (ester CO), 163.6 (carbamate CO), 152.7 (C-1), 135.7 (benzyl C-1), 128.7 (benzyl C-3 and benzyl C-5), 128.5 (benzyl C-2 and benzyl C-6), 128.3 (benzyl C-4), 115.9 (C-2), 78.7 (oxetanyl C-2), 67.5 (oxetanyl C-4) and 52.7 (methyl);  $m/z$  (ES) 300.2 (100%, MNa<sup>+</sup>).

### Methyl 2-amino-2-(oxetan-3-yl)acetate, **183**



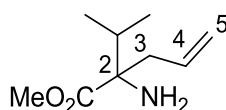
Hydrogen was bubbled through a suspension of Pd(OH)<sub>2</sub>/C (217 mg, 5 mol%) and alkene **182** (1.71 g, 6.17 mmol) in 1:1 MeOH–DCM (120 mL, ~0.05 M) and the reaction mixture was stirred at room temperature overnight before being filtered through Celite. The solvent was concentrated *in vacuo* and the residue was purified by basic SCX cartridge to yield the amino ester<sup>91</sup> **183** (530 mg, 59%) as a yellow oil,  $R_f = 0.54$  (5:95 MeOH–DCM);  $\delta_H$  (500 MHz, CDCl<sub>3</sub>) 4.84–4.69 (2H, m, oxetanyl 2-H<sub>a</sub> and oxetanyl 4-H<sub>a</sub>), 4.67–4.57 (2H, m, oxetanyl 2-H<sub>b</sub> and oxetanyl 4-H<sub>b</sub>), 3.76 (1H, d,  $J$  9.2, 2-H), 3.72 (3H, s, methyl), 3.24–3.10 (1H, m, oxetanyl 1-H) and 1.59 (2H, br s, NH<sub>2</sub>);  $\delta_C$  (126 MHz, CDCl<sub>3</sub>) 174.6 (C-1), 74.3 (oxetanyl C-2), 74.1 (oxetanyl C-4), 56.5 (C-2), 51.9 (methyl) and 39.1 (oxetanyl C-1);  $m/z$  (ES) 146.5 (100%, MH<sup>+</sup>).

### Methyl 2-amino-2-(2-fluorophenyl)acetate, **188**



Thionyl chloride (0.470 mL, 6.50 mmol) was added dropwise to a suspension of 2-fluorophenyl amino acid (1.00 g, 5.91 mmol) in MeOH (20 mL, ~0.3 M) at –10 °C. The resulting mixture was stirred at reflux overnight, before being concentrated *in vacuo* and recrystallized from MeOH–Et<sub>2</sub>O to yield the amino ester salt<sup>92</sup> **188** (1.13 g, 87%) as an amorphous yellow solid,  $R_f = 0.64$  (30:70 Petrol–EtOAc);  $\delta_H$  (500 MHz, MeOD) 7.59 (1H, dddd,  $J$  8.4, 7.6, 5.4 and 1.7, fluorophenyl 4-H), 7.54 (1H, td,  $J$  7.6 and 1.6, fluorophenyl 3-H), 7.36 (1H, td,  $J$  7.6, and 1.0, fluorophenyl 5-H), 7.32 (1H, ddd,  $J$  10.1, 8.4 and 0.9, fluorophenyl 6-H), 5.47 (1H, s, 2-H) and 3.87 (3H, s, methyl).

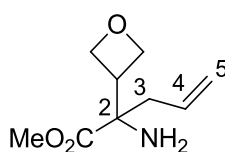
### Methyl 2-amino-2-isopropyl pent-4-enoate, **175**



By general procedure P, valine methyl ester hydrochloride (2.00 g, 11.9 mmol) gave the allylated *amino ester* **175** (1.53 g, 75%) as a brown oil which was used without

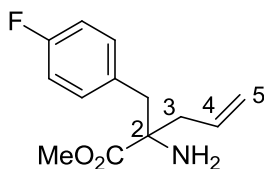
further purification,  $R_f = 0.37$  (30:70 Petrol-EtOAc);  $\nu_{\max}/\text{cm}^{-1}$  (ATR) 2964, 1730, 1436, 1213, 1160 and 1134;  $\delta_{\text{H}}$  (500 MHz,  $\text{CDCl}_3$ ) 5.53 (1H, dddd,  $J$  16.7, 9.9, 8.4 and 6.5, 4-H), 5.04-4.94 (2H, m, 5-H<sub>2</sub>), 3.58 (3H, s, methyl), 2.39 (1H, dd,  $J$  13.4 and 6.5 3-H<sub>a</sub>), 2.15 (1H, dd,  $J$  13.4 and 8.4, 3-H<sub>b</sub>), 1.89 (1H, hept,  $J$  6.9, isopropyl 2-H), 1.58 (2H, br s,  $\text{NH}_2$ ), 0.82 (3H, d,  $J$  6.9, isopropyl-Me<sub>A</sub>) and 0.72 (3H, d,  $J$  6.9, isopropyl-Me<sub>B</sub>);  $\delta_{\text{C}}$  (126 MHz,  $\text{CDCl}_3$ ) 177.1 (CO), 133.2 (C-4), 119.3 (C-5), 64.2 (C-2), 51.9 (methyl), 42.1 (C-3), 35.4 (isopropyl C-2), 17.8 (isopropyl-Me<sub>A</sub>) and 16.2 (isopropyl-Me<sub>B</sub>); HRMS found  $\text{MH}^+$ , 172.1366.  $\text{C}_9\text{H}_{17}\text{NO}_2$  requires  $\text{MH}$ , 172.1337.

### Methyl 2-amino-2-(oxetan-3-yl)pent-4-enoate, **184**



By general procedure P, amino ester **183** (126 mg, 0.870 mmol) gave the allylated *amino ester* **184** (67.0 mg, 42%) as a yellow oil which was used without further purification,  $R_f = 0.69$  (50:50 Petrol-EtOAc);  $\nu_{\max}/\text{cm}^{-1}$  (ATR) 2952, 2879, 1727, 1436, 1216, 977 and 918;  $\delta_{\text{H}}$  (300 MHz,  $\text{CDCl}_3$ ) 5.61-5.36 (1H, m, 5-H<sub>a</sub>), 5.03-5.01 (1H, m, 4-H), 5.00-4.93 (1H, m, 5-H<sub>b</sub>), 4.60-4.50 (3H, m, 2-H<sub>a</sub> and oxetanyl 4-H<sub>2</sub>), 4.41 (1H, t,  $J$  6.6, oxetanyl 2-H<sub>b</sub>), 3.57 (3H, s, methyl), 3.33-3.14 (1H, m, oxetanyl 1-H), 2.30 (1H, ddt,  $J$  13.5, 6.5 and 1.2, 3-H<sub>a</sub>), 2.05 (1H, dd,  $J$  13.5 and 8.2, 3-H<sub>b</sub>) and 1.64 (2H, br s,  $\text{NH}_2$ );  $\delta_{\text{C}}$  (126 MHz,  $\text{CDCl}_3$ ) 175.6 (C-1), 132.1 (C-4), 119.6 (C-5), 72.4 (oxetanyl C-2), 72.1 (oxetanyl C-4), 60.3 (C-2), 52.1 (methyl), 42.1 (oxetanyl C-1) and 41.5 (C-3); HRMS found  $\text{MH}^+$ , 186.1155.  $\text{C}_9\text{H}_{15}\text{NO}_3$  requires  $\text{MH}$ , 186.1130.

### Methyl-2-amino-2-[(4-fluorophenyl)methyl]pent-4-enoate, **186**

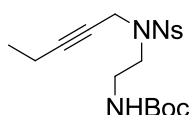


By general procedure P (but excluding addition of  $\text{Et}_3\text{N}$ ), 4-fluoro-DL-phenylalaninemethyl ester hydrochloride (500 mg, 2.14 mmol) gave the allylated *amino ester* **186** (282 mg, 56%) as a yellow oil which was used without further purification,  $R_f = 0.54$  (5:95 MeOH-DCM);  $\nu_{\max}/\text{cm}^{-1}$  (ATR) 2952, 2919, 1732, 1509, 1441, 1219 and 840;  $\delta_{\text{H}}$  (500 MHz,  $\text{CDCl}_3$ ) 7.22-7.07 (2H, m, fluorophenyl 2-H and fluorophenyl 6-H), 7.04-6.91 (2H, m, fluorophenyl 3-H and fluorophenyl 5-H), 5.71 (1H, dddd,  $J$  16.7, 10.0, 8.5

and 6.4, 4-H), 5.25-5.15 (2H, m, 5-H<sub>2</sub>), 3.72 (3H, s, methyl), 3.16 (1H, d, *J* 13.4, benzylic-H<sub>a</sub>), 2.78 (1H, d, *J* 13.4, benzylic-H<sub>b</sub>), 2.72 (1H, dd, *J* 13.5 and 6.4, 3-H<sub>a</sub>) and 2.33 (1H, dd, *J* 13.5 and 8.5, 3-H<sub>b</sub>),  $\delta_c$  (126 MHz, CDCl<sub>3</sub>) 176.4 (C-1), 162.1 (d, *J* 245.3, fluorophenyl C-4), 132.3 (C-4), 131.9 (d, *J* 3.3, fluorophenyl C-1), 131.4 (d, *J* 7.9, fluorophenyl C-2 and fluorophenyl C-6), 119.9 (C-5), 115.3 (d, *J* 21.2, fluorophenyl C-3 and fluorophenyl C-5), 61.9 (C-2), 52.0 (methyl), 44.9 (benzylic-C) and 44.3 (C-3);  $\delta_F$  (282 MHz, CDCl<sub>3</sub>) -115.9; HRMS found MH<sup>+</sup>, 238.1264. C<sub>13</sub>H<sub>16</sub>FNO<sub>2</sub> requires *MH*, 238.1243.

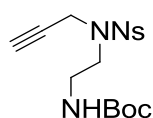
## 5.5 Connection of Building Blocks

### *tert*-Butyl-*N*-{2-[*N*-(pent-2'-yn-1'-yl)(2-nitrophenyl)sulfonamido]ethyl}carbamate, **31**



By general procedure F, pentynyl sulfonamide **29** (4.84 g, 18.0 mmol) and cyclic sulfamidate **30** (3.66 g, 16.4 mmol) gave a crude residue which was purified by flash chromatography (SiO<sub>2</sub>, 25:25:50 Petrol-Et<sub>2</sub>O-CHCl<sub>3</sub>) to yield the sulfonamide<sup>44</sup> **31** (3.78 g, 56%) as a yellow solid, *R<sub>f</sub>* = 0.65 (50:50 Petrol-EtOAc);  $\nu_{\max}$ /cm<sup>-1</sup> (ATR) 3419 (br), 2978, 2937, 1708, 1545, 1366 and 1167;  $\delta_H$  (500 MHz, CDCl<sub>3</sub>) 8.06 (1H, dd, *J* 7.4 and 1.8, nitrophenyl 3-H), 7.72-7.65 (2H, m, nitrophenyl 4-H and 5-H), 7.63 (1H, dd, *J* 7.4 and 1.8, nitrophenyl 6-H), 4.82 (1H, s, NH), 4.20 (2H, s, pentynyl 1-H<sub>2</sub>), 3.51 (2H, t, *J* 5.8, 2-H<sub>2</sub>), 3.36 (2H, q, *J* 5.8, 1-H<sub>2</sub>), 2.04 (2H, q, *J* 7.5, pentynyl 4-H<sub>2</sub>), 1.44 (9H, s, Boc) and 0.98 (3H, t, *J* 7.5, pentynyl 5-H<sub>3</sub>);  $\delta_c$  (126 MHz, CDCl<sub>3</sub>) 148.5 (C-2), 133.7 (C-5), 133.0 (C-1), 131.6 (C-4), 131.2 (C-6), 124.2 (C-3), 88.2 (pentynyl C-2), 79.7 (Boc), 72.3 (pentynyl C-3), 46.7 (pentynyl C-1), 38.3 (ethyl C-1), 37.6 (ethyl C-2), 28.5 (Boc), 13.7 (pentynyl C-5) and 12.3 (pentynyl C-4), Boc CO not observed; *m/z* (ES) 420.2 (100%, MNa<sup>+</sup>).

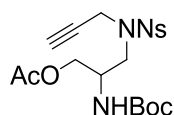
### *tert*-Butyl-*N*-{2-[*N*-(prop-2-yn-1-yl)(2-nitrophenyl)sulfonamido]ethyl}carbamate, **100**



By general procedure F, propargyl sulfonamide **99** (5.98 g, 24.9 mmol) and cyclic sulfamidate **30** (5.05 g, 22.6 mmol) gave a crude residue which was purified by flash chromatography (SiO<sub>2</sub>, 100% DCM) to yield the sulfonamide<sup>44</sup> **100** (8.15 g, 94%) as a

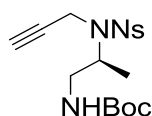
yellow solid,  $R_f = 0.41$  (100% DCM);  $\nu_{\max}/\text{cm}^{-1}$  (ATR) 3289, 2978, 1697, 1591, 1543, 1365, 1163 and 589;  $\delta_{\text{H}}$  (500 MHz,  $\text{CDCl}_3$ ) 8.07 (1H, dd,  $J$  7.4 and 1.7, nitrophenyl 3-H), 7.76-7.68 (2H, m, nitrophenyl 4-H and nitrophenyl 5-H), 7.66 (1H, dd,  $J$  7.4 and 1.7, nitrophenyl 6-H), 4.88 (1H, br s, NH), 4.27 (2H, d,  $J$  2.2, propargyl 1- $\text{H}_2$ ), 3.55 (2H, t,  $J$  5.9, 2- $\text{H}_2$ ), 3.43-3.33 (2H, m, 1- $\text{H}_2$ ), 2.22 (1H, t,  $J$  2.2, propargyl 3-H) and 1.44 (9H, s, Boc);  $\delta_{\text{C}}$  (126 MHz,  $\text{CDCl}_3$ ) 171.1 (Boc CO), 148.3 (nitrophenyl C-2), 133.8 (nitrophenyl C-5), 132.6 (nitrophenyl C-1), 131.7 (nitrophenyl C-4), 131.0 (nitrophenyl C-6), 124.2 (nitrophenyl C-3), 79.6 (Boc), 77.3 (propargyl C-2), 74.2 (propargyl C-3), 46.7 (C-2), 38.0 (C-1), 37.0 (propargyl C-1) and 28.3 (Boc);  $m/z$  (ES) 406.1 (100%,  $\text{MNa}^+$ ).

**2-[[*tert*-Butoxy)carbonyl]amino]-3-[*N*-(prop-2-yn-1-yl)2-nitrobenzene sulfonamido]propyl acetate, **104****



By general procedure F, propargyl sulfonamide **99** and cyclic sulfamidate **95** (3.38 g, 11.5 mmol) gave a crude residue which was purified by flash chromatography ( $\text{SiO}_2$ , 10:90  $\text{Et}_2\text{O}$ -DCM) to yield the sulfonamide<sup>44</sup> **104** (3.05 g, 58%) as an orange amorphous solid,  $R_f = 0.48$  (10:90  $\text{Et}_2\text{O}$ -DCM);  $\delta_{\text{H}}$  (500 MHz,  $\text{CDCl}_3$ ) 8.07 (1H, dd,  $J$  7.6 and 1.7, nitrophenyl 3-H), 7.78-7.69 (2H, m, nitrophenyl 4-H and nitrophenyl 5-H), 7.65 (1H, dd,  $J$  7.4 and 1.7, nitrophenyl 6-H), 4.91 (1H, d,  $J$  7.9, NH), 4.42 (1H, d,  $J$  18.7, propargyl 1- $\text{H}_a$ ), 4.25 (1H, dd,  $J$  18.7 and 2.4, propargyl 1- $\text{H}_b$ ), 4.23-4.12 (3H, m, 2-H and 3- $\text{H}_2$ ), 3.67 (1H, dd,  $J$  13.7 and 10.0, 1- $\text{H}_a$ ), 3.55-3.37 (1H, m, 1- $\text{H}_b$ ), 2.19 (1H, t,  $J$  2.4, propargyl 3-H), 2.14 (3H, s, methyl) and 1.46 (9H, s, Boc);  $\delta_{\text{C}}$  (126 MHz,  $\text{CDCl}_3$ ) 170.8 (acetyl CO), 155.6 (Boc CO), 148.3 (nitrophenyl C-2), 133.9 (nitrophenyl C-5), 132.6 (nitrophenyl C-1), 131.7 (nitrophenyl C-4), 131.0 (nitrophenyl C-6), 124.2 (nitrophenyl C-3), 80.1 (Boc), 76.2 (propargyl C-3), 74.5 (propargyl C-2), 64.1 (propargyl C-1), 47.4 (C-1), 46.7 (C-2), 36.8 (C-3), 28.3 (methyl) and 20.7 (Boc);  $m/z$  (ES) 356.0 (100%) and 478.1 (43%,  $\text{MNa}^+$ ).

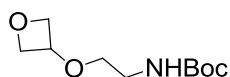
***tert*-Butyl-*N*-{(2*S*)-2-[*N*-(prop-2-yn-1-yl)(2-nitrophenyl)sulfonamido]propyl} carbamate, **102****



By general procedure F, propargyl sulfonamide **99** (2.63 g, 11.0 mmol) and cyclic sulfamidate **91** (2.36 g, 9.95 mmol) gave a crude residue which was purified by flash

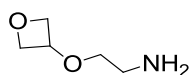
chromatography (SiO<sub>2</sub>, 100% DCM) to yield the *sulfonamide* **102** (1.92 g, 49%) as a yellow amorphous solid,  $R_f = 0.14$  (100% DCM);  $\nu_{\max}/\text{cm}^{-1}$  (ATR) 3428 (br), 3291, 2979, 1706, 1544, 1367, 1159 and 584;  $[\alpha]_{\text{D}}^{28} -39$  ( $c = 0.28$ , MeOH);  $\delta_{\text{H}}$  (500 MHz, CDCl<sub>3</sub>) 8.15 (1H, dd,  $J$  7.4 and 1.6, nitrophenyl 3-H), 7.73-7.66 (2H, m, nitrophenyl 4-H and nitrophenyl 5-H), 7.64 (1H, dd,  $J$  7.2 and 2.0, nitrophenyl 6-H), 4.90 (1H, t,  $J$  6.7, NH), 4.19 (1H, dd,  $J$  18.9 and 2.4, propargyl 1-H<sub>a</sub>), 4.16-4.07 (2H, m, propargyl 1-H<sub>b</sub> and 2-H), 3.28 (2H, app t,  $J$  6.7, 1-H<sub>2</sub>), 2.21 (1H, t,  $J$  4.2, propargyl 3-H), 1.40 (9H, s, Boc) and 1.20 (3H, d,  $J$  6.8, methyl);  $\delta_{\text{C}}$  (126 MHz, CDCl<sub>3</sub>) 155.9 (CO), 147.9 (nitrophenyl C-2), 133.7 (nitrophenyl C-5), 133.6 (nitrophenyl C-1), 131.9 (nitrophenyl C-4), 131.7 (nitrophenyl C-6), 124.2 (nitrophenyl C-3), 72.8 (propargyl C-2), 54.3 (C-2), 43.2 (C-1), 32.0 (propargyl C-1), 28.4 (Boc), 16.1 (methyl) and 14.1 (propargyl C-3), Boc quaternary carbons not observed; HRMS found  $\text{MH}^+$ , 398.1380. C<sub>17</sub>H<sub>23</sub>N<sub>3</sub>O<sub>6</sub>S requires  $\text{MH}$ , 398.1386.

### ***tert*-Butyl *N*-[2-(oxetan-3-yloxy)ethyl]carbamate, **245****



By general procedure F, 3-oxetan-ol (0.310 mL, 4.93 mmol) and cyclic sulfamidate **30** (1.00 g, 4.48 mmol) gave a crude product which was purified by flash chromatography (SiO<sub>2</sub>, 20:30:50 Petrol–Et<sub>2</sub>O–CHCl<sub>3</sub>) to yield the *protected amine* **245** (400 mg, 41%) as a colourless oil,  $R_f = 0.59$  (30:70 Petrol–EtOAc);  $\nu_{\max}/\text{cm}^{-1}$  (ATR) 3338, 2973, 2872, 1690, 1513, 1248, 1166, 1115 and 968;  $\delta_{\text{H}}$  (500 MHz, CDCl<sub>3</sub>) 4.92 (1H, br s, NH), 4.83-4.77 (2H, m, oxetanyl 2-H<sub>a</sub> and oxetanyl 4-H<sub>a</sub>), 4.65-4.60 (2H, m, oxetanyl 2-H<sub>b</sub> and oxetanyl 4-H<sub>b</sub>), 4.60-4.53 (1H, m, oxetanyl 1-H), 3.45 (2H, t,  $J$  5.1, 2-H<sub>2</sub>), 3.34 (2H, dd,  $J$  9.9 and 4.7, 1-H<sub>2</sub>) and 1.48 (9H, s, Boc);  $\delta_{\text{C}}$  (126 MHz, CDCl<sub>3</sub>) 155.9 (CO), 79.5 (Boc), 78.6 (oxetanyl C-2 and oxetanyl C-4), 72.5 (oxetanyl C-1), 67.8 (C-2), 40.5 (C-1) and 28.4 (Boc); HRMS found  $\text{MH}^+$ , 218.1386. C<sub>10</sub>H<sub>19</sub>NO<sub>4</sub> requires  $\text{MH}$ , 218.1392.

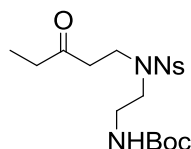
### **2-(Oxetan-3-yloxy)ethyl amine, **246****



By general procedure Y, amine **245** (400 mg, 1.84 mmol) gave a crude product which was purified by flash chromatography (SiO<sub>2</sub>, 100% EtOAc) to yield the *deprotected amine* **246** (215 mg, 100%) as a colourless oil,  $R_f = 0.22$  (100% EtOAc);  $\nu_{\max}/\text{cm}^{-1}$  (ATR) 3305 (br), 2942, 2883, 1706, 1156, 909 and 727;  $\delta_{\text{H}}$  (500 MHz, MeOD) 3.76 (2H, t,  $J$  5.4, 2-H<sub>2</sub>), 3.67 (2H, dd,  $J$  11.6 and 4.5, oxetanyl 2-H<sub>a</sub> and oxetanyl 4-H<sub>a</sub>), 3.60 (2H, dd,  $J$  11.6 and 5.8, oxetanyl 2-H<sub>b</sub> and oxetanyl 4-H<sub>b</sub>), 3.52 (2H, t,  $J$  5.4, 1-H<sub>2</sub>) and 3.47 (1H, tt,  $J$  5.8 and 4.5,

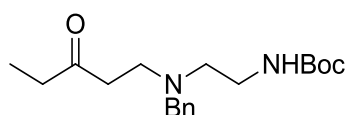
oxetanyl 1-H);  $\delta_c$  (126 MHz, MeOD) 82.9 (oxetanyl C-1), 68.9 (C-2), 62.5 (oxetanyl C-2 and oxetanyl C-4) and 41.2 (C-1); HRMS found  $MNa^+$ , 140.0315.  $C_5H_{11}NO_2$  requires  $MNa$ , 140.0687.

### ***tert*-Butyl-*N*-{2-[*N*-(3'-oxopentyl)(2-nitrophenyl)sulfonamido]ethyl}carbamate, **32****



By general procedure G, the sulfonamide **31** (3.78 g, 9.19 mmol) gave a crude product which was purified by flash chromatography ( $SiO_2$ , 50:50 Petrol–EtOAc) to yield the ketone<sup>44</sup> **32** (3.39 g, 86%) as an orange solid,  $R_f$  = 0.26 (50:50 Petrol–EtOAc);  $\nu_{max}/cm^{-1}$  (ATR) 3403 (br), 2978, 1709, 1544, 1367 and 1164;  $\delta_H$  (500 MHz,  $CDCl_3$ ) 8.01 (1H, d,  $J$  7.3, 3-H), 7.76-7.67 (2H, m, 4-H and 5-H), 7.63 (1H, d,  $J$  7.3, 6-H), 4.85 (1H, t,  $J$  6.3, NH), 3.56 (2H, t,  $J$  6.3, ethyl 2- $H_2$ ), 3.40 (2H, t,  $J$  6.5, oxopentyl 2- $H_2$ ), 3.31 (2H, q,  $J$  6.3, ethyl 1- $H_2$ ), 2.81 (2H, t,  $J$  6.5, oxopentyl 1- $H_2$ ), 2.43 (2H, q,  $J$  7.3, oxopentyl 4- $H_2$ ), 1.43 (9H, s, Boc) and 1.03 (3H, t,  $J$  7.3, oxopentyl 5- $H_3$ );  $\delta_c$  (126 MHz,  $CDCl_3$ ) 209.3 (oxopentyl C-3), 133.9 (nitrophenyl C-5), 132.7 (nitrophenyl C-1), 131.9 (nitrophenyl C-4), 131.2 (nitrophenyl C-6), 124.4 (nitrophenyl C-3), 48.5 (C-2), 43.5 (oxopentyl C-2), 41.7 (C-1), 39.3 (oxopentyl C-1), 36.4 (oxopentyl C-4), 28.5 (Boc) and 7.7 (oxopentyl C-5), Boc quaternary carbons and nitrophenyl C-2 not observed;  $m/z$  (ES) 452.1 (100%,  $MNa^+$ ).

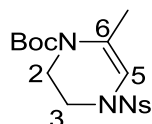
### ***tert*-Butyl *N*-{2-[benzyl(3-oxypentyl)amino]ethyl}carbamate, **126****



Ethyl vinyl ketone (1.50 mL, 15.2 mmol) was added dropwise to a solution of diamine **125** (1.90 g, 7.59 mmol) in EtOH (15 mL, 0.5 M) at room temperature and stirred overnight. The reaction mixture was concentrated *in vacuo* and purified by flash chromatography ( $SiO_2$ , 60:40 Petrol–EtOAc) to yield the *amino ketone* **126** (1.24 g, 49%) as a colourless oil,  $R_f$  = 0.58 (30:70 Petrol–EtOAc);  $\nu_{max}/cm^{-1}$  (ATR) 3352 (br), 2974, 2809, 1705, 1495, 1167 and 736;  $\delta_H$  (500 MHz,  $CDCl_3$ ) 7.35-7.30 (2H, m, benzyl 3-H and benzyl 5-H), 7.30-7.23 (3H, m, benzyl 2-H, benzyl 4-H and benzyl 6-H), 4.95 (1H, s, NH), 3.58 (2H, s, benzylic- $H_2$ ), 3.24-3.17 (2H, m, 1- $H_2$ ), 2.81 (2H, t,  $J$  6.9, oxopentyl 1- $H_2$ ), 2.62-2.48 (4H, m, 2- $H_2$  and oxopentyl 2- $H_2$ ), 2.38 (2H, q,  $J$  7.3, oxopentyl 4- $H_2$ ), 1.46 (9H, s, Boc) and 1.05 (3H, t,  $J$  7.3, oxopentyl 5- $H_3$ );  $\delta_c$  (126 MHz,  $CDCl_3$ ) 210.7 (oxopentyl C-3), 156.0 (Boc), 139.0 (benzyl C-1), 128.8 (benzyl C-3 and benzyl C-5), 128.3 (benzyl C-2 and benzyl C-6),

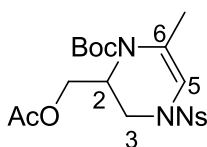
127.1 (C-4), 78.9 (Boc), 58.7 (oxopentyl C-1), 53.3 (C-1), 48.7 (benzylic-C), 40.2 (C-2), 38.1 (oxopentyl C-2), 36.2 (oxopentyl C-4), 28.5 (Boc) and 7.6 (oxopentyl C-5); HRMS found  $MH^+$ , 335.2350.  $C_{19}H_{30}N_2O_3$  requires  $MH$ , 335.2334.

***tert*-Butyl-6-methyl-4-[(2-nitrophenyl)sulfonyl]-1,2,3,4-tetrahydropyrazine-1-carbamate, **101****



By general procedure H, the sulfonamide **100** (3.69 g, 9.62 mmol) gave a crude residue which was purified by flash chromatography ( $SiO_2$ , 70:30 Petrol–EtOAc) to yield the tetrahydropyrazine<sup>44</sup> **101** (2.84 g, 77%) as a yellow solid,  $R_f$  = 0.61 (50:50 Petrol–EtOAc);  $\nu_{max}/cm^{-1}$  (ATR) 2977, 2933, 1702, 1455, 1369, 1171 and 776;  $\delta_H$  (500 MHz,  $CDCl_3$ ) 7.99 (1H, dd,  $J$  7.4 and 1.7, nitrophenyl 3-H), 7.78-7.70 (2H, m, nitrophenyl 4-H and nitrophenyl 5-H), 7.66 (1H, dd,  $J$  7.4 and 1.7, nitrophenyl 6-H), 6.01 (1H, s, 5-H), 3.68-3.64 (2H, m, 3- $H_2$ ), 3.64-3.60 (2H, m, 2- $H_2$ ), 2.09 (3H, s, methyl) and 1.50 (9H, s, Boc);  $\delta_C$  (126 MHz,  $CDCl_3$ ) 152.5 (Boc CO), 148.3 (nitrophenyl C-2), 134.0 (nitrophenyl C-5), 131.7 (nitrophenyl C-4), 131.3 (nitrophenyl C-1), 130.7 (nitrophenyl C-6), 124.2 (nitrophenyl C-3), 120.2 (C-6), 108.0 (C-5), 81.7 (Boc), 44.6 (C-3), 41.6 (C-2), 28.3 (Boc) and 20.1 (methyl);  $m/z$  (ES) 406.1 (100%,  $MNa^+$ ).

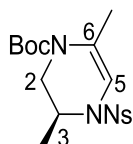
***tert*-Butyl 2-[(acetyloxy)methyl]-6-methyl-4-(2-nitrobenzenesulfonyl)-1,2,3,4-tetrahydropyrazine-1-carboxylate, **105****



By general procedure H, the sulfonamide **104** (2.25 g, 4.94 mmol) gave a crude residue which was purified by flash chromatography ( $SiO_2$ , 100% DCM) to yield the tetrahydropyrazine **105** (1.65 g, 73%) as a yellow oil,  $R_f$  = 0.65 (10:90  $Et_2O$ –DCM);  $\delta_H$  (500 MHz,  $CDCl_3$ ) 8.02 (1H, dd,  $J$  7.6 and 1.6, nitrophenyl 3-H), 7.81-7.71 (2H, m, nitrophenyl 4-H and nitrophenyl 5-H), 7.68 (1H, dd,  $J$  7.5 and 1.7, nitrophenyl 6-H), 6.03 (1H, s, 5-H), 4.88-4.71 (1H, m, 2-H), 4.09 (1H, app dt,  $J$  12.5 and 1.7, 2-methyl- $H_a$ ), 3.97 (1H, dd,  $J$  11.1 and 7.4, 3- $H_a$ ), 3.88 (1H, dd,  $J$  11.1 and 7.3, 3- $H_b$ ), 3.30 (1H, dd,  $J$  12.5 and 3.4, 2-methyl- $H_b$ ), 2.10 (3H, s, acetyl), 2.02 (3H, s, 6-methyl) and 1.50 (9H, s, Boc);  $\delta_C$  (126 MHz,  $CDCl_3$ ) 170.4 (acetyl CO), 152.3 (Boc CO), 148.1 (nitrophenyl C-2), 134.2 (nitrophenyl C-5), 131.8

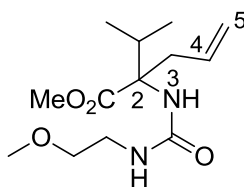
(nitrophenyl C-4), 131.2 (nitrophenyl C-1), 130.7 (nitrophenyl C-6), 124.4 (nitrophenyl C-3), 116.6 (C-6), 107.5 (C-5), 82.1 (Boc), 60.5 (2-methyl), 48.2 (C-2), 44.2 (C-3), 28.2 (Boc), 20.7 (acetyl) and 20.4 (C-6); HRMS found  $MH^+$ , 456.1552.  $C_{19}H_{25}N_3O_8S$  requires  $MH$ , 456.1440.

***tert*-Butyl-(3*S*)-3,6-dimethyl-4-[(2-nitrophenyl)sulfonyl]-1,2,3,4-tetrahydropyrazine-1-carbamate, **103****



By general procedure H, the sulfonamide **102** (1.92 g, 4.83 mmol) gave a crude residue which was purified by flash chromatography ( $SiO_2$ , 30:20:50 Petrol-Et<sub>2</sub>O-CHCl<sub>3</sub>) to give the *tetrahydropyrazine* **103** (1.82 g, 95%) as an orange oil,  $R_f = 0.81$  (30:70 Petrol-EtOAc);  $\nu_{max}/cm^{-1}$  (ATR) 3099, 2977, 2933, 1701, 1545, 1366, 1246 and 1176;  $[\alpha]_D^{28}$  182 ( $c = 0.060$ , MeOH);  $\delta_H$  (500 MHz, CDCl<sub>3</sub>) 8.07-7.93 (1H, m, nitrophenyl 3-H), 7.80-7.69 (2H, m, nitrophenyl 4-H and nitrophenyl 5-H), 7.68-7.60 (1H, m, nitrophenyl 6-H), 5.95 (1H, app t,  $J$  1.1, 5-H), 4.36-4.27 (1H, m, 3-H), 4.19 (1H, dd,  $J$  13.1 and 1.9, 2-H<sub>a</sub>), 2.58 (1H, dd,  $J$  13.1 and 2.3, 2-H<sub>b</sub>), 2.11 (3H, d,  $J$  1.1, 6-methyl), 1.50 (9H, s, Boc) and 1.17 (3H, d,  $J$  6.6, 3-methyl);  $\delta_C$  (126 MHz, CDCl<sub>3</sub>) 153.2 (CO), 148.3 (nitrophenyl C-2), 133.9 (nitrophenyl C-5), 131.7 (nitrophenyl C-1), 131.6 (nitrophenyl C-4), 130.8 (nitrophenyl C-6), 124.2 (nitrophenyl C-3), 119.5 (C-6), 106.5 (C-5), 81.5 (Boc), 49.8 (C-3), 46.1 (C-2), 28.2 (Boc), 20.0 (6-methyl) and 17.1 (3-methyl); HRMS found  $MH^+$ , 398.1387.  $C_{17}H_{23}N_3O_6S$  requires  $MH$ , 398.1386.

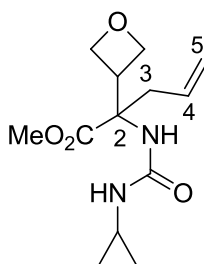
**Methyl 2-[[[(2-methoxyethyl)carbamoyl]amino]-2-(prop-2-yl)pent-4-enoate], **189****



By general procedure Q, 2-methoxyethyl isocyanate (70.0  $\mu$ L, 0.780 mmol) and amino ester **175** (89.4 mg, 0.520 mmol) gave a crude residue which was purified by flash chromatography ( $SiO_2$ , 50:50 Petrol-EtOAc) to yield the *urea* **189** (82.5 mg, 58%) as a colourless amorphous solid,  $R_f = 0.31$  (30:70 Petrol-EtOAc);  $\nu_{max}/cm^{-1}$  (ATR) 3351 (br), 2933, 2880, 1732, 1635, 1555, 1227 and 1121;  $\delta_H$  (500 MHz, CDCl<sub>3</sub>) 5.76-5.60 (1H, m, 4-H), 5.53 (1H, s, NH), 5.15-4.98 (2H, m, 5-H<sub>2</sub>), 4.84 (1H, s, methoxyethyl 1-NH), 3.78 (3H, s,

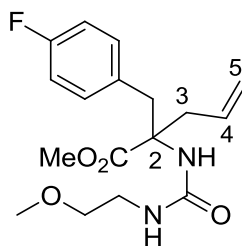
methyl), 3.48 (2H, t,  $J$  5.0, methoxyethyl 2-H<sub>2</sub>), 3.39 (3H, s, methoxyethyl 4-H<sub>3</sub>), 3.37-3.33 (2H, m, methoxyethyl 1-H<sub>2</sub>), 3.31 (1H, dd,  $J$  13.9 and 7.2, 3-H<sub>a</sub>), 2.74 (1H, dd,  $J$  13.9 and 7.4, 3-H<sub>b</sub>), 2.56 (1H, app hept,  $J$  6.9, isopropyl 2-H), 1.00 (3H, d,  $J$  6.9, isopropyl-Me<sub>A</sub>) and 0.93 (3H, d,  $J$  6.9, isopropyl-Me<sub>B</sub>);  $\delta_c$  (126 MHz, CDCl<sub>3</sub>) 173.8 (C-1), 156.6 (urea CO), 133.9 (C-4), 117.8 (C-5), 72.2 (methoxyethyl C-2), 67.5 (C-2), 58.6 (methyl), 51.9 (methoxyethyl C-4), 40.4 (methoxyethyl C-1), 36.9 (C-3), 33.9 (isopropyl C-2), 17.8 (isopropyl-Me<sub>A</sub>) and 17.7 (isopropyl-Me<sub>B</sub>); HRMS found MH<sup>+</sup>, 273.1833. C<sub>13</sub>H<sub>24</sub>N<sub>2</sub>O<sub>4</sub> requires  $MH$ , 273.1814.

### 3 Cyclopropyl-5-(oxetan-3-yl)-5-(prop-2-en-1-yl)imidazolidine-2,4-dione, **191**



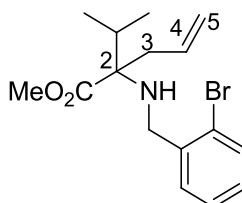
By general procedure Q, isocyanato cyclopropane (50.0  $\mu$ L, 1.05 mmol) and amino ester **184** (130 mg, 0.700 mmol) gave a crude residue which was purified by flash chromatography (SiO<sub>2</sub>, 100% EtOAc) to yield the *urea* **191** (75.8 mg, 40%) as a colourless amorphous solid,  $R_f$  = 0.13 (100% EtOAc);  $\nu_{max}$ / cm<sup>-1</sup> (ATR) 3358 (br), 2956, 2888, 1734, 1646, 1557 and 1226;  $\delta_H$  (500 MHz, CDCl<sub>3</sub>) 6.00 (1H, s, 2-NH), 5.82-5.65 (1H, m, 4-H), 5.21 (1H, d,  $J$  6.0, 5-H<sub>a</sub>), 5.18 (1H, s, cyclopropyl-NH), 4.80 (1H, t,  $J$  6.7, oxetanyl 2-H<sub>a</sub>), 4.78-4.70 (3H, m, 5-H<sub>b</sub> and oxetanyl 4-H<sub>2</sub>), 4.64 (1H, t,  $J$  6.8, oxetanyl 2-H<sub>b</sub>), 3.98-3.88 (1H, m, oxetanyl 1-H), 3.83 (3H, s, methyl), 3.00 (1H, dd,  $J$  13.9 and 8.0, 3-H<sub>a</sub>), 2.72 (1H, dd,  $J$  13.9 and 6.8, 3-H<sub>b</sub>), 2.50 (1H, tt,  $J$  6.8 and 3.6, cyclopropyl 1-H), 0.86-0.70 (2H, m, cyclopropyl 2-H<sub>2</sub>) and 0.68-0.56 (2H, m, cyclopropyl 3-H<sub>2</sub>);  $\delta_c$  (126 MHz, CDCl<sub>3</sub>) 173.1 (C-1), 157.8 (urea CO), 132.2 (C-4), 119.8 (C-5), 73.2 (oxetanyl C-2), 72.9 (oxetanyl C-4), 62.5 (C-2), 52.8 (methyl), 41.2 (oxetanyl C-1), 37.6 (C-3), 22.6 (cyclopropyl C-1), 7.7 (cyclopropyl C-2) and 7.5 (cyclopropyl C-3); HRMS found MH<sup>+</sup>, 269.1508. C<sub>13</sub>H<sub>20</sub>N<sub>2</sub>O<sub>4</sub> requires  $MH$ , 269.1501.

**Methyl 2-[(4-fluorophenyl)methyl]-2-[[2-methoxyethyl]carbamoyl]amino}pent-4-enoate, **190****



By general procedure Q, 2-methoxyethyl isocyanate (0.160 mL, 1.79 mmol) and amino ester **186** (282 mg, 1.19 mmol) gave a crude residue which was purified by flash chromatography (SiO<sub>2</sub>, 50:50 Petrol–EtOAc) to yield the *urea* **190** (210 mg, 52%) as a colourless amorphous solid,  $R_f = 0.42$  (30:70 Petrol–EtOAc);  $\nu_{\max}/\text{cm}^{-1}$  (ATR) 3344 (br), 2930, 1740, 1636, 1556, 1509 and 1221;  $\delta_{\text{H}}$  (500 MHz, CDCl<sub>3</sub>) 6.98–6.92 (2H, m, fluorophenyl 2-H and fluorophenyl 6-H), 6.88–6.82 (2H, m, fluorophenyl 3-H and fluorophenyl 5-H), 5.58 (1H, ddt,  $J$  17.3, 10.1 and 7.4, 4-H), 5.17 (1H, s, urea NH), 5.09–4.90 (2H, m, 5-H<sub>2</sub>), 4.63 (1H, t,  $J$  5.5, methoxyethyl 1-NH), 3.68 (3H, s, methyl), 3.65 (1H, d,  $J$  13.6, benzylic-H<sub>a</sub>), 3.38 (2H, t,  $J$  5.0, methoxyethyl 2-H<sub>2</sub>), 3.33–3.19 (6H, m, 3-H<sub>a</sub>, methoxyethyl 1-H<sub>2</sub> and methoxyethyl 4-H<sub>3</sub>), 3.02 (1H, d,  $J$  13.6, benzylic-H<sub>b</sub>) and 2.49 (1H, dd,  $J$  13.8 and 7.7, 3-H<sub>b</sub>);  $\delta_{\text{C}}$  (126 MHz, CDCl<sub>3</sub>) 173.6 (C-1), 161.9 (d,  $J$  244.8 Hz, fluorophenyl C-4), 156.5 (urea CO), 132.7 (C-4), 132.5 (d,  $J$  3.3, fluorophenyl C-1), 131.3 (d,  $J$  7.9, fluorophenyl C-2 and fluorophenyl C-6), 118.8 (C-5), 114.9 (d,  $J$  21.1, fluorophenyl C-3 and fluorophenyl C-5), 72.1 (methoxyethyl C-2), 65.4 (C-2), 58.7 (methyl), 52.5 (methoxyethyl C-4), 40.3 (benzylic C) and 40.2 (C-3 and methoxyethyl C-1);  $\delta_{\text{F}}$  (282 MHz, CDCl<sub>3</sub>) –116.3; HRMS found MH<sup>+</sup>, 339.1744. C<sub>17</sub>H<sub>23</sub>FN<sub>2</sub>O<sub>4</sub> requires *MH*, 339.1720.

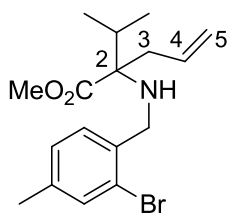
**Methyl 2-[[2-(2-bromophenyl)methyl]amino]-2-(propan-2-yl)pent-4-enoate, **194****



2-Bromobenzaldehyde (2.12 mL, 18.2 mmol) was added to the amino ester **175** (1.56 g, 9.11 mmol) in DCM (40 mL, ~0.2 M) in the presence of 4 Å mol. sieves (312 mg, 0.2 w/w). NaBH(OAc)<sub>3</sub> (7.73 g, 36.4 mmol) was added and the mixture stirred at reflux overnight. The mixture was concentrated *in vacuo* and the residue was purified by flash chromatography (SiO<sub>2</sub>, 95:5 Petrol–EtOAc), then again (SiO<sub>2</sub>, 95:5 Petrol–EtOAc) to yield

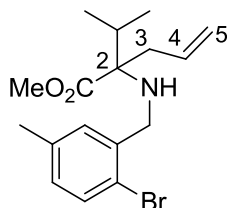
the *alkylated amine* **194** (2.07 g, 67%) as a yellow oil,  $R_f = 0.76$  (80:20 Petrol–EtOAc);  $\nu_{\max}/\text{cm}^{-1}$  (ATR) 2962, 1725, 1464, 1437, 1212 and 1025;  $\delta_{\text{H}}$  (500 MHz,  $\text{CDCl}_3$ ) 7.59-7.49 (2H, m, bromobenzyl 3-H and 6-H), 7.34-7.28 (1H, m, bromobenzyl 4-H), 7.12 (1H, app td,  $J$  7.7, 1.6, bromobenzyl 5-H), 6.06-5.89 (1H, m, 4-H), 5.18 (1H, dd,  $J$  17.2 and 1.4, 5- $\text{H}_a$ ), 5.13 (1H, dd,  $J$  10.2 and 0.8, 5- $\text{H}_b$ ), 3.87 (1H, d,  $J$  13.0, benzylic- $\text{H}_a$ ), 3.79-3.72 (4H, m, methyl and benzylic- $\text{H}_b$ ), 2.72 (1H, ddt,  $J$  15.0, 6.3 and 1.4, 3- $\text{H}_a$ ), 2.67-2.55 (1H, m, 3- $\text{H}_b$ ), 2.13 (1H, hept,  $J$  6.9, isopropyl 2-H), 2.03 (1H, s, NH) and 1.00 (6H, d,  $J$  6.9, isopropyl- $\text{Me}_A$  and isopropyl- $\text{Me}_B$ );  $\delta_{\text{C}}$  (126 MHz,  $\text{CDCl}_3$ ) 175.1, (CO), 139.9 (bromobenzyl C-2), 134.3 (bromobenzyl C-3), 132.6 (C-4), 130.2 (bromobenzyl C-6), 128.4 (bromobenzyl C-4), 127.6 (bromobenzyl C-5), 123.9 (bromobenzyl C-1), 117.7 (C-5), 67.7 (C-2), 51.5 (methyl), 47.3 (benzylic-C), 36.4 (C-3), 33.8 (isopropyl C-2), 17.8 (isopropyl- $\text{Me}_A$ ) and 17.2 (isopropyl- $\text{Me}_B$ ); HRMS found  $\text{MH}^+$ , 340.1011.  $\text{C}_{16}\text{H}_{22}\text{BrNO}_2$  requires  $\text{MH}$ , 340.0912.

**Methyl 2-[[[2-bromo-4-methylphenyl)methyl]amino]-2-(propan-2-yl)pent-4-enoate, 269**



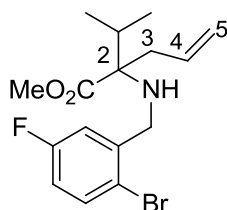
By general procedure N, amino ester **175** (430 mg, 2.51 mmol) and 2-bromo-4-methylbenzaldehyde (1.00 g, 5.02 mmol) gave a crude residue which was purified by flash chromatography ( $\text{SiO}_2$ , 95:5 Petrol–EtOAc) to yield the *alkylated amine* **269** (590 mg, 66%) as a colourless oil,  $R_f = 0.57$  (90:10 Petrol–EtOAc);  $\nu_{\max}/\text{cm}^{-1}$  (ATR) 3073, 2964, 2877, 1725, 1464, 1433, 1212 and 1141;  $\delta_{\text{H}}$  (400 MHz,  $\text{CDCl}_3$ ) 7.41-7.36 (2H, m, bromobenzyl 5-H and bromobenzyl 6-H), 7.10 (1H, d,  $J$  7.8, bromobenzyl 3-H), 6.03-5.89 (1H, m, 4-H), 5.23-5.14 (1H, m, 5- $\text{H}_a$ ), 5.12 (1H, d,  $J$  10.1, 5- $\text{H}_b$ ), 3.81 (1H, d,  $J$  12.7, benzylic- $\text{H}_a$ ), 3.74 (3H, s, methyl), 3.69 (1H, d,  $J$  12.7, benzylic- $\text{H}_b$ ), 2.71 (1H, dd,  $J$  15.0 and 6.3, 3- $\text{H}_a$ ), 2.62 (1H, dd,  $J$  15.0 and 7.8, 3- $\text{H}_b$ ), 2.33 (3H, s, tolyl), 2.18-2.06 (1H, m, isopropyl 2-H), 1.97 (1H, br s, NH) and 0.98 (6H, d,  $J$  6.9, isopropyl- $\text{Me}_A$  and isopropyl- $\text{Me}_B$ );  $\delta_{\text{C}}$  (101 MHz,  $\text{CDCl}_3$ ) 175.2 (C-1), 138.5 (bromobenzyl C-1), 136.8 (bromobenzyl C-2), 134.3 (C-4), 133.0 (bromobenzyl C-6), 130.1 (bromobenzyl C-5), 128.3 (bromobenzyl C-3), 123.7 (bromobenzyl C-4), 117.6 (C-5), 67.7 (C-2), 51.5 (methyl), 47.0 (benzylic-C), 36.3 (C-3), 33.8 (isopropyl C-2), 20.7 (tolyl), 17.8 (isopropyl- $\text{Me}_A$ ) and 17.2 (isopropyl- $\text{Me}_B$ ); HRMS found  $\text{MH}^+$ , 354.1085.  $\text{C}_{17}\text{H}_{24}\text{BrNO}_2$  requires  $\text{MH}$ , 354.1068.

**Methyl 2-[[2-(2-bromo-5-methylphenyl)methyl]amino]-2-(propan-2-yl)pent-4-enoate, 270**



By general procedure N, amino ester **175** (430 mg, 2.51 mmol) and 2-bromo-5-methylbenzaldehyde (1.00 g, 5.02 mmol) gave a crude residue which was purified by flash chromatography (SiO<sub>2</sub>, 90:10 Petrol–EtOAc) to yield the *alkylated amine* **270** (710 mg, 80%) as a colourless oil,  $R_f = 0.53$  (90:10 Petrol–EtOAc);  $\nu_{\max}/\text{cm}^{-1}$  (ATR) 3356, 3075, 2964, 1726, 1466, 1212, 1024 and 807;  $\delta_{\text{H}}$  (400 MHz, CDCl<sub>3</sub>) 7.19 (1H, d,  $J$  8.1, bromobenzyl 3-H), 7.08 (1H, d,  $J$  1.9, bromobenzyl 6-H), 6.72 (1H, dd,  $J$  8.1 and 1.9, bromobenzyl 4-H), 5.81-5.68 (1H, m, 4-H), 5.00-4.93 (1H, m, 5-H<sub>A</sub>), 4.93-4.88 (1H, m, 5-H<sub>B</sub>), 3.59 (1H, d,  $J$  12.6, benzylic-H<sub>A</sub>), 3.53 (3H, s, methyl), 3.50-3.43 (1H, m, benzylic-H<sub>B</sub>), 2.50 (1H, dd,  $J$  15.0 and 6.3, 3-H<sub>A</sub>), 2.40 (1H, dd,  $J$  15.0 and 7.8, 3-H<sub>B</sub>), 2.10 (3H, s, tolyl), 1.97-1.86 (1H, m, isopropyl 2-H), 1.78 (1H, br s, NH) and 0.77 (6H, d,  $J$  6.9, isopropyl-Me<sub>A</sub> and isopropyl-Me<sub>B</sub>);  $\delta_{\text{C}}$  (101 MHz, CDCl<sub>3</sub>) 175.1 (C-1), 139.3 (bromobenzyl C-1), 137.4 (bromobenzyl C-2), 134.3 (C-4), 132.3 (bromobenzyl C-3), 131.1 (bromobenzyl C-6), 129.3 (bromobenzyl C-4), 120.6 (bromobenzyl C-5), 117.7 (C-5), 67.7 (C-2), 51.5 (methyl), 47.3 (benzylic-C), 36.3 (C-3), 33.7 (isopropyl C-2), 21.0 (tolyl), 17.8 (isopropyl-Me<sub>A</sub>) and 17.2 (isopropyl-Me<sub>B</sub>); HRMS found  $\text{MH}^+$ , 354.1083. C<sub>17</sub>H<sub>24</sub>BrNO<sub>2</sub> requires  $MH$ , 354.1068.

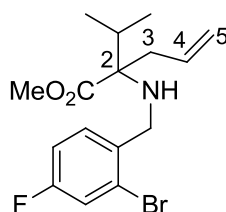
**Methyl 2-[[2-(2-bromo-5-fluorophenyl)methyl]amino]-2-(propan-2-yl)pent-4-enoate, 271**



By general procedure N, amino ester **175** (500 mg, 2.92 mmol) and 2-bromo-5-fluorobenzaldehyde (1.19 g, 5.84 mmol) gave a crude residue which was purified by flash chromatography (SiO<sub>2</sub>, 95:5 Petrol–EtOAc) to yield the *alkylated amine* **271** (670 mg, 64%) as a colourless oil,  $R_f = 0.69$  (90:10 Petrol–EtOAc);  $\nu_{\max}/\text{cm}^{-1}$  (ATR) 3074, 2966, 1727, 1464, 1434, 1215 and 1142;  $\delta_{\text{H}}$  (400 MHz, CDCl<sub>3</sub>) 7.25 (1H, dd,  $J$  8.7 and 5.3, bromobenzyl 6-H), 7.13 (1H, dd,  $J$  8.7 and 3.1, bromobenzyl 3-H), 6.63 (1H, td,  $J$  8.7 and 3.1, bromobenzyl

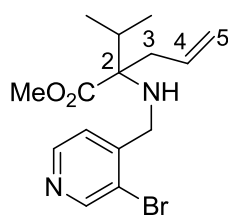
4-H), 5.74-5.61 (1H, m, 4-H), 4.97-4.85 (2H, m, 5-H<sub>2</sub>), 3.62-3.49 (5H, m, benzylic-H<sub>2</sub> and methyl), 2.46 (1H, dd, *J* 15.0 and 6.4, 3-H<sub>a</sub>), 2.38 (1H, dd, *J* 15.0 and 7.8, 3-H<sub>b</sub>), 1.95-1.84 (1H, m, isopropyl 2-H), 1.76 (1H, br s, NH) and 0.77 (6H, d, *J* 6.9, isopropyl-Me<sub>A</sub> and isopropyl-Me<sub>B</sub>);  $\delta_c$  (101 MHz, CDCl<sub>3</sub>) 175.1 (C-1), 162.2 (d, *J* 246.2, bromobenzyl C-5), 142.4 (d, *J* 7.3, bromobenzyl C-1), 134.1 (C-4), 133.5 (d, *J* 8.0, bromobenzyl C-6), 117.9 (C-5), 117.4 (d, *J* 3.0, bromobenzyl C-2), 116.9 (d, *J* 23.5, bromobenzyl C-3), 115.3 (d, *J* 22.7, bromobenzyl C-4), 67.7 (C-2), 51.6 (methyl), 47.0 (benzylic -C), 36.6 (C-3), 34.0 (isopropyl C-2), 17.8 (isopropyl-Me<sub>A</sub>) and 17.2 (isopropyl-Me<sub>B</sub>);  $\delta_F$  (376 MHz, CDCl<sub>3</sub>) -114.6; HRMS found MH<sup>+</sup>, 358.0834. C<sub>16</sub>H<sub>21</sub>BrFNO<sub>2</sub> requires *MH*, 358.0818.

**Methyl 2-[[[(2-bromo-4-fluorophenyl)methyl]amino]-2-(propan-2-yl)pent-4-enoate, 272**



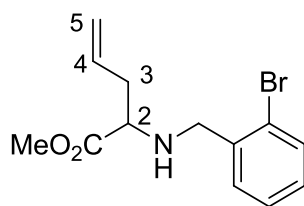
By general procedure N, amino ester **175** (500 mg, 2.92 mmol) and 2-bromo-4-fluorobenzaldehyde (1.19 g, 5.84 mmol) gave a crude residue which was purified by flash chromatography (SiO<sub>2</sub>, 90:10 Petrol-EtOAc) to yield the *alkylated amine 272* (700 mg, 67%) as a colourless oil, *R<sub>f</sub>* = 0.53 (90:10 Petrol-EtOAc);  $\nu_{max}$ / cm<sup>-1</sup> (ATR) 3356, 3074, 2966, 1726, 1598, 1484, 1215 and 857;  $\delta_H$  (400 MHz, CDCl<sub>3</sub>) 7.51 (1H, dd, *J* 8.3 and 6.2, bromobenzyl 3-H), 7.28 (1H, dd, *J* 8.3 and 2.6, bromobenzyl 6-H), 7.02 (1H, td, *J* 8.3 and 2.6, bromobenzyl 5-H), 6.01-5.83 (1H, m, 4-H), 5.16 (1H, dd, *J* 17.2 and 1.5, 5-H<sub>a</sub>), 5.13-5.07 (1H, m, 5-H<sub>b</sub>), 3.81 (1H, d, *J* 13.0, benzylic-H<sub>a</sub>), 3.75 (3H, s, methyl), 3.70 (1H, d, *J* 13.0, benzylic-H<sub>b</sub>), 2.69 (1H, dd, *J* 15.0 and 6.3, 3-H<sub>a</sub>), 2.60 (1H, dd, *J* 15.0 and 7.8, 3-H<sub>b</sub>), 2.17-2.05 (1H, m, isopropyl 2-H), 1.95 (1H, br s, NH) and 0.98 (6H, d, *J* 6.9, isopropyl-Me<sub>A</sub> and isopropyl-Me<sub>B</sub>);  $\delta_c$  (101 MHz, CDCl<sub>3</sub>) 175.0 (C-1), 161.3 (d, *J* 249.3, bromobenzyl C-4), 135.9 (d, *J* 3.5, bromobenzyl C-2), 134.2 (C-4), 131.1 (d, *J* 8.3, bromobenzyl C-3), 123.6 (d, *J* 9.5, bromobenzyl C-1), 119.7 (d, *J* 24.3, bromobenzyl C-6), 117.7 (C-5), 114.5 (d, *J* 20.6, bromobenzyl C-5), 67.7 (C-2), 51.5 (methyl), 46.6 (benzylic-C), 36.4 (C-3), 33.9 (isopropyl C-2), 17.8 (isopropyl-Me<sub>A</sub>) and 17.2 (isopropyl-Me<sub>B</sub>);  $\delta_F$  (376 MHz, CDCl<sub>3</sub>) -114.1; HRMS found MH<sup>+</sup>, 358.0832. C<sub>16</sub>H<sub>21</sub>BrFNO<sub>2</sub> requires *MH*, 358.0818.

### Methyl 2-(((3-bromopyridin-4-yl)methyl)amino)-2-isopropylpent-4-enoate, 273



By general procedure N, amino ester **175** (461 mg, 2.69 mmol) and 3-bromo-4-pyridine carboxaldehyde (1.00 g, 5.38 mmol) gave a crude residue which was purified by flash chromatography (SiO<sub>2</sub>, 80:20 Petrol–EtOAc) to yield the *alkylated amine* **273** (520 mg, 57%) as a colourless oil,  $R_f = 0.16$  (90:10 Petrol–EtOAc);  $\nu_{\max}/\text{cm}^{-1}$  (ATR) 3075, 2965, 2877, 1727, 1468, 1434, 1218 and 1022;  $\delta_{\text{H}}$  (400 MHz, CDCl<sub>3</sub>) 8.42 (1H, s, bromopyridyl 2-H), 8.27 (1H, d,  $J$  4.9, bromopyridyl 6-H), 7.35 (1H, d,  $J$  4.9, bromopyridyl 5-H), 5.78–5.51 (1H, m, 4-H), 4.89 (2H, t,  $J$  13.4, 5-H<sub>2</sub>), 3.59 (2H, d,  $J$  6.5, benzylic-H<sub>2</sub>), 3.53 (3H, s, methyl), 2.44 (1H, dd,  $J$  15.0 and 6.4, 3-H<sub>a</sub>), 2.36 (1H, dd,  $J$  15.0 and 7.9, 3-H<sub>b</sub>), 1.94–1.84 (1H, m, isopropyl 2-H), 1.77 (1H, br s, NH) and 0.77 (6H, d,  $J$  6.9, isopropyl-Me<sub>A</sub> and isopropyl-Me<sub>B</sub>);  $\delta_{\text{C}}$  (101 MHz, CDCl<sub>3</sub>) 175.0 (CO), 151.4 (bromopyridyl C-2), 149.2 (bromopyridyl C-3), 148.4 (bromopyridyl C-6), 133.9 (C-4), 124.2 (bromopyridyl C-5), 121.9 (bromopyridyl C-4), 118.1 (C-5), 67.7 (C-2), 51.7 (methyl), 46.3 (benzylic-C), 36.8 (C-3), 34.1 (isopropyl C-2), 17.8 (isopropyl-Me<sub>A</sub> and 17.2 (isopropyl-Me<sub>B</sub>); HRMS found  $MH^+$ , 341.1004. C<sub>15</sub>H<sub>21</sub>BrN<sub>2</sub>O<sub>2</sub> requires  $MH$ , 341.0864.

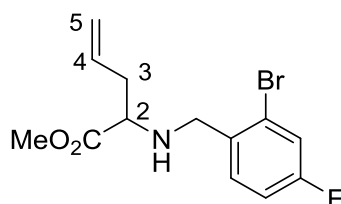
### Methyl 2-(((2-bromophenyl)methyl)amino)pent-4-enoate, 275



Et<sub>3</sub>N (0.420 mL, 3.02 mmol) was added to a mixture of methyl 2-aminopent-4-enoate hydrochloride (500 mg, 3.02 mmol) and bromobenzaldehyde (1.12 g, 6.04 mmol), which by general procedure N, gave a crude residue which was purified by flash chromatography (SiO<sub>2</sub>, 95:5 Petrol–EtOAc) to yield the *alkylated amine* **275** (560 mg, 62%) as a colourless oil,  $R_f = 0.45$  (80:20 Petrol–EtOAc);  $\nu_{\max}/\text{cm}^{-1}$  (ATR) 3331 (br), 3073, 2980, 2949, 2841, 1733, 1435, 1195 and 748;  $\delta_{\text{H}}$  (400 MHz, CDCl<sub>3</sub>) 7.55 (1H, d,  $J$  7.6, bromobenzyl 6-H), 7.43 (1H, dd,  $J$  7.6 and 1.6, bromobenzyl 3-H), 7.29 (1H, t,  $J$  7.6, bromobenzyl 4-H), 7.13 (1H, td,  $J$  7.6 and 1.6, bromobenzyl 5-H), 5.78 (1H, ddt,  $J$  17.2, 10.1 and 7.1, 4-H), 5.17–5.12 (1H, m, 5-H<sub>a</sub>), 5.12–5.09 (1H, m, 5-H<sub>b</sub>), 3.93 (1H, d,  $J$  14.0, benzylic-

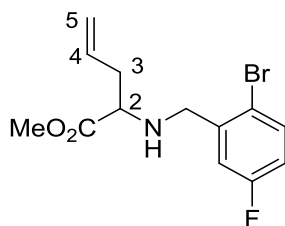
H<sub>a</sub>), 3.79 (1H, d, *J* 14.0, benzylic-H<sub>b</sub>), 3.72 (3H, s, methyl), 3.40 (1H, t, *J* 6.5, 2-H), 2.54-2.40 (2H, m, 3-H<sub>2</sub>) and 2.06 (1H, br s, NH); δ<sub>c</sub> (101 MHz, CDCl<sub>3</sub>) 174.7 (C-1), 138.8 (bromobenzyl C-2), 133.6 (C-4), 132.8 (bromobenzyl C-6), 130.2 (bromobenzyl C-3), 128.7 (bromobenzyl C-4), 127.4 (bromobenzyl C-5), 124.1 (bromobenzyl C-1), 118.2 (C-5), 60.4 (methyl), 51.9 (benzylic-C), 51.7 (C-2) and 37.7 (C-3); HRMS found MH<sup>+</sup>, 298.0452. C<sub>13</sub>H<sub>16</sub>BrNO<sub>2</sub> requires *MH*, 298.0442.

### Methyl 2-[(2-bromo-4-fluorophenyl)methyl]amino}pent-4-enoate, 276



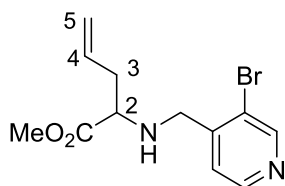
Et<sub>3</sub>N (0.420 mL, 3.02 mmol) was added to a mixture of methyl 2-aminopent-4-enoate hydrochloride (500 mg, 3.02 mmol) and 2-bromo-4-fluoro benzaldehyde (1.23 g, 6.04 mmol), which by general procedure N, gave a crude residue which was purified by flash chromatography (SiO<sub>2</sub>, 95:5 to 85:15 Petrol–EtOAc) to yield the *alkylated amine* **276** (440 mg, 46%) as a colourless oil, *R*<sub>f</sub> = 0.40 (80:20 Petrol–EtOAc); ν<sub>max</sub>/ cm<sup>-1</sup> (ATR) 3077, 2950, 2842, 1734, 1484, 1220, 1172, 876 and 858; δ<sub>H</sub> (400 MHz, CDCl<sub>3</sub>) 7.41 (1H, dd, *J* 8.4 and 6.1, bromobenzyl 3-H), 7.30 (1H, dd, *J* 8.4 and 2.6, bromobenzyl 6-H), 7.02 (1H, td, *J* 8.4 and 2.6, bromobenzyl 5-H), 5.85-5.70 (1H, m, 4-H), 5.17-5.12 (1H, m, 5-H<sub>a</sub>), 5.12-5.09 (1H, m, 5-H<sub>b</sub>), 3.89 (1H, d, *J* 14.0, benzylic-H<sub>a</sub>), 3.81-3.68 (4H, m, benzylic-H<sub>b</sub> and methyl), 3.37 (1H, t, *J* 6.5, 2-H), 2.53-2.37 (2H, m, 3-H<sub>2</sub>) and 1.97 (1H, br s, NH); δ<sub>c</sub> (101 MHz, CDCl<sub>3</sub>) 174.7 (C-1), 161.5 (d, *J* 250.1, bromobenzyl C-4), 134.7 (bromobenzyl C-2), 133.5 (C-4), 131.0 (d, *J* 8.2, bromobenzyl C-3), 123.9 (d, *J* 9.3, bromobenzyl C-1), 119.9 (d, *J* 24.3, bromobenzyl C-6), 118.2 (C-5), 114.4 (d, *J* 20.6, bromobenzyl C-5), 60.3 (C-2), 51.8 (methyl), 51.1 (benzylic-C) and 37.7 (C-3); δ<sub>F</sub> (376 MHz, CDCl<sub>3</sub>) -113.7; HRMS found MH<sup>+</sup>, 316.0410. C<sub>13</sub>H<sub>15</sub>BrFNO<sub>2</sub> requires *MH*, 316.0348.

### Methyl 2-[[2-bromo-5-fluorophenyl)methyl]amino]pent-4-enoate, 277



Et<sub>3</sub>N (0.420 mL, 3.02 mmol) was added to a mixture of methyl 2-aminopent-4-enoate hydrochloride (500 mg, 3.02 mmol) and 2-bromo-5-fluoro benzaldehyde (1.23 g, 6.04 mmol), which by general procedure N, gave a crude residue which was purified by flash chromatography (SiO<sub>2</sub>, 95:5 to 80:20 Petrol–EtOAc) to yield the *alkylated amine* **277** (480 mg, 50%) as a colourless oil,  $R_f = 0.73$  (70:30 Petrol–EtOAc);  $\nu_{\max}/\text{cm}^{-1}$  (ATR) 3345 (br), 3077, 2951, 2843, 1734, 1464, 1435, 1197 and 1149;  $\delta_{\text{H}}$  (400 MHz, CDCl<sub>3</sub>) 7.47 (1H, dd,  $J$  8.9 and 5.3, bromobenzyl 6-H), 7.24 (1H, dd,  $J$  8.9 and 3.1, bromobenzyl 3-H), 6.85 (1H, td,  $J$  8.9 and 3.1, bromobenzyl 4-H), 5.87–5.71 (1H, m, 4-H), 5.20–5.09 (2H, m, 5-H<sub>2</sub>), 3.90 (1H, d,  $J$  14.8, benzylic-H<sub>a</sub>), 3.76–3.68 (4H, m, benzylic-H<sub>b</sub> and methyl), 3.38 (1H, t,  $J$  6.4, 2-H), 2.54–2.39 (2H, m, 3-H<sub>2</sub>) and 2.00 (1H, br s, NH);  $\delta_{\text{C}}$  (101 MHz, CDCl<sub>3</sub>) 174.7 (C-1), 162.1 (d,  $J$  246.7, bromobenzyl C-5), 141.2 (d,  $J$  7.1, bromobenzyl C-1), 133.7 (d,  $J$  8.0, bromobenzyl C-6), 133.4 (C-4), 118.3 (C-5), 117.6 (d,  $J$  3.1, bromobenzyl C-2), 116.8 (d,  $J$  23.6, bromobenzyl C-3), 115.5 (d,  $J$  22.6, bromobenzyl C-4), 60.4 (methyl), 51.8 (C-2), 51.5 (benzylic-C) and 37.7 (C-3);  $\delta_{\text{F}}$  (376 MHz, CDCl<sub>3</sub>) –114.7; HRMS found MH<sup>+</sup>, 316.0345. C<sub>13</sub>H<sub>15</sub>BrFNO<sub>2</sub> requires  $MH$ , 316.0348.

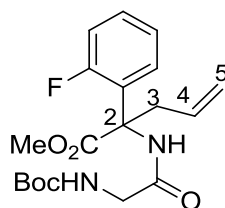
### Methyl 2-[[3-bromopyridin-4-yl)methyl]amino]pent-4-enoate, 278



Et<sub>3</sub>N (0.420 mL, 3.02 mmol) was added to a mixture of methyl 2-aminopent-4-enoate hydrochloride (500 mg, 3.02 mmol) and 3-bromo-4-pyridine carboxaldehyde (1.12 g, 6.04 mmol), which by general procedure N, gave a crude residue which was purified by flash chromatography (SiO<sub>2</sub>, 70:30 Petrol–EtOAc) to yield the *alkylated amine* **278** (490 mg, 54%) as a colourless oil,  $R_f = 0.44$  (70:30 Petrol–EtOAc);  $\nu_{\max}/\text{cm}^{-1}$  (ATR) 3322 (br), 2950, 1734, 1198, 1171, 1147, 1016 and 991;  $\delta_{\text{H}}$  (400 MHz, CDCl<sub>3</sub>) 8.57 (1H, s, bromopyridyl 2-H), 8.41 (1H, d,  $J$  5.0, bromopyridyl 6-H), 7.39 (1H, dd,  $J$  5.0 and 0.8, bromopyridyl 5-H), 5.84–5.64 (1H, m, 4-H), 5.14–5.02 (2H, m, 5-H<sub>2</sub>), 3.86 (1H, dd,  $J$  15.7

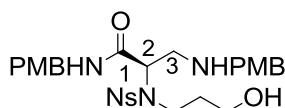
and 0.9, benzylic-H<sub>a</sub>), 3.68-3.59 (4H, m, benzylic-H<sub>b</sub> and methyl), 3.29 (1H, dd, *J* 6.7 and 6.0, 2-H), 2.50-2.29 (2H, m, 3-H<sub>2</sub>) and 1.91 (1H, br s, NH);  $\delta_c$  (101 MHz, CDCl<sub>3</sub>) 174.6 (C-1), 151.6 (bromopyridyl C-2), 148.4 (bromopyridyl C-6), 148.0 (bromopyridyl C-3), 133.3 (C-4), 124.0 (bromopyridyl C-5), 122.0 (bromopyridyl C-4), 118.5 (C-5), 60.5 (methyl), 51.9 (C-2), 50.6 (benzylic-C) and 37.7 (C-3); HRMS found MH<sup>+</sup>, 299.0352. C<sub>12</sub>H<sub>15</sub>BrN<sub>2</sub>O<sub>2</sub> requires *MH*, 299.0395.

**Methyl 2-(2-[[*tert*-butoxy]carbonyl]amino)acetamido)-2-(2-fluorophenyl)pent-4-enoate, 193**



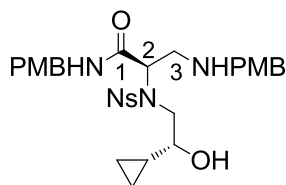
By general procedure P, the methyl ester **188** (560 mg, 2.55 mmol) gave the crude allylated amino ester. TBTU (732 mg, 2.28 mmol) was added to a stirred solution of *N*-Boc-glycine (399 mg, 2.28 mmol) in DCM (15.0 mL, ~0.1 M). The crude amino ester (340 mg, 1.52 mmol) and Et<sub>3</sub>N (0.320 mL, 2.28 mmol) was added and the reaction mixture was stirred overnight, before being extracted with DCM (3 × 20 mL), and washed with water (20 mL) and brine (20 mL). The combined organic layers were dried (MgSO<sub>4</sub>) and concentrated *in vacuo* before being purified by flash chromatography (SiO<sub>2</sub>, 50:50 Petrol–EtOAc) to yield the *amide* **193** (520 mg, 54% over two steps) as a yellow oil, *R*<sub>f</sub> = 0.78 (40:60 Petrol–EtOAc);  $\nu_{\max}$ /cm<sup>-1</sup> (ATR) 3390, 2979, 1682, 1491, 1231 and 1164;  $\delta_H$  (500 MHz, CDCl<sub>3</sub>) 7.65 (1H, td, *J* 8.0 and 1.1, fluorophenyl 4-H), 7.50 (1H, s, NH), 7.35-7.30 (1H, m, fluorophenyl 3-H), 7.21 (1H, td, *J* 8.0 and 1.0, fluorophenyl 5-H), 7.03 (1H, ddd, *J* 11.7, 8.0 and 1.1, fluorophenyl 6-H), 5.75-5.65 (1H, m, 4-H), 5.20 (1H, d, *J* 2.6, 5-H<sub>a</sub>), 5.17 (1H, app s, 5-H<sub>b</sub>), 5.06 (1H, br s, glycine-H<sub>a</sub>), 3.91 (1H, dd, *J* 13.3 and 6.5, 3-H<sub>a</sub>), 3.84-3.70 (4H, m, methyl and glycine-H<sub>b</sub>), 2.92 (1H, dd, *J* 13.3 and 8.0, 3-H<sub>b</sub>) and 1.48 (9H, s, Boc);  $\delta_c$  (126 MHz, CDCl<sub>3</sub>) 172.1 (ester-CO), 167.8 (glycine C-1), 159.1 (fluorophenyl C-2), 131.4 (C-4), 129.9 (d, *J* 8.9, fluorophenyl C-4), 128.9 (d, *J* 3.2, fluorophenyl C-3), 126.8 (fluorophenyl C-1), 123.8 (d, *J* 3.4, fluorophenyl C-5), 119.9 (C-5), 115.8 (d, *J* 22.2, fluorophenyl C-6), 62.3 (C-2), 53.3 (methyl), 45.0 (glycine C-2), 37.2 (C-3) and 28.3 (Boc), Boc quaternary carbons not observed;  $\delta_F$  (282 MHz, CDCl<sub>3</sub>) -113.9; HRMS found MH<sup>+</sup>, 381.1827. C<sub>19</sub>H<sub>25</sub>FN<sub>2</sub>O<sub>5</sub> requires *MH*, 381.1826.

**(2R)-2-[N-(3-Hydroxypropyl)2-nitrobenzenesulfonamido]-N-[(4-methoxyphenyl)methyl]-3-[[4-methoxyphenyl)methyl]amino}propanamide, 232**



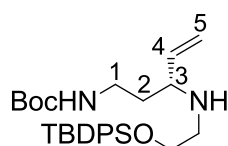
By general procedure F, propargyl sulfonamide **223** (169 mg, 0.650 mmol) and cyclic sulfamidate **S-54** (240 mg, 0.590 mmol) gave a crude residue which was purified by flash chromatography (SiO<sub>2</sub>, 100% EtOAc) to yield the *sulfonamide* **232** (110 mg, 32%) as a yellow oil,  $R_f = 0.24$  (100% EtOAc);  $\nu_{\max}/\text{cm}^{-1}$  (ATR) 3392 (br), 2936, 2837, 1667, 1542, 1512 and 1247;  $[\alpha]_D^{27}$  121 ( $c = 0.057$ , CHCl<sub>3</sub>);  $\delta_H$  (500 MHz, CDCl<sub>3</sub>) 8.20-8.14 (1H, m, nitrophenyl 3-H), 8.09 (1H, t,  $J$  5.1, 1-NH), 7.69-7.61 (2H, m, nitrophenyl 4-H and nitrophenyl 5-H), 7.56-7.49 (1H, m nitrophenyl 6-H), 7.17 (2H, d,  $J$  8.6, 1-PMB 2-H and 3-PMB 2-H), 7.03 (2H, d,  $J$  8.6, 1-PMB 6-H and 3-PMB 6-H), 6.87 (2H, d,  $J$  8.6, 1-PMB 3-H and 3-PMB 3-H), 6.80 (2H, d,  $J$  8.6, 1-PMB 5-H and 3-PMB 5-H), 4.53 (1H, dd,  $J$  8.5 and 6.0, 2-H), 4.37-4.24 (2H, m, 1-benzylic-H<sub>2</sub>), 3.83 (3H, s, 1-PMB-methyl), 3.82 (3H, s, 3-PMB-methyl), 3.69 (1H, d,  $J$  12.8, 3-benzylic-H<sub>a</sub>), 3.65 (1H, d,  $J$  12.8, 3-benzylic-H<sub>b</sub>), 3.59 (2H, t,  $J$  5.7, hydroxypropyl 3-H<sub>2</sub>), 3.53 (2H, t,  $J$  7.1, hydroxypropyl 1-H<sub>2</sub>), 3.16 (1H, dd,  $J$  12.2 and 8.5, 3-H<sub>a</sub>), 3.06 (1H, dd,  $J$  12.2 and 6.0, 3-H<sub>b</sub>), 2.13 (2H, br s, 3-NH and OH) and 1.90-1.71 (2H, m, hydroxypropyl 2-H<sub>2</sub>);  $\delta_C$  (126 MHz, CDCl<sub>3</sub>) 169.1 (C-1), 159.1 (1-PMB C-4), 158.9 (3-PMB C-4), 147.9 (nitrophenyl C-2), 133.7 (nitrophenyl C-5), 133.0 (nitrophenyl C-1), 131.8 (nitrophenyl C-4), 131.2 (nitrophenyl C-6), 131.0 (1-PMB C-1), 129.8 (3-PMB C-1), 129.4 (1-PMB C-2 and 3-PMB C-2), 129.2 (1-PMB C-6 and 3-PMB C-6), 124.2 (nitrophenyl C-3), 114.1 (1-PMB C-3 and 3-PMB C-3), 113.9 (1-PMB C-5 and 3-PMB C-5), 59.5 (C-2), 59.3 (hydroxypropyl C-3), 55.31 (1-PMB methyl), 55.28 (3-PMB methyl), 52.9 (3-PMB benzylic-C), 49.0 (hydroxypropyl C-1), 43.8 (C-3), 43.1 (1-PMB benzylic-C) and 32.7 (hydroxypropyl C-2); HRMS found MH<sup>+</sup>, 587.2207. C<sub>28</sub>H<sub>34</sub>N<sub>4</sub>O<sub>8</sub>S requires *MH*, 587.2175.

**(2R)-2-{N-[(2R)-2-Cyclopropyl-2-hydroxyethyl]-2-nitrobenzenesulfonamido}-N-[[4-methoxyphenyl)methyl]-3-[[[(4-methoxyphenyl)methyl]amino}propanamide, **234****



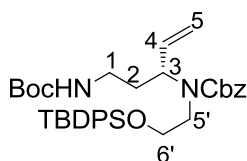
By general procedure F, sulfonamide **230** (370 mg, 1.29 mmol) and cyclic sulfamidate **S-54** (476 mg, 1.17 mmol) gave a crude residue which was purified by flash chromatography (SiO<sub>2</sub>, 30:70 Petrol–EtOAc) to yield the *sulfonamide* **234** (177 mg, 25%) as a yellow oil,  $R_f = 0.12$  (30:70 Petrol–EtOAc);  $\nu_{\max}/\text{cm}^{-1}$  (ATR) 3378 (br), 2927, 1542, 1514, 1249, 1177 and 1025;  $[\alpha]_{\text{D}}^{25}$  12 ( $c = 1.1$ , CHCl<sub>3</sub>);  $\delta_{\text{H}}$  (500 MHz, CDCl<sub>3</sub>) 8.03 (1H, t,  $J$  5.2, 1-NH), 7.95 (1H, dd,  $J$  7.5 and 1.6, nitrophenyl 3-H), 7.45-7.38 (2H, m, nitrophenyl 4-H and nitrophenyl 5-H), 7.32 (1H, dd,  $J$  7.5 and 1.6, nitrophenyl 6-H), 6.91 (2H, d,  $J$  8.6, 1-PMB 3-H and 1-PMB 5-H), 6.84 (2H, d,  $J$  8.5, 3-PMB 3-H and 3-PMB 5-H), 6.62 (2H, d,  $J$  8.6, 1-PMB 2-H and 1-PMB 6-H), 6.57 (2H, d,  $J$  8.5, 3-PMB 2-H and 3-PMB 6-H), 4.42 (1H, t,  $J$  7.3, 3-NH), 4.07 (2H, d,  $J$  5.2, 1-PMB benzylic-H<sub>2</sub>), 3.59 (3H, s, 1-PMB methyl), 3.57 (3H, s, 3-PMB methyl), 3.57-3.54 (1H, m, 2-H), 3.54-3.43 (3H, m, 3-H<sub>2</sub> and ethyl 1-H<sub>a</sub>), 3.13 (1H, dd,  $J$  15.1 and 10.1, ethyl 1-H<sub>b</sub>), 3.01-2.92 (3H, m, 3-PMB benzylic-H<sub>2</sub> and ethyl 2-H), 0.55-0.47 (1H, m, cyclopropyl 1-H), 0.30-0.19 (2H, m, cyclopropyl 2-H<sub>2</sub>), 0.14-0.08 (1H, m, cyclopropyl 3-H<sub>a</sub>) and 0.07-0.00 (1H, m, cyclopropyl 3-H<sub>b</sub>);  $\delta_{\text{C}}$  (126 MHz, CDCl<sub>3</sub>) 169.6 (C-1), 159.2 (1-PMB C-4), 159.1 (3-PMB C-4), 148.0 (nitrophenyl C-2), 133.8 (nitrophenyl C-5), 133.0 (nitrophenyl C-1), 132.1 (nitrophenyl C-4), 131.4 (nitrophenyl C-6), 129.8 (1-PMB C-3 and 1-PMB C-5), 129.7 (1-PMB C-1 and 3-PMB C-1), 129.2 (3-PMB C-3 and 3-PMB C-5), 124.1 (nitrophenyl C-3), 114.13 (1-PMB C-2 and 1-PMB C-6), 114.06 (3-PMB C-2 and 3-PMB C-6), 73.6 (ethyl C-2), 59.4 (C-2), 55.31 (1-PMB methyl), 55.28 (3-PMB methyl), 53.1 (C-3), 52.7 (ethyl C-1), 49.2 (3-PMB benzylic-C), 43.2 (1-PMB benzylic-C), 15.2 (cyclopropyl C-1), 2.5 (cyclopropyl C-2) and 1.7 (cyclopropyl C-3); HRMS found MH<sup>+</sup>, 613.2335. C<sub>30</sub>H<sub>36</sub>N<sub>4</sub>O<sub>8</sub>S requires *MH*, 613.2332.

***tert*-Butyl *N*-[(3*R*)-3-({2-[(*tert*-butyldiphenylsilyl)oxy]ethyl}amino)pent-4-en-1-yl] carbamate, **57****



By general procedure I, allylic carbonate **45** (1.00 g, 3.86 mmol), amine **56** (1.50 g, 1.3 mmol), and phosphoramidite **S-21** (83.7 mg, 4 mol%) gave a crude residue which was purified by flash chromatography (SiO<sub>2</sub>, 70:30 Petrol–EtOAc) to give the *alkene* **57** (790 mg, 42%) as a yellow oil,  $R_f = 0.44$  (50:50 Petrol–EtOAc);  $\nu_{\max}/\text{cm}^{-1}$  (ATR) 3341 (br), 2930, 1698, 1505, 1248, 1169 and 1109;  $[\alpha]_D^{25} -2.9$  ( $c = 0.39$ , CHCl<sub>3</sub>);  $\delta_H$  (500 MHz, CDCl<sub>3</sub>) 7.72–7.67 (4H, m, phenyl 3-H and phenyl 5-H), 7.49–7.38 (6H, m, phenyl 2-H, phenyl 4-H and phenyl 6-H), 5.72–5.57 (1H, m, 4-H), 5.18–5.11 (2H, m, 5-H<sub>2</sub>), 5.10 (1H, br s, NH), 3.84–3.74 (2H, m, ethyl 2-H<sub>2</sub>), 3.25 (1H, dt,  $J$  12.5 and 5.8, 1-H<sub>a</sub>), 3.17 (1H, dt,  $J$  19.1 and 6.5, 1-H<sub>b</sub>), 3.10 (1H, dd,  $J$  13.8 and 6.9, 3-H), 2.85–2.77 (1H, m, ethyl 1-H<sub>a</sub>), 2.64 (1H, dt,  $J$  11.9 and 5.0, ethyl 1-H<sub>b</sub>), 1.66 (2H, dd,  $J$  13.8 and 6.5, 2-H<sub>2</sub>), 1.46 (9H, s, Boc) and 1.08 (9H, s, *t*Bu);  $\delta_C$  (126 MHz, CDCl<sub>3</sub>) 156.0 (CO), 140.4 (C-4), 135.6 (phenyl C-3 and phenyl C-5), 133.7 (1H, d,  $J$  2.5, phenyl C-1), 129.7 (phenyl C-4), 127.70 (phenyl C-2), 127.69 (phenyl C-6), 116.2 (C-5), 63.3 (ethyl C-2), 60.0 (C-3), 48.8 (ethyl C-1), 38.0 (C-1), 35.3 (C-2), 28.5 (Boc), 26.9 (*t*Bu) and 19.2 (Si-C); HRMS found MH<sup>+</sup>, 483.3139. C<sub>28</sub>H<sub>42</sub>N<sub>2</sub>O<sub>3</sub>Si requires  $MH$ , 483.3043.

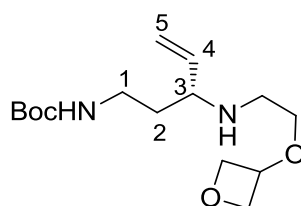
***tert*-Butyl *N*-[(3*R*)-3-(9,9-dimethyl-3-oxo-1,8,8-triphenyl-2,7-dioxa-4-aza-8-siladecan-4-yl)pent-4-en-1-yl]carbamate, **247****



By general procedure J, amine **57** (395 mg, 0.820 mmol) gave the *protected amine* **247** (450 mg, 89%) as a yellow oil which was used without further purification,  $R_f = 0.70$  (70:30 Petrol–EtOAc);  $\nu_{\max}/\text{cm}^{-1}$  (ATR) 3347, 2890, 2857, 1697, 1412, 1168 and 1111;  $[\alpha]_D^{25} 5.5$  ( $c = 1.7$ , CHCl<sub>3</sub>);  $\delta_H$  (501 MHz, MeOD) 7.47 (4H, d,  $J$  7.4, phenyl 3-H and phenyl 5-H), 7.30–7.24 (2H, m, phenyl 4-H), 7.21 (4H, t,  $J$  7.4, phenyl 2-H and phenyl 6-H), 7.16–7.05 (4H, m, benzyl-H), 5.64 (1H, ddd,  $J$  17.1, 10.5 and 6.4, 4-H), 4.98–4.85 (4H, m, 5-H<sub>2</sub> and siladecanyl 1-H<sub>2</sub>), 4.22 (1H, dd,  $J$  13.0 and 7.0, 1-H<sub>a</sub>), 3.66–3.51 (2H, m, siladecanyl 6-H<sub>2</sub>), 3.26–3.16 (2H, m, siladecanyl 5-H<sub>2</sub>), 2.90–2.70 (2H, m, 1-H<sub>b</sub> and 3-H), 1.63–1.54 (2H,

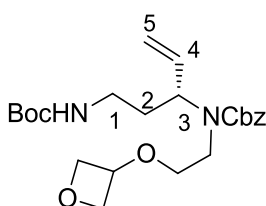
m, 2-H<sub>2</sub>), 1.25 (9H, s, Boc) and 0.87 (9H, s, <sup>t</sup>Bu);  $\delta_c$  (126 MHz, MeOD) 158.1 (siladecanyl C-3), 157.9 (CO), 138.1 (C-4), 137.9 (benzyl C-1), 136.6 (phenyl C-3 and phenyl C-5), 134.8 (phenyl C-1), 130.8 (phenyl C-4), 129.4 (benzyl C-3 and benzyl C-5), 129.0 (benzyl C-4), 128.8 (benzyl C-2 and benzyl C-6), 128.7 (phenyl C-2), 128.7 (phenyl C-6), 117.4 (C-5), 68.3 (siladecanyl C-1), 61.4 (siladecanyl C-6), 58.3 (C-3), 47.5 (siladecanyl C-5), 38.6 (C-1), 33.2 (C-2), 28.8 (Boc), 27.4 (<sup>t</sup>Bu) and 19.9 (Si-C); HRMS found MH<sup>+</sup>, 617.3429. C<sub>36</sub>H<sub>48</sub>N<sub>2</sub>O<sub>5</sub>Si requires *MH*, 617.3410.

***tert*-Butyl *N*-[(3*R*)-3-{[2-(oxetan-3-yloxy)ethyl]amino}pent-4-en-1-yl]carbamate, **248****



By general procedure I, the amine **246** (90.0 mg, 0.770 mmol), allylic carbonate **45** (154 mg, 0.590 mmol) and phosphoramidite **S-21** (12.8 mg, 4 mol%) gave a crude residue which was purified by flash chromatography (SiO<sub>2</sub>, 5:95 MeOH–DCM) and then again (SiO<sub>2</sub>, 5:95 MeOH–DCM) to give the *alkene* **248** (30.0 mg, 17%) as a yellow oil, *R<sub>f</sub>* = 0.16 (5:95 MeOH–DCM);  $\nu_{\max}$ / cm<sup>-1</sup> (ATR) 3314 (br), 2960, 2930, 1693, 1511, 1249 and 1170;  $[\alpha]_D^{25}$  –4.9 (*c* = 0.16, CHCl<sub>3</sub>);  $\delta_H$  (500 MHz, MeOD) 5.59–5.48 (1H, m, 4-H), 5.24–5.15 (2H, m, 5-H<sub>2</sub>), 3.15 (1H, dd, *J* 13.2 and 8.4, 3-H), 3.09–2.99 (1H, m, 1-H<sub>a</sub>), 2.92 (1H, dt, *J* 14.0 and 7.1, 1-H<sub>b</sub>), 2.67–2.58 (1H, m, ethyl 2-H<sub>a</sub>), 2.55–2.45 (1H, m, ethyl 2-H<sub>b</sub>), 1.71 (1H, td, *J* 13.2 and 7.1, 2-H<sub>a</sub>), 1.52 (1H, ddd, *J* 20.6, 13.2 and 7.1, 2-H<sub>b</sub>), 1.48–1.39 (2H, m, ethyl 1-H<sub>2</sub>), 1.34 (9H, s, Boc), 1.28 (2H, dd, *J* 15.0 and 7.4, oxetanyl 2-H<sub>a</sub> and oxetanyl 4-H<sub>a</sub>) and 0.85 (3H, app t, *J* 7.4, oxetanyl 1-H, oxetanyl 2-H<sub>b</sub> and oxetanyl 4-H<sub>b</sub>);  $\delta_c$  (126 MHz, MeOD) 158.6 (CO), 138.1 (C-4), 120.2 (C-5), 80.1 (Boc), 60.8 (C-3), 47.3 (C-1), 37.9 (ethyl C-2), 35.2 (C-2), 31.4 (ethyl C-1), 28.7 (Boc), 21.2 (oxetanyl C-2 and oxetanyl C-4) and 14.1 (oxetanyl C-1); HRMS found MH<sup>+</sup>, 301.2124. C<sub>15</sub>H<sub>28</sub>N<sub>2</sub>O<sub>4</sub> requires *MH*, 301.2127.

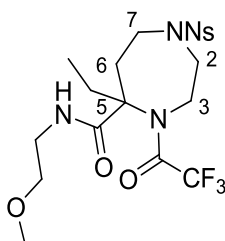
***tert*-Butyl *N*-[(3*R*)-3-[[*(benzyloxy)*carbonyl][2-(oxetan-3-yl)oxy]ethyl]amino}pent-4-en-1-yl]carbamate, **249****



By general procedure J, amine **248** (70.0 mg, 0.230 mmol) gave a crude residue which was purified by flash chromatography (SiO<sub>2</sub>, 50:50 Petrol–EtOAc) to give the *protected amine* **249** (81.4 mg, 81%) as a yellow oil,  $R_f = 0.76$  (70:30 Petrol–EtOAc);  $\nu_{\max}/\text{cm}^{-1}$  (ATR) 2961, 2933, 2873, 2495, 1663, 1414, 1155 and 698;  $[\alpha]_D^{20} 32$  ( $c = 0.597$ , CHCl<sub>3</sub>);  $\delta_H$  (501 MHz, MeOD) 7.28–7.22 (4H, m, benzyl 2-H, benzyl 3-H, benzyl 5-H and benzyl 6-H), 7.21–7.17 (1H, m, benzyl 4-H), 5.81 (1H, ddd,  $J$  17.1, 10.7 and 6.6, 4-H), 5.07 (1H, d,  $J$  10.7, 5-H<sub>a</sub>), 5.06–5.04 (1H, m, 5-H<sub>b</sub>), 5.02 (2H, app d,  $J$  3.3, benzylic-H<sub>2</sub>), 4.27 (1H, dd,  $J$  13.3 and 6.6, 3-H), 3.06 (2H, app td,  $J$  7.2 and 2.7, ethyl 1-H<sub>2</sub>), 2.99–2.87 (2H, m, 1-H<sub>2</sub>), 1.75 (2H, app q,  $J$  7.1, 2-H<sub>2</sub>), 1.48–1.40 (2H, m, ethyl 2-H<sub>2</sub>), 1.32 (9H, s, Boc), 1.22–1.13 (2H, m, oxetanyl 2-H<sub>a</sub> and oxetanyl 3-H) and 0.78 (3H, app t,  $J$  7.4, oxetanyl 2-H<sub>b</sub> and oxetanyl 4-H<sub>2</sub>);  $\delta_C$  (126 MHz, MeOD) 158.2 (Boc), 158.0 (CO), 138.4 (C-4), 138.1 (benzyl C-1), 129.4 (benzyl C-2 and benzyl C-6), 129.0 (benzyl C-3 and benzyl C-5), 128.9 (benzyl C-4), 117.1 (C-5), 68.2 (benzylic-C), 58.7 (C-3), 46.2 (ethyl C-1), 38.8 (C-1), 33.4 (C-2), 32.9 (ethyl C-2), 28.7 (Boc), 21.1 (oxetanyl C-2 and oxetanyl C-4) and 13.9 (oxetanyl C-3), Boc quaternary carbon not observed.

## 5.6 Synthesis of Scaffolds

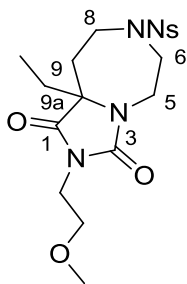
### ***N*-Methoxyethyl-5-ethyl-1-[(2-nitrophenyl)sulfonyl]-4-(trifluoroacetyl)-1,4-diazepane-5-carboxamide, **51****



By general procedure K, ketone **32** (450 mg, 1.05 mmol) and 2-methoxyethyl isocyanide (179 mg, 2.10 mmol) gave a crude product which was purified by flash chromatography (SiO<sub>2</sub>, 30:70 Petrol–EtOAc) to yield the *diazepane* **51** (380 mg, 71%) as a yellow oil,  $R_f = 0.26$  (20:80 Petrol–EtOAc);  $\nu_{\max}/\text{cm}^{-1}$  (ATR) 3280 (br), 2937, 1742, 1698,

1682, 1545, 1372 and 1162;  $\delta_{\text{H}}$  (500 MHz,  $\text{CDCl}_3$ ) 8.01-7.92 (1H, m, nitrophenyl 3-H), 7.77-7.63 (3H, m, nitrophenyl 4-H, nitrophenyl 5-H and nitrophenyl 6-H), 5.99 (1H, t,  $J$  4.7, NH), 4.20 (1H, dd,  $J$  16.5 and 5.9, 3- $\text{H}_a$ ), 4.15-4.03 (1H, m, 2- $\text{H}_a$ ), 3.86 (1H, dd,  $J$  14.1 and 6.7, 7- $\text{H}_a$ ), 3.63-3.54 (1H, m, 7- $\text{H}_b$ ), 3.53-3.43 (4H, m, 2- $\text{H}_b$ , 3- $\text{H}_b$  and methoxyethyl 1- $\text{H}_2$ ), 3.42-3.30 (5H, m, methoxyethyl 2- $\text{H}_2$  and methoxyethyl 4- $\text{H}_3$ ), 2.72-2.51 (2H, m, ethyl 1- $\text{H}_2$ ), 1.93 (1H, dd,  $J$  18.7 and 6.7, 6- $\text{H}_a$ ), 1.65 (1H, dt,  $J$  18.7 and 7.3, 6- $\text{H}_b$ ) and 0.93 (3H, t,  $J$  7.2, ethyl 2- $\text{H}_3$ );  $\delta_{\text{C}}$  (126 MHz,  $\text{CDCl}_3$ ) 170.9 (amide CO), 148.1 (nitrophenyl C-2), 133.8 (nitrophenyl C-5), 132.6 nitrophenyl (C-1), 131.9 (nitrophenyl C-4), 130.6 (nitrophenyl C-6), 124.4 (nitrophenyl C-3), 70.8 (C-3), 69.2 (C-5), 58.8 (methoxyethyl C-4), 49.9 (C-2), 48.4 (C-7), 44.0 (methoxyethyl C-1), 39.6 (methoxyethyl C-2), 37.3 (ethyl C-1), 26.9 (C-6) and 7.9 (ethyl C-2), trifluoroacetyl carbons not observed;  $\delta_{\text{F}}$  (282 MHz,  $\text{CDCl}_3$ ) -68.4; HRMS found  $\text{MH}^+$ , 511.1485.  $\text{C}_{19}\text{H}_{25}\text{F}_3\text{N}_4\text{O}_7\text{S}$  requires  $\text{MH}$ , 511.1474.

**9a-Ethyl-2-(2-methoxyethyl)-7-(2-nitrophenylsulfonyl)-octahydro-1H-imidazolidino[1,5-d][1,4]diazepine-1,3-dione, 106**

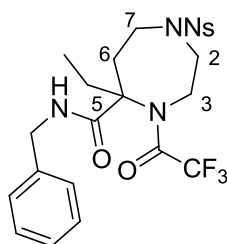


$\text{K}_2\text{CO}_3$  (1.02 g, 7.40 mmol) was added to a solution of the diazepane **51** (380 mg, 0.740 mmol) in MeOH (18.5 mL, 0.04 M) and water (8.22 mL, 0.09 M). The reaction mixture was stirred at room temperature overnight before being concentrated *in vacuo*, diluted with water (20 mL) and extracted with EtOAc ( $3 \times 20$  mL). The combined organic phases were washed with brine (20 mL), dried ( $\text{MgSO}_4$ ) and concentrated *in vacuo*. The residue was purified by flash chromatography ( $\text{SiO}_2$ , 30:70 Petrol-EtOAc) to yield the *hydantoin* **106** (280 mg, 86%) as a yellow oil,  $R_f = 0.26$  (20:80 Petrol-EtOAc);  $\nu_{\text{max}}$ /  $\text{cm}^{-1}$  (ATR) 2936, 1769, 1708, 1544, 1451, 1368 and 1165;  $\delta_{\text{H}}$  (500 MHz,  $\text{CDCl}_3$ ) 8.01 (1H, dd,  $J$  7.6 and 1.6, nitrophenyl 3-H), 7.77-7.69 (2H, m, nitrophenyl 4-H and nitrophenyl 5-H), 7.67 (1H, dd,  $J$  7.2 and 1.8, nitrophenyl 6-H), 4.25-4.16 (1H, m, 5- $\text{H}_a$ ), 3.91-3.82 (2H, m, 6- $\text{H}_a$  and 8- $\text{H}_a$ ), 3.81-3.70 (2H, m, methoxyethyl 1- $\text{H}_2$ ), 3.62-3.55 (2H, m, 6- $\text{H}_b$  and 8- $\text{H}_b$ ), 3.32 (3H, s, methoxyethyl 4- $\text{H}_3$ ), 3.19-3.09 (2H, m, methoxyethyl 2- $\text{H}_2$ ), 2.69-2.57 (2H, m, 5- $\text{H}_b$  and 9- $\text{H}_a$ ), 2.11-2.02 (1H, m, 9- $\text{H}_b$ ), 1.92 (1H, dq,  $J$  14.6 and 7.3, ethyl 1- $\text{H}_a$ ), 1.74 (1H, dq,  $J$  14.6 and 7.3, ethyl 1- $\text{H}_b$ ) and 0.80 (3H, t,  $J$  7.3, ethyl 2- $\text{H}_3$ );  $\delta_{\text{C}}$  (126 MHz,  $\text{CDCl}_3$ ) 175.3 (C-1), 156.4 (C-3), 147.9 (nitrophenyl C-2), 133.9 (nitrophenyl C-5), 132.6 (nitrophenyl C-1),

131.8 (nitrophenyl C-4), 130.9 (nitrophenyl C-6), 124.4 (nitrophenyl C-3), 68.5 (C-5), 68.1 (C-9a), 58.5 (methoxyethyl C-4), 48.0 (C-6), 44.8 (C-8), 41.7 (methoxyethyl C-1), 39.4 (methoxyethyl C-2), 38.3 (ethyl C-1), 29.0 (C-9) and 7.3 (ethyl C-2); HRMS found  $MH^+$ , 441.1446.  $C_{18}H_{24}N_4O_7S$  requires  $MH$ , 441.1444.

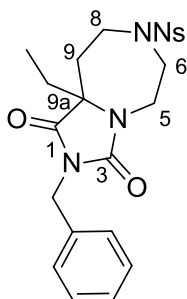
Analysis of the HMBC spectrum showed correlations between C-3 and 5- $H_a$ , C-3 and methoxyethyl 1- $H_2$ , C-3 and methoxyethyl 2- $H_2$ .

### ***N*-Benzyl-5-ethyl-1-[(2-nitrophenyl)sulfonyl]-4-(trifluoroacetyl)-1,4-diazepane-5-carboxamide, 33**



By general procedure K, ketone **32** (700 mg, 1.63 mmol) and benzyl isocyanide (0.400 mL, 3.26 mmol) gave a crude product which was purified by flash chromatography ( $SiO_2$ , 60:40 DCM-EtOAc) to yield the diazepane<sup>44</sup> **33** (710 mg, 80%) as a colourless amorphous solid,  $R_f$  = 0.44 (50:50 Petrol-EtOAc);  $\nu_{max}/cm^{-1}$  (ATR) 3422 (br), 2977, 1695, 1666, 1543, 1371 and 1152;  $\delta_H$  (500 MHz,  $CDCl_3$ ) 7.97 (1H, dd,  $J$  10.1 and 4.9, nitrophenyl 3-H), 7.78-7.70 (2H, m, nitrophenyl 4-H and 5-H), 7.68 (1H, dd,  $J$  7.4 and 1.6, nitrophenyl 6-H), 7.41-7.26 (5H, m, benzyl-H), 5.92 (1H, t,  $J$  5.2, NH), 4.54-4.39 (2H, m, benzylic- $H_2$ ), 4.25 (1H, dd,  $J$  16.8 and 5.7, 3- $H_a$ ), 4.11 (1H, dd,  $J$  14.4 and 5.7, 2- $H_a$ ), 3.90 (1H, dd,  $J$  14.8 and 7.0, 7- $H_a$ ), 3.64 (1H, dd,  $J$  14.8 and 10.7, 7- $H_b$ ), 3.52 (1H, dd,  $J$  16.8 and 9.0, 3- $H_b$ ), 3.39 (1H, dd,  $J$  14.4 and 9.0, 2- $H_b$ ), 2.76-2.56 (2H, m, ethyl 1- $H_2$ ), 1.94 (1H, dd,  $J$  16.8 and 7.0, 6- $H_a$ ), 1.69-1.58 (1H, m, 6- $H_b$ ) and 0.96 (3H, t,  $J$  7.2, ethyl 2- $H_3$ );  $\delta_C$  (126 MHz,  $CDCl_3$ ) 170.7 (amide CO), 157.0 (app d,  $J$  35.5, trifluoroacetyl C-1) 148.1 (nitrophenyl C-2), 137.8 (benzyl C-1), 133.9 (nitrophenyl C-5), 132.5 (nitrophenyl C-1), 131.9 (nitrophenyl C-4), 130.5 (nitrophenyl C-6), 128.9 (benzyl C-3 and benzyl C-5), 127.7 (benzyl C-2, benzyl C-4 and benzyl C-6), 124.5 (nitrophenyl C-3), 116.3 (q,  $J$  287.9, trifluoroacetyl C-2), 69.2 (C-5), 49.8 (benzylic-C), 48.5 (C-3), 44.0 (C-2), 43.9 (C-7), 37.4 (ethyl C-1), 26.9 (C-6) and 7.9 (ethyl C-2);  $\delta_F$  (282 MHz,  $CDCl_3$ ) -68.3;  $m/z$  (ES) 565.2 (100%,  $MNa^+$ ).

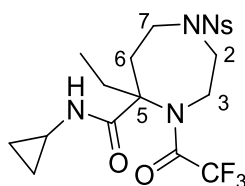
**2-Benzyl-9a-ethyl-7-(2-nitrophenylsulfonyl)-octahydro-1H-imidazolidino[1,5-d][1,4]diazepine-1,3-dione, 107**



$K_2CO_3$  (1.60 g, 11.6 mmol) was added to a solution of the diazepane **33** (630 mg, 1.16 mmol) in MeOH (30 mL, ~0.04 M) and water (13 mL, 0.09 M). The reaction mixture was stirred at room temperature overnight before being concentrated *in vacuo*, diluted with water (30 mL) and extracted with EtOAc (3 × 30 mL). The combined organic phases were washed with brine (30 mL), dried ( $MgSO_4$ ) and concentrated *in vacuo*. The residue was purified by flash chromatography ( $SiO_2$ , 40:60 Petrol–EtOAc) to yield the *hydantoin* **107** (200 mg, 36%) as a yellow solid, m.p. 145-147 °C;  $R_f$  = 0.43 (20:80 Petrol–EtOAc);  $\nu_{max}/cm^{-1}$  (ATR) 2927, 1767, 1709, 1544, 1449, 1366 and 1165;  $\delta_H$  (500 MHz,  $CDCl_3$ ) 8.01 (1H, m, nitrophenyl 3-H), 7.86-7.60 (3H, m, nitrophenyl 4-H, nitrophenyl 5-H and nitrophenyl 6-H), 7.50-7.18 (5H, m, benzyl-H), 4.74-4.63 (2H, m, benzylic- $H_2$ ), 4.28-4.15 (1H, m, 5- $H_a$ ), 3.97-3.77 (2H, m, 6- $H_a$  and 8- $H_a$ ), 3.23-3.04 (2H, m, 6- $H_b$  and 5- $H_b$ ), 2.68-2.48 (2H, m, 8- $H_b$  and 9- $H_a$ ), 2.13-2.00 (1H, m, 9- $H_b$ ), 1.89 (1H, dq,  $J$  14.7 and 7.4, ethyl 1- $H_a$ ), 1.73 (1H, dq,  $J$  14.7 and 7.4, ethyl 1- $H_b$ ) and 0.64 (3H, t,  $J$  7.4, ethyl 2- $H_3$ );  $\delta_C$  (126 MHz,  $CDCl_3$ ) 175.0 (C-1), 156.2 (C-3), 147.9 (nitrophenyl C-2), 136.0 (benzyl C-1), 133.9 (nitrophenyl C-5), 132.5 (nitrophenyl C-1), 131.8 (nitrophenyl C-4), 130.9 (nitrophenyl C-6), 128.7 (benzyl C-3 and benzyl C-5), 128.5 (benzyl C-2 and benzyl C-6), 128.0 (benzyl C-4), 124.4 (nitrophenyl C-3), 67.9 (C-9a), 48.1 (benzylic-C), 44.9 (C-5), 42.7 (C-6), 41.8 (C-8), 39.2 (ethyl C-1), 29.1 (C-9) and 7.3 (ethyl C-2); HRMS found  $MH^+$ , 473.1490.  $C_{22}H_{24}N_4O_6S$  requires  $MH$ , 473.1495.

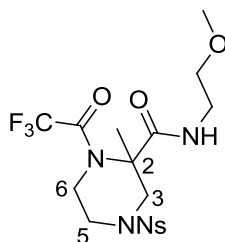
Analysis of the HMBC spectrum showed correlations between C-3 and benzylic- $H_2$ , C-3 and 5- $H_a$ , C-3 and 5- $H_b$ .

***N*-Cyclopropyl-5-ethyl-1-[(2-nitrophenyl)sulfonyl]-4-(trifluoroacetyl)-1,4-diazepane-5-carboxamide, 108**



By general procedure K, ketone **32** (910 mg, 2.12 mmol) and cyclopropyl isocyanide (0.340 mL, 4.24 mmol) gave a crude product which was purified by flash chromatography (SiO<sub>2</sub>, 50:50 Petrol–EtOAc) to yield the *diazepane* **108** (690 mg, 66%) as a colourless amorphous solid, *R*<sub>f</sub> = 0.36 (30:70 Petrol–EtOAc);  $\nu_{\max}$ / cm<sup>-1</sup> (ATR) 3401 (br), 2975, 1693, 1664, 1543, 1451, 1370, 1143 and 729;  $\delta_{\text{H}}$  (500 MHz, CDCl<sub>3</sub>) 7.87 (1H, dd, *J* 7.3 and 1.9, nitrophenyl 3-H), 7.68-7.61 (2H, m, nitrophenyl 4-H and nitrophenyl 5-H), 7.59 (1H, dd, *J* 7.5 and 1.7, nitrophenyl 6-H), 5.75 (1H, s, NH), 4.13 (1H, dd, *J* 16.7 and 5.7, 3-H<sub>a</sub>), 4.01 (1H, dd, *J* 14.3 and 5.7, 2-H<sub>a</sub>), 3.78 (1H, dd, *J* 14.7 and 6.8, 7-H<sub>a</sub>), 3.53 (1H, dd, *J* 14.7 and 10.7, 7-H<sub>b</sub>), 3.39 (1H, dd, *J* 16.7 and 8.9, 3-H<sub>b</sub>), 3.29 (1H, dd, *J* 14.3 and 8.9, 2-H<sub>b</sub>), 2.61-2.54 (1H, m, cyclopropyl 1-H), 2.53-2.44 (2H, m, ethyl 1-H<sub>a</sub> and ethyl 1-H<sub>b</sub>), 1.78 (1H, dd, *J* 16.4 and 6.8, 6-H<sub>a</sub>), 1.54-1.42 (1H, m, 6-H<sub>b</sub>), 0.85 (3H, t, *J* 7.4, ethyl 2-H<sub>3</sub>), 0.73-0.63 (2H, m, cyclopropyl 2-H<sub>2</sub>), 0.51-0.44 (1H, m, cyclopropyl 3-H<sub>a</sub>) and 0.40-0.31 (1H, m, cyclopropyl 3-H<sub>b</sub>);  $\delta_{\text{C}}$  (126 MHz, CDCl<sub>3</sub>) 172.3 (amide CO), 157.0 (app d, *J* 35.6, trifluoroacetyl C-1), 148.1 (nitrophenyl C-2), 133.9 (nitrophenyl C-5), 132.5 (nitrophenyl C-1), 132.0 (nitrophenyl C-4), 130.5 (nitrophenyl C-6), 124.4 (nitrophenyl C-3), 116.3 (q, *J* 288.4, trifluoroacetyl C-2), 68.9 (C-5), 49.8 (C-3), 48.4 (C-2), 43.9 (C-7), 37.1 (C-6), 26.8 (ethyl C-1), 22.9 (cyclopropyl C-1), 7.8 (cyclopropyl C-2), 6.8 (cyclopropyl C-3) and 6.4 (ethyl C-2);  $\delta_{\text{F}}$  (282 MHz, CDCl<sub>3</sub>) -68.4; HRMS found MH<sup>+</sup>, 493.1363. C<sub>19</sub>H<sub>23</sub>F<sub>3</sub>N<sub>4</sub>O<sub>6</sub>S requires *MH*, 493.1368.

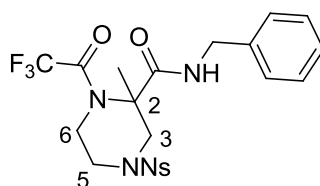
***N*-Methoxyethyl-2-methyl-4-[(2-nitrophenyl)sulfonyl]-1-(trifluoroacetyl)piperazine-2-carboxamide, 110**



By general procedure K, tetrahydropyrazine **101** (564 mg, 1.47 mmol) and 2-methoxyethyl isocyanide (250 mg, 2.94 mmol) gave a crude product which was purified

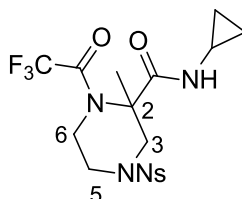
by flash chromatography (SiO<sub>2</sub>, 40:60 Petrol–EtOAc) to yield the *piperazine* **110** (680 mg, 96%) as a yellow oil,  $R_f = 0.43$  (30:70 Petrol–EtOAc);  $\nu_{\max}/\text{cm}^{-1}$  (ATR) 3358 (br), 2927, 1719, 1545, 1370, 1168 and 555;  $\delta_{\text{H}}$  (500 MHz, CDCl<sub>3</sub>) 8.04–8.00 (1H, m, nitrophenyl 3-H), 7.78–7.70 (2H, m, nitrophenyl 4-H and nitrophenyl 5-H), 7.70–7.62 (1H, m, nitrophenyl 6-H), 6.57 (1H, br s, NH), 4.06 (1H, dt,  $J$  15.4 and 2.0, 5-H<sub>a</sub>), 3.65–3.57 (1H, m, 5-H<sub>b</sub>), 3.55–3.48 (4H, m, 3-H<sub>a</sub> and methoxyethyl 2-H<sub>2</sub>), 3.46 (3H, s, methoxyethyl 4-H<sub>3</sub>), 3.43–3.37 (1H, m, 6-H<sub>a</sub>), 3.29–3.17 (2H, m, methoxyethyl 1-H<sub>2</sub>), 2.98 (1H, d,  $J$  12.9, 3-H<sub>b</sub>), 1.50–1.45 (1H, m, 6-H<sub>b</sub>) and 1.39 (3H, s, methyl);  $\delta_{\text{C}}$  (126 MHz, CDCl<sub>3</sub>) 173.9 (amide CO), 148.2 (nitrophenyl C-2), 133.8 (nitrophenyl C-5), 131.8 (nitrophenyl C-1), 131.7 (nitrophenyl C-4), 131.3 (nitrophenyl C-6), 124.2 (nitrophenyl C-3), 69.7 (C-5), 59.9 (C-2), 59.2 (methoxyethyl C-4), 51.0 (C-3), 45.4 (methoxyethyl C-2), 40.1 (C-6), 38.6 (methoxyethyl C-1) and 19.5 (methyl), trifluoroacetyl carbons not observed;  $\delta_{\text{F}}$  (282 MHz, CDCl<sub>3</sub>) -81.6; HRMS found MH<sup>+</sup>, 483.1122. C<sub>17</sub>H<sub>21</sub>F<sub>3</sub>N<sub>4</sub>O<sub>7</sub>S requires *MH*, 483.1161.

***N*-Benzyl-2-methyl-4-[(2-nitrophenyl)sulfonyl]-1-(trifluoroacetyl)piperazine-2-carboxamide, 109**



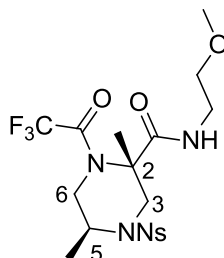
By general procedure K, tetrahydropyrazine **101** (650 mg, 1.70 mmol) and benzyl isocyanide (0.41 mL, 3.40 mmol) gave a crude product which was purified by flash chromatography (SiO<sub>2</sub>, 80:20 DCM–Et<sub>2</sub>O) to yield the piperazine<sup>44</sup> **109** (750 mg, 86%) as a colourless amorphous solid,  $R_f = 0.53$  (30:70 Petrol–EtOAc);  $\nu_{\max}/\text{cm}^{-1}$  (ATR) 3368 (br), 2937, 1699, 1673, 1542, 1370, 1216, 1145 and 732;  $\delta_{\text{H}}$  (500 MHz, CDCl<sub>3</sub>) 8.03 (1H, dd,  $J$  7.6 and 1.2, nitrophenyl 3-H), 7.81–7.72 (2H, m, nitrophenyl 4-H and nitrophenyl 5-H), 7.70 (1H, dd,  $J$  7.6 and 1.3, nitrophenyl 6-H), 7.43–7.35 (2H, m, benzyl 3-H and benzyl 5-H), 7.34–7.25 (3H, m, benzyl 2-H, benzyl 4-H and benzyl 6-H), 6.20 (1H, t,  $J$  5.0, NH), 4.52–4.36 (2H, m, benzylic-H<sub>2</sub>), 4.03–3.92 (1H, m, 5-H<sub>a</sub>), 3.88–3.75 (3H, m, 3-H<sub>a</sub>, 5-H<sub>b</sub> and 6-H<sub>a</sub>), 3.70 (1H, d,  $J$  13.8, 3-H<sub>b</sub>), 3.59–3.46 (1H, m, 6-H<sub>b</sub>) and 1.72 (3H, s, methyl);  $\delta_{\text{C}}$  (126 MHz, CDCl<sub>3</sub>) 169.2 (amide CO), 156.9 (q,  $J$  36.6, trifluoroacetyl C-1), 148.1 (nitrophenyl C-2), 137.4 (nitrophenyl C-1), 134.3 (nitrophenyl C-5), 132.0 (nitrophenyl C-4), 131.4 (benzyl C-1), 131.2 (nitrophenyl C-6), 128.8 (benzyl C-3 and benzyl C-5), 127.8 (benzyl C-2 and benzyl C-6), 127.7 (benzyl C-4), 124.5 (nitrophenyl C-3), 115.9 (q,  $J$  288.5, trifluoroacetyl C-2), 64.3 (C-2), 51.8 (C-3), 44.3 (C-5), 44.2 (C-6), 41.4 (benzylic-C) and 18.2 (methyl);  $\delta_{\text{F}}$  (282 MHz, CDCl<sub>3</sub>) -69.6;  $m/z$  (ES) 515.1 (100%, MNa<sup>+</sup>).

***N*-Cyclopropyl-2-methyl-4-[(2-nitrobenzene)sulfonyl]-1-(trifluoroacetyl)piperazine-2-carboxamide, **111****



By general procedure K, tetrahydropyrazine **101** (810 mg, 2.11 mmol) and cyclopropyl isocyanide (0.340 mL, 4.22 mmol) gave a crude residue which was purified by flash chromatography (SiO<sub>2</sub>, 40:60 Petrol–EtOAc) to yield the *piperazine* **111** (680 mg, 69%) as a colourless amorphous solid, *R*<sub>f</sub> = 0.48 (30:70 Petrol–EtOAc); *v*<sub>max</sub>/ cm<sup>-1</sup> (ATR) 3341 (br), 3015, 1699, 1543, 1363, 1215 and 1144;  $\delta$ <sub>H</sub> (500 MHz, CDCl<sub>3</sub>) 8.04 (1H, dd, *J* 7.6 and 1.7, nitrophenyl 3-H), 7.81-7.73 (2H, m, nitrophenyl 4-H and nitrophenyl 5-H), 7.71 (1H, dd, *J* 7.5 and 1.7, nitrophenyl 6-H), 6.04 (1H, s, NH), 4.02-3.90 (1H, m, 5-H<sub>a</sub>), 3.83-3.71 (3H, m, 3-H<sub>a</sub>, 5-H<sub>b</sub> and 6-H<sub>a</sub>), 3.63 (1H, d, *J* 13.8, 3-H<sub>b</sub>), 3.58-3.51 (1H, m, 6-H<sub>b</sub>), 2.67-2.57 (1H, m, cyclopropyl 1-H), 1.66 (3H, s, methyl), 0.81-0.71 (2H, m, cyclopropyl 2-H<sub>2</sub>) and 0.60-0.51 (2H, m, cyclopropyl 3-H<sub>2</sub>);  $\delta$ <sub>C</sub> (126 MHz, CDCl<sub>3</sub>) 170.7 (CO), 156.9 (q, *J* 30.6, trifluoroacetyl C-1), 148.1 (nitrophenyl C-2), 134.3 (nitrophenyl C-5), 132.0 (nitrophenyl C-4), 131.5 (nitrophenyl C-1), 131.2 (nitrophenyl C-6), 124.5 (nitrophenyl C-3), 115.8 (app d, *J* 288.2, trifluoroacetyl C-2), 64.1 (C-2), 51.6 (C-5), 44.3 (C-3), 41.2 (q, *J* 4.1, C-6), 23.1 (cyclopropyl C-1), 18.0 (methyl), 6.6 (cyclopropyl C-2) and 6.4 (cyclopropyl C-3);  $\delta$ <sub>F</sub> (282 MHz, CDCl<sub>3</sub>) -69.7; HRMS found MH<sup>+</sup>, 465.1063. C<sub>17</sub>H<sub>19</sub>F<sub>3</sub>N<sub>4</sub>O<sub>6</sub>S requires *MH*, 465.1055.

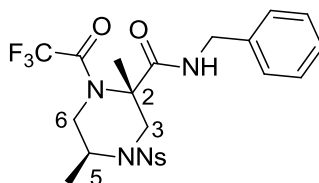
***N*-Methoxyethyl-(2*S*,5*S*)-2,5-(dimethyl)-4-[(2-nitrobenzene)sulfonyl]-1-(trifluoroacetyl)piperazine-2-carboxamide, **113****



By general procedure K, tetrahydropyrazine **103** (584 mg, 1.47 mmol) and 2-methoxyethyl isocyanide (250 mg, 2.94 mmol) gave a crude residue which was purified by flash chromatography (SiO<sub>2</sub>, 10:90 Petrol–EtOAc) to yield the *piperazine* **113** (590 mg, 81%) as a colourless amorphous solid, *R*<sub>f</sub> = 0.37 (10:90 Petrol–EtOAc); *v*<sub>max</sub>/ cm<sup>-1</sup> (ATR)

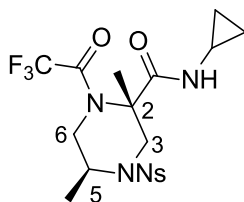
3368, 2934, 1700, 1543, 1361, 1216 and 1154, ;  $[\alpha]_D^{22}$  92 ( $c = 0.16$ ,  $\text{CHCl}_3$ );  $\delta_H$  (500 MHz,  $\text{CDCl}_3$ ) 8.12 (1H, dd,  $J$  6.9 and 2.4, nitrophenyl 3-H), 7.80-7.71 (3H, m, nitrophenyl 4-H, nitrophenyl 5-H and nitrophenyl 6-H), 6.28 (1H, t,  $J$  5.0, NH), 4.43-4.33 (1H, m, 5-H), 3.95-3.91 (2H, m, 3-H<sub>2</sub>), 3.52-3.43 (4H, m, 6-H<sub>2</sub> and methoxyethyl 1-H<sub>2</sub>), 3.43-3.37 (1H, m, methoxyethyl 2-H<sub>a</sub>), 3.36 (3H, s, methoxyethyl 4-H<sub>3</sub>), 3.22-3.13 (1H, m, methoxyethyl 2-H<sub>b</sub>), 1.73 (3H, s, 2-methyl) and 1.28 (3H, d,  $J$  6.4, 5-methyl);  $\delta_C$  (126 MHz,  $\text{CDCl}_3$ ) 169.1 (CO), 148.0 (nitrophenyl C-2), 134.0 (nitrophenyl C-5), 133.6 (nitrophenyl C-1), 132.1 (nitrophenyl C-4), 131.4 (nitrophenyl C-6), 124.6 (nitrophenyl C-3), 70.6 (C-3), 64.9 (C-2), 58.7 (C-5), 51.1 (methoxyethyl C-4), 49.8 (C-6), 46.6 (methoxyethyl C-1), 39.6 (methoxyethyl C-2), 18.7 (2-methyl) and 18.0 (5-methyl), trifluoroacetyl carbons not observed;  $\delta_F$  (282 MHz,  $\text{CDCl}_3$ ) -69.3; HRMS found  $\text{MH}^+$ , 497.1332.  $\text{C}_{18}\text{H}_{23}\text{F}_3\text{N}_4\text{O}_7\text{S}$  requires  $\text{MH}$ , 497.1318.

***N*-Benzyl-(2*S*,5*S*)-2,5-(dimethyl)-4-[(2-nitrobenzene)sulfonyl]-1-(trifluoroacetyl) piperazine-2-carboxamide, **112****



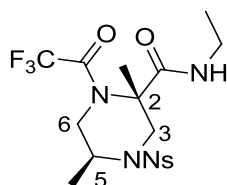
By general procedure K, tetrahydropyrazine **103** (350 mg, 0.880 mmol) and benzyl isocyanide (0.210 mL, 1.76 mmol) gave a crude residue which was purified by flash chromatography ( $\text{SiO}_2$ , 30:70 Petrol-EtOAc) to yield the *piperazine* **112** (356 mg, 77%) as a colourless amorphous solid,  $R_f = 0.40$  (30:70 Petrol-EtOAc);  $\nu_{\text{max}}$ /  $\text{cm}^{-1}$  (ATR) 3367 (br), 2935, 1699, 1543, 1362, 1216 and 1154;  $[\alpha]_D^{28}$  49 ( $c = 0.050$ , MeOH);  $\delta_H$  (500 MHz,  $\text{CDCl}_3$ ) 8.15-8.10 (1H, m, nitrophenyl 3-H), 7.81-7.73 (2H, m, nitrophenyl 4-H and nitrophenyl 5-H), 7.73-7.68 (1H, m, nitrophenyl 6-H), 7.39-7.33 (2H, m, benzyl 3-H and benzyl 5-H), 7.32-7.25 (4H, m, benzyl 2-H, benzyl 4-H and benzyl 6-H), 6.18 (1H, t,  $J$  5.3, NH), 4.52 (1H, dd,  $J$  14.9 and 5.3, benzylic-H<sub>a</sub>), 4.37-4.31 (1H, m, 5-H), 4.28 (1H, dd,  $J$  14.9 and 5.3, benzylic-H<sub>b</sub>), 3.99 (1H, d,  $J$  14.2, 3-H<sub>a</sub>), 3.90 (1H, dd,  $J$  14.7 and 4.7, 6-H<sub>a</sub>), 3.57-3.47 (2H, m, 3-H<sub>b</sub> and 6-H<sub>b</sub>) and 1.31-1.27 (6H, m, 2-methyl and 5-methyl);  $\delta_C$  (126 MHz,  $\text{CDCl}_3$ ) 169.2 (CO), 157.3 (app d,  $J$  36.3, trifluoroacetyl C-1), 137.5 (nitrophenyl C-2), 134.1 (nitrophenyl C-4), 133.3 (nitrophenyl C-1), 132.1 (nitrophenyl C-5), 131.4 (nitrophenyl C-6), 128.7 (benzyl C-3 and benzyl C-5), 127.7 (benzyl C-2 and benzyl C-6), 127.6 (benzyl C-4), 124.6 (nitrophenyl C-3), 115.9 (app d,  $J$  288.5, trifluoroacetyl C-2), 64.9 (C-2), 51.0 (C-5), 49.9 (C-3), 46.8 (C-6), 44.2 (benzylic-C), 19.0 (2-methyl) and 18.0 (5-methyl);  $\delta_F$  (282 MHz,  $\text{CDCl}_3$ ) -69.2; HRMS found  $\text{MH}^+$ , 529.1376.  $\text{C}_{22}\text{H}_{23}\text{F}_3\text{N}_4\text{O}_6\text{S}$  requires  $\text{MH}$ , 529.1368.

**(2*S*, 5*S*)-*N*-Cyclopropyl-2,5-dimethyl-4-(2-nitrobenzenesulfonyl)-1-(trifluoroacetyl)piperazine-2-carboxamide, 114**



By general procedure K, tetrahydropyrazine **103** (1.36 g, 3.42 mmol) and cyclopropyl isocyanide (0.550 mL, 6.84 mmol) gave a crude residue which was purified by flash chromatography (SiO<sub>2</sub>, 40:60 Petrol–EtOAc) to yield the *piperazine* **114** (800 mg, 49%) as a white amorphous solid,  $R_f = 0.30$  (40:60 Petrol–EtOAc);  $\nu_{\max}/\text{cm}^{-1}$  (ATR) 3350 (br), 3096, 3013, 2936, 1698, 1543, 1363, 1216, 1150, 735 and 580;  $[\alpha]_D^{20}$  107 ( $c = 2.78$ , CHCl<sub>3</sub>);  $\delta_H$  (500 MHz, CDCl<sub>3</sub>) 8.14-8.09 (1H, m, nitrophenyl 3-H), 7.80-7.75 (2H, m, nitrophenyl 4-H and nitrophenyl 5-H), 7.75-7.72 (1H, m, nitrophenyl 6-H), 6.09 (1H, s, NH), 4.40-4.31 (1H, m, 5-H), 3.96-3.87 (2H, m, 3-H<sub>a</sub> and 6-H<sub>a</sub>), 3.46 (1H, d,  $J$  14.5, 6-H<sub>b</sub>), 3.40 (1H, dd,  $J$  14.8 and 7.6, 3-H<sub>b</sub>), 2.47-2.33 (1H, m, cyclopropyl 1-H), 1.66 (3H, s, 2-methyl), 1.23 (3H, d,  $J$  6.3, 5-methyl), 0.74-0.62 (2H, m, cyclopropyl 2-H<sub>2</sub>) and 0.60-0.47 (2H, m, cyclopropyl 3-H<sub>2</sub>);  $\delta_C$  (126 MHz, CDCl<sub>3</sub>) 171.2 (CO), 156.9 (q,  $J$  36.3, trifluoroacetyl C-1), 147.9 (nitrophenyl C-1), 134.2 (nitrophenyl C-5), 133.5 (nitrophenyl C-2), 132.3 (nitrophenyl C-4), 131.4 (nitrophenyl C-6), 124.7 (nitrophenyl C-3), 115.8 (q,  $J$  288.3, trifluoroacetyl C-2), 64.7 (C-2), 51.1 (C-5), 49.5 (C-3), 46.4 (d,  $J$  3.6, C-6), 22.9 (cyclopropyl C-1), 18.4 (2-methyl), 17.7 (5-methyl) 6.3 (cyclopropyl C-2) and 6.2 (cyclopropyl C-3);  $\delta_F$  (282 MHz, CDCl<sub>3</sub>) -69.3; HRMS found MH<sup>+</sup>, 479.1320. C<sub>18</sub>H<sub>21</sub>F<sub>3</sub>N<sub>4</sub>O<sub>6</sub>S requires  $MH$ , 479.1212.

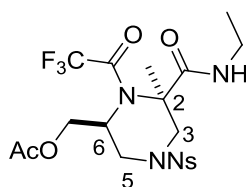
***N*-Ethyl-(2*S*,5*S*)-2,5-(dimethyl)-4-[(2-nitrobenzene)sulfonyl]-1-(trifluoroacetyl)piperazine-2-carboxamide, 115**



By general procedure K, tetrahydropyrazine **103** (220 mg, 0.550 mmol) and ethyl isocyanide (60.6 mg, 1.10 mmol) gave a crude residue which was purified by flash chromatography (SiO<sub>2</sub>, 30:70 Petrol–EtOAc) to yield the *piperazine* **115** (182 mg, 71%) as a colourless amorphous solid,  $R_f = 0.49$  (30:70 Petrol–EtOAc);  $\nu_{\max}/\text{cm}^{-1}$  (ATR) 3368, 2980, 2938, 1698, 1667, 1541, 1357 and 1139;  $[\alpha]_D^{23}$  77 ( $c = 0.31$ , CHCl<sub>3</sub>);  $\delta_H$  (500 MHz, CDCl<sub>3</sub>)

8.10 (1H, dd, *J* 7.1 and 1.6, nitrophenyl 3-H), 7.84-7.67 (3H, m, nitrophenyl 4-H, nitrophenyl 5-H and nitrophenyl 6-H), 5.92 (1H, t, *J* 5.0, NH), 4.42-4.24 (1H, m, 5-H), 4.02-3.85 (2H, m, 3-H<sub>2</sub>), 3.58-3.43 (2H, m, 6-H<sub>2</sub>), 3.34-3.21 (1H, m, ethyl 1-H<sub>a</sub>), 3.21-3.07 (1H, m, ethyl 1-H<sub>b</sub>), 1.72 (3H, s, 2-methyl), 1.26 (3H, app t, *J* 6.4, 5-methyl) and 1.12 (3H, t, *J* 7.2, ethyl 2-H<sub>3</sub>);  $\delta_c$  (126 MHz, CDCl<sub>3</sub>) 169.0 (CO), 157.1 (app d, *J* 36.4, trifluoroacetyl C-1), 148.0 (nitrophenyl C-2), 134.2 (nitrophenyl C-5), 133.3 (nitrophenyl C-1), 132.2 (nitrophenyl C-4), 131.3 (nitrophenyl C-6), 124.5 (nitrophenyl C-3), 115.9 (q, *J* 288.5, trifluoroacetyl C-2), 64.9 (C-2), 51.0 (C-5), 49.8 (C-3), 46.7 (app d, *J* 3.6, C-6), 35.1 (ethyl C-1), 18.8 (2-methyl), 17.9 (5-methyl) and 14.3 (ethyl C-2);  $\delta_f$  (282 MHz, CDCl<sub>3</sub>) -69.2; HRMS found MH<sup>+</sup>, 467.1222. C<sub>17</sub>H<sub>21</sub>F<sub>3</sub>N<sub>4</sub>O<sub>6</sub>S requires *MH*, 467.1212.

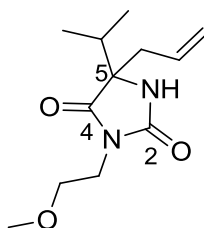
**[6-(Ethylcarbamoyl)-6-methyl-4-(2-nitrobenzenesulfonyl)-1-(trifluoroacetyl) piperazin-2-yl]methyl acetate, 116**



By general procedure K (with an additional 12 eq. TFA), tetrahydropyrazine **105** (1.03 g, 2.27 mmol) and ethyl isocyanide (250 mg, 4.54 mmol) gave a crude residue which was purified by flash chromatography (SiO<sub>2</sub>, 50:50 Petrol–EtOAc) the again (SiO<sub>2</sub>, 20:80 Et<sub>2</sub>O–DCM) to yield the *piperazine* **116** (580 mg, 49%) as a pale yellow solid, m.p. 85-87 °C; *R<sub>f</sub>* = 0.41 (50:50 Petrol–EtOAc);  $\nu_{max}$ / cm<sup>-1</sup> (ATR) 3275 (br), 2989, 2944, 1722, 1546, 1372 and 1168;  $\delta_H$  (500 MHz, CDCl<sub>3</sub>) 8.04 (1H, dd, *J* 7.6 and 1.5, nitrophenyl 3-H), 7.82-7.72 (2H, m, nitrophenyl 4-H and nitrophenyl 5-H), 7.70 (1H, dd, *J* 7.5 and 1.5, nitrophenyl 6-H), 4.83 (1H, s, NH), 4.28-4.19 (1H, m, 6-H), 4.14 (1H, dd, *J* 10.9 and 5.9, 6-methyl-H<sub>a</sub>), 4.06-3.97 (1H, m, 5-H<sub>a</sub>), 3.54-3.48 (1H, m, 5-H<sub>b</sub>), 3.47-3.38 (3H, m, 3-H<sub>2</sub> and 6-methyl-H<sub>b</sub>), 3.34-3.24 (2H, m, ethyl 1-H<sub>2</sub>), 2.10 (3H, s, acetyl), 1.46 (3H, s, 2-methyl) and 1.22 (3H, t, *J* 7.2, ethyl 2-H<sub>3</sub>);  $\delta_c$  (126 MHz, CDCl<sub>3</sub>) 173.5 (acetyl CO), 170.7 (amide CO), 148.1 (nitrophenyl C-2), 134.3 (nitrophenyl C-5), 132.0 (nitrophenyl C-4), 131.5 (nitrophenyl C-6), 131.3 (nitrophenyl C-1), 124.5 (nitrophenyl C-3), 121.8 (app d, *J* 288.2, trifluoroacetyl C-2), 64.0 (C-5), 59.1 (C-2), 51.2 (6-methyl), 47.0 (C-6), 45.7 (C-3), 35.8 (ethyl C-1), 24.0 (acetyl), 20.8 (2-methyl), and 13.1 (ethyl C-2), trifluoroacetyl C-1 not observed;  $\delta_f$  (282 MHz, CDCl<sub>3</sub>) -82.4; HRMS found MH<sup>+</sup>, 525.1197. C<sub>19</sub>H<sub>23</sub>F<sub>3</sub>N<sub>4</sub>O<sub>8</sub>S requires *MH*, 525.1267.

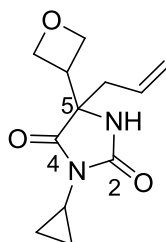
Stereochemistry has been determined where analysis of the NOESY spectrum showed correlation between the 6-H and 2-methyl protons.

**3-(2-Methoxyethyl)-5-(prop-2-en-1-yl)-5-(propan-2-yl)imidazolidine-2,4-dione, 195**



By general procedure R, the urea **189** (82.5 mg, 0.300 mmol) gave a crude residue which was purified by flash chromatography (SiO<sub>2</sub>, 5:95 MeOH–DCM) to yield the *hydantoin* **195** (48.6 mg, 67%) as a colourless amorphous solid  $R_f = 0.55$  (10:90 MeOH–DCM);  $\nu_{\max}/\text{cm}^{-1}$  (ATR) 3276 (br), 2967, 1771, 1708, 1448 and 1119;  $\delta_{\text{H}}$  (500 MHz, CDCl<sub>3</sub>) 5.73–5.63 (1H, m, propenyl 2-H), 5.21–5.13 (2H, m propenyl 3-H<sub>2</sub>), 3.74–3.67 (2H, m, methoxyethyl 2-H<sub>2</sub>), 3.56 (2H, t,  $J$  5.7, methoxyethyl 1-H<sub>2</sub>), 3.35 (3H, s, methoxyethyl 4-H<sub>3</sub>), 2.59–2.45 (2H, m, propenyl 1-H<sub>2</sub>), 2.10 (1H, hept,  $J$  6.9, propyl 2-H), 1.00 (3H, d,  $J$  6.9, propyl 1-H<sub>2</sub>) and 0.94 (3H, d,  $J$  6.9, propyl 3-H<sub>2</sub>);  $\delta_{\text{C}}$  (126 MHz, CDCl<sub>3</sub>) 175.4 (C-4), 157.1 (C-2), 130.7 (propenyl C-2), 120.2 (propenyl C-3), 68.8 (methoxyethyl C-2), 67.9 (C-5), 58.3 (methoxyethyl C-4), 39.3 (methoxyethyl C-1), 37.7 (propenyl C-1), 33.6 (propyl C-2), 16.7 (propyl C-1) and 16.3 (propyl C-3); HRMS found MH<sup>+</sup>, 241.1554. C<sub>12</sub>H<sub>20</sub>N<sub>2</sub>O<sub>3</sub> requires MH, 241.1552.

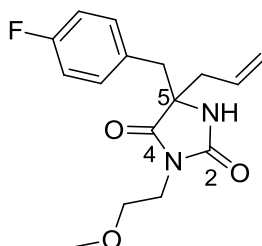
**3-Cyclopropyl-5-(oxetane-3-yl)-5-(prop-2-en-1-yl)imidazolidine-2,4-dione, 197**



By general procedure R, the urea **191** (75.8 mg, 0.280 mmol) gave a crude residue which was purified by flash chromatography (SiO<sub>2</sub>, 100% EtOAc) to yield the *hydantoin* **197** (61.0 mg, 92%) as a yellow oil,  $R_f = 0.58$  (10:90 MeOH–DCM);  $\delta_{\text{H}}$  (501 MHz, CDCl<sub>3</sub>) 6.17 (1H, s, NH), 5.71–5.53 (1H, m, propenyl 2-H), 5.24–5.12 (2H, m, propenyl 3-H<sub>2</sub>), 4.80 (1H, dd,  $J$  8.3 and 6.5, oxetanyl 2-H<sub>a</sub>), 4.66 (1H, dd,  $J$  8.3 and 6.5, oxetanyl 4-H<sub>a</sub>), 4.43 (2H, app t,  $J$  6.5, oxetanyl 2-H<sub>b</sub> and oxetanyl 4-H<sub>b</sub>), 3.47 (1H, tt,  $J$  8.3 and 6.5, oxetanyl 1-H), 2.66–2.54 (1H, m, cyclopropyl 1-H), 2.41 (1H, dd,  $J$  13.9 and 7.7, propenyl 1-H<sub>a</sub>), 2.32 (1H, dd,  $J$  13.9 and 7.1, propenyl 1-H<sub>b</sub>), 0.99–0.94 (2H, m, cyclopropyl 2-H<sub>2</sub>) and 0.93–0.87 (2H, m, cyclopropyl 3-H<sub>2</sub>);  $\delta_{\text{C}}$  (126 MHz, CDCl<sub>3</sub>) 174.3 (C-4), 157.0 (C-2), 129.5 (propenyl C-2),

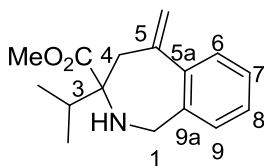
121.3 (propenyl C-3), 72.1 (oxetanyl C-2), 71.3 (oxetanyl C-4), 63.6 (C-5), 40.2 (oxetanyl C-1), 39.3 (propenyl C-1), 21.8 (cyclopropyl C-1), 5.0 (cyclopropyl C-2) and 4.9 (cyclopropyl C-3).

**5-[(4-Fluorophenyl)methyl]-3-(2-methoxyethyl)-5-(prop-2-en-1-yl)imidazolidine-2,4-dione, **196****



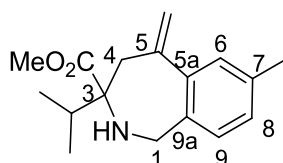
By general procedure R, the urea **190** (210 mg, 0.621 mmol) gave a crude residue which was purified by flash chromatography (SiO<sub>2</sub>, 50:50 Petrol-EtOAc) to yield the *hydantoin* **196** (153 mg, 80%) as a colourless solid, m.p. 49-51 °C; *R<sub>f</sub>* = 0.38 (50:50 Petrol-EtOAc); *v*<sub>max</sub>/cm<sup>-1</sup> (ATR) 3273 (br), 2928, 1771, 1706, 1509, 1449 and 1223; *δ*<sub>H</sub> (500 MHz, CDCl<sub>3</sub>) 7.19-7.09 (2H, m, fluorophenyl 2-H and fluorophenyl 6-H), 7.07-6.88 (2H, m, trifluoroacetyl 3-H and fluorophenyl 5-H), 6.19 (1H, s, NH), 5.77-5.60 (1H, m, propenyl 3-H<sub>a</sub>), 5.24-5.22 (1H, m, propenyl 3-H<sub>b</sub>), 5.21-5.17 (1H, m, propenyl 2-H), 3.52 (2H, t, *J* 5.9, methoxyethyl 1-H<sub>2</sub>), 3.35-3.27 (2H, m, methoxyethyl 2-H<sub>2</sub>), 3.25 (3H, s, methoxyethyl 4-H<sub>3</sub>), 3.11 (1H, d, *J* 13.9, benzylic-H<sub>a</sub>), 2.90 (1H, d, *J* 13.9, benzylic-H<sub>b</sub>), 2.65 (1H, dd, *J* 14.0 and 7.3, propenyl 1-H<sub>a</sub>) and 2.48 (1H, dd, *J* 14.0 and 7.4, propenyl 1-H<sub>b</sub>); *δ*<sub>C</sub> (126 MHz, CDCl<sub>3</sub>) 175.0 (C-4), 162.2 (d, *J* 246.2, fluorophenyl C-4), 156.8 (C-2), 131.8 (d, *J* 7.9, fluorophenyl C-2 and fluorophenyl C-6), 130.2 (propenyl C-2), 129.9 (d, *J* 2.8, fluorophenyl C-1), 121.1 (propenyl C-3), 115.3 (d, *J* 21.4, fluorophenyl C-3 and fluorophenyl C-5), 68.7 (methoxyethyl C-1), 65.7 (C-5), 58.6 (methoxyethyl C-4), 41.5 (methoxyethyl C-2), 41.0 (methyl) and 37.8 (propenyl C-1); *δ*<sub>F</sub> (282 MHz, CDCl<sub>3</sub>) -115.1; HRMS found *MH*<sup>+</sup>, 307.1488. C<sub>16</sub>H<sub>19</sub>FN<sub>2</sub>O<sub>3</sub> requires *MH*, 307.1458.

**Methyl 5-methylidene-3-(propan-2-yl)-2,3,4,5-tetrahydro-1H-2-benzazepine-3-carboxylate, 199**



By general procedure S, the amino ester **194** (518 mg, 1.52 mmol) gave a crude residue which was purified by flash chromatography (SiO<sub>2</sub>, 70:30 Petrol–EtOAc) to yield the *tetrahydrobenzazepine* **199** (300 mg, 76%) as a yellow oil, *R<sub>f</sub>* = 0.79 (40:60 Petrol–EtOAc);  $\nu_{\max}/\text{cm}^{-1}$  (ATR) 2949, 1727, 1464, 1433, 1202 and 1242;  $\delta_{\text{H}}$  (500 MHz, CDCl<sub>3</sub>) 7.45–7.39 (1H, m, 9-H), 7.23–7.16 (2H, m, 7-H and 8-H), 7.11–7.05 (1H, m, 6-H), 5.40 (1H, d, *J* 1.4, alkene-H<sub>a</sub>), 5.07 (1H, app s, alkene-H<sub>b</sub>), 4.06 (1H, d, *J* 16.5, 1-H<sub>a</sub>), 3.97 (1H, d, *J* 16.5, 1-H<sub>b</sub>), 3.74 (3H, s, methyl), 3.02 (1H, d, *J* 14.0, 4-H<sub>a</sub>), 2.87 (1H, d, *J* 14.0, 4-H<sub>b</sub>), 2.19–2.03 (1H, m, isopropyl 2-H), 1.02 (3H, d, *J* 4.0, isopropyl-Me<sub>A</sub>) and 1.00 (3H, d, *J* 4.0, isopropyl-Me<sub>B</sub>);  $\delta_{\text{C}}$  (126 MHz, CDCl<sub>3</sub>) 175.3 (CO), 145.3 (C-5a), 140.3 (C-9a), 139.6 (C-5), 127.9 (C-9), 127.7 (C-8), 127.4 (C-7), 126.8 (C-6), 115.4 (alkene), 69.3 (C-3), 51.6 (methyl), 49.2 (C-1), 40.6 (C-4), 34.9 (isopropyl C-2), 18.2 (isopropyl-Me<sub>A</sub>) and 17.1 (isopropyl-Me<sub>B</sub>); HRMS found MH<sup>+</sup>, 260.1772. C<sub>16</sub>H<sub>21</sub>NO<sub>2</sub> requires *MH*, 260.1650.

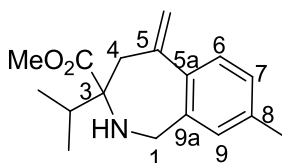
**Methyl 7-methyl-5-methylidene-3-(propan-2-yl)-2,3,4,5-tetrahydro-1H-2-benzazepine-3-carboxylate, 279**



By general procedure S, amino ester **269** (590 mg, 1.67 mmol) gave a crude residue which was purified by flash chromatography (SiO<sub>2</sub>, 80:20 Petrol–EtOAc) to yield the *tetrahydrobenzazepine* **279** (370 mg, 81%) as a yellow oil, *R<sub>f</sub>* = 0.65 (70:30 Petrol–EtOAc);  $\nu_{\max}/\text{cm}^{-1}$  (ATR) 3356, 3082, 2950, 1731, 1464, 1203, 1172, 890 and 811;  $\delta_{\text{H}}$  (300 MHz, CDCl<sub>3</sub>) 7.21 (1H, s, 6-H), 7.02–6.93 (2H, m, 8-H and 9-H), 5.37 (1H, d, *J* 1.6, alkene-H<sub>a</sub>), 5.03 (1H, app s, alkene-H<sub>b</sub>), 4.00 (1H, d, *J* 16.4, 1-H<sub>a</sub>), 3.91 (1H, d, *J* 16.4, 1-H<sub>b</sub>), 3.72 (3H, s, methyl), 2.99 (1H, d, *J* 13.8, 4-H<sub>a</sub>), 2.83 (1H, d, *J* 13.8, 4-H<sub>b</sub>), 2.33 (3H, s, tolyl), 2.14–1.99 (1H, m, isopropyl 2-H), 1.02–0.96 (6H, m, isopropyl-Me<sub>A</sub> and isopropyl-Me<sub>B</sub>);  $\delta_{\text{C}}$  (101 MHz, CDCl<sub>3</sub>) 145.4 (C-5), 145.2 (C-7), 138.9 (C-9a), 136.2 (C-5a), 128.3 (C-6), 128.0 (C-9), 127.8 (C-8), 115.1 (alkene), 69.3 (C-3), 51.6 (methyl), 48.9 (C-1), 40.7 (C-4), 34.9

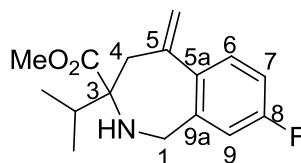
(isopropyl C-2), 21.0 (tolyl), 18.1 (isopropyl-Me<sub>A</sub>) and 17.1 (isopropyl-Me<sub>B</sub>); HRMS found MH<sup>+</sup>, 274.1821. C<sub>17</sub>H<sub>23</sub>NO<sub>2</sub> requires *MH*, 274.1807.

**Methyl 8-methyl-5-methylidene-3-(propan-2-yl)-2,3,4,5-tetrahydro-1H-2-benzazepine-3-carboxylate, 280**



By general procedure S, amino ester **270** (710 mg, 2.00 mmol) gave a crude residue which was purified by flash chromatography (SiO<sub>2</sub>, 80:20 Petrol–EtOAc) to yield the *tetrahydrobenzazepine* **280** (480 mg, 88%) as a yellow oil, *R*<sub>f</sub> = 0.62 (70:30 Petrol–EtOAc);  $\nu_{\max}$ / cm<sup>-1</sup> (ATR) 3359, 2950, 1728, 1463, 1201, 907 and 731;  $\delta_{\text{H}}$  (400 MHz, CDCl<sub>3</sub>) 7.31 (1H, d, *J* 7.8, 6-H), 7.00 (1H, d, *J* 7.8, 7-H), 6.88 (1H, s, 9-H), 5.35 (1H, d, *J* 1.5, alkene-H<sub>a</sub>), 5.01 (1H, app s, alkene-H<sub>b</sub>), 4.01 (1H, d, *J* 16.5, 1-H<sub>a</sub>), 3.91 (1H, d, *J* 16.5, 1-H<sub>b</sub>), 3.73 (3H, s, methyl), 2.98 (1H, d, *J* 13.9, 4-H<sub>a</sub>), 2.84 (1H, d, *J* 13.9, 4-H<sub>b</sub>), 2.32 (3H, s, tolyl), 2.15–2.00 (1H, m, isopropyl 2-H), 1.02–0.97 (6H, m, isopropyl-Me<sub>A</sub> and isopropyl-Me<sub>B</sub>);  $\delta_{\text{C}}$  (101 MHz, CDCl<sub>3</sub>) 175.4 (CO), 145.1 (C-5), 139.7 (C-9a), 137.4 (C-8), 137.1 (C-5a), 128.6 (C-6), 127.6 (C-7), 127.5 (C-9), 114.6 (alkene), 69.3 (C-3), 51.6 (methyl), 49.2 (C-1), 40.8 (C-4), 34.9 (isopropyl C-2), 20.9 (tolyl), 18.2 (isopropyl-Me<sub>A</sub>) and 17.1 (isopropyl-Me<sub>B</sub>); HRMS found MH<sup>+</sup>, 274.1826. C<sub>17</sub>H<sub>23</sub>NO<sub>2</sub> requires *MH*, 274.1807.

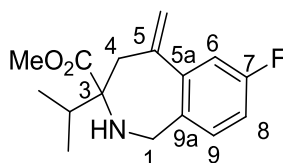
**Methyl 8-fluoro-5-methylidene-3-(propan-2-yl)-2,3,4,5-tetrahydro-1H-2-benzazepine-3-carboxylate, 281**



By general procedure S, amino ester **271** (670 mg, 1.87 mmol) gave a crude residue which was purified by flash chromatography (SiO<sub>2</sub>, 80:20 Petrol–EtOAc) to yield the *tetrahydrobenzazepine* **281** (470 mg, 91%) as a yellow oil, *R*<sub>f</sub> = 0.75 (70:30 Petrol–EtOAc);  $\nu_{\max}$ / cm<sup>-1</sup> (ATR) 3359, 3084, 2952, 1728, 1465, 1219, 1201 and 1128;  $\delta_{\text{H}}$  (300 MHz, CDCl<sub>3</sub>) 7.36 (1H, dd, *J* 8.6 and 5.7, 6-H), 6.87 (1H, td, *J* 8.6 and 2.7, 7-H), 6.77 (1H, dd, *J* 8.6 and 2.7, 9-H), 5.33 (1H, d, *J* 1.4, alkene-H<sub>a</sub>), 5.03 (1H, app s, alkene-H<sub>b</sub>), 4.01 (1H, d, *J* 16.7, 1-H<sub>a</sub>), 3.90 (1H, d, *J* 16.7, 1-H<sub>b</sub>), 3.73 (3H, s, methyl), 2.97 (1H, d, *J* 14.0, 4-H<sub>a</sub>), 2.82 (1H, d, *J* 14.0, 4-H<sub>b</sub>), 2.15–1.97 (1H, m, isopropyl 2-H), 1.04–0.95 (6H, m, isopropyl-

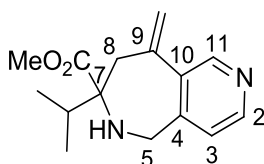
Me<sub>A</sub> and isopropyl-Me<sub>B</sub>);  $\delta_c$  (101 MHz, CDCl<sub>3</sub>) 175.3 (CO), 163.2 (C-8), 144.4 (C-5), 142.0 (C-9a), 136.3 (C-5a), 129.4 (d, *J* 8.0, C-6), 115.3 (alkene), 114.3 (d, *J* 21.3, C-7), 113.4 (d, *J* 21.1, C-9), 69.2 (C-3), 51.7 (methyl), 49.0 (C-1), 40.6 (C-4), 34.8 (isopropyl C-2), 18.1 (isopropyl-Me<sub>A</sub>) and 17.1 (isopropyl-Me<sub>B</sub>);  $\delta_f$  (376 MHz, CDCl<sub>3</sub>) -115.9; HRMS found MH<sup>+</sup>, 278.1570. C<sub>16</sub>H<sub>20</sub>FNO<sub>2</sub> requires *MH*, 278.1556.

**Methyl 7-fluoro-5-methylidene-3-(propan-2-yl)-2,3,4,5-tetrahydro-1H-2-benzazepine-3-carboxylate, 282**



By general procedure S, amino ester **272** (700 mg, 1.95 mmol) gave a crude residue which was purified by flash chromatography (SiO<sub>2</sub>, 80:20 Petrol-EtOAc) to yield the *tetrahydrobenzazepine* **282** (500 mg, 92%) as a yellow oil, *R<sub>f</sub>* = 0.62 (70:30 Petrol-EtOAc);  $\nu_{\max}$ /cm<sup>-1</sup> (ATR) 3358, 2952, 1727, 1580, 1214, 1127, 904 and 731;  $\delta_H$  (400 MHz, CDCl<sub>3</sub>) 7.00 (1H, dd, *J* 8.3 and 2.7, 9-H), 6.93 (1H, dd, *J* 8.3 and 5.8, 6-H), 6.77 (1H, td, *J* 8.3 and 2.7, 8-H), 5.30 (1H, d, *J* 1.2, alkene-H<sub>a</sub>), 5.01 (1H, app s, alkene-H<sub>b</sub>), 3.91 (1H, d, *J* 16.4, 1-H<sub>a</sub>), 3.81 (1H, d, *J* 16.4, 1-H<sub>b</sub>), 3.64 (3H, s, methyl), 2.89 (1H, d, *J* 14.0, 4-H<sub>a</sub>), 2.75 (1H, d, *J* 14.0, 4-H<sub>b</sub>), 2.04-1.93 (1H, m, isopropyl 2-H), 0.93-0.87 (6H, m, isopropyl-Me<sub>A</sub> and isopropyl-Me<sub>B</sub>);  $\delta_c$  (101 MHz, CDCl<sub>3</sub>) 175.3 (CO), 161.66 (d, *J* 243.8, C-7), 144.5 (d, *J* 1.9, C-5), 142.25 (d, *J* 7.2, C-9a), 135.6 (C-5a), 129.3 (d, *J* 8.2, C-9), 116.4 (alkene), 114.2 (d, *J* 22.0, C-6), 113.9 (d, *J* 21.3, C-8), 69.2 (C-3), 51.7 (methyl), 48.6 (C-1), 40.2 (C-4), 34.9 (isopropyl C-2), 18.1 (isopropyl-Me<sub>A</sub>) and 17.0 (isopropyl-Me<sub>B</sub>);  $\delta_f$  (376 MHz, CDCl<sub>3</sub>) -117.0; HRMS found MH<sup>+</sup>, 278.1573. C<sub>16</sub>H<sub>20</sub>FNO<sub>2</sub> requires *MH*, 278.1556.

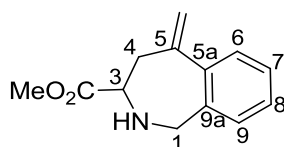
**Methyl 7-isopropyl-9-methylene-6,7,8,9-tetrahydro-5H-pyrido[4,3-c]azepine-7-carboxylate, 283**



By general procedure S, amino ester **273** (520 mg, 1.52 mmol) gave a crude residue which was purified by flash chromatography (SiO<sub>2</sub>, 10:90 MeOH-EtOAc) to yield the *tetrahydrobenzazepine* **283** (360 mg, 91%) as a yellow oil, *R<sub>f</sub>* = 0.61 (20:80 MeOH-EtOAc);  $\nu_{\max}$ /cm<sup>-1</sup> (ATR) 3359 (br), 2952, 2878, 1727, 1204 and 1130;  $\delta_H$  (400 MHz, CDCl<sub>3</sub>)

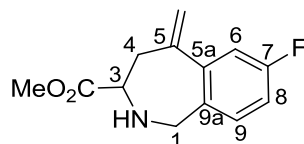
8.61 (1H, s, 11-H), 8.37 (1H, d, *J* 5.0, 2-H), 6.97 (1H, d, *J* 5.0, 3-H), 5.48 (1H, d, *J* 0.8, alkene-H<sub>a</sub>), 5.13 (1H, app s, alkene-H<sub>b</sub>), 4.03 (1H, d, *J* 17.1, 5-H<sub>a</sub>), 3.94 (1H, d, *J* 17.1, 5-H<sub>b</sub>), 3.76 (3H, s, methyl), 2.99 (1H, d, *J* 13.9, 8-H<sub>a</sub>), 2.85 (1H, d, *J* 13.9, 8-H<sub>b</sub>), 2.22-2.00 (1H, m, isopropyl 2-H) and 1.00 (6H, t, *J* 7.2, isopropyl-Me<sub>A</sub> and isopropyl-Me<sub>B</sub>);  $\delta_c$  (101 MHz, CDCl<sub>3</sub>) 175.0 (CO), 148.5 (C-11), 148.3 (C-2), 148.1 (C-9), 141.9 (C-4), 135.7 (C-10), 122.1 (C-3), 116.4 (alkene-C), 69.3 (C-7), 51.8 (methyl), 48.3 (C-5), 40.7 (C-8), 34.6 (isopropyl C-2), 18.1 (isopropyl-Me<sub>A</sub>) and 17.1 (isopropyl-Me<sub>B</sub>); HRMS found MH<sup>+</sup>, 261.1620. C<sub>15</sub>H<sub>20</sub>N<sub>2</sub>O<sub>2</sub> requires *MH*, 261.1603.

### Methyl 5-methylidene-2,3,4,5-tetrahydro-1*H*-2-benzazepine-3-carboxylate, **284**



By general procedure S, amino ester **275** (360 mg, 1.21 mmol) gave a crude residue which was purified by flash chromatography (SiO<sub>2</sub>, 40:60 Petrol–EtOAc) to yield the *tetrahydrobenzazepine* **284** (150 mg, 57%) as a yellow oil, *R<sub>f</sub>* = 0.20 (60:40 Petrol–EtOAc);  $\nu_{\max}$ /cm<sup>-1</sup> (ATR) 3346 (br), 3063, 3015, 2950, 2846, 1736, 1434, 1200, 1172, 774 and 744;  $\delta_H$  (400 MHz, CDCl<sub>3</sub>) 7.28-7.23 (1H, m, 9-H), 7.17-7.09 (2H, m, 7-H and 8-H), 7.05-7.01 (1H, m, 6-H), 5.18 (1H, d, *J* 1.5, alkene-H<sub>a</sub>), 5.10 (1H, app s, alkene-H<sub>b</sub>), 4.02 (1H, d, *J* 15.9, 1-H<sub>a</sub>), 3.87 (1H, d, *J* 15.9, 1-H<sub>b</sub>), 3.75 (1H, dd, *J* 9.4 and 4.4, 3-H), 3.69 (3H, s, methyl), 2.90 (1H, dd, *J* 13.4 and 4.4, 4-H<sub>a</sub>), 2.56 (1H, dd, *J* 13.4 and 9.4, 4-H<sub>b</sub>) and 1.99 (1H, br s, NH);  $\delta_c$  (101 MHz, CDCl<sub>3</sub>) 173.6 (CO), 146.8 (C-5), 141.7 (C-9a), 139.2 (C-5a), 128.2 (C-9), 128.0 (C-8), 127.5 (C-7), 127.2 (C-6), 116.0 (alkene), 62.6 (C-3), 52.1 (methyl), 51.5 (C-1) and 40.4 (C-4); HRMS found MH<sup>+</sup>, 218.1183. C<sub>13</sub>H<sub>15</sub>NO<sub>2</sub> requires *MH*, 218.1181.

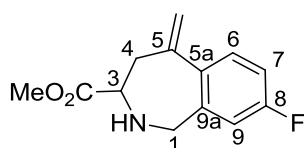
### Methyl 7-fluoro-5-methylidene-2,3,4,5-tetrahydro-1*H*-2-benzazepine-3-carboxylate, **285**



By general procedure S, amino ester **276** (440 mg, 1.39 mmol) gave a crude residue which was purified by flash chromatography (SiO<sub>2</sub>, 50:50 Petrol–EtOAc) to yield the *tetrahydrobenzazepine* **285** (170 mg, 52%) as a yellow oil, *R<sub>f</sub>* = 0.19 (50:50 Petrol–EtOAc);  $\nu_{\max}$ /cm<sup>-1</sup> (ATR) 3347, 2952, 1737, 1582, 1436, 1276, 1213 and 1173;  $\delta_H$  (400 MHz, CDCl<sub>3</sub>) 7.11-7.01 (2H, m, 6-H and 9-H), 6.89 (1H, td, *J* 8.3 and 2.7, 8-H), 5.28 (1H, d, *J*

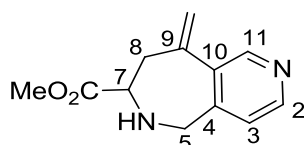
1.4, alkene-H<sub>a</sub>), 5.23 (1H, app s, alkene-H<sub>b</sub>), 4.08 (1H, d, *J* 15.8, 1-H<sub>a</sub>), 3.92 (1H, d, *J* 15.8, 1-H<sub>b</sub>), 3.83 (1H, dd, *J* 9.3 and 4.3, 3-H), 3.78 (3H, s, methyl), 2.98 (1H, dd, *J* 13.5 and 4.3, 4-H<sub>a</sub>), 2.64 (1H, dd, *J* 13.5 and 9.3, 4-H<sub>b</sub>) and 2.00 (1H, br s, NH);  $\delta_{\text{C}}$  (101 MHz, CDCl<sub>3</sub>) 173.4 (CO), 161.8 (d, *J* 245.2, C-7), 145.9 (C-9a), 143.7 (d, *J* 7.3, C-5), 135.1 (C-5a), 129.6 (d, *J* 8.1, C-9), 116.9 (alkene), 115.0 (d, *J* 22.0, C-6), 113.8 (d, *J* 21.1, C-8), 62.5 (C-3), 52.1 (methyl), 50.8 (C-1) and 40.1 (C-4);  $\delta_{\text{F}}$  (376 MHz, CDCl<sub>3</sub>) -116.3; HRMS found MH<sup>+</sup>, 236.1099. C<sub>13</sub>H<sub>14</sub>FNO<sub>2</sub> requires *MH*, 236.1087.

**Methyl 8-fluoro-5-methylidene-2,3,4,5-tetrahydro-1H-2-benzazepine-3-carboxylate, 286**



By general procedure S, amino ester **277** (480 mg, 1.52 mmol) gave a crude residue which was purified by flash chromatography (SiO<sub>2</sub>, 40:60 Petrol-EtOAc) to yield the *tetrahydrobenzazepine* **286** (300 mg, 84%) as a yellow oil, *R<sub>f</sub>* = 0.36 (40:60 Petrol-EtOAc);  $\nu_{\text{max}}$ /cm<sup>-1</sup> (ATR) 3340 (br), 3081, 2952, 2845, 1736, 1492, 1272 and 1219;  $\delta_{\text{H}}$  (400 MHz, CDCl<sub>3</sub>) 7.21 (1H, dd, *J* 8.8 and 6.0, 9-H), 6.81 (1H, td, *J* 8.8 and 2.6, 6-H), 6.74 (1H, dd, *J* 8.8 and 2.5, 7-H), 5.15 (1H, d, *J* 1.1, alkene-H<sub>a</sub>), 5.08 (1H, app s, alkene-H<sub>b</sub>), 3.98 (1H, d, *J* 16.0, 1-H<sub>a</sub>), 3.84 (1H, d, *J* 16.0, 1-H<sub>b</sub>), 3.74 (1H, dd, *J* 9.3 and 4.5, 3-H), 3.69 (3H, s, methyl), 2.88 (1H, dd, *J* 13.4 and 4.5, 4-H<sub>a</sub>) and 2.54 (1H, dd, *J* 13.4 and 9.3, 4-H<sub>b</sub>);  $\delta_{\text{C}}$  (101 MHz, CDCl<sub>3</sub>) 173.4 (CO), 161.9 (d, *J* 247.1, C-8), 145.8 (C-5), 141.5 (C-9a), 137.6 (C-5a), 129.9 (d, *J* 8.0, C-9), 116.0 (alkene), 114.7 (d, *J* 21.4, C-6), 113.6 (d, *J* 20.9, C-7), 62.4 (C-3), 52.1 (methyl), 51.2 (C-1) and 40.2 (C-4);  $\delta_{\text{F}}$  (376 MHz, CDCl<sub>3</sub>) -115.7; HRMS found MH<sup>+</sup>, 236.1101. C<sub>13</sub>H<sub>14</sub>FNO<sub>2</sub> requires *MH*, 236.1087.

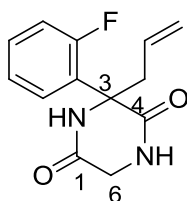
**Methyl 9-methylene-6,7,8,9-tetrahydro-5H-pyrido[4,3-c]azepine-7-carboxylate, 287**



By general procedure S, amino ester **278** (490 mg, 1.64 mmol) gave a crude residue which was purified by flash chromatography (SiO<sub>2</sub>, 100% EtOAc to 10:90 MeOH-EtOAc) to yield the *tetrahydrobenzazepine* **287** (290 mg, 81%) as a yellow oil, *R<sub>f</sub>* = 0.28 (10:90 MeOH-EtOAc);  $\nu_{\text{max}}$ /cm<sup>-1</sup> (ATR) 3342 (br), 2951, 1736, 1435, 1274, 1207 and 1157;

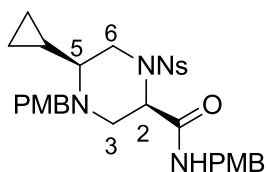
$\delta_{\text{H}}$  (400 MHz,  $\text{CDCl}_3$ ) 8.57 (1H, s, 11-H), 8.43 (1H, d,  $J$  4.9, 2-H), 7.03 (1H, d,  $J$  4.9, 3-H), 5.37 (1H, d,  $J$  1.0, alkene- $\text{H}_a$ ), 5.27 (1H, app s, alkene- $\text{H}_b$ ), 4.14 (1H, d,  $J$  16.5, 5- $\text{H}_a$ ), 3.96 (1H, d,  $J$  16.5, 5- $\text{H}_b$ ), 3.86 (1H, dd,  $J$  9.1 and 4.9, 7-H), 3.80 (3H, s, methyl), 3.01 (1H, dd,  $J$  13.5 and 4.9, 8- $\text{H}_a$ ) and 2.68 (1H, dd,  $J$  13.5 and 9.1, 8- $\text{H}_b$ );  $\delta_{\text{C}}$  (101 MHz,  $\text{CDCl}_3$ ) 173.3 (CO), 148.7 (C-11), 147.7 (C-2), 142.9 (C-9), 136.7 (C-4), 132.1 (C-10), 122.2 (C-3), 117.1 (alkene), 62.0 (C-7), 52.2 (methyl), 50.4 (C-5) and 40.0 (C-8); HRMS found  $\text{MH}^+$ , 219.1141.  $\text{C}_{12}\text{H}_{14}\text{N}_2\text{O}_2$  requires  $\text{MH}$ , 219.1133.

### 3-(2-Fluorophenyl)-3-(prop-2-en-1-yl)piperazine-2,5-dione, **198**



TFA (1.05 mL, 13.7 mmol) was added to a stirred solution of amide **193** (520 mg, 1.37 mmol) in DCM (15.0 mL,  $\sim 0.1$  M) at  $0^\circ\text{C}$  and stirred for 10 min before being warmed to room temperature and stirred overnight. The reaction mixture was concentrated *in vacuo* and dissolved in DMF (30 mL,  $\sim 0.05$  M).  $\text{Cs}_2\text{CO}_3$  (893 mg, 2.74 mmol) was added and the reaction mixture heated at reflux for 1 hr, before being concentrated *in vacuo*. The residue was purified by flash chromatography ( $\text{SiO}_2$ , 5:95 MeOH–DCM) to yield the piperazine **198** (250 mg, 71%) as an amorphous pale orange solid,  $R_f = 0.50$  (10:90 MeOH–DCM);  $\nu_{\text{max}}/\text{cm}^{-1}$  (ATR) 3195, 3078, 2923, 1678, 1453 and 773;  $\delta_{\text{H}}$  (501 MHz, MeOD) 7.43 (1H, td,  $J$  8.0 and 1.4, fluorophenyl 4-H), 7.30 (1H, dddd,  $J$  8.0, 7.4, 5.2 and 1.7, fluorophenyl 3-H), 7.13 (1H, td,  $J$  8.0 and 1.2, fluorophenyl 5-H), 7.05 (1H, ddd,  $J$  12.2, 8.0 and 1.4, fluorophenyl 6-H), 5.84–5.72 (1H, m, propenyl 2-H), 5.24–5.16 (2H, m, propenyl 3- $\text{H}_2$ ), 3.86 (2H, d,  $J$  0.5, 6- $\text{H}_2$ ), 3.08 (1H, dd,  $J$  13.3 and 6.7, propenyl 1- $\text{H}_a$ ) and 2.80 (1H, dd,  $J$  13.3 and 7.7, propenyl 1- $\text{H}_b$ );  $\delta_{\text{C}}$  (126 MHz, MeOD) 169.9 (C-1), 167.8 (C-4), 163.2 (fluorophenyl C-2), 132.4 (propenyl C-2), 131.6 (d,  $J$  9.0, fluorophenyl C-4), 129.8 (d,  $J$  10.7, fluorophenyl C-1), 128.7 (d,  $J$  3.1, fluorophenyl C-3), 125.4 (d,  $J$  3.4, fluorophenyl C-5), 121.8 (propenyl C-3), 117.2 (d,  $J$  22.4, fluorophenyl C-6), 62.7 (C-3), 45.7 (C-6) and 42.8 (propenyl C-1);  $\delta_{\text{F}}$  (282 MHz,  $\text{CDCl}_3$ )  $-112.8$ ; HRMS found  $\text{MH}^+$ , 249.1035.  $\text{C}_{13}\text{H}_{13}\text{FN}_2\text{O}_2$  requires  $\text{MH}$ , 249.1039.

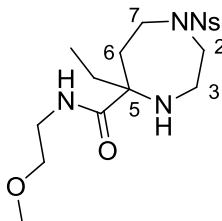
**(2*R*, 5*S*)-5-Cyclopropyl-*N*, 4-bis[(4-methoxyphenyl)methyl]-1-(2-nitrobenzene sulfonyl)piperazine-2-carboxamide, **235****



DEAD (59.0  $\mu$ L, 0.370 mmol) was added dropwise to a solution of the alcohol **234** (177 mg, 0.290 mmol),  $\text{PPh}_3$  (106 mg, 0.406 mmol) in THF (5.80 mL, 0.05 M) at 0  $^\circ\text{C}$ . The resulting solution was warmed to room temperature and stirred overnight, before being concentrated *in vacuo* and purified by flash chromatography ( $\text{SiO}_2$ , 50:50 Petrol–EtOAc) then again ( $\text{SiO}_2$ , 60:40 Petrol–EtOAc), before being purified by mass-directed preparative HPLC to yield the *piperazine* **235** (14.6 mg, 8%) as a yellow oil,  $R_f = 0.71$  (30:70 Petrol–EtOAc);  $\delta_{\text{H}}$  (500 MHz,  $\text{CDCl}_3$ ) 8.12 (1H, d,  $J$  7.6, nitrophenyl 3-H), 7.76 (1H, t,  $J$  7.6, nitrophenyl 4-H), 7.62 (1H, t,  $J$  7.6, nitrophenyl 5-H), 7.51 (1H, d,  $J$  7.6, nitrophenyl 6-H), 7.08 (2H, d,  $J$  8.4, 2-PMB 3-H and 2-PMB 5-H), 7.00 (2H, d,  $J$  8.4, 4-PMB 3-H and 4-PMB 5-H), 6.78 (4H, dd,  $J$  12.6 and 8.4, 2-PMB 2-H, 2-PMB 6-H, 4-PMB 2-H and 4-PMB 6-H), 4.39 (1H, app s, 2-H), 4.30 (1H, dd,  $J$  14.4 and 5.5, 2-benzylic- $\text{H}_a$ ), 4.13 (1H, dd,  $J$  14.4 and 5.5, 2-benzylic- $\text{H}_b$ ), 3.90 (1H, d,  $J$  13.2, 4-benzylic- $\text{H}_a$ ), 3.80 (3H, s, 2-PMB methyl), 3.78-3.76 (4H, m, 4-PMB methyl and 6- $\text{H}_a$ ), 3.63 (1H, d,  $J$  13.2, 4-benzylic- $\text{H}_b$ ), 3.49 (1H, dd,  $J$  13.0 and 2.9, 6- $\text{H}_b$ ), 3.22 (1H, d,  $J$  12.3, 3- $\text{H}_a$ ), 3.15 (1H, dd,  $J$  12.3 and 4.2, 3- $\text{H}_b$ ), 1.94 (1H, d,  $J$  10.0, 5-H), 1.24-1.10 (1H, m, cyclopropyl 1-H), 0.75-0.61 (1H, m, cyclopropyl 2- $\text{H}_a$ ), 0.35-0.22 (2H, m, cyclopropyl 2- $\text{H}_b$  and cyclopropyl 4- $\text{H}_a$ ) and -0.09--0.22 (1H, m, cyclopropyl 4- $\text{H}_b$ );  $\delta_{\text{C}}$  (126 MHz,  $\text{CDCl}_3$ ) 168.2 (CO), 159.1 (2-PMB C-4), 159.0 (4-PMB C-4), 147.5 (nitrophenyl C-2), 133.9 (nitrophenyl C-5), 133.1 (nitrophenyl C-1), 132.1 (nitrophenyl C-4), 132.1 (nitrophenyl C-6), 130.1 (2-PMB C-1 and 4-PMB C-1), 129.9 (2-PMB C-3 and 2-PMB C-5), 129.3 (4-PMB C-3 and 4-PMB C-5), 124.6 (nitrophenyl C-3), 114.2 (2-PMB C-2 and 2-PMB C-6), 113.9 (4-PMB C-2 and 4-PMB C-6), 61.8 (C-5), 58.5 (C-6), 56.7 (C-2), 55.5 (2-PMB methyl), 55.3 (4-PMB methyl), 48.5 (4-PMB benzylic-C), 46.3 (C-3), 43.2 (2-PMB benzylic-C), 6.9 (cyclopropyl C-2), 4.8 (cyclopropyl C-1) and 0.8 (cyclopropyl C-4).

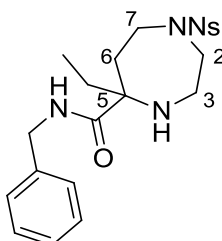
## 5.7 Synthesis of Fragments

### ***N*-Methoxyethyl-5-ethyl-1-[(2-nitrophenyl)sulfonyl]-1,4-diazepane-5-carboxamide, **130****



By general procedure L, the protected diazepane **51** (379 mg, 0.740 mmol) gave a crude residue which was purified by flash chromatography (SiO<sub>2</sub>, 100% EtOAc) to yield the *deprotected diazepane* **130** (239 mg, 78%) as a yellow oil,  $R_f = 0.09$  (30:70 Petrol–EtOAc);  $\nu_{\max}/\text{cm}^{-1}$  (ATR) 3383, 3285, 2933, 1714, 1639, 1605, 1544, 1345, 1272 and 577;  $\delta_{\text{H}}$  (500 MHz, CDCl<sub>3</sub>) 8.03 (1H, d,  $J$  7.9, nitrophenyl 3-H), 7.95 (1H, br s, amide NH), 7.74–7.68 (2H, m, nitrophenyl 4-H and nitrophenyl 5-H), 7.65 (1H, d,  $J$  8.4, nitrophenyl 6-H), 3.71–3.56 (2H, m, 2-H<sub>a</sub> and 3-H<sub>a</sub>), 3.50–3.41 (4H, m, 2-H<sub>b</sub>, 3-H<sub>b</sub> and 7-H<sub>2</sub>), 3.39–3.29 (4H, m, methoxyethyl 2-H<sub>a</sub> and methoxyethyl 4-H<sub>3</sub>), 3.24–3.10 (2H, m, methoxyethyl 1-H<sub>2</sub>), 2.98 (1H, dd,  $J$  14.7 and 6.6, methoxyethyl 2-H<sub>b</sub>), 2.38 (1H, dd,  $J$  15.8 and 8.4, ethyl 1-H<sub>a</sub>), 1.97 (1H, dd,  $J$  15.8 and 8.4, ethyl 1-H<sub>b</sub>), 1.89–1.77 (1H, m, 6-H<sub>a</sub>), 1.65 (1H, br s, NH), 1.60–1.47 (1H, m, 6-H<sub>b</sub>) and 0.84 (3H, app t,  $J$  8.4, ethyl 2-H<sub>3</sub>);  $\delta_{\text{C}}$  (126 MHz, CDCl<sub>3</sub>) 175.1 (amide CO), 148.0 (nitrophenyl C-2), 133.5 (nitrophenyl C-5), 132.9 (nitrophenyl C-1), 131.6 (nitrophenyl C-4), 131.0 (nitrophenyl C-6), 124.1 (nitrophenyl C-3), 71.4 (C-3), 65.3 (C-5), 58.7 (methoxyethyl C-4), 51.7 (C-2), 44.2 (C-7), 44.0 (methoxyethyl C-1), 39.0 (methoxyethyl C-2), 37.7 (ethyl C-1), 31.9 (C-6) and 8.1 (ethyl C-2); HRMS found  $\text{MH}^+$ , 415.1717. C<sub>17</sub>H<sub>26</sub>N<sub>4</sub>O<sub>6</sub>S requires  $\text{MH}$ , 415.1651.

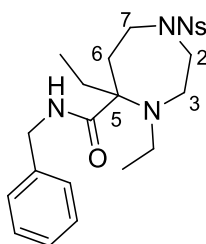
### ***N*-Benzyl-5-ethyl-1-[(2-nitrophenyl)sulfonyl]-1,4-diazepane-5-carboxamide, **117****



By general procedure L, the protected diazepane **33** (890 mg, 1.64 mmol) gave a crude residue which was purified by flash chromatography (SiO<sub>2</sub>, 40:60 Petrol–EtOAc) to yield the *deprotected diazepane* **117** (250 mg, 34%) as a yellow oil,  $R_f = 0.18$  (40:60

Petrol–EtOAc);  $\nu_{\max}/\text{cm}^{-1}$  (ATR) 3349 (br), 2932, 1653, 1543, 1454, 1370, 1163 and 577;  $\delta_{\text{H}}$  (500 MHz,  $\text{CDCl}_3$ ) 8.03 (1H, dd,  $J$  7.6 and 1.7, nitrophenyl 3-H), 7.99 (1H, t,  $J$  5.7, NH), 7.77-7.68 (2H, m, nitrophenyl 4-H and nitrophenyl 5-H), 7.66 (1H, dd,  $J$  7.4 and 1.7, nitrophenyl 6-H), 7.43-7.20 (5H, m, benzyl-H), 4.49 (1H, dd,  $J$  14.7 and 5.7, benzylic- $\text{H}_a$ ), 4.42 (1H, dd,  $J$  14.7 and 5.7, benzylic- $\text{H}_b$ ), 3.73-3.55 (2H, m, 2- $\text{H}_a$  and 3- $\text{H}_a$ ), 3.35 (1H, dd,  $J$  13.9 and 7.2, 7- $\text{H}_a$ ), 3.25 (1H, dd,  $J$  13.9 and 9.1, 7- $\text{H}_b$ ), 3.16 (1H, dd,  $J$  14.9 and 6.5, 3- $\text{H}_b$ ), 2.98 (1H, dd,  $J$  14.9 and 6.2, 2- $\text{H}_b$ ), 2.43 (1H, dd,  $J$  15.5 and 8.1, ethyl 1- $\text{H}_a$ ), 2.02 (1H, dd,  $J$  15.5 and 8.1, ethyl 1- $\text{H}_b$ ), 1.87 (1H, td,  $J$  15.1 and 7.2, 6- $\text{H}_a$ ), 1.70-1.55 (1H, m, 6- $\text{H}_b$ ) and 0.86 (3H, app t,  $J$  8.1, ethyl 2- $\text{H}_3$ );  $\delta_{\text{C}}$  (75 MHz,  $\text{CDCl}_3$ ) 148.0 (nitrophenyl C-2), 138.4 (benzyl C-1), 133.6 (nitrophenyl C-5), 132.7 (nitrophenyl C-1), 131.7 (nitrophenyl C-4), 131.0 (nitrophenyl C-6), 128.7 (benzyl C-3 and benzyl C-5), 127.7 (benzyl C-2 and benzyl C-6), 127.5 (benzyl C-4), 124.2 (nitrophenyl C-3), 65.7 (C-5), 51.0 (C-3), 44.3 (benzylic-C), 44.0 (C-2), 43.5 (C-7), 37.2 (C-6), 31.9 (ethyl C-1) and 8.2 (ethyl C-2), amide CO not observed; HRMS found  $\text{MH}^+$ , 447.1721.  $\text{C}_{21}\text{H}_{26}\text{N}_4\text{O}_5\text{S}$  requires  $\text{MH}$ , 447.1702.

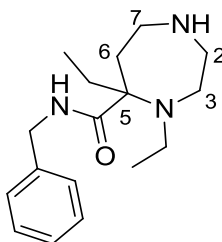
***N*-Benzyl-5-ethyl-1-[(2-nitrophenyl)sulfonyl]-4-(ethyl)-1,4-diazepane-5-carboxamide, 118**



By general procedure M, acetaldehyde (0.130 mL, 2.24 mmol) and diazepane **117** (250 mg, 0.560 mmol) gave a crude residue which was purified by flash chromatography ( $\text{SiO}_2$ , 30:70 Petrol–EtOAc) to yield the alkylated *diazepane* **118** (170 mg, 64%) as a yellow oil,  $R_f = 0.66$  (30:70 Petrol–EtOAc);  $\nu_{\max}/\text{cm}^{-1}$  (ATR) 3371 (br), 2968, 1662, 1542, 1501, 1362, 1162, 729 and 575;  $\delta_{\text{H}}$  (500 MHz,  $\text{CDCl}_3$ ) 7.98 (1H, dd,  $J$  7.6 and 1.6, nitrophenyl 3-H), 7.74-7.66 (2H, m, nitrophenyl 4-H and nitrophenyl 5-H), 7.63 (1H, dd,  $J$  7.5 and 1.6, nitrophenyl 6-H), 7.57 (1H, t,  $J$  5.8, NH), 7.36-7.32 (2H, m, benzyl 3-H and benzyl 5-H), 7.31-7.26 (3H, m, benzyl 2-H, benzyl 4-H and benzyl 6-H), 4.51 (1H, dd,  $J$  14.6 and 5.8, benzylic- $\text{H}_a$ ), 4.38 (1H, dd,  $J$  14.6 and 5.8, benzylic- $\text{H}_b$ ), 3.90 (1H, dd,  $J$  13.0 and 6.8, 2- $\text{H}_a$ ), 3.75 (1H, dd,  $J$  14.7 and 7.1, 7- $\text{H}_a$ ), 3.22 (1H, ddd,  $J$  15.4, 7.6 and 2.4, 2- $\text{H}_a$ ), 3.15 (1H, dd,  $J$  14.7 and 9.7, 7- $\text{H}_b$ ), 2.97 (1H, ddd,  $J$  13.0, 7.6 and 2.6, 3- $\text{H}_b$ ), 2.82 (1H, ddd,  $J$  15.4, 6.8 and 2.6, 2- $\text{H}_b$ ), 2.71-2.51 (2H, m, 4-ethyl 1- $\text{H}_2$ ), 2.29 (1H, dd,  $J$  15.6 and 7.4, 5-ethyl 1- $\text{H}_a$ ), 2.08-2.03 (1H, m, 5-ethyl 1- $\text{H}_b$ ), 1.92-1.70 (2H, m, 6- $\text{H}_2$ ) and 0.97 (6H, t,  $J$  7.4, 4-ethyl 2- $\text{H}_3$  and 5-ethyl 2- $\text{H}_3$ );  $\delta_{\text{C}}$  (126 MHz,  $\text{CDCl}_3$ ) 175.0 (amide CO), 148.1 (nitrophenyl C-2), 138.5

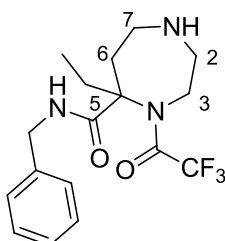
(benzyl C-1), 133.5 (nitrophenyl C-5), 132.7 (nitrophenyl C-1), 131.6 (nitrophenyl C-4), 130.8 (nitrophenyl C-6), 128.7 (benzyl C-3 and benzyl C-5), 127.8 (benzyl C-2 and benzyl C-6), 127.5 (benzyl C-4), 124.1 (nitrophenyl C-3), 69.5 (C-5), 49.2 (4-ethyl C-1), 46.4 (C-2), 43.7 (benzylic-C), 43.5 (C-3), 43.0 (C-7), 35.6 (C-6), 28.5 (5-ethyl C-1), 14.2 (4-ethyl C-2) and 9.5 (5-ethyl C-2); HRMS found  $MH^+$ , 475.2028.  $C_{23}H_{30}N_4O_5S$  requires  $MH$ , 475.2015.

### ***N*-Benzyl-5-ethyl-4-(ethyl)-1,4-diazepane-5-carboxamide, 119**



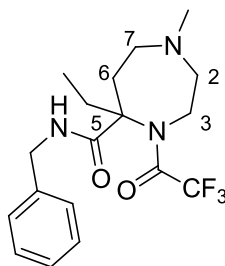
By general procedure O, the protected diazepane **118** (170 mg, 0.358 mmol) gave a crude residue which was purified by basic SCX cartridge to yield the *deprotected* diazepane **119** (70.4 mg, 68%) as a yellow oil,  $R_f = 0.64$  (10:90 MeOH-DCM);  $\nu_{max}/cm^{-1}$  (ATR) 3361 (br), 2967, 2934, 2854, 1657, 1503, 1455 and 700;  $\delta_H$  (500 MHz,  $CDCl_3$ ) 7.87 (1H, t,  $J$  5.4, NH), 7.40-7.34 (2H, m, benzyl 3-H and benzyl 5-H), 7.33-7.30 (3H, m, benzyl 2-H, benzyl 4-H and benzyl 6-H), 4.58 (1H, dd,  $J$  14.6 and 6.7, benzylic- $H_a$ ), 4.35 (1H, dd,  $J$  14.6 and 5.4, benzylic- $H_b$ ), 3.27-3.19 (2H, m, 2- $H_a$  and 3- $H_a$ ), 3.12 (1H, dd,  $J$  14.0 and 7.1, 7- $H_a$ ), 2.96 (1H, dd,  $J$  12.6 and 9.7, 2- $H_b$ ), 2.77-2.68 (2H, m, 7- $H_b$  and 3- $H_b$ ), 2.61-2.52 (2H, m, 4-ethyl 1- $H_a$  and 5-ethyl 1- $H_a$ ), 2.26-2.12 (2H, m, 5-ethyl 1- $H_b$  and 6- $H_a$ ), 2.01 (1H, dq,  $J$  15.3 and 7.8, 4-ethyl 1- $H_b$ ), 1.81 (1H, td,  $J$  14.8 and 7.1, 6- $H_b$ ), 1.09 (3H, app t,  $J$  7.8, 4-ethyl 2- $H_3$ ) and 0.94 (3H, t,  $J$  7.0 5-ethyl 2- $H_3$ );  $\delta_C$  (126 MHz,  $CDCl_3$ ) 176.1 (CO), 138.6 (benzyl C-1), 128.8 (benzyl C-3 and benzyl C-5), 127.8 (benzyl C-2 and benzyl C-6), 127.5 (benzyl C-4), 68.9 (C-5), 52.0 (C-3), 47.9 (C-2), 45.6 (C-7), 43.6 (benzylic-C), 43.6 (4-ethyl C-1), 38.0 (5-ethyl C-1), 27.0 (C-6), 14.5 (4-ethyl C-2) and 9.6 (5-ethyl C-2); HRMS found  $MH^+$ , 290.2247.  $C_{17}H_{27}N_3O$  requires  $MH$ , 290.2232.

## ***N*-Benzyl-5-ethyl-4-(trifluoroacetyl)-1,4-diazepane-5-carboxamide, 120**



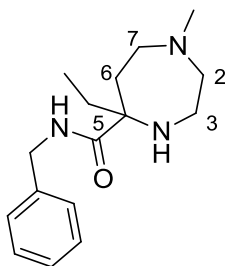
By general procedure K (with an additional 6 eq. TFA), ketone **126** (533 mg, 1.60 mmol) and benzyl isocyanide (0.387 mL, 3.19 mmol) gave a crude residue which was purified by flash chromatography (SiO<sub>2</sub>, 60:40 DCM–EtOAc). Ammonium formate (578 mg, 9.16 mmol) and 20% Pd(OH)<sub>2</sub>/C (128 mg, 10 mol%) was added to a solution of the crude piperazine (820 mg, 1.83 mmol) in EtOH (20 mL, 0.1 M). The resulting mixture was stirred at 70 °C for 4 hr before being cooled to room temperature and filtered through Celite. The filtrate was concentrated *in vacuo* and the residue was diluted with sat. NaHCO<sub>3</sub> (20 mL) and DCM (20 mL). The aqueous layer was extracted with DCM (3 × 20 mL) and the combined organic layers were dried (MgSO<sub>4</sub>) and concentrated *in vacuo*. The residue was purified by flash chromatography (SiO<sub>2</sub>, 40:60 Petrol–EtOAc) to yield the *deprotected piperazine* **120** (230 mg, 40% over two steps) as a yellow oil, *R*<sub>f</sub> = 0.67 (30:70 Petrol–EtOAc);  $\nu_{\text{max}}$ / cm<sup>-1</sup> (ATR) 3340 (br), 2936, 1680, 1455, 1177, 1135 and 698;  $\delta_{\text{H}}$  (501 MHz, DMSO) 8.25 (1H, app q, *J* 4.2, NH), 7.34-7.24 (4H, m, benzyl 2-H, benzyl 3-H, benzyl 5-H and benzyl 6-H), 7.23-7.18 (1H, m, benzyl 4-H), 4.36-4.27 (2H, m, benzylic-H<sub>2</sub>), 3.70-3.55 (1H, m, 3-H<sub>a</sub>), 3.55-3.43 (3H, m, 2-H<sub>a</sub> and 7-H<sub>2</sub>), 2.97 (1H, dt, *J* 14.6 and 3.7, 6-H<sub>a</sub>), 2.84-2.63 (2H, m, 6-H<sub>b</sub> and 3-H<sub>b</sub>), 2.30 (0.5H, dd, *J* 15.2 and 6.2, 2-H<sub>b</sub>), 2.21 (0.5H, dd, *J* 15.3 and 6.6, 2-H<sub>b</sub>), 1.72-1.66 (1H, m, *J* 14.0 and 7.0, NH), 1.60-1.48 (2H, m, ethyl 1-H<sub>2</sub>) and 0.74 (3H, t, *J* 7.5, ethyl 2-H<sub>3</sub>);  $\delta_{\text{C}}$  (126 MHz, DMSO) 174.7 (CO), 174.5 (CO), 139.8 (benzyl C-1), 128.2 (benzyl C-3 and benzyl C-5), 127.24 (benzyl C-2), 127.22 (benzyl C-6), 126.7 (benzyl C-4), 64.3 (C-5), 64.2 (C-5), 49.7 (C-3), 49.4 (C-3), 43.4 (benzylic-C), 42.4 (C-2), 42.2 (C-7), 42.1 (C-7), 37.1 (C-6), 32.6 (ethyl C-1), 32.4 (ethyl C-1) and 8.1 (ethyl C-2), trifluoroacetyl carbons not observed;  $\delta_{\text{F}}$  (282 MHz, DMSO) -67.6 and -67.8; HRMS found MH<sup>+</sup>, 358.1757. C<sub>17</sub>H<sub>22</sub>F<sub>3</sub>N<sub>3</sub>O<sub>2</sub> requires *MH*, 358.1742.

**N-Benzyl-5-ethyl-methyl-4-(trifluoroacetyl)-1,4-diazepane-5-carboxamide, 128**



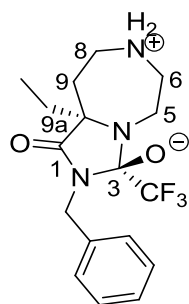
Acetic acid (0.180 mL, 3.08 mmol) was added to a solution of piperazine **120** (274 mg, 0.770 mmol), 37% formaldehyde (86.0  $\mu$ L, 1.16 mmol) and zinc dust (101 mg, 1.54 mmol) in dioxane (3.85 mL, 0.2 M). The resulting mixture was stirred at 30 °C for 6 hr and at room temperature overnight, before being filtered and concentrated *in vacuo*. Sat. NaHCO<sub>3</sub> (5 mL) was added to basify the mixture before the aqueous layer was extracted with DCM (3  $\times$  5 mL). The combined organic phases were washed with water (5 mL), brine (5 mL), dried (MgSO<sub>4</sub>) and concentrated *in vacuo*. The residue was purified by flash chromatography (SiO<sub>2</sub>, 50:50 Petrol–EtOAc) to yield the alkylated *piperazine* **128** (102 mg, 36%) as a yellow oil,  $R_f = 0.67$  (30:70 Petrol–EtOAc);  $\nu_{\max}/\text{cm}^{-1}$  (ATR) 3367, 2970, 2938, 1683, 1507, 1173 and 1139;  $\delta_{\text{H}}$  (501 MHz, MeOD) 7.27-7.17 (4H, m, benzyl 2-H, benzyl 3-H, benzyl 5-H and benzyl 6-H), 7.16-7.10 (1H, m, benzyl 4-H), 4.32 (1H, d,  $J$  14.9, benzylic-H<sub>a</sub>), 4.27 (1H, d,  $J$  14.9, benzylic-H<sub>b</sub>), 3.97-3.86 (1H, m, 3-H<sub>a</sub>), 3.83 (0.5H, dd,  $J$  14.1 and 7.1, 2-H<sub>a</sub>), 3.68 (0.5H, dd,  $J$  15.7 and 5.9, 2-H<sub>a</sub>), 3.44-3.30 (1H, m, 7-H<sub>a</sub>), 3.19-3.13 (1H, m, 6-H<sub>a</sub>), 3.03-2.95 (2H, m, 3-H<sub>b</sub> and 7-H<sub>b</sub>), 2.38-2.35 (2H, m, 2-H<sub>b</sub> and methyl), 2.27 (2H, s, methyl), 1.72-1.63 (1H, m, 6-H<sub>b</sub>), 1.60-1.50 (2H, m, ethyl 1-H<sub>2</sub>) and 0.72 (3H, td,  $J$  7.5 and 2.6, ethyl 2-H<sub>3</sub>);  $\delta_{\text{C}}$  (126 MHz, MeOD) 140.2 (app d,  $J$  4.8, trifluoroacetyl C-1), 129.4 (benzyl C-3 and benzyl C-5), 128.9 (benzyl C-2 and benzyl C-6), 128.2 (benzyl C-4), 118.1 (app d,  $J$  287.0, trifluoroacetyl C-2), 70.4 (C-5) 51.3 (C-3), 50.3 (C-2), 44.2 (benzylic-C), 43.2 (C-7), 34.9 (methyl), 34.6 (methyl), 33.1 (C-6), 32.4 (C-6), 32.3 (ethyl C-1), 31.8 (ethyl C-1) and 9.3 (ethyl C-3), amide CO and benzyl C-1 not observed; HRMS found MH<sup>+</sup>, 372.1913. C<sub>18</sub>H<sub>24</sub>F<sub>3</sub>N<sub>3</sub>O<sub>2</sub> requires MH, 372.1899.

## ***N*-Benzyl-5-ethyl-methyl-1,4-diazepane-5-carboxamide, 129**



By general procedure L (with an additional 14 eq. NaBH<sub>4</sub>), the protected piperazine **128** (21.0 mg, 57.0 μmol) gave the *deprotected piperazine* **129** (12.9 mg, 82%) as a yellow oil which was used without further purification, *R*<sub>f</sub> = 0.77 (30:70 MeOH–DCM); *v*<sub>max</sub>/ cm<sup>-1</sup> (ATR) 3335 (br), 2937, 2808, 1652, 1498, 1454 and 699; δ<sub>H</sub> (500 MHz, CDCl<sub>3</sub>) 7.89 (1H, s, NH), 7.33–7.17 (5H, m, benzyl-H), 4.43–4.34 (2H, m, *J* 14.7 and 5.8, benzylic-H<sub>2</sub>), 3.10 (1H, dd, *J* 14.5 and 8.5, 3-H<sub>a</sub>), 2.97 (1H, dd, *J* 12.5 and 5.5, 2-H<sub>a</sub>), 2.87 (1H, dd, *J* 13.3 and 7.1, 7-H<sub>a</sub>), 2.75–2.62 (2H, m, 2-H<sub>b</sub> and 7-H<sub>b</sub>), 2.58 (1H, dd, *J* 14.5 and 5.5, 3-H<sub>b</sub>), 2.34 (3H, s, methyl), 2.11 (1H, dd, *J* 15.1 and 6.8, 6-H<sub>a</sub>), 1.92–1.78 (2H, m, ethyl 1-H<sub>2</sub>), 1.76–1.64 (1H, m, 6-H<sub>b</sub>) and 0.93 (3H, t, *J* 7.5, ethyl 2-H<sub>3</sub>); δ<sub>C</sub> (126 MHz, CDCl<sub>3</sub>) 176.0 (CO), 138.8 (benzyl C-1), 128.7 (benzyl C-3 and benzyl C-5), 127.8 (benzyl C-2 and benzyl C-6), 127.4 (benzyl C-4), 68.5 (C-5), 54.6 (C-3), 51.0 (C-2), 44.1 (C-7), 43.5 (benzylic-C), 39.7 (methyl), 38.5 (C-6), 27.8 (ethyl C-1) and 9.3 (ethyl C-2); HRMS found MH<sup>+</sup>, 276.2186. C<sub>16</sub>H<sub>25</sub>N<sub>3</sub>O requires *MH*, 276.2076.

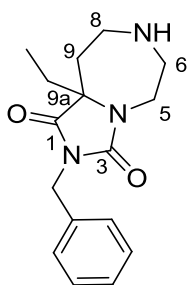
## **2-Benzyl-9a-ethyl-1-oxo-3-(trifluoromethyl)-octahydro-1*H*-imidazolidino[1,5-*d*][1,4]diazepin-7-ium-3-olate, 121**



K<sub>2</sub>CO<sub>3</sub> (271 mg, 1.96 mmol) was added to a stirred solution of the protected piperazine **33** (710 mg, 1.31 mmol) and PhSH (0.200 mL, 1.96 mmol) in MeCN (13.1 mL, 0.1 M), and the mixture was stirred at room temperature overnight. Excess K<sub>2</sub>CO<sub>3</sub> was removed by filtration and the reaction mixture was concentrated *in vacuo*. The residue was purified by flash chromatography (SiO<sub>2</sub>, 10:90 MeOH–DCM) to yield the *zwitterion* **121** (330 mg, 70%) as a colourless solid, m.p. 140–142 °C; *R*<sub>f</sub> = 0.32 (10:90 MeOH–DCM);

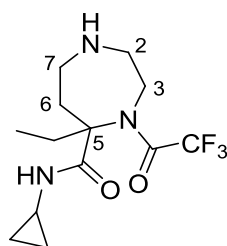
$\nu_{\max}/\text{cm}^{-1}$  (ATR) 3305 (br), 2963, 2936, 2880, 1707, 1453, 1294 and 1164;  $\delta_{\text{H}}$  (500 MHz,  $\text{CDCl}_3$ ) 7.44 (2H, d,  $J$  7.3, benzyl 3-H and benzyl 5-H), 7.35-7.30 (2H, m, benzyl 2-H and benzyl 6-H), 7.28-7.22 (1H, m, benzyl 4-H), 4.70 (1H, d,  $J$  15.4, benzylic- $\text{H}_a$ ), 4.65 (1H, d,  $J$  15.3, benzylic- $\text{H}_b$ ), 3.73-3.62 (1H, m, 5- $\text{H}_a$ ), 3.16 (1H, ddd,  $J$  15.9, 7.3 and 3.4, 6- $\text{H}_a$ ), 2.95-2.85 (3H, m, 6- $\text{H}_b$  and 8- $\text{H}_2$ ), 2.85-2.78 (1H, m, 5- $\text{H}_b$ ), 2.09-1.94 (3H, m, 9- $\text{H}_2$  and NH), 1.78 (1H, dq,  $J$  14.8 and 7.4, ethyl 1- $\text{H}_a$ ), 1.61 (1H, dq,  $J$  14.8 and 7.4, ethyl 1- $\text{H}_b$ ) and 0.91 (3H, t,  $J$  7.4, ethyl 3- $\text{H}_3$ );  $\delta_{\text{C}}$  (126 MHz,  $\text{CDCl}_3$ ) 174.8 (CO), 137.5 (benzyl C-1), 128.5 (benzyl C-3 and benzyl C-5), 128.1 (benzyl C-2 and benzyl C-6), 127.1 (benzyl C-4), 122.6 (app d,  $J$  289.7, C-3), 96.9 (app d,  $J$  33.0, trifluoromethyl), 67.2 (C-9 $_a$ ), 43.8 (benzylic-C), 41.9 (C-5), 40.8 (C-6), 40.1 (C-8), 34.5 (ethyl C-1), 30.5 (C-9) and 8.1 (ethyl C-2);  $\delta_{\text{F}}$  (282 MHz,  $\text{CDCl}_3$ ) -79.8; HRMS found  $\text{MH}^+$ , 358.1732.  $\text{C}_{17}\text{H}_{22}\text{F}_3\text{N}_3\text{O}_2$  requires  $\text{MH}$ , 358.1742.

**2-Benzyl-9a-ethyl-octahydro-1H-imidazolidino[1,5-d][1,4]diazepine-1,3-dione, 122**



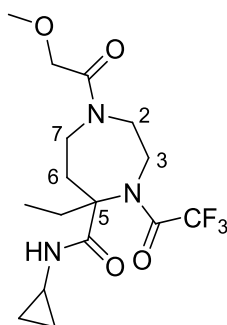
$\text{K}_2\text{CO}_3$  (522 mg, 3.78 mmol) was added to a solution of the zwitterion **121** (270 mg, 0.760 mmol) in EtOH (3.80 mL, 0.2 M) and stirred at 70 °C for 4 hr. The reaction mixture was concentrated *in vacuo*, diluted with water (5 mL) and extracted with EtOAc (3 × 5 mL). The combined organic phases were washed with brine (5 mL), dried ( $\text{MgSO}_4$ ) and concentrated *in vacuo*. The residue was purified by flash chromatography ( $\text{SiO}_2$ , 10:90 MeOH-DCM) to yield the *hydantoin* **122** (89.1 mg, 41%) as a yellow oil,  $R_f$  = 0.24 (10:90 MeOH-DCM);  $\nu_{\max}/\text{cm}^{-1}$  (ATR) 3341 (br), 2967, 2937, 1764, 1703, 1448 and 1350;  $\delta_{\text{H}}$  (501 MHz,  $\text{CDCl}_3$ ) 7.42-7.36 (2H, m, benzyl 3-H and benzyl 5-H), 7.34-7.23 (3H, m, benzyl 2-H, benzyl 4-H and benzyl 6-H), 4.71-4.63 (2H, m, benzylic- $\text{H}_2$ ), 4.10-4.00 (1H, m, 5- $\text{H}_a$ ), 3.00-2.83 (4H, m, 5- $\text{H}_b$ , 6- $\text{H}_2$  and 8- $\text{H}_a$ ), 2.51 (1H, dd,  $J$  15.2 and 6.4, 8- $\text{H}_b$ ), 2.18 (1H, dd,  $J$  14.7 and 10.7, 9- $\text{H}_a$ ), 1.84 (1 H, dq,  $J$  14.6 and 7.4, ethyl 1- $\text{H}_a$ ), 1.74 (1H, ddd,  $J$  14.7, 10.8 and 1.3, 9- $\text{H}_b$ ), 1.69-1.58 (2H, m, ethyl 1- $\text{H}_b$  and NH) and 0.62 (3H, t,  $J$  7.4, ethyl 2- $\text{H}_3$ );  $\delta_{\text{C}}$  (126 MHz,  $\text{CDCl}_3$ ) 175.8 (C-1), 156.6 (C-3), 136.4 (benzyl C-1), 128.6 (benzyl C-4), 128.5 (benzyl C-3 and benzyl C-5), 127.8 (benzyl C-2 and benzyl C-6), 68.5 (C-9 $_a$ ), 48.2 (benzylic-C), 44.9 (C-5), 43.2 (C-6), 42.5 (C-8), 41.5 (ethyl C-1), 29.8 (C-9) and 7.4 (ethyl C-2); HRMS found  $\text{MH}^+$ , 288.1716.  $\text{C}_{16}\text{H}_{21}\text{N}_3\text{O}_2$  requires  $\text{MH}$ , 288.1712.

### ***N*-Cyclopropyl-5-ethyl-4-(trifluoroacetyl)-1,4-diazepane-5-carboxamide, 133**



By general procedure O, the protected diazepane **108** (520 mg, 1.06 mmol) gave a crude residue which was purified by basic SCX cartridge to yield the *deprotected diazepane* **133** (320 mg, 98%) as an orange amorphous solid  $R_f = 0.76$  (20:80 MeOH-DCM);  $\nu_{\max}/\text{cm}^{-1}$  (ATR) 3340 (br), 2968, 2937, 1682, 1512, 1460, 1181 and 1139;  $\delta_{\text{H}}$  (500 MHz,  $\text{CDCl}_3$ ) 7.66 (0.55H, s, NH), 7.53 (0.45H, s, NH), 3.97 (0.45H, dd,  $J$  14.2, 8.0, 3- $\text{H}_a$ ), 3.90 (0.55H, dd,  $J$  13.1, 8.9, 3- $\text{H}_a$ ), 3.84-3.66 (1H, m, 2- $\text{H}_a$ ), 3.64-3.53 (1.55H, m, 7- $\text{H}_a$  and 7- $\text{H}_b$ ), 3.41 (0.45H, dd,  $J$  14.4, 9.2, 7- $\text{H}_b$ ), 3.23-3.15 (0.55H, m, 3- $\text{H}_b$ ), 3.14-3.06 (0.45H, m, 3- $\text{H}_b$ ), 3.04-2.93 (1H, m, 2- $\text{H}_b$ ), 2.82-2.72 (1H, m, cyclopropyl 1-H), 2.55 (0.55H, dd,  $J$  15.3, 7.0, cyclopropyl 2- $\text{H}_a$ ), 2.43 (0.45H, dd,  $J$  15.5, 7.7, cyclopropyl 2- $\text{H}_b$ ), 1.95-1.76 (2H, m, cyclopropyl 2- $\text{H}_b$  and 6- $\text{H}_a$ ), 1.73-1.51 (1H, m, 6- $\text{H}_b$ ), 0.93-0.78 (5H, m, cyclopropyl 3- $\text{H}_2$  and ethyl 2- $\text{H}_3$ ) and 0.58-0.44 (2H, m, ethyl 1- $\text{H}_2$ );  $\delta_{\text{C}}$  (126 MHz,  $\text{CDCl}_3$ ) 156.5 (app d,  $J$  35.0, trifluoroacetyl C-1), 116.6 (q,  $J$  288.0, trifluoroacetyl C-2), 65.3 (C-5), 65.1 (C-5), 43.9 (C-3), 43.18 (C-2), 43.15 (C-2), 42.8 (C-7), 42.5 (C-7), 32.6 (C-6), 31.9 (C-6), 22.6 (cyclopropyl C-1), 22.5 (cyclopropyl C-1), 8.2 (ethyl C-2), 8.2 (ethyl C-2), 6.6 (cyclopropyl C-2), 6.5 (cyclopropyl C-3), 6.48 (ethyl C-1) and 6.47 (ethyl C-1), amide CO not observed;  $\delta_{\text{F}}$  (282 MHz,  $\text{CDCl}_3$ ) -68.6; HRMS found  $\text{MH}^+$ , 308.1613.  $\text{C}_{13}\text{H}_{20}\text{F}_3\text{N}_3\text{O}_2$  requires  $\text{MH}$ , 308.1586.

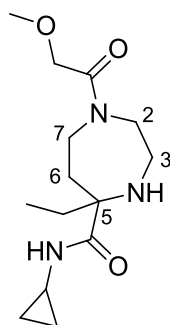
### ***N*-Cyclopropyl-5-ethyl-(methoxyacetyl)-4-(trifluoroacetyl)-1,4-diazepane-5-carboxamide, 134**



By general procedure T, the diazepane **133** (269 mg, 0.880 mmol) and methoxyacetyl chloride (0.160 mL, 1.75 mmol) gave a crude residue which was purified

by flash chromatography (SiO<sub>2</sub>, 10:90 MeOH–DCM) to yield the acylated *diazepane* **134** (258 mg, 78%) as a yellow oil,  $R_f = 0.70$  (10:90 MeOH–DCM);  $\nu_{\max}/\text{cm}^{-1}$  (ATR) 3327 (br), 2948, 1688, 1656, 1461, 1208, 1182 and 1142;  $\delta_{\text{H}}$  (500 MHz, CDCl<sub>3</sub>) 5.81 (1H, d,  $J$  8.3, NH), 4.64 (0.5H, dd,  $J$  13.1 and 4.7, 3-H<sub>a</sub>), 4.46 (0.5H, dd,  $J$  14.4 and 6.9, 3-H<sub>a</sub>), 4.29–4.19 (1H, m, methoxyacetyl 2-H<sub>a</sub>), 4.18–4.07 (1H, m, 2-H<sub>a</sub>), 4.05–3.96 (1H, m, methoxyacetyl 2-H<sub>b</sub>), 3.91–3.79 (1H, m, 7-H<sub>a</sub>), 3.63–3.55 (1H, m, 7-H<sub>b</sub>), 3.50 (1.4H, s, methoxyacetyl 4-H<sub>3</sub>), 3.48 (1.6H, s, methoxyacetyl 4-H<sub>3</sub>), 3.33–3.23 (1H, m, 3-H<sub>b</sub>), 3.22–3.15 (1H, m, 2-H<sub>b</sub>), 2.77–2.68 (1H, m, cyclopropyl 1-H), 2.63–2.49 (1H, m, ethyl 1-H<sub>a</sub>), 2.24 (1H, ddd,  $J$  15.4, 10.1 and 5.2, 6-H<sub>a</sub>), 1.96 (0.5H, dd,  $J$  16.3 and 6.9, ethyl 1-H<sub>b</sub>), 1.88 (0.5H, dd,  $J$  16.2 and 6.7, ethyl 1-H<sub>b</sub>), 1.60–1.53 (1H, m, 6-H<sub>b</sub>), 0.93–0.90 (3H, m, ethyl 2-H<sub>3</sub>), 0.87–0.75 (2H, m, cyclopropyl 2-H<sub>2</sub>), 0.63–0.54 (1H, m, cyclopropyl 3-H<sub>a</sub>), 0.51–0.42 (1H, m, cyclopropyl 3-H<sub>b</sub>);  $\delta_{\text{C}}$  (126 MHz, CDCl<sub>3</sub>) 173.91 (amide CO), 173.87 (amide CO), 170.34 (methoxyacetyl CO), 170.27 (methoxyacetyl CO), 73.4 (C-3), 73.2 (C-3), 67.0 (C-5), 66.8 (C-5), 59.11 (methoxyacetyl C-4), 59.09 (methoxyacetyl C-4), 48.7 (methoxyacetyl C-2), 48.4 (methoxyacetyl C-2), 47.5 (C-2), 42.0 (C-7), 36.6 (ethyl C-1), 36.0 (ethyl C-1), 27.5 (C-6), 27.3 (C-6), 22.9 (cyclopropyl C-1), 8.1 (ethyl C-2), 6.99 (cyclopropyl C-2), 6.96 (cyclopropyl C-2), 6.4 (cyclopropyl C-3), 6.3 (cyclopropyl C-3), trifluoroacetyl carbons not observed;  $\delta_{\text{F}}$  (282 MHz, CDCl<sub>3</sub>) -68.0, -68.1; HRMS found MH<sup>+</sup>, 380.1790. C<sub>16</sub>H<sub>24</sub>F<sub>3</sub>N<sub>3</sub>O<sub>4</sub> requires  $MH$ , 380.1797.

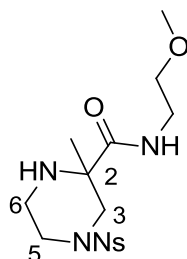
### ***N*-Cyclopropyl-5-ethyl-(methoxyacetyl)-1,4-diazepane-5-carboxamide, 135**



By general procedure L, the protected piperazine **134** (170 mg, 0.450 mmol) gave a crude residue which was purified by basic SCX cartridge to yield the *deprotected piperazine* **135** (29.0 mg, 27%) as a yellow oil in 70% purity,  $\nu_{\max}/\text{cm}^{-1}$  (ATR) 3323 (br), 2931, 1640, 1457 and 1122;  $\delta_{\text{H}}$  (500 MHz, CDCl<sub>3</sub>) 7.87 (1H, s, NH), 4.16 (1H, d,  $J$  4.4, methoxyacetyl 1-H<sub>a</sub>), 3.74 (1H, ddd,  $J$  14.2, 5.6 and 2.9, 3-H<sub>a</sub>), 3.67–3.54 (1H, m, methoxyacetyl 1-H<sub>b</sub>), 3.54–3.47 (1H, m, 2-H<sub>a</sub>), 3.45 (2H, s, methoxyacetyl 4-H<sub>3</sub>), 3.43 (1H, s, methoxyacetyl 4-H<sub>3</sub>), 3.36–3.27 (1H, m, 3-H<sub>b</sub>), 3.13 (1H, ddd,  $J$  14.8, 5.8 and 2.9, 7-H<sub>a</sub>), 2.96 (1H, ddd,  $J$  14.8, 8.5 and 2.9, 7-H<sub>b</sub>), 2.82–2.69 (1H, m, cyclopropyl 1-H), 2.56–2.43 (1H, m, 2-H<sub>b</sub>), 1.94–1.84 (1H, m, ethyl 1-H<sub>a</sub>), 1.83–1.74 (1H, m, 6-H<sub>a</sub>), 1.73–1.61 (1H, m, 6-H<sub>b</sub>),

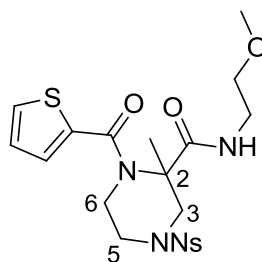
0.89 (2H, t,  $J$  7.5, ethyl 2-H<sub>3</sub>), 0.87-0.78 (4H, m, cyclopropyl 2-H<sub>2</sub>, ethyl 1-H<sub>b</sub> and ethyl 2-H<sub>3</sub>) and 0.56-0.48 (2H, m, cyclopropyl 3-H<sub>2</sub>);  $\delta_c$  (126 MHz, CDCl<sub>3</sub>) 174.4 (5-CO), 169.0 (1-CO), 71.4 (C-3), 65.4 (C-5), 59.2 (methoxyacetyl C-4), 46.5 (methoxyacetyl C-1), 43.6 (C-2), 42.6 (C-7), 36.4 (ethyl C-1), 33.2 (C-6), 22.6 (cyclopropyl C-1), 8.3 (ethyl C-2), 6.5 (cyclopropyl C-2) and 6.4 (cyclopropyl C-3); HRMS found MH<sup>+</sup>, 284.1982. C<sub>14</sub>H<sub>25</sub>N<sub>3</sub>O<sub>3</sub> requires *MH*, 284.1974.

***N*-Methoxyethyl-2-methyl-4-[(2-nitrophenyl)sulfonyl]piperazine-2-carboxamide, 143**



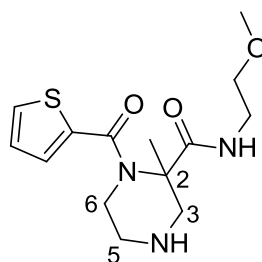
By general procedure L, the protected piperazine **110** (450 mg, 0.930 mmol) gave the *deprotected piperazine* **143** (240 mg, 67%) as a yellow oil which was used without further purification,  $R_f$  = 0.38 (5:95 MeOH-DCM);  $\nu_{max}$ / cm<sup>-1</sup> (ATR) 3335 (br), 2930, 1667, 1543, 1372, 1166, 1125 and 577;  $\delta_H$  (500 MHz, CDCl<sub>3</sub>) 8.12-8.07 (1H, m, nitrophenyl 3-H), 7.77-7.72 (2H, m, nitrophenyl 4-H and nitrophenyl 5-H), 7.72-7.67 (1H, m, nitrophenyl 6-H), 7.39-7.31 (1H, m, NH), 4.09 (1H, d,  $J$  12.8, 3-H<sub>a</sub>), 3.74-3.65 (1H, m, 5-H<sub>a</sub>), 3.45-3.39 (4H, m, 5-H<sub>b</sub>, 6-H<sub>2</sub> and methoxyethyl 2-H<sub>a</sub>), 3.37 (3H, s, methoxyethyl 4-H<sub>3</sub>), 3.14-3.09 (1H, m, methoxyethyl 2-H<sub>b</sub>), 3.09-3.00 (2H, m, methoxyethyl 1-H<sub>2</sub>), 2.89 (1H, d,  $J$  12.8, 3-H<sub>b</sub>) and 1.35 (3H, s, methyl);  $\delta_c$  (126 MHz, CDCl<sub>3</sub>) 171.8 (CO), 148.2 (nitrophenyl C-2), 133.8 (nitrophenyl C-5), 131.8 (nitrophenyl C-1), 131.8 (nitrophenyl C-4), 131.7 (nitrophenyl C-6), 124.3 (nitrophenyl C-3), 70.9 (C-3), 58.8 (methoxyethyl C-4), 58.7 (C-2), 51.4 (C-5), 45.1 (C-6), 41.8 (methoxyethyl C-2), 39.3 (methoxyethyl C-1) and 24.1 (methyl); HRMS found MH<sup>+</sup>, 387.1155. C<sub>15</sub>H<sub>22</sub>N<sub>4</sub>O<sub>6</sub>S requires *MH*, 387.1338.

***N*-Methoxyethyl-2-methyl-4-[(2-nitrobenzene)sulfonyl]-1-(2-thiophenecarbonyl)piperazine-2-carboxamide, **144****



By general procedure T, the piperazine **143** (348 mg, 0.900 mmol) gave a crude residue which was purified by mass-directed preparative HPLC to yield the acylated piperazine **144** (185 mg, 41%) as a yellow oil,  $R_f = 0.54$  (10:90 MeOH-DCM);  $\nu_{\max}/\text{cm}^{-1}$  (ATR) 3352, 2933, 2894, 1669, 1630, 1542, 1361 and 1163;  $\delta_{\text{H}}$  (500 MHz,  $\text{CDCl}_3$ ) 8.12-8.05 (1H, m, nitrophenyl 3-H), 7.80-7.73 (2H, m, nitrophenyl 4-H and nitrophenyl 5-H), 7.73-7.69 (1H, m, nitrophenyl 6-H), 7.54 (1H, dd,  $J$  5.0 and 1.0, thiophene 5-H), 7.45 (1H, dd,  $J$  3.7 and 1.0, thiophene 3-H), 7.10 (1H, dd,  $J$  5.0 and 3.7, thiophene 4-H), 6.68 (1H, t,  $J$  4.9, NH), 4.00 (1H, ddd,  $J$  14.0, 6.6 and 3.7, 5- $\text{H}_a$ ), 3.86 (1H, ddd,  $J$  14.0, 7.8 and 3.6, 5- $\text{H}_b$ ), 3.78 (1H, d,  $J$  13.0, 3- $\text{H}_a$ ), 3.70 (1H, ddd,  $J$  11.1, 6.6 and 3.6, 6- $\text{H}_a$ ), 3.57 (1H, ddd,  $J$  11.1, 7.8 and 3.7, 6- $\text{H}_b$ ), 3.51 (3H, s, methoxyethyl 4- $\text{H}_3$ ), 3.49-3.45 (2H, m, methoxyethyl 1- $\text{H}_2$ ), 3.44-3.41 (1H, m, 3- $\text{H}_b$ ), 3.41-3.30 (2H, m, methoxyethyl 2- $\text{H}_2$ ) and 3.27 (3H, s, methyl);  $\delta_{\text{C}}$  (126 MHz,  $\text{CDCl}_3$ ) 171.1 (2-CO), 166.8 (1-CO), 148.1 (nitrophenyl C-2), 137.2 (nitrophenyl C-1), 134.0 (nitrophenyl C-5), 131.9 (nitrophenyl C-4), 131.8 (thiophene C-1), 131.5 (nitrophenyl C-6), 130.4 (thiophene C-4 and thiophene C-5), 127.3 (thiophene C-3), 124.4 (nitrophenyl C-3), 70.9 (C-5), 63.1 (C-2), 58.7 (methoxyethyl C-4), 52.7 (C-3), 45.6 (C-6), 45.3 (methoxyethyl C-1), 39.5 (methoxyethyl C-2) and 18.9 (methyl); HRMS found  $\text{MH}^+$ , 497.1182.  $\text{C}_{20}\text{H}_{24}\text{N}_4\text{O}_7\text{S}_2$  requires  $\text{MH}$ , 497.1164.

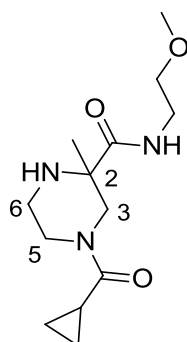
***N*-Methoxyethyl-2-methyl-1-(2-thiophenecarbonyl)piperazine-2-carboxamide, **145****



By general procedure O, the protected piperazine **144** (185 mg, 0.37 mmol) gave a crude residue which was purified by flash chromatography ( $\text{SiO}_2$ , 10:90 MeOH-DCM) to

yield the *deprotected piperazine* **145** (105 mg, 91%) as a yellow oil,  $R_f = 0.43$  (10:90 MeOH–DCM);  $\nu_{\max}/\text{cm}^{-1}$  (ATR) 3318 (br), 2931, 2874, 1625, 1522, 1422 and 1374;  $\delta_{\text{H}}$  (500 MHz,  $\text{CDCl}_3$ ) 7.58 (1H, s, NH), 7.55 (1H, dd,  $J$  5.0 and 1.0, thiophene 5-H), 7.47 (1H, dd,  $J$  3.7 and 1.0, thiophene 3-H), 7.11 (1H, dd,  $J$  5.0 and 3.7, thiophene 4-H), 3.87 (1H, dt,  $J$  14.0 and 3.9, 5- $\text{H}_a$ ), 3.54–3.49 (4H, m, 3- $\text{H}_a$ , 5- $\text{H}_b$  and 6- $\text{H}_2$ ), 3.49–3.45 (1H, m, methoxyethyl 2- $\text{H}_a$ ), 3.35 (3H, s, methoxyethyl 4- $\text{H}_3$ ), 3.34–3.26 (1H, m, methoxyethyl 2- $\text{H}_b$ ), 3.05 (2H, dd,  $J$  6.3 and 4.1, methoxyethyl 1- $\text{H}_2$ ), 2.74 (1H, d,  $J$  13.6, 3- $\text{H}_b$ ) and 1.65 (3H, s, methyl);  $\delta_{\text{C}}$  (126 MHz,  $\text{CDCl}_3$ ) 173.7 (2-CO), 168.3 (1-CO), 138.3 (thiophene C-1), 130.6 (thiophene C-4), 130.5 (thiophene C-5), 127.3 (thiophene C-3), 71.2 (C-5), 62.8 (C-2), 58.8 (methoxyethyl C-4), 54.7 (C-6), 48.1 (C-3), 45.1 (methoxyethyl C-2), 39.2 (methoxyethyl C-1) and 21.3 (methyl); HRMS found  $\text{MH}^+$ , 312.1398.  $\text{C}_{14}\text{H}_{21}\text{N}_3\text{O}_3\text{S}$  requires  $\text{MH}$ , 312.1382.

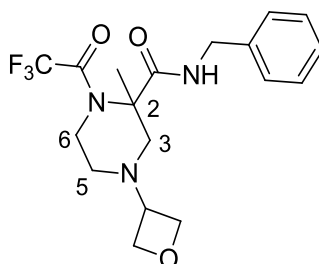
***N*-Methoxyethyl-2-methyl-4-cyclopropanecarbonyl-piperazine-2-carboxamide,  
148**



By general procedure O, the protected piperazine **110** (306 mg, 0.634 mmol) gave a crude residue which was purified by basic SCX cartridge to give the crude deprotected piperazine (162 mg, 0.545 mmol). This was combined with cyclopropanecarbonyl chloride (99.0  $\mu\text{L}$ , 1.09 mmol) and subjected to general procedure T to give the crude acylated piperazine (224 mg, 0.610 mmol) which by general procedure L gave a crude product which was purified by basic SCX cartridge, and later by mass-directed preparative HPLC to yield the *deprotected piperazine* **148** (72.1 mg, 43% over three steps) as a yellow oil,  $R_f = 0.60$  (10:90 MeOH–DCM);  $\nu_{\max}/\text{cm}^{-1}$  (ATR) 3299 (br), 2928, 2874, 1614, 1437, 1121 and 1091;  $\delta_{\text{H}}$  (501 MHz, MeOD) 4.65–4.55 (1H, m, methoxyethyl 2- $\text{H}_a$ ), 4.03 (1H, d,  $J$  9.4, 3- $\text{H}_a$ ), 3.46–3.42 (3H, m, 5- $\text{H}_2$  and methoxyethyl 2- $\text{H}_b$ ), 3.41–3.37 (1H, m, 3- $\text{H}_b$ ), 3.36–3.34 (1H, m, methoxyethyl 1- $\text{H}_a$ ), 3.33 (3H, s, methoxyethyl 4- $\text{H}_3$ ), 2.99 (1H, d,  $J$  13.4, 6- $\text{H}_a$ ), 2.91 (1H, dt,  $J$  13.4 and 3.0, 6- $\text{H}_b$ ), 2.74 (1H, dt,  $J$  10.3 and 2.8, methoxyethyl 1- $\text{H}_b$ ), 2.09–1.99 (1H, m, cyclopropyl 1-H), 1.24 (3H, s, methyl), 0.95–0.88 (1H, m, cyclopropyl 2- $\text{H}_a$ ) and 0.83–0.73 (3H, m, cyclopropyl 2- $\text{H}_b$  and cyclopropyl 3- $\text{H}_2$ );  $\delta_{\text{C}}$  (126 MHz, MeOD) 176.4 (4-CO), 174.6 (2-CO), 71.8 (C-3), 58.9 (methoxyethyl C-4), 53.2 (C-5), 43.7

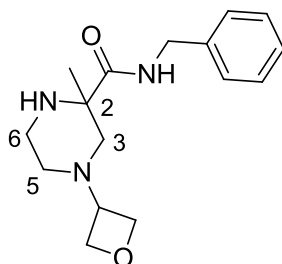
(methoxyethyl C-2), 42.6 (methoxyethyl C-1), 40.1 (C-6), 25.0 (cyclopropyl C-1), 11.8 (methyl), 8.2 (cyclopropyl C-2) and 7.6 (cyclopropyl C-3); HRMS found  $MH^+$ , 270.1843.  $C_{13}H_{23}N_3O_3$  requires  $MH$ , 270.1817.

### ***N*-Benzyl-2-methyl-4-oxetane-1-(trifluoroacetyl)piperazine-2-carboxamide, 137**



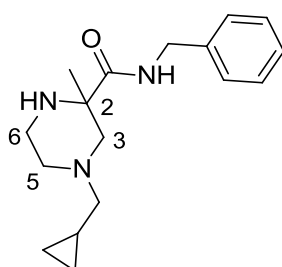
By general procedure O, the protected piperazine **109** (550 mg, 1.07 mmol) gave a crude residue which was purified by flash chromatography ( $SiO_2$ , 10:90 MeOH–DCM). Oxetane-3-one (90.0  $\mu$ L, 1.42 mmol) was added to a solution of the crude deprotected piperazine (389 mg, 1.18 mmol) in THF (2.36 mL, 0.5 M).  $NaBH(OAc)_3$  (500 mg, 2.36 mmol) was slowly added at 0 °C and the solution was warmed to room temperature and stirred overnight. The solvent was removed *in vacuo* and the residue was diluted with water (5 mL) and EtOAc (5 mL). The aqueous layer was extracted with EtOAc (3  $\times$  5 mL) and the combined organic layers were washed with brine (5 mL), dried ( $MgSO_4$ ) and concentrated *in vacuo*. The residue was purified by flash chromatography ( $SiO_2$ , 5:95 MeOH–DCM) to yield the alkylated piperazine **137** (409 mg, 98% over two steps) as a colourless amorphous solid,  $R_f$  = 0.30 (5:95 MeOH–DCM);  $\nu_{max}$ /  $cm^{-1}$  (ATR) 3327 (br), 2949, 2876, 1701, 1669, 1208 and 1146;  $\delta_H$  (500 MHz,  $CDCl_3$ ) 7.42–7.30 (5H, m, benzyl-H), 6.30 (1H, t,  $J$  5.5, NH), 4.67 (2H, td,  $J$  6.6 and 4.5, oxetanyl 2- $H_a$  and oxetanyl 4- $H_a$ ), 4.57–4.51 (2H, m, oxetanyl 2- $H_b$  and oxetanyl 4- $H_b$ ), 4.50 (2H, d,  $J$  5.5, benzylic- $H_2$ ), 3.88 (1H, dt,  $J$  13.1 and 4.0, 6- $H_a$ ), 3.63–3.54 (2H, m, 3- $H_a$  and 6- $H_b$ ), 2.67 (1H, d,  $J$  11.9, 3- $H_b$ ), 2.64 (1H, td,  $J$  4.5 and 1.5, oxetanyl 1-H), 2.59 (1H, dd,  $J$  11.1 and 4.0, 5- $H_a$ ), 2.52 (1H, dd,  $J$  11.1 and 1.4, 5- $H_b$ ) and 1.68 (3H, s, methyl);  $\delta_C$  (126 MHz,  $CDCl_3$ ) 170.6 (CO), 138.0 (benzyl C-1), 128.8 (benzyl C-3 and benzyl C-5), 127.9 (benzyl C-2 and benzyl C-6), 127.7 (benzyl C-4), 75.0 (oxetanyl C-4), 74.8 (oxetanyl C-2), 63.3 (C-6), 58.3 (oxetanyl 1-H), 57.8 (C-3), 48.1 (benzylic-C), 44.1 (C-5) and 17.9 (methyl), trifluoroacetyl carbons not observed;  $\delta_F$  (282 MHz,  $CDCl_3$ ) -69.2; HRMS found  $MH^+$ , 386.1711.  $C_{18}H_{22}F_3N_3O_3$  requires  $MH$ , 386.1691.

### ***N*-Benzyl-2-methyl-4-oxetanepiperazine-2-carboxamide, 138**



By general procedure L, the protected piperazine **137** (409 mg, 1.06 mmol) gave the deprotected piperazine **138** (238 mg, 78%) as a yellow oil which was used without further purification,  $R_f = 0.64$  (10:90 MeOH–DCM);  $\nu_{\max}/\text{cm}^{-1}$  (ATR) 3308 (br), 2946, 2872, 1655, 1517, 973 and 698;  $\delta_{\text{H}}$  (500 MHz,  $\text{CDCl}_3$ ) 7.96 (1H, t,  $J$  5.6, NH), 7.40–7.33 (4H, m, benzyl 2-H, benzyl 3-H, benzyl 5-H and benzyl 6-H), 7.33–7.30 (1H, m, benzyl 4-H), 4.67 (2H, dd,  $J$  6.6 and 1.6, oxetanyl 2- $\text{H}_a$  and oxetanyl 4- $\text{H}_a$ ), 4.63 (2H, app dd,  $J$  7.7 and 6.6, oxetanyl 2- $\text{H}_b$  and oxetanyl 4- $\text{H}_b$ ), 4.57 (1H, dd,  $J$  14.8 and 5.6, benzylic- $\text{H}_a$ ), 4.47 (1H, dd,  $J$  14.8 and 5.6, benzylic- $\text{H}_b$ ), 3.52–3.43 (1H, m, oxetanyl 1-H), 3.25 (1H, dd,  $J$  11.1 and 1.2, 3- $\text{H}_a$ ), 2.96–2.84 (2H, m, 5- $\text{H}_2$ ), 2.55 (1H, ddd,  $J$  10.9, 4.2 and 2.8, 6- $\text{H}_a$ ), 1.90 (1H, td,  $J$  10.9 and 3.5, 6- $\text{H}_b$ ), 1.74 (1H, d,  $J$  11.1, 3- $\text{H}_b$ ) and 1.28 (3H, s, methyl);  $\delta_{\text{C}}$  (126 MHz,  $\text{CDCl}_3$ ) 174.4 (CO), 138.7 (benzyl C-1), 128.7 (benzyl C-3 and benzyl C-5), 127.7 (benzyl C-2 and benzyl C-6), 127.3 (benzyl C-4), 75.4 (oxetanyl C-2), 75.2 (oxetanyl C-4), 59.0 (oxetanyl C-1), 57.8 (C-2), 57.2 (C-5), 50.1 (C-3), 43.4 (benzylic-C), 42.3 (C-6) and 25.6 (methyl); HRMS found  $\text{MH}^+$ , 290.1898.  $\text{C}_{16}\text{H}_{23}\text{N}_3\text{O}_2$  requires  $\text{MH}$ , 290.1868.

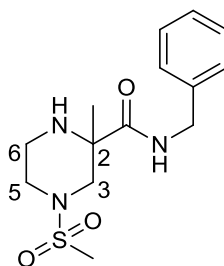
### ***N*-Benzyl-2-methyl-4-(cyclopropylmethyl)piperazine-2-carboxamide, 140**



By general procedure O, the protected piperazine **109** (70.1 mg, 0.136 mmol) gave a crude residue which was purified by flash chromatography ( $\text{SiO}_2$ , 10:90 MeOH–DCM) to give the crude deprotected piperazine (49.5 mg, 0.150 mmol). This was combined with cyclopropane carboxaldehyde (0.450 mL, 0.600 mmol) which by general procedure M, gave the crude alkylated piperazine (50.2 mg, 0.130 mmol). This was then subjected to general procedure L (with an additional 21 eq.  $\text{NaBH}_4$ ) to give a crude residue which was purified by mass-directed preparative HPLC to yield the deprotected piperazine

**140** (9.60 mg, 24% over three steps) as a yellow oil,  $R_f = 0.49$  (10:90 MeOH–DCM);  $\nu_{\max}/\text{cm}^{-1}$  (ATR) 3285 (br), 2926, 2785, 1654, 1521, 1454 and 698;  $\delta_{\text{H}}$  (500 MHz,  $\text{CDCl}_3$ ) 8.12 (1H, t,  $J$  5.2, NH), 7.36–7.27 (5H, m, benzyl-H), 6.07 (1H, s, NH), 4.50 (1H, dd,  $J$  14.8 and 5.2, benzylic- $\text{H}_a$ ), 4.45 (1H, dd,  $J$  14.8 and 5.2, benzylic- $\text{H}_b$ ), 3.60 (1H, d,  $J$  12.2, 3- $\text{H}_a$ ), 3.09–2.95 (3H, m, 5- $\text{H}_a$  and 6- $\text{H}_2$ ), 2.53–2.41 (3H, m, 5- $\text{H}_b$  and 4-methyl), 2.38 (1H, d,  $J$  12.2, 3- $\text{H}_b$ ), 1.38 (3H, s, 2-methyl), 1.02–0.79 (1H, m, cyclopropyl 1-H), 0.68–0.40 (2H, m, cyclopropyl 2- $\text{H}_2$ ) and 0.35–0.02 (2H, m, cyclopropyl 3- $\text{H}_2$ );  $\delta_{\text{C}}$  (126 MHz,  $\text{CDCl}_3$ ) 173.2 (CO), 138.2 (benzyl C-1), 128.7 (benzyl C-3 and benzyl C-5), 127.8 (benzyl C-2 and benzyl C-6), 127.5 (benzyl C-4), 62.5 (C-3), 57.9 (C-2), 57.7 (C-6), 51.6 (C-5), 43.7 (benzylic-C), 40.8 (4-methyl), 25.0 (2-methyl), 7.1 (cyclopropyl C-1), 4.4 (cyclopropyl C-2) and 3.8 (cyclopropyl C-3); HRMS found  $\text{MH}^+$ , 288.2093.  $\text{C}_{17}\text{H}_{25}\text{N}_3\text{O}$  requires  $\text{MH}$ , 288.2076.

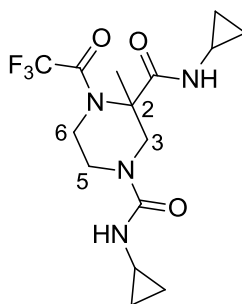
### **N-Benzyl-4-methanesulfonyl-2-methylpiperazine-2-carboxamide, 142**



By general procedure O, the protected piperazine **109** (1.53 g, 2.97 mmol) gave the crude deprotected piperazine which was dissolved in DCM (30 mL, 0.1 M) and methanesulfonyl chloride (0.330 mL, 4.33 mmol) was added at 0 °C. The reaction was warmed to room temperature and stirred overnight before more methanesulfonyl chloride (0.990 mL, 13.0 mmol) and DMAP (35.0 mg, 0.288 mmol) was added. Water (30 mL) was added and the aqueous layer was extracted with DCM (3 × 30 mL). The combined organic phases were washed with brine (30 mL), dried ( $\text{MgSO}_4$ ) and concentrated *in vacuo* to give a residue which was purified by flash chromatography ( $\text{SiO}_2$ , 80:20  $\text{Et}_2\text{O}$ –DCM) to yield the crude decorated piperazine. By general procedure L, the crude decorated piperazine gave the *deprotected piperazine 142* (169 mg, 18% over three steps) as a yellow oil,  $R_f = 0.41$  (20:20:60 MeOH–Petrol–EtOAc);  $\nu_{\max}/\text{cm}^{-1}$  (ATR) 3329 (br), 2927, 1664, 1518, 1324 and 1153;  $\delta_{\text{H}}$  (500 MHz,  $\text{CDCl}_3$ ) 7.48 (1H, t,  $J$  6.4, NH), 7.41–7.34 (2H, m, benzyl 3-H and benzyl 5-H), 7.33–7.26 (3H, m, benzyl 2-H, benzyl 4-H and benzyl 6-H), 4.51 (1H, dd,  $J$  14.8 and 6.4, benzylic- $\text{H}_a$ ), 4.46 (1H, dd,  $J$  14.8 and 6.4, benzylic- $\text{H}_b$ ), 4.19 (1H, dd,  $J$  12.2 and 1.5, 3- $\text{H}_a$ ), 3.64–3.54 (1H, m, 5- $\text{H}_a$ ), 2.97 (1H, dt,  $J$  13.3 and 2.8, 5- $\text{H}_b$ ), 2.89 (3H, s,  $\text{SO}_2$ -methyl), 2.87–2.80 (1H, m, 6- $\text{H}_a$ ), 2.75 (1H, td,  $J$  11.2 and 2.8, 6- $\text{H}_b$ ), 2.61 (1H, d,  $J$  12.2, 3- $\text{H}_b$ ) and 1.33 (3H, s, 2-methyl);  $\delta_{\text{C}}$  (126 MHz,  $\text{CDCl}_3$ ) 173.2 (CO), 138.3

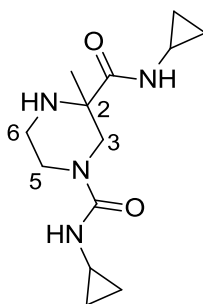
(benzyl C-1), 128.7 (benzyl C-3 and benzyl C-5), 127.7 (benzyl C-2 and benzyl C-6), 127.5 (benzyl C-4), 58.3 (C-2), 52.1 (C-3), 45.1 (C-5), 43.6 (benzylic-C), 42.3 (C-6), 37.4 (SO<sub>2</sub>-methyl) and 25.1 (2-methyl); HRMS found MH<sup>+</sup>, 312.1417. C<sub>14</sub>H<sub>21</sub>N<sub>3</sub>O<sub>3</sub>S requires MH, 312.1382.

**N2-Cyclopropyl-N4-cyclopropyl-(2-methyl)-1-(trifluoroacetyl)piperazine-1,4-dicarboxamide, 150**



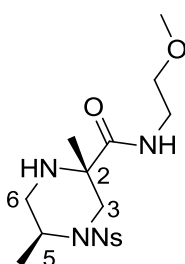
By general procedure O, the protected piperazine **111** (340 mg, 0.73 mmol) gave a crude residue which was purified by flash chromatography (SiO<sub>2</sub>, 10:90 MeOH–DCM) to give the crude deprotected piperazine (129 mg, 0.460 mmol). This was combined with cyclopropyl isocyanate (57.0 mg, 0.690 mmol) and subjected to general procedure Q (excluding addition of Et<sub>3</sub>N) to give a crude residue which was purified by flash chromatography (SiO<sub>2</sub>, 5:95 MeOH–DCM) to yield the *urea* **150** (42.4 mg, 16% over two steps) as a yellow oil, *R*<sub>f</sub> = 0.67 (5:95 MeOH–DCM); *v*<sub>max</sub>/ cm<sup>-1</sup> (ATR) 2978, 1744, 1696, 1544, 1367, 1347 and 1180; *δ*<sub>H</sub> (500 MHz, MeOD) 4.08-3.99 (1H, m, 3-H<sub>a</sub>), 3.97-3.87 (2H, m, 5-H<sub>a</sub> and 6-H<sub>a</sub>), 3.69 (1H, d, *J* 14.3, 3-H<sub>b</sub>), 3.62 (1H, ddd, *J* 12.6, 8.3 and 4.4, 5-H<sub>b</sub>), 3.49 (1H, ddd, *J* 10.9, 6.4 and 4.2, 6-H<sub>b</sub>), 2.65-2.49 (2H, m, 2-cyclopropyl 1-H and 4-cyclopropyl 1-H), 1.59 (3H, s, methyl), 0.75-0.67 (4H, m, 2-cyclopropyl 2-H<sub>2</sub> and 4-cyclopropyl 2-H<sub>2</sub>), 0.61-0.55 (2H, m, 2-cyclopropyl 3-H<sub>2</sub>) and 0.53-0.49 (2H, m, 4-cyclopropyl 3-H<sub>2</sub>); *δ*<sub>C</sub> (126 MHz, MeOD) 173.9 (amide CO), 160.7 (urea CO), 157.3 (q, *J* 37.2, trifluoroacetyl C-1), 117.4 (app d, *J* 287.3, trifluoroacetyl C-2), 66.8 (C-2), 48.0 (C-3), 44.1 (C-5), 41.6 (q, *J* 4.0, C-6), 24.1 (2-cyclopropyl C-1), 23.7 (4-cyclopropyl C-1), 18.7 (methyl), 6.9 (2-cyclopropyl C-2), 6.8 (4-cyclopropyl C-2), 6.5 (2-cyclopropyl C-3) and 6.4 (4-cyclopropyl C-3).

## **N2-Cyclopropyl-N4-cyclopropyl-(2-methyl)-piperazine-1,4-dicarboxamide, 151**



By general procedure L, the protected piperazine **150** (42.4 mg, 0.120 mmol) gave a crude residue which was purified by basic SCX cartridge to yield the *deprotected piperazine* **151** (19.5 mg, 61%) as a yellow oil;  $R_f = 0.34$  (10:90 MeOH-DCM);  $\nu_{\max}/\text{cm}^{-1}$  (ATR) 3307 (br), 2928, 2855, 1645, 1529, 1455 and 1272;  $\delta_{\text{H}}$  (500 MHz, MeOD) 4.89 (2H, s, NH), 4.29-4.17 (1H, m, 3-H<sub>a</sub>), 3.85-3.75 (1H, m, 3-H<sub>b</sub>), 2.88-2.78 (2H, m, 5-H<sub>2</sub>), 2.76-2.66 (2H, m, 6-H<sub>2</sub>), 2.66-2.60 (1H, m, 2-cyclopropyl 1-H), 2.60-2.53 (1H, m, 4-cyclopropyl 1-H), 1.20 (3H, d,  $J$  4.7, methyl), 0.82-0.74 (2H, m, 2-cyclopropyl 2-H<sub>2</sub>), 0.73-0.65 (2H, m, 4-cyclopropyl 2-H<sub>2</sub>) and 0.61-0.44 (4H, m, 2-cyclopropyl 3-H<sub>2</sub> and 4-cyclopropyl 3-H<sub>2</sub>);  $\delta_{\text{C}}$  (126 MHz, MeOD) 178.5 (amide CO), 160.9 (urea CO), 59.5 (C-2), 51.5 (C-3), 44.7 (C-5), 43.0 (C-6), 24.7 (2-cyclopropyl C-1), 24.1 (4-cyclopropyl C-1), 23.4 (methyl), 7.1 (2-cyclopropyl C-2 and 2-cyclopropyl C-3), 6.6 (4-cyclopropyl C-2) and 6.4 (4-cyclopropyl C-3); HRMS found  $\text{MH}^+$ , 267.1823.  $\text{C}_{13}\text{H}_{22}\text{N}_4\text{O}_2$  requires  $\text{MH}$ , 267.1821.

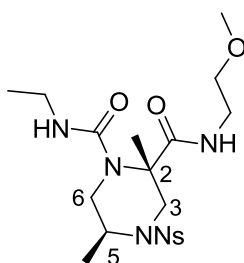
## **N-Methoxyethyl-(2S,5S)-2,5-(dimethyl)-4-[(2-nitrobenzene)sulfonyl]piperazine-2-carboxamide, 157**



By general procedure L, the protected piperazine **113** (590 mg, 1.19 mmol) gave a crude residue which was purified by flash chromatography ( $\text{SiO}_2$ , 10:90 Petrol-EtOAc) to yield the *deprotected piperazine* **157** (220 mg, 46%) as a yellow oil,  $R_f = 0.70$  (10:90 MeOH-DCM);  $\nu_{\max}/\text{cm}^{-1}$  (ATR) 3351 (br), 2975, 2931, 1665, 1540, 1348, 1156 and 577;  $[\alpha]_{\text{D}}^{27} -6.7$  ( $c = 0.063$ ,  $\text{CHCl}_3$ );  $\delta_{\text{H}}$  (500 MHz,  $\text{CDCl}_3$ ) 8.25-8.18 (1H, m, nitrophenyl 3-H), 7.81-7.67 (3H, m, nitrophenyl 4-H, nitrophenyl 5-H and nitrophenyl 6-H), 7.46 (1H, t,  $J$  5.8, NH), 4.12-4.04 (2H, m, methoxyethyl 1-H<sub>2</sub>), 3.39-3.35 (1H, m, 5-H), 3.34 (3H, s,

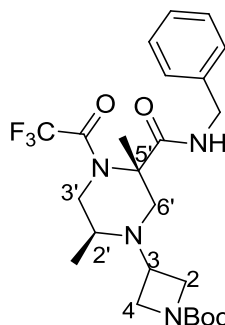
methoxyethyl 4-H<sub>3</sub>), 3.33-3.27 (2H, m, methoxyethyl 2-H<sub>2</sub>), 3.26-3.21 (1H, m, 3-H<sub>a</sub>), 3.19 (1H, dd, *J* 14.3 and 4.2, 6-H<sub>a</sub>), 2.85 (1H, d, *J* 13.1, 3-H<sub>b</sub>), 2.69 (1H, dd, *J* 14.3 and 1.1, 6-H<sub>b</sub>), 1.31 (3H, d, *J* 6.6, 5-methyl) and 1.20 (3H, s, 2-methyl);  $\delta_c$  (126 MHz, CDCl<sub>3</sub>) 172.3 (CO), 133.4 (nitrophenyl C-5), 133.3 (nitrophenyl C-1), 132.2 (nitrophenyl C-4), 131.8 (nitrophenyl C-6), 124.3 (nitrophenyl C-3), 71.1 (methoxyethyl C-1), 58.7 (C-5), 57.6 (C-2), 46.68 (C-3), 46.67 (methoxyethyl C-2), 45.0 (methoxyethyl C-4), 39.0 (C-6), 25.9 (5-methyl) and 14.8 (2-methyl), nitrophenyl C-2 not observed; HRMS found MH<sup>+</sup>, 401.1514. C<sub>16</sub>H<sub>24</sub>N<sub>4</sub>O<sub>6</sub>S requires *MH*, 401.1495.

**(2*S*, 5*S*)-*N*1-Ethyl-*N*2-(2-methoxyethyl)-(2,5-dimethyl)-4[(2-nitrobenzene) sulfonyl]piperazine-1,2-dicarboxamide, **158****



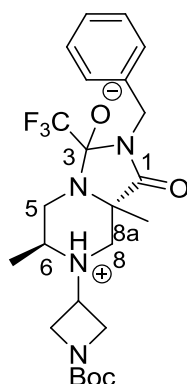
By general procedure Q (with additional 1.5 eq. isocyanate), ethyl isocyanate (60.0  $\mu$ L, 0.820 mmol) and piperazine **157** (110 mg, 0.270 mmol) gave a crude residue which was purified by flash chromatography (SiO<sub>2</sub>, 100% EtOAc) to yield the *urea* **158** (89.0 mg, 70%) as a yellow oil, *R<sub>f</sub>* = 0.37 (10:90 MeOH-DCM);  $\nu_{\max}$ /cm<sup>-1</sup> (ATR) 3342 (br), 2973, 2931, 1653, 1539, 1352, 1157, and 576;  $[\alpha]_D^{23}$  104 (*c* = 0.14, CHCl<sub>3</sub>);  $\delta_H$  (500 MHz, CDCl<sub>3</sub>) 8.10-8.04 (1H, m, nitrophenyl 3-H), 7.68-7.60 (3H, m, nitrophenyl 4-H, nitrophenyl 5-H and nitrophenyl 6-H), 7.11 (1H, t, *J* 5.8, amide NH), 4.75 (1H, t, *J* 4.7, urea NH), 4.29-4.19 (1H, m, 5-H), 3.97 (1H, dd, *J* 14.2 and 5.6, 6-H<sub>a</sub>), 3.90 (1H, d, *J* 14.5, 3-H<sub>a</sub>), 3.49 (1H, dt, *J* 19.5 and 5.8, methoxyethyl 1-H<sub>a</sub>), 3.39 (2H, t, *J* 5.8, methoxyethyl 2-H<sub>2</sub>), 3.26 (3H, s, methoxyethyl 4-H<sub>3</sub>), 3.20-3.11 (4H, m, 3-H<sub>b</sub>, methoxyethyl 1-H<sub>b</sub> and ethyl 1-H<sub>2</sub>), 2.84 (1H, dd, *J* 14.2 and 8.6, 6-H<sub>b</sub>), 1.41 (3H, s, 2-methyl), 1.05 (3H, t, *J* 7.2, ethyl 2-H<sub>3</sub>) and 0.96 (3H, d, *J* 6.3, 5-methyl);  $\delta_c$  (126 MHz, CDCl<sub>3</sub>) 172.2 (amide CO), 158.9 (urea CO), 135.0 (nitrophenyl C-1), 133.7 (nitrophenyl C-5), 132.1 (nitrophenyl C-4), 131.4 (nitrophenyl C-6), 124.6 (nitrophenyl C-3), 70.5 (C-3), 63.4 (C-2), 58.6 (C-5), 51.3 (methoxyethyl C-4), 50.0 (methoxyethyl C-1), 46.3 (methoxyethyl C-2), 39.4 (ethyl C-1), 35.9 (C-6), 19.1 (2-methyl), 16.5 (ethyl C-2) and 15.2 (5-methyl), nitrophenyl C-2 not observed; HRMS found MH<sup>+</sup>, 472.1888. C<sub>19</sub>H<sub>29</sub>N<sub>5</sub>O<sub>7</sub>S requires *MH*, 472.1866.

***tert*-Butyl 3-[(2*S*, 5*S*)-5-(benzylcarbamoyl)-2,5-dimethyl-4-(trifluoroacetyl)piperazine-1-yl]azetidine-1-carboxylate, **153****



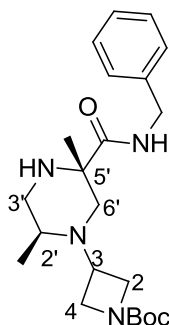
By general procedure O, the protected piperazine **112** (770 mg, 1.46 mmol) gave a residue which was purified by flash chromatography (SiO<sub>2</sub>, 5:95 to 10:90 MeOH–DCM) to yield the crude product. The crude deprotected piperazine was combined with Boc-azetidinone (1.00 g, 5.84 mmol) and by general procedure M, gave a crude residue which was purified by flash chromatography (SiO<sub>2</sub>, 50:50 Petrol–EtOAc) to give the *decorated piperazine* **153** (90.0 mg, 12% over two steps) as a yellow oil, *R*<sub>f</sub> = 0.24 (40:60 Petrol–EtOAc);  $\nu_{\max}$ /cm<sup>-1</sup> (ATR) 3347 (br), 2976, 1695, 1412, 1392 and 1143;  $[\alpha]_{\text{D}}^{25}$  39 (c = 0.77, CHCl<sub>3</sub>);  $\delta_{\text{H}}$  (500 MHz, CDCl<sub>3</sub>) 7.39–7.33 (2H, m, benzyl 3-H and benzyl 5-H), 7.33–7.27 (3H, m, benzyl 2-H, benzyl 4-H and benzyl 6-H), 6.54 (1H, t, *J* 5.2, NH), 4.60 (1H, dd, *J* 14.4 and 5.2, benzylic-H<sub>a</sub>), 4.35 (1H, dd, *J* 14.4 and 5.2, benzylic-H<sub>b</sub>), 4.21–4.10 (1H, m, 2-H<sub>a</sub>), 4.00–3.93 (1H, m, 2-H<sub>b</sub>), 3.88 (1H, dd, *J* 13.0 and 3.9, piperazine 3-H<sub>a</sub>), 3.83 (1H, dd, *J* 9.2 and 4.3, 4-H<sub>a</sub>), 3.75 (1H, dd, *J* 9.2 and 5.6, 4-H<sub>b</sub>), 3.71 (1H, dd, *J* 8.6 and 5.7, piperazine 3-H<sub>b</sub>), 3.60–3.54 (1H, m, 3-H), 3.24–3.11 (1H, m, piperazine 2-H), 2.81–2.73 (2H, m, piperazine 6-H<sub>2</sub>), 1.61 (3H, s, piperazine 5-methyl), 1.47 (9H, s, Boc) and 1.01 (3H, d, *J* 5.9, piperazine 2-methyl);  $\delta_{\text{C}}$  (101 MHz, CDCl<sub>3</sub>) 170.7 (Boc), 156.0 (amide CO), 138.0 (benzyl C-1), 129.0 (benzyl C-3 and benzyl C-5), 128.0 (benzyl C-2 and benzyl C-6), 128.0 (benzyl C-4), 79.9 (Boc), 64.0 (piperazine C-5), 60.4 (azetidine C-2), 53.4 (azetidine C-4), 52.7 (piperazine C-2), 51.0 (piperazine C-6), 49.7 (C-3), 46.9 (piperazine C-3), 43.9 (benzylic-C), 28.4 (Boc), 17.1 (piperazine 5-methyl) and 14.2 (piperazine 2-methyl), trifluoroacetyl carbons not observed; HRMS found MH<sup>+</sup>, 499.2558. C<sub>24</sub>H<sub>33</sub>F<sub>3</sub>N<sub>4</sub>O<sub>4</sub> requires *MH*, 499.2532.

**(6*S*, 8*aS*)-2-Benzyl-7-{1-[(*tert*-butoxy)carbonyl]azetidino-3-yl}-6,8*a*-dimethyl-1-oxo-3-(trifluoromethyl)-octahydroimidazolidino[1,5-*a*]piperazin-7-ium-3-olate, 156**



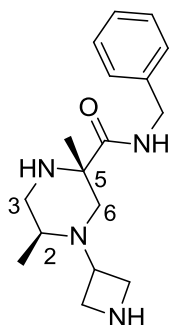
By general procedure O, the protected piperazine **112** (770 mg, 1.46 mmol) gave a residue which was purified by flash chromatography (SiO<sub>2</sub>, 5:95 to 10:90 MeOH–DCM) to yield the crude product. The crude deprotected piperazine was combined with Boc-azetidino (1.00 g, 5.84 mmol) and by general procedure M, gave a crude residue which was purified by flash chromatography (SiO<sub>2</sub>, 50:50 Petrol–EtOAc) to give the *piperaziniumolate* **156** (450 mg, 62% over two steps) as a yellow oil, *R*<sub>f</sub> = 0.24 (40:60 Petrol–EtOAc);  $\nu_{\text{max}}$ / cm<sup>-1</sup> (ATR) 3217, 2978, 1699, 1412, 1366 and 1163;  $[\alpha]_{\text{D}}^{25}$  41 (*c* = 0.45, CHCl<sub>3</sub>);  $\delta_{\text{H}}$  (500 MHz, CDCl<sub>3</sub>) 7.38 (2H, d, *J* 7.3, benzyl 3-H and benzyl 5-H), 7.33 (2H, t, *J* 7.3, benzyl 2-H and benzyl 6-H), 7.29-7.25 (1H, m, benzyl 4-H), 4.85 (1H, d, *J* 15.2, benzylic-H<sub>a</sub>), 4.44 (1H, d, *J* 15.2, benzylic-H<sub>b</sub>), 3.96-3.91 (1H, m, 5-H<sub>a</sub>), 3.85 (1H, t, *J* 7.4, azetidine 2-H<sub>a</sub>), 3.60-3.52 (3H, m, azetidine 2-H<sub>b</sub> and 4-H<sub>2</sub>), 3.45 (1H, dt, *J* 13.1 and 7.4, azetidine 3-H), 3.18 (1H, dd, *J* 14.3 and 5.3, 6-H), 2.67 (1H, d, *J* 12.7, 8-H<sub>a</sub>), 2.56 (1H, dd, *J* 15.6 and 8.3, 5-H<sub>b</sub>), 2.34 (1H, d, *J* 12.7, 8-H<sub>b</sub>), 1.48 (9H, s, Boc), 1.34 (3H, s, 8<sub>a</sub>-methyl) and 0.86 (3H, d, *J* 5.3, 6-methyl);  $\delta_{\text{C}}$  (126 MHz, CDCl<sub>3</sub>) 175.9 (Boc), 155.8 (C-1), 137.0 (benzyl C-1), 128.5 (benzyl C-3 and benzyl C-5), 128.3 (benzyl C-2 and benzyl C-6), 127.7 (benzyl C-4), 97.5 (C-4), 79.8 (Boc), 62.6 (C-8<sub>a</sub>), 51.3 (C-6), 49.0 (azetidine C-3), 47.6 (C-8), 45.29 (C-5), 45.28 (azetidine C-2 and azetidine C-4), 43.8 (benzylic-C), 28.4 (Boc), 21.0 (8<sub>a</sub>-methyl) and 11.5 (6-methyl); HRMS found MH<sup>+</sup>, 499.2545. C<sub>24</sub>H<sub>33</sub>F<sub>3</sub>N<sub>4</sub>O<sub>4</sub> requires *MH*, 499.2532.

***tert*-Butyl 3-[(2*S*, 5*S*)-5-(benzylcarbamoyl)-2,5-dimethylpiperazine-1-yl]azetidine-1-carboxylate, **154****



By general procedure L, the piperaziniumolate **156** (450 mg, 0.900 mmol) gave the *deprotected piperazine* **154** (362 mg, 100%) as a yellow oil,  $R_f = 0.28$  (10:90 MeOH-DCM);  $\nu_{\max}/\text{cm}^{-1}$  (ATR) 2984, 1735, 1372, 1236, 1044, 915 and 727;  $[\alpha]_D^{25}$  105 ( $c = 0.37$ ,  $\text{CHCl}_3$ );  $\delta_H$  (501 MHz,  $\text{CDCl}_3$ ) 7.77 (1H, t,  $J$  5.7, NH), 7.36-7.31 (2H, m benzyl 3-H and benzyl 5-H), 7.31-7.24 (3H, m, benzyl 2-H, benzyl 4-H and benzyl 6-H), 4.52 (1H, dd,  $J$  14.8 and 5.7, benzylic- $H_a$ ), 4.43 (1H, dd,  $J$  14.8 and 5.7, benzylic- $H_b$ ), 3.91-3.79 (4H, m, 2- $H_2$  and 4- $H_2$ ), 3.41-3.32 (1H, m, 3-H), 3.07-2.97 (2H, m, piperazine 3- $H_a$  and piperazine 6- $H_a$ ), 2.71-2.63 (1H, m, piperazine 2-H), 2.58 (1H, dd,  $J$  13.2 and 3.0, piperazine 3- $H_b$ ), 2.28 (1H, d,  $J$  11.6, piperazine 6- $H_b$ ), 1.53 (1H, br s, NH), 1.44 (9H, s, Boc), 1.28 (3H, s, piperazine 5-methyl) and 0.94 (3H, d,  $J$  6.7, piperazine 2-methyl);  $\delta_C$  (126 MHz,  $\text{CDCl}_3$ ) 174.5 (Boc), 156.3 (amide CO), 138.8 (benzyl C-1), 128.6 (benzyl C-3 and benzyl C-5), 127.6 (benzyl C-2 and benzyl C-6), 127.3 (benzyl C-4), 79.2 (Boc), 57.8 (piperazine C-5), 56.0 (C-2 and C-4), 53.9 (C-3), 51.0 (piperazine C-2), 48.9 (piperazine C-6), 48.1 ((piperazine C-3), 43.4 (benzylic-C), 28.4 (Boc), 25.1 (piperazine 5-methyl) and 9.1 (piperazine 2-methyl); HRMS found  $\text{MH}^+$ , 403.2733.  $\text{C}_{22}\text{H}_{34}\text{N}_4\text{O}_3$  requires  $\text{MH}$ , 403.2709.

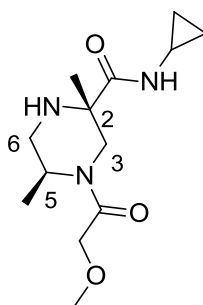
**[(2*S*, 5*S*)-5-(Benzylcarbamoyl)-2,5-dimethylpiperazin-1-yl]azetidine-1-carboxylate, **155****



By general procedure Y, the protected azetidine **154** (362 mg, 0.900 mmol) gave the *deprotected azetidine* **155** (230 mg, 84%) as a yellow oil,  $R_f = 0.43$  (20:80 sat.  $\text{NH}_3$  in

MeOH-DCM);  $\nu_{\max}/\text{cm}^{-1}$  (ATR) 3296 (br), 2962, 2931, 1653, 1518, 1453, 1367, 1175 and 697;  $[\alpha]_{\text{D}}^{24}$  21 ( $c = 1.77$ ,  $\text{CHCl}_3$ );  $\delta_{\text{H}}$  (500 MHz, MeOD) 7.38-7.33 (4H, m, benzyl 2-H, benzyl 3-H, benzyl 5-H and benzyl 6-H), 7.31-7.25 (1H, m, benzyl 4-H), 4.51-4.39 (2H, m, benzylic- $\text{H}_2$ ), 3.69-3.58 (2H, m, azetidine 2- $\text{H}_2$ ), 3.56-3.42 (3H, m, azetidine 1-H and azetidine 4- $\text{H}_2$ ), 3.02 (1H, dd,  $J$  13.8 and 4.5, 3- $\text{H}_a$ ), 2.89 (1H, d,  $J$  11.6, 6- $\text{H}_a$ ), 2.66-2.60 (2H, m, 2-H and 3- $\text{H}_b$ ), 2.28 (1H, d,  $J$  11.6, 6- $\text{H}_b$ ), 1.28 (3H, s, 5-methyl) and 0.99 (3H, d,  $J$  6.5, 2-methyl);  $\delta_{\text{C}}$  (126 MHz, MeOD) 177.5 (CO), 140.1 (benzyl C-1), 129.5 (benzyl C-3 and benzyl C-5), 128.4 (benzyl C-2 and benzyl C-6), 128.1 (benzyl C-4), 58.8 (C-5), 57.0 (azetidine C-1), 53.0 (azetidine C-2), 51.5 (azetidine C-4), 50.9 (C-2), 50.1 (C-3), 48.7 (C-6), 44.0 (benzylic-C), 24.9 (5-methyl) and 9.8 (2-methyl); HRMS found  $\text{MH}^+$ , 303.2209.  $\text{C}_{17}\text{H}_{26}\text{N}_4\text{O}$  requires  $\text{MH}$ , 303.2185.

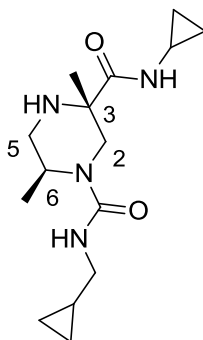
**[(2*S*, 5*S*)-*N*-Cyclopropyl-4-(2-methoxyacetyl)-2,5-dimethylpiperazine-2-carboxamide, 162**



By general procedure O, the protected piperazine **114** (400 mg, 0.835 mmol) gave a residue which was purified by flash chromatography ( $\text{SiO}_2$ , 20:80 MeOH-DCM) to yield the crude deprotected piperazine which was combined with methoxyacetyl chloride (0.150 mL, 1.60 mmol) and by general procedure T, gave a crude residue which was purified by flash chromatography ( $\text{SiO}_2$ , 10:90 MeOH-DCM). By general procedure L, the crude decorated piperazine gave a crude residue which was purified by flash chromatography ( $\text{SiO}_2$ , 100% EtOAc) then again ( $\text{SiO}_2$ , 30:70 Petrol-EtOAc) to yield *piperazine* **162** (43.1 mg, 19% over three steps) as a yellow oil,  $R_f = 0.33$  (10:90 MeOH-DCM);  $\nu_{\max}/\text{cm}^{-1}$  (ATR) 3300 (br), 2975, 2930, 1639, 1454, 1267, 1170 and 1116;  $[\alpha]_{\text{D}}^{20}$  57 ( $c = 0.085$ ,  $\text{CHCl}_3$ );  $\delta_{\text{H}}$  (400 MHz,  $\text{CDCl}_3$ ) 7.32 (1H, s, cyclopropyl-NH), 5.52 (1H, s, NH), 4.38 (1H, d,  $J$  14.8, 3- $\text{H}_a$ ), 4.00 (2H, s, methoxyacetyl 2- $\text{H}_2$ ), 3.98-3.92 (1H, m, 5-H), 3.34 (3H, s, methoxyacetyl 4- $\text{H}_3$ ), 2.97 (1H, dd,  $J$  13.6 and 1.6, 6- $\text{H}_a$ ), 2.91 (1H, d,  $J$  14.8, 3- $\text{H}_b$ ), 2.74-2.64 (1H, m, cyclopropyl 1-H), 2.55 (1H, dd,  $J$  13.6 and 3.2, 6- $\text{H}_b$ ), 1.40-1.26 (6H, m, 2-methyl and 5-methyl), 0.69 (2H, dt,  $J$  7.4 and 3.8, cyclopropyl 2- $\text{H}_2$ ), 0.48-0.42 (1H, m, cyclopropyl 3- $\text{H}_a$ ) and 0.41-0.34 (1H, m, cyclopropyl 3- $\text{H}_b$ );  $\delta_{\text{C}}$  (101 MHz,  $\text{CDCl}_3$ ) 176.4

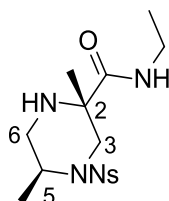
(methoxyacetyl C-1), 168.6 (CO), 71.5 (methoxyacetyl C-2), 64.8 (C-2), 59.2 (methoxyacetyl C-4), 49.2 (C-5), 47.0 (C-6), 43.8 (C-3), 23.3 (cyclopropyl C-1), 23.2 (2-methyl), 15.2 (5-methyl), 6.5 (cyclopropyl C-2) and 6.0 (cyclopropyl C-3); HRMS found  $MH^+$ , 270.1828.  $C_{13}H_{23}N_3O_3$  requires  $MH$ , 270.1817.

**[(3*S*, 6*S*)-*N*3-Cyclopropyl-*N*1-(cyclopropylmethyl)-3,6-dimethylpiperazine-1,3-dicarboxamide, **164****



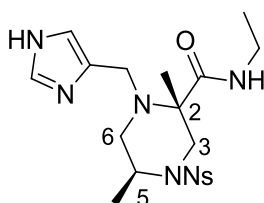
By general procedure O, the protected piperazine **114** (400 mg, 0.835 mmol) gave a residue which was purified by flash chromatography ( $SiO_2$ , 20:80 MeOH-DCM) to yield the crude deprotected piperazine which was combined with cyclopropylmethyl isocyanate (117 mg, 1.20 mmol) and by general procedure Q, gave a crude residue which was purified by flash chromatography ( $SiO_2$ , 100% EtOAc). By general procedure L, the crude decorated piperazine gave a crude residue which was purified by flash chromatography ( $SiO_2$ , 10:90 MeOH-DCM) to yield *piperazine* **164** (65.7 mg, 26% over three steps) as a yellow oil,  $R_f = 0.34$  (10:90 MeOH-DCM);  $\nu_{max}/cm^{-1}$  (ATR) 3300 (br), 2970, 2926, 2488, 1607, 1452, 1432 and 1173;  $[\alpha]_D^{20}$  124 ( $c = 0.182$ ,  $CHCl_3$ );  $\delta_H$  (400 MHz, MeOD) 4.00 (1H, d,  $J$  13.7, NH), 3.87-3.77 (1H, m, 6-H), 3.11 (1H, dt,  $J$  3.1 and 1.5, cyclopropyl 1-H), 2.87-2.74 (2H, m, cyclopropyl methyl- $H_2$ ), 2.62-2.53 (2H, m, 2- $H_a$  and 5- $H_a$ ), 2.49-2.44 (1H, m, 2- $H_b$ ), 2.42 (1H, dd,  $J$  13.7 and 2.0, 5- $H_b$ ), 1.01-0.94 (6H, m, 3-methyl and 6-methyl), 0.86-0.71 (1H, m, cyclopropyl methyl 1-H), 0.58-0.44 (2H, m, cyclopropyl 2- $H_2$ ), 0.34-0.22 (4H, m, cyclopropyl 3- $H_2$  and cyclopropyl methyl 2- $H_2$ ) and 0.04-0.00 (2H, m, cyclopropyl methyl 3- $H_2$ );  $\delta_C$  (101 MHz, MeOD) 176.5 (6-CO), 157.7 (3-CO), 57.1 (C-3), 45.0 (cyclopropyl methyl), 44.2 (C-6), 44.1 (C-2), 43.3 (C-5), 22.9 (3-methyl), 21.1 (cyclopropyl C-1), 12.1 (6-methyl), 9.9 (cyclopropyl methyl C-1), 4.3 (cyclopropyl C-2), 4.2 (cyclopropyl C-3), 1.43 (cyclopropyl methyl C-2) and 1.41 (cyclopropyl methyl C-3); HRMS found  $MH^+$ , 295.2293.  $C_{15}H_{26}N_4O_2$  requires  $MH$ , 295.2134.

***N*-Ethyl-(2*S*,5*S*)-2,5-(dimethyl)-4-[(2-nitrobenzene)sulfonyl]piperazine-2-carboxamide, **165****



By general procedure L, the protected piperazine **115** (182 mg, 0.390 mmol) gave a crude residue which was purified by flash chromatography (SiO<sub>2</sub>, 5:95 MeOH–DCM) to yield the *deprotected piperazine* **165** (75.2 mg, 52%) as a yellow oil, *R*<sub>f</sub> = 0.67 (5:95 MeOH–DCM);  $\nu_{\text{max}}$ / cm<sup>-1</sup> (ATR) 3351 (br), 2974, 2933, 1662, 1542, 1373, 1349 and 1157;  $[\alpha]_{\text{D}}^{23}$  122 (*c* = 0.23, CHCl<sub>3</sub>);  $\delta_{\text{H}}$  (500 MHz, CDCl<sub>3</sub>) 8.25-8.16 (1H, m, nitrophenyl 3-H), 7.81-7.71 (3H, m, nitrophenyl 4-H, nitrophenyl 5-H and nitrophenyl 6-H), 7.10 (1H, t, *J* 3.7, NH), 4.14-4.05 (2H, m, 3-H<sub>a</sub> and 5-H), 3.18 (1H, dd, *J* 14.2 and 4.2, 6-H<sub>a</sub>), 3.15-3.05 (2H, m, ethyl 1-H<sub>2</sub>), 2.87 (1H, d, *J* 13.2, 3-H<sub>b</sub>), 2.67 (1H, dd, *J* 14.2 and 1.1, 6-H<sub>b</sub>), 1.31 (3H, d, *J* 6.8, 5-methyl), 1.19 (3H, s, 2-methyl) and 1.02 (3H, t, *J* 7.3, ethyl 2-H<sub>3</sub>);  $\delta_{\text{C}}$  (126 MHz, CDCl<sub>3</sub>) 172.0 (CO), 147.6 (nitrophenyl C-2), 133.4 (nitrophenyl C-5), 133.3 (nitrophenyl C-1), 132.2 (nitrophenyl C-4), 131.8 (nitrophenyl C-6), 124.3 (nitrophenyl C-5), 57.5 (C-2), 46.8 (C-3), 46.7 (C-5), 45.0 (ethyl C-1), 34.2 (C-6), 25.9 (5-methyl), 14.8 (2-methyl) and 14.6 (ethyl C-2); HRMS found MH<sup>+</sup>, 371.1415. C<sub>15</sub>H<sub>22</sub>N<sub>4</sub>O<sub>5</sub>S requires *MH*, 371.1389.

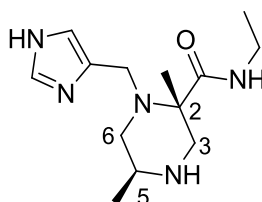
***N*-Ethyl-(2*S*,5*S*)-2,5-(dimethyl)-4-[(2-nitrobenzene)sulfonyl]-1-(1*H*-imidazole-4-ylmethyl)piperazine-2-carboxamide, **168****



Acetic acid (27.0  $\mu$ L, 0.480 mmol) and NaBH(OAc)<sub>3</sub> (271 mg, 1.28 mmol) were added to a solution of the piperazine **165** (118 mg, 0.320 mmol) and 4-imidazolecarboxaldehyde (61.5 mg, 0.640 mmol) in DCE (1.07 mL, 0.3 M), and stirred overnight. More 4-imidazolecarboxaldehyde (61.5 mg, 0.640 mmol) and NaBH(OAc)<sub>3</sub> (203 mg, 0.960 mmol) were added in two portions over the next two days. The reaction mixture was diluted with DCM (5 mL) and sat. NaHCO<sub>3</sub> (5 mL). The aqueous layer was extracted with DCM (3  $\times$  5 mL) and the combined organic layers were washed with brine (5 mL), dried (MgSO<sub>4</sub>) and concentrated *in vacuo*. The residue was purified by basic SCX

cartridge and then twice by flash chromatography (SiO<sub>2</sub>, 5:95 sat. NH<sub>3</sub> in MeOH–DCM) to yield the alkylated *piperazine* **168** (20.4 mg, 14%) as a colourless amorphous solid,  $R_f = 0.15$  (10:90 MeOH–DCM);  $\nu_{\max}/\text{cm}^{-1}$  (ATR) 3213 (br), 2972, 1738, 1651, 1542, 1370, 1350 and 1158;  $[\alpha]_{\text{D}}^{23} 129$  ( $c = 0.060$ , CHCl<sub>3</sub>);  $\delta_{\text{H}}$  (500 MHz, CDCl<sub>3</sub>) 8.11–7.93 (2H, m, nitrophenyl 3-H and imidazole 2-H), 7.78–7.53 (4H, m, nitrophenyl 4-H, nitrophenyl 5-H, nitrophenyl 6-H and imidazole 5-H), 7.00 (1H, s, amide NH), 4.12–3.94 (1H, m, 5-H), 3.84 (1H, d,  $J$  14.4, 3-H<sub>a</sub>), 3.68 (1H, d,  $J$  14.3, 1-methyl-H<sub>a</sub>), 3.58 (1H, d,  $J$  14.3, 1-methyl-H<sub>b</sub>), 3.51 (1H, s, imidazole NH), 3.31 (1H, d,  $J$  14.4, 3-H<sub>b</sub>), 3.28–3.17 (1H, m, ethyl 1-H<sub>a</sub>), 3.14–3.02 (1H, m, ethyl-1-H<sub>b</sub>), 2.92 (1H, dd,  $J$  12.8 and 5.9, 6-H<sub>a</sub>), 2.42 (1H, dd,  $J$  12.8 and 8.2, 6-H<sub>b</sub>), 1.35 (3H, s, 2-methyl), 1.11 (3H, t,  $J$  7.3, ethyl 2-H<sub>3</sub>) and 0.96 (3H, d,  $J$  6.4, 5-methyl);  $\delta_{\text{C}}$  (126 MHz, CDCl<sub>3</sub>) 173.6 (CO), 147.8 (nitrophenyl C-2), 135.4 (imidazole C-2 and imidazole C-5), 134.7 (nitrophenyl C-1), 133.5 (nitrophenyl C-5), 131.9 (nitrophenyl C-4), 130.9 (nitrophenyl C-6), 124.3 (nitrophenyl C-3), 63.4 (C-2), 52.4 (C-5), 50.5 (C-3), 49.7 (1-methyl), 47.2 (ethyl C-1), 34.5 (C-6), 16.2 (2-methyl), 15.6 (ethyl C-2) and 14.4 (C-5), imidazole C-4 not observed; HRMS found MH<sup>+</sup>, 451.1785. C<sub>19</sub>H<sub>26</sub>N<sub>6</sub>O<sub>5</sub>S requires *MH*, 451.1763.

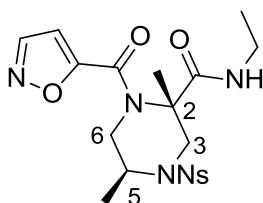
***N*-Ethyl-(2*S*,5*S*)-2,5-(dimethyl)-1-(1*H*-imidazole-4-ylmethyl)piperazine-2-carboxamide, **169****



By general procedure O, the protected piperazine **168** (68.4 mg, 0.150 mmol) gave a crude residue which was purified by basic SCX cartridge and then by flash chromatography (SiO<sub>2</sub>, 10:90 sat. NH<sub>3</sub> in MeOH–DCM) to yield the *deprotected piperazine* **169** (23.5 mg, 59%) as a colourless amorphous solid,  $R_f = 0.50$  (20:80 MeOH–DCM);  $\nu_{\max}/\text{cm}^{-1}$  (ATR) 3189 (br), 2972, 2831, 1644, 1516, 1154, 1089 and 731;  $[\alpha]_{\text{D}}^{24} -26$  ( $c = 0.10$ , CHCl<sub>3</sub>);  $\delta_{\text{H}}$  (500 MHz, CDCl<sub>3</sub>) 8.18 (1H, s, imidazole 2-H), 7.56 (1H, s, imidazole 5-H), 6.81 (1H, s, NH), 3.45 (1H, d,  $J$  13.9, 3-H<sub>a</sub>), 3.34–3.18 (2H, m, 6-H<sub>a</sub> and ethyl 1-H<sub>a</sub>), 3.05 (1H, d,  $J$  13.9, 3-H<sub>b</sub>), 2.89 (1H, d,  $J$  12.6, 1-methyl-H<sub>a</sub>), 2.82 (1H, d,  $J$  12.6, 1-methyl-H<sub>b</sub>), 2.76–2.68 (1H, m, ethyl 1-H<sub>b</sub>), 2.63 (1H, dd,  $J$  11.5 and 3.1, 6-H<sub>b</sub>), 1.86 (1H, app t,  $J$  11.1, 5-H), 1.26 (3H, s, 2-methyl), 1.09 (3H, t,  $J$  7.3, ethyl 2-H<sub>3</sub>) and 0.94 (3H, d,  $J$  6.4, 5-methyl);  $\delta_{\text{C}}$  (126 MHz, CDCl<sub>3</sub>) 175.9 (CO), 135.2 (imidazole C-2 and imidazole C-5), 62.9 (C-2), 56.8 (C-3), 54.0 (C-5), 50.9 (1-methyl), 50.3 (ethyl C-1), 34.3 (C-1), 19.6 (2-methyl), 14.7 (ethyl C-2)

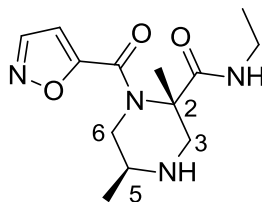
and 9.7 (5-methyl), imidazole C-4 not observed; HRMS found  $MH^+$ , 266.2009.  $C_{13}H_{23}N_5O$  requires  $MH$ , 266.1981.

***N*-Ethyl-(2*S*,5*S*)-2,5-(dimethyl)-4[(2-nitrobenzene)sulfonyl]-1-(isoxazole-5-carbonyl) piperazine-2-carboxamide, **166****



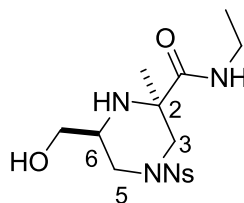
$Et_3N$  (0.110 mL, 0.800 mmol) and isoxazole-5-carbonyl chloride (60.0  $\mu$ L, 0.600 mmol) were added to a solution of piperazine **165** (75.2 mg, 0.200 mmol) in DCM (10 mL, 0.02 M), and stirred at room temperature overnight. The reaction mixture was diluted with sat.  $NaHCO_3$  (10 mL) and the aqueous layer was extracted with DCM ( $3 \times 10$  mL). The combined organic layers were washed with water (10 mL), brine (10 mL), dried ( $MgSO_4$ ) and concentrated *in vacuo*. The residue was purified by flash chromatography ( $SiO_2$ , 10:90 MeOH-DCM) and then again ( $SiO_2$ , 5:95 MeOH-DCM) to yield the acylated piperazine **166** (50 mg, 54%) as a yellow oil,  $R_f = 0.41$  (10:90 MeOH-DCM);  $\nu_{max}/cm^{-1}$  (ATR) 3289 (br), 2981, 1738, 1652, 1543, 1408 and 732;  $[\alpha]_D^{23}$  28 ( $c = 0.15$ ,  $CHCl_3$ );  $\delta_H$  (500 MHz,  $CDCl_3$ ) 8.28 (1H, d,  $J$  1.8, isoxazole 3-H), 8.15-8.02 (1H, m, nitrophenyl 3-H), 7.71-7.60 (3H, m, nitrophenyl 4-H, nitrophenyl 5-H and nitrophenyl 6-H), 6.81 (1H, d,  $J$  1.8, isoxazole 4-H), 6.14 (1H, t,  $J$  5.1, NH), 4.40-4.26 (1H, m, 5-H), 3.94 (1H, d,  $J$  14.2, 3- $H_a$ ), 3.81 (1H, dd,  $J$  14.4 and 4.7, 6- $H_a$ ), 3.48 (1H, dd,  $J$  14.4 and 6.0, 6- $H_b$ ), 3.30 (1H, d,  $J$  14.2, 3- $H_b$ ), 3.22-3.09 (1H, m, ethyl 1- $H_a$ ), 3.09-2.99 (1H, m, ethyl 1- $H_b$ ), 1.63 (3H, s, 2-methyl), 1.24 (3H, d,  $J$  6.5, 5-methyl) and 1.00 (3H, t,  $J$  7.3, ethyl 2- $H_3$ );  $\delta_C$  (126 MHz,  $CDCl_3$ ) 169.8 (amide CO), 163.3 (isoxazole CO), 159.5 (isoxazole C-5), 150.5 (isoxazole C-3), 147.8 (nitrophenyl C-2), 133.9 (nitrophenyl C-5), 133.8 (nitrophenyl C-1), 132.1 (nitrophenyl C-6), 131.7 (nitrophenyl C-4), 124.6 (nitrophenyl C-3), 109.0 (isoxazole C-4), 64.4 (C-2), 50.7 (C-5), 49.0 (C-3), 48.6 (C-6), 34.9 (ethyl C-1), 20.2 (3-methyl), 16.8 (5-methyl) and 14.4 (ethyl C-2); HRMS found  $MH^+$ , 466.1417.  $C_{19}H_{23}N_5O_7S$  requires  $MH$ , 466.1396.

***N*-Ethyl-(2*S*,5*S*)-2,5-(dimethyl)-1-(isoxazole-5-carbonyl)piperazine-2-carboxamide, 167**



By general procedure O, the protected piperazine **166** (45.0 mg, 97.0  $\mu\text{mol}$ ) gave a crude residue which was purified by flash chromatography ( $\text{SiO}_2$ , 10:90 MeOH–DCM) and again ( $\text{SiO}_2$ , 5:95 MeOH–DCM) to yield the *deprotected* piperazine **167** (7.20 mg, 26%) as a yellow oil,  $R_f = 0.71$  (10:90 MeOH–DCM);  $\nu_{\text{max}}/\text{cm}^{-1}$  (ATR) 3327 (br), 2975, 2932, 1645, 1532, 1442 and 1378;  $[\alpha]_{\text{D}}^{28} 7.7$  ( $c = 0.073$ ,  $\text{CHCl}_3$ );  $\delta_{\text{H}}$  (501 MHz, MeOD) 8.40 (1H, d,  $J$  1.9, isoxazole 3-H), 6.71 (1H, d,  $J$  1.9, isoxazole 4-H), 3.76 (1H, dd,  $J$  13.6 and 3.9, 3- $\text{H}_a$ ), 3.16–3.09 (2H, m, ethyl 1- $\text{H}_2$ ), 3.03–2.98 (1H, m, 5-H), 2.96 (1H, d,  $J$  13.6, 3- $\text{H}_b$ ), 2.83 (1H, d,  $J$  11.0, 6- $\text{H}_a$ ), 2.80 (1H, d,  $J$  11.0, 6- $\text{H}_b$ ), 1.47 (3H, s, 2-methyl) and 1.03–0.98 (6H, m, ethyl 2- $\text{H}_3$  and 5-methyl);  $\delta_{\text{C}}$  (126 MHz, MeOD) 174.7 (amide CO), 164.2 (isoxazole CO), 161.5 (isoxazole C-5), 151.5 (isoxazole C-3), 107.8 (isoxazole C-4), 62.3 (C-2), 55.0 (C-3), 50.4 (C-5), 49.9 (ethyl C-1), 35.6 (C-6), 18.9 (2-methyl), 16.1 (5-methyl) and 14.7 (ethyl C-2); HRMS found  $\text{MH}^+$ , 281.1636.  $\text{C}_{13}\text{H}_{20}\text{N}_4\text{O}_3$  requires  $\text{MH}$ , 281.1613.

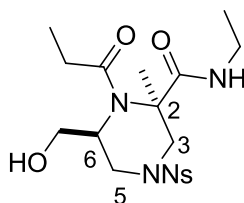
***N*-Ethyl-6-(hydroxymethyl)-2-methyl-4-(2-nitrobenzenesulfonyl)piperazine-2-carboxamide, 171**



By general procedure L (with an additional 7 eq.  $\text{NaBH}_4$  and heating at reflux for 4 hr), the protected piperazine **116** (290 mg, 0.555 mmol) gave a crude residue which was purified by flash chromatography ( $\text{SiO}_2$ , 5:95 MeOH–DCM) to yield the *deprotected* piperazine **171** (112 mg, 53%) as a yellow oil,  $R_f = 0.38$  (10:90 MeOH–DCM);  $\nu_{\text{max}}/\text{cm}^{-1}$  (ATR) 3359 (br), 2931, 1652, 1544, 1373, 1355, 1165 and 587;  $\delta_{\text{H}}$  (500 MHz,  $\text{CDCl}_3$ ) 8.10 (1H, dd,  $J$  5.6 and 3.4, nitrophenyl 3-H), 7.76 (2H, dd,  $J$  5.6 and 3.1, nitrophenyl 4-H and nitrophenyl 5-H), 7.69 (1H, dd,  $J$  5.6 and 3.1, nitrophenyl 6-H), 6.81 (1H, s, NH), 4.25 (1H, d,  $J$  12.8, 3- $\text{H}_a$ ), 3.84 (1H, d,  $J$  11.5, 6-methyl- $\text{H}_a$ ), 3.74 (1H, dd,  $J$  11.1 and 3.5, 5- $\text{H}_a$ ), 3.66 (1H, dd,  $J$  11.1 and 4.1, 5- $\text{H}_b$ ), 3.31–3.18 (2H, m, ethyl 1- $\text{H}_2$ ), 3.05–2.98 (1H, m, 6-H), 2.70

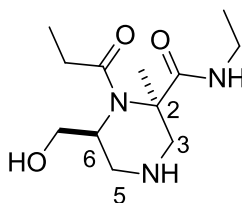
(1H, app t, *J* 11.5, 6-methyl-H<sub>b</sub>), 2.59 (1H, d, *J* 12.8, 3-H<sub>b</sub>), 1.94 (1H, br s, NH), 1.62 (1H, br s, OH), 1.26 (3H, s, 2-methyl) and 1.11 (3H, t, *J* 7.2, ethyl 2-H<sub>3</sub>);  $\delta_c$  (126 MHz, CDCl<sub>3</sub>) 172.7 (CO), 133.8 (nitrophenyl C-5), 131.8 (nitrophenyl C-4), 131.6 (nitrophenyl C-6), 124.2 (nitrophenyl C-3), 63.7 (C-3), 58.4 (C-2), 52.8 (C-6), 51.1 (6-methyl C-1), 47.0 (C-5), 34.5 (ethyl C-1), 25.8 (2-methyl) and 14.6 (ethyl C-2), nitrophenyl C-1 and nitrophenyl C-2 not observed; HRMS found MH<sup>+</sup>, 387.1363. C<sub>15</sub>H<sub>22</sub>N<sub>4</sub>O<sub>6</sub>S requires *MH*, 387.1338.

***N*-Ethyl-6-(hydroxymethyl)-2-methyl-4-(2-nitrobenzenesulfonyl)-1-propanoyl piperazine-2-carboxamide, 172**



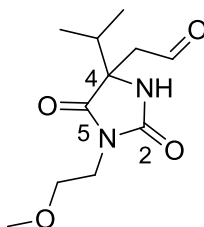
Propionyl chloride (29.0  $\mu$ L, 0.320 mmol) was added to a solution of piperazine **171** (112 mg, 0.290 mmol) and DIPEA (0.150 mL, 0.870 mmol) in THF (5.80 mL, 0.05 M). The reaction mixture was stirred at room temperature overnight before being concentrated *in vacuo*. The residue was purified by flash chromatography (SiO<sub>2</sub>, 10:90 MeOH–DCM) to yield the decorated *piperazine* **172** (65.1 mg, 51%) as a yellow oil, *R<sub>f</sub>* = 0.75 (10:90 MeOH–DCM);  $\nu_{\max}$ /cm<sup>-1</sup> (ATR) 3368 (br), 2979, 1737, 1665, 1545, 1373, 1168 and 587;  $\delta_H$  (500 MHz, CDCl<sub>3</sub>) 8.06-8.00 (1H, m, nitrophenyl 3-H), 7.70-7.64 (2H, m, nitrophenyl 5-H and nitrophenyl 6-H), 7.63-7.58 (1H, m, nitrophenyl 4-H), 6.73 (1H, t, *J* 5.3, NH), 4.18 (1H, dd, *J* 12.7 and 1.3, 5-H<sub>a</sub>), 4.04 (1H, dd, *J* 11.3 and 6.2, ethyl 1-H<sub>a</sub>), 3.99 (1H, dd, *J* 11.3 and 6.2, ethyl 1-H<sub>b</sub>), 3.79 (1H, ddd, *J* 12.1, 3.3 and 1.3, 6-H), 3.18-3.02 (3H, m, 3-H<sub>2</sub> and 5-H<sub>b</sub>), 2.56-2.40 (2H, m, 6-methyl), 2.32 (2H, q, *J* 7.6, propanoyl 2-H<sub>2</sub>), 1.53 (1H, br s, OH), 1.14 (3H, s, 2-methyl), 1.10 (3H, t, *J* 7.6, propanoyl 3-H<sub>3</sub>) and 0.98 (3H, t, *J* 6.2, ethyl 2-H<sub>3</sub>);  $\delta_c$  (126 MHz, CDCl<sub>3</sub>) 173.9 (1-CO), 172.2 (2-CO), 133.6 (nitrophenyl C-5), 132.1 (nitrophenyl C-1), 131.7 (nitrophenyl C-4), 131.6 (nitrophenyl C-6), 124.2 (nitrophenyl C-3), 64.8 (C-5), 58.4 (C-2), 51.3 (ethyl C-1), 50.8 (C-6), 47.4 (C-3), 34.4 (6-methyl), 27.4 (propanoyl C-2), 25.7 (2-methyl), 14.5 (propanoyl C-3) and 9.0 (ethyl C-2), nitrophenyl C-2 not observed; HRMS found MH<sup>+</sup>, 443.1624. C<sub>18</sub>H<sub>26</sub>N<sub>4</sub>O<sub>7</sub>S requires *MH*, 443.1600.

### ***N*-Ethyl-6-(hydroxymethyl)-2-methyl-1-propanoylpiperazine-2-carboxamide, 173**



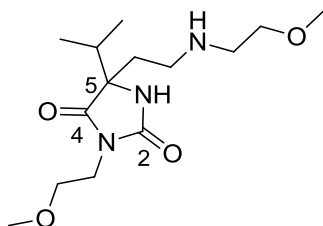
By general procedure O, the protected piperazine **172** (57.5 mg, 0.130 mmol) gave a crude residue which was purified by flash chromatography (SiO<sub>2</sub>, 10:90 MeOH–DCM) to yield the *deprotected piperazine* **173** (29.9 mg, 89%) as a yellow oil,  $R_f = 0.23$  (10:90 MeOH–DCM);  $\nu_{\max}/\text{cm}^{-1}$  (ATR) 3309 (br), 2971, 1735, 1644, 1527, 1185 and 805;  $\delta_{\text{H}}$  (500 MHz, CDCl<sub>3</sub>) 7.42 (1H, t,  $J$  5.0, NH), 3.93 (2H, qd,  $J$  11.3 and 5.0, ethyl 1-H<sub>2</sub>), 3.57 (1H, d,  $J$  12.6, 3-H<sub>a</sub>), 3.31–3.19 (2H, m, 5-H<sub>2</sub>), 2.98–2.83 (2H, m, 6-methyl), 2.35–2.27 (3H, m, 6-H and propanoyl 2-H<sub>2</sub>), 2.25 (1H, d,  $J$  12.6, 3-H<sub>b</sub>), 1.11 (3H, s, 2-methyl) and 1.11–1.06 (6H, m, ethyl 2-H<sub>3</sub> and propanoyl 3-H<sub>3</sub>);  $\delta_{\text{C}}$  (126 MHz, CDCl<sub>3</sub>) 174.3 (1-CO), 174.0 (2-CO), 65.7 (ethyl C-1), 57.6 (C-2), 52.7 (C-3), 51.5 (C-6), 48.2 (C-5), 34.0 (6-methyl), 27.4 (propanoyl C-1), 26.0 (2-methyl), 14.8 (ethyl C-2) and 9.0 (propanoyl C-3); HRMS found  $\text{MH}^+$ , 258.1853. C<sub>12</sub>H<sub>23</sub>N<sub>3</sub>O<sub>3</sub> requires  $\text{MH}$ , 258.1817.

### **2-[1-(2-Methoxyethyl)-2,5-dioxo-4-(propan-2-yl)imidazolidin-4-yl]acetaldehyde, 200**



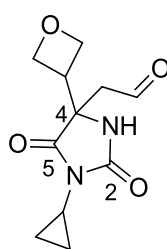
By general procedure U, the hydantoin **195** (48.6 mg, 0.200 mmol) gave the *aldehyde* **200** (34.6 mg, 71%) as a yellow oil which was used without further purification,  $R_f = 0.54$  (10:90 MeOH–DCM);  $\nu_{\max}/\text{cm}^{-1}$  (ATR) 3288 (br), 2967, 1773, 1706, 1449, 1345 and 1151;  $\delta_{\text{H}}$  (500 MHz, CDCl<sub>3</sub>) 9.63–9.53 (1H, m, acetaldehyde 2-H), 6.17 (1H, s, NH), 3.73–3.59 (2H, m, methoxyethyl 2-H<sub>2</sub>), 3.51 (2H, t,  $J$  5.7, methoxyethyl 1-H<sub>2</sub>), 3.26 (3H, s, methoxyethyl 4-H<sub>3</sub>), 2.96 (1H, dd,  $J$  17.7 and 1.8, acetaldehyde 1-H<sub>a</sub>), 2.81 (1H, d,  $J$  17.7, acetaldehyde 1-H<sub>b</sub>), 2.10–1.97 (1H, m, propyl 2-H), 0.91 (3H, d,  $J$  6.9, propyl 1-H<sub>3</sub>), 0.86 (3H, d,  $J$  6.8, propyl 3-H<sub>3</sub>);  $\delta_{\text{C}}$  (126 MHz, CDCl<sub>3</sub>) 197.9 (acetaldehyde C-2), 175.3 (C-5), 157.3 (C-2), 68.7 (methoxyethyl C-2), 64.6 (C-4), 58.5 (methoxyethyl C-4), 47.5 (methoxyethyl C-1), 38.0 (acetaldehyde C-1), 34.2 (propyl C-2), 16.4 (propyl C-1) and 16.3 (propyl C-3); HRMS found  $\text{MH}^+$ , 243.1337. C<sub>11</sub>H<sub>18</sub>N<sub>2</sub>O<sub>4</sub> requires  $\text{MH}$ , 243.1345.

**3-(2-Methoxyethyl)-5-{2-[(2-methoxyethyl)amino]ethyl}-5-(propan-2-yl)imidazolidine-2,4-dione, **201****



By general procedure M, 2-methoxyethyl amine (50.0  $\mu$ L, 0.560 mmol) and aldehyde **200** (34.6 mg, 0.140 mmol) gave the decorated *hydantoin* **201** (41.2 mg, 100%) as a yellow oil which did not require further purification,  $R_f = 0.17$  (10:90 MeOH-DCM);  $\nu_{\max}/\text{cm}^{-1}$  (ATR) 2918 (br), 1770, 1708, 1447 and 1117;  $\delta_{\text{H}}$  (500 MHz,  $\text{CDCl}_3$ ) 3.61 (2H, t,  $J$  5.6, 3-methoxyethyl 2- $\text{H}_2$ ), 3.51-3.46 (2H, m, 3-methoxyethyl 1- $\text{H}_2$ ), 3.40 (2H, t,  $J$  4.8, 5-methoxyethyl 2- $\text{H}_2$ ), 3.27 (3H, s, 3-methoxyethyl 4- $\text{H}_3$ ), 3.25 (3H, s, 5-methoxyethyl 4- $\text{H}_3$ ), 2.74-2.69 (2H, m, 5-methoxyethyl 1- $\text{H}_2$ ), 2.67-2.55 (2H, m, aminoethyl 2- $\text{H}_2$ ), 2.01-1.87 (3H, m, aminoethyl 1- $\text{H}_2$  and propyl 2- $\text{H}$ ), 0.89 (3H, d,  $J$  6.9, propyl 1- $\text{H}_3$ ) and 0.84 (3H, d,  $J$  6.7, propyl 3- $\text{H}_3$ );  $\delta_{\text{C}}$  (126 MHz,  $\text{CDCl}_3$ ) 176.22 (C-4), 157.4 (C-2), 70.8 (3-methoxyethyl C-2), 68.8 (3-methoxyethyl C-1), 67.2 (C-5), 58.8 (5-methoxyethyl C-4), 58.4 (3-methoxyethyl C-4), 48.7 (5-methoxyethyl C-2), 44.1 (5-methoxyethyl C-1), 37.7 (aminoethyl C-2), 34.1 (propyl C-2), 33.4 (aminoethyl C-1), 16.5 (propyl C-1) and 16.4 (propyl C-3); HRMS found  $\text{MH}^+$ , 302.2105.  $\text{C}_{14}\text{H}_{27}\text{N}_3\text{O}_4$  requires  $\text{MH}$ , 302.2080.

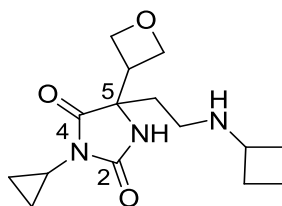
**2-[1-Cyclopropyl-4(oxetane-3-yl)-2,5-dioxoimidazolidin-4-yl] acetaldehyde, **202****



By general procedure U, the hydantoin **197** (61.0 mg, 0.258 mmol) gave *aldehyde* **202** (53.9 mg, 88%) as a colourless oil which was used without further purification,  $R_f = 0.54$  (10:90 MeOH-DCM);  $\nu_{\max}/\text{cm}^{-1}$  (ATR) 3277 (br), 2921, 1773, 1710 and 1434;  $\delta_{\text{H}}$  (500 MHz,  $\text{CDCl}_3$ ) 9.57 (1H, s, acetaldehyde 2- $\text{H}$ ), 6.35 (1H, s, NH), 4.72-4.67 (1H, m, oxetanyl 2- $\text{H}_a$ ), 4.58-4.53 (1H, m, oxetanyl 4- $\text{H}_a$ ), 4.42 (1H, t,  $J$  6.8, oxetanyl 2- $\text{H}_b$ ), 4.37 (1H, t,  $J$  6.8, oxetanyl 4- $\text{H}_b$ ), 3.42-3.31 (1H, m, cyclopropyl 1- $\text{H}$ ), 2.95-2.83 (1H, m, oxetanyl 1- $\text{H}$ ), 2.78 (1H, d,  $J$  18.5, acetaldehyde 1- $\text{H}_a$ ), 2.60-2.56 (1H, m, acetaldehyde 1- $\text{H}_b$ ) and 0.96-0.89 (4H, m, cyclopropyl 2- $\text{H}_2$  and cyclopropyl 3- $\text{H}_2$ );  $\delta_{\text{C}}$  (126 MHz,  $\text{CDCl}_3$ ) 196.7

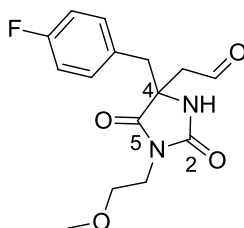
(acetaldehyde C-2), 174.0 (C-5), 156.8 (C-2), 71.9 (oxetanyl C-2), 70.6 (oxetanyl C-4), 60.1 (C-4), 47.2 (acetaldehyde C-1), 40.7 (cyclopropyl C-1), 22.0 (oxetanyl C-1), 4.94 (cyclopropyl C-2) and 4.88 (cyclopropyl C-3); HRMS found  $MH^+$ , 239.1022.  $C_{11}H_{14}N_2O_4$  requires  $MH$ , 239.1032.

**5-[2-(Cyclobutylamino)ethyl]-3-cyclopropyl-5-(oxetan-3-yl)imidazolidino-2,4-dione, **203****



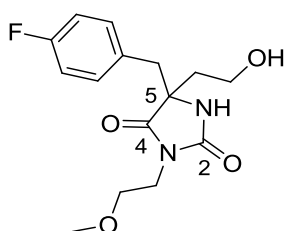
By general procedure M, cyclobutylamine (77.0  $\mu$ L, 0.904 mmol) and aldehyde **202** (53.9 mg, 0.226 mmol) gave a crude residue which was purified by flash chromatography ( $SiO_2$ , 5:95 MeOH-DCM) to yield the decorated *hydantoin* **203** (45.5 mg, 69%) as a yellow oil,  $R_f$  = 0.63 (20:80 MeOH-DCM);  $\nu_{max}/cm^{-1}$  (ATR) 3319 (br), 2943, 2832, 1448 and 1023;  $\delta_H$  (500 MHz, MeOD) 3.39-3.35 (1H, m, oxetanyl 2- $H_a$ ), 3.27 (1H, dd,  $J$  10.9 and 8.8, oxetanyl 4- $H_a$ ), 3.12-3.03 (2H, m, ethyl 2- $H_2$ ), 3.01 (1H, dd,  $J$  12.2 and 3.5, oxetanyl 2- $H_b$ ), 2.52 (1H, ddd,  $J$  11.0, 6.9 and 4.4, cyclopropyl 1-H), 2.41 (1H, ddd,  $J$  12.6, 9.9 and 5.8, oxetanyl 1-H), 2.26-2.18 (1H, m, ethyl 1- $H_a$ ), 2.18-2.12 (2H, m, cyclobutyl 1-H and cyclobutyl 2- $H_a$ ), 2.09 (1H, dd,  $J$  13.8 and 4.3, cyclobutyl 2- $H_b$ ), 2.06-1.99 (2H, m, cyclobutyl 4- $H_2$ ), 1.89 (1H, t,  $J$  12.4, oxetanyl 4- $H_b$ ), 1.83-1.74 (2H, m, cyclobutyl 3- $H_2$ ), 1.71 (1H, dt,  $J$  13.9 and 2.0, ethyl 1- $H_b$ ) and 0.97-0.81 (4H, m, cyclopropyl 2- $H_2$  and cyclopropyl 3- $H_2$ );  $\delta_C$  (126 MHz, MeOD) 178.7 (C-2), 159.3 (C-4), 69.1 (C-5), 61.30 (oxetanyl C-2), 61.25 (cyclobutyl C-1), 48.5 (oxetanyl C-4), 46.2 (ethyl C-2), 43.5 (oxetanyl C-1), 34.7 (ethyl C-1), 27.5 (cyclobutyl C-2 and cyclobutyl C-4), 22.1 (cyclopropyl C-1), 14.8 (cyclobutyl C-3), 5.7 (cyclopropyl C-2) and 5.3 (cyclopropyl C-3); HRMS found  $MH^+$ , 294.1829.  $C_{15}H_{23}N_3O_3$  requires  $MH$ , 294.1817.

**2-{4-[(4-Fluorophenyl)methyl]-1-(2-methoxyethyl)-2,5-dioximidazolidin-4-yl} acetaldehyde, **204****



By general procedure U, the hydantoin **196** (76.6 mg, 0.250 mmol) gave the *aldehyde* **204** (37.7 mg, 49%) as a yellow oil which was used without further purification,  $R_f = 0.29$  (5:95 MeOH–DCM);  $\nu_{\max}/\text{cm}^{-1}$  (ATR) 3274 (br), 2929, 1701, 1450, 1222 and 1114;  $\delta_H$  (500 MHz,  $\text{CDCl}_3$ ) 9.65 (1H, s, acetaldehyde 2-H), 7.09–7.01 (2H, m, fluorophenyl 3-H and fluorophenyl 6-H), 6.96–6.84 (2H, m, fluorophenyl 4-H and fluorophenyl 5-H), 6.30 (1H, s, NH), 3.43 (2H, t,  $J$  5.9, methoxyethyl 2- $\text{H}_2$ ), 3.26–3.18 (2H, m, methoxyethyl 1- $\text{H}_2$ ), 3.17 (3H, s, methoxyethyl 4- $\text{H}_3$ ), 3.05 (1H, d,  $J$  18.6, 4-methyl- $\text{H}_a$ ), 3.00 (1H, d,  $J$  13.7, acetaldehyde 1- $\text{H}_a$ ), 2.95 (1H, d,  $J$  13.7, acetaldehyde 1- $\text{H}_b$ ) and 2.88 (1H, d,  $J$  18.6, 4-methyl- $\text{H}_b$ );  $\delta_C$  (126 MHz,  $\text{CDCl}_3$ ) 198.0 (acetaldehyde C-2), 174.5 (C-5), 162.4 (d,  $J$  246.5, fluorophenyl C-4), 156.4 (C-2), 131.8 (d,  $J$  8.0, fluorophenyl C-2 and fluorophenyl C-6), 129.1 (d,  $J$  3.3, fluorophenyl C-1), 115.4 (d,  $J$  21.4, fluorophenyl C-3 and fluorophenyl C-5), 68.6 (methoxyethyl C-2), 62.4 (C-4), 58.6 (methoxyethyl C-4), 48.8 (methoxyethyl C-1), 41.2 (4-methyl) and 37.9 (acetaldehyde C-1); HRMS found  $\text{MH}^+$ , 309.1310.  $\text{C}_{15}\text{H}_{17}\text{FN}_2\text{O}_4$  requires  $\text{MH}$ , 309.1250.

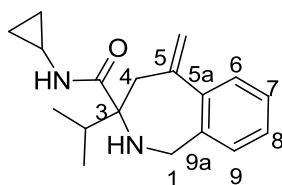
**5-[(4-Fluorophenyl)methyl]-5-(2-hydroxyethyl)-3-(2-methoxyethyl)imidazolidine-2,4-dione, **205****



$\text{NaBH}_4$  (9.23 mg, 0.244 mmol) was added to a solution of the aldehyde **204** (37.7 mg, 0.122 mmol) in MeOH (1.22 mL, 0.1 M) at 0 °C. The reaction mixture was stirred at room temperature overnight before the solvent was removed *in vacuo* and the residue was treated with water (2 mL). The aqueous layer was extracted with EtOAc (3 × 2 mL) and the combined organic phases were dried ( $\text{MgSO}_4$ ) and concentrated *in vacuo*. The crude residue was purified by flash chromatography ( $\text{SiO}_2$ , 5:95 MeOH–DCM) to yield the

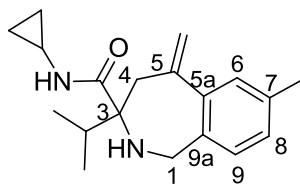
*alcohol* **205** (25.9 mg, 68%) as a yellow oil,  $R_f = 0.57$  (10:90 MeOH–DCM);  $\nu_{\max}/\text{cm}^{-1}$  (ATR) 3288 (br), 2927, 1697, 1509, 1449, 1221, 1115 and 1051;  $\delta_{\text{H}}$  (500 MHz,  $\text{CDCl}_3$ ) 7.07 (2H, dd,  $J$  8.4 and 5.5, fluorophenyl 2-H and fluorophenyl 6-H), 6.89 (2H, app t,  $J$  8.4, fluorophenyl 3-H and fluorophenyl 5-H), 6.17 (1H, s, NH), 3.83–3.64 (2H, m, hydroxyethyl 2-H<sub>2</sub>), 3.48–3.36 (2H, m, methoxyethyl 2-H<sub>2</sub>), 3.32–3.20 (2H, m, methoxyethyl 1-H<sub>2</sub>), 3.17 (3H, s, methoxyethyl 4-H<sub>3</sub>), 2.99 (1H, d,  $J$  13.7, 5-methyl-H<sub>a</sub>), 2.89 (1H, d,  $J$  13.7, 5-methyl-H<sub>b</sub>), 2.16 (1H, ddd,  $J$  14.7, 9.1 and 5.0, hydroxyethyl 1-H<sub>a</sub>), 1.88 (1H, dt,  $J$  14.7 and 4.3, hydroxyethyl 1-H<sub>b</sub>) and 1.66 (1H, s, OH);  $\delta_{\text{C}}$  (126 MHz,  $\text{CDCl}_3$ ) 175.9 (C-4), 162.2 (d,  $J$  246.0, fluorophenyl C-4), 156.8 (C-2), 131.9 (d,  $J$  8.0, fluorophenyl C-2 and fluorophenyl C-6), 129.7 (d,  $J$  3.4, fluorophenyl C-1), 115.3 (d,  $J$  21.3 fluorophenyl C-3 and fluorophenyl C-5), 68.6 (hydroxyethyl C-2), 64.8 (C-5), 58.6 (methoxyethyl C-4), 58.1 (methoxyethyl C-2), 41.6 (methoxyethyl C-1), 38.5 (5-methyl) and 37.6 (hydroxyethyl C-1);  $\delta_{\text{F}}$  (282 MHz,  $\text{CDCl}_3$ ) –115.2; HRMS found  $\text{MH}^+$ , 311.1417.  $\text{C}_{15}\text{H}_{19}\text{FN}_2\text{O}_4$  requires  $MH$ , 311.1407.

***N*-Cyclopropyl-5-methylidene-3-(propan-2-yl)-2,3,4,5-tetrahydro-1*H*-2-benzazepine-3-carboxamide, **211****



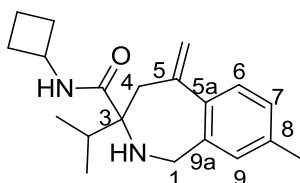
By general procedure V, the amino ester **199** (394 mg, 1.52 mmol) and cyclopropylamine (1.05 mL, 15.2 mmol) gave a crude residue which was purified by flash chromatography ( $\text{SiO}_2$ , 60:40 Petrol–EtOAc) to yield the *amide* **211** (200 mg, 46%) as a yellow oil,  $R_f = 0.47$  (50:50 Petrol–EtOAc);  $\nu_{\max}/\text{cm}^{-1}$  (ATR) 3336 (br), 2963, 2929, 1660, 1504, 1455 and 773;  $\delta_{\text{H}}$  (500 MHz,  $\text{CDCl}_3$ ) 7.54–7.46 (2H, m, 9-H and NH), 7.21 (2H, app dt,  $J$  19.1 and 7.3, 7-H and 8-H), 7.05 (1H, d,  $J$  7.3, 6-H), 5.47 (1H, s, alkene-H<sub>a</sub>), 5.14 (1H, s, alkene-H<sub>b</sub>), 4.12 (1H, d,  $J$  16.5, 1-H<sub>a</sub>), 3.94 (1H, d,  $J$  16.5, 1-H<sub>b</sub>), 3.05–2.94 (2H, m, 4-H<sub>2</sub>), 2.76–2.65 (1H, m, cyclopropyl 1-H), 2.11 (1H, hept, 6.9, isopropyl 2-H), 1.76 (1H, s, NH), 1.08 (3H, d,  $J$  6.9, isopropyl-Me<sub>A</sub>), 0.99 (3H, d,  $J$  6.9, isopropyl-Me<sub>B</sub>), 0.83–0.68 (2H, m, cyclopropyl 2-H<sub>2</sub>) and 0.49–0.37 (2H, m, cyclopropyl 3-H<sub>2</sub>);  $\delta_{\text{C}}$  (126 MHz,  $\text{CDCl}_3$ ) 175.4 (CO), 144.2 (C-5a), 140.0 (C-9a and C-5), 128.0 (C-9), 127.7 (C-7), 127.3 (C-8), 127.1 (C-6), 116.2 (alkene), 67.3 (C-3), 49.2 (C-1), 39.6 (C-4), 33.9 (cyclopropyl C-1), 22.1 (isopropyl C-2), 18.5 (isopropyl-Me<sub>A</sub>), 17.3 (isopropyl-Me<sub>B</sub>), 6.6 (cyclopropyl C-2) and 6.4 (cyclopropyl C-3); HRMS found  $\text{MH}^+$ , 285.1978.  $\text{C}_{18}\text{H}_{24}\text{N}_2\text{O}$  requires  $MH$ , 285.1967.

***N*-Cyclopropyl-7-methyl-5-methylidene-3-(propan-2-yl)-2,3,4,5-tetrahydro-1*H*-2-benzazepine-3-carboxamide, 288**



By general procedure V, the amino ester **279** (370 mg, 1.35 mmol) and cyclopropylamine (0.94 mL, 13.5 mmol) gave a crude residue which was purified by flash chromatography (SiO<sub>2</sub>, 50:50 Petrol–EtOAc) to yield the *amide* **288** (80.0 mg, 20%) as a colourless oil,  $R_f = 0.35$  (50:50 Petrol–EtOAc);  $\nu_{\max}/\text{cm}^{-1}$  (ATR) 3331 (br), 3086, 3010, 2963, 1661, 1496, 1457, 890 and 813;  $\delta_{\text{H}}$  (400 MHz, CDCl<sub>3</sub>) 7.41 (1H, br s, NH), 7.21 (1H, s, 6-H), 6.93–6.88 (1H, m, 8-H), 6.84 (1H, d,  $J$  7.7, 9-H), 5.37 (1H, d,  $J$  1.2, alkene-H<sub>a</sub>), 5.02 (1H, app s, alkene-H<sub>b</sub>), 3.97 (1H, d,  $J$  16.4, 1-H<sub>a</sub>), 3.79 (1H, d,  $J$  16.4, 1-H<sub>b</sub>), 2.90 (1H, d,  $J$  14.0, 4-H<sub>a</sub>), 2.86 (1H, d,  $J$  14.0, 4-H<sub>b</sub>), 2.65–2.55 (1H, m, cyclopropyl 1-H), 2.25 (3H, s, tolyl), 2.04–1.95 (1H, m, isopropyl 2-H), 1.54 (1H, br s, NH), 0.97 (3H, d,  $J$  6.9, isopropyl-Me<sub>A</sub>), 0.88 (3H, d,  $J$  6.9, isopropyl-Me<sub>B</sub>), 0.72–0.60 (2H, m, cyclopropyl 2-H<sub>2</sub>) and 0.38–0.29 (2H, m, cyclopropyl 3-H<sub>2</sub>);  $\delta_{\text{C}}$  (101 MHz, CDCl<sub>3</sub>) 175.5 (CO), 144.3 (C-5), 139.8 (C-9a), 136.6 (C-5a), 136.5 (C-7), 128.2 (C-6), 128.0 (C-9), 127.9 (C-8), 115.8 (alkene), 67.1 (C-3), 48.8 (C-1), 39.6 (C-4), 33.9 (isopropyl C-2), 22.0 (tolyl), 21.0 (cyclopropyl C-1), 18.5 (isopropyl-Me<sub>A</sub>), 17.2 (isopropyl-Me<sub>B</sub>), 6.6 (cyclopropyl C-2) and 6.3 (cyclopropyl C-3); HRMS found  $MH^+$ , 299.2137. C<sub>19</sub>H<sub>26</sub>N<sub>2</sub>O requires  $MH$ , 299.2123.

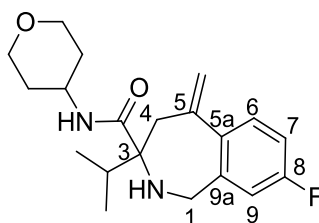
***N*-Cyclobutyl-8-methyl-5-methylidene-3-(propan-2-yl)-2,3,4,5-tetrahydro-1*H*-2-benzazepine-3-carboxamide, 289**



By general procedure V, the amino ester **280** (480 mg, 1.76 mmol) and cyclobutylamine (1.50 mL, 17.6 mmol) gave a crude residue which was purified by flash chromatography (SiO<sub>2</sub>, 60:40 Petrol–EtOAc) to yield the *amide* **289** (210 mg, 38%) as an amorphous orange solid,  $R_f = 0.72$  (50:50 Petrol–EtOAc);  $\nu_{\max}/\text{cm}^{-1}$  (ATR) 3331 (br), 2966, 2939, 2873, 1656, 1498, 896 and 728;  $\delta_{\text{H}}$  (400 MHz, CDCl<sub>3</sub>) 7.61 (1H, d,  $J$  8.5, NH), 7.38 (1H, d,  $J$  7.9, 6-H), 7.03 (1H, d,  $J$  7.9, 7-H), 6.88 (1H, s, 9-H), 5.43 (1H, d,  $J$  1.5, alkene-H<sub>a</sub>), 5.05 (1H, d,  $J$  1.5, alkene-H<sub>b</sub>), 4.37 (1H, h,  $J$  8.2, cyclobutyl 1-H), 4.08 (1H, d,  $J$  16.6, 1-H<sub>a</sub>),

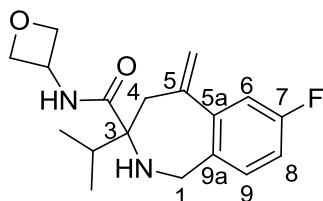
3.92 (1H, d, *J* 16.6, 1-H<sub>b</sub>), 3.00 (1H, d, *J* 14.0, 4-H<sub>a</sub>), 2.91 (1H, d, *J* 14.0, 4-H<sub>b</sub>), 2.41-2.26 (5H, m, tolyl and cyclobutyl 2-H<sub>2</sub>), 2.08 (1H, hept, *J* 6.9, isopropyl 2-H), 1.92-1.76 (2H, m, cyclobutyl 4-H<sub>2</sub>), 1.75-1.62 (3H, m, cyclobutyl 3-H<sub>2</sub> and NH), 1.06 (3H, d, *J* 6.9, isopropyl Me<sub>A</sub>) and 1.00 (3H, d, *J* 6.9, isopropyl-Me<sub>B</sub>);  $\delta_c$  (101 MHz, CDCl<sub>3</sub>) 172.9 (CO), 144.0 (C-5), 139.5 (C-9a), 137.1 (C-8), 137.0 (C-5a), 128.6 (C-6), 127.7 (C-7), 127.6 (C-9), 115.3 (alkene), 67.0 (C-3), 49.1 (C-1), 44.2 (cyclobutyl C-1), 39.7 (C-4), 33.7 (isopropyl C-2), 31.37 (cyclobutyl C-2), 31.35 (cyclobutyl C-4), 20.9 (tolyl), 18.6 (isopropyl-Me<sub>A</sub>), 17.3 (isopropyl-Me<sub>B</sub>) and 15.2 (cyclobutyl C-3); HRMS found MH<sup>+</sup>, 313.2279. C<sub>20</sub>H<sub>28</sub>N<sub>2</sub>O requires *MH*, 313.2280.

***N*-Tetrahydropyran-8-fluoro-5-methylidene-3-(propan-2-yl)-2,3,4,5-tetrahydro-1*H*-2-benzazepine-3-carboxamide, **290****



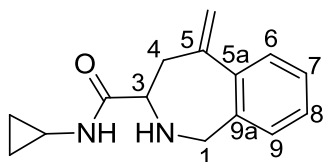
By general procedure V, the amino ester **281** (470 mg, 1.69 mmol) and 4-aminotetrahydropyran (1.75 mL, 16.9 mmol) gave a crude residue which was purified by flash chromatography (SiO<sub>2</sub>, 40:60 Petrol–EtOAc) to yield the *amide* **290** (420 mg, 72%) as a colourless oil, *R*<sub>f</sub> = 0.23 (50:50 Petrol–EtOAc);  $\nu_{\max}/\text{cm}^{-1}$  (ATR) 3326 (br), 3083, 2958, 2846, 1656, 1493, 1142 and 731;  $\delta_H$  (400 MHz, CDCl<sub>3</sub>) 7.43 (1H, dd, *J* 8.6 and 5.8, 9-H), 7.39 (1H, d, *J* 8.4, NH), 6.91 (1H, td, *J* 8.6 and 2.6, 7-H), 6.76 (1H, dd, *J* 8.6 and 2.6, 6-H), 5.40 (1H, d, *J* 1.0, alkene-H<sub>a</sub>), 5.09 (1H, app s, alkene-H<sub>b</sub>), 4.08 (1H, d, *J* 16.6, 1-H<sub>a</sub>), 4.02-3.87 (4H, m, 1-H<sub>b</sub>, THP 1-H and THP 3-H<sub>2</sub>), 3.56-3.44 (2H, m, THP 5-H<sub>2</sub>), 2.99 (1H, d, *J* 14.1, 4-H<sub>a</sub>), 2.94 (1H, d, *J* 14.1, 4-H<sub>b</sub>), 2.14-2.07 (1H, m, isopropyl 2-H), 1.92-1.85 (1H, m, THP 2-H<sub>a</sub>), 1.84-1.76 (1H, m, THP 2-H<sub>b</sub>), 1.69 (1H, br s, NH), 1.55-1.39 (2H, m, THP 6-H<sub>2</sub>), 1.06 (3H, d, *J* 6.9, isopropyl-Me<sub>A</sub>) and 1.00 (3H, d, *J* 6.9, isopropyl-Me<sub>B</sub>);  $\delta_c$  (101 MHz, CDCl<sub>3</sub>) 172.8 (CO), 160.6 (C-8), 143.3 (C-5), 141.5 (d, *J* 6.2, C-9a), 136.1 (d, *J* 3.3, C-5a), 129.4 (d, *J* 7.9, C-6), 116.0 (alkene), 114.4 (d, *J* 21.2, C-7), 113.8 (d, *J* 21.1, C-9), 67.1 (C-3), 66.8 (THP C-3), 60.4 (THP C-5), 48.9 (C-1), 45.1 (THP C-1), 39.6 (C-4), 33.8 (isopropyl C-2), 33.5 (THP C-2), 33.2 (THP C-6), 18.5 (isopropyl-Me<sub>A</sub>) and 17.2 (isopropyl-Me<sub>B</sub>);  $\delta_F$  (376 MHz, CDCl<sub>3</sub>) –115.8; HRMS found MH<sup>+</sup>, 347.2150. C<sub>20</sub>H<sub>27</sub>FN<sub>2</sub>O<sub>2</sub> requires *MH*, 347.2135.

**7-Fluoro-5-methylidene-N-(oxetan-3-yl)-3-(propan-2-yl)-2,3,4,5-tetrahydro-1H-2-benzazepine-3-carboxamide, 291**



By general procedure V, the amino ester **282** (500 mg, 1.80 mmol) and 4-aminooxetane (1.26 mL, 18.0 mmol) gave a crude residue which was purified by flash chromatography (SiO<sub>2</sub>, 50:50 Petrol–EtOAc), then again (SiO<sub>2</sub>, 20:80 Petrol–EtOAc) to yield the *amide* **291** (210 mg, 37%) as a colourless oil,  $R_f = 0.24$  (40:60 Petrol–EtOAc);  $\nu_{\max}/\text{cm}^{-1}$  (ATR) 3323 (br), 2962, 2876, 1659, 1491, 1206, 974 and 875;  $\delta_{\text{H}}$  (400 MHz, CDCl<sub>3</sub>) 8.05 (1H, d,  $J$  7.7, NH), 7.17 (1H, dd,  $J$  9.2 and 2.7, 9-H), 7.03 (1H, dd,  $J$  9.2 and 5.8, 6-H), 6.89 (1H, td,  $J$  9.2 and 2.7, 8-H), 5.46 (1H, d,  $J$  1.2, alkene-H<sub>a</sub>), 5.15–5.11 (1H, m, alkene-H<sub>b</sub>), 5.07–4.97 (1H, m, oxetanyl 3-H), 4.95 (1H, t,  $J$  6.9, oxetanyl 2-H<sub>a</sub>), 4.91 (1H, t,  $J$  6.9, oxetanyl 2-H<sub>b</sub>), 4.50 (1H, t,  $J$  6.2, oxetanyl 4-H<sub>a</sub>), 4.41 (1H, t,  $J$  6.2, oxetanyl 4-H<sub>b</sub>), 4.19–4.11 (1H, m, 1-H<sub>a</sub>), 3.93 (1H, d,  $J$  16.3, 1-H<sub>b</sub>), 3.00 (1H, dd,  $J$  14.1 and 0.9, 4-H<sub>a</sub>), 2.93 (1H, dd,  $J$  14.1 and 0.8, 4-H<sub>b</sub>), 2.18–2.09 (1H, m, isopropyl 2-H) and 1.03 (6H, t,  $J$  6.9, isopropyl-Me<sub>A</sub> and isopropyl-Me<sub>B</sub>);  $\delta_{\text{C}}$  (101 MHz, CDCl<sub>3</sub>) 173.8 (CO), 163.1 (C-7), 143.3 (d,  $J$  2.2, C-5a), 141.8 (C-5), 134.9 (d,  $J$  3.0, C-9a), 129.6 (d,  $J$  8.1, C-9), 117.1 (alkene), 114.2 (d,  $J$  8.2, C-6), 113.9 (d,  $J$  7.5, C-8), 78.80 (oxetanyl C-7), 78.75 (oxetanyl C-4), 67.3 (C-3), 48.5 (C-1), 44.3 (oxetanyl C-3), 39.3 (C-4), 34.0 (isopropyl C-2), 18.4 (isopropyl-Me<sub>A</sub>) and 17.2 (isopropyl-Me<sub>B</sub>);  $\delta_{\text{F}}$  (376 MHz, CDCl<sub>3</sub>) –116.2; HRMS found MH<sup>+</sup>, 319.1836. C<sub>18</sub>H<sub>23</sub>FN<sub>2</sub>O<sub>2</sub> requires *MH*, 319.1822.

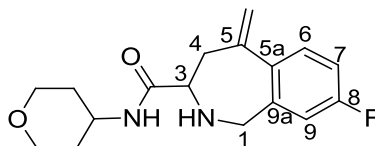
**N-Cyclopropyl-5-methylidene-2,3,4,5-tetrahydro-1H-2-benzazepine-3-carboxamide, 292**



By general procedure V, the amino ester **284** (140 mg, 0.640 mmol) and cyclopropylamine (0.44 mL, 6.40 mmol) gave a crude residue which was purified by flash chromatography (SiO<sub>2</sub>, 100% EtOAc) to yield the *amide* **292** (60.0 mg, 39%) as a red oil,  $R_f = 0.50$  (10:90 MeOH–EtOAc);  $\nu_{\max}/\text{cm}^{-1}$  (ATR) 3286 (br), 3065, 3011, 2926, 2852, 1651, 1509, 904, 773 and 729;  $\delta_{\text{H}}$  (400 MHz, CDCl<sub>3</sub>) 7.32 (1H, dd,  $J$  7.3 and 1.6, 9-H), 7.27 (1H, br

s, NH), 7.18-7.08 (2H, m, 7-H and 8-H), 6.99 (1H, dd, *J* 7.5 and 1.3, 6-H), 5.22 (1H, d, *J* 1.5, alkene-H<sub>a</sub>), 5.10 (1H, d, *J* 0.7, alkene-H<sub>b</sub>), 3.90 (2H, s, 1-H<sub>2</sub>), 3.49 (1H, dd, *J* 9.5 and 4.8, 3-H), 3.10 (1H, dd, *J* 13.9 and 4.8, 4-H<sub>a</sub>), 2.70-2.61 (1H, m, cyclopropyl 1-H), 2.56 (1H, dd, *J* 13.9 and 9.5, 4-H<sub>b</sub>), 1.74 (1H, br s, NH), 0.72-0.66 (2H, m, cyclopropyl 2-H<sub>2</sub>) and 0.44-0.38 (2H, m, cyclopropyl 3-H<sub>2</sub>);  $\delta_c$  (101 MHz, CDCl<sub>3</sub>) 174.4 (CO), 146.6 (C-5), 141.3 (C-9a), 138.8 (C-5a), 128.2 (C-9), 128.0 (C-8), 127.4 (C-7), 127.3 (C-6), 115.7 (alkene), 62.7 (C-3), 51.1 (C-1), 38.8 (C-4), 22.2 (cyclopropyl C-1), 6.5 (cyclopropyl C-2) and 6.3 (cyclopropyl C-3); HRMS found MH<sup>+</sup>, 243.1507. C<sub>15</sub>H<sub>18</sub>N<sub>2</sub>O requires *MH*, 243.1497.

**8-Fluoro-5-methylene-*N*-(tetrahydro-2*H*-pyran-4-yl)-2,3,4,5-tetrahydro-1*H*-benzo[*c*]azepine-3-carboxamide, 294**

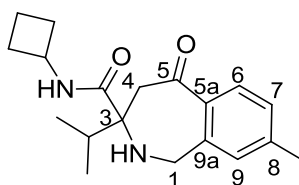


By general procedure V, the amino ester **286** (300 mg, 1.28 mmol) and 4-aminotetrahydropyran (1.00 g, 9.89 mmol) gave a crude residue which was purified by flash chromatography (SiO<sub>2</sub>, 10:90 to 20:80 MeOH–EtOAc) to yield the *amide* **294** (70.9 mg, 18%) as a yellow oil, *R<sub>f</sub>* = 0.18 (10:90 MeOH–EtOAc);  $\nu_{\max}$ / cm<sup>-1</sup> (ATR) 3307 (br), 2927, 2847, 1655, 1513, 1493 and 1140;  $\delta_H$  (400 MHz, CDCl<sub>3</sub>) 7.34 (1 H, dd, *J* 8.8 and 5.7, 9-H), 7.23 (1 H, br s, NH), 6.89 (1 H, td, *J* 8.8 and 2.7, 7-H), 6.77 (1 H, dd, *J* 8.8 and 2.7, 6-H), 5.24 (1 H, d, *J* 1.5, alkene-H<sub>a</sub>), 5.14 (1 H, app s, alkene-H<sub>b</sub>), 4.01-3.86 (5 H, m, 1-H<sub>2</sub>, THP 1-H and THP 2-H<sub>2</sub>), 3.57 (1 H, dd, *J* 9.2 and 4.9, 3-H), 3.52-3.39 (2 H, m, THP 6-H<sub>2</sub>), 3.14 (1 H, dd, *J* 13.9 and 4.9, 4-H<sub>a</sub>), 2.60 (1 H, dd, *J* 13.9 and 9.2, 4-H<sub>b</sub>), 1.95 (1 H, br s, NH), 1.91-1.77 (2 H, m, THP 3-H<sub>2</sub>) and 1.57-1.35 (2 H, m, THP 5-H<sub>2</sub>);  $\delta_c$  (101 MHz, CDCl<sub>3</sub>) 172.0 (CO), 161.9 (d, *J* 246.8, C-8), 145.5 (C-5), 141.0 (d, *J* 6.5, C-9a), 137.1 (d, *J* 3.2, C-5a), 130.0 (d, *J* 7.6, C-9), 115.7 (alkene), 114.6 (d, *J* 21.7, C-7), 113.9 (d, *J* 20.7, C-6), 66.8 (THP C-2 and THP C-6), 62.4 (THP C-4), 50.7 (C-1), 45.2 (C-3), 38.8 (C-4), 33.2 (THP C-3) and 33.1 (THP C-5); HRMS found MH<sup>+</sup>, 305.1683. C<sub>17</sub>H<sub>21</sub>FN<sub>2</sub>O<sub>2</sub> requires *MH*, 305.1665.



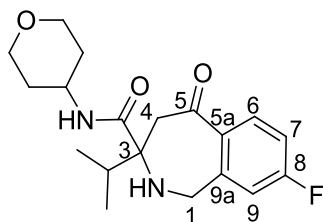
6-H<sub>a</sub>), 3.77 (1H, d, *J* 15.1, 6-H<sub>b</sub>), 2.37 (3H, s, tolyl), 2.35-2.29 (1H, m, OH), 2.19-2.10 (2H, m, 11-H<sub>2</sub>), 2.10-2.05 (1H, m, isopropyl 2-H), 1.06-0.99 (1H, m, cyclopropyl 1-H), 0.98-0.93 (6H, m, isopropyl-Me<sub>A</sub> and isopropyl-Me<sub>B</sub>) and 0.70-0.46 (4H, m, cyclopropyl 2-H<sub>2</sub> and cyclopropyl 3-H<sub>2</sub>);  $\delta_C$  (101 MHz, CDCl<sub>3</sub>) 199.0 (C-1<sub>open</sub>), 176.3 (C-3), 141.9 (C-10a), 137.1 (C-6a), 132.54 (C-9), 130.6 (C-7), 128.6 (C-8), 125.4 (C-10), 90.0 (C-1<sub>closed</sub>), 68.1 (C-4), 50.7 (C-6), 45.6 (C-11), 32.4 (isopropyl C-2), 22.0 (tolyl), 21.3 (cyclopropyl C-1), 18.7 (isopropyl-Me<sub>A</sub>), 16.5 (isopropyl-Me<sub>B</sub>), 4.3 (cyclopropyl C-2) and 3.7 (cyclopropyl C-3); HRMS found MH<sup>+</sup>, 301.1926. C<sub>18</sub>H<sub>24</sub>N<sub>2</sub>O<sub>2</sub> requires *MH*, 301.1916.

***N*-Cyclobutyl-3-isopropyl-8-methyl-5-oxo-2,3,4,5-tetrahydro-1*H*-benzo[*c*]azepine-3-carboxamide, 214ba**



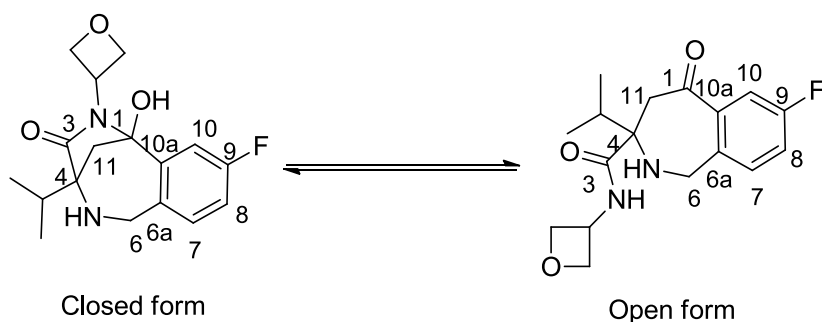
By general procedure X, alkene **289** (210 mg, 0.670 mmol) gave a crude residue which was purified by flash chromatography (SiO<sub>2</sub>, 40:60 Petrol–EtOAc) to give the *ketone* **214ba** (140 mg, 66%,  $\geq$  98% open form) as an amorphous orange solid, *R<sub>f</sub>* = 0.54 (30:70 Petrol–EtOAc);  $\nu_{max/}$  cm<sup>-1</sup> (ATR) 3332 (br), 2967, 2874, 1671, 1606, 1508 and 1298;  $\delta_H$  (400 MHz, CDCl<sub>3</sub>) 7.88 (1H, d, *J* 7.9, 6-H), 7.61 (1H, d, *J* 8.6, NH), 7.18 (1H, d, *J* 7.9, 7-H), 7.08-7.03 (1H, m, 9-H), 4.29-4.16 (2H, m, alkene-H<sub>a</sub> and cyclobutyl 1-H), 4.09 (1H, d, *J* 15.8, alkene-H<sub>b</sub>), 3.38 (1H, d, *J* 14.5, 1-H<sub>a</sub>), 3.18 (1H, d, *J* 14.5, 1-H<sub>b</sub>), 2.40 (3H, s, tolyl), 2.35-2.23 (1H, m, cyclobutyl 2-H<sub>a</sub>), 2.22-2.13 (1H, m, cyclobutyl 2-H<sub>b</sub>), 2.00-1.89 (1H, m, isopropyl 2-H), 1.84-1.75 (1H, m, cyclobutyl 3-H<sub>a</sub>), 1.73-1.60 (3H, m, cyclobutyl 3-H<sub>b</sub> and cyclobutyl 4-H<sub>2</sub>), 1.04 (3H, d, *J* 6.9, isopropyl-Me<sub>A</sub>) and 0.96 (3H, d, *J* 6.9, isopropyl-Me<sub>B</sub>);  $\delta_C$  (101 MHz, CDCl<sub>3</sub>) 199.3 (C-5), 172.4 (CO), 143.4 (C-9a), 143.3 (C-8), 134.6 (C-5a), 129.6 (C-6), 129.4 (C-7), 128.5 (C-9), 64.9 (C-3), 49.6 (C-1), 47.8 (C-4), 44.2 (cyclobutyl C-1), 36.1 (isopropyl C-2), 31.2 (cyclobutyl C-2), 31.1 (cyclobutyl C-4), 21.5 (tolyl), 18.3 (isopropyl-Me<sub>A</sub>), 17.2 (isopropyl-Me<sub>B</sub>) and 15.1 (cyclobutyl C-3); HRMS found MH<sup>+</sup>, 315.2089. C<sub>19</sub>H<sub>26</sub>N<sub>2</sub>O<sub>2</sub> requires *MH*, 315.2072.

**8-Fluoro-3-isopropyl-5-oxo-*N*-(tetrahydro-2*H*-pyran-4-yl)-2,3,4,5-tetrahydro-1*H*-benzo[*c*]azepine-3-carboxamide, 214ca**



By general procedure X, alkene **290** (420 mg, 1.21 mmol) gave a crude residue which was purified by flash chromatography (SiO<sub>2</sub>, 40:60 Petrol–EtOAc) to give the *ketone* **214ca** (350 mg, 83%,  $\geq$  98% open form) as a brown oil,  $R_f$  = 0.35 (20:80 Petrol–EtOAc);  $\nu_{\max}$ / cm<sup>-1</sup> (ATR) 3330 (br), 2960, 2848, 1672, 1509, 1250, 1089 and 729;  $\delta_H$  (400 MHz, CDCl<sub>3</sub>) 7.96 (1H, dd,  $J$  8.7 and 5.9, 6-H), 7.37 (1H, d,  $J$  8.2, NH), 7.02 (1H, td,  $J$  8.7 and 2.5, 7-H), 6.91 (1H, dd,  $J$  8.7 and 2.4, 9-H), 4.22 (1H, d,  $J$  15.7, 1-H<sub>a</sub>), 4.05 (1H, d,  $J$  15.7, 1-H<sub>b</sub>), 3.92-3.73 (3H, m, THP 1-H and THP 3-H<sub>2</sub>), 3.44-3.35 (2H, m, THP 5-H<sub>2</sub>), 3.33 (1H, d,  $J$  14.7, 4-H<sub>a</sub>), 3.17 (1H, d,  $J$  14.7, 4-H<sub>b</sub>), 2.01-1.93 (1H, m, isopropyl 2-H), 1.81-1.73 (1H, m, THP 2-H<sub>a</sub>), 1.57-1.48 (1H, m, THP 2-H<sub>b</sub>), 1.37 (1H, ddd,  $J$  23.8, 11.3 and 4.5, THP 6-H<sub>a</sub>), 1.00 (3H, d,  $J$  6.9, isopropyl-Me<sub>A</sub>), 0.95 (3H, d,  $J$  6.9, isopropyl-Me<sub>B</sub>) and 0.91-0.85 (1H, m, THP 6-H<sub>b</sub>);  $\delta_C$  (101 MHz, CDCl<sub>3</sub>) 197.8 (C-5), 172.6 (CO), 163.6 (C-8), 145.9 (C-9a), 133.5 (d,  $J$  2.9, C-5a), 132.5 (d,  $J$  9.4, C-6), 115.5 (d,  $J$  21.8, C-7), 115.0 (d,  $J$  21.3, C-9), 66.7 (THP C-3), 64.9 (C-3), 60.4 (THP C-5), 49.3 (C-1), 47.6 (C-4), 45.1 (THP C-1), 36.0 (isopropyl C-2), 33.2 (THP C-2), 32.9 (THP C-6), 18.1 (isopropyl-Me<sub>A</sub>) and 17.0 (isopropyl-Me<sub>B</sub>);  $\delta_F$  (376 MHz, CDCl<sub>3</sub>) -106.0; HRMS found MH<sup>+</sup>, 349.1934. C<sub>19</sub>H<sub>25</sub>FN<sub>2</sub>O<sub>3</sub> requires *MH*, 349.1927.

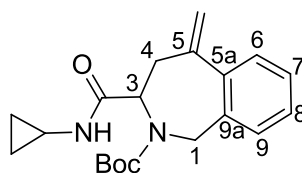
**9-Fluoro-1-hydroxy-4-isopropyl-2-(oxetan-3-yl)-1,2,5,6-tetrahydro-1,4-methanobenzo[*f*] [1,4]diazocin-3(4*H*)-one, 214f**



By general procedure X, alkene **291** (210 mg, 0.660 mmol) gave a crude residue which was purified by flash chromatography (SiO<sub>2</sub>, 50:50 to 10:90 Petrol–EtOAc) to yield the crude imine which was used as a mixture of ketone and hemiaminal. NaBH(OAc)<sub>3</sub>

(560 mg, 2.64 mmol) was added to a solution of the crude imine in DCM (6.60 mL, 0.1 M) and the reaction was stirred at room temperature overnight. Water (10 mL) was added and the aqueous layer was extracted with DCM (3 × 10 mL). The combined organic layers were washed with water (10 mL), brine (10 mL), dried (MgSO<sub>4</sub>) and concentrated *in vacuo*. The residue was purified by flash chromatography (SiO<sub>2</sub>, 10:90 Petrol–EtOAc to 10:90 MeOH–EtOAc) to give the *tetrahydrobenzazepine* **214f** (34.5 mg, 16% over two steps, 70:30 closed : open forms) as a yellow oil,  $R_f = 0.22$  (100% EtOAc);  $\nu_{\max}/\text{cm}^{-1}$  (ATR) 3322 (br), 2963, 2877, 1680, 1491, 1305, 1274 and 974;  $\delta_{\text{H}}$  (400 MHz, CDCl<sub>3</sub>) 8.00 (1H, d,  $J$  6.9, NH), 7.55 (1H, dd,  $J$  8.6, 2.8, 7-H<sub>open</sub>), 7.42 (1H, dd,  $J$  9.1 and 2.8, 7-H<sub>closed</sub>), 7.21-7.16 (1H, m, 10-H<sub>open</sub>), 7.11 (1H, dd,  $J$  8.6 and 2.8, 8-H<sub>open</sub>), 7.06 (1H, dd,  $J$  9.1 and 5.6, 10-H<sub>closed</sub>), 6.85 (1H, td,  $J$  9.1 and 2.8, 8-H<sub>closed</sub>), 5.06 (1H, dd,  $J$  7.5 and 6.1, oxetanyl 2-H<sub>a</sub>), 4.99 (1H, dd,  $J$  7.5 and 6.2, oxetanyl 2-H<sub>b</sub>), 4.85-4.76 (2H, m, oxetanyl 3-H<sub>open</sub>), 4.69-4.59 (1H, m, oxetanyl 3-H<sub>closed</sub>), 4.56-4.40 (2H, m, oxetanyl 4-H<sub>2closed</sub>), 4.15-3.98 (2 H, m, oxetanyl 4-H<sub>2open</sub>), 3.88 (1H, d,  $J$  15.4, 6-H<sub>a</sub> closed), 3.77 (1H, d,  $J$  15.4, 6-H<sub>b</sub> closed), 3.28 (1H, d,  $J$  14.7, 6-H<sub>a</sub> open), 3.12 (1H, d,  $J$  14.7, 6-H<sub>b</sub> open), 2.12 (2H, s, 11-H<sub>2</sub> closed), 2.07-2.00 (1H, m, isopropyl 2-H closed), 1.98 (2H, s, 11-H<sub>2</sub> open), 1.95-1.85 (1H, m, isopropyl 2-H open), 0.94 (3H, d,  $J$  6.9, isopropyl-Me<sub>A</sub> open), 0.93-0.88 (6 H, m, isopropyl-Me<sub>A</sub> closed and isopropyl-Me<sub>B</sub> closed) and 0.87-0.72 (3H, m, isopropyl-Me<sub>B</sub> open);  $\delta_{\text{C}}$  (101 MHz, CDCl<sub>3</sub>) 175.3 (C-3), 160.3 (d,  $J$  107.8, C-9), 143.7 (d,  $J$  6.6, C-10a), 132.2 (d,  $J$  7.6, C-7 closed), 131.3 (d,  $J$  3.4, C-7 open), 130.8 (d,  $J$  7.4, C-6a), 119.6 (d,  $J$  21.8, C-10 open), 115.8 (d,  $J$  22.6, C-8 open), 114.7 (d,  $J$  21.0, C-10 closed), 113.0 (d,  $J$  24.2, C-8 closed), 78.6 (oxetanyl C-2 open), 78.4 (oxetanyl C-4 open), 75.6 (oxetanyl C-2 closed), 75.2 (oxetanyl C-4 closed), 68.6 (C-4 closed), 65.0 (C-4 open), 50.3 (C-6 closed), 48.7 (C-6 open), 47.3 (C-11 open), 46.4 (C-11 closed), 46.1 (oxetanyl C-1 closed), 44.3 (oxetanyl C-1 open), 36.1 (isopropyl C-2 open), 32.3 (isopropyl C-2 closed), 18.7 (isopropyl-Me<sub>A</sub> closed), 18.1 (isopropyl-Me<sub>A</sub> open), 17.1 (isopropyl-Me<sub>B</sub> open) and 16.5 (isopropyl-Me<sub>B</sub> closed); numbering of the compound has been completed using the closed major form;  $\delta_{\text{F}}$  (282 MHz, CDCl<sub>3</sub>) – 113.5 and –113.8; HRMS found MH<sup>+</sup>, 321.1622. C<sub>17</sub>H<sub>21</sub>FN<sub>2</sub>O<sub>3</sub> requires *MH*, 321.1614.

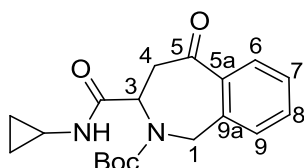
***tert*-Butyl 3-(cyclopropylcarbamoyl)-5-methylidene-2,3,4,5-tetrahydro-1H-2-benzazepine-2-carboxylate, 295**



Boc<sub>2</sub>O (28.4 mg, 0.130 mmol) was added to a solution of amine **292** (30.0 mg, 0.124 mmol) in DCM (1.24 mL, 0.1 M), and the resulting solution was stirred at room

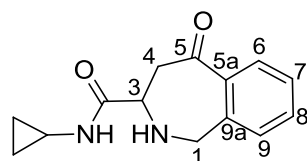
temperature overnight before being concentrated *in vacuo*. The residue was purified by flash chromatography (SiO<sub>2</sub>, 30:70 Petrol–EtOAc) to give the protected *tetrahydrobenzazepine* **295** (29.7 mg, 70%) as a colourless oil, *R<sub>f</sub>* = 0.62 (30:70 Petrol–EtOAc);  $\nu_{\max}/\text{cm}^{-1}$  (ATR) 3305 (br), 3066, 3007, 2976, 2929, 1692, 1659, 1538, 1411 and 1162;  $\delta_{\text{H}}$  (400 MHz, CDCl<sub>3</sub>, 333 K) 7.44 (1H, d, *J* 6.8, 9-H), 7.25–7.15 (2H, m, 7-H and 8-H), 7.09 (1H, d, *J* 6.5, 6-H), 6.45 (1H, br s, NH), 5.36 (1H, s, alkene-H<sub>a</sub>), 5.18 (1H, s, alkene-H<sub>b</sub>), 4.68 (1H, dd, *J* 10.9 and 6.0, 3-H), 4.55 (1H, d, *J* 16.5, 1-H<sub>a</sub>), 4.40 (1H, d, *J* 16.5, 1-H<sub>b</sub>), 3.15–2.84 (2H, m, 4-H<sub>2</sub>), 2.78–2.65 (1H, m, cyclopropyl 1-H), 1.38 (2H, s, Boc, rotamer A), 1.26 (7H, s, Boc, rotamer B), 0.78 (2H, d, *J* 6.8, cyclopropyl 2-H<sub>2</sub>) and 0.59–0.38 (2H, m, cyclopropyl 3-H<sub>2</sub>);  $\delta_{\text{C}}$  (101 MHz, CDCl<sub>3</sub>) 188.4 (Boc), 172.3 (CO), 144.5 (C-5), 139.1 (C-9a), 136.5 (C-5a), 128.0 (C-9), 127.8 (C-8), 127.4 (C-7), 127.3 (C-6), 116.5 (alkene), 80.8 (Boc), 59.7 (C-3), 48.3 (C-1), 35.7, (C-4) 28.1 (Boc), 22.5 (cyclopropyl C-1) and 6.6 (cyclopropyl C-2 and cyclopropyl C-3); HRMS found MH<sup>+</sup>, 343.2009. C<sub>20</sub>H<sub>26</sub>N<sub>2</sub>O<sub>3</sub> requires *MH*, 343.2021.

***tert*-Butyl 3-(cyclopropylcarbamoyl)-5-oxo-4,5-dihydro-1*H*-benzo[*c*]azepine-2(3*H*)-carboxylate, 214ka**



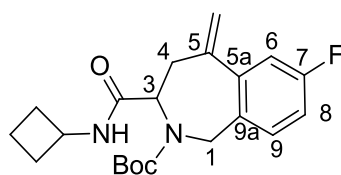
By general procedure U, alkene **295** (161 mg, 0.47 mmol) gave a crude residue which was purified by flash chromatography (SiO<sub>2</sub>, 30:70 Petrol–EtOAc) then again (SiO<sub>2</sub>, 50:50 Petrol–EtOAc) to give the *ketone* **214ka** (110 mg, 68%) as a yellow oil, *R<sub>f</sub>* = 0.47 (30:70 Petrol–EtOAc);  $\nu_{\max}/\text{cm}^{-1}$  (ATR) 3305 (br), 2976, 2932, 1662, 1392, 1366, 1156 and 730;  $\delta_{\text{H}}$  (501 MHz, CDCl<sub>3</sub>) 7.97 (1H, d, *J* 7.6, 9-H), 7.47 (1H, td, *J* 7.6 and 1.4, 8-H), 7.38 (1H, t, *J* 7.6, 7-H), 7.34–7.28 (1H, m, 6-H), 4.91–4.69 (2H, m, 1-H<sub>a</sub> and 3-H), 4.62 (1H, d, *J* 10.2, 1-H<sub>b</sub>), 3.59 (1H, t, *J* 13.5, 4-H<sub>a</sub>), 3.01 (1H, dd, *J* 13.5 and 4.6, 4-H<sub>b</sub>), 2.80–2.69 (1H, m, cyclopropyl 1-H), 1.35 (9H, s, Boc), 0.83–0.71 (2H, m, cyclopropyl 2-H<sub>2</sub>) and 0.58–0.39 (2H, m, cyclopropyl 3-H<sub>2</sub>);  $\delta_{\text{C}}$  (101 MHz, CDCl<sub>3</sub>) 198.6 (C-5), 171.3 (CO), 155.4 (Boc), 141.6 (C-5a), 132.5 (C-9a), 129.4 (C-9), 129.3 (C-8), 128.6 (C-7), 127.9 (C-6), 81.5 (Boc), 53.6 (C-3), 48.1 (C-1), 28.1 (C-4), 23.8 (Boc), 22.6 (cyclopropyl C-1) and 6.7 (cyclopropyl C-2 and cyclopropyl C-3); HRMS found MH<sup>+</sup>, 345.1802. C<sub>19</sub>H<sub>24</sub>N<sub>2</sub>O<sub>4</sub> requires *MH*, 345.1814.

***N*-Cyclopropyl-5-oxo-2,3,4,5-tetrahydro-1*H*-benzo[*c*]azepine-3-carboxamide, 214ga**



By general procedure Y, the protected hemiaminal **214ka** (50.0 mg, 0.150 mmol) gave a crude residue which was purified by flash chromatography (SiO<sub>2</sub>, 5:95 MeOH–EtOAc) to give the *ketone* **214ga** (22.1 mg, 60%, ≥ 98% open form) as a yellow oil, *R<sub>f</sub>* = 0.73 (20:80 MeOH–EtOAc);  $\nu_{\max}$ / cm<sup>-1</sup> (ATR) 3315 (br), 3009, 2925, 2854, 1673, 1513, 1284 and 770;  $\delta_{\text{H}}$  (400 MHz, CDCl<sub>3</sub>) 7.82–7.78 (1H, m, 9-H), 7.39 (1H, t, *J* 7.5, 8-H), 7.35 (1H, br s, NH), 7.31 (1H, td, *J* 7.5 and 0.9, 7-H), 7.15 (1H, d, *J* 7.5, 6-H), 4.09 (1H, d, *J* 16.1, 1-H<sub>a</sub>), 4.04 (1H, d, *J* 16.1, 1-H<sub>b</sub>), 3.67 (1H, dd, *J* 9.9 and 4.4, 3-H), 3.25 (1H, dd, *J* 14.7 and 4.4, 4-H<sub>a</sub>), 3.09 (1H, dd, *J* 14.7 and 9.9, 4-H<sub>b</sub>), 2.61 (1H, tq, *J* 7.4 and 3.8, cyclopropyl 1-H), 1.89 (1H, br s, NH), 0.73–0.63 (2H, m, cyclopropyl 2-H<sub>2</sub>) and 0.43–0.26 (2H, m, cyclopropyl 3-H<sub>2</sub>);  $\delta_{\text{C}}$  (101 MHz, CDCl<sub>3</sub>) 200.5 (C-5), 173.7 (CO), 142.2 (C-5a), 137.7 (C-9a), 132.5 (C-9), 129.2 (C-8), 128.5 (C-7), 127.9 (C-6), 55.7 (C-3), 49.2 (C-1), 44.5 (C-4), 22.3 (cyclopropyl C-1), 6.5 (cyclopropyl C-2) and 6.4 (cyclopropyl C-3); HRMS found MH<sup>+</sup>, 245.1283. C<sub>14</sub>H<sub>16</sub>N<sub>2</sub>O<sub>2</sub> requires *MH*, 245.1290.

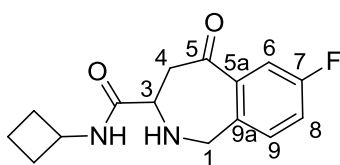
***tert*-Butyl 3-(cyclobutylcarbamoyl)-7-fluoro-5-methylene-4,5-dihydro-1*H*-benzo[*c*]azepine-2(3*H*)-carboxylate, 296**



By general procedure V, the amino ester **285** (170 mg, 0.720 mmol) and cyclobutylamine (0.610 mL, 7.20 mmol) gave a crude residue which was purified by flash chromatography (SiO<sub>2</sub>, 5:95 MeOH–EtOAc) and then again (SiO<sub>2</sub>, 5:95 MeOH–EtOAc) to yield the crude amide. Boc<sub>2</sub>O (50.4 mg, 0.231 mmol) was added to a solution of crude amide (59.2 mg, 0.22mmol) in DCM (2.20 mL, 0.1 M), and the resulting mixture was stirred at room temperature overnight before being concentrated *in vacuo*. The residue was purified by flash chromatography (SiO<sub>2</sub>, 20:80 Petrol–EtOAc) to give the protected *tetrahydrobenzazepine* **296** (82.0 mg, 31% over two steps) as a colourless oil, *R<sub>f</sub>* = 0.79 (10:90 Petrol–EtOAc);  $\nu_{\max}$ / cm<sup>-1</sup> (ATR) 3312 (br), 2978, 2939, 1657, 1368, 1212, 1161, 1118 and 1070;  $\delta_{\text{H}}$  (400 MHz, CDCl<sub>3</sub>, 333K) 7.05 (1H, dd, *J* 9.2 and 2.5, 9-H), 6.99 (1H, br

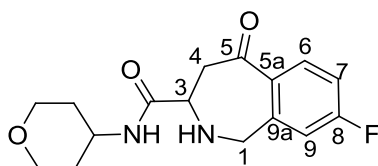
s, 6-H), 6.80 (1H, td,  $J$  9.2 and 2.6, 8-H), 6.30 (1H, br s, NH), 5.29 (1H, s, alkene-H<sub>a</sub>), 5.15 (1H, s, alkene-H<sub>b</sub>), 4.55 (2H, s, 1-H<sub>2</sub>), 4.38-4.19 (2H, m, cyclobutyl 1-H and 3-H), 3.03-2.65 (2H, m, 4-H<sub>2</sub>), 2.39-2.20 (2H, m, cyclobutyl 2-H<sub>2</sub>), 1.88-1.71 (2H, m, cyclobutyl 4-H<sub>2</sub>), 1.70-1.59 (2H, m, cyclobutyl 3-H<sub>2</sub>), 1.45 (7H, s, Boc, rotamer A) and 1.39 (2H, s, Boc, rotamer B);  $\delta_c$  (101 MHz, CDCl<sub>3</sub>) 177.24 (CO), 169.7 (Boc), 162.0 (d,  $J$  245.0, C-7), 146.8 (C-5), 144.0 (C-9a), 141.4 (C-5a), 129.6 (C-9), 119.7 (C-6), 117.1 (alkene), 114.3 (d,  $J$  22.2, C-8), 85.0 (Boc), 47.4 (C-1), 44.8 (C-3 and cyclobutyl C-1), 35.6 (C-4), 31.2 (cyclobutyl C-2), 31.1 (cyclobutyl C-4), 28.2 (Boc), 27.4 (Boc) and 15.1 (cyclobutyl C-3); HRMS found MH<sup>+</sup>, 375.2075. C<sub>21</sub>H<sub>27</sub>FN<sub>2</sub>O<sub>3</sub> requires *MH*, 375.2084.

***N*-Cyclobutyl-7-fluoro-5-oxo-2,3,4,5-tetrahydro-1*H*-benzo[*c*]azepine-3-carboxamide, 214ia**



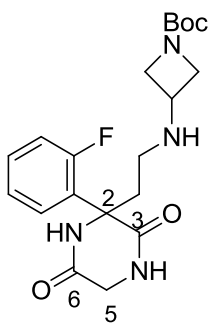
By general procedure U, alkene **296** (82.0 mg, 0.22 mmol) gave a crude ketone which by general procedure Y, gave a crude residue which was purified by flash chromatography (SiO<sub>2</sub>, 5:95 MeOH–EtOAc) to give the *ketone* **214ia** (60.8 mg, 100% over two steps,  $\geq$  98% open form) as a dark brown oil,  $R_f$  = 0.59 (10:90 MeOH–EtOAc);  $\nu_{\max}/\text{cm}^{-1}$  (ATR) 3077 (br), 2953, 1671, 1447, 1201 and 1137;  $\delta_H$  (400 MHz, MeOD) 7.60-7.55 (2H, m, 6-H and 9-H), 7.43 (1H, td,  $J$  8.2 and 2.8, 8-H), 4.65 (1H, d,  $J$  14.8, 1-H<sub>a</sub>), 4.56 (1H, d,  $J$  14.8, 1-H<sub>b</sub>), 4.28-4.16 (2H, m, 3-H and cyclobutyl 1-H), 3.48 (1H, dd,  $J$  18.3 and 9.9, 4-H<sub>a</sub>), 3.33-3.28 (1H, m, 4-H<sub>b</sub>), 2.31-2.19 (2H, m, cyclobutyl 2-H<sub>2</sub>), 1.98-1.87 (2H, m, cyclobutyl 4-H<sub>2</sub>) and 1.80-1.69 (3H, m, cyclobutyl 3-H<sub>2</sub> and NH);  $\delta_c$  (101 MHz, MeOD) 195.5 (C-5), 164.0 (d,  $J$  355.6, C-7), 139.4 (C-9a), 133.5 (d,  $J$  8.1, C-9), 127.6 (d,  $J$  3.4, C-5a), 120.2 (d,  $J$  22.0, C-6), 115.3 (d,  $J$  23.5, C-8), 53.2 (cyclobutyl C-1), 45.04 (C-3), 45.03 (C-1), 41.4 (C-4), 29.7 (cyclobutyl C-2 and cyclobutyl C-4) and 14.6 (cyclobutyl C-3);  $\delta_F$  (282 MHz, CDCl<sub>3</sub>) -72.9 and -73.1; HRMS found MH<sup>+</sup>, 277.1346. C<sub>15</sub>H<sub>17</sub>FN<sub>2</sub>O<sub>2</sub> requires *MH*, 277.1352.

**8-Fluoro-5-oxo-N-(tetrahydro-2H-pyran-4-yl)-2,3,4,5-tetrahydro-1H-benzo[c]azepine-3-carboxamide, 214ha**



Boc<sub>2</sub>O (52.7 mg, 0.240 mmol) was added to a solution of amine **294** (70.9 mg, 0.230 mmol) in DCM (2.30 mL, 0.1 M), and the resulting solution was stirred at room temperature overnight before being concentrated *in vacuo*. The residue was purified by flash chromatography (SiO<sub>2</sub>, 10:90 Petrol-EtOAc) to give the crude tetrahydrobenzazepine which was subjected to general procedures U followed by Y. This gave a crude residue which was purified by flash chromatography (SiO<sub>2</sub>, 5:95 to 20:80 MeOH-EtOAc) to give the *ketone* **214ha** (70.4 mg, 100% over three steps,  $\geq$  98% open form) as a dark brown oil,  $R_f$  = 0.60 (20:80 MeOH-EtOAc);  $\nu_{\max}$ / cm<sup>-1</sup> (ATR) 3415 (br), 2959, 2858, 2400, 1671, 1441, 1203, 1182 and 1133;  $\delta_H$  (400 MHz, MeOD) 7.89-7.82 (1H, m, 9-H), 7.26-7.17 (2H, m, 6-H and 7-H), 4.53 (1H, d,  $J$  14.9, 1-H<sub>a</sub>), 4.46 (1H, d,  $J$  14.9, 1-H<sub>b</sub>), 4.16-4.06 (1H, m, THP 4-H), 3.88-3.64 (4H, m, THP 2-H<sub>2</sub> and THP 6-H<sub>2</sub>), 3.41-3.28 (3H, m, 3-H and 4-H<sub>2</sub>), 1.74-1.60 (2H, m, THP 3-H<sub>2</sub>) and 1.47-1.31 (2H, m, THP 5-H<sub>2</sub>);  $\delta_C$  (101 MHz, MeOD) 195.3 (C-5), 166.7 (CO), 165.3 (d,  $J$  216.7, C-8), 132.1 (d,  $J$  9.6, C-6), 117.8 (d,  $J$  23.4, C-7), 116.8 (d,  $J$  22.0, C-9), 66.1 (THP C-2 and THP C-6), 53.5 (THP C-4), 46.3 (C-3), 45.5 (C-1), 41.7 (C-4), 31.9 (THP C-3) and 31.9 (THP C-5), aromatic quaternary carbons not observed;  $\delta_F$  (376 MHz, MeOD) -77.0; HRMS found MH<sup>+</sup>, 307.1457. C<sub>16</sub>H<sub>19</sub>FN<sub>2</sub>O<sub>3</sub> requires *MH*, 307.1458.

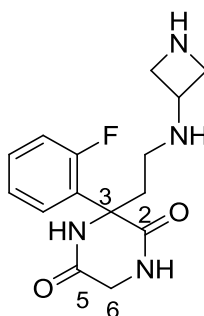
***tert*-Butyl 3-({2-[(2-fluorophenyl)-3,6-dioxopiperazin-2-yl]ethyl}amino)azetidine-1-carboxylate, 207**



By general procedure W, alkene **198** (125 mg, 0.500 mmol) gave the crude aldehyde which was combined with 1-Boc-3-(amino)azetidine (344 mg, 2.00 mmol) and by general procedure M, gave a crude residue which was purified by flash

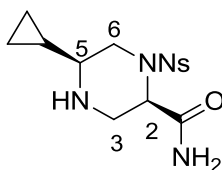
chromatography (SiO<sub>2</sub>, 10:90 MeOH–DCM) to give the *decorated piperazine* **207** (46.0 mg, 23% over two steps) as a yellow oil,  $R_f = 0.44$  (30:70 MeOH–DCM);  $\nu_{\max}/\text{cm}^{-1}$  (ATR) 3364 (br), 2483, 2071, 1677, 1414, 1119 and 972;  $\delta_{\text{H}}$  (501 MHz, MeOD) 7.31–7.24 (1H, m, fluorophenyl 4-H), 7.13 (1H, td,  $J$  8.0 and 1.7, fluorophenyl 3-H), 7.07 (1H, ddd,  $J$  11.9, 8.0 and 1.0, fluorophenyl 5-H), 7.02 (1H, td,  $J$  8.0 and 1.2, fluorophenyl 6-H), 4.78–4.70 (1H, m, azetidine 1-H), 4.10–4.01 (3H, m, azetidine 2-H<sub>2</sub> and azetidine 4-H<sub>a</sub>), 4.00–3.89 (1H, m, azetidine 4-H<sub>b</sub>), 3.57 (1H, td,  $J$  9.4 and 2.3, ethyl 2-H<sub>a</sub>), 3.36 (2H, s, 5-H<sub>2</sub>), 3.25 (1H, dt,  $J$  9.4 and 7.6, ethyl 2-H<sub>b</sub>), 2.89 (1H, dt,  $J$  13.0 and 9.0, ethyl 1-H<sub>a</sub>), 2.44 (1H, ddt,  $J$  13.0, 7.6 and 2.3, ethyl 1-H<sub>b</sub>) and 1.29 (9H, s, Boc);  $\delta_{\text{C}}$  (126 MHz, MeOD) 173.8 (C-3), 170.5 (Boc), 162.4 (d,  $J$  248.2, fluorophenyl C-2), 157.9 (C-6), 131.9 (d,  $J$  8.8, fluorophenyl C-4), 129.2 (d,  $J$  3.3, fluorophenyl C-3), 127.2 (d,  $J$  12.0, fluorophenyl C-1), 125.4 (d,  $J$  3.4, fluorophenyl C-5), 117.9 (d,  $J$  22.2, fluorophenyl C-6), 81.3 (Boc), 65.1 (C-3), 53.7 (azetidine C-2 and azetidine C-4), 44.0 (azetidine C-1), 43.0 (C-5), 41.7 (ethyl C-2), 32.9 (1H, d,  $J$  2.7, ethyl C-1) and 28.5 (Boc); HRMS found  $\text{MH}^+$ , 407.2092. C<sub>20</sub>H<sub>27</sub>FN<sub>4</sub>O<sub>4</sub> requires  $MH$ , 407.2094.

### 3-{2-[(Azetidin-3-yl)amino]ethyl}-3-(2-fluorophenyl)piperazine-2,5-dione, **208**



By general procedure Y, the protected amine **207** (46.0 mg, 0.110 mmol) gave the *piperazine* **208** (20.3 mg, 60%) as a yellow oil,  $\nu_{\max}/\text{cm}^{-1}$  (ATR) 3269 (br), 2951, 2934, 1711, 1553 and 1438;  $\delta_{\text{H}}$  (500 MHz, MeOD) 7.51–7.40 (1H, m, fluorophenyl 4-H), 7.30 (1H, td,  $J$  8.1 and 1.6, fluorophenyl 3-H), 7.25 (1H, ddd,  $J$  11.9, 8.1 and 0.9, fluorophenyl 5-H), 7.22–7.18 (1H, m, fluorophenyl 6-H), 5.12–5.03 (1H, m, azetidine 3-H), 4.02 (1H, t,  $J$  7.7, azetidine 2-H<sub>a</sub>), 3.91 (1H, t,  $J$  7.7, azetidine 2-H<sub>b</sub>), 3.84–3.70 (3H, m, azetidine 4-H<sub>2</sub> and ethyl 2-H<sub>a</sub>), 3.44 (1H, dd,  $J$  17.4 and 7.9, ethyl 2-H<sub>b</sub>), 3.34–3.26 (2H, m, 6-H<sub>2</sub>), 3.07 (1H, dt,  $J$  13.1 and 8.9, ethyl 1-H<sub>a</sub>) and 2.66–2.56 (1H, m, ethyl 1-H<sub>b</sub>);  $\delta_{\text{C}}$  (126 MHz, MeOD) 174.9 (C-2), 173.5 (C-5), 162.5 (d,  $J$  248.1, fluorophenyl C-2), 131.8 (d,  $J$  8.8, fluorophenyl C-4), 129.3 (d,  $J$  3.4, fluorophenyl C-3), 127.6 (d,  $J$  12.0, fluorophenyl C-1), 125.4 (d,  $J$  3.3, fluorophenyl C-5), 117.9 (d,  $J$  22.3, fluorophenyl C-6), 65.0 (C-3), 51.2 (azetidine C-2 and azetidine C-4), 48.3 (azetidine C-3), 45.1 (C-6), 41.8 (ethyl C-2) and 32.9 (ethyl C-1); HRMS found  $\text{MH}^+$ , 307.1567. C<sub>15</sub>H<sub>19</sub>FN<sub>4</sub>O<sub>2</sub> requires  $MH$ , 307.1570.

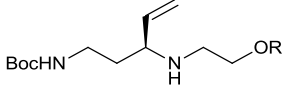
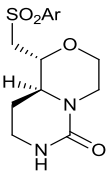
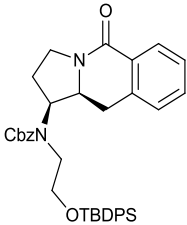
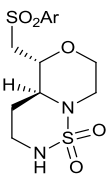
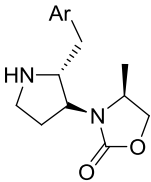
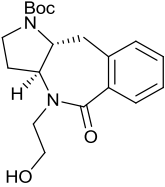
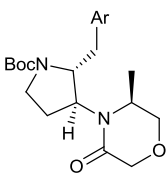
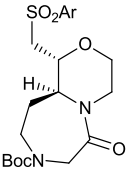
**(2R, 5S)-5-Cyclopropyl-1-(2-nitrobenzenesulfonyl)piperazine-2-carboxamide, 236**

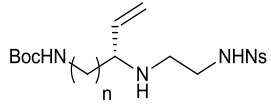
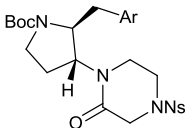
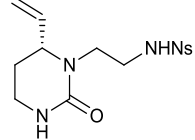
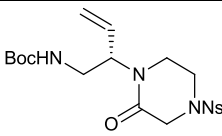
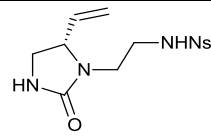
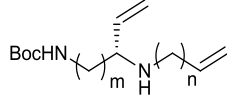
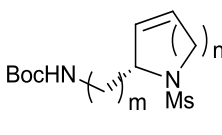
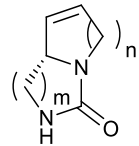
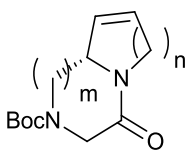
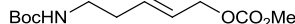
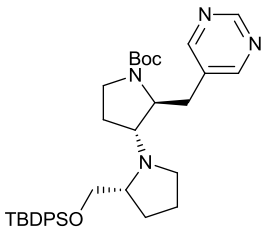
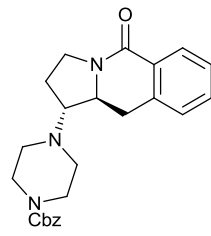
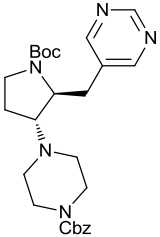


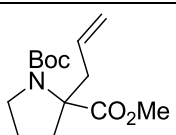
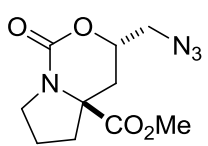
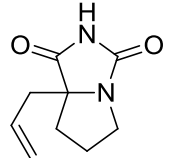
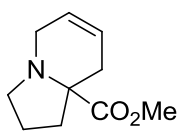
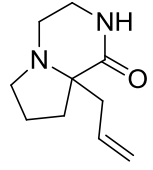
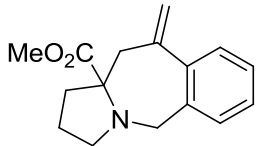
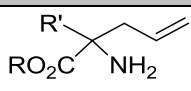
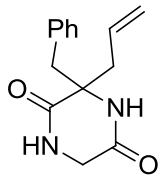
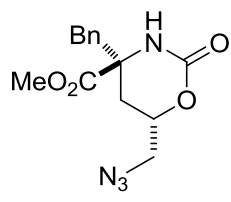
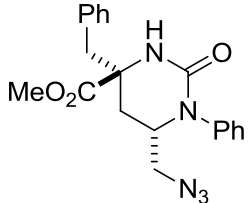
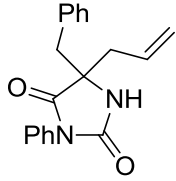
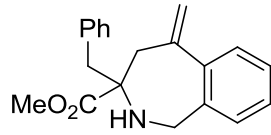
A solution of the protected piperazine **235** (14.6 mg, 250  $\mu\text{mol}$ ) and CAN (54.8 mg, 0.100 mmol) in MeCN (0.250 mL, 0.1 M) and water (80.0  $\mu\text{L}$ , 0.3 M) was stirred at room temperature overnight before more CAN (54.8 mg, 0.100 mmol) was added. The reaction mixture was concentrated *in vacuo* before being purified by mass-directed preparative HPLC to yield the *deprotected piperazine* **236** (6.10 mg, 69%) as a yellow oil,  $R_f = 0.72$  (30:70 MeOH-DCM);  $\nu_{\text{max}}/\text{cm}^{-1}$  (ATR) 3327 (br), 3195 (br), 2928, 1677, 1543, 1369 and 1170;  $[\alpha]_{\text{D}}^{25}$  158 ( $c = 0.15$ ,  $\text{CHCl}_3$ );  $\delta_{\text{H}}$  (501 MHz, MeOD) 8.12-8.07 (1H, m, nitrophenyl 3-H), 7.78-7.70 (3H, m, nitrophenyl 4-H, nitrophenyl 5-H and nitrophenyl 6-H), 4.52 (1H, app s, 2-H), 3.76-3.69 (1H, m, 6-H<sub>a</sub>), 3.61 (1H, d,  $J$  13.2, 6-H<sub>b</sub>), 3.54-3.46 (1H, m, 3-H<sub>a</sub>), 3.39-3.29 (1H, m, 3-H<sub>b</sub>), 2.17 (1H, d,  $J$  7.8, NH), 1.27-1.12 (1H, m, 5-H), 0.96-0.89 (1H, m, cyclopropyl 1-H), 0.47-0.39 (1H, m, cyclopropyl 2-H<sub>a</sub>), 0.31-0.19 (1H, m, cyclopropyl 2-H<sub>b</sub>) and 0.13-0.04 (2H, m, cyclopropyl 4-H<sub>2</sub>);  $\delta_{\text{C}}$  (126 MHz, MeOD) 147.1 (nitrophenyl C-2), 135.7 (nitrophenyl C-5), 133.33 (nitrophenyl C-1), 133.29 (nitrophenyl C-4), 132.5 (nitrophenyl C-6), 125.7 (nitrophenyl C-3), 58.5 (C-5), 55.6 (C-2), 46.9 (C-6), 42.2 (C-3), 12.4 (cyclopropyl C-1), 4.8 (cyclopropyl C-2) and 4.2 (cyclopropyl C-4); HRMS found  $\text{MH}^+$ , 355.1079.  $\text{C}_{14}\text{H}_{18}\text{N}_4\text{O}_5\text{S}$  requires  $\text{MH}$ , 355.1076.

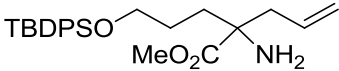
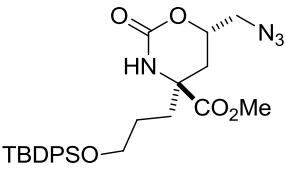
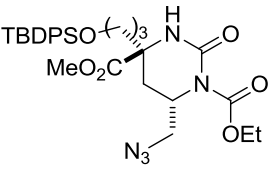
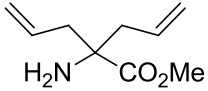
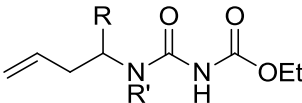
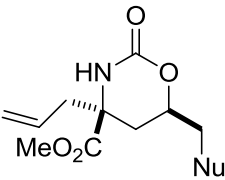
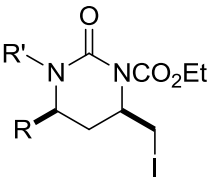
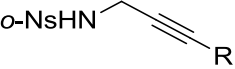
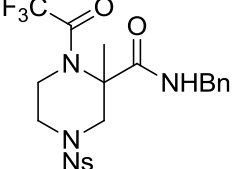
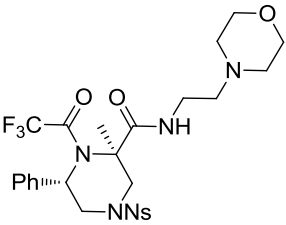
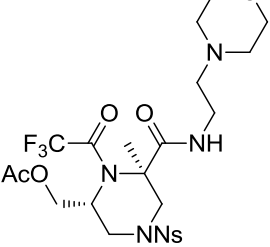
## Appendix

**Table 31** Methodologies for the formation, and available yields of exemplified scaffolds formed using previously established chemistry in Leeds. This information was gathered in order to identify a range of scaffolds which could be formed in reasonable yields, as well as reliable methodology for their synthesis. A full description can be found in Section 2.2.1.

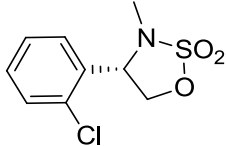
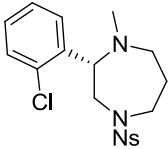
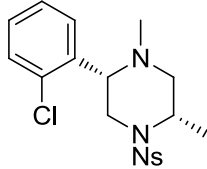
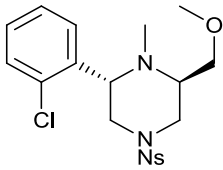
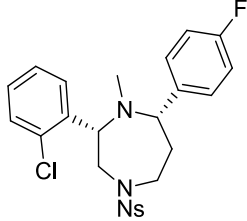
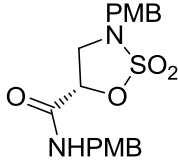
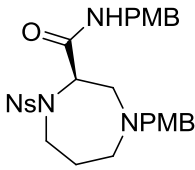
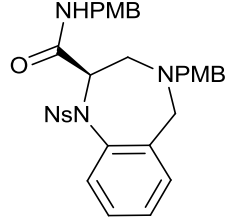
<b>Iridium Chemistry<sup>41</sup></b>		<b>Starting Material:</b>	
			
<b>Method / Yield</b>	<b>Exemplified Scaffold</b>	<b>Method / Yield</b>	<b>Exemplified Scaffold</b>
i) Iodine-mediated morpholine formation ii) CDI-urea formation  40%		i) Amino-arylation ii) Lactamisation  77%	
i) Iodine-mediated morpholine formation ii) Sulfurea formation		i) CDI-carbamate formation ii) Amino-arylation  66-90%	
i) Aminoarylation ii) Lactamisation  38%		i) Keto-morpholine formation ii) Amino-arylation × 2  83%	
i) Iodine-mediated morpholine formation ii) Keto-piperazine formation			

<b>Iridium Chemistry</b>		 <b>Starting Material:</b> $n = 1, 2$	
<b>Method / Yield</b>	<b>Exemplified Scaffold</b>	<b>Method / Yield</b>	<b>Exemplified Scaffold</b>
i) Ketopiperazine formation ii) Amino-arylation × 2 (Not compatible with Ns)		CDI-urea formation  49%	
Ketopiperazine formation  95%		CDI-urea formation  57%	
<b>Iridium Chemistry</b>		 <b>Starting Material:</b> $m, n = 1, 2$	
<b>Method / Yield</b>	<b>Exemplified Scaffold</b>	<b>Method / Yield</b>	<b>Exemplified Scaffold</b>
RCM $m=1, n=1, 72\%$ $m=1, n=2, 54\%$ $m=2, n=1, 54\%$ $m=2, n=2, 72\%$		i) CDI-urea formation ii) RCM $m=1, n=1, 51\%$ $m=1, n=2$ $m=2, n=1, 67\%$ $m=2, n=2, 50\%$	
i) Ketopiperazine formation ii) RCM $m=1, n=1$ $m=1, n=2, 67\%$ $m=2, n=1$ $m=2, n=2, 72\%$			
<b>Iridium Chemistry</b>		<b>Starting Material:</b> 	
<b>Method / Yield</b>	<b>Exemplified Scaffold</b>	<b>Method / Yield</b>	<b>Exemplified Scaffold</b>
i) Allylic amination ii) Amino-arylation  53-83%		i) Allylic amination ii) Amino-arylation iii) Lactamisation  68%	
i) Allylic amination ii) Amino-arylation  74-80%			

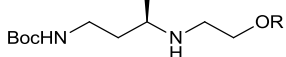
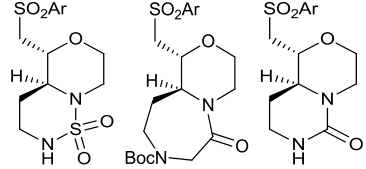
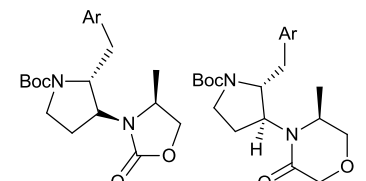
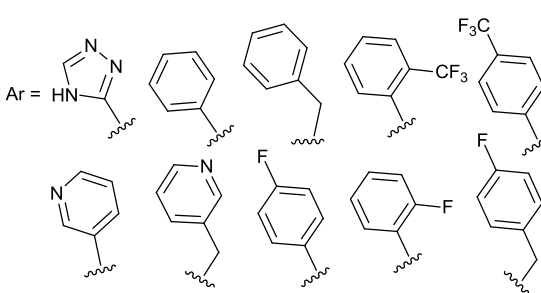
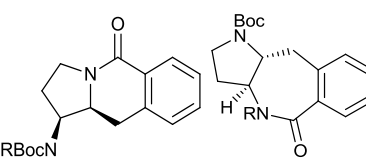
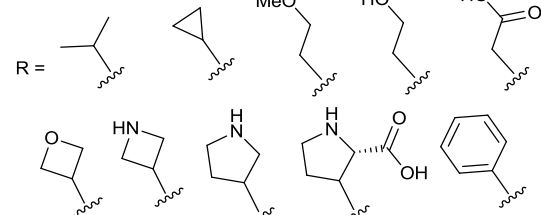
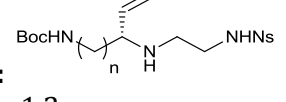
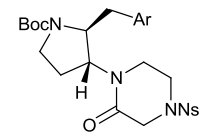
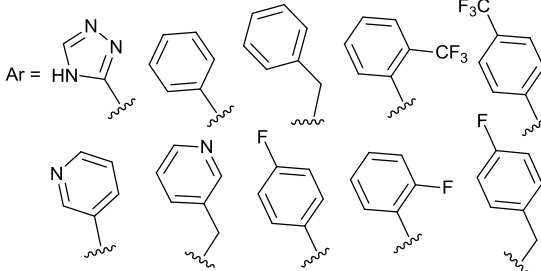
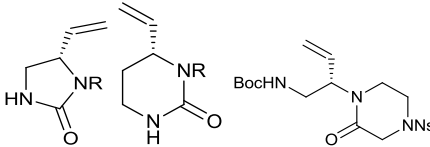
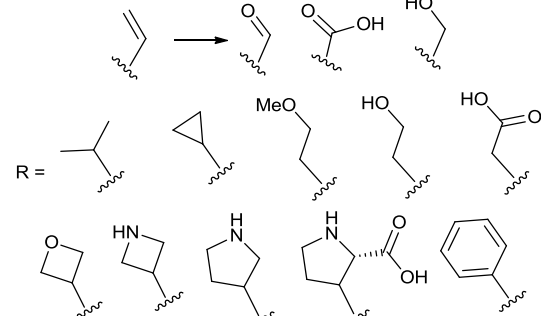
<b>Amino Acid Chemistry</b> <sup>43</sup>		<b>Starting Material:</b> 	
<b>Method / Yield</b>	<b>Exemplified Scaffold</b>	<b>Method / Yield</b>	<b>Exemplified Scaffold</b>
Iodine-mediated carbamate formation 53%		i) Urea formation ii) Hydantoin formation 86%	
i) <i>N</i> -allylation ii) RCM 77%		i) Reductive amination ii) Keto-piperazine formation 63%	
i) Reductive amination ii) Heck 54%			
<b>Amino Acid Chemistry</b>		<b>Starting Material:</b>  R, R' = Bn, Me	
<b>Method / Yield</b>	<b>Exemplified Scaffold</b>	<b>Method / Yield</b>	<b>Exemplified Scaffold</b>
i) Amide formation ii) Diketopiperazine formation 93%		i) Boc-protection ii) Iodine-mediated carbamate formation 88%	
i) Urea formation ii) Iodine-mediated cyclisation 86%		i) <i>N</i> -allylation ii) RCM 68%	
i) Urea formation ii) Hydantoin formation 86%		i) Reductive amination ii) Heck 97%	

<b>Amino Acid Chemistry</b>		<b>Starting Material:</b> 	
<b>Method / Yield</b>	<b>Exemplified Scaffold</b>	<b>Method / Yield</b>	<b>Exemplified Scaffold</b>
i) Boc-protection ii) Iodine-mediated carbamate formation  80%		i) Urea formation ii) Iodine-mediated cyclisation  67%	
<b>Amino Acid Chemistry</b>		<b>Urea Chemistry</b> <sup>43</sup>	
<b>Starting Material:</b> 		<b>Starting Material:</b> 	
<b>Method / Yield</b>	<b>Exemplified Scaffold</b>	<b>Method / Yield</b>	<b>Exemplified Scaffold</b>
i) Boc-protection ii) Iodine-mediated cyclisation iii) Nucleophilic displacement  78-80%		Iodine-mediated cyclisation  64-80%	
<b>Ugi Chemistry</b> <sup>44</sup>		<b>Starting Material:</b>  R = H, Et	
<b>Method / Yield</b>	<b>Exemplified Scaffold</b> <sup>viii</sup>	<b>Method / Yield</b>	<b>Exemplified Scaffold</b>
i) Cyclic sulfamidate ring opening ii) Alkyne hydration iii) Ugi reaction  71%		i) Cyclic sulfamidate ring opening ii) Au-mediated hydroamination iii) Ugi reaction  70%	
i) Cyclic sulfamidate ring opening ii) Au-mediated hydroamination iii) Ugi reaction  28%		i) Cyclic sulfamidate ring opening ii) Au-mediated hydroamination iii) Ugi reaction  65%	

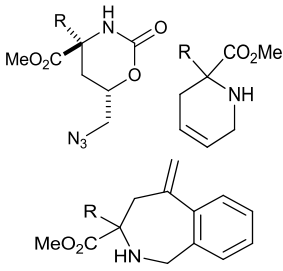
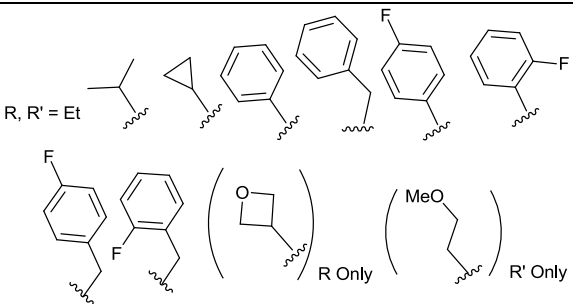
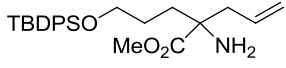
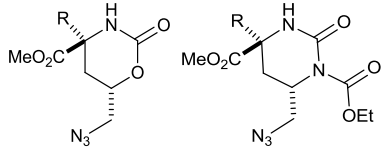
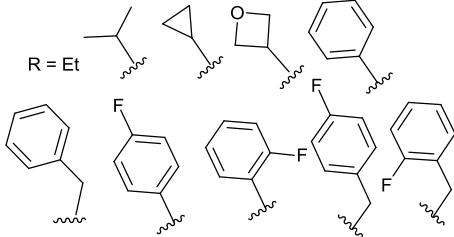
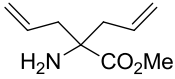
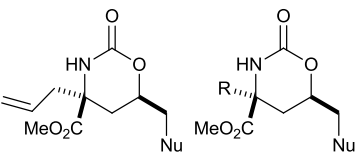
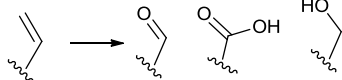
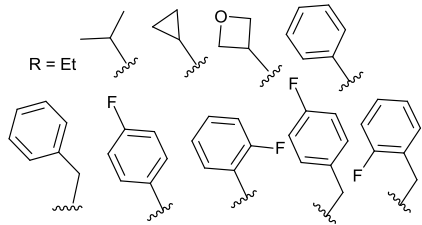
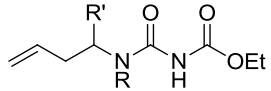
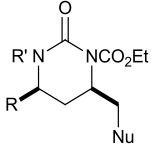
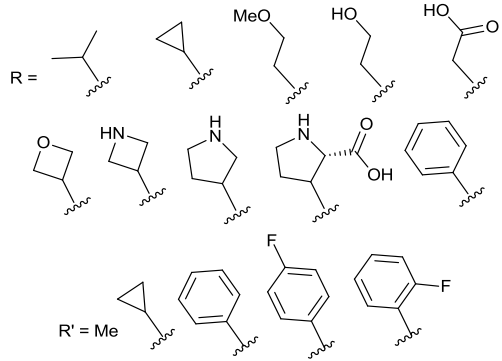
<sup>viii</sup> *o*-Ns refers to 2-nitrobenzenesulfonamide whereas Ns refers to 4-nitrobenzenesulfonamide from here onwards.

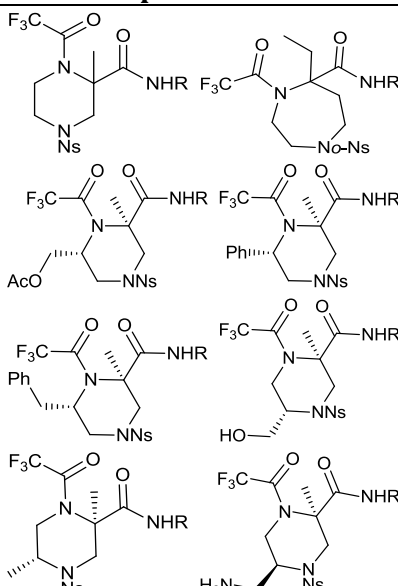
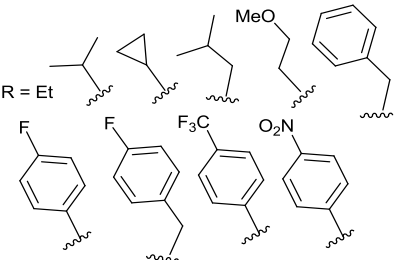
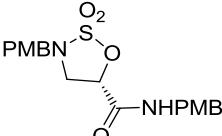
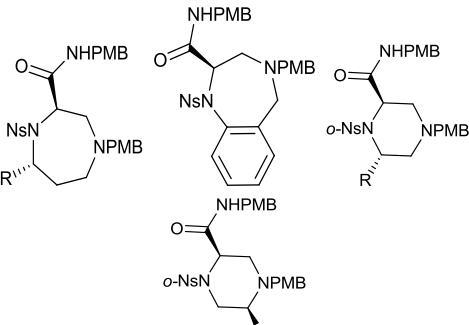
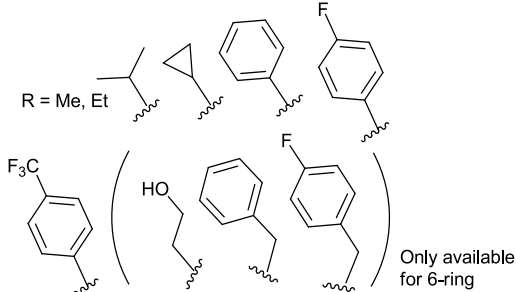
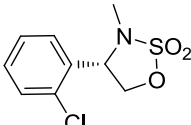
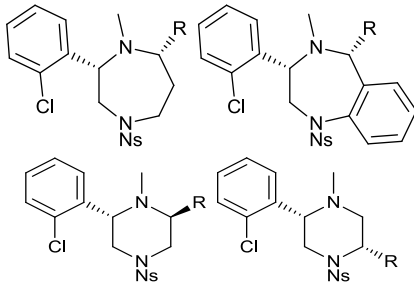
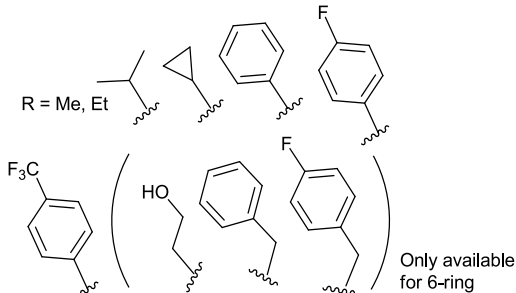
<b>Mitsunobu Chemistry</b> <sup>42</sup>		 <b>Starting Material:</b>	
<b>Method / Yield</b>	<b>Exemplified Scaffold</b>	<b>Method / Yield</b>	<b>Exemplified Scaffold</b>
i) Cyclic sulfamidate ring opening ii) Mitsunobu reaction  87%		i) Cyclic sulfamidate ring opening ii) Mitsunobu reaction  44%	
i) Cyclic sulfamidate ring opening ii) Mitsunobu reaction  55%		i) Cyclic sulfamidate ring opening ii) Mitsunobu reaction  80%	
<b>Mitsunobu Chemistry</b>		 <b>Starting Material:</b>	
<b>Method / Yield</b>	<b>Exemplified Scaffold</b>	<b>Method / Yield</b>	<b>Exemplified Scaffold</b>
i) Cyclic sulfamidate ring opening ii) Mitsunobu reaction  38%		i) Cyclic sulfamidate ring opening ii) Mitsunobu reaction  28%	

**Table 32** Alternative building blocks used and functional group interconversions applied for each exemplified scaffold, in the enumeration of the virtual library. This shows the range of transformations applied to each exemplified scaffold in the generation of a library of virtual scaffolds. A full description can be found in Section 2.2.2.

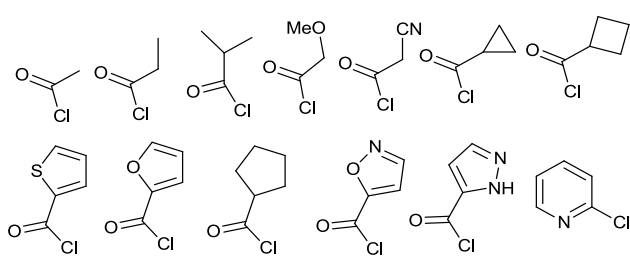
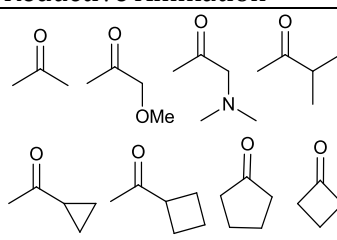
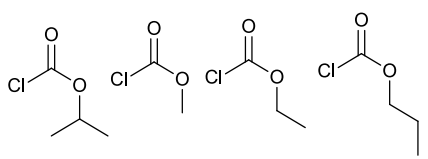
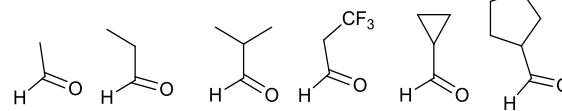
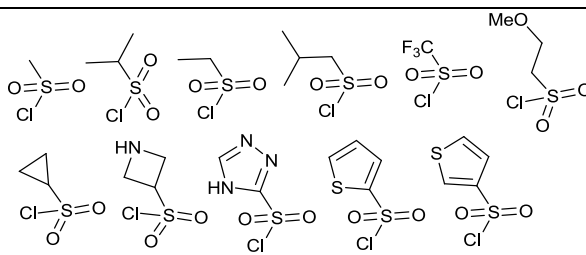
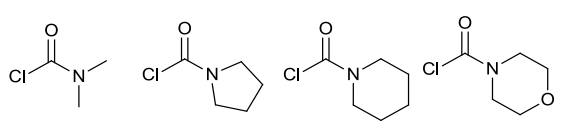
<p style="text-align: center;"><b>Iridium Chemistry</b></p>	<p style="text-align: center;"><b>Starting Material:</b></p> 
<p style="text-align: center;"><b>Exemplified Scaffold</b></p>	<p style="text-align: center;"><b>Alternative Building Blocks</b></p>
 	
	<p style="text-align: center;"><b>R =</b></p> 
<p style="text-align: center;"><b>Iridium Chemistry</b></p>	<p style="text-align: center;"><b>Starting Material:</b></p>  <p style="text-align: center;"><math>n=1,2</math></p>
<p style="text-align: center;"><b>Exemplified Scaffold</b></p>	<p style="text-align: center;"><b>Alternative Building Blocks and Functional Group Interconversions</b></p>
	
	<p style="text-align: center;"><b>R =</b></p> 



	
<p><b>Amino Acid Chemistry</b></p>	<p><b>Starting Material:</b> </p>
<p><b>Exemplified Scaffold</b></p>	<p><b>Alternative Building Blocks</b></p>
	
<p><b>Amino Acid Chemistry</b></p>	<p><b>Starting Material:</b> </p>
<p><b>Exemplified Scaffold</b></p>	<p><b>Alternative Building Blocks and Functional Group Interconversions</b></p>
	<p>Nu = CN, NO<sub>2</sub>, I, N<sub>3</sub>, NH<sub>2</sub>, SPh</p>  
<p><b>Amino Acid Chemistry</b></p>	<p><b>Starting Material:</b> </p>
<p><b>Exemplified Scaffold</b></p>	<p><b>Alternative Building Blocks</b></p>
	<p>Nu = CN, NO<sub>2</sub>, I, N<sub>3</sub>, NH<sub>2</sub>, SPh</p> 

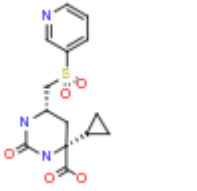
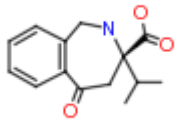
<p align="center"><b>Ugi Chemistry</b></p>	<p align="center"><b>Starting Material:</b>  <math>\text{o-NsHN}-\text{CH}_2-\text{C}\equiv\text{C}-\text{R}</math>  <math>\text{R} = \text{H, Et}</math></p>
<p align="center"><b>Exemplified Scaffold</b></p> 	<p align="center"><b>Alternative Building Blocks</b></p> 
<p align="center"><b>Mitsunobu Chemistry</b></p>	<p align="center"><b>Starting Material:</b></p> 
<p align="center"><b>Exemplified Scaffold</b></p> 	<p align="center"><b>Alternative Building Blocks</b></p> 
<p align="center"><b>Mitsunobu Chemistry</b></p>	<p align="center"><b>Starting Material:</b></p> 
<p align="center"><b>Exemplified Scaffold</b></p> 	<p align="center"><b>Alternative Building Blocks</b></p> 

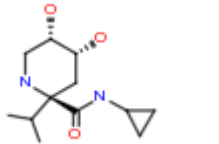
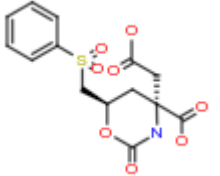
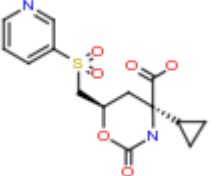
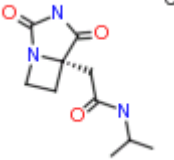
**Table 33** Derivatisations applied to virtual scaffolds in the enumeration of the virtual fragment library. Derivatisation adds complexity and shape diversity to the virtual scaffolds and removes any reactive functionality by reacting them with capping groups, improving fragment properties. A full description can be found in Section 2.2.3.

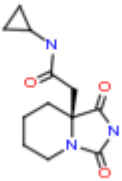
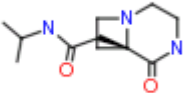
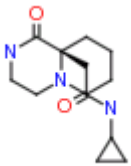
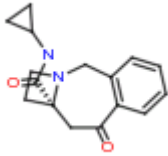
<b>Secondary Amine Decorations</b>	
<b>Amide Formation</b>	<b>Reductive Amination</b>
	
<b>Carbamate Formation</b>	
	
<b>Sulfonamide Formation</b>	<b>Urea Formation</b>
	

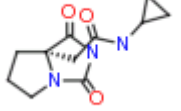
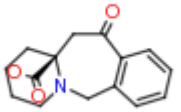
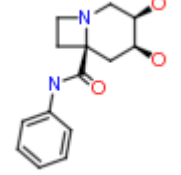
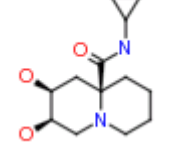


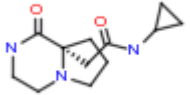
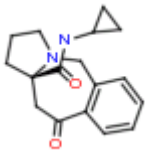
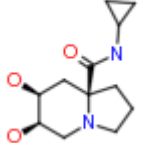
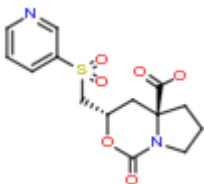
**Table 34** Percentage of molecules belonging to HA (heavy atom) ranges 16-20, 18-22 and 20-24, of the total number of fragments derivatised from each scaffold (identified by the chemistry used in a key step, with some differentiated by the ring size of the product *e.g.* “Mitsunobu 6” refers to a scaffold formed using Mitsunobu chemistry in a key step to form a product with a 6-membered ring), shown using an exemplar fragment (hydrogens omitted by PLP). Maximum scaffold coverage is desired in order to incorporate the most diverse range of virtual fragments, thus, “0% coverage” of a scaffold by each of the three HA ranges has been highlighted and noted. It was on this basis that the heavy atom range 18-22 was chosen for fragment identification, as it contained the least number of scaffolds with “0% coverage,” *i.e.* covered the highest number of scaffolds. A full description can be found in Section 2.3.

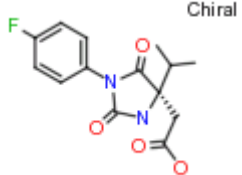
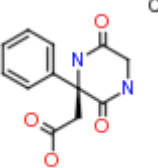
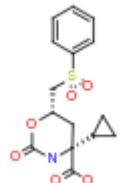
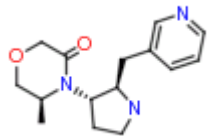
Scaffold ID	Exemplar fragment	No. fragments based on scaffold	16-20 HA	Percentage of total fragments	18-22 HA	Percentage of total fragments	20-24 HA	Percentage of total fragments
amino acid scaffold-1		128	6	4.7%	50	39.1%	122	95.3%
amino acid scaffold-11	 Chiral	530	16	3.0%	192	36.2%	520	98.1%

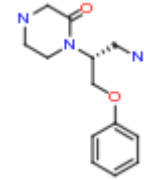
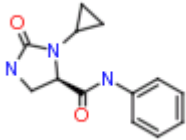
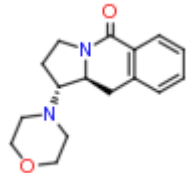
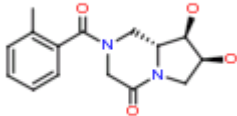
amino acid scaffold-12		2604	808	31.0%	1516	58.2%	2088	80.2%
amino acid scaffold-13		74	4	5.4%	30	40.5%	71	95.9%
amino acid scaffold-14		128	6	4.7%	50	39.1%	122	95.3%
amino acid scaffold-15		56	56	100%	10	17.9%	0	0%

amino acid scaffold-16	 Chiral	66	66	100%	56	84.8%	10	15.2%
amino acid scaffold-17	 Chiral	56	56	100%	10	17.9%	0	0%
amino acid scaffold-18	 Chiral	66	66	100%	56	84.8%	10	15.2%
amino acid scaffold-19	 Chiral	62	14	22.6%	60	96.8%	60	96.8%

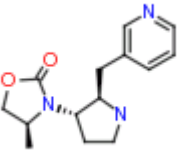
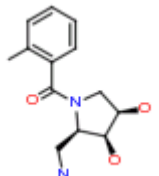
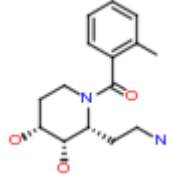
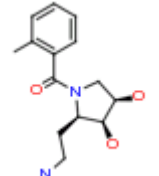
amino acid scaffold-2	<p>Chiral</p> 	64	64	100%	32	50%	0	0%
amino acid scaffold-20	<p>Chiral</p> 	62	2	3.2%	14	22.6%	60	96.8%
amino acid scaffold-21		12	12	100%	5	41.7%	0	0%
amino acid scaffold-22		12	12	100%	12	100%	5	41.7%

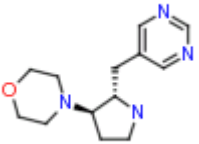
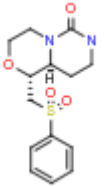
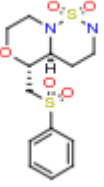
amino acid scaffold-3	 <p style="text-align: center;">Chiral</p>	64	64	100%	32	50%	0	0%
amino acid scaffold-4	 <p style="text-align: center;">Chiral</p>	62	2	3.2%	44	71.0%	60	96.8%
amino acid scaffold-5		12	12	100%	10	83.3%	0	0%
amino acid scaffold-6		20	1	5.0%	9	45.0%	19	95.0%

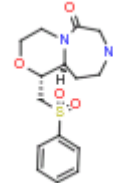
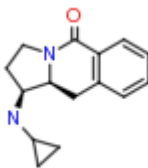
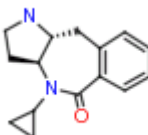
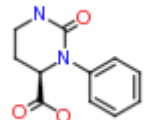
amino acid scaffold-7	 <p>Chiral</p>	1782	284	15.9%	814	45.7%	1672	93.8%
amino acid scaffold-8	 <p>Chiral</p>	614	244	39.7%	388	63.2%	434	70.7%
amino acid scaffold-9		6	0	0%	0	0%	6	100%
Ir scaffold-1		106	4	3.8%	22	20.8%	105	99.1%

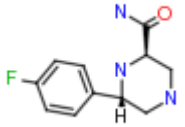
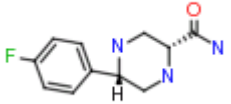
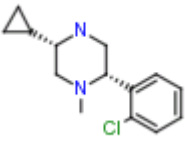
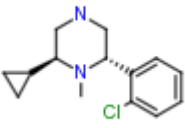
Ir scaffold-10		176	165	93.8%	106	60.2%	31	17.6%
Ir scaffold-11		779	579	74.3%	464	59.6%	300	38.5%
Ir scaffold-12		26	5	19.2%	10	38.5%	23	88.5%
Ir scaffold-14		72	69	95.8%	42	58.3%	8	11.1%

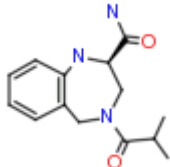
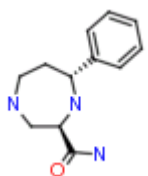
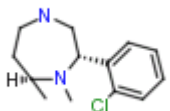
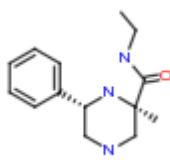
Ir scaffold-16		77	54	70.1%	69	89.6%	42	54.5%
Ir scaffold-18		76	68	89.5%	59	77.6%	23	30.3%
Ir scaffold-19		76	68	89.5%	59	77.6%	23	30.3%
Ir scaffold-2		416	15	3.6%	84	20.2%	411	98.8%

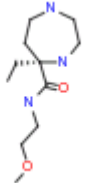
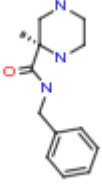
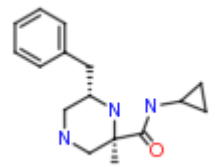
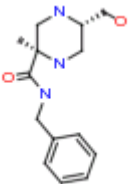
Ir scaffold-21		213	11	5.2%	46	21.6%	209	98.1%
Ir scaffold-22	 Chiral	46	46	100%	6	13.0%	0	0%
Ir scaffold-23	 Chiral	122	118	96.7%	46	37.7%	6	4.9%
Ir scaffold-24	 Chiral	84	84	100%	16	19.0%	4	4.8%

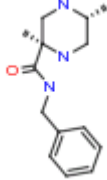
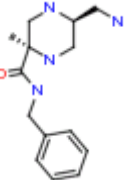
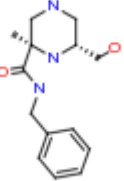
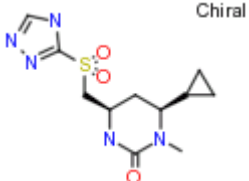
Ir scaffold-25	 Chiral	84	84	100%	16	19.0%	4	4.8%
Ir scaffold-3		500	75	15.0%	231	46.2%	466	93.2%
Ir scaffold-4		8	1	12.5%	7	87.5%	8	100%
Ir scaffold-5		8	0	0%	3	37.5%	8	100%

Ir scaffold-6		22	0	0%	4	18.2%	22	100%
Ir scaffold-7		399	20	5.0%	94	23.6%	389	97.5%
Ir scaffold-8		420	20	4.8%	104	24.8%	410	97.6%
Ir scaffold-9		824	548	66.5%	543	65.9%	382	46.4%

Mitsunobu 6 scaffold-1		1315	783	59.5%	751	57.1%	660	50.2%
Mitsunobu 6 scaffold-2		1315	783	59.5%	751	57.1%	660	50.2%
Mitsunobu 6 scaffold-3		414	80	19.3%	251	60.6%	379	91.5%
Mitsunobu 6 scaffold-4		414	80	19.3%	251	60.6%	379	91.5%

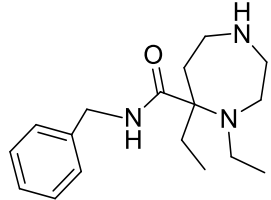
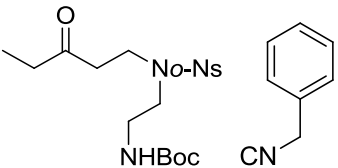
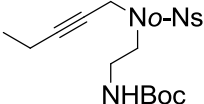
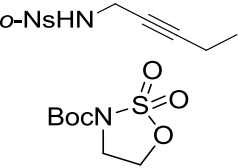
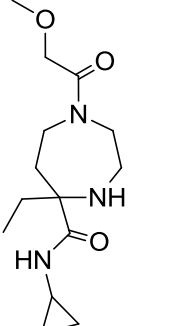
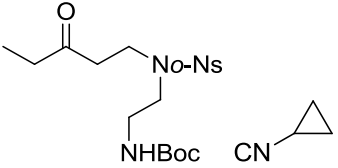
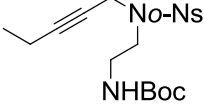
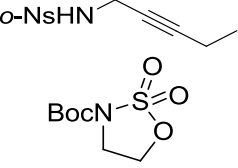
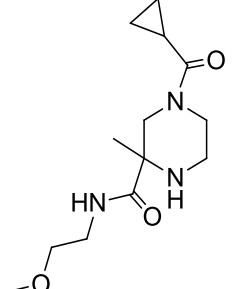
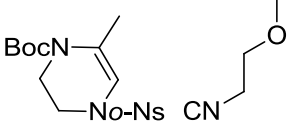
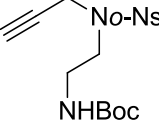
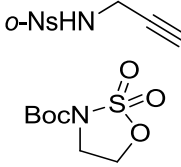
Mitsunobu 7 scaffold-1		77	54	70.1%	69	89.6%	42	54.5%
Mitsunobu 7 scaffold-2		896	476	53.1%	541	60.4%	515	57.5%
Mitsunobu 7 scaffold-4		220	28	12.7%	113	51.4%	208	94.5%
Ugi scaffold-1		334	13	3.9%	71	21.3%	329	98.5%

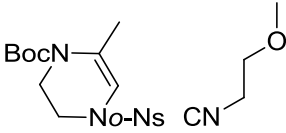
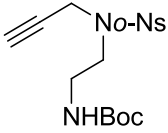
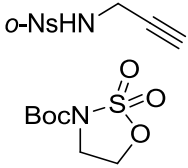
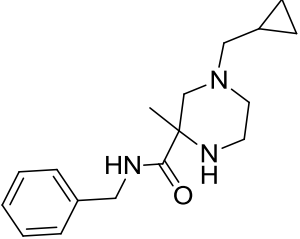
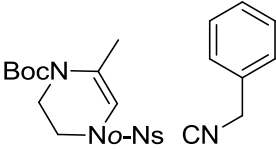
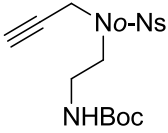
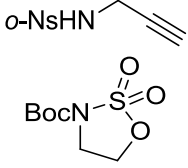
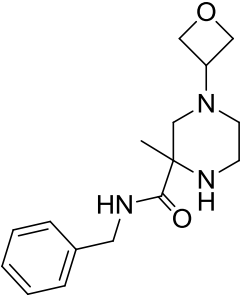
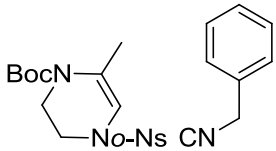
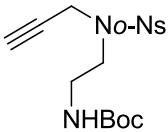
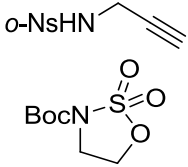
Ugi scaffold-2		959	329	34.3%	661	68.9%	793	82.7%
Ugi scaffold-3		1257	661	52.6%	793	63.1%	763	60.7%
Ugi scaffold-4		171	5	2.9%	29	17.0%	170	99.4%
Ugi scaffold-5		1064	387	36.4%	727	68.3%	860	80.8%

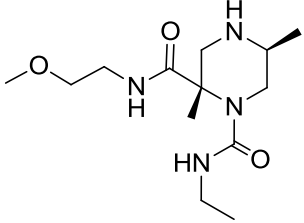
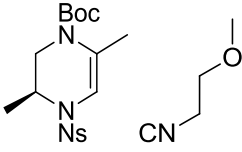
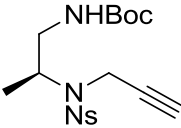
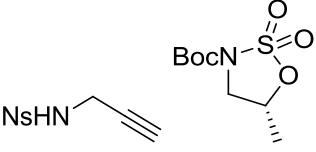
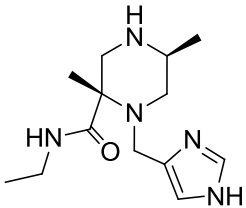
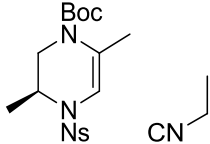
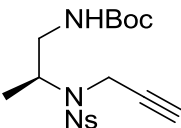
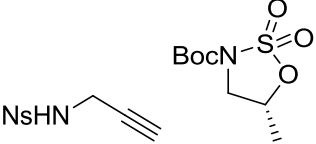
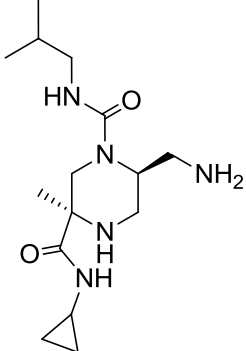
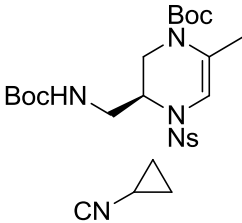
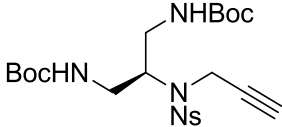
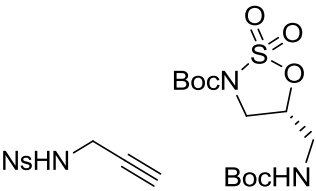
Ugi scaffold-6		1107	510	46.1%	757	68.4%	786	71.0%
Ugi scaffold-7		959	329	34.3%	661	68.9%	793	82.7%
Ugi scaffold-8		1064	387	36.4%	727	68.3%	860	80.8%
urea scaffold-1	 Chiral	395	37	9.4%	141	35.7%	373	94.4%
<b>Total</b>		22975	8771	38.2%	12715	55.3%	16703	72.7%

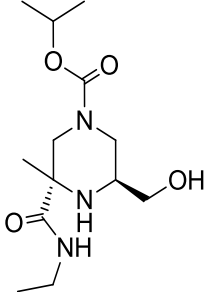
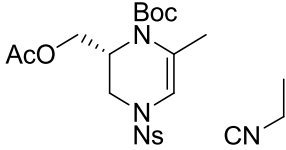
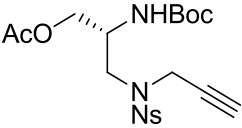
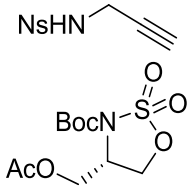
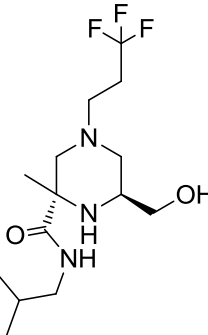
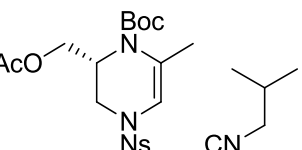
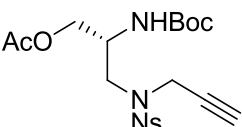
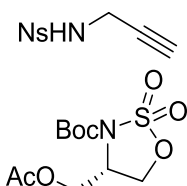
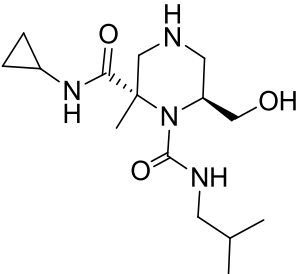
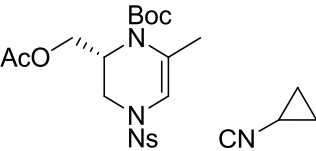
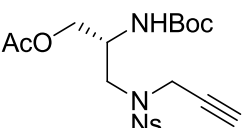
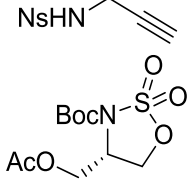
**Table 35** Retrosynthetic analysis of compounds from two selected libraries after applying a simulated annealing PLP protocol for the generation of a shape-diverse fragment library. The fragment as well as key intermediates and building blocks can be seen; the key reactions which take place are also summarised. Molecules produced by run 1 were taken forward for synthesis due to their chemistry being more developed than molecules from run 2. A full description can be found in Section 2.6.2.

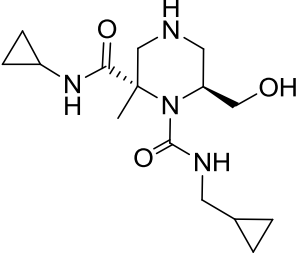
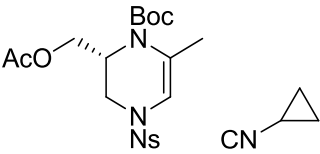
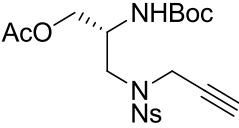
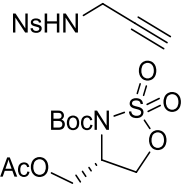
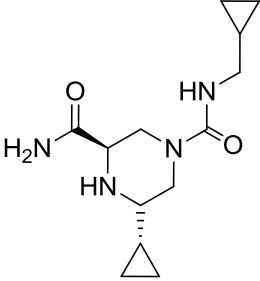
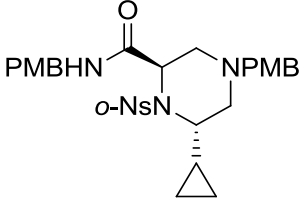
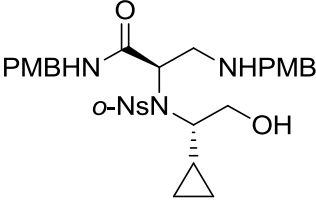
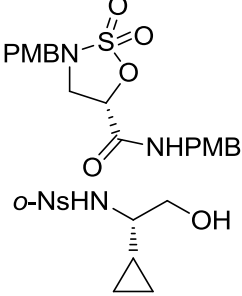
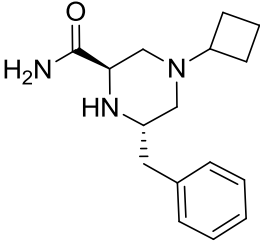
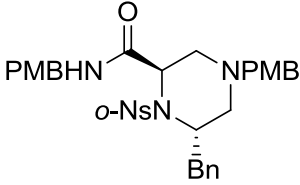
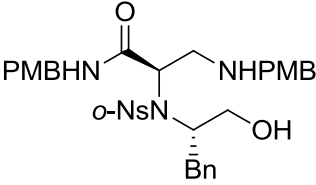
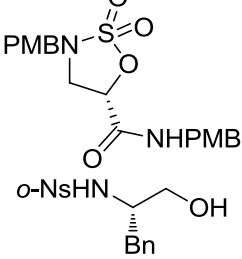
Virtual Fragment (Run 1)	Key Intermediate	Key Intermediate	Building Blocks	Reactions Occurred
				Allylic amination CDI-urea formation
				N-allylation RCM
				Cyclic sulfamidate ring opening Alkyne hydration Ugi reaction

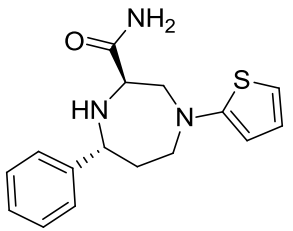
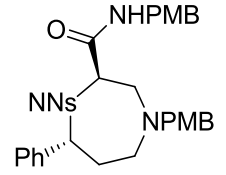
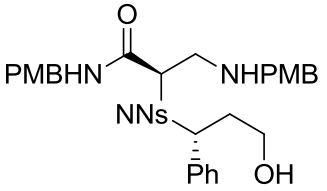
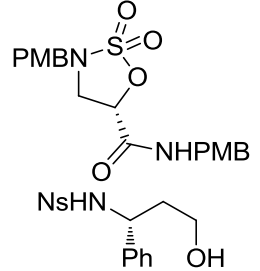
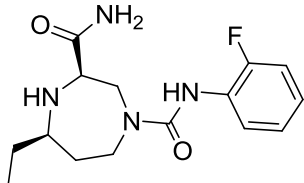
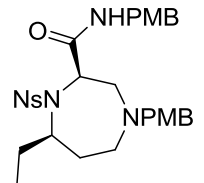
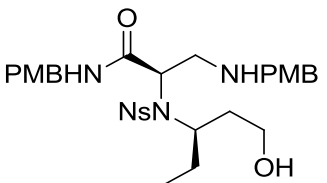
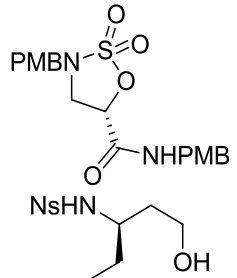
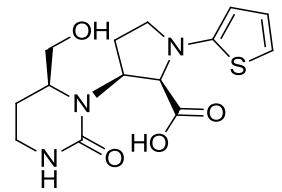
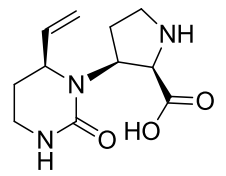
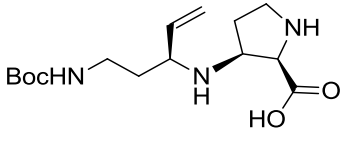
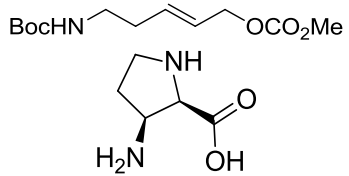
				<p>Cyclic sulfamidate ring opening</p> <p>Alkyne hydration</p> <p>Ugi reaction</p>
				<p>Cyclic sulfamidate ring opening</p> <p>Alkyne hydration</p> <p>Ugi reaction</p>
				<p>Cyclic sulfamidate ring opening</p> <p>Au-mediated hydroamination</p> <p>Ugi reaction</p>

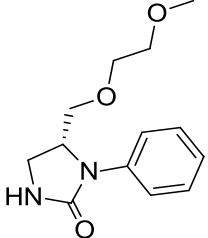
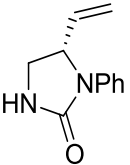
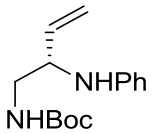
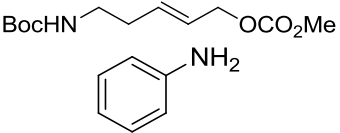
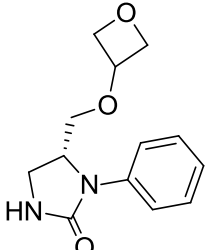
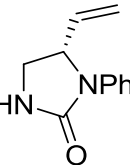
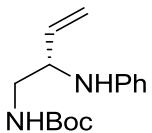
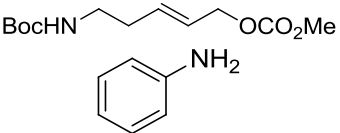
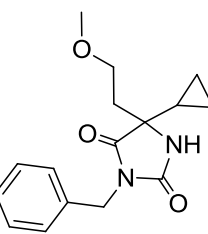
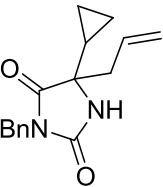
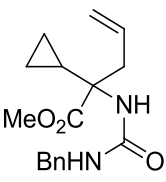
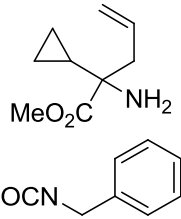
				<p>Cyclic sulfamidate ring opening</p> <p>Au-mediated hydroamination</p> <p>Ugi reaction</p>
				<p>Cyclic sulfamidate ring opening</p> <p>Au-mediated hydroamination</p> <p>Ugi reaction</p>
				<p>Cyclic sulfamidate ring opening</p> <p>Au-mediated hydroamination</p> <p>Ugi reaction</p>

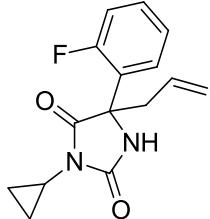
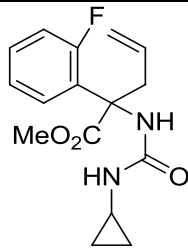
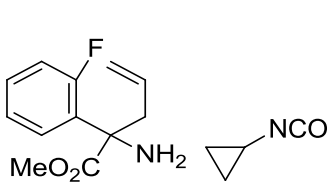
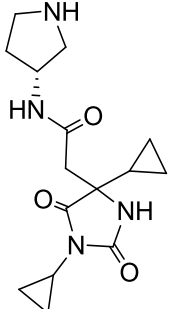
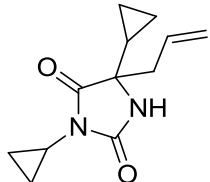
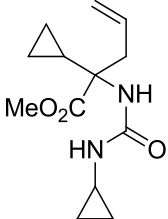
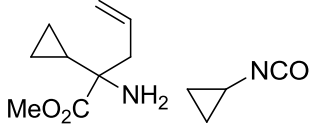
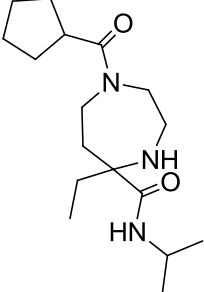
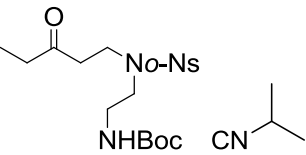
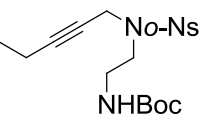
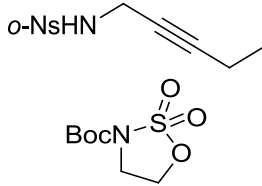
				<p>Cyclic sulfamidate ring opening</p> <p>Au-mediated hydroamination</p> <p>Ugi reaction</p>
				<p>Cyclic sulfamidate ring opening</p> <p>Au-mediated hydroamination</p> <p>Ugi reaction</p>
				<p>Cyclic sulfamidate ring opening</p> <p>Au-mediated hydroamination</p> <p>Ugi reaction</p>

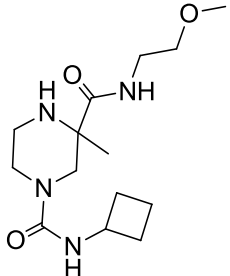
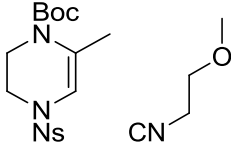
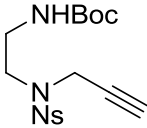
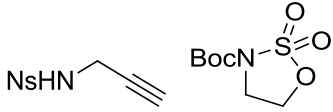
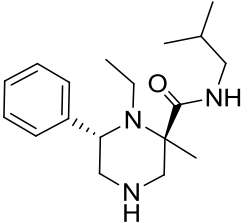
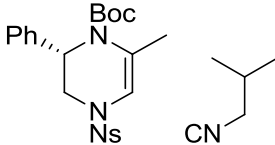
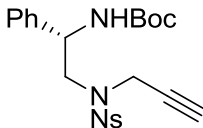
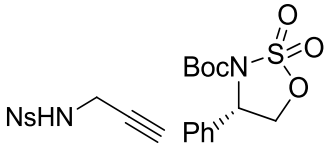
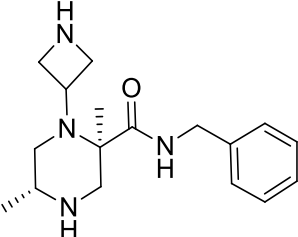
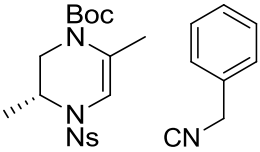
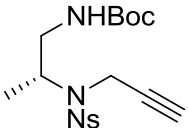
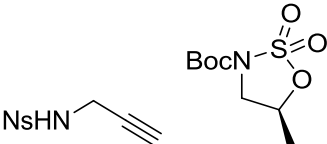
				<p>Cyclic sulfamidate ring opening</p> <p>Au-mediated hydroamination</p> <p>Ugi reaction</p>
				<p>Cyclic sulfamidate ring opening</p> <p>Au-mediated hydroamination</p> <p>Ugi reaction</p>
				<p>Cyclic sulfamidate ring opening</p> <p>Au-mediated hydroamination</p> <p>Ugi reaction</p>

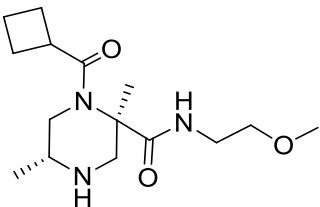
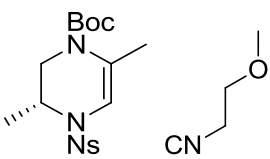
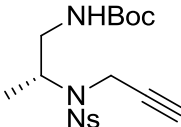
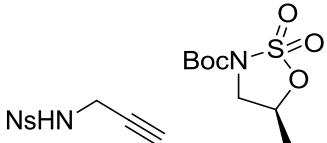
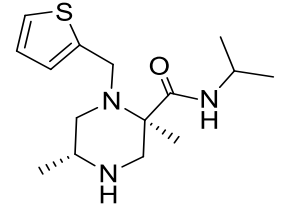
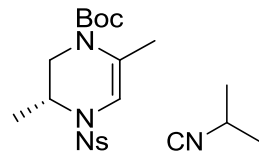
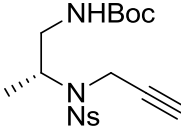
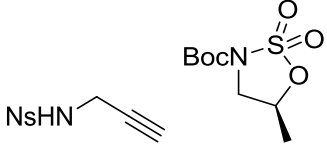
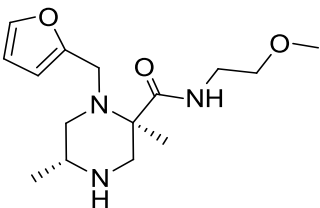
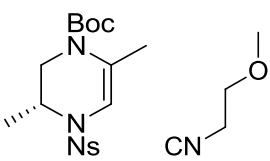
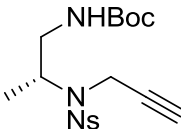
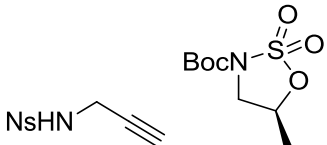
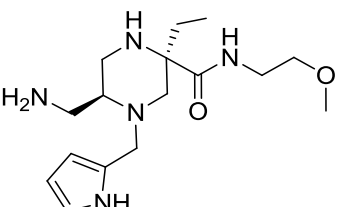
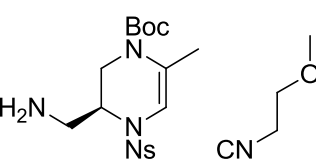
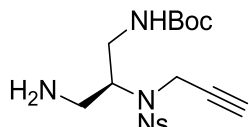
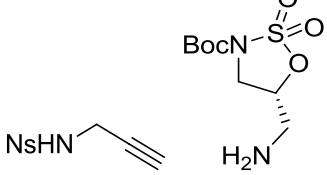
				<p>Cyclic sulfamidate ring opening</p> <p>Au-mediated hydroamination</p> <p>Ugi reaction</p>
				<p>Cyclic sulfamidate ring opening</p> <p>Mitsunobu reaction</p>
				<p>Cyclic sulfamidate ring opening</p> <p>Mitsunobu reaction</p>

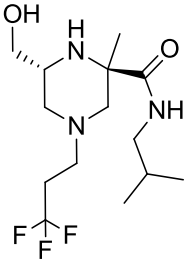
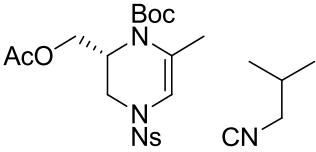
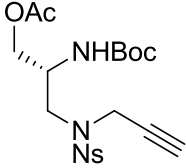
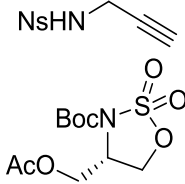
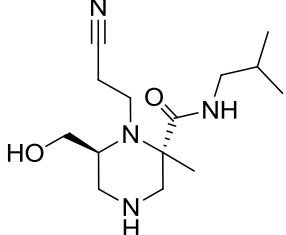
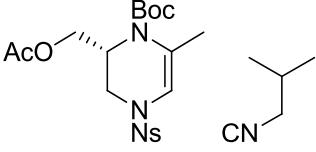
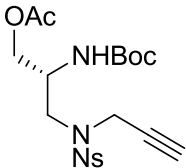
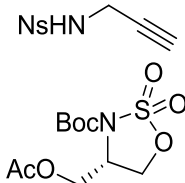
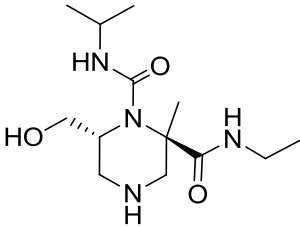
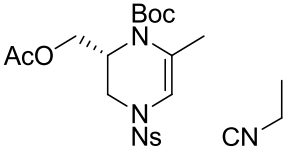
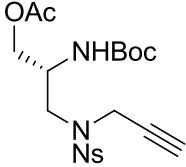
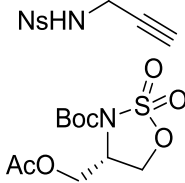
				Cyclic sulfamidate ring opening Mitsunobu reaction
				Cyclic sulfamidate ring opening Mitsunobu reaction
<b>Virtual Fragment (Run 2)</b>	<b>Key Intermediate</b>	<b>Key Intermediate</b>	<b>Building Blocks</b>	<b>Reactions Occurred</b>
				Allylic amination CDI-urea formation

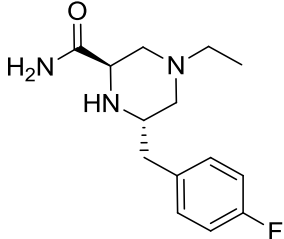
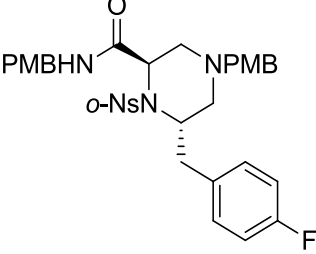
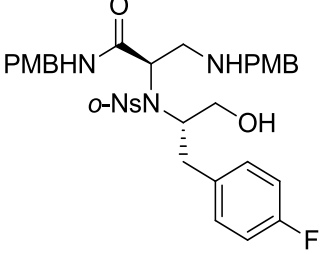
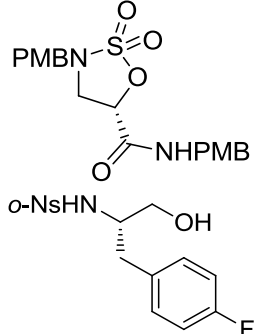
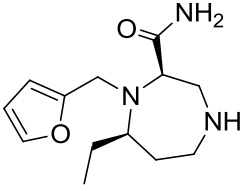
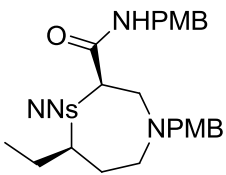
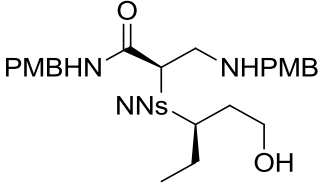
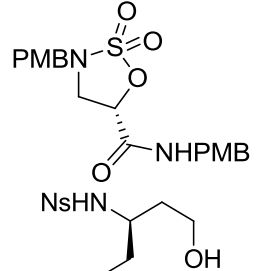
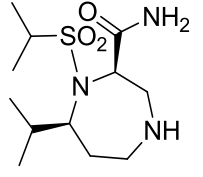
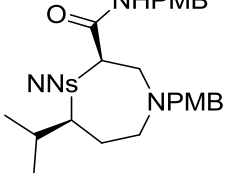
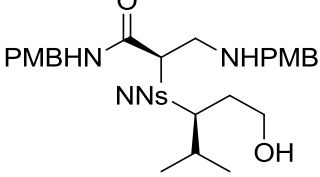
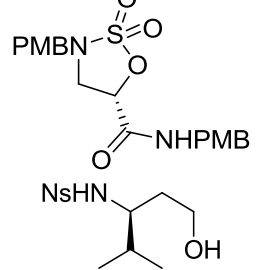
				<p>Allylic amination CDI-urea formation</p>
				<p>Allylic amination CDI-urea formation</p>
				<p>Urea formation Hydantoin formation</p>

				<p>Urea formation Hydantoin formation</p>
				<p>Urea formation Hydantoin formation</p>
				<p>Cyclic sulfamidate ring opening Alkyne hydration Ugi reaction</p>

				<p>Cyclic sulfamidate ring opening</p> <p>Au-mediated hydroamination</p> <p>Ugi reaction</p>
				<p>Cyclic sulfamidate ring opening</p> <p>Au-mediated hydroamination</p> <p>Ugi reaction</p>
				<p>Cyclic sulfamidate ring opening</p> <p>Au-mediated hydroamination</p> <p>Ugi reaction</p>

				Cyclic sulfamidate ring opening Au-mediated hydroamination Ugi reaction
				Cyclic sulfamidate ring opening Au-mediated hydroamination Ugi reaction
				Cyclic sulfamidate ring opening Au-mediated hydroamination Ugi reaction
				Cyclic sulfamidate ring opening Au-mediated hydroamination Ugi reaction

				<p>Cyclic sulfamidate ring opening</p> <p>Au-mediated hydroamination</p> <p>Ugi reaction</p>
				<p>Cyclic sulfamidate ring opening</p> <p>Au-mediated hydroamination</p> <p>Ugi reaction</p>
				<p>Cyclic sulfamidate ring opening</p> <p>Au-mediated hydroamination</p> <p>Ugi reaction</p>

				<p>Cyclic sulfamidate ring opening</p> <p>Mitsunobu reaction</p>
				<p>Cyclic sulfamidate ring opening</p> <p>Mitsunobu reaction</p>
				<p>Cyclic sulfamidate ring opening</p> <p>Mitsunobu reaction</p>

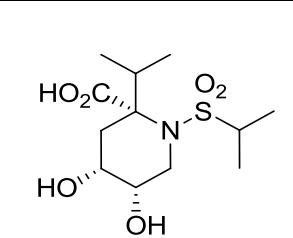
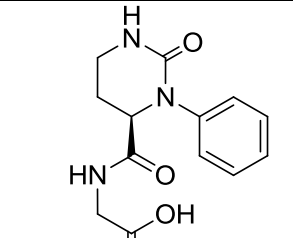
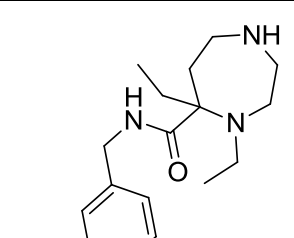
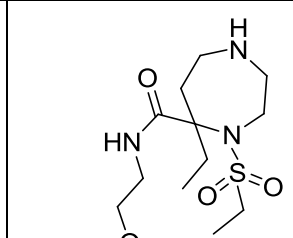
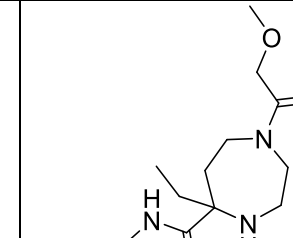
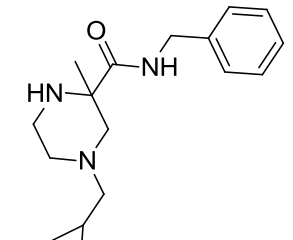
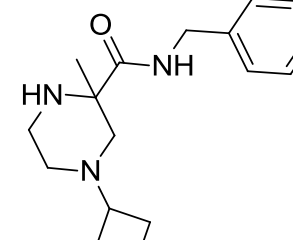
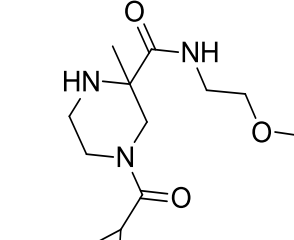
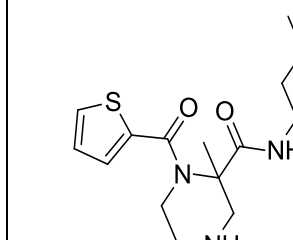
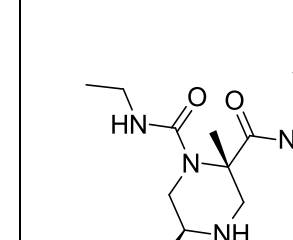
**Table 36** For each framework type in the random library of 80 fragments, the frequency of compounds containing the framework has been summarised, as well as the corresponding frequency of compounds containing the same framework in the combined library of 73,031 fragments. The frameworks were ordered in decreasing frequency of compounds present in the random library of 80, and those frequencies were then normalised in order to make them independent of the library size. This was done in order to compare the relationship between frequencies of frameworks in a random library of 80 fragments and the combined library. A full description can be found in Section 2.7.2.

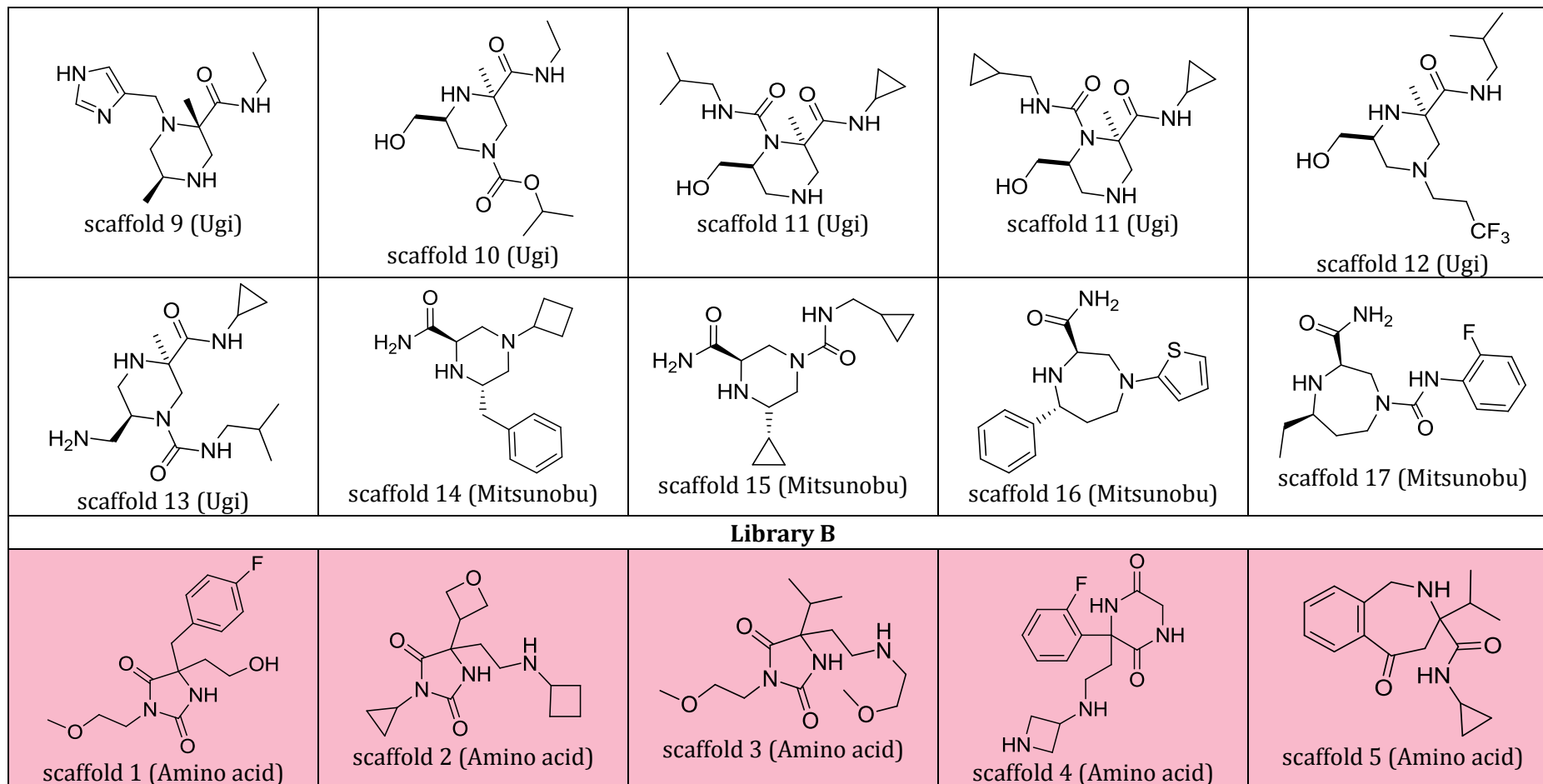
Framework (Smiles)	Frequency in Random Library of 80	Normalised Frequency	Frequency in Combined Library of 73,031	Normalised Frequency
C1CCCCC1	8	0.1000	6714	0.0919
C(CC1CCCCC1)C2CCCCC2	6	0.0750	3156	0.0432
C1CCC(CC1)C2CCCCC2	3	0.0375	2331	0.0319
C(C1CCCC1)C2CCCCC2	3	0.0375	2209	0.0302
C(C1CCCCC1)C2CCCCC2	3	0.0375	2498	0.0342
C(CC1CCCCC1)CC2CCCCC2	3	0.0375	2809	0.0385
C1CCCCC1	2	0.0250	328	0.0045
C(CCC1CCCC1)CC2CCCC2	1	0.0125	338	0.0046
C(CCC1CCCCC1)CC2CC2	1	0.0125	117	0.0016
C(CC1CCC2CCCCC2C1)C3CC3	1	0.0125	19	0.0003
C(CC1CC1)CC2CCCCC2	1	0.0125	131	0.0018
C(CCC1CCCC1)CCC2CCCCC2	1	0.0125	1589	0.0218
C1CCC(CC1)C2CC3C4CCC(C4)C3C2	1	0.0125	65	0.0009
C(CC1CCC(C1)C2CC2)C3CCCC3	1	0.0125	17	0.0002
C(CC1CCCCC1)CC2CCC3CCCC23	1	0.0125	58	0.0008
C(C1CCCCC1)C2CCCC3CCCC23	1	0.0125	95	0.0013
C(CCCC1CCCCC1)CCC2CC2	1	0.0125	92	0.0013

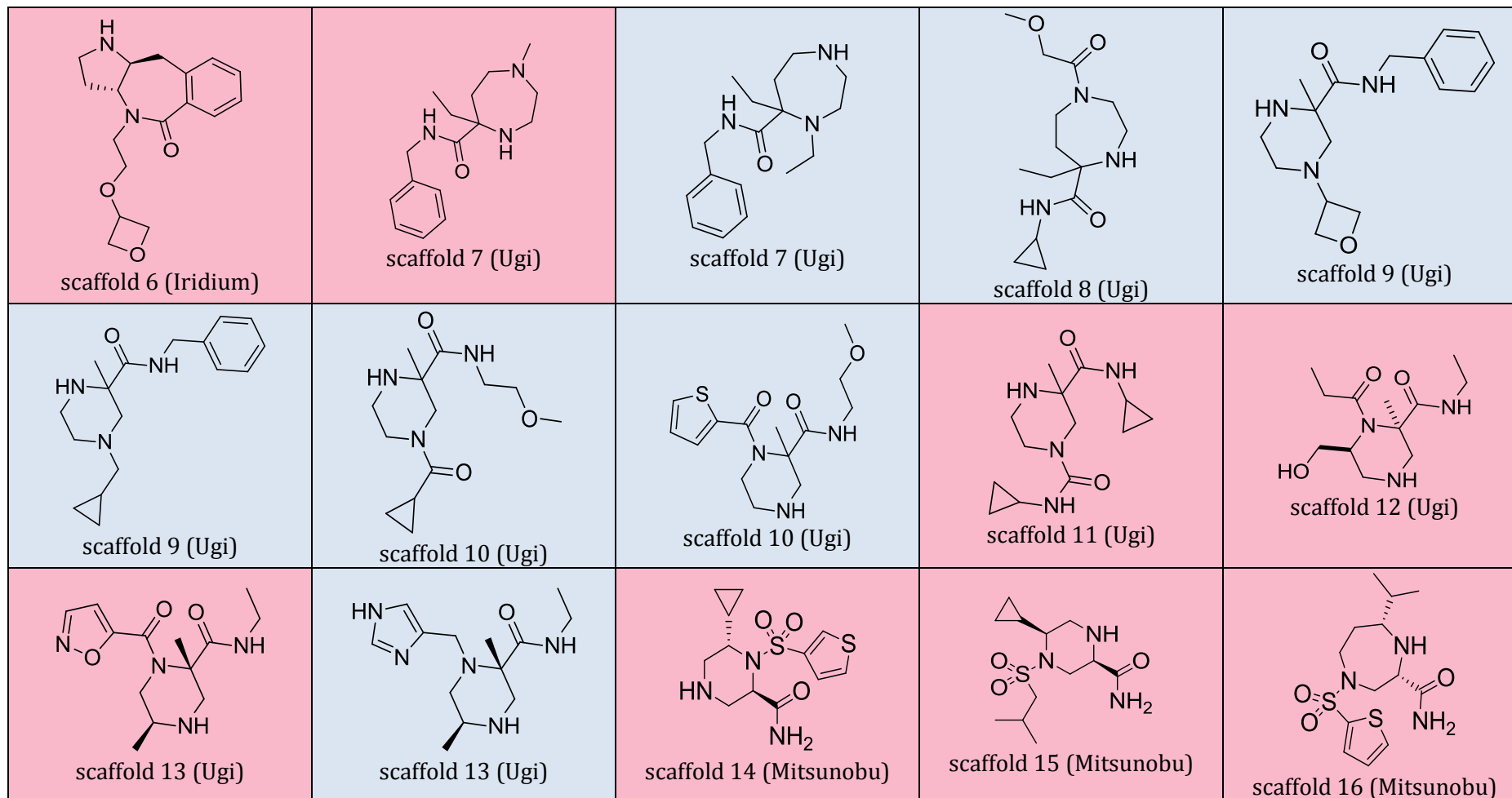
C(C1CCCC1)C2CCC(CC2)C3CCCCC3	1	0.0125	128	0.0018
C(CC1CCCC1)CC2CC3CCC2C3	1	0.0125	7	0.0001
C(CC(C1CCCC1)C2CCCC2)CC3CCCC3	1	0.0125	21	0.0003
C(C1CCCC1)C2CCCC3CCCCC23	1	0.0125	104	0.0014
C(C1CCCC1)C2CCCC3CCCC23	1	0.0125	18	0.0002
C(C1CCCC1)C2CCCC3C4CCCCC4CC23	1	0.0125	1	0
C(CC1CCCC1)CC2CCCCC2	1	0.0125	2307	0.0316
C(CC1CC2CCCCC2C1)C3CCCC3	1	0.0125	174	0.0024
C(C1CCCC1)C2CCCC(C2)C3CCCCC3	1	0.0125	108	0.0015
C(CC1CCCC1C2CC2)C3CCCCC3	1	0.0125	7	0.0001
C(C1CCCCC1)C2CCC(C2)C3CCCCC3	1	0.0125	286	0.0039
C(C1CCCC1)C2CCCC2C3CCCC3	1	0.0125	95	0.0013
C(CCCC1CCCC1)CCC2CCCCC2	1	0.0125	593	0.0081
C(CC1CCC(C1)C2CCCCC2)C3CC3	1	0.0125	20	0.0003
C(CC1CCC2CCCC2C1)C3CCCC3	1	0.0125	161	0.0022
C(C1CCCCC1)C2CCC(C2)C3CCCCC3	1	0.0125	102	0.0014
C(CC1CCC1)CC2CCCC2	1	0.0125	34	0.0005
C(CC1CCC1)CC2CC3CCCCC3CC4CCCC24	1	0.0125	2	0
C(CC1CCCCC1CC2CC2)C3CC3	1	0.0125	20	0.0003
C(C1CCCC1)C2CCC3CCCC3CC2	1	0.0125	8	0.0001
C1CCC(CC1)C2CCCCC2C3CCCC3	1	0.0125	54	0.0007
C1CCCC(CC1)C2CC2	1	0.0125	6	0.0001
C(CC1CCCCC1C2CCCC2)C3CC3	1	0.0125	5	0.0001
C1CCC2CCCCC2CC1	1	0.0125	139	0.0019
C(C1CCC1)C2CCCCC2	1	0.0125	38	0.0005
C1CCCC(CC1)C2CCC2	1	0.0125	24	0.0003
C(CC1CCCCC1)C2CC2	1	0.0125	426	0.0058

C(CC1CCCC1)CC2CCC3CCCC3C2	1	0.0125	213	0.0029
C1CCC(CC1)C2CCC3CCCC3C2	1	0.0125	323	0.0044
C(CC1CCC2CCCC12)C3CCCC3	1	0.0125	240	0.0033
C1CCCCCCC2CCCCC2CCCCC1	1	0.0125	4	0.0001
C1CCCC(CC1)C2CCCC2	1	0.0125	61	0.0008
C(CCC1CC2CCCC2C1)CC3CCCC3	1	0.0125	114	0.0016
C(CCC1CCCC1)CC2CCCC2	1	0.0125	2299	0.0315
C(CC1CCCC1)CC2CCC3CCCC3C2	1	0.0125	209	0.0029
C1CCC(CC1)C2CCC(C2)C3CCCC3	1	0.0125	140	0.0019
C1CCC2CCCC2C1	1	0.0125	1437	0.0197
C(CC(C1CCCC1)C2CCCC2)CC3CCCC3	1	0.0125	21	0.0003
C(CC1CCCC1)C2CCCC2	1	0.0125	2343	0.0321
C1CCC(C1)C2CC3CCC(C4CCCC4)C3C2	1	0.0125	11	0.0002
C(CC1CCCC1)CC2CCCC(CC3CC3)C2	1	0.0125	1	0
C1CCC2CC3CCCC3CC2C1	1	0.0125	99	0.0014

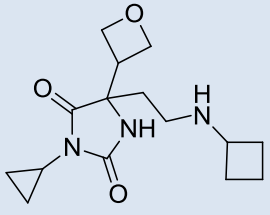
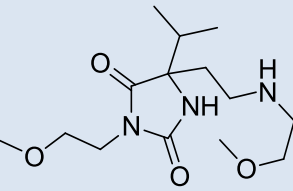
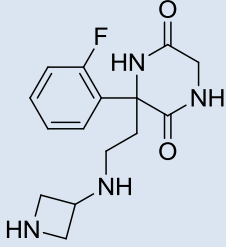
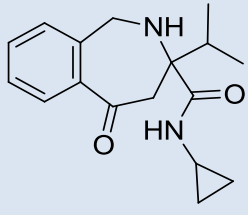
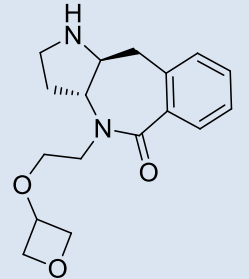
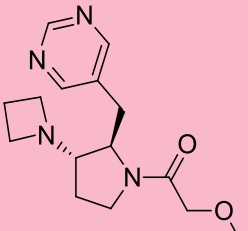
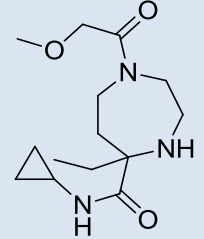
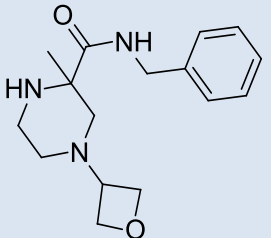
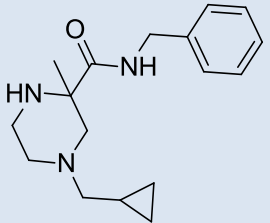
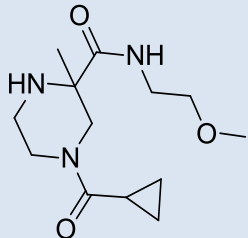
**Table 37 A:** Library A, the original library of 20 fragments selected from the Leeds virtual fragment library; **B:** Library B, the second library of 20 fragments selected from the Leeds virtual fragment library. Fragments in blue are from Library A and fragments in pink are new; **C:** Library C, the third library of 20 fragments selected from the Leeds virtual fragment library. Fragments in blue are from Libraries A and B and fragments in pink are new; **D:** Library D, the final library of 20 fragments selected from the Leeds virtual fragment library which was eventually synthesised. Fragments in blue are from Libraries A, B and C and fragments in pink are new. Each fragment has been labelled with the scaffold from which they originate as well as the chemistry used for their key stage for formation. A full description can be found in Section 3.2

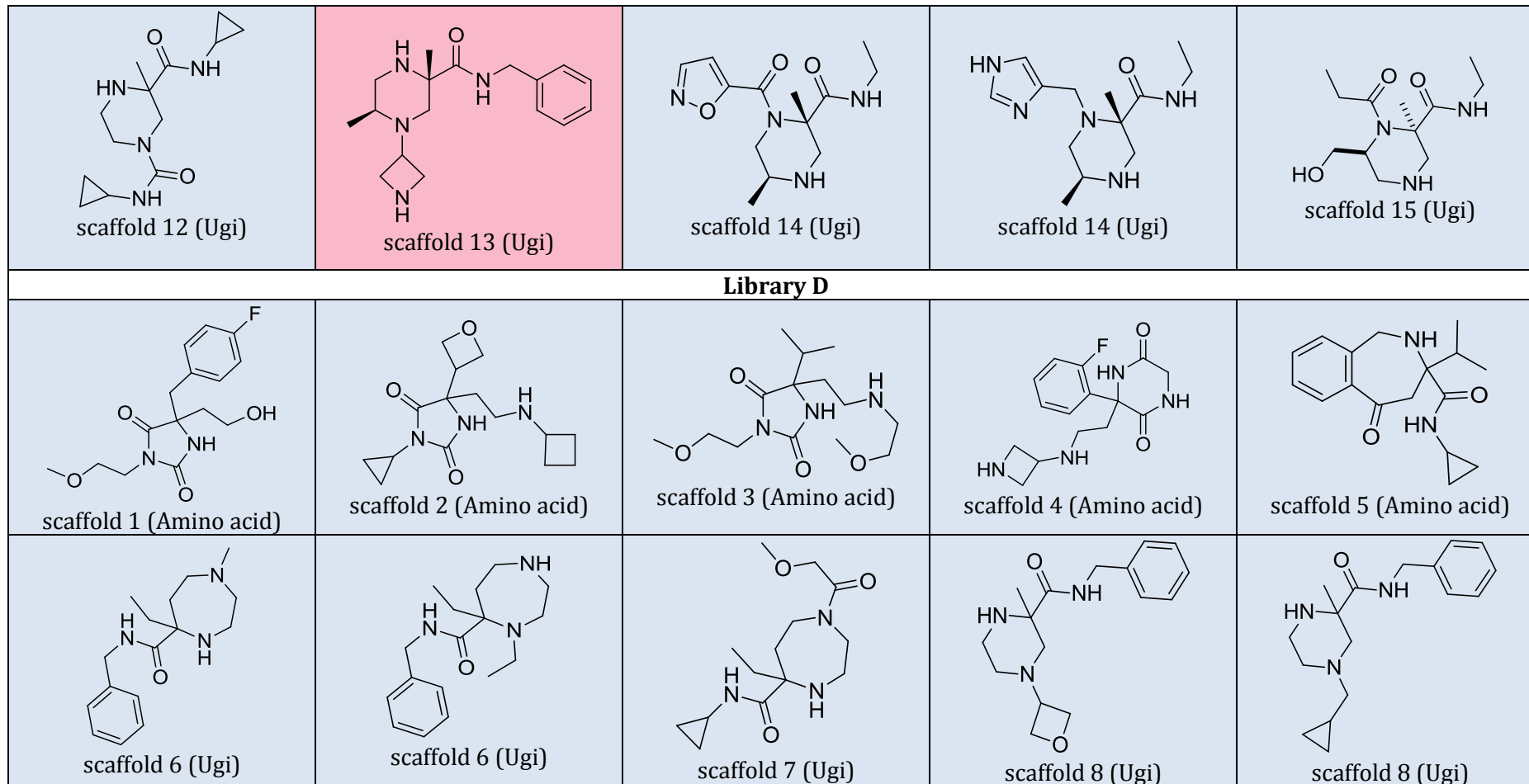
Library A				
 <p>scaffold 1 (Amino acid)</p>	 <p>scaffold 2 (Iridium)</p>	 <p>scaffold 3 (Ugi)</p>	 <p>scaffold 4 (Ugi)</p>	 <p>scaffold 5 (Ugi)</p>
 <p>scaffold 6 (Ugi)</p>	 <p>scaffold 6 (Ugi)</p>	 <p>scaffold 7 (Ugi)</p>	 <p>scaffold 7 (Ugi)</p>	 <p>scaffold 8 (Ugi)</p>

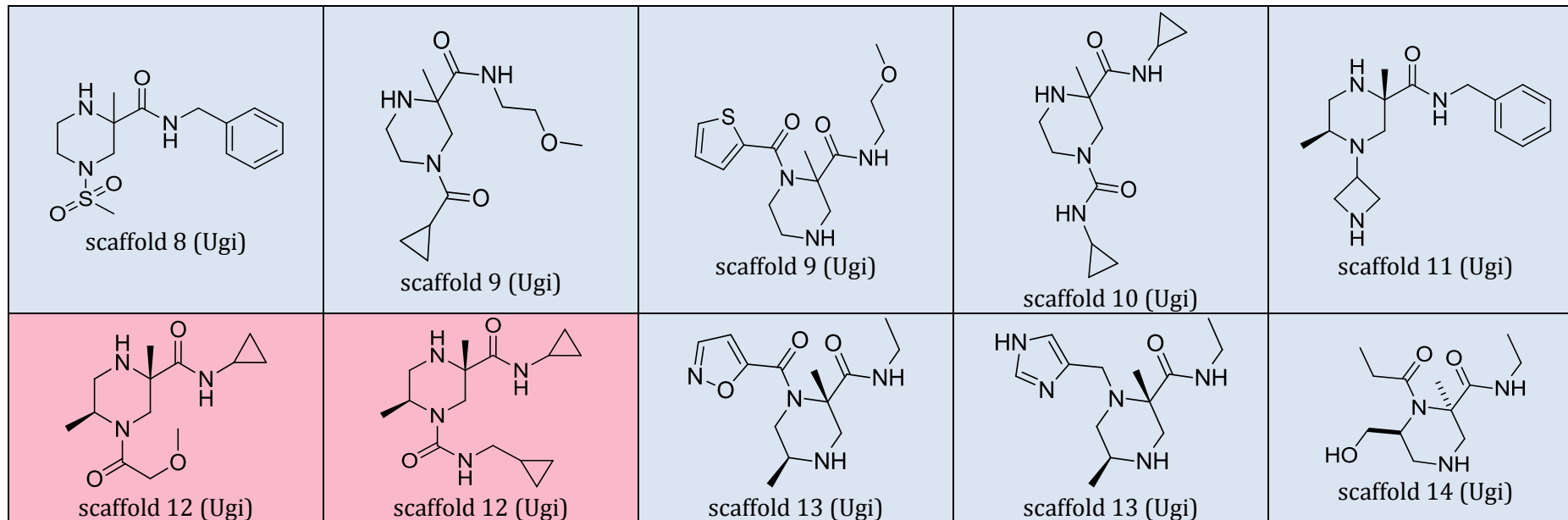




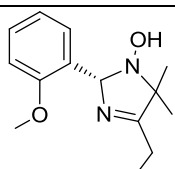
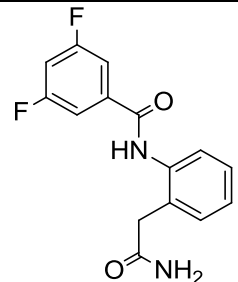
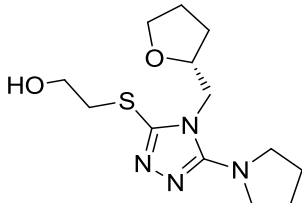
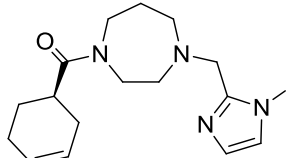
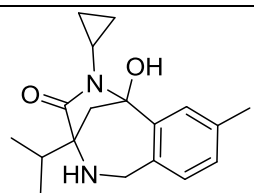
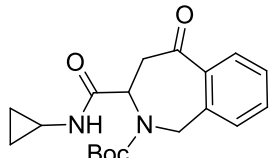
Library C

 <p>scaffold 1 (Amino acid)</p>	 <p>scaffold 2 (Amino acid)</p>	 <p>scaffold 3 (Amino acid)</p>	 <p>scaffold 4 (Amino acid)</p>	 <p>scaffold 5 (Amino acid)</p>
 <p>scaffold 6 (Iridium)</p>	 <p>scaffold 7 (Iridium)</p>	 <p>scaffold 8 (Ugi)</p>	 <p>scaffold 8 (Ugi)</p>	 <p>scaffold 9 (Ugi)</p>
 <p>scaffold 10 (Ugi)</p>	 <p>scaffold 10 (Ugi)</p>	 <p>scaffold 10 (Ugi)</p>	 <p>scaffold 11 (Ugi)</p>	 <p>scaffold 11 (Ugi)</p>





**Table 38** Other hits identified from the screen of 60 commercial molecules and 10 Leeds analogues against Aurora A. The sites targeted by each fragment has been described along with quality of their observed crystal densities. A full description can be found in Section 4.3.2.

Structure	Site of Target	Comment
<i>ZINC Commercial Library</i>		
	1	Weak crystal density and orientation unclear.
	1	Reasonable crystal density and exists in two conformations.
	2	Reasonable crystal density but tail of fragment unclear.
	2	Weak crystal density.
<i>Leeds Library</i>		
	1	Weak crystal density, fragment orientation unclear.
	1	Weak crystal density, fragment orientation unclear.

## References

1. Murray, C. W. & Rees, D. C. The rise of fragment-based drug discovery. *Nat. Chem.* **1**, 187–192 (2009).
2. Roughley, S. D. & Jordan, A. M. The medicinal chemist's toolbox: An analysis of reactions used in the pursuit of drug candidates. *J. Med. Chem* **54**, 3451–3479 (2011).
3. Churcher, I., Nadin, A. & Hattotuwigama, C. Lead-oriented synthesis: A new opportunity for synthetic chemistry. *Angew. Chem. Int. Ed.* **51**, 1114–1122 (2012).
4. Lipinski, C. A., Lombardo, F., Dominy, B. W. & Feeney, P. J. Experimental and computational approaches to estimate solubility and permeability in drug discovery and development settings. *Adv. Drug Deliv. Rev.* **46**, 3–26 (2001).
5. MacLellan, P. & Nelson, A. A conceptual framework for analysing and planning synthetic approaches to diverse lead-like scaffolds. *Chem. Commun.* **49**, 2383–2393 (2013).
6. Lovering, F., Bikker, J. & Humblet, C. Escape from flatland: Increasing saturation as an approach to improving clinical success. *J. Med. Chem.* **52**, 6752–6756 (2009).
7. Hann, M. M. & Oprea, T. I. Pursuing the leadlikeness concept in pharmaceutical research. *Curr. Op. Chem. Biol.* **8**, 255–263 (2004).
8. Wassermann, A. M. *et al.* Efficient search of chemical space: Navigating from fragments to structurally diverse chemotypes. *J. Med. Chem* **56**, 8879–8891 (2013).
9. Lehn, J. Dynamic combinatorial chemistry and virtual combinatorial libraries. *Chem. Eur. J.* **2**, 2455–2463 (1999).
10. Terrett, N. K., Gardner, M., Gordon, D. W., Kobylecki, R. J. & Steele, J. Drug discovery by combinatorial chemistry- the development of a novel method for the rapid synthesis of single compounds. *Chem. Eur. J.* **3**, 1917–2463 (1997).
11. Lowe, G. Combinatorial Chemistry. *Chem. Soc. Rev.* **24**, 309–317 (1995).
12. Persidis, A. High-throughput screening. *Nat. Biotechnol.* **16**, 488–489 (1998).
13. Oprea, T. I. Virtual screening in lead discovery: A viewpoint. *Molecules* **7**, 51–62 (2002).
14. Rishton, G. M. Reactive compounds and in vitro false positives in HTS. *Drug Discov. Today* **2**, 382–384 (1997).
15. Oprea, T. I., Zamora, I. & Svensson, P. *Combinatorial library design and evaluation for drug design.* (2001).
16. Morley, A. D. *et al.* Fragment-based hit identification: Thinking in 3D. *Drug Discov. Today* **18**, 1221–1227 (2013).
17. Kirkpatrick, P. & Ellis, C. Chemical Space. *Nature* **432**, 823 (2004).
18. Reddy, V. P. in *Organofluorine Compounds in Biology and Medicine* 265–300 (2015).
19. Souers, A. J. *et al.* ABT-199, A potent and selective BCL-2 inhibitor, achieves antitumor activity while sparing platelets. *Nat Med* **19**, 202–208 (2013).
20. Hajduk, P. J. Fragment-based drug design: How big is too big? *J. Med. Chem* **49**, 6972–6976 (2006).
21. Wyatt, P. G. *et al.* Identification of AT7519, a novel cyclin dependent kinase inhibitor using fragment-based X-ray crystallography and structure based drug design. *J. Med. Chem.* **51**, 4986–4999 (2008).
22. Erlanson, D. A., McDowell, R. S. & O'Brien, T. Fragment-based drug discovery. *J. Med. Chem* **47**, 3463–3482 (2004).

23. Leach, A. R. & Hann, M. M. Molecular complexity and fragment-based drug discovery: Ten years on. *Curr. Op. Chem. Biol.* **15**, 489–496 (2011).
24. Hajduk, P. J. & Greer, J. A decade of fragment-based drug design: Strategic advances and lessons learned. *Nat Rev Drug Discov* **6**, 211–219 (2007).
25. Shepherd, C. A., Hopkins, A. L. & Navratilova, I. Fragment screening by SPR and advanced application to GPCRs. *Prog. Biophys. Mol. Biol.* **116**, 113–123 (2014).
26. Silvestre, H. L., Blundell, T. L., Abell, C. & Ciulli, A. Integrated biophysical approach to fragment screening and validation for fragment-based lead discovery. *Proc. Natl. Acad. Sci.* **110**, 12984–12989 (2013).
27. Cooper, M. A. Optical biosensors in drug discovery. *Nat Rev Drug Discov* **1**, 515–528 (2002).
28. Navratilova, I. & Hopkins, A. L. Fragment screening by surface plasmon resonance. *ACS Med. Chem. Lett.* **1**, 44–48 (2010).
29. Dalvit, C. NMR methods in fragment screening: Theory and a comparison with other biophysical techniques. *Drug Discov. Today* **14**, 1051–1057 (2009).
30. Hämäläinen, M. D. *et al.* Label-free primary screening and affinity ranking of fragment libraries using parallel analysis of protein panels. *J. Biomol. Screen.* **13**, 202–209 (2008).
31. Navratilova, I. *et al.* Thermodynamic benchmark study using Biacore technology. *Anal. Biochem.* **364**, 67–77 (2007).
32. Moore, J. M. NMR screening in drug discovery. *Curr. Opin. Biotechnol.* **10**, 54–58 (1999).
33. Jhoti, H., Cleasby, A., Verdonk, M. & Williams, G. Fragment-based screening using X-ray crystallography and NMR spectroscopy. *Curr. Opin. Chem. Biol.* **11**, 485–493 (2007).
34. Nienaber, V. L. *et al.* Discovering novel ligands for macromolecules using X-ray crystallographic screening. *Nat Biotech* **18**, 1105–1108 (2000).
35. Blum, L. C. & Reymond, J. L. 970 Million druglike small molecules for virtual screening in the chemical universe database GDB-13. *J. Am. Chem. Soc.* **131**, 8732–8733 (2009).
36. Jhoti, H., Williams, G., Rees, D. C. & Murray, C. W. The ‘rule of three’ for fragment-based drug discovery: Where are we now? *Nat Rev Drug Discov* **12**, 644 (2013).
37. Collins, K. D., Rühling, A., Lied, F. & Glorius, F. Rapid assessment of protecting-group stability by using a robustness screen. *Chem. Eur. J.* **20**, 3800–3805 (2014).
38. Nie, F. *et al.* A multidimensional diversity-oriented synthesis strategy for structurally diverse and complex macrocycles. *Angew. Chemie Int. Ed.* **55**, 11139–11143 (2016).
39. Hung, A. W. *et al.* Route to three-dimensional fragments using diversity-oriented synthesis. *Proc. Natl. Acad. Sci.* **108**, 6799–6804 (2011).
40. Ruijter, E., Scheffelaar, R. & Orru, R. V. A. Multicomponent reaction design in the quest for molecular complexity and diversity. *Angew. Chem. Int. Ed.* **50**, 6234–6246 (2011).
41. Doveston, R. G. *et al.* A unified lead-oriented synthesis of over fifty molecular scaffolds. *Org. Biomol. Chem.* **13**, 859–865 (2015).
42. James, T. *et al.* A modular lead-oriented synthesis of diverse piperazine, 1,4-diazepane and 1,5-diazocane scaffolds. *Org. Biomol. Chem.* **12**, 2584–2591 (2014).
43. Foley, D. J., Doveston, R. G., Churcher, I., Nelson, A. & Marsden, S. P. A systematic approach to diverse, lead-like scaffolds from  $\alpha$ ,  $\alpha$ -disubstituted amino acids. *Chem. Commun.* **51**, 11174–11177 (2015).

44. James, T., Simpson, I., Grant, J. A., Sridharan, V. & Nelson, A. Modular, gold-catalyzed approach to the synthesis of lead-like piperazine scaffolds. *Org. Lett.* **15**, 6094–6097 (2013).
45. Brown, N. & Jacoby, E. On scaffolds and hopping in medicinal chemistry. *Mini-Rev. Med. Chem* **6**, 1217–1229 (2006).
46. Lipkus, A. *et al.* Structural diversity of organic chemistry. A scaffold analysis of the CAS registry. *J. Org. Chem* **73**, 4443–4451 (2008).
47. Krier, M., Bret, G. & Rognan, D. Assessing the scaffold diversity of screening libraries. *J. Chem. Inf. Model.* **46**, 512–524 (2006).
48. Burke, M. D., Berger, E. M. & Schreiber, S. L. Generating diverse skeletons of small molecules combinatorially. *Science*. **302**, 613–618 (2003).
49. Brustle, M. *et al.* Descriptors, physical properties, and drug-likeness. *J. Med. Chem* **45**, 3345–3355 (2002).
50. Sauer, W. H. B. & Schwarz, M. K. Molecular shape diversity of combinatorial libraries: A prerequisite for broad bioactivity. *J. Chem. Inf. Comput. Sci.* **43**, 987–1003 (2003).
51. Haigh, J. A., Pickup, B. T., Grant, J. A. & Nicholls, A. Small molecule shape-fingerprints. *J. Chem. Inf. Model.* **45**, 673–684 (2005).
52. Flower, D. On the properties of bit string-based measures of chemical similarity. *J. Chem. Inf. Comput. Sci.* **38**, 379–386 (1998).
53. Leung, C. S., Leung, S. S. F., Tirado-Rives, J. & Jorgensen, W. L. Methyl effects on protein ligand binding. *J. Med. Chem.* **55**, 4489–4500 (2012).
54. vandeWaterbeemd, H., Camenisch, G., Folkers, G. & Raevsky, O. A. Estimation of Caco-2 cell permeability using calculated molecular descriptors. *QSAR* **15**, 480–490 (1996).
55. Good, A. C., Hermsmeier, M. A. & Hindle, S. A. Measuring CAMD technique performance: A virtual screening case study in the design of validation experiments. *J. Comput. Aided Mol. Des.* **18**, 529–536 (2004).
56. Grant, J. A., Gallardo, M. A. & Pickup, B. T. A fast method of molecular shape comparison: A simple application of a Gaussian description of molecular shape. *J. Comput. Chem.* **17**, 1653–1666 (1996).
57. Nikolova, N. & Jaworska, J. Approaches to measure chemical similarity. *QSAR Comb. Sci.* **22**, 1006–1026 (2003).
58. Fontaine, F., Bolton, E. & Borodina, Y. Fast 3D shape screening of large chemical databases through alignment-recycling. *Chem. Cent. J.* **1**, 12 (2007).
59. Irwin, J. J., Sterling, T., Mysinger, M. M., Bolstad, E. S. & Coleman, R. G. ZINC: A free tool to discover chemistry for biology. *J. Chem. Inf. Model.* **52**, 1757–1768 (2012).
60. Gasteiger, J., Rudolph, C. & Sadowski, J. Automatic generation of 3D-atomic coordinates for organic molecules. *Tetrahedron Comput. Methodol.* **3**, 537–547 (1990).
61. Deepak, M. S., Roland, F. & Haufe, G. Highly efficient stereoconservative amidation and deamidation of  $\alpha$ -amino acids. (2004).
62. Bower, J. F. *et al.* N-Heterocycle construction via cyclic sulfamidates. Applications in synthesis. *Org. Biomol. Chem.* **8**, 1505 (2010).
63. Williams, A. J., Chakthong, S., Gray, D., Lawrence, R. M. & Gallagher, T. 1,2-Cyclic sulfamidates as versatile precursors to thiomorpholines and piperazines. (2003).
64. Das, R. & Chakraborty, D. Silver triflate catalyzed acetylation of alcohols, thiols, phenols, and amines. *Synthesis (Stuttg)*. **2011**, 1621–1625 (2011).
65. Nicolai, S. & Waser, J. Pd(0)-Catalyzed oxy- and aminoalkynylation of olefins for the synthesis of tetrahydrofurans and pyrrolidines. *Org. Lett.* **13**, 6324–6327 (2011).

66. Han, J., Xu, B. & Hammond, G. B. Highly efficient Cu(I)-catalyzed synthesis of N - Heterocycles through a cyclization-triggered addition of alkynes. *J. Am. Chem. Soc.* **132**, 916–917 (2010).
67. Weyrauch, J. P. *et al.* Cyclization of propargylic amides: Mild access to oxazole derivatives. *Chem. - A Eur. J.* **16**, 956–963 (2010).
68. Stephen, A., Hashmi, K., Weyrauch, J. P., Frey, W. & Bats, J. W. Gold catalysis: Mild conditions for the synthesis of oxazoles from N-propargylcarboxamides and mechanistic aspects. (2004).
69. Hashmi, K., Stephen, A., Molinari, L., Rominger, F. & Oeser, T. Gold catalysis: Products and intermediates obtained from N-propargylcarboxamides bearing additional substituents on nitrogen. *European J. Org. Chem.* **2011**, 2256–2264 (2011).
70. Tsukano, C. *et al.* Platinum catalyzed 7-endo cyclization of internal alkynyl amides and its application to synthesis of the caprazamycin core. *Org. Biomol. Chem.* **10**, 6074 (2012).
71. Hansmann, M. M., Rudolph, M., Rominger, F., Hashmi, K. & Stephen, A. Mechanistic switch in dual gold catalysis of diynes: C(sp<sup>3</sup>)-H activation through bifurcation-vinylidene versus carbene pathways. *Angew. Chemie Int. Ed.* **52**, 2593–2598 (2013).
72. Li, Z., Brouwer, C. & He, C. Gold-catalyzed organic transformations. *Chem. Rev.* **108**, 3239–3265 (2008).
73. Ito, H., Harada, T., Ohmiya, H. & Sawamura, M. Intramolecular hydroamination of alkynic sulfonamides catalyzed by a gold–triethynylphosphine complex: Construction of azepine frameworks by 7- exo - dig cyclization. *Beilstein J. Org. Chem.* **7**, 951–959 (2011).
74. Zhang, Y., Donahue, J. P. & Li, C.-J. Gold(III)-catalyzed double hydroamination of o-alkynylaniline with terminal alkynes leading to N-vinylindoles. (2007).
75. Kang, J.-E., Kim, H.-B., Lee, J.-W. & Shin, S. Gold(I)-Catalyzed intramolecular hydroamination of alkyne with trichloroacetimidates. (2006).
76. Müller, T. E. *et al.* Developing transition-metal catalysts for the intramolecular hydroamination of alkynes. (1999).
77. Sanudo, M., García-Valverde, M., Marcaccini, S. B. & Torroba, T. A. A diastereoselective synthesis of pseudopeptidic hydantoins. *Tetrahedron* **68**, 2621–2629 (2012).
78. Lin, J., Cammarata, V. & Worley, S. D. Infrared characterization of biocidal nylon. *Polymer (Guildf)*. **42**, 7903–7906 (2001).
79. Ruider, S. A., Müller, S. & Carreira, E. M. Ring expansion of 3-oxetanone-derived spirocycles: Facile synthesis of saturated nitrogen heterocycles. *Angew. Chemie Int. Ed.* **52**, 11908–11911 (2013).
80. Lokey, S. & Turner, R. Use of trifluoroacetamide for N-terminal protection. (2013).
81. Green, T. W. & Wuts, P. G. M. *Protective Groups in Organic Synthesis*. (1999).
82. Abdel-Magid, A. F., Kenneth G. Carson, Bruce D. Harris, Cynthia A. Maryanoff & Shah, R. D. Reductive Amination of Aldehydes and Ketones with Sodium Triacetoxyborohydride. Studies on Direct and Indirect Reductive Amination Procedures1. (1996).
83. Cardullo, F. *et al.* Deprotection of o-nitrobenzenesulfonyl (nosyl) derivatives of amines mediated by a solid-supported thiol. *SYNLETT* **19**, 2996–2998 (2005).
84. Firth, J. D. *et al.* Exploitation of the Ugi–Joullié reaction in the synthesis of libraries of drug-like bicyclic hydantoins. *Synthesis (Stuttg)*. **47**, 2391–2406. (2015).
85. Meshram, G. A. & Patil, V. D. A simple and efficient method for sulfonylation of amines, alcohols and phenols with cupric oxide under mild conditions. *Tetrahedron Lett.* **50**, 1117–1121 (2009).

86. Charrier, J. D. *et al.* WO2010/54398 A1. (2010).
87. Phukan, K., Ganguly, M. & Devi, N. Mild and useful method for N-acylation of amines. *Synth. Commun.* **39**, 2694–2701 (2009).
88. Carnaroglio, D. *et al.* One-pot sequential synthesis of isocyanates and urea derivatives via a microwave-assisted Staudinger–aza-Wittig reaction. *Beilstein J. Org. Chem.* **9**, 2378–2386 (2013).
89. Confalone, P. N., Huie, E. M., Ko, S. S. & Cole, G. M. Design and synthesis of potential DNA cross-linking reagents based on the anthramycin class of minor groove binding compounds. *J. Org. Chem.* **53**, 482–487 (1988).
90. Trost, B. M. & Ariza, X. Enantioselective allylations of azlactones with unsymmetrical acyclic allyl esters. *J. Am. Chem. Soc.* **121**, 10727–10737 (1999).
91. Moldes, M. T., Costantino, G., Marinozzi, M. & Pellicciari, R. Synthesis and preliminary biological evaluation at the glycineB site of (+)- and (-)-3-oxetanylglycine, novel non-proteinogenic amino acids. *Farm.* **56**, 609–613 (2001).
92. Bregman, H. *et al.* WO2013134079 (A1). (2013).
93. De Clercq, E. New developments in anti-HIV chemotherapy. *Biochim. Biophys. Acta - Mol. Basis Dis.* **1587**, 258–275 (2002).
94. Al-Warhi, T. I., Al-Hazimi, H. M. A. & El-Faham, A. Recent development in peptide coupling reagents. *J. Saudi Chem. Soc.* **16**, 97–116 (2012).
95. Dunetz, J. R., Magano, J. & Weisenburger, G. A. Large-scale applications of amide coupling Reagents for the synthesis of pharmaceuticals. *Org. Process Res. Dev.* **20**, 140–177 (2016).
96. Tom, N. J., Simon, W. M., Frost, H. N. & Ewing, M. Deprotection of a primary Boc group under basic conditions. *Tetrahedron Letters* **45**, (2004).
97. Mizoroki, T., Mori, K. & Ozaki, A. Arylation of olefin with aryl iodide catalyzed by palladium. *Bull. Chem. Soc. Jpn.* **44**, 581–581 (1971).
98. Schiaffo, C. E. & Dussault, P. H. Ozonolysis in solvent/water mixtures: Direct conversion of alkenes to aldehydes and ketones. *J. Org. Chem.* **73**, 4688–4690 (2008).
99. Pappo, R., Allen, Jr., D. S., Lemieux, R. U. & Johnson, W. S. Osmium tetroxide-catalyzed periodate oxidation of olefinic bonds. *J. Org. Chem.* **21**, 478–479 (1956).
100. Breuning, M., Steiner, M., Mehler, C., Paasche, A. & Hein, D. A flexible route to chiral 2-endo-substituted 9-oxabispindines and their application in the enantioselective oxidation of secondary alcohols. *J. Org. Chem.* **74**, 1407–1410 (2009).
101. Donohoe, T. J., Callens, C. K. A., Flores, A., Lacy, A. R. & Rathi, A. H. Recent developments in methodology for the direct oxyamination of olefins. *Chem. - A Eur. J.* **17**, 58–76 (2011).
102. Lucet, D., Le Gall, T. & Mioskowski, C. The chemistry of vicinal diamines. *Angew. Chemie Int. Ed.* **37**, 2580–2627 (1998).
103. Saha, N., Biswas, T. & Chattopadhyay, S. K. Enantiodivergent synthetic entry to the quinolizidine alkaloid lasubine II. *Org. Lett.* **13**, 5128–5131 (2011).
104. Chaumontet, M., Piccardi, R. & Baudoin, O. Synthesis of 3,4-dihydroisoquinolines by a C(sp<sup>3</sup>)-H activation/electrocyclization strategy: Total synthesis of coralydine. *Angew. Chemie Int. Ed.* **48**, 179–182 (2009).
105. Masamune, S., Choy, W., Petersen, J. S. & Sita, L. R. Double asymmetric synthesis and a new strategy for stereochemical control in organic synthesis. *Angew. Chemie Int. Ed. English* **24**, 1–30 (1985).
106. Heathcock, C. H. & White, C. T. Use of double stereodifferentiation to enhance 1,2 diastereoselection in aldol condensations of chiral aldehydes. *J. Am. Chem. Soc.* **101**, 7076–7077 (1979).

107. Annadi, K. & Wee, A. G. H. Ceric ammonium nitrate oxidation of N-(p-methoxybenzyl)lactams: Competing formation of N-(hydroxymethyl) $\delta$ -lactams. *ARKIVOC* **6**, 108–126 (2014).
108. Wang, D. & Astruc, D. The golden age of transfer hydrogenation. *Chem. Rev.* **115**, 6621–6686 (2015).
109. Chen, L.-Y. *et al.* 2,3-Dichloro-5,6-dicyanobenzoquinone (DDQ) mediated oxidationdehydrogenation of 2-aryl-3,4-dihydro-2H-benzopyrans: Synthesis of 2-arylbenzopyran-4-ones. *ARKIVOC* **11**, 64–76 (2010).
110. Porto, R. S., Vasconcellos, M. L., Ventura, E. & Coelho, F. Diastereoselective epoxidation of allylic diols derived from Baylis-Hillman adducts. *Synthesis (Stuttg)*. 2297–2306 (2005).
111. in *Comprehensive Organic Name Reactions and Reagents* (John Wiley & Sons, Inc., 2010).
112. Gawande, M. B., Polshettiwar, V., Varma, R. S. & Jayaram, R. V. An efficient and chemoselective Cbz-protection of amines using silica–sulfuric acid at room temperature. *Tetrahedron Lett.* **48**, 8170–8173 (2007).
113. Cox, O. B. *et al.* A poised fragment library enables rapid synthetic expansion yielding the first reported inhibitors of PHIP(2), an atypical bromodomain. *Chem. Sci.* **7**, 2322–2330 (2016).
114. Hall, R. J., Mortenson, P. N. & Murray, C. W. Efficient exploration of chemical space by fragment-based screening. *Prog. Biophys. Mol. Biol.* **116**, 82–91 (2014).
115. Pearce, N. *et al.* A multi-crystal method for extracting obscured signal from crystallographic electron density. *bioRxiv* (2016).
116. Keen, N. & Taylor, S. Aurora-kinase inhibitors as anticancer agents. *Nat Rev Cancer* **4**, 927–936 (2004).
117. Bischoff, J. R. & Plowman, G. D. The Aurora/Ipl1p kinase family: Regulators of chromosome segregation and cytokinesis. *Trends Cell Biol.* **9**, 454–459 (1999).
118. Janeček, M. *et al.* Allosteric modulation of AURKA kinase activity by a small-molecule inhibitor of its protein-protein interaction with TPX2. *Sci. Rep.* **6**, 28528 (2016).
119. Emsley, P., Lohkamp, B., Scott, W. G. & Cowtan, K. Features and development of Coot. *Acta Crystallogr. Sect. D Biol. Crystallogr.* **66**, 486–501 (2010).
120. Mao, J. C., Wan, B. S., Wang, R. L., Wu, F. & Lu, S. W. Concise synthesis of novel practical sulfamide–amine alcohols for the enantioselective addition of diethylzinc to aldehydes. *J. Org. Chem* **69**, 9123–9127 (2004).
121. Jin, W., Li, X. C. & Wan, B. A highly diastereo- and enantioselective copper(I)-catalyzed Henry reaction using a bis(sulfonamide)-diamine ligand. *J. Org. Chem* **76**, 484–491 (2011).
122. Jin, W., Li, X., Huang, Y., Wu, F. & Wan, B. A highly effective bis(sulfonamide)-diamine ligand: A unique chiral skeleton for the enantioselective Cu-catalyzed Henry reaction. *Chem. Eur. J.* **16**, 8259–8261 (2010).
123. van Lingen, H. L. *et al.* An efficient synthesis of 1-naphthylbis(oxazoline) and exploration of the scope in asymmetric catalysis. *Eur. J. Org. Chem.* 317–324 (2003).
124. Dollinger, H. *et al.* US2007/287704 A1. (2007).
125. Majik, M. S., Parameswaran, P. S. & Tilve, S. G. Total synthesis of (–)- and (+)-tedanalactam. *J. Org. Chem* **74**, 6378–6381 (2009).
126. Jenkins, T., Husfeld, C., Seroogy, J. & Wray, J. US2011/262355 A1. (2011).
127. Canne, L. E., Winston, R. L. & Ken, S. B. H. Synthesis of a versatile purification handle for use with Boc chemistry solid phase peptide synthesis. *Tetrahedron Lett.* **38**, 3361–3364 (1997).

128. Henderson, J. A. & Phillips, A. J. Total synthesis of aburatubolactam A. *Angew. Chem. Int. Ed.* **47**, 8499–8501 (2008).
129. Yokoyama, H., Ejiri, H., Miyazawa, M., Yamaguchi, S. & Hirai, Y. Asymmetric synthesis of fagomine. *Tetrahedron: Asymmetry* **18**, 852–856 (2007).
130. Tosatti, P. Metal-Catalysed Asymmetric Allylic Substitution Reactions for Array Synthesis. **Ph.D.**, (University of Leeds, 2011).